

**Aus der Abteilung für Klinische Pharmakologie
Direktor: Prof. Dr. med. S. Endres**

**Medizinische Klinik und Poliklinik IV
Klinikum der Universität
Ludwig-Maximilians-Universität München
Direktor: Prof. Dr. med M. Reincke**

**Molekulare Mechanismen der Entzündung:
Pro- und anti-inflammatorische Faktoren und deren
Bedeutung für Pathophysiologie und Therapie
entzündlicher Erkrankungen**

**Habilitationsschrift
vorgelegt von
Dr. med. Arndt Schottelius
2018**

Inhaltsverzeichnis

Abkürzungsverzeichnis.....	3
1. Pro- und anti-inflammatorische Faktoren und deren Rolle bei Entstehung und Kontrolle der Entzündung.....	4
2. Entzündungserkrankungen können mit therapeutischen Antikörpern und kleinmolekularen Substanzen erfolgreich behandelt werden.....	6
3. Zusammenfassung und Ausblick.....	9
4. Literaturverzeichnis.....	10
Lebenslauf.....	14
Verzeichnis der Veröffentlichungen.....	21
Anhang.....	24

Abkürzungsverzeichnis

NF- κ B

IL-10

TNF- α

GM-CSF

Nukleärer Faktor kappa B

Interleukin-10

Tumor-Nekrose-Faktor- α

Granulozyten-Makrophagen-Kolonie-stimulierender Faktor

1. Pro- und anti-inflammatorische Faktoren und deren Rolle bei Entstehung und Kontrolle der Entzündung

Viele Entzündungserkrankungen sind durch eine überschießende und unkontrollierte Ausschüttung von pro-inflammatorischen Zytokinen charakterisiert. Einer der zentralen Regulatoren einer vermehrten Ausschüttung dieser entzündlichen Zytokine ist der Nukleäre Faktor kappa B (NF- κ B). NF- κ B ist ein Transkriptionsfaktor der die Transkription einer Reihe von Genen reguliert, die in der Entzündung und bei der Entstehung von Krebs eine zentrale Rolle spielen. Eine Dysregulation von NF- κ B spielt eine wichtige Rolle bei chronisch entzündlichen Erkrankungen wie etwa der rheumatoiden Arthritis, der Psoriasis oder chronisch entzündlicher Darmerkrankungen. So werden zum Beispiel viele pro-entzündliche Zytokine – wie etwa IL-1 β , TNF- α , IL-2, IL-6, IL-8 und auch IL-12 - transkriptionell durch NF- κ B reguliert, die bei der Pathogenese chronisch-entzündlicher Darmerkrankungen wie Morbus Crohn oder Colitis ulcerosa zentral beteiligt sind (Schottelius und Baldwin, 1999). Bei diesen Patienten wurde die aktivierte Form von NF- κ B in der entzündeten Mukosa gefunden (Schreiber, Nikolaus et al. 1998). Auch andere Transkriptionsfaktoren wie etwa *Signal Transducer and Activator of Transcription* (STAT) 1 wurden im entzündeten Gewebe von Patienten mit Colitis ulcerosa gefunden (Schreiber, Rosenstiel, Hampe, Schottelius et al. 2002). Während in der Entzündung und in undifferenzierten intestinalen Epithelzellen IL-1 β NF- κ B stark induzieren kann, geht diese IL-1 β -induzierte NF- κ B Aktivierung interessanterweise mit zunehmender Zelldifferenzierung verloren (Böcker, Schottelius, Watson, Holt, Licato, Brenner, Sartor, Jobin 2000).

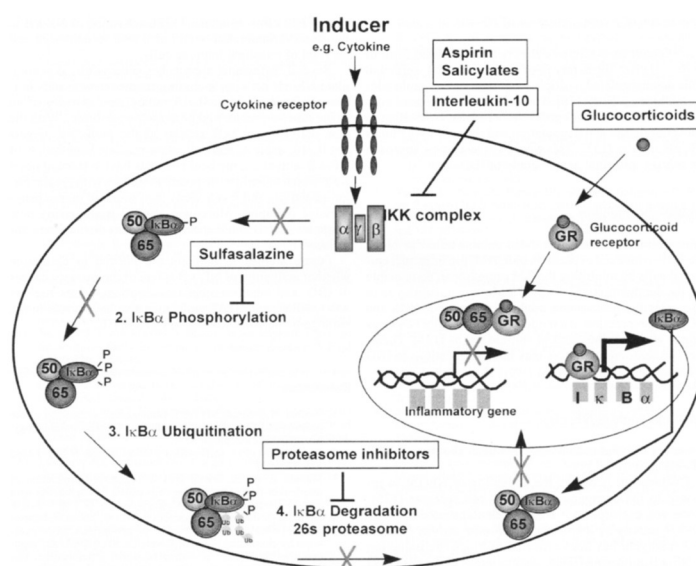


Abbildung 1: Effekte verschiedener anti-entzündlicher Wirkstoffe auf NF- κ B

Glukokortikoide binden an den Glukokortikoid-Rezeptor, der direkt an den p65/p50 Heterodimer binden und diesen inhibieren kann (Transrepression). Glukokortikoide inhibieren NF- κ B auch durch die Induktion von I κ B α (Schottelius and Baldwin, 1999)

NF- κ B wird in vielen Krebsarten konstitutiv aktiviert gefunden, wo es verschiedene Tumor-fördernde Wirkungen ausübt. Diese Tumor-fördernde Wirkung wird weiterhin durch die Beobachtung unterstützt, dass Patienten mit einer chronischen Entzündung ein höheres

Krebsrisiko haben. So ist etwa die chronische Entzündung bei den chronisch-entzündlichen Darmerkrankungen (CED) ein Risikofaktor für das CED-assoziierte kolorektale Karzinom (KRK), das etwa 5% aller kolorektalen Karzinome ausmacht (Schottelius, Dinter et al. 2006; Schottelius und Dinter 2006). Obwohl die molekularen Mechanismen der Verbindung zwischen CED und KRK nicht gut verstanden sind, weisen präklinische Modelle auf eine Rolle des Transkriptionsfaktors NF- κ B hin. Zum einen reguliert NF- κ B die Expression verschiedener Zytokine und moduliert dadurch den Entzündungsprozess in CED. Zum anderen stimuliert NF- κ B die Proliferation von Tumorzellen und verlängert deren Überleben durch die Regulation anti-apoptotischer Gene (Chu, McKinsey, Liu et al.). Zudem konnte gezeigt werden, dass die meisten Karzinogene und Tumor-Promotoren NF- κ B aktivieren, während chemopräventive Stoffe generell diesen Transkriptionsfaktor hemmen. In der Tat gibt es vielfältige Hinweise dafür, dass NF- κ B Krebs erzeugen könnte. Dazu zählen die Erkenntnisse, dass NF- κ B-kontrollierte Gene Onkogene sein können, und dass dieser Transkriptionsfaktor die Apoptose, die Zell-Zyklus Progression, sowie die Zellproliferation und möglicherweise auch die Zelldifferenzierung kontrolliert (Baldwin 1996). So stimuliert etwa onkogenes H-Ras über PI3K und Akt die transkriptionelle Aktivität von NF- κ B und unterdrückt dadurch die Apoptose (Madrid, Wang, Guttridge, Schottelius und Baldwin, 2000).

Das pro-entzündliche Zytokin TNF- α , ein starker NF- κ B Aktivator, ist in den chronisch-entzündlichen Darmerkrankungen, der rheumatoiden Arthritis und in der Psoriasis ein Hauptfaktor in der Entzündungs-Pathogenese (Übersicht in Schottelius, Moldawer, Dinarello, Asadullah, Sterry, Edwards, 2004). Ähnlich wie IL-1, ist TNF- α ein zentraler Regulator der angeborenen Immunität. Die durch TNF- α vermittelte Entzündungsantwort wird über IL-1, aber auch über mehr distale pro-inflammatorische Zytokine vermittelt, darunter IL-1, IL-4, IL-6, IL-12, IL-18 oder IFN γ . Die Expression von TNF- α wird durch verschiedenste Stimuli induziert, darunter Viren, Bakterien, Tumor-Zellen, Komplement und eine Reihe von Zytokinen (Übersicht in Schottelius, Moldawer, Dinarello et al. 2004). Eine der Signalkaskaden, die durch diese Stimuli zur Produktion und Ausschüttung von TNF- α führen, wird über die Kinase p38 und die darunter liegende Mitogen-aktivierte Protein Kinase-aktivierte Protein Kinase 2 (MK2) vermittelt. Die pharmakologische Blockierung dieser Kinasen ist auch das Ziel therapeutischer Ansätze mit niedermolekularen Substanzen.

Ein wichtiger Bestandteil jeder Entzündung ist die Einwanderung von Leukozyten in das entzündete Gewebe. Die Einwanderung der Leukozyten ist durch eine Kaskade von Aktivierungsschritten charakterisiert, an deren Anfang das Anhaften der Zellen an die Innenwand der betroffenen Gefäße steht (Springer 1994). Hierbei erkennen E- und P-Selektine auf der Gefäßoberfläche bestimmte Karbohydrat-Epitope auf der Oberfläche der Leukozyten, welche für ihre Funktionalität durch Fukosyltransferasen zuvor fukosyliert worden sein müssen (de Vries, Knegtel, Holmes et al. 2001; Maly, Thall, Petryniak et al. 1996; Schottelius, Hamann und Asadullah 2003; Syrbe, Jennrich, Schottelius et al. 2004).

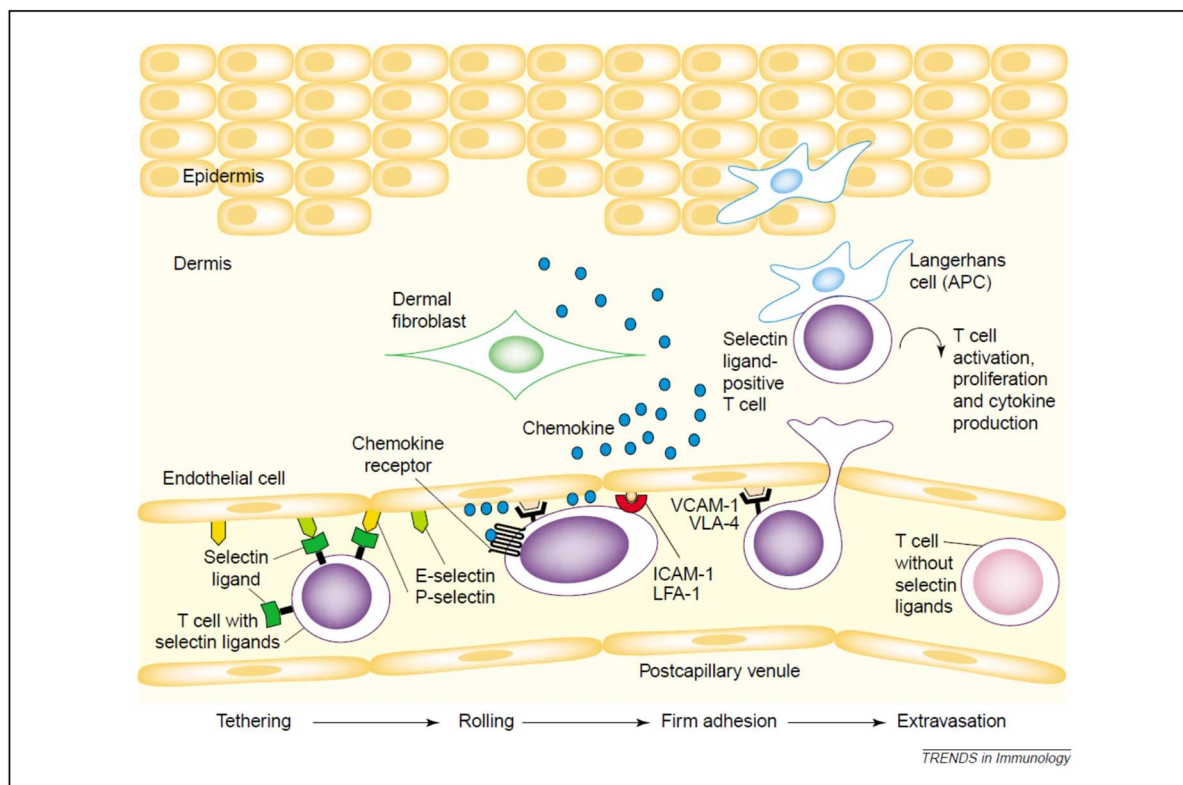


Abbildung 2: Rollen und Extravasation von Memory T Zellen in der kutanen Entzündung (Schottelius et al, Trends in Immunology 2003)

Die Fukosyltransferase VII scheint besonders für die kutane Immunität wichtig zu sein, da Knock-out-Studien in FucVII^{-/-} Mäusen eine stark verminderte Entzündung in Hautentzündungsmodellen zeigen konnten (Schottelius, Lowe und Asadullah 2002; Schottelius, Asadullah und Hamann 2004).

Darüber hinaus spielen Chemokine und ihre Rezeptoren bei der Einwanderung von Leukozyten in das entzündete Gewebe eine bedeutende Rolle. So konnte in entzündlichen Hauterkrankungen, wie etwa der Psoriasis, den Chemokin-Rezeptoren CCR4 und CCR10 eine Schlüsselrolle für die hautspezifische Einwanderung von T-Zellen zugeschrieben werden (Reiss, Proudfoot und Power, 2001).

2. Entzündungserkrankungen können mit therapeutischen Antikörpern und kleinmolekularen Substanzen erfolgreich behandelt werden

Viele Faktoren, die der Entzündung entgegenwirken, üben ihre anti-inflammatorische Wirkung zumindest teilweise durch die Unterdrückung von NF- κ B aus. So werden seit vielen Jahren Glukokortikoide erfolgreich in der Behandlung chronisch entzündlicher Erkrankungen therapeutisch eingesetzt. Die starke therapeutische Wirkung von Glukokortikoiden kann durch ihre Hemmung von NF- κ B als einen der Hauptregulatoren der Entzündung erklärt werden (Scheinmann 1995). Der größte Teil der anti-inflammatorischen Wirkung von Glukokortikoiden wird durch einen Transrepressions-Mechanismus ausgeübt, bei dem die Expression pro-entzündlicher Faktoren auch durch eine Hemmung von NF- κ B vermittelt wird. Da Glukokortikoide nach längerer Gabe jedoch auch Nebenwirkungen, wie etwa eine zunehmende Atrophie der Haut hervorrufen können, hat sich die pharmakologische

Forschung in der Industrie lange Zeit mit der Suche nach neuartigen sogenannten dissoziierten Glukokortikoid-Rezeptor Agonisten befasst und auch solche Substanzen identifizieren können (Schäcke und Schottelius 2004). Diese SEGRAs (*selective glucocorticoid receptor agonists*) Substanzen zeigen eine gesteigerte Transrepression bei verringerter Transaktivierung und konnten hierdurch in Entzündungsmodellen eine Verringerung von Nebenwirkungen bei erhaltener anti-entzündlicher Wirksamkeit zeigen.

Offenbar spielt auch die Sensitivität der Glukokortikoid-Rezeptoren in verschiedenen Entzündungserkrankungen eine Rolle beim Ansprechen der Therapie mit Glukokortikoiden. So konnte beispielsweise in peripheren mononukleären Zellen von Patienten mit chronisch entzündlichen Darmerkrankungen eine höhere Expression des Glukokortikoid-Rezeptors mit erhöhter Dissoziationskonstante als Zeichen niedriger Affinität festgestellt werden. Diese Beobachtung könnte mit einer verringerten Sensitivität gegenüber exogenen und endogenen Glukokortikoiden erklärt werden (Schottelius, Wedel, Weltrich et al. 2000).

Auch für das anti-inflammatorische Zytokin IL-10 konnte gezeigt werden, dass es andere pro-inflammatorische Zytokine zumindest teilweise durch eine Inhibierung von NF- κ B unterdrückt. Diese IL-10-vermittelte Blockade von NF- κ B wird über eine Hemmung der I κ B Kinase und durch eine Blockade der DNA-Bindung von NF- κ B vermittelt (Schottelius, Mayo, Sartor und Baldwin et al. 1999). Zusätzlich induziert IL-10 auch eine selektive Induktion der nukleären Translokation und DNA-Bindung von NF- κ B-inhibierenden p50 Homodimeren (Driessler, Venstrom, Sabat, Asadullah und Schottelius 2003).

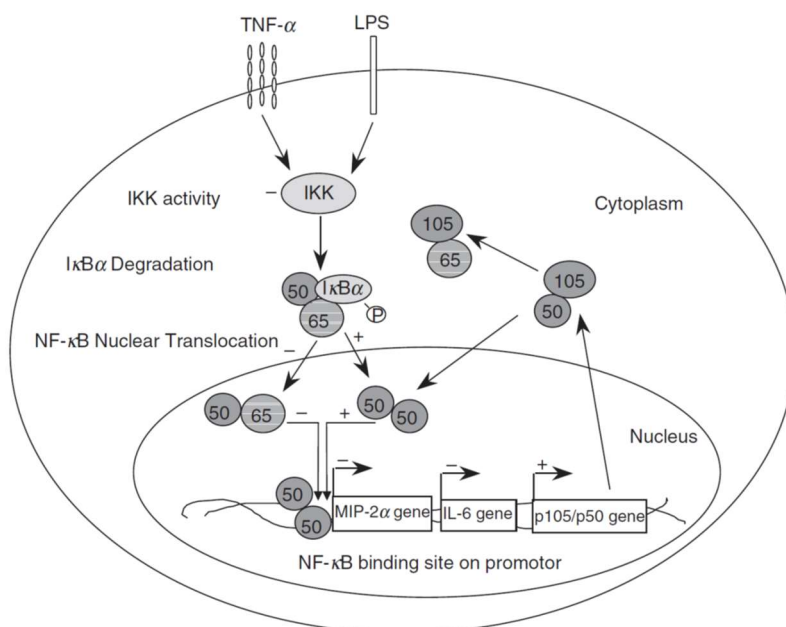


Abbildung 3: Schema der IL-10 vermittelten Inhibierung von NF- κ . Inhibition der IKK Aktivität und Stabilisierung von I κ B α , damit Inhibition der nukleären Translokation von p65/p50 Heterodimeren. Selektive Expression von p105/p50 Heterodimeren und nukleäre Translokation von repressiven p50 Homodimeren (Schottelius et al 1999; Driessler und Schottelius 2004)

Welche zentrale Rolle TNF- α bei Entzündungserkrankungen spielt, zeigt der große therapeutische Erfolg beim Einsatz von monoklonalen Antikörpern wie Infliximab oder Adalimumab, die dieses pro-inflammatorische Zytokin sehr effektiv neutralisieren (Übersicht in Schottelius, Asadullah, Sterry, Edwards 2006). Bei der Behandlung der rheumatoiden Arthritis und der multiplen Sklerose werden neuerdings auch neutralisierende monoklonale Antikörper gegen das pro-entzündliche Zytokin GM-CSF mit Erfolg klinisch getestet (Behrens, Tak, Ostergaard, Schottelius und Burkhardt et al. 2014; Schottelius 2013). GM-CSF wird in Patienten mit rheumatoider Arthritis in höherer Konzentration im entzündeten synovialen Gewebe und der Synovialflüssigkeit gefunden (Alvaro-Gracia, Zvaifler, Brown et al 1991; Wright, Bucknall, Moods et al. 2012). Patienten, die GM-CSF als supportive Therapie erhielten, erfuhren eine Verschlimmerung ihrer rheumatoiden Arthritis (de Vries, Willemse, Biesma et al. 1991). Sowohl die Inhibierung des Zytokins GM-CSF durch einen neutralisierenden Antikörper, wie auch die Inhibition der Signaltransduktion durch Blockade des GM-CSF Rezeptors haben erste erfolgsversprechende therapeutische Wirkungen gezeigt (Behrens, Tak, Ostergaard, Schottelius und Burkhardt et al 2014; Burmester, Weinblatt, McInnes 2011). Derzeit werden beide therapeutischen anti-GM-CSF/GM-CSF-Rezeptor Ansätze in Phase II/III Studien weiter geprüft. Präklinisch konnte der Einsatz von monoklonalen Antikörpern gegen die Chemokin-Rezeptoren CCR4 und CCR10 in der Maus effektiv das spezifische Einwandern von T-Zellen in die entzündete Haut verhindern (Wang, Fujita, Schottelius et al. 2010).

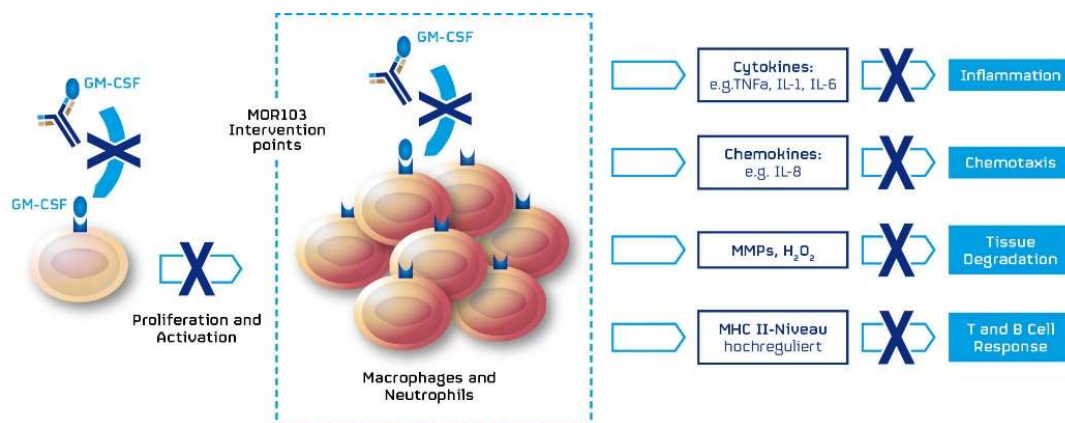


Abbildung 4: Wirkungsmechanismen des gegen GM-CSF gerichteten monoklonalen Antikörpers MOR103 (Webseite der MorphoSys AG).

Neben monoklonalen Antikörpern sind auch eine Reihe von neuartigen anti-entzündlichen Lipid-Mediator Analogen und niedermolekularen Substanzen auf ihre Wirksamkeit in Tiermodellen der Entzündung getestet worden. So zeigen etwa Lipoxin A4 Analoge eine starke anti-inflammatorische Wirkung in Modellen der Hautentzündung (Schottelius, Giesen, Asadullah et al. 2002; Guildford, Baumann, Skuballa, Schottelius et al. 2004). Auch niedermolekulare Inhibitoren der (*Mitogen-activated protein kinase-activated*) MAP Kinase 2 haben gute anti-entzündliche Effekte in Hautentzündungsmodellen zeigen können (Schottelius, Zügel, Döcke et al. 2010). Die pharmazeutische Industrie hat zudem versucht, niedermolekulare Substanzen zur Inhibierung der Fukosyltransferase VII zu identifizieren (von Ahsen, Voigtmann, Klotz, Schottelius et al. 2007).

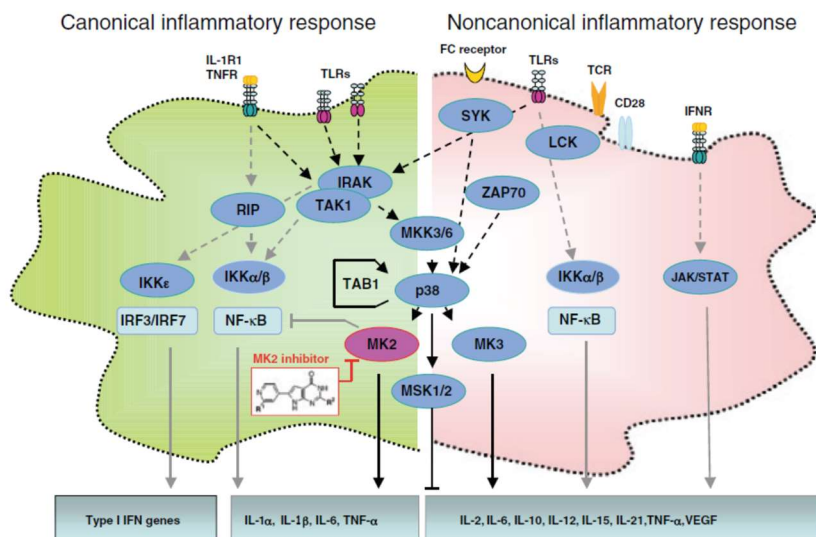


Abbildung 5: MK-2 liegt in der Signalkaskade unterhalb p38 und ist an der Produktion von TNF α und anderen pro-entzündlichen Zytokinen beteiligt (canonical and non-canonical activation of the p38 pathway, Fyhrquist et al 2010)

3. Zusammenfassung und Ausblick

Die durchgeführten Arbeiten beschreiben wichtige molekulare Mechanismen der Pathogenese häufiger Entzündungskrankheiten. Der anti-entzündliche Mechanismus des zentralen entzündungshemmenden Zytokins IL-10 konnte entschlüsselt werden. Diese Erkenntnisse haben auch zur Erforschung und präklinischen Entwicklung neuartiger niedermolekularer Substanzen für die Behandlung entzündlicher Hauterkrankungen und anderer Entzündungserkrankungen geführt.

In der Behandlung der rheumatoiden Arthritis konnten erste bedeutende therapeutische Erfolge durch den Einsatz eines neuen gegen GM-CSF gerichteten monoklonalen Antikörpers erzielt werden. Diese Substanz hat auch erste erfolgsversprechende Daten in der multiplen Sklerose erzielt und wird nun in weiteren klinischen Studien in der rheumatoiden Arthritis und der entzündlichen Osteoarthritis der Hand an Patienten erprobt.

Literaturverzeichnis

1. Alvaro-Gracia JM, Zvaifler NJ, Brown CB, Kaushansky K, Firestein GS (1991). Cytokines in chronic inflammatory arthritis. VI. Analysis of the synovial cells involved in granulocyte-macrophage colony-stimulating factor production and gene expression in rheumatoid arthritis and its regulation by IL-1 and tumor necrosis factor-alpha. *J Immunol* 146, 3365-3371.
2. Baldwin, AS (1996) The NF-kappa B and I kappa B proteins: new discoveries and insights. *Annu Rev Immunol* 14, 649-683.
3. Behrens F, Tak PP, Ostergaard M, Stoilov R, Wiland P, Huizinga TW, Berenfs VY, Vladeva S, Rech J, Rubbert-Roth A, Korkosz M, Rekalov D, Zupanets IA, Ejbjerg BJ, Geiseler J, Fresenius J, Korolkiewicz RP, Schottelius AJ, Burkhardt H. (last authors contributed equally) (2015). MOR103, a human monoclonal antibody to granulocyte-macrophage colony-stimulating factor, in the treatment of patients with moderate rheumatoid arthritis: results of a phase Ib/IIa randomised, double-blind, placebo-controlled, dose-escalation trial. *Ann Rheum Dis* 74, 1058-1064.
4. Böcker U, Schottelius A, Watson J, Holt L, Licato L, Brenner DA, Sartor RB and Jobin C (2000). Cellular differentiation causes a selective down-regulation of interleukin (IL)-1 beta mediated NF-kappa B activation and IL-8 gene expression in intestinal epithelial cells. *J Biol Chem* 275, 12207-12213.
5. Burmester GR, Weinblatt ME, McInnes IB, Porter D, Barbarash O, Vatutin M, Szombati I, Esfandiari E, Sleeman MA, Kane CD, Cavet G, Wang B, Godwood A, Magrini F; EARTH Study Group (2013). Efficacy and safety of mavrilimumab in subjects with rheumatoid arthritis. *Ann Rheum Dis* 72, 1445-52.
6. Chu ZL, McKinsey TA, Liu L, Gentry JJ, Malim MH, Ballard DW (1997) Suppression of tumor necrosis factor-induced cell death by inhibitor of apoptosis c-IAP2 is under NF-kappaB control. *Proc Natl Acad Sci U S A* 94, 10057-10062.
7. de Vries T, Knegtel RM, Holmes EH, Macher BA. (2001). Fucosyltransferases: structure/function studies. *Glycobiol* 11, 119R-128R.
8. de Vries EG, Willems PH, Biesma B, Stern AC, Limburg PC, Vellenga E (1991). Flare-up of rheumatoid arthritis during GM-CSF treatment after chemotherapy. *Lancet* 338, 517-518.
9. Driessler F, Venstrom K, Sabat R, Asadullah K and Schottelius AJ (2003). Molecular mechanisms of Interleukin-10 to inhibit NF-kappa B activity: a role for p50. *Clinical Experiment Immunol*, 135, 64-73.

10. Fyhrquist N, Matikainen S, Lauerma A (2010). MK2 signaling: lessons on tissue specificity in modulation of inflammation. *J Invest Dermatol* 130, 342-344.
11. Guildford WJ, Bauman JG, Skuballa W, Bauer S, Wei GP, Davey D, Schaefer C, Mallari C, Terkelsen J, Tseng JL, Shen J, Subramanyam B, Schottelius AJ and Parkinson J (2004). Novel 3-oxa lipoxin A4 analogues with enhanced chemical and metabolic stability have anti-inflammatory activity in vivo. *J Med Chem*, 47, 2157-2165.
12. Madrid LV, Wang CY, Guttridge DC, Schottelius AJ and Baldwin Jr AS (2000). Akt suppresses apoptosis by stimulating the transactivation potential of the RelA/p65 subunit of NF-kappa B. *Mol Cell Biol* 20, 1626-1638.
13. Malý P, Thall A, Petryniak B, Rogers CE, Smith PL, Marks RM, Kelly RJ, Gersten KM, Cheng G, Saunders TL, Camper SA, Camphausen RT, Sullivan FX, Isogai Y, Hindsgaul O, von Andrian UH, Lowe JB (1996). The alpha(1,3)fucosyltransferase Fuc-TVII controls leukocyte trafficking through an essential role in L-, E-, and P-selectin ligand biosynthesis. *Cell* 86, 643-653.
14. Reiss Y, Proudfoot AE, Power CA, Campbell JJ, Butcher EC (2001). CC chemokine receptor (CCR)4 and the CCR10 ligand cutaneous T cell-attracting chemokine (CTACK) in lymphocyte trafficking to inflamed skin. *J Exp Med.* 19, 1541-1547.
15. Schäcke H, Schottelius A, Hennekes H, Strehlke P, Jaroch S, Schmees N, Rehwinkel H, Döcke W-D and Asadullah K (2004). SEGRAs: a novel class of anti-inflammatory compounds. *Proc Nat Acad of Sci USA* 101, 227-232.
16. Schäcke H, Hennekes H, Schottelius A, Jaroch S, Lehmann M, Schmees N, Rehwinkel H, and Asadullah K (2002). Dissociation of transactivation from transrepression activity by selective glucocorticoid receptor agonists (SEGRAs) leads to separation of therapeutic effects from certain side effects – SEGRAs: a novel class of anti-inflammatory compounds. *Ernst Schering Research Foundation Workshop* 40, 357-371.
17. Schottelius A, Wedel S, Weltrich R, Rohde W, Buttgereit F, Schreiber S and Lochs H (2000). Higher expression of glucocorticoid receptor in peripheral mononuclear cells in inflammatory bowel disease. *Am J Gastroenterol* 95, 1994-1999.
18. Schottelius A, Mayo M, Sartor RB and Baldwin AS (1999). Interleukin-10 signaling blocks inhibitor of κ B kinase activity and Nuclear Factor κ B DNA-binding. *J Biol Chem* 274, 31868-31874
19. Schottelius A and Baldwin AS. In Stallmach et al (1999). Mechanisms and clinical efficacy of Interleukin-10. *Falk Symposium 104 - Induction and Modulation of Gastrointestinal Inflammation*, Kluwer Academic Publishers, Lancaster, UK.

20. Schottelius A, Mayo M, Sartor RB and Baldwin AS. In Rogler et al (1999). Interleukin-10 inhibits nuclear factor kappa B by distinct mechanisms. *Falk Symposium 111 – IBD at the End of its First Century*, Kluwer Academic Publishers, Lancaster, UK.
21. Schottelius A and Baldwin AS (1999). A role for transcription factor NF-kappa B in intestinal inflammation. *Internat J Colorect Dis* 14, 18-28.
22. Schottelius AJ and Dinter H (2006). Cytokines, NF-κB, microenvironment, intestinal inflammation and cancer. *Cancer Treat Res*, 130, 67-87.
23. Schottelius A and Dinter H, Dalglish A and Haeffner B (2006). Cytokines, NF-κB, microenvironment, intestinal inflammation and cancer. *The Link between Inflammation and Cancer – Wounds that do not heal*, Springer US.
24. Schottelius AJ, Moldawer LL, Dinarello C, Asadullah K, Sterry W, and Edwards, CK III (2004). Biology of Tumor Necrosis Factor-α (TNFα) – implications for psoriasis. *Exp Dermatol*, 13, 193-222.
25. Schottelius A, Asadullah K, Sterry W and Edwards C III. In Asadullah and Sterry (2006). Anti-TNFα therapy in dermatology. *Cytokine and Anti-Cytokine Therapy in Dermatology*, Transworld Research Network, Kerala, India.
26. Schottelius AJ, Giesen C, Asadullah K, Bauman J, Guilford W, Perez HD, Fierro I, Colgan S, Serhan CN and Parkinson JF (2002). An aspirin-triggered Lipoxin A4 stable analog displays a unique topical anti-inflammatory profile. *J Immunol* 169, 7063-7070.
27. Schottelius AJ, Zügel U, Döcke WD, Zollner TM, Röse L, Mengel A, Buchmann B, Becker A, Grütz G, Naundorf S, Friedrich A, Gaestel M, Asadullah K. (2010). The role of mitogen-activated protein kinase-activated protein kinase 2 in the p38/TNF-alpha pathway of systemic and cutaneous inflammation. *J Invest Dermatol* 130, 481-489.
28. Schottelius A, Hamann A and Asadullah K (2003). Role of fucosyltransferases in leukocyte trafficking: major impact for cutaneous immunity. *Trends Immunol* 24, 101-104.
29. Schottelius A. (2013). The role of GM-CSF in multiple sclerosis. *Drug Res* 63 Suppl 1: S8.
30. Schottelius A, Lowe JB and Asadullah K (2002). Deficiency of alpha (1,3) Fucosyltransferase VII has distinct effects in Th1 and Th2 models of skin inflammation. *J Invest Dermatol* 119, 207–350, Abstract 678.
31. Schreiber S, Rosenstiel P, Hampe J, Nikolaus S, Groessner B, Schottelius A, Kühbacher T, Hämling J, Fölsch UR and Seegert D (2002). Activation of Signal Transducer and Activator of Transcription (STAT) 1 in human chronic inflammatory bowel disease. *Gut* 51, 379-385.

32. Schreiber S, Nikolaus S and Hampe J (1998). Activation of nuclear factor kappa B in inflammatory bowel disease. *Gut* 42, 477-484.
33. Schreiber S und Schottelius A. In Fölsch/Kochsiek/Schmidt (2000). Pathophysiology of Inflammatory Bowel Disease. *Pathophysiologie des Menschen*, Springer Verlag Heidelberg.
34. Syrbe U, Jennrich S, Schottelius A, Richter A, Radbruch A and Hamann A (2004). Differential regulation of P-selectin ligand expression in naïve versus memory T cells: evidence for epigenetic regulation of involved glycosyltransferase genes. *Blood*, 104, 3243-3248.
35. Von Ahsen O, Voigtmann U, Klotz M, Nifantiev N, Schottelius A, Ernst A, Müller-Tiemann B, Parczyk K. (2008). A miniaturized high-throughput screening assay for fucosyltransferase VII. *Anal Biochem* 372, 96-105.
36. Wang X, Fujita M, Prado R, Tousson A, Hsu HC, Schottelius A, Kelly DR, Yang PA, Wu Q, Chen J, Xu H, Elmets CA, Mountz JD, Edwards CK 3rd. (2010). Visualizing CD4 T-cell migration into inflamed skin and its inhibition by CCR4/CCR10 blockades using in vivo imaging model. *Brit J Dermatol*, 162, 487-96.
37. Wright HL, Bucknall RC, Moots RJ, Edwards SW (2012). Analysis of SF and plasma cytokines provides insights into the mechanisms of inflammatory arthritis and may predict response to therapy. *Rheumatology*, 51, 451-459.

CURRICULUM VITAE

Dr. med. Arndt J. G. Schottelius

PROFESSIONAL EXPERIENCE

Kymab Ltd, Cambridge, UK

Executive Vice President of Research & Development

05/2017 – present

- Responsible for technology development, antibody discovery research, preclinical and clinical development
- 3 development programs (anti-OX40L in autoimmune diseases, anti-ICOS in cancer and anti-BMP6 anemia of chronic inflammation)
- 12 discovery programs in different stages of development

MorphoSys AG, Munich/Martinsried

Chief Development Officer (CDO)/

Entwicklungsvorstand

12/2008 – 04/2017

- Built all development functions and hired exceptional functional leaders for preclinical development, clinical research, clinical operations, drug safety, regulatory affairs, quality assurance and project management; leading CDO area of more than 70 people
- Responsibility for all strategic and operational tasks within proprietary development
- Responsible for Proprietary Development Budget exceeding € 75m
- Proprietary Research and Development Portfolio encompasses 14 programs:
 - MOR208 (anti-CD19 Fc enhanced mAb; ongoing Phase II studies in B-cell malignancies)
 - MOR202 (anti-CD 38 mAb; ongoing Phase II studies in multiple myeloma)
 - MOR209 (anti-PSMA/CD3 bispecific mAb; ongoing Phase I in castrate resistant prostate cancer)
 - MOR106 (target not disclosed; ongoing Phase I in inflammation)
 - MOR107 (Angiotensin Type II receptor agonist peptide; Phase I planned in 2016; fibrosis)
 - MOR103/ GSK3196165 (anti-GM-CSF mAb; out-licensed to GSK; ongoing Phase IIb in RA and Phase IIa in inflammatory hand osteoarthritis)
 - Immuno-Oncology program (MHC-associated peptides; collaboration with Immatics)
 - Immuno-Oncology program (target not disclosed; collaboration with Merck Serono)
 - Six discovery stage programs (targets not disclosed)
- Brought five therapeutic antibody programs into clinical development and in close collaboration with Chief Scientific Officer advanced discovery programs into preclinical development
- Developed human monoclonal antibody directed against GM-CSF (MOR103) to strong clinical proof-of-concept Phase IIa data in RA and established first positive Phase Ib safety data in MS leading to attractive partnership deal with GSK
- Established strong preclinical data for human antibody directed against CD38 (MOR202) in multiple myeloma and brought into Phase I/IIa leading to highly attractive co-development partnership with Celgene. Advanced program to robust clinical proof-of-concept. Leading efforts to design and implement pivotal combination study for anti-CD38 mAb program in multiple myeloma. Championed efforts to develop anti-CD38 in autoimmune disease.
- Instrumental in in-licensing humanized anti-CD19 Fc-enhanced monoclonal antibody (Xmab 5574/MOR208) and anti-PSMA/CD-3 bispecific mAb (ES414/MOR209) to broaden portfolio. Part of Joint Steering Committee moving the program into Phase I in prostate cancer patients.
- Drove strategic direction and development of MOR208 program into multiple fully sponsored monotherapy and combination therapy Phase II trials in CLL, ALL and NHL as well as

investigator sponsored studies in CLL and ALL. Led all efforts to design, achieve regulatory clearance and implement fast-to-market development path with Phase II/III pivotal combination study in DLBCL

- Successfully interacted with FDA and European authorities to achieve Orphan Drug and Fast-track designations for MOR208 anti-CD19 in the US and Europe
- Built network of and close interaction with top thought leaders in indications relevant for portfolio
- Responsible liaison and regular strategic reviews with Chief Scientific Advisor to MorphoSys
- Implemented Strategic Scientific Advisory Board with top thought leaders from US and Europe
- Very close collaboration with Business Development (co-lead) in selecting, reviewing and executing in-licensing projects and in partnering own proprietary programs

- Member and active participation in Joint Development Committees with GSK (MOR103 anti-GM-CSF), with Celgene during active partnership with MOR202 (anti-CD38) and with Emergent Biosolutions for MOR209 (anti-PSMA/CD3)
- Regular active participation of major international scientific conferences and scientific advisory board meetings for proprietary programs (immunology/inflammation/auto-immune & oncology/hem-onc/immuno-oncology)
- Implemented robust quality management system and SOPs for all development areas resulting in multiple successful and smooth authority GCP & GMP inspections
- Built highly functional and scalable project management system and team structures securing strong project leadership, team collaboration, execution on timelines and within budget
- Implemented and chair Development Review Committee (regular rigorous strategic and technical review of all preclinical and clinical programs in proprietary development; review of GLP-tox studies, preclinical disease model data, indication selection, designs and plans for early and late stage clinical studies, CTA/IND packages and other authority submissions)
- Executive member of Portfolio Management Group and instrumental in implementing of portfolio reviews
- Management Board position further includes the following responsibilities:
 - Setting overall strategy for the company
 - Selection of targets and lead indications for discovery programs
 - Active participation and decision making in regular cost center and budget reviews
 - Direction and prioritization of in-licensing and M&A projects
 - Executive presentations and updates to supervisory board and Science & Technology Committee
 - Representing the company at investor meetings and regular direct interactions with investors and analysts at major healthcare conferences in the US and Europe

Genentech, South San Francisco, CA

Medical Director, Immunology Tissue Growth & Repair Clinical Development 8/2007 – 12/2008

Clinical Scientist & Medical Monitor for Phase III studies with Rituximab & Ocrelizumab in RA

- Medical Monitoring of IMAGE & FILM studies
- Management of Quintile's medical monitoring activities
- Ongoing response to questions & assessment of issues which require input or intervention by sponsor (e.g. queries from sites/IRBs regarding ICFs)
- Biweekly review of study-specific data from the safety database and the review of IND safety reports for the Rituxan and 2H7 immunology programs
- Interface with and facilitation of study and program-specific issues between the global partners, GNE staff and CRO
- Regular participation in Rituxan & 2H7 RA Clinical Study Team (CST) meetings
- Development and review of study-related documents including those specified as CST deliverables
- Analysis and interpretation of study specific data
- Assembled pre-meeting package and Type C meeting with FDA to discuss utility of MRI in RA

Genentech, South San Francisco, CA

Director, Immunology Tissue Growth & Repair Early Development

1/2005-8/2007

Directing pre-clinical development of all protein, antibody and small molecule therapeutics in the areas of immunology and tissue growth & repair (ITGR)

- Providing scientific and strategic guidance and oversight to Early Development Teams and guiding all activities to IND-filing (including research studies, assay development, PK/PD studies, safety studies, CMC activities, indication selection, generation of target product profile, clinical development strategy and plan, diagnostic strategy and plan, market assessment & strategy, program valuation including costs, timelines, peak revenues and net present value)
- Providing intensive hands-on interactions with Early Development Team Leaders and management to ensure programs achieve development milestones and product values are maximized
- Overall accountability for IND filings with FDA
- Overseeing budgeting, planning processes and staffing on ITGR Early Development Teams

Major Accomplishments at Genentech

1/2005-12/2008

Direction & Leadership of Early Development Teams

- Directed early development and successful IND-submissions of two therapeutic antibodies for asthma and systemic lupus erythematosus.
 - HAE1 (high affinity anti-IgE mAb for mild to moderate asthma)
 - Anti-IFNalpha (active systemic lupus)
- Directed seven additional early development projects towards IND-submission
 - Anti-beta7 etrolizumab; now in Phase III for ulcerative colitis
 - Anti-OX40L (asthma)
 - Anti-BR3 (rheumatoid arthritis)
 - Anti-CD4 (rheumatoid arthritis, lupus and multiple sclerosis)
 - STIgMA (age-related macular degeneration)
 - Anti-Abeta crenezumab; now in Phase III for Alzheimer's Disease
 - Anti-oxLDL (diabetic patients with history of myocardial infarction)
- Co-led effort to create pre-Early Development Core Teams to enable a smooth transition from Late Stage Research into Early Development
- As Early Development Team Leader led development assessment of anti-IL13 lebrikizumab therapeutic antibody (Tanox) and successfully gained *Portfolio Planning Committee* approval for clinical development in asthma; now in Phase III for severe asthma
- As Diagnostic Subteam Leader initiated diagnostic program for the discovery and development of predictive biomarkers in the anti-IgE franchise
- Built ITGR Early Development group and hired two full-time Early Development Team Leader
- Supervised staff of 4-6 Early Development Team Leaders, who lead all pre-clinical development activities on an Early Development Project Team (including 4 Senior Scientists and one Associate Director)

Membership in key executive review committees & Sponsorship for Early Development Teams

- Influenced company key research & development and strategic portfolio management decisions as member of *Immunology Tissue Growth & Repair Development Review Committee* and *Research Review Committee* (ad-hoc)
- Sponsorship for all ITGR Early Development Teams at pre-IND Development Review Committee and IND Strategic Review Committee presentations
- Sponsorship for *Development Sciences Information Technology Systems Governance Committee*, which defined and managed the IT strategy & prioritizes, executes and integrates IT initiatives
- Provided guidance to teams for diagnostic and imaging strategies and plans as member of *Diagnostic Coordination Committee* and *Imaging Council*

Early Development Portfolio Management

- Co-developed and applied tier system for Early Development project prioritization

- Co-designed and implemented Early Development Pipeline tool with key milestones, project background and links to monthly project reports
- Co-chaired quarterly pre-PUB review of Early Development programs

Business Development Activities

- Served as the Development Sciences SPOC for multiple business development opportunities in ITGR; coordinated pre-clinical due diligence activities on several business development teams

Direction/Guidance in Strategic Alliances

- Membership of Joint Development Committee with TolerRx (anti-CD4 mAb) – reviewed and negotiated material production, pre-clinical plans and clinical development plans and timelines
- In collaboration with Alliance Management clarified JRCS/JDCC responsibilities and transition process for anti-OX40L project and guided team through transition
- Facilitated and maintained open communication with development partners (TolerRx & Roche)

Process Improvements

- Streamlined IND construction and review process for large and small molecules, resulting in more efficient process and shorter timelines to IND
- Led cross-functional initiative to streamline development assessment process for Early Development projects to improve efficiency in generation of target product profiles, clinical development plans and program valuations

Innovation & Leadership Development

- Led initiative to support innovation and scientific leadership in Development Sciences Organization
- Initiated scientific leadership goals and designed & implemented scientific leadership development program in Development Sciences (“*Leading Scientific Innovation*”)

Education & Training

- Led initiative to improve education and training on early development teams
- Designed and rolled-out new Early Development educational forum and supportive web-based tools (*Early Development Case Studies*)
- Co-designed and implemented Early Development Website containing tool kit with key guidance documents and templates to guide and train Early Development Teams

Berlex Biosciences, Richmond, CA

2003 – 2005

Subsidiary of Schering AG

Senior Scientist and Acting Head, Research Business Area Dermatology

Discovery and pre-clinical development of antibody and small molecule inhibitors for the treatment of inflammatory diseases

- Hired key scientific personal to establish new inflammation/dermatology group at Berlex
- Designed and implemented new laboratory for dermatology research group
- Established network and collaborations with key opinion leaders in dermatology and inflammation
- Initiated concept research proposal and led project team with the aim to identify a bispecific monoclonal antibody directed against CCR4 and CCR10 to treat inflammatory skin diseases
- Initiated immunizations and fusions, set up external collaborations to establish a novel animal model to screen leukocyte trafficking

Schering AG, Berlin, Germany (today part of Bayer AG)

1999 - 2003

Scientist, Research Business Area Dermatology

Discovery and pre-clinical development of small molecule inhibitors for the treatment of inflammation/autoimmune diseases and inflammatory skin diseases.

- Led and coordinated all *in vivo* screening of Selective Glucocorticoid Receptor Agonist compounds; successful identification of potential development candidates; establishment of clinical biomarkers

- and co-development of new formulations
- Initiated concept research project and led project team for the identification of a lead compound to inhibit a glykosyltransferase for the treatment of inflammatory skin diseases. Coordinated all research activities in chemistry and biology; project received high priority status
- Led *in vivo* activities for several projects (stable Lipoxin A4 analogue, kinase inhibitors, IL-10 inducers, chemokine receptor antagonist) to identify compounds with efficacy in inflammatory disease
- Member of the *Review Board* for internal research projects
- Member of the *Business Development Team* (interdisciplinary team formed by the Business Unit Dermatology with one representative from the functions Marketing, Clinical Development and Research with the task to establish business development strategies for a specific indication)
- Organization of an international workshop of the *Ernst Schering Research Foundation* with key opinion leaders in the field (“Leukocyte Trafficking: Role of Fucosyltransferases and Selectins”)

Charité University Hospital, Berlin, Germany **1995 - 1997**
Resident physician, 4th Medical Department for Gastroenterology, Hepatology & Endocrinology

- Residency training in internal medicine
- Research association with the Mucosal Immunology Group (Mentor: Stefan Schreiber, M.D.)
- Investigated the regulation of glucocorticoid receptor expression in inflammatory bowel disease
- Studied regulation of the NF- κ B/I κ B and STAT1 Systems in Patients with IBD
- Subinvestigator in two treatment protocols using human recombinant Interleukin-10 (Essex Pharma/Schering-Plough) in steroid refractory Crohns disease and ulcerative colitis and studying function and regulation of NF- κ B in steroid refractory disease

EDUCATION

High School Diploma, Clymer, New York (AFS Exchange Program)	1984
Graduation from German High School	1986

Medical School: **1988 – 95**

- Albert-Ludwigs-University Freiburg, Germany
- Doctoral thesis: “Expression and Structure of the p53 Tumor Suppressor Gene in Cells of Acute Myeloid Leukemia”,
Department of Hematology/Oncology, University Freiburg Medical Center
 (grade “*magna cum laude*”).
- Study Year at the Royal Free Hospital School of Medicine, London, UK 1992 - 93
- Final year medical school: Eberhard-Karls-University Tübingen 1994 - 95
- Electives in Basle, Switzerland and New York City
- Graduation, M.D. 1995

POSTGRADUATE TRAINING AND FELLOWSHIP APPOINTMENTS

Postdoctoral Fellow, Laboratory of Albert S. Baldwin, Jr., Ph.D., Professor of Biology, Associate Director, Lineberger Comprehensive Cancer Center, University of North Carolina, Chapel Hill, NC, USA	1997 - 99
---	-----------

- Close cooperation with R. Balfour Sartor, M.D., Center for IBD Research and Advanced Treatment, UNC
- Studying the molecular mechanisms involved in the inhibition of NF- κ B by IL-10
- Elucidating the role of intrinsic IL-10 in regulating NF- κ B activation and apoptosis in the IL-10 knock-out mouse

ACADEMIC HONORS AND AWARDS

Selection for the <i>American Field Service (AFS) Exchange Program</i>	1983 - 84
Scholarship of the <i>German National Scholarship Foundation</i> (<i>“Studienstiftung des deutschen Volkes”</i>)	1990 - 95
Research Fellowship Award by the <i>Crohn’s & Colitis Foundation of America</i>	1998 - 99

PROFESSIONAL MEMBERSHIPS

American Association of Immunology
American College of Rheumatology
American Society of Clinical Oncology
Society for Immunotherapy of Cancer

LEADERSHIP & DRUG DEVELOPMENT TRAINING

- Member of the *“Support & Challenge Group”* (Schering AG): highly selective participation for intense training in project leadership skills/management
- Project Management Courses (Berlex): Leadership, Teambuilding, Negotiation skills and Problem Solving
- *“Developing the Strategic Leader”* (Center for Creative Leadership), Colorado Springs, CO
- *“Leading Scientific Innovation”* (Genentech): Designed and initiated program for scientific leaders to foster innovation and creativity
- *Advanced Course in Immunology*, Stanford University
- *Toxicology in the Nonclinical Development of Drugs and Biologics* (PERI), Baltimore, MD
- *Leadership and Strategy in Pharmaceuticals and Biotech*, Harvard Business School, Boston, MA

INVITED LECTURES/ORAL PRESENTATIONS

Mechanisms and Clinical Efficacy of Interleukin-10

Falk Symposium 104 - Induction and Modulation of Gastrointestinal Inflammation, Saarbrücken, Germany March 5 -7 1998

Anti-Inflammatory Cross-Talk Into the NF- κ B System

Etiology and Pathophysiology of Chronic Intestinal Inflammation, Ferring Workshop, University of Kiel Medical Center, Germany March 20 1998

Molecular Mechanisms for the Inhibition of NF- κ B by IL-10

53th Meeting of the German Society for Digestive Diseases and Metabolism, Kiel, Germany September 1-6 1998

IL-10 Inhibits NF- κ B Activity and Renders HT-29 Cells Sensitive to TNF- α Induced Apoptosis

University of Heidelberg Medical Center, Germany March 1 1999

Role of NF- κ B in Cancer and Apoptosis

55th Meeting of the German Society for Digestive Diseases and Metabolism, Hamburg, Germany September 1-6 2000

Broad Topical Efficacy of a Stable Lipoxin A₄ Analog in Skin Inflammation

Meeting of the Society for Dermatological Research, Hamburg, Germany, February 15-17 2001

Pathophysiology and Therapy of Rheumatoid Arthritis/Novel targets in autoimmunity

Clinical Immunology Lecture Series, Charité University Hospital, Berlin, Germany, February 2003

Selective Glucocorticoid Receptor Agonists

“Trends and perspectives for the therapy of inflammatory skin disorders” Symposium organized by CRBA

Dermatology, Schering AG/Berlex, Berkely, USA, October 2003

Targeting the NF- κ B Pathway for Inflammatory Disease

Navigating the NF- κ B Pathway for Drug Development, Conference, American Conference Institute, Boston, October 27-28, 2004

Decision-Making in Early Drug Development, Invited Presentation at the German-American Business Association, San Francisco, February 8, 2006

Monoclonal Antibodies as Key Growth Components, 8th annual bioLogic Europe 2007 conference, Geneva, Switzerland, June 11-14, 2007

Early Drug Development, Lecture during course "Introduction to Biotechnology" (Prof. Cliff Wang), Stanford University, May 10, 2008

Reverse Brain Drain, Going Public Conference, Munich, Germany, April 17, 2009

Decision making on location for clinical development, 26th DGPharMed (German Association for Pharmaceutical Medicine) Conference, Cologne, Germany, March 2010

[besser durchgehend Kleinschreibung der Titel, wie ab hier nach unten]

The development of therapeutic antibodies at MorphoSys, Life Sciences Conference at Bird&Bird law firm, Munich, November 18, 2010

Optimized antibodies for the therapy of leukemias: MOR208, a new compound for the treatment of cancer, German Science Day, Berlin, February 2012

Anti-GM-CSF antibodies in multiple sclerosis, Symposium Paul-Martini Foundation, Berlin November 2013

Autoimmune disease: finding early differentiation in crowded markets, Panelist at Panel Discussion BioEurope, Turine, March 2014

Early clinical development and timely decision-making, Yearly Convention of the German Association of Pharmaceutical Medicine, Berlin, March 2015

How to Grow a Sustainable Biotech Company? Three Success Stories, Panelist at Panel Discussion Bio International Convention, Philadelphia, June 2105

Verzeichnis der Veröffentlichungen

1. Originalarbeiten als Erst- oder Letztautor

1. Behrens F, Tak PP, Ostergaard M, Stoilov R, Wiland P, Huizinga TW, Berenfus VY, Vladeva S, Rech J, Rubbert-Roth A, Korkosz M, Rekalov D, Zupanets IA, Ejbjerg BJ, Geiseler J, Fresenius J, Korolkiewicz RP, **Schottelius AJ***, Burkhardt H* (*last authors contributed equally) (2015). MOR103, a human monoclonal antibody to granulocyte-macrophage colony-stimulating factor, in the treatment of patients with moderate rheumatoid arthritis: results of a phase Ib/IIa randomised, double-blind, placebo-controlled, dose-escalation trial. *Annals Rheumatic Diseases* 74, 1058-1064. (Impact Factor IF 10.3)

2. **Schottelius AJ**, Zügel U, Döcke WD, Zollner TM, Röse L, Mengel A, Buchmann B, Becker A, Grütz G, Naundorf S, Friedrich A, Gaestel M, Asadullah K (2010). The role of mitogen-activated protein kinase-activated protein kinase 2 in the p38/TNF-alpha pathway of systemic and cutaneous inflammation. *Journal of Investigative Dermatology* 130, 481-489. (IF 7.2)

3. Driessler F, Venstrom K, Sabat R, Asadullah K and **Schottelius AJ** (2003). Molecular mechanisms of interleukin-10 to inhibit NF-kappa B activity: a role for p50. *Clinical Experimental Immunology* 135, 64-73. (IF 3.1)

4. **Schottelius AJ**, Giesen C, Asadullah K, Bauman J, Guilford W, Perez HD, Fierro I, Colgan S, Serhan CN and Parkinson JF (2002). An Aspirin-triggered Lipoxin A4 stable analog displays a unique topical anti-inflammatory profile. *Journal of Immunology* 169, 7063-7070. (IF 4.9)

5. **Schottelius A**, Wedel S, Weltrich R, Rohde W, Buttgerit F, Schreiber S and Lochs H (2000). Higher expression of glucocorticoid receptor in peripheral mononuclear cells in inflammatory bowel disease. *American Journal of Gastroenterology* 95, 1994-1999. (IF 10.7)

6. **Schottelius A**, Mayo M, Sartor RB and Baldwin AS (1999). Interleukin-10 signaling blocks inhibitor of κ B kinase activity and Nuclear Factor κ B DNA-binding. *Journal of Biological Chemistry* 274, 31868-31874. (IF 4.5)

7. **Schottelius A**, Brennscheidt U, Ludwig WD, Mertelsmann RH, Herrmann F and Lübbert M (1994). Mechanisms of p53 alteration in acute leukemias. *Leukemia* 8, 1673-1681. (IF 12.1)

2. Originalarbeiten als Koautor

8. Wang X, Fujita M, Prado R, Tousson A, Hsu HC, **Schottelius A**, Kelly DR, Yang PA, Wu Q, Chen J, Xu H, Elmets CA, Mountz JD, Edwards CK 3rd. (2010). Visualizing CD4 T-cell migration into inflamed skin and its inhibition by CCR4/CCR10 blockades using in vivo imaging model. *British Journal of Dermatology* 162, 487-96. (IF 4.2)

9. Ahsen O, Voigtmann U, Klotz M, Nifantiev N, **Schottelius A**, Ernst A, Müller-Tiemann B, Parczyk K. (2008). A miniaturized high-throughput screening assay for fucosyltransferase VII. *Analytical Biochemistry* 372, 96-105. (IF 2.2)

10. Guildford WJ, Bauman JG, Skuballa W, Bauer S, Wei GP, Davey D, Schaefer D, Mallari C, Terkelsen J, Tseng JL, Shen J, Subramanyam B, **Schottelius AJ** and Parkinson JF (2004). Novel 3-oxa lipoxin A4 analogues with enhanced chemical and metabolic stability have anti-inflammatory activity in vivo.

Journal of Medicinal Chemistry, 47, 2157-2165. (IF 5.4)

11. Schäcke H, **Schottelius A**, Hennekes H, Strehlke P, Jaroch S, Schmees N, Rehwinkel H, Döcke WD and Asadullah K (2004). Dissociation of transactivation from transrepression activity by selective glucocorticoid receptor agonists (SEGRAs) leads to separation of therapeutic effects from certain side effects – SEGRAs: a novel class of anti-inflammatory compounds.

Proceedings of the National Academy of Sciences 101, 227-232. (IF 9.4)

12. Syrbe U, Jennrich S, **Schottelius A**, Richter A, Radbruch A and Hamann A (2004). Differential regulation of P-selectin ligand expression in naïve versus memory T cells: evidence for epigenetic regulation of involved glycosyltransferase genes.

Blood 104, 3243-3248. (IF 11.8)

13. Schreiber S, Rosenstiel P, Hampe J, Nikolaus S, Groessner B, **Schottelius A**, Kühbacher T, Hämling J, Fölsch UR and Seegert D (2002). Activation of Signal Transducer and Activator of Transcription (STAT) 1 in human chronic inflammatory bowel disease.

Gut 51, 379-385. (IF 14.6)

14. Schäcke H, Hennekes H, **Schottelius A**, Jaroch S, Lehmann M, Schmees N, Rehwinkel H, and Asadullah K (2002). SEGRAs: a novel class of anti-inflammatory compounds.

Ernst Schering Research Foundation Workshop 40, 357-371. (IF 2.1)

15. Böcker U, **Schottelius A**, Watson J, Holt L, Licato L, Brenner DA, Sartor RB and Jobin C (2000). Cellular differentiation causes a selective down-regulation of interleukin (IL)-1 beta mediated NF-kappa B activation and IL-8 gene expression in intestinal epithelial cells.

Journal of Biological Chemistry 275, 12207-12213. (IF 4.5)

16. Madrid LV, Wang CY, Guttridge DC, **Schottelius AJ** and Baldwin AS Jr (2000). Akt suppresses apoptosis by stimulating the transactivation potential of the RelA/p65 subunit of NF-kappa B.

Molecular Cellular Biology 20, 1626-1638. (IF 4.7)

17. Ohta T, Michel JJ, **Schottelius AJ** and Xiong Y (1999). ROC1, a homolog of APC11, represents a family of cullin partners with associated ubiquitin ligase activity.

Molecular Cell 3, 535-541. (IF 14.0)

3. Übersichtsartikel

1. **Schottelius A** (2013). The role of GM-CSF in multiple sclerosis.
Drug Research 63 Suppl 1: S8. (IF 0.7)
2. **Schottelius AJ** and Dinter H (2006). Cytokines, NF- κ B, microenvironment, intestinal inflammation and cancer.
Cancer Treat Res 130, 67-87. (IF 3.3)
3. **Schottelius AJ**, Moldawer LL, Dinarello C, Asadullah K, Sterry W, and Edwards CK, III (2004). Biology of tumor Necrosis Factor- α (TNF α) – implications for psoriasis.
Experimental Dermatology, 13, 193-222. (IF 2.6)
4. **Schottelius A**, Hamann A and Asadullah K (2003). Role of fucosyltransferases in leukocyte trafficking: major impact for cutaneous immunity.
Trends in Immunology 24, 101-104. (IF 11.4)
5. **Schottelius A** and Baldwin AS (1999). A role for transcription factor NF-kappa B in intestinal inflammation.
International Journal of Colorectal Disease 14, 18-28. (IF 2.4)

Sum Impact Factors 1. – 3. : 147.2

4. Buchkapitel

1. **Schottelius A** and Dinter H, Cytokines, NF- κ B, microenvironment, intestinal inflammation and cancer. In Dalgleish A and Haeffner B (2006) *The Link between Inflammation and Cancer – Wounds that do not heal*, Springer US
2. **Schottelius A**, Asadullah K, Sterry W and Edwards C III, Anti-TNF α therapy in dermatology In Asadullah and Sterry (2006): *Cytokine and Anti-Cytokine Therapy in Dermatology*, Transworld Research Network, Kerala, India
3. **Schottelius A** “*Leukocyte Trafficking: Role of Fucosyltransferases and Selectins*”, Ernst Schering Research Foundation Workshop; Editors: **Schottelius A**, Asadullah K and Hamann A (2004)
4. Schreiber S und **Schottelius A**, *Pathophysiology of Inflammatory Bowel Disease*
In Fölsch/Kochsiek/Schmidt (2000): *Pathophysiologie des Menschen*, Springer Verlag Heidelberg
5. **Schottelius A** and Baldwin AS, Mechanisms and Clinical Efficacy of Interleukin-10
In Stallmach et al (1999): *Falk Symposium 104 - Induction and Modulation of Gastrointestinal Inflammation*, Kluwer Academic Publishers, Lancaster, UK
6. **Schottelius A**, Mayo M, Sartor RB and Baldwin AS
Interleukin-10 inhibits nuclear factor kappa B by distinct mechanisms
In Rogler et al (1999): *Falk Symposium 111 – IBD at the End of its First Century*, Kluwer Academic Publishers, Lancaster, UK

Anhang

1. **Schottelius A**, Brennscheidt U, Ludwig WD, Mertelsmann RH, Herrmann F and Lübbert M (1994). Mechanisms of p53 alteration in acute leukemias. *Leukemia* 8, 1673-1681.
2. **Schottelius A**, Mayo M, Sartor RB and Baldwin AS (1999). Interleukin-10 signaling blocks inhibitor of κ B kinase activity and Nuclear Factor κ B DNA-binding. *Journal of Biological Chemistry* 274, 31868-31874.
3. Ohta T, Michel JJ, **Schottelius AJ** and Xiong Y (1999). ROC1, a homolog of APC11, represents a family of cullin partners with associated ubiquitin ligase activity. *Molecular Cell* 3, 535-541.
4. **Schottelius A**, Wedel S, Weltrich R, Rohde W, Buttgerit F, Schreiber S and Lochs H (2000). Higher expression of glucocorticoid receptor in peripheral mononuclear cells in inflammatory bowel disease. *American Journal of Gastroenterology* 95, 1994-1999.
5. Böcker U, **Schottelius A**, Watson J, Holt L, Licato L, Brenner DA, Sartor RB and Jobin C (2000). Cellular differentiation causes a selective down-regulation of interleukin (IL)-1 beta mediated NF-kappa B activation and IL-8 gene expression in intestinal epithelial cells. *Journal of Biological Chemistry* 275, 12207-12213.
6. Madrid LV, Wang CY, Guttridge DC, **Schottelius AJ** and Baldwin AS Jr (2000). Akt suppresses apoptosis by stimulating the transactivation potential of the RelA/p65 subunit of NF-kappa B. *Molecular Cellular Biology* 20, 1626-1638.
7. **Schottelius AJ**, Giesen C, Asadullah K, Bauman J, Guilford W, Perez HD, Fierro I, Colgan S, Serhan CN and Parkinson JF (2002). An Aspirin-triggered Lipoxin A4 stable analog displays a unique topical anti-inflammatory profile. *Journal of Immunology* 169, 7063-7070.
8. Schreiber S, Rosenstiel P, Hampe J, Nikolaus S, Groessner B, **Schottelius A**, Kühbacher T, Hämling J, Fölsch UR and Seegert D (2002). Activation of Signal Transducer and Activator (STAT) 1 in human chronic inflammatory bowel disease. *Gut* 51, 379-385.
9. Schäcke H, Hennekes H, **Schottelius A**, Jaroch S, Lehmann M, Schmees N, Rehwinkel H, and Asadullah K (2002). SEGRAs: a novel class of anti-inflammatory compounds. *Ernst Schering Research Foundation Workshop* 40, 357-371.
10. Driessler F, Venstrom K, Sabat R, Asadullah K and **Schottelius AJ** (2003). Molecular mechanisms of interleukin-10 to inhibit NF-kappa B activity: a role for p50. *Clinical Experimental Immunology* 135, 64-73.
11. Syrbe U, Jennrich S, **Schottelius A**, Richter A, Radbruch A and Hamann A (2004). Differential regulation of P-selectin ligand expression in naïve versus memory T cells: evidence for epigenetic regulation of involved glycosyltransferase genes. *Blood* 104, 3243-3248.

12. Schäcke H, **Schottelius A**, Hennekes H, Strehlke P, Jaroch S, Schmees N, Rehwinkel H, Döcke WD and Asadullah K (2004). Dissociation of transactivation from transrepression activity by selective glucocorticoid receptor agonists (SEGRAs) leads to separation of therapeutic effects from certain side effects – SEGRAs: a novel class of anti-inflammatory compounds.
Proceedings of the National Academy of Sciences 101, 227-232.
13. Guildford WJ, Bauman JG, Skuballa W, Bauer S, Wei GP, Davey D, Schaefer D, Mallari C, Terkelsen J, Tseng JL, Shen J, Subramanyam B, **Schottelius AJ** and Parkinson JF (2004). Novel 3-oxa lipoxin A4 analogues with enhanced chemical and metabolic stability have anti-inflammatory activity in vivo.
Journal of Medicinal Chemistry, 47, 2157-2165.
14. Ahsen O, Voigtmann U, Klotz M, Nifantiev N, **Schottelius A**, Ernst A, Müller-Tiemann B, Parczyk K. (2008). A miniaturized high-throughput screening assay for fucosyltransferase VII.
Analytical Biochemistry 372, 96-105.
15. **Schottelius AJ**, Zügel U, Döcke WD, Zollner TM, Röse L, Mengel A, Buchmann B, Becker A, Grütz G, Naundorf S, Friedrich A, Gaestel M, Asadullah K (2010). The role of mitogen-activated protein kinase-activated protein kinase 2 in the p38/TNF-alpha pathway of systemic and cutaneous inflammation.
Journal of Investigative Dermatology 130, 481-489.
16. Wang X, Fujita M, Prado R, Tousson A, Hsu HC, **Schottelius A**, Kelly DR, Yang PA, Wu Q, Chen J, Xu H, Elmets CA, Mountz JD, Edwards CK 3rd. (2010). Visualizing CD4 T-cell migration into inflamed skin and its inhibition by CCR4/CCR10 blockades using in vivo imaging model.
British Journal of Dermatology 162, 487-96.
17. Behrens F, Tak PP, Ostergaard M, Stoilov R, Wiland P, Huizinga TW, Berenfus VY, Vladeva S, Rech J, Rubbert-Roth A, Korkosz M, Rekalov D, Zupanets IA, Ejbjerg BJ, Geiseler J, Fresenius J, Korolkiewicz RP, **Schottelius AJ***, Burkhardt H* (*last authors contributed equally) (2015). MOR103, a human monoclonal antibody to granulocyte-macrophage colony-stimulating factor, in the treatment of patients with moderate rheumatoid arthritis: results of a phase Ib/IIa randomised, double-blind, placebo-controlled, dose-escalation trial.
Annals Rheumatic Diseases 74, 1058-1064.

Mechanisms of p53 Alteration in Acute Leukemias

Arndt Schottelius¹, Ulrich Brennscheidt¹, Wolf-Dieter Ludwig², Roland H. Mertelsmann¹, Friedhelm Herrmann^{1,2}, and Michael Lübbert¹

¹Department of Hematology/Oncology, University of Freiburg Medical Center, ²Department of Medical Oncology and Applied Molecular Biology, University Hospital "Rudolf Virchow", Free University Berlin, and Max-Delbrück Center for Molecular Medicine, Berlin, Germany

Disruption of normal p53 expression is the most frequent genetic change occurring in various human solid tumors; it is mostly due to sequence alterations of the p53 coding region by missense mutations or to loss of an entire, functional allele of this gene. In the present study, possible mechanisms resulting in a disruption of regulated expression of wild-type p53 were examined in acute leukemias of either lymphoid (ALL) or myeloid (AML) phenotype. p53 transcript accumulation, nucleotide sequence and gene structure were analyzed in primary leukemic cells from 50 patients. p53-specific transcripts were detected in 26/26 cases of ALL and 16/23 cases of AML using reverse transcriptase (RT)-PCR. Sequencing of transcripts did not reveal any point mutations or deletions. Heterozygosity at a polymorphic *Bgl*I site within intron 1 was found in 4/28 leukemic samples, and loss of one allele was noted in one of these. In addition, a novel, leukemia-associated structural abnormality located within the 5' flanking region of the p53 gene and associated with the loss of heterozygosity was observed in cells from this patient with ALL. The MDM2 gene which inactivates p53 by binding to it was neither amplified nor rearranged in 28 leukemias studied. Thus, disruption of regulated p53 expression resulting in lack of detectable p53 mRNA even by RT-PCR occurs in about 30% of cases of AML; however, p53 alterations typical for human solid tumors are an infrequent event in most types of human acute leukemias.

INTRODUCTION

The 53-kDa nuclear phosphoprotein termed p53 (1,2) is involved in growth control of normal cells (Ref. 3 and references therein). It can act as a transcriptional activator and bind to DNA in a sequence-specific manner (4–7). p53 also binds to several viral antigens, including large T antigen of SV40, of human papilloma virus and human adenovirus antigens (8,9). Recently, binding of p53 to a cellular gene product, MDM2, which is frequently amplified and overexpressed in sarcomas, has been demonstrated (10). p53 was initially thought to be an oncogene due to its overexpression in many different tumor types (2,11–14). More recently it has become clear that normal p53 can function as a suppressor of malignant transformation *in vitro* (15), and *in vivo* (16).

Alterations of p53 coding nucleotide sequence (mostly missense mutations) and intronic sequence (splice site mutations) are the most frequent genetic changes in sporadic human malignancies (3). Studies on the diversity of inactivation mechanisms of normal p53 have been conducted on various types of human solid tumors (reviewed in (17)). Point mutations or small deletions within the highly conserved portions of the p53 coding sequence occur with a high frequency

in a variety of solid tumors (18–29); loss of one allele of p53, or of part of the entire short arm of human chromosome 17 harboring this gene (30), frequently occurs in cancers of the colon, breast, lung and brain (18,19). Furthermore, gene rearrangements or deletions resulting in the complete loss of coding sequence have been noted in primary tumors originating from the mesenchyme (25,26,31), in hepatocellular carcinoma (27), murine erythroleukemia (32,33), and infrequently in chronic myelogenous leukemia (34–36). Mechanisms of inactivation can occur at different levels in the same type of tumor, and may contribute to the initiation, maintenance or progression of the malignant state (26).

Others as well as ourselves have demonstrated that p53 is differentially expressed in leukemia cells of lymphoid and myeloid phenotype, respectively (37–40). Primary cells and cell lines of lymphoid origin always disclosed p53 transcripts, whereas those from patients with myeloid leukemias expressed p53 mRNA and p53 protein in about 50% of cases. In these studies, p53 mRNA expression was examined by Northern blot analyses. In the present study we confirmed and extended these results by examining p53 mRNA expression in a series of patients with acute leukemias of either lymphoid (ALL) or myeloid lineage (AML) by employing the highly sensitive transcript detection of reverse transcription combined with polymerase chain reaction (RT-PCR). All ALL samples disclosed p53 transcripts, whereas in c. 30% of AML, no p53 expression was detectable even by this highly sensitive assay.

p53 transcript nucleotide sequence, structure and copy number of the p53 and MDM2 (41) genes were also determined in primary leukemic cells from these patients. None of the primary leukemia samples disclosed point mutations or amplifications; however, in a case of ALL, a structural alteration was detected which was located 5' of the p53 coding region and associated with loss of heterozygosity of the p53 gene.

MATERIALS AND METHODS

Cells

After obtaining informed consent, mononuclear cells were isolated from heparinized venous blood or bone marrow from 26 patients with ALL and 23 patients with AML using density centrifugation. ALL subtypes were c-ALL ($n = 8$), pre-pre-B-ALL ($n = 3$), pre-B-ALL ($n = 7$), B-ALL ($n = 3$), T-ALL ($n = 5$); AML subtypes are shown in Table 1. All cell preparations contained >85% leukemic cells as judged by inspection of Wright-Giemsa stained slide preparations. In addition, cells were characterized by immunocytochemistry using a panel of monoclonal antibodies directed against various myeloid- and lymphoid-associated surface markers.

Received March 3, 1994. Accepted June 17, 1994.

Correspondence to: Michael Lübbert, Dept of Hematology/Oncology, University of Freiburg Medical Center, Hugstetter Str 55, D-79106 Freiburg, Germany

LEUKEMIA

© 1994 Macmillan Press Ltd

Table 1 Expression and Structure of the p53 Gene in Primary Acute Myeloid Leukemic Cells

Patient no.	Sex	Age	Cells	FAB	5'p53	3'p53	β_2 MG	BglII RFLP
1	M	54	BM	M5	+/wt	+/wt	ND	11/9.5
2	M	74	BM	M4	+/wt	+/wt	ND	11
3	F	31	BM	M5b	+/wt	+/wt	+	11
4	M	58	BM	M4	+/wt	ND	ND	ND
5	F	56	BM	M1	+/ND	+/ND	ND	ND
6	F	37	pb	M2	+/wt	+/wt	ND	11
7	M	57	pb	M2	+/wt	+/wt	ND	11
8	F	66	pb	M4	+/wt	+/wt	+	ND
9	F	24	pb	M3	+/wt	+/wt	+	11
10	M	53	pb	M2	-	-	+	ND
11	M	58	BM	M2	-	-	ND	ND
12	F	41	BM	M1	-	-	ND	ND
13	F	81	BM	M1	+/wt	+/wt	+	ND
14	F	64	BM	M1	+/wt	+/wt	ND	ND
15	M	50	BM	M2	+/wt	+/wt	ND	11
16	F	71	BM	M2	+/wt	+/wt	ND	ND
17	M	50	BM	M1	-	-	+	ND
18	M	52	pb	M4	+/wt	+/wt	+	11
19	F	43	pb	M5	+/wt	+/wt	+	11/9.5
20	F	19	BM	M4	-	-	+	ND
21	M	45	BM	M4	-	-	ND	ND
22	F	38	BM	M2	+/wt	+/wt	-	11
23	M	66	BM	M4	-	-	+	ND

+, transcript fragment detectable by RT-PCR and gel electrophoresis; -, no transcript detectable; BM, bone marrow as source of leukemic cells; FAB, phenotype of leukemia according to the French-American-British Cooperative Group classification (64); PB, peripheral blood as source for leukemic cells; ND, not done; β_2 MG, amplification of a β_2 -microglobulin specific transcript fragment by RT-PCR as described in Materials and Methods; wt, only the wild-type, p53 cDNA sequence was detectable by direct sequencing of PCR products. BglII RFLP, presence of the polymorphic (54) 11.0-kb allele ('11'), the 9.5-kb allele ('9.5') or both, as detected by Southern blot; p53 5' mRNA, transcript fragment amplified from codons 78 through 227; p53 3' mRNA, transcript fragment amplified from codons 214 through 310.

Reverse Transcription and Polymerase Chain Reaction (RT-PCR)

Total RNA was isolated from mononuclear cells by ultracentrifugation over a 5.4 M CsCl gradient after lysis of cells in guanidium isothiocyanate as described by Chirgwin *et al.* (42). Aliquots of 3 μ g of total RNA were used for first strand cDNA synthesis at 42°C, 60 min in a reaction primed by random hexamer (100 μ M; Pharmacia, Stockholm, Sweden), was transcribed by Moloney murine leukemia virus reverse transcriptase (RT, 200 U; Gibco BRL, Stockholm, Sweden) in the presence of 200 μ M dNTPs (Pharmacia) in a 30 μ l reaction volume. After 60 min, RT reaction was terminated by heating of samples to 94°C for 5 min. Polymerase chain reaction (PCR) was performed, with 25 to 30 cycles of denaturing (94°C, 30 sec), annealing (56°C, 15 sec) and extension (72°C, 30 sec) in the presence of 200 μ M dNTPs, 2.5 mM MgCl₂, 10 mM Tris pH 8.4, 1.5 U Taq DNA polymerase (Perkin-Elmer, Langen, Germany). At 30 cycles or less, amplification occurs in an exponential manner and may be suitable for quantitative expression analysis, whereas with more cycles, the amplification process enters a linear and finally plateau phase and is not suitable for exact quantification of transcripts (43). In cases where no amplification product was visualized under UV-transillumination of ethidium bromide-stained gels after 30 cycles, PCR was repeated until 40 cycles were completed (linear amplification). At least three independent repetitions of these amplifications were performed. The following primers were used:

444 (5' CAGCTCTACACCGGGCGGCCCTGCACCAG 3', sense) and 446 (5' GAGCCAACCTCAGCGGCTCATAGGGCACC 3', antisense) for amplification of exons 4-7 of p53 mRNA.

448 (5' TAGTGTGGTGGTCCCTATGAGCCC 3', sense) and 716 (5' TTCTGCAGTCTCGCTTAGTGCTCC 3', antisense) for amplification of exons 6-9 of p53 mRNA (see Figure 1).

As a control for intact RNA, efficient reverse transcription and lack of inhibitory contaminants in the reactions, a 100-bp fragment of β_2 -microglobulin mRNA was amplified in selected cases, either in the same tube or in a sister reaction, using primers

450 (5' ACCCCCACTGAAAAGATGAGTAT 3', sense) and 452 (5' ATGATGCTGCTTACATGTCTCGAT 3', antisense) (44).

All temperature-dependent reactions were performed in a DNA thermal cycler (Perkin Elmer/Cetus). Great care was taken to avoid false PCR results through contamination or carry-over. Specifically, controls used to detect potential false-positive results were: (i) several RT reactions of each experiment were performed without the addition of template RNA and were amplified as described above; and (ii) a mock RT reaction was carried out in the absence of RT but with a positive control RNA (peripheral blood lymphocytes from a normal donor which had been cultured with phytohemagglutinin (2 μ g/ml) for 24 h and expressed p53 mRNA); PCR was then performed as described above. One tenth of each PCR reaction was electrophoresed on 3% NuSieve/1% agarose gel and blotted onto Zetaprobe membrane (Bio-Rad, Richmond, CA,

USA) by alkaline transfer after soaking the gel in HCl (0.25 N) for 15 min. Detection of specific hybrids was achieved by utilizing the enhanced chemiluminescence of luminol (ECL) oxidation catalyzed by horseradish peroxidase. In brief, filters were hybridized with probing oligonucleotides 443 (5' TCTGTCCCTTCCCAGAAAACC 3') for the 5' segment, and 446 for the 3' segment of the p53 mRNA) that had been 3'-end-labeled with a fluorescein-dUTP tail using TdT. Prehybridization, hybridization and antibody-mediated autoradiography of luminol oxidation were performed according to instructions given by the manufacturer (Amersham Buehler, Braunschweig, Germany).

DNA Sequencing of PCR Products

PCR products were separated from excess oligonucleotides and unincorporated dNTPs by centrifugation through Amicon columns (100 micron membrane) at 10 000 r.p.m. for 10 min and concentrated by ethanol precipitation. PCR products were redissolved in H₂O and processed for DNA sequencing by chain termination (45), using a modified DNA polymerase (Sequenase; US Biochemical, Cleveland, OH, USA) as described previously (46). In brief, 30–50 ng of DNA were annealed to 20 pmoles of sequencing primer oligonucleotide 443 or 445 (5' CGAAAAGTGTCTGTCATCC 3'), as internal primers for the PCR product spanning p53 exons 4–7, or the oligos 448 and 716 which were also used to amplify the portion covering exons 6–9. Annealing was performed in the presence of 0.5% NP-40, 5 μ Ci ³⁵S-dATP, 1 μ l of 100 mM DTT (47). After termination of each sequencing reaction and denaturing by boiling for 2 min, 1/2 reaction volume was loaded onto denaturing 6% polyacrylamide/urea gels and electrophoresed at 50°C. Gels were dried and exposed to Kodak X-AR 5 film at room temperature for 2–6 days. Labeling efficiency of strand fragments yielded an average readability of gels from starting between 10 and 30 bp from the 3' border of the sequencing primer.

Southern Blotting

DNA was isolated by cesium-chloride density centrifugation (42), further purified by proteinase K digestion and ammonium acetate precipitations (48), and restricted according to specifications given by the manufacturer (New England Biolabs, Beverly, MA, USA). Aliquots of cleaved DNA were size-separated on agarose gels, blotted and hybridized as described (40). For probing of the p53 gene, the 1670-bp *HindIII/EcoRI* cDNA fragment (complementary to 3' of exon 1 through exon 11, Ref. 49), or the 350-bp *BamHI/XbaI* DNA fragment covering the 5' flanking region and part of exon 1 (50) were used (both kindly provided by Phil Koeffler, Cedars Sinai Medical Center, Los Angeles, CA, USA). The 912-bp *XhoI/XhoI* fragment of a human colon MDM2 cDNA (51) was kindly provided by Bert Vogelstein, Johns Hopkins Oncology Center, Baltimore, MD, USA. As controls for completeness of digestion, and loss or amplification of gene copies, cDNA probes for human macrophage colony-stimulating factor (M-CSF) (kindly provided by Peter Ralph, Cetus, Emeryville, CA, USA) and Interleukin (IL-3) (provided by D. Krumwieh, Behringwerke Marburg, Germany) were used for rehybridization of stripped filters. Probes were labeled to high specific activity by random-priming (52), purified from unincorporated ³²P-dCTP by chromatography, denatured in 2 mg of sheared salmon sperm DNA by boiling and chilling, and added to hybridization solution (10⁹ c.p.m./ml). Hybridization was car-

ried out for 16–24 h at 42°C in a hybridization oven under constant slow rotation. Filters were washed in decreasing concentration of SSC to a final stringency of 0.25 \times SSC, 65°C for 15 min. Filters were autoradiographed at –70°C onto Kodak XR-5 film in the presence of an intensifying screen (Cronex Lightning Plus) for 2–5 days.

RESULTS

p53-Specific Transcripts are Consistently Detectable in Primary Leukemic Cells of Lymphoid but not Myeloid Phenotype

Primary cells from patients with acute leukemias of either lymphoid (ALL), or myeloid (AML) phenotype were examined for mRNA expression of the p53 gene using the highly sensitive assay of RT-PCR. Two separate but overlapping transcript fragments (35-bp overlap), each interrupted by several intervening sequences, and together encompassing ~700 bp of the central portion of p53 coding sequence (exons 4–9) were amplified from cDNA (Figure 1). The region spanned by both PCR products encompasses four evolutionarily highly conserved regions and 'hotspot' segments for point mutations in solid tumors. As a positive control for efficient reverse transcription and PCR, β_2 -microglobulin mRNA sequences were also amplified from selected samples. By this semi-quantitative but highly sensitive approach, expression of p53 was detectable in normal human bone marrow samples from four different donors, and in 26/26 samples of ALL cells (Figure 2). In contrast, expression of these transcript fragments was detectable in 16/23 samples of AML but could not be disclosed in the remaining seven (Figure 2b, Table 1).

In order to examine p53 transcripts for possible alterations of their nucleotide sequence, direct DNA sequencing of both PCR products was performed. In initial experiments both regions were amplified and directly sequenced from lymphocyte RNA from a healthy donor, and from the myeloma cell line U266 with a known mutation of the p53 coding region (53). As shown in Figure 3, the altered p53 transcript exhibiting a G to A nucleotide substitution at the first position of codon 161 could readily be detected by this assay. We next sequenced RT-PCR products from 25 samples of ALL and 15 cell samples of AML. However, by this approach only the wild-type nucleotide sequence was detectable in these cells (Table 1).

Novel Structural Alteration Located 5' of the p53 Coding Region and Associated with Loss of Heterozygosity in a Case of Acute Lymphocytic Leukemia

Primary leukemia samples were probed for possible alterations of the p53 gene outside the highly conserved regions of the coding sequence. Southern blot analyses were performed on selected samples using various restriction enzymes and DNA probes for both the 5' and 3' regions of the gene. Several aberrations from the expected 'germline' restriction patterns were noted. Firstly, the known *BglII* RFLP located within the 3' portion of intron 1 of p53 (54) was observed in 2/14 cases of ALL and 2/10 patients with AML (Figure 4, Table 1). In three of these, the two *BglII* alleles represented by the 9.5-kb and 11.0-kb fragments were represented in equimolar amounts, as indicated by similar band intensities. In one of the ALL patients, however, the 9.5-kb band was 5- to 6-fold

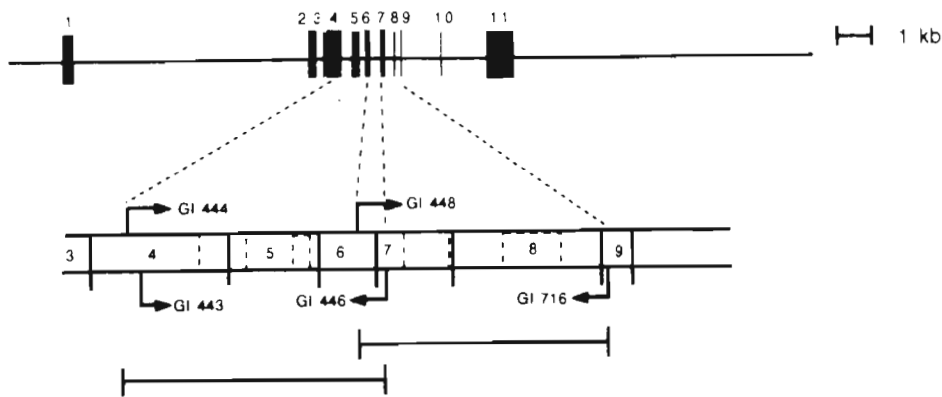


Figure 1 RT-PCR amplification and sequencing strategy of p53 mRNA. Upper panel, genomic structure of p53; black bars indicate exon sequences. Middle panel, central portion of p53 coding sequence; numbers indicate exons, shaded boxes lined by broken lines indicate highly conserved regions, arrows indicate oligonucleotides used for PCR (444, 446, 448, 716) and sequencing (443, 446, 448, 716). Lower panel, RT-PCR products spanning codons 78-227 (exons 4-7, 445 bp) and 214-310 (exons 6-9, 289 bp), respectively

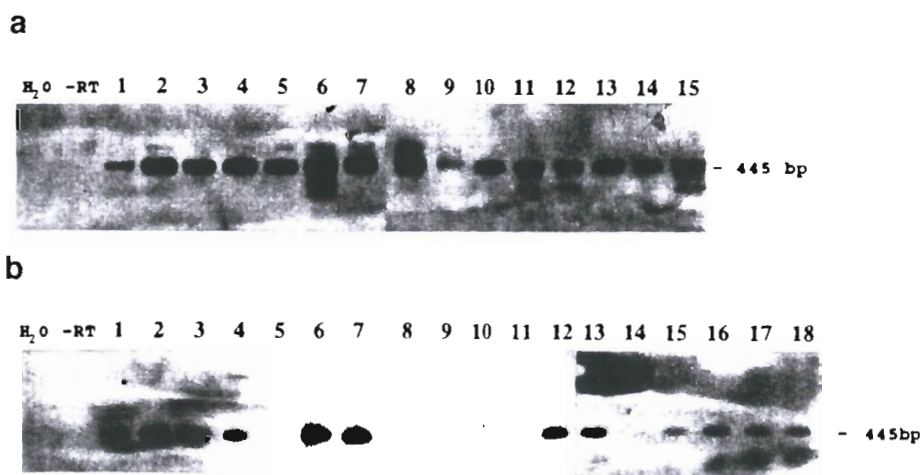


Figure 2 p53 mRNA expression by acute leukemia cells from patients with ALL (panel a) and AML (panel b). A 445-bp fragment of p53 mRNA was amplified by RT-PCR, blotted and hybridized to non-radioactive probe as described in Materials and Methods. (a) H₂O, mock RT-PCR reaction with H₂O added instead of RNA; -RT, mock RT-PCR reaction with RNA from lectin-activated peripheral blood lymphocytes from healthy donor, but no reverse transcriptase added; lane 1-14, cells from patients with ALL; lane 15, lectin-activated peripheral blood lymphocytes from healthy donor. (b) lanes 1-3, 5-12, 14-18, leukemic cells from patients with AML; lane 4, normal human bone marrow cells; lane 13, lectin-activated peripheral blood lymphocytes

more intense than the 11-kb band (Figure 4b, lane 3). Examination of peripheral blood mononuclear cells isolated from the same patient in remission showed heterozygosity as indicated by similar intensity of both bands. The observed diminution of the allele represented by the 11.0-kb band thus indicates a loss of heterozygosity (LOH) for the p53 gene in the leukemic cells. This suggests no resultant loss of one p53 allele but doubling of the remaining allele by mitotic recombination after loss of heterozygosity. Of note, the abnormal karyotype of the leukemic cells of this patient (56, XX, +X, +4, +10, +12, +13, +14, +15, +18, +21, +21) did not reveal alterations of chromosome 17.

In the same patient, a novel 8-kb band was observed after restriction of DNA from leukemic cells with *EcoRI* and hybridization with the 5'-specific p53 probe (Figure 5), whereas the expected, germline 3.8-kb *EcoRI* band was diminished 5- to 6-fold in intensity. This ratio was unchanged even with an excess of restriction enzyme, and control hybridizations with other pBR322-derived probes ruled out

partial digestion or plasmid contamination. Other restriction digests visualizing the 5' p53 region or hybridization with the pR4-2 p53 cDNA probe did not disclose an abnormal pattern. This alteration is not an RFLP since it was not detectable in non-leukemic, remission peripheral blood lymphocytes of the same patient (Figure 5, lane 2).

Lack of MDM2 Gene Amplification in Acute Leukemias

A high incidence of gene amplification of the MDM2 locus has recently been reported in mesenchymal tumors (31,55). We therefore probed for possible amplification of this gene in ten DNA samples of AML and 14 samples of ALL. However, neither gene amplification nor aberrant restriction fragments were detected by Southern blot using four different restriction enzymes (not shown).

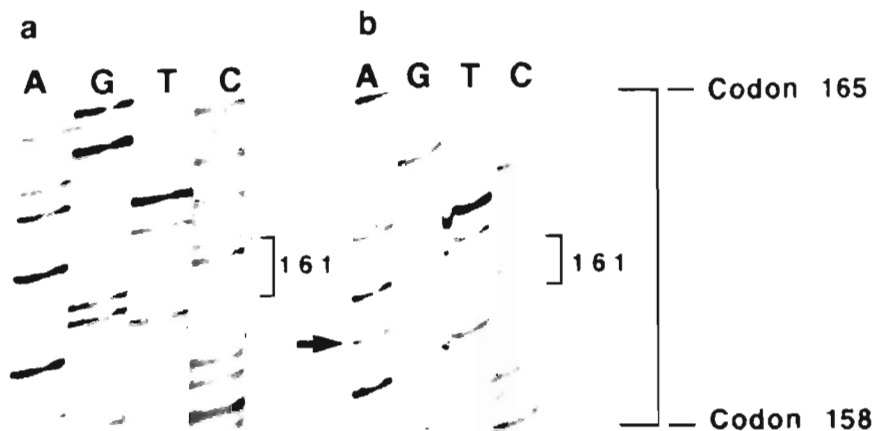


Figure 3 Expression of mutated p53 transcript by U-266 myeloma cell line. Total RNA was extracted from PHA-treated normal peripheral blood lymphocytes (left) and U-266 cells (right), reverse transcribed into cDNA, amplified by PCR using oligonucleotides 444 and 446 (see Figure 1) and directly sequenced using the internal primer 443

DISCUSSION

Studies in different systems have shown that disruption of synthesis of normal, 'wild-type' p53 can occur on several levels (18,19,26,27). With regard to hematologic malignancies, others as well as ourselves have noted that differential p53 expression occurs depending on the cell phenotype (37-40); p53 gene rearrangements infrequently occur in primary CML cells (34-36) and point mutations within the mutational 'hot-spot' regions of this gene (located within the highly conserved areas of the coding region) are an infrequent event (56-58).

In the present study, we wished to examine primary leukemic blast cells representing the myeloid and lymphoid lineages for differential expression of p53 and possible alterations by use of the very sensitive and specific assay of RT-PCR. p53 transcripts were consistently detectable in light-density normal human bone marrow cells, as well as in leukemic cells of lymphoid but not myeloid phenotype. We cannot rule out the possibility that in some samples, the wild-type transcript sequence detected originated from small numbers of residual normal hematopoietic cells, whereas the leukemic cells did not express p53 at all or expressed only very low levels of an altered transcript.

Direct sequencing of PCR products containing the 'hot-spot' regions did not reveal point mutations as observed in other tumor types. Direct sequencing of PCR product will visualize sequence alterations present in the majority of cells (see Figure 3). However, mutations present in only a small subpopulation of leukemic cells might not be detected due to sensitivity limits of this assay. These data, in agreement with others (54,57), suggest that, at least in the region analyzed by us, p53 alterations occur only infrequently in primary cells from these groups of diseases. This excludes ALL of FAB L3 subtype, Burkitt's lymphomas and acute T-cell leukemias (56,59). Furthermore, a small subgroup of AML with monosomy of the short arm of chromosome 17 (harboring the p53 gene) has a higher incidence of mutations (58). None of the AML samples studied by us had loss of an allele of chromosome 17 as indicated by gene copy number.

Southern blot analysis of p53 gene structure in primary leukemias disclosed heterozygosity at a *Bgl*II RFLP in 4/24 cases. In one of these, mitotic recombination had resulted in loss of heterozygosity (LOH) of the p53 gene and in duplication of the remaining allele. In malignant but not normal hemato-

poietic cells of this patient, an additional, novel band mapping to the 5' flanking region of the p53 was noted. Both genetic tags did not co-segregate, since the novel *Eco*RI band was absent in non-leukemic cells. The sequence of a cosmid clone covering this region contains an *Eco*RI restriction site ~4.2 kb upstream of the 3.8 kb *Eco*RI/*Eco*RI fragment visualized by the 5' p53 probe (49). In leukemic cells from patient 15, this *Eco*RI restriction site upstream of the 3.8-kb *Eco*RI/*Eco*RI fragment is apparently deleted, either by a point mutation or a small deletion within this region. Determining the exact type of sequence alteration necessitates analysis of this region by PCR; however, nucleotide sequence information of this region is unavailable at present. These results show that leukemia-associated alterations of p53 can occur outside the coding and intronic regions of this gene.

Our data on primary cells from acute leukemia are in stark contrast to recent reports showing that cell lines derived from myeloid (59) and lymphoid (60) leukemias have a high incidence of p53 mutations. This suggests that these alterations may have arisen *in vitro*, during or after establishment of permanent growth of these cells in culture. Laumann *et al.* (61) have noted that in different passages of the Jurkat T-lymphoblastic cell line, *in vitro* evolution of several, different point mutations had occurred, also emphasizing the genetic instability of the p53 gene during *in vitro* culture of hemopoietic cells.

In summary, these results strengthen the notion that mutations within the highly conserved portions of the p53 coding region occur infrequently in most types of AML and ALL. In addition the MDM2 gene is not amplified in these leukemias, similar to findings obtained in myelodysplastic syndrome (37,62). However, mRNA expression does not occur in a subgroup of AML and in spite of normal gene structure, p53 may have a dominant role in the negative regulation of cell proliferation. Simplistically, one could speculate that in cases of AML where no p53 is expressed, this might result in dysregulated, and thus spurred, proliferation. Conversely, p53 expression is increased during normal myeloid differentiation, and reconstruction of p53 expression in K562 myeloblastic/erythroblastic cells which lack p53 expression has resulted in partial maturation of these cells (63). Further studies are necessary to unravel the role of p53 in the processes of decreased proliferation and increased differentiation

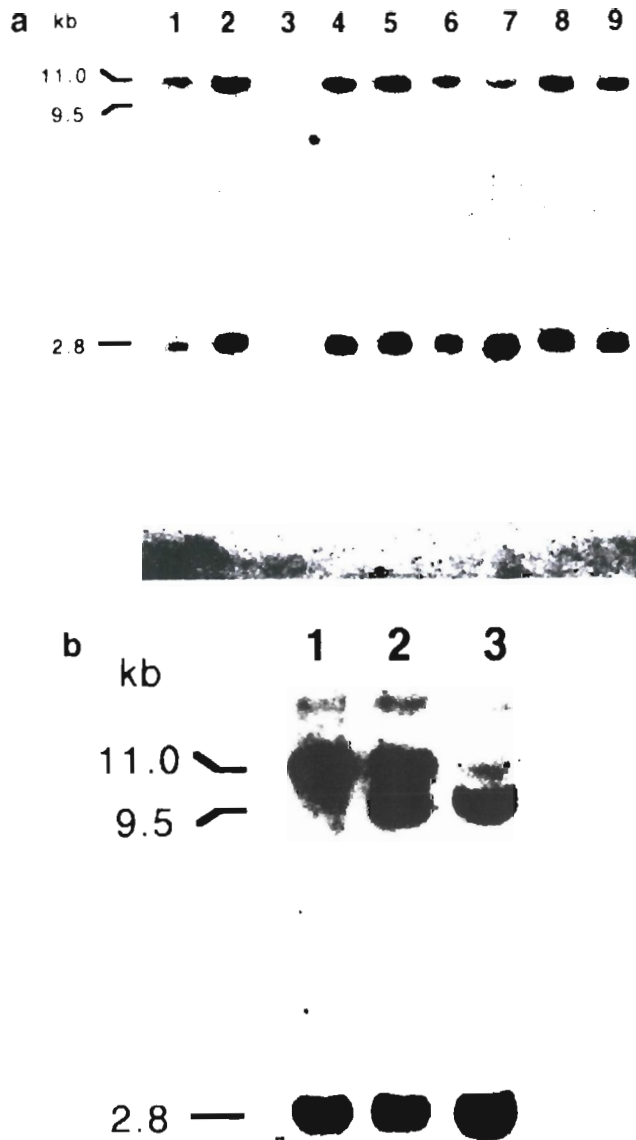


Figure 4 *Bgl*II restriction fragment length polymorphism of p53 first intron in lymphoid and myeloid acute leukemias. (a) DNAs from ALL patient 1 (lane 1), patient 2 (lane 2), patient 3 (lane 3), patient 10 (lane 4), patient 14 (lane 5), patient 17 (lane 6), patient 20 (lane 7), patient 23 (lane 8), from normal lymphocytes (lane 9) were digested to completion with *Bgl*II, analyzed by blotting and hybridization to the pR4-2 p53 cDNA probe (covering the bulk of the p53 coding region) as described in Materials and Methods. *Hind*III-digested Lambda DNA was used as molecular weight marker. (b) DNA was extracted from leukemic cells of a patient with non-Hodgkin's lymphoma (lane 1), remission peripheral blood lymphocytes from patient 15 (lane 2), leukemic cells from patient 15 (lane 3), and processed as described in (a).

during normal myelopoiesis, and their disruption in leukemic cells which are blocked in maturation.

Acknowledgements. Supported by Grant W 48/92/Lü1 from Deutsche Krebshilfe. We wish to thank Johanna Römmelt, Regina Ruszynski and Christine Martens for expert technical

assistance; Thomas Boehm, Freiburg, Germany, and Carl Miller, Los Angeles, CA, USA, for helpful discussions; and David Iggo, ICRF, Herts, UK for advice with RT-PCR. Dr Filber-Brillinger, Luitpold-Krankenhaus, Würzburg, Germany kindly provided remission peripheral blood samples, clinical and cytogenetic data from ALL patient 15.

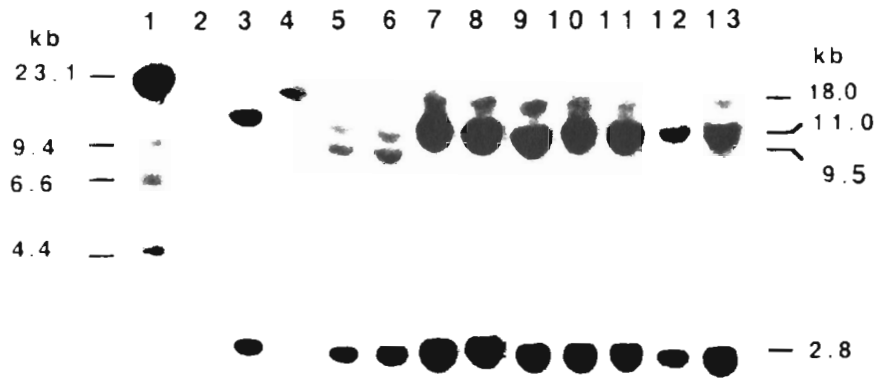


Figure 4 DNAs were extracted from normal peripheral blood lymphocytes (lane 3), from promyelocytic HL-60 cells which have gross deletions of one p53 allele and loss of the other allele (lane 4; Ref. 65), and from AML patients 19 (lane 5), 1 (lane 6), 2 (lane 7), 3 (lane 8), 7 (lane 9), 22 (lane 10), 9 (lane 11), 11 (lane 12), and 18 (lane 13), and processed as described in (a). Lane 1: *Hind*III digested lambda DNA

REFERENCES

1. Lane DP, Crawford LV. T-antigen is bound to a host protein in SV40-transformed cells. *Nature* **1979**;278:261-263.
2. Linzer DH, Levine AJ. Characterization of a 54 K dalton cellular SV40 tumor antigen present in SV40 transformed cells and uninfected embryonal carcinoma cells. *Cell* **1979**;17:43-52.
3. Levine AJ, Momand J, Finlay CA. The p53 tumour suppressor gene. *Nature* **1991**;351:453-456.
4. Raycroft L, Wu H, Lozano G. Transcriptional activation by wild-type but not transforming mutants of the p53 anti-oncogene. *Science* **1990**;249:1049-1051.
5. O'Rourke RW, Miller CW, Kato GJ, Simon KI, Chen D-L, Dang CV, Koeffler HP. A potential transcriptional activation element in the p53 protein. *Oncogene* **1990**;5:1829-1832.
6. El-Deiry WS, Kern SE, Pietenpol JA, Kinzler KW, Vogelstein B. Definition of a consensus binding site for p53. *Nature Genet* **1992**;1:45-49.
7. Kern SE, Kinzler KW, Bruskin A, Jarosz D, Friedman P, Prives C, Vogelstein B. Identification of p53 as a sequence-specific DNA-binding protein. *Science* **1991**;252:1708-1711.
8. Werness BA, Levine AJ, Howley PM. Association of human papillomavirus types 16 and 18 E6 proteins with p53. *Science* **1990**;248:76-79.
9. Yew PR, Berk AJ. Inhibition of p53 transactivation required for transformation by adenovirus early 1B protein. *Nature* **1992**;357:82-85.
10. Momand J, Zambetti GP, Olson DC, George DL, Levine AJ. The mdm-2 oncogene product forms a complex with the p53 protein and inhibits p53-mediated transactivation. *Cell* **1992**;69:1237-1245.
11. Dippold WG, Jay G, DeLeo AB, Khoury G, Old LJ. p53 transformation-related protein: detection by monoclonal antibody in mouse and human cells. *Proc Natl Acad Sci USA* **1981**;78:1695-1699.
12. Parada LF, Land H, Weinberg RA, Woli D, Rotter V. Cooperation between genes encoding p53 tumor antigen and ras in cellular transformation. *Nature* **1984**;312:649-651.
13. Eliyahu D, Raz A, Gruss P, Givol D, Oren M. Participation of p53 cellular tumour antigen in transformation of normal embryonic cells. *Nature* **1984**;312:646-649.
14. Jenkins J. Cellular immortalization by a cDNA clone encoding the transformation-associated phosphoprotein p53. *Nature* **1984**;312:646-649.
15. Finlay CA, Hinds PW, Levine AJ. The p53 proto-oncogene can act as a suppressor of transformation. *Cell* **1989**;57:1083-1093.
16. Donehower LA, Harvey M, Slagle BL, McArthur MJ, Montgomery Jr CA, Burel JS, Bradley A. Mice deficient for p53 are developmentally

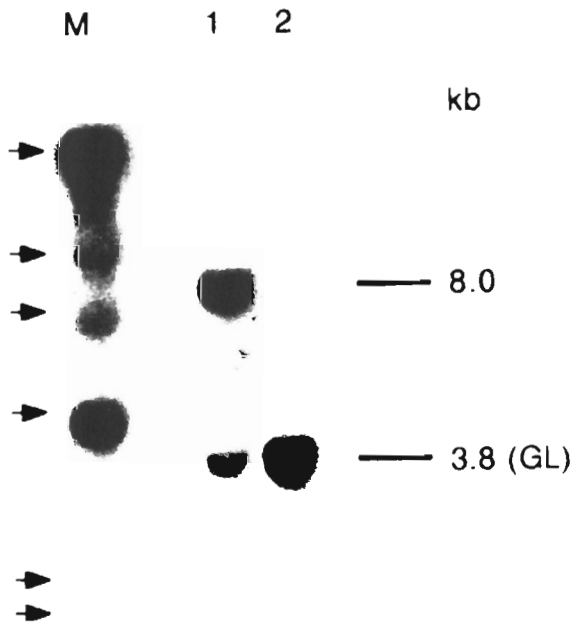


Figure 5 Structural alteration in the 5' flanking region of the p53 gene of a patient with common (c-)ALL. DNAs from leukemic cells (lane 1) and from remission peripheral blood lymphocytes (lane 2) of patient 15 were cleaved with *Eco*RI, Southern blotted and hybridized to the p53 probe pBT53 (complementary to the 5' flanking p53 region and exon II). M, lambda *Hind*III DNA; GL, expected germline band

- tally normal but susceptible to spontaneous tumours. *Nature* **1992**;356:215-221.
17. Hollstein M, Sidransky D, Vogelstein B, Harris CC. p53 mutations in human cancers. *Science* **1991**;253:49-53.
 18. Nigro JM, Baker SJ, Preisinger AC, Jessup JM, Hostetter R, Cleary K, Bigner SH, Davidson N, Baylin S, Devilee P, Glover T, Collins FS, Weston A, Modali R, Harris CC, Vogelstein B. Mutations in the p53 gene occur in diverse human tumour types. *Nature* **1989**;342:705-708.
 19. Rodrigues NR, Rowan A, Smith MEF, Kerr IB, Bodmer WF, Gannon JV, Lane DP. p53 mutations in colorectal cancer. *Proc Natl Acad Sci USA* **1990**;87:7555-7559.
 20. Bartek J, Iggo R, Gannon J, Lane DP. Genetic and immunochemical analysis of mutant p53 in human breast cancer cell lines. *Oncogene* **1990**;5:893-899.
 21. Takahashi T, D'Amico D, Chiba I, Buchhagen DL, Minna JD. Identification of intronic point mutations as an alternative mechanism for p53 inactivation in lung cancer. *J Clin Invest* **1990**;86:363-369.
 22. Iggo R, Gatter K, Bartek J, Lane D, Harris AL. Increased expression of mutant forms of p53 oncogene in primary lung cancer. *Lancet* **1990**;335:675-679.
 23. Chiba I, Takahashi T, Nau MM, D'Amico D, Curiel DT, Mitsudomi T, Buchhagen DL, Carbone D, Piantadosi S, Koga H, Reisman PT, Slamon DJ, Holmes EC, Minna JD. Mutations in the p53 gene are frequent in primary, resected non-small cell lung cancer. *Oncogene* **1990**;5:1603-1610.
 24. Sameshima Y, Akiyama T, Mori N, Mizoguchi H, Toyoshima K, Sugimura T, Terada M, Yokota J. Point mutation of the p53 gene resulting in splicing inhibition in small cell lung carcinoma. *Biochem Biophys Res Comm* **1990**;173:697-703.
 25. Miller CW, Aslo A, Tsay C, Slamon D, Ishizaki K, Toguchida J, Yamamuro T, Lampkin B, Koeffler HP. Frequency and structure of p53 rearrangements in human osteosarcoma. *Cancer Res* **1990**;50:7950-7954.
 26. Mulligan LM, Matlashewski GJ, Scoble HJ, Cavenee WK. Mechanisms of p53 loss in human sarcomas. *Proc Natl Acad Sci USA* **1990**;87:5863-5867.
 27. Bressan B, Galvin KM, Liang TJ, Isselbacher KJ, Wands JR, Ozturk M. Abnormal structure and expression of p53 gene in human hepatocellular carcinoma. *Proc Natl Acad Sci USA* **1990**;87:1973-1977.
 28. Scorsoni KA, Zhou Y-Z, Butel JS, Slagle BL. p53 mutations cluster at codon 249 in hepatitis B virus-positive hepatocellular carcinomas from China. *Cancer Res* **1992**;52:1635-1638.
 29. Sidransky D, Eschenbach AV, Tsai YC, Jones P, Summerhayes I, Marshall F, Paul M, Green P, Hamilton SR, Frost P, Vogelstein B. Identification of p53 gene mutations in bladder cancers and urine samples. *Science* **1991**;252:706-709.
 30. Miller CW, Mohandas T, Wolf D, Prokocimer M, Rotter V, Koeffler HP. Human p53 localized to short arm of chromosome 17. *Nature* **1986**;319:783-784.
 31. Masuda H, Miller CW, Koeffler HP, Battifora H, Cline MJ. Rearrangement of the p53 gene is common in human osteogenic sarcomas. *Proc Natl Acad Sci USA* **1987**;84:7716-7719.
 32. David YB, Pridoux VR, Chow V, Benchimol S, Bernstein A. Inactivation of the p53 oncogene by internal deletion or retroviral integration in erythroleukemic cell lines induced by friend leukemia virus. *Oncogene* **1988**;3:179-185.
 33. Hicks GC, Mowat M. Integration of friend murine leukemia virus into both alleles of the p53 oncogene in an erythroleukemic cell line. *J Virol* **1988**;62:4752-4755.
 34. Ahuja H, Bar-Eli M, Advani SH, Benchimol S, Cline MJ. Alterations in the p53 gene and the clonal evolution of the blast crisis of chronic myelocytic leukemia. *Proc Natl Acad Sci USA* **1989**;86:6783-6787.
 35. Kelman Z, Prokocimer M, Peller S, Kahn Y, Rechavi G, Manor Y, Cohen A, Rotter V. Rearrangements in the p53 gene in Philadelphia chromosome-positive chronic myelogenous leukemia. *Blood* **1989**;74:2318-2324.
 36. Mashal R, Shtalid M, Talpaz M, Kantarjian H, Smith L, Beran M, Cork A, Trujillo J, Guterman J, Deisseroth A. Rearrangement and expression of p53 in the chronic phase and blast crisis of chronic myelogenous leukemia. *Blood* **1990**;75:180-189.
 37. Smith LJ, McCulloch EA, Benchimol S. Expression of the p53 oncogene in acute myeloblastic leukemia. *J Exp Med* **1986**;164:751-761.
 38. Prokocimer M, Shaklai M, Ben-Bassat H, Wolf D, Goldfinger N, Rotter V. Expression of p53 in human leukemia and lymphoma. *Blood* **1986**;68:113-118.
 39. Koeffler HP, Miller CW, Nicolson MA, Ranyard J, Bosselman RA. Increased expression of p53 protein in human leukemia cells. *Proc Natl Acad Sci USA* **1986**;83:4035-4039.
 40. Lübbert M, Miller CW, Crawford L, Koeffler HP. p53 in chronic myelogenous leukemia: study of regulation of differential expression. *J Exp Med* **1988**;167:873-886.
 41. Buese-Ramos CE, Yang Y, DeLeon E, McCown P, Stass SA, Albitar M. The human MDM-2 oncogene is overexpressed in leukemias. *Blood* **1993**;82:2617-2623.
 42. Chirgwin JM, Przybyla AE, MacDonald RJ, Rutter WJ. Isolation of biologically active ribonucleic acid from sources enriched in ribonuclease. *Biochemistry* **1979**;18:5294-5299.
 43. Noonan KE, Beck C, Holzmayer TA, Chin JE, Wunder JS, Andrlis IL, Gazdar AF, Willman CL, Griffith B, Von Hoff DD, Roninson IB. Quantitative analysis of MDR1 (multidrug resistance) gene expression in human tumors by polymerase chain reaction. *Proc Natl Acad Sci USA* **1990**;87:7160-7164.
 44. Bonifer R, Neumann C, Mertelsmann R, Herrmann F. Interleukin-5 expressing allergen-specific T cells in patients with house dust mite sensitization: analysis at a clonal level. In: Freund M, Link H, Schmidt RE, Welte K, eds. *Cytokines in hemopoiesis, oncology, and AIDS ii*. Berlin, Heidelberg: Springer Verlag, **1992**:465-472.
 45. Sanger F, Nicklen S, Coulson AR. DNA sequencing with chain-terminating inhibitors. *Proc Natl Acad Sci USA* **1977**;74:5463-5465.
 46. Lübbert M, Mirro J, McCormick F, Kitchingman G, Mertelsmann R, Herrmann F, Koeffler HP. Prevalence of N-ras mutations in children with myelodysplastic syndromes and acute myeloid leukemia. *Oncogene* **1992**;7:263-268.
 47. Bachmann B, Lücke W, Hunsmann G. Improvement of PCR amplified DNA sequencing with the aid of detergents. *Nucleic Acids Res* **1990**;18:1309.
 48. Hardy KJ, Peterlin BM, Atchison RE, Stobo JD. Regulation of expression of the human interferon τ gene. *Proc Natl Acad Sci USA* **1985**;82:8173-8176.
 49. Lamb P, Crawford L. Characterization of the human p53 gene. *Mol Cell Biol* **1986**;6:1379-1385.
 50. Harlow E, Williamson NM, Ralston R, Heitman DM, Adams TE. Molecular cloning and *in vitro* expression of a cDNA clone for human cellular tumor antigen p53. *Mol Cell Biol* **1985**;5:1601-1610.
 51. Oliner JD, Kinzler KW, Meltzer PS, George DL, Vogelstein B. Amplification of a gene encoding a p53-associated protein in human sarcomas. *Nature* **1992**;358:80-83.
 52. Feinberg AP, Vogelstein B. A technique for radiolabeling DNA restriction endonuclease fragments to high specificity. *Anal Biochem* **1983**;132:6-13.
 53. Mazars G-R, Pontier M, Zhang X-G, Jourdan M, Bataille R, Theillet C, Klein B. Mutations of the p53 gene in human myeloma cell lines. *Oncogene* **1992**;7:1015-1018.
 54. Buchman VL, Chumakov PM, Ninkina NN, Samarina OP, Georgiev GP. A variation in the structure of the protein-coding region of the human p53 gene. *Gene* **1988**;70:245-252.
 55. Ladanyi M, Cha C, Lewis R, Jhanwar SC, Huvos AG, Healey JH. MDM2 gene amplification in metastatic osteosarcoma. *Cancer Res* **1993**;53:16-18.
 56. Gaidano G, Ballerini P, Gong JZ, Inghirami G, Neri A, Newcom EW, Magrath IT, Knowles DM, Dalla-Favera R. p53 mutation in human lymphoid malignancies: association with Burkitt's lymphoma and chronic lymphocytic leukemia. *Proc Natl Acad Sci USA* **1991**;88:5413-5417.
 57. Sakashita A, Hattori T, Miller CW, Suzushima H, Asou N, Takatsuki K, Koeffler HP. Mutations of the p53 gene in adult T-cell leukemia. *Blood* **1992**;79:477-480.
 58. Fenaux P, Jonveaux O, Quiquandon I, Lai JL, Pignion JM, Loucheux-Lefevre MH, Batters F, Berger R, Kerckaert JP. p53 gene mutations in acute myeloid leukemia with 17p monosomy. *Blood* **1991**;78:1652-1657.
 59. Sugimoto K, Toyoshima H, Sakai R, Miyagawa K, Hagiwara K.

- Frequent mutations in human myeloid leukemia cell lines. *Blood* **1992**;79:2378-2383.
60. Cheng J, Haas M. Frequent mutations in the p53 tumor suppressor gene in human leukemia T cell lines. *Mol Cell Biol* **1990**;10:5502-5509.
 61. Laumann R, Lückner M, Tesch H. Point mutations in the conserved regions of the p53 tumour suppressor gene do not account for the transforming process in the Jurkat acute lymphoblastic leukemia T cells. *Leukemia* **1992**;6:227-228.
 62. Preudhomme C, Quesnel B, Vachee A, Lepelley P, Collin-D'Hooghe M, Wattel E, Fenaux P. Absence of amplification on MDM2 gene, a regulator of p53 function, in myelodysplastic syndromes. *Leukemia* **1993**;7:1291-1293.
 63. Feinstein E, Gale RP, Reed J, Canaani E. Expression of the normal p53 gene induces differentiation of K562 cells. *Oncogene* **1992**;7:1853-1857.
 64. Bennett JM, Catovsky D, Daniel M-T, Flandrin G, Galton DAG, Gralnick HR, Sultan C. Proposed revised criteria for the classification of acute myeloid leukemia. *Ann Intern Med* **1985**;103:620-625.
 65. Wolf D, Rotter V. Major deletions in the gene encoding the p53 tumor antigen cause lack of p53 expression in HL-60 cells. *Proc Natl Acad Sci USA* **1985**;82:790-794.

Interleukin-10 Signaling Blocks Inhibitor of κ B Kinase Activity and Nuclear Factor κ B DNA Binding*

(Received for publication, May 23, 1999, and in revised form, August 9, 1999)

Arndt J. G. Schottelius[‡]§, Marty W. Mayo[‡], R. Balfour Sartor[‡]§, and Albert S. Baldwin, Jr.[‡]§¶

From the [‡]Lineberger Comprehensive Cancer Center, [¶]Department of Biology, and [§]Center for Gastrointestinal Biology and Disease, University of North Carolina, Chapel Hill, North Carolina 27599-7295

The transcription factor nuclear factor κ B (NF- κ B) coordinates the activation of numerous genes in response to pathogens and proinflammatory cytokines and is, therefore, pivotal in the development of acute and chronic inflammatory diseases. In its inactive state, NF- κ B is constitutively present in the cytoplasm as a p50-p65 heterodimer bound to its inhibitory protein I κ B. Proinflammatory cytokines, such as tumor necrosis factor (TNF), activate NF- κ B by stimulating the activity of the I κ B kinases (IKKs) which phosphorylate I κ B α on serine residues 32 and 36, targeting it for rapid degradation by the 26 S proteasome. This enables the release and nuclear translocation of the NF- κ B complex and activation of gene transcription. Interleukin-10 (IL-10) is a pleiotropic cytokine that controls inflammatory processes by suppressing the production of proinflammatory cytokines which are known to be transcriptionally controlled by NF- κ B. Conflicting data exists on the effects of IL-10 on TNF- and LPS-induced NF- κ B activity in human monocytes and the molecular mechanisms involved have not been elucidated. In this study, we show that IL-10 functions to block NF- κ B activity at two levels: 1) through the suppression of IKK activity and 2) through the inhibition of NF- κ B DNA binding activity. This is the first evidence of an anti-inflammatory protein inhibiting IKK activity and demonstrates that IKK is a logical target for blocking inflammatory diseases.

Interleukin-10 (IL-10)¹ is a pleiotropic cytokine produced by many cell types including monocytes/macrophages, cells that play a critical role in the inflammatory process (1–3). The anti-inflammatory effect of IL-10 is achieved through the suppressed production of macrophage inflammatory proteins such as IL-1, IL-6, IL-8, IL-12, TNF, granulocyte-macrophage colony stimulating factor, granulocyte colony stimulating factor, MHC class II molecules, B7, and intercellular adhesion molecule-1 (3–10) and through diminishing Th1 cell activity by suppres-

sion of IL-2 and interferon- γ (11). Evidence for the *in vivo* role of IL-10 as an important immunoregulator with potent anti-inflammatory and immunosuppressive activities comes from the observation that IL-10-deficient mice develop chronic enterocolitis with similarities to inflammatory bowel disease (12). IL-10 treatment has shown benefits in models of induced colitis (13–15) and arthritis (14, 16), as well as in models of experimental autoimmune encephalomyelitis, pancreatitis, diabetes mellitus, and experimental endotoxemia *in vivo* (17–20). Moreover, patients suffering from Crohn's disease display clinical improvement following IL-10 treatment (21, 22).

Some molecular mechanisms of monocyte deactivation by IL-10 have been described. IL-10 was found to inhibit protein-tyrosine kinase activation induced by LPS binding to the CD14 receptor and to consequently block the downstream Ras signaling pathway (23). Moreover, IL-10 has been shown to interfere with protein-tyrosine kinase-dependent CD40 signaling controlling IL-1 β synthesis in monocytes (24).

Many of the proinflammatory cytokines and costimulatory proteins demonstrated to be suppressed by IL-10 are known to be regulated by the transcription factor NF- κ B (25). Furthermore, NF- κ B also has a role in IL-10 gene expression (26). Classical NF- κ B, a heterodimer composed of p50 and p65 subunits, is a potent activator of gene expression (25, 27, 28). NF- κ B resides in the cytoplasm as an inactive complex bound to the inhibitor protein I κ B (27). In response to a variety of extracellular stimuli, such as IL-1 β , TNF, LPS, or phorbol esters, I κ B proteins are rapidly phosphorylated by the recently identified I κ B kinase (IKK) complex. IKK-induced phosphorylation of I κ B occurs on residues Ser³² and Ser³⁶ for I κ B α and on Ser¹⁹ and Ser²³ for I κ B β (25, 29, 30) which targets these inhibitory proteins for rapid polyubiquitination and degradation through the 26 S proteasome (31). This results in liberation of NF- κ B from I κ B and subsequent translocation of NF- κ B to the nucleus where it regulates gene transcription. The recent identification of the kinases responsible for I κ B phosphorylation is a critical step for understanding the mechanisms of NF- κ B activation. The cytokine-responsive I κ B kinase complex is composed of stoichiometric amounts of IKK- α and IKK- β and the recently discovered IKK γ /NEMO (32). IKK γ preferentially interacts with IKK β and is required for the activation of the IKK complex (29, 32–36). Further evidence that IKK α and IKK β are required for the functional IKK complex is supported by experiments which demonstrate that the overexpression of IKK α or IKK β activated an NF- κ B-dependent reporter, whereas dominant negative mutants of IKK α or IKK β inhibited TNF- or IL-1-induced NF- κ B activation (29, 33–36).

Although IL-10 has been found to inhibit the activity of NF- κ B in monocytes/macrophages and T cells, results from different groups have been variable as to whether the block occurs at the level of I κ B (37–40, 44). Furthermore, no molecular mechanisms have been elucidated which may control

* This work was supported by National Institutes of Health Grant AI35098 (to A. S. B.), the University of North Carolina Comprehensive Center for Inflammatory Disorders, a Crohn's and Colitis Foundation of America research fellowship award (to A. J. G. S.), and National Institutes of Health Grants CA75080 (to M. W. M.) and ROI DK 47700 (to R. B. S.). The costs of publication of this article were defrayed in part by the payment of page charges. This article must therefore be hereby marked "advertisement" in accordance with 18 U.S.C. Section 1734 solely to indicate this fact.

¶ To whom correspondence should be addressed: Lineberger Comprehensive Cancer Center, University of North Carolina, Chapel Hill, NC 27599-7295. Tel.: 919-966-3695; Fax: 919-966-0444; E-mail: jhall@med.unc.edu.

¹ The abbreviations used are: IL, interleukin; TNF, tumor necrosis factor; MHC, major histocompatibility complex; LPS, lipopolysaccharide; NF- κ B, nuclear factor κ B; I κ B, inhibitor of κ B; IKK, I κ B kinase; EMSA, electrophoretic mobility shift assay; PAGE, polyacrylamide gel electrophoresis.

NF- κ B activity in response to IL-10. Our data provides evidence that IL-10 inhibits TNF-induced NF- κ B activity by blocking TNF-induced IKK activity, thus inhibiting degradation of I κ B and the subsequent NF- κ B nuclear translocation. Additionally, a second mechanism appears to be functional: IL-10 signaling blocks the ability of translocated NF- κ B to bind to DNA.

EXPERIMENTAL PROCEDURES

Cell Culture and Treatments—The human monocytic cell lines THP-1 (TIB202) and U937 (CRL-1593) were obtained from the American Type Culture Collection (ATCC) and were cultured at 37 °C in RPMI 1640 containing L-glutamine (Life Technologies, Inc., Gaithersburg, MD), supplemented with 10% fetal bovine serum and antibiotics (Life Technologies). Media for THP-1 cells was additionally supplemented with HEPES (pH 7.8) to a final concentration of 20 mM and with 2-mercaptoethanol (Life Technologies, Inc.) to a final concentration of 5.5×10^{-5} M. The human intestinal epithelial cell line HT-29 (HTB 38) was obtained from ATCC and was cultured at 37 °C in McCoy's 5A Media supplemented with 10% fetal bovine serum and antibiotics.

Recombinant human TNF was purchased from Promega (Madison, WI). Recombinant human IL-10 was purchased from R&D Systems (Minneapolis, MN). Stock solutions were found to have less than 0.1 μ g of endotoxin/1 μ g of cytokine as determined by the LAL method. LPS (from *Escherichia coli* Serotype 055:B5) was purchased from Sigma. Cells were grown to a density of 1×10^6 cells/ml and stimulated with TNF or LPS, in the presence or absence of IL-10. After the indicated time periods, cells were harvested and processed for electrophoretic mobility shift assays, Western blot analysis, or I κ B kinase assays.

Electrophoretic Mobility Shift Assays (EMSA)—Nuclear extracts for EMSAs were prepared as described previously (41). 0.05% of Nonidet P-40 was used to extract nuclei. 8 μ g of extract were incubated for 20 min in a total of 20 μ l containing 1 μ g of poly(dI-dC) with $4-6 \times 10^4$ cpm of a 32 P-labeled oligonucleotide probe containing a κ B site from the class I MHC promoter (5'-CAGGGCTGGGGATTCCCCATCTCCACAGTTTCACATTC-3'). The final buffer concentration was 10 mM Tris-HCl (pH 7.7), 50 mM NaCl, 0.5 mM EDTA, 1 mM dithiothreitol, 10% glycerol. Complexes were resolved on a 5% polyacrylamide gel in Tris glycine buffer (25 mM Tris, 190 mM glycine, 1 mM EDTA) at 25 mA for 2-3 h at room temperature. Dried gels were exposed on film for 15-48 h. For supershift analysis, antibodies against specific NF- κ B subunits were added to the nuclear extract and incubated for 15 min prior to the addition of poly(dI-dC) and labeled oligonucleotide probe. The following antibodies were used for supershift analysis: p65 (Rockland, Boyertown, PA), p50 (NLS, Santa Cruz Biotechnology), and c-Rel (C, Santa Cruz Biotechnology).

Transfections and Luciferase Assays—For transient transfections of THP-1 cells, cells were divided the day prior to transfection. THP-1 cells were transiently transfected with the 3 \times κ B luciferase reporter plasmid, containing three copies of the MHC class I NF- κ B consensus site or were transfected with a mutant 3 \times κ B (mut3 \times κ B) luciferase reporter, which is no longer transcriptionally activated by NF- κ B. On the day of transfection, cells were collected and washed with $\times 1$ phosphate-buffered saline. A total of 5 μ g of plasmid DNA was incubated in a total volume of 500 μ l of suspension Tris-buffered saline containing 25 mM Tris-Cl (pH 7.4), 137 mM NaCl, 5 mM KCl, 0.6 mM Na₂HPO₄, 0.7 mM CaCl₂, 0.5 mM MgCl₂. 500 μ l of suspension Tris-buffered saline were combined with 500 μ l of diethylaminoethyl-dextran (DEAE-dextran) (Sigma) to a final concentration of 100 mg/ml. This mixture was added to the pelleted cells that were carefully resuspended and incubated for 60 min at 37 °C. Cells were then washed with suspension Tris-buffered saline and medium and were resuspended in 10 ml of complete medium. After a period of 48 h, IL-10 was added 60 min prior to stimulation with TNF for an additional 5 h. Cell extracts were prepared and luciferase activity was monitored as described previously (41). HT-29 cells were transfected with SuperFect Transfection Reagent (Qiagen GmbH, Hilden, Germany) as recommended by the manufacturer.

Northern Blot Analysis—Total RNA was isolated using the RNeasy Mini Kit as recommended by the manufacturer (Qiagen Inc., Valencia, CA). RNA samples were fractionated on an agarose gel and transferred overnight onto a nylon filter. The next day RNA was cross-linked with a UV cross-linker (Stratagene, La Jolla, Ca). For detection of I κ B α and IL-8 mRNAs, blots were hybridized in QuickHyb buffer supplemented with 100 μ g of salmon sperm DNA as recommended by the manufacturer (Stratagene, La Jolla, Ca). All probes were generated with a random primed labeling kit (Amersham Pharmacia Biotech) in the presence of [α - 32 P]dCTP (NEN Life Science Products Inc.). DNA prod-

ucts were purified over micro-Sephadex G-50 columns (Life Technologies), boiled, and added to the hybridization mixture. Washes were performed twice in $2 \times$ SSC, 0.1% SDS for 10 min at room temperature, followed by two washes in $0.1 \times$ SSC, 0.1% SDS for 20 min at 65 °C. Membranes were then exposed to film overnight.

Western Blot Analysis—Nuclear and cytoplasmic extracts were prepared as described previously (41). Equal amounts of extracts were subjected to SDS-PAGE electrophoresis and transferred to nitrocellulose membranes (Schleicher & Schuell). Blocking was performed in 5% nonfat dry milk, $1 \times$ TBST (25 mM Tris-HCl, pH 8.0, 125 mM NaCl, 0.1% Tween 20). Primary and secondary antibodies were diluted in 0.25% bovine serum albumin, $1 \times$ TBST and incubations proceeded for 30 min at room temperature. Washes were performed in $1 \times$ TBST for 5 min and repeated 3 times. Specific proteins were visualized by enhanced chemiluminescence (Amersham Pharmacia Biotech). Antibodies for I κ B α (C-21), I κ B β (C-20), I κ B ϵ (M-121), and p50 (NLS) were obtained from Santa Cruz Biotechnology. The antibody for p65 was obtained from Rockland.

I κ B α Kinase Assay—Cells were treated with TNF for various times without or with prior incubation with IL-10. Whole cell extracts were immunoprecipitated with an antibody against IKK- β (gift of Dr. F. Mercurio, Signal Pharmaceuticals) and the immunoprecipitates subjected to an IKK activity assay (36), using GST-I κ B α (1-54) WT (4 μ g) or a mutated form of I κ B α (S32T,S36T) as substrates. Samples were subjected to SDS-PAGE and gels were dyed with Gelcode Blue stain (Pierce Inc.) for equal loading control. Bands were quantitated on a PhosphorImager System (Storm 840; Molecular Dynamics Inc., Sunnydale, CA).

RESULTS

IL-10 Inhibits TNF-induced Proinflammatory IL-8 Cytokine Production and NF- κ B-dependent Transcription in Human Monocytic and Intestinal Epithelial Cells—To investigate whether the anti-inflammatory effects of IL-10 are mediated through the ability of this cytokine to inhibit NF- κ B, we chose to use the human monocytic cell lines THP-1 and U937 and the human intestinal epithelial cell line HT-29 as *in vitro* models. To elucidate whether IL-10 induced a similar effect in THP-1, U937, and HT-29 cells as previously demonstrated in peripheral blood mononuclear cells (7), cells were stimulated with TNF or LPS in either the presence or absence of human recombinant IL-10. Stimulation with TNF or LPS for 8 h led to an increase in IL-8 production in THP-1, U937, and HT-29 cells, which was inhibited by the addition of IL-10 (data not shown).

Since it has been well established that TNF up-regulates IL-8 transcription through an NF- κ B-dependent mechanism (42), we wanted to determine whether IL-10 inhibited transcriptional activation of NF- κ B. THP-1 and HT-29 cells were transiently transfected with the 3 \times κ B luciferase reporter plasmid, containing three copies of the MHC class I NF- κ B consensus site. To ensure that luciferase activities were specific for NF- κ B-dependent transcription, experiments were also performed in parallel using the mutant 3 \times κ B (mut 3 \times κ B) luciferase reporter, which is not transcriptionally activated by NF- κ B (43). Forty-eight hours after transfection, cells were treated with TNF in either the presence or absence of IL-10, harvested 5 h following addition of TNF, and assayed for NF- κ B-dependent transcription. As shown in Fig. 1A, TNF induced the transcriptional activity of NF- κ B approximately 20-fold in THP-1 cells (*left panel*) and approximately 35-fold in HT-29 cells (*right panel*). However, pretreatment with IL-10 strongly inhibited the TNF-induced NF- κ B activity in both THP-1 and HT-29 cells (Fig. 1A). The ability of IL-10 to modulate NF- κ B transcriptional activity was specific, since transfection experiments were normalized to the mut 3 \times κ B luciferase reporter (Fig. 1A, *left and right panels*).

Since IL-10 repressed an NF- κ B responsive reporter in transient transfection assays, we wanted to determine whether IL-10 would also block the ability of TNF to up-regulate NF- κ B responsive gene expression. To experimentally address this question, Northern blot analysis for I κ B α and IL-8 (both NF-

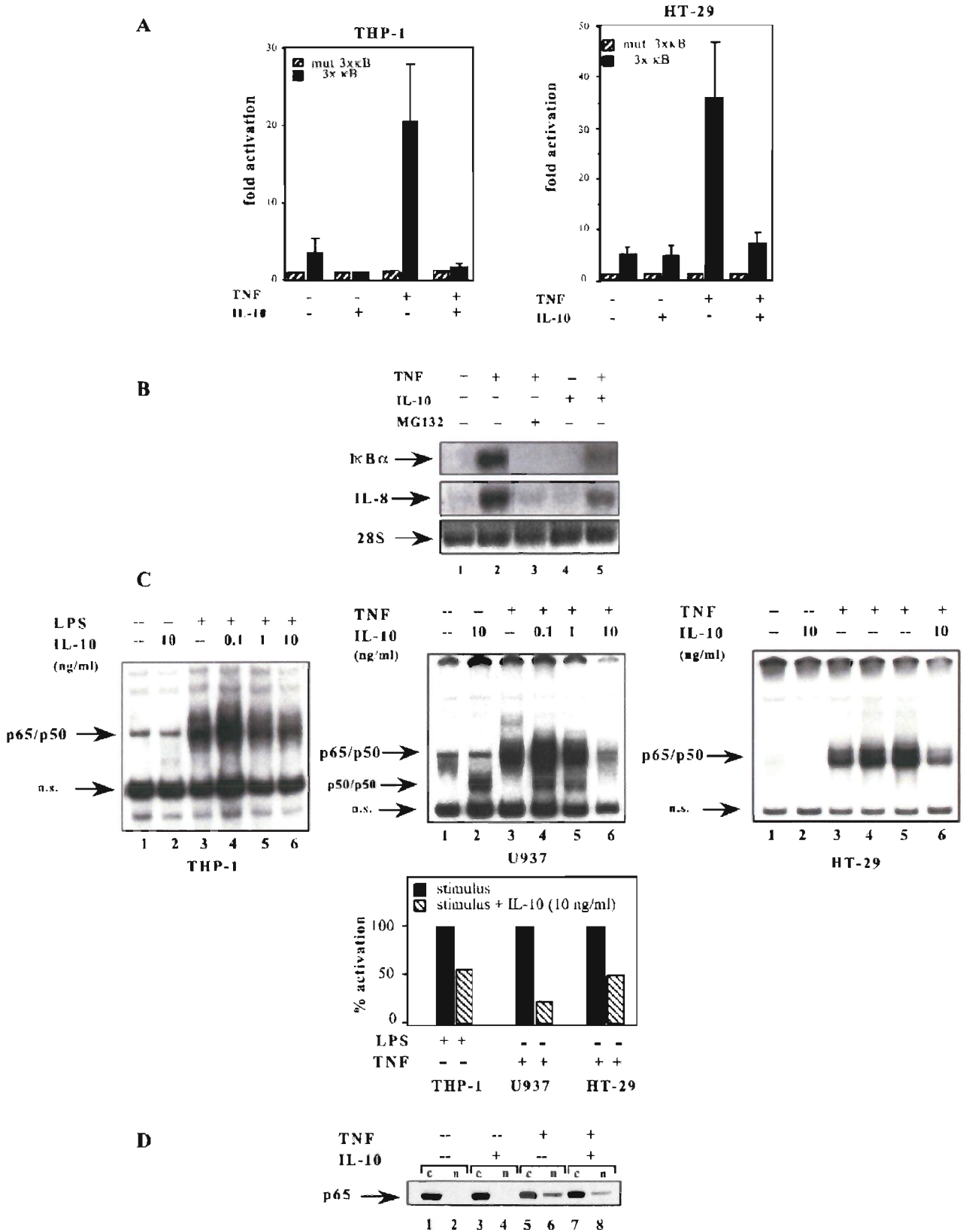


FIG. 1. A, IL-10 inhibits NF- κ B dependent transcription in human monocytic and intestinal epithelial cells. THP-1 and HT-29 cells were transfected with the 3 κ B-Luc or mut 3 κ B-Luc construct by the DEAE-dextran method (THP-1) or with Superfect (HT-29). 48 h after transfection cells were exposed to TNF (2 ng/ml) in the presence or absence of IL-10 (100 ng/ml) for 5 h. Cells were then lysed and the cytosolic extracts (100 μ g) were used in luciferase assays to determine activity. Fold induction is relative to luciferase activity in cells transfected with mut 3 κ B-Luc. Data is expressed as the mean of two independent experiments \pm S.E. **B**, IL-10 suppresses TNF-induced steady state I κ B α mRNA levels. THP-1

κ B-regulated genes) was performed. Total RNA was prepared from THP-1 cells that had been treated with TNF alone, with TNF plus IL-10, or with TNF plus the NF- κ B inhibitor MG 132 (55). TNF-treated cells displayed a strong increase in both I κ B α and IL-8 gene expression (Fig. 1B, lanes 1 and 2, upper and middle panels). However, I κ B α and IL-8 mRNA levels were suppressed approximately 60% in cells that had been pretreated by IL-10 and subsequently stimulated with TNF (Fig. 1B, lane 5, upper and middle panels). As predicted, pretreatment with the NF- κ B inhibitor MG 132 suppressed TNF-induced I κ B α and IL-8 mRNA levels almost completely (Fig. 1B, lanes 2 and 3, upper and middle panels). These results indicate that IL-10 is capable of inhibiting TNF-induced expression of two endogenous, NF- κ B-regulated genes.

Inhibition of NF- κ B DNA Binding Activity by IL-10—To assess whether IL-10 inhibited NF- κ B-dependent transcription through the suppression of DNA binding, EMSAs were performed. Nuclear extracts were prepared from cells treated with TNF or LPS in the presence or absence of IL-10 and nuclear proteins were analyzed for their ability to recognize a ³²P-labeled NF- κ B consensus site. Analysis of nuclear extracts from TNF- or LPS-stimulated cells demonstrated an increase in NF- κ B DNA binding activity as compared with nuclear extracts from unstimulated cells (Fig. 1C, compare lane 1 to 3, left, middle, and right panels). Pretreatment with IL-10 inhibited TNF- and LPS-induced DNA binding in a dose-dependent manner (Fig. 1C, lanes 4–6, left and middle panels). IL-10 induced its effects on NF- κ B DNA binding by specifically affecting the p65/p50 heterodimer complex, as determined by antibody supershift experiments (data not shown). Even though IL-10 blocked both TNF- and LPS-induced NF- κ B DNA binding, the ability of IL-10 to inhibit NF- κ B was greater in response to TNF than in response to LPS. Importantly, IL-10 inhibited TNF-induced NF- κ B DNA binding activity to a similar level in both THP-1 and U937 cells (Fig. 1C and data not shown). Although we observed a similar inhibitory effect on NF- κ B DNA binding activity in HT-29 cells following TNF stimulation, this effect was not as dramatic as observed for monocytic cells (Fig. 1C).

IL-10 Inhibits NF- κ B Nuclear Translocation by Preventing TNF-induced Degradation of I κ B α —The primary level of control of NF- κ B is through its interaction with the inhibitor protein I κ B. Thus, one mechanism to explain the ability of IL-10 to inhibit NF- κ B activity is by the ability of this anti-inflammatory cytokine to inhibit nuclear translocation of NF- κ B by blocking I κ B α degradation in response to TNF stimulation. To experimentally address this question, THP-1 cells were stimulated with TNF for 15 min in either the presence or absence of IL-10, cytoplasmic and nuclear proteins were isolated, and Western blot analysis was performed to determine whether IL-10 addition effected nuclear translocation of the p65 protein. As shown in Fig. 1D, p65 was predominantly cytoplasmically localized in unstimulated cells (Fig. 1D, lanes 1

and 2) and in cells treated with IL-10 alone (lanes 3 and 4). Cells stimulated with TNF (15 min) demonstrated an increase in nuclear translocation of p65 (lanes 5 and 6). In contrast, cells pretreated with IL-10 and then stimulated with TNF for 15 min demonstrated a reduction in nuclear p65 (Fig. 1D, compare lanes 7 and 8 with lanes 5 and 6). To further elucidate if the IL-10-induced block of p65 nuclear translocation was caused by the ability of this cytokine to interfere with TNF-induced degradation of I κ B α , cytoplasmic extracts of cells stimulated with TNF for various times in the absence or presence of IL-10 were subjected to Western blot analysis. Immunoblot analysis for I κ B α demonstrated that treatment with TNF resulted in a time-dependent degradation of I κ B α . In contrast, pretreatment with IL-10 prevented I κ B α degradation up to 15 min following the addition of TNF (Fig. 2A). However, IL-10 failed to prevent TNF-induced degradation of I κ B α 30 min post-stimulation (Fig. 2A, lane 11). The fact that I κ B α reaccumulates following degradation is not explained by the inability of IL-10 to block NF- κ B activation since IL-10 blocks the induction of I κ B α mRNA (see Fig. 1B). Differences in I κ B α protein levels observed in TNF and IL-10 treated cells were not due to differences in protein loading since immunoblot analysis demonstrated similar levels of p50 expression (Fig. 2A). These results indicate that single dose pretreatment with IL-10 transiently blocks I κ B α degradation in response to TNF stimulation (see "Discussion").

IL-10 Blocks the TNF Induced Activation of the I κ B Kinase—Since TNF-mediated activation of NF- κ B has been shown to require the IKK-induced phosphorylation of I κ B α (29, 33–36), we wanted to determine if IL-10 inhibited NF- κ B by targeting the IKK complex. In order to measure TNF-induced IKK activity, IKK was immunoprecipitated from whole cell extracts and used in an *in vitro* kinase assay to measure the ability of IKK to phosphorylate a GST-I κ B α substrate containing serine residues 32 and 36. The specificity of the IKK assay was determined by the inability to phosphorylate a GST-I κ B α S32T/S36T mutant in which serine residues 32 and 36 have been converted to threonine residues. As shown in Fig. 2B, TNF addition induced IKK activity in a time-dependent fashion in U937 cells. Maximum IKK activity in response to TNF addition was observed within 10 min, and was greatly diminished within 30 min post-TNF stimulation. However, TNF-induced IKK activity was inhibited by IL-10, with peak effects at 5 and 10 min post-TNF stimulation (Fig. 2B). Note that the quantification of relative IKK activity shown in Fig. 2B is derived from comparison to time T₀' and is not a direct comparison of IKK activity between the two experimental conditions at a particular time point. The ability of TNF to induce IKK activity was specific for serine residues 32 and 36, since the GST-I κ B α S32T/S36T mutant could not be phosphorylated in the kinase assays (Fig. 2B). Although similar kinetics of TNF-induced IKK activity were seen in both THP-1 and U937 cells (Fig. 2, B, C, and D), the inhibitory effects of IL-10 in THP-1 cells (Fig. 2C) were much more pronounced in comparison to U937 cells (com-

cells were left untreated (lane 1), treated with IL-10 (10 ng/ml) alone (lane 4), treated with TNF (10 ng/ml) for 2 h without (lane 2) or with a 1-h pretreatment with MG 132 (100 μ M) (lane 3) or IL-10 (10 ng/ml) (lane 5). Total RNA was extracted and subjected to Northern blot analysis and probed for I κ B α and IL-8. Equal loading of RNA was confirmed by visualizing the 28 S RNA. The data is representative of two independent experiments. C, IL-10 inhibits NF- κ B DNA binding activity in monocytic and intestinal epithelial cells. THP-1 cells (left panel) were stimulated with LPS (10 μ g/ml) for 60 min without (lane 3) or with a 5-min pretreatment with various doses of IL-10 (0.1–10 ng/ml) (lanes 4–6). U937 cells (middle panel) were stimulated with TNF (10 ng/ml) for 15 min without (lane 3) or with a 5-min pretreatment with various doses of IL-10 (0.1–10 ng/ml) (lanes 4–6). HT-29 cells (right panel) were stimulated with varying doses of TNF (2 ng/ml, lane 3; 10 ng/ml, lane 4; 50 ng/ml, lane 5) for 30 min without (lanes 3–5) or with a 5-min pretreatment with IL-10 (10 ng/ml) (lane 6). Nuclear proteins were extracted and assayed for NF- κ B DNA binding activity in EMSA. The ability of IL-10 to inhibit NF- κ B DNA binding activity was greater in response to TNF (80% inhibition in U937 cells; 50% inhibition in HT-29 cells) than in response to LPS (45% in THP-1 cells) (lower panel). D, inhibition of NF- κ B DNA binding activity by IL-10 under conditions of TNF treatment up to 15 min is caused by a block in p65 nuclear translocation. Nuclear (n) and cytoplasmic (c) extracts of THP-1 cells that were left untreated (lanes 1 and 2), treated with IL-10 (10 ng/ml) alone (lanes 3 and 4), or treated with TNF (10 ng/ml) without (lanes 5 and 6) or with a 5-min pretreatment with IL-10 (10 ng/ml) (lanes 7 and 8) were loaded adjacent and subjected to SDS-PAGE followed by p65 immunoblotting and compared for the induction or inhibition of p65 nuclear translocation.

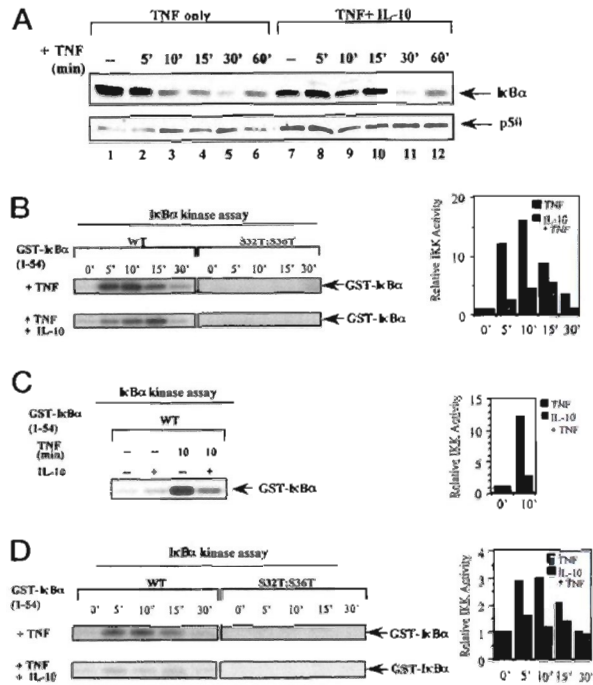


FIG. 2. IL-10 prevents TNF-induced degradation of I κ B α by blocking I κ B kinase activity. *A*, THP-1 cells were left untreated (lane 1), treated with IL-10 (10 ng/ml) alone (lane 7), or treated with TNF (10 ng/ml) without (lanes 2–6) or with a 5-min IL-10 pretreatment (10 ng/ml) (lanes 8–12) for the times indicated. Equivalent amounts of cytoplasmic extracts were analyzed by Western blot using antibodies against I κ B α . Immunoblotting for p50 demonstrated equal loading of protein (lower panel). One representative experiment of three experiments is shown. *B*, U937 cells were treated with TNF (10 ng/ml) for various times. Whole cell extracts were immunoprecipitated with an antibody against IKK β and the immunoprecipitates subjected to an IKK activity assay. GST-I κ B α (1–54) WT (4 μ g) or a mutated form of GST-I κ B α (S32T,S36T) was used as substrate. Western blotting for IKK was performed as a loading control (not shown). Comassie Blue staining of gels showed equal loading of the GST-I κ B α substrate (not shown). IKK activity as quantitated by PhosphorImager analysis (Molecular Dynamics) was normalized to activity of untreated cells and expressed as fold induction. The data is representative of three independent experiments. *C*, anti-IKK β immunoprecipitates from whole cell extracts of THP-1 cells were left untreated, treated with IL-10 (10 ng/ml), or were stimulated with TNF (10 ng/ml) for 10 min without or with a 5-min pretreatment with IL-10 (10 ng/ml) and examined for IKK activity. WT GST-I κ B α was used as substrate. TNF-induced IKK activity in THP-1 cells is expressed as fold induction after normalization to activity of untreated cells. The data is representative of three independent experiments. *D*, I κ B α kinase assay with anti-IKK β immunoprecipitates from whole cell extracts of THP-1 cells that were treated with low dose TNF (2 ng/ml) without or with an IL-10 pretreatment.

pare with Fig. 2*B*). IL-10-mediated inhibition of IKK activity was also observed when cells were treated with lower doses of TNF (2 ng/ml) (Fig. 2*D*). Although the kinetics of the IKK activity occurs quite rapidly and persists for only 30 min following TNF stimulation, our results clearly demonstrate that IL-10 controls NF- κ B activity in part through the regulation of the IKK complex.

IL-10 Inhibits NF- κ B DNA Binding After Prolonged TNF Stimulation—Since IL-10 inhibited NF- κ B-dependent transcription in transient transfection experiments up to 5 h post-TNF stimulation (Fig. 1*A*), we wanted to determine whether IL-10 could also inhibit NF- κ B activity at later time points of TNF stimulation. Interestingly, IL-10 significantly blocked NF- κ B DNA binding following longer TNF treatment (Fig. 3*A*). Inhibition of DNA binding at these later time points of TNF did not coincide with the same time frame in which IL-10 inhibited IKK activity (Fig. 2, *B* and *D*, and data not shown) and inhib-

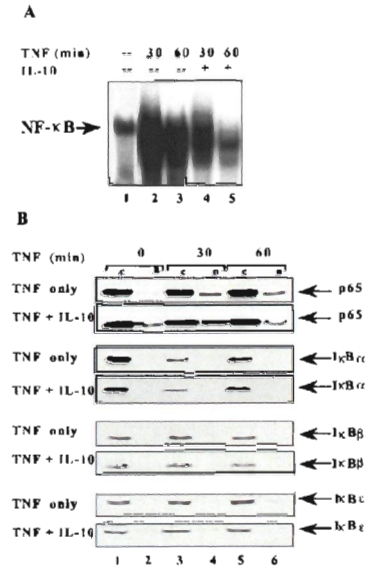


FIG. 3. IL-10-mediated inhibition of NF- κ B DNA binding upon longer TNF treatment is independent of blocking p65 nuclear translocation. *A*, 10^7 THP-1 cells were stimulated with TNF (10 ng/ml) for 30 and 60 min without (lanes 2 and 3) or with a 5-min IL-10 pretreatment (10 ng/ml) (lanes 4 and 5). Nuclear proteins were extracted and assayed for NF- κ B DNA binding activity by EMSA. *B*, equal amounts of cytoplasmic (*c*) and nuclear (*n*) proteins of THP-1 cells of the same experiment as in *A* were loaded adjacent and subjected to SDS-PAGE followed by immunoblotting for p65, I κ B α , I κ B β , and I κ B ϵ . Extracts of cells that were left untreated (lanes 1 and 2, first panel) or treated with TNF (10 ng/ml) for 30 and 60 min (lanes 3–6, first panel) were compared with extracts of cells treated with IL-10 alone (10 ng/ml) (lanes 1 and 2, second panel) or cells pretreated with IL-10 (10 ng/ml) before a 30- and 60-min treatment with TNF (lanes 3–6, second panel) for the induction or inhibition of p65 nuclear translocation and for the cellular distribution of I κ B α , I κ B β , and I κ B ϵ .

ited I κ B α degradation (Fig. 2*A*). In order to determine whether IL-10 was inhibiting DNA binding activity of NF- κ B at these later time points through mechanisms involving nuclear translocation of p65, Western blot analysis was performed. Western blot analysis for p65 of cytoplasmic and nuclear extracts of TNF-treated cells with or without the pretreatment of IL-10 revealed that the inhibition of NF- κ B DNA binding under these conditions was not due to a block of NF- κ B nuclear translocation (Fig. 3*B*). Similar amounts of nuclear p65 were detected in cells treated with TNF for 30 and 60 min regardless of the addition of IL-10 (Fig. 3*B*, upper panels, compare nuclear levels of p65 at the 30- and 60-min time points). These data indicate that even under situations where p65 is nuclear there is an inhibition of NF- κ B DNA binding activity by IL-10. To determine whether the I κ B proteins, I κ B α , I κ B β , and I κ B ϵ , play a role in inhibiting NF- κ B DNA binding in response to IL-10, cytoplasmic and nuclear proteins were assayed for I κ B proteins by Western blot analysis. Analysis of nuclear extracts failed to demonstrate an accumulation of I κ B proteins (α , β , and ϵ) following IL-10 treatment, suggesting that the inhibitory action of IL-10 on NF- κ B DNA binding is not mediated by increased nuclear levels of these inhibitory molecules.

DISCUSSION

Interleukin-10 controls inflammatory processes by suppressing the production of proinflammatory cytokines which are known to be transcriptionally controlled by NF- κ B. Although IL-10 has been found to inhibit the activity of NF- κ B in various cell types, results from different groups have been variable and no molecular mechanisms have been elucidated which may control NF- κ B activity in response to IL-10. We wanted to

investigate whether the anti-inflammatory effects of this cytokine are mediated through its ability to inhibit NF- κ B. In agreement with previous studies (7), stimulation with TNF or LPS led to an increase in IL-8 production, which was inhibited by IL-10 addition. TNF-induced IL-8 production is regulated through an NF- κ B-dependent mechanism (42). In transient transfection experiments we show that IL-10 was able to specifically inhibit NF- κ B-dependent transcription (Fig. 1A). These results indicate that IL-10 not only inhibits TNF-induced IL-8 cytokine production, as previously reported for human neutrophils (7), but also inhibits the transcriptional activity of NF- κ B in monocytic and intestinal epithelial cells. Consistent with previous reports (40), our data indicate that NF- κ B-dependent transcriptional regulation is a target for the anti-inflammatory actions of IL-10. This finding is further supported by the observation that IL-10 pretreatment was able to suppress TNF-induced mRNA levels for I κ B α and IL-8, which are both positively up-regulated by the NF- κ B transcription factor (Fig. 1B).

Although it has been previously established that IL-10 inhibits NF- κ B activity (37, 39, 40), the mechanisms governing this process have not been fully elucidated. Here we demonstrate that pretreatment with IL-10 inhibits TNF-induced and LPS-induced DNA binding of NF- κ B in a dose-dependent manner and specifically affects the p65/p50 heterodimer complex (Fig. 1C). Importantly, the ability of IL-10 to block DNA binding activity of NF- κ B was not limited to one type of inflammatory stimulus, nor was it a cell-specific phenomenon, since IL-10 inhibited TNF and LPS-induced NF- κ B activity in both U937 and THP-1 monocytic cells. This is further supported by our observation that IL-10 also inhibited TNF-induced NF- κ B activity in HT-29 intestinal epithelial cells, although to a lesser extent than in monocytic cells. Interestingly, the extent of IL-10's inhibitory effects was also dependent on the activating stimulus, since IL-10 inhibited TNF-induced NF- κ B activity to a greater degree than it inhibited LPS-stimulated NF- κ B activity in monocytic cells. These results indicate that IL-10 functions to block the signal transduction pathway required for induction of NF- κ B DNA binding activity. Our data is supported by studies in human peripheral blood mononuclear cells (37) and murine macrophages (40) that have demonstrated the ability of IL-10 to block LPS-induced NF- κ B DNA binding, but is in contrast to other studies in human monocytes (38) in which IL-10 was not able to block LPS-induced activation of NF- κ B DNA binding. These differences might arise from different cell types used in the studies (peripheral blood mononuclear cells *versus* monocytes) or the concentrations of LPS that were used. In agreement with our results, Wang *et al.* (37) also demonstrated the ability of IL-10 to block TNF-induced NF- κ B DNA binding in human peripheral blood mononuclear cells using similar doses of TNF and IL-10.

The potential inhibition of I κ B degradation in response to cytokine stimulation would be one mechanism to explain the ability of IL-10 to inhibit NF- κ B. We report here that IL-10 inhibits NF- κ B nuclear translocation by preventing TNF-induced degradation of I κ B α (Fig. 2A). Pretreatment with IL-10 prevented I κ B α degradation up to 15 min following the addition of TNF but failed to prevent TNF-induced degradation of I κ B α 30 min post-stimulation. These results indicate that IL-10 can induce its inhibitory effects on NF- κ B, at least in part, by delaying TNF-induced degradation of I κ B α (also see below).

It has recently been established that IKK phosphorylates I κ B α on serine residues 32 and 36, and that this phosphorylation is the prerequisite for ubiquitination and proteasome-dependent degradation of I κ B, thus liberating NF- κ B and allowing it to translocate to the nucleus (25, 27). Here we demonstrate that IL-10 blocks the TNF-induced activation of

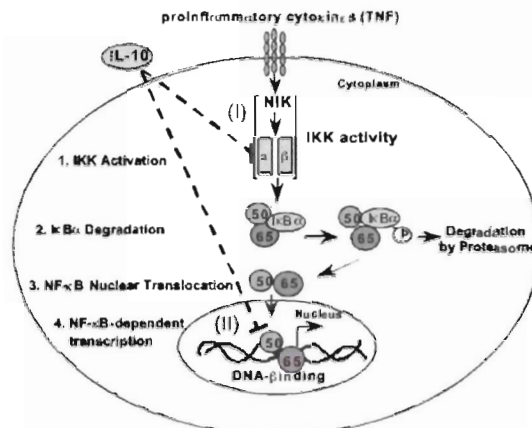


FIG. 4. Scheme explaining mechanisms of IL-10-mediated inhibition of NF- κ B activity. *I*, in the absence of IL-10, TNF activates the I κ B kinase (IKK), which phosphorylates the inhibitory protein I κ B α on serine residues 32 and 36. *2*, phosphorylated I κ B α , which functions to sequester the inactive p65/p50 heterodimer in the cytoplasm, is then ubiquitinated and degraded by the 26 S proteasome. *3*, degradation of I κ B α frees the p65/p50 heterodimer, which then can translocate to the nucleus, where it transcriptionally regulates NF- κ B dependent genes (*4*). In the presence of IL-10, NF- κ B is regulated by dual mechanisms. (*I*), upon short term exposure to TNF, pretreatment with IL-10 blocks TNF-induced IKK activity, thus inhibiting phosphorylation and degradation of I κ B α . The preserved I κ B α continues to bind NF- κ B in the cytoplasm, which prohibits NF- κ B nuclear translocation and NF- κ B dependent transcription. (*II*), upon longer exposure to TNF, pretreatment with IL-10 can directly block NF- κ B DNA binding by a mechanism that is independent of NF- κ B nuclear translocation.

the I κ B kinase up to 80% with peak effects at 5 and 10 min post-TNF stimulation (Fig. 2, B-D). To our knowledge, this is the first demonstration of a cytokine-mediated inhibition of IKK activity and identifies, in part, the molecular target through which IL-10 inhibits NF- κ B activation. The specific blockade of IKK has recently been identified as the molecular target of aspirin- and sodium salicylate-mediated inhibition of NF- κ B activity (45) and further emphasizes IKK as a crucial target of anti-inflammatory drugs. It is important to point out that even though IL-10 has dramatic inhibitory effects in both THP-1 and U937 cells with respect to NF- κ B activity, we found that the inhibitory effects of IL-10 on IKK activity were more pronounced on THP-1 cells (Fig. 2, B, C, and D). Currently we are investigating whether the level of IL-10 receptor expression in these cell lines could account for the differences in IKK inhibition mediated by IL-10.

We demonstrate that IL-10 is able to block NF- κ B DNA binding after prolonged TNF stimulation, however, under these conditions the inhibition of NF- κ B activity was not caused by a block of NF- κ B nuclear translocation (Fig. 3, A and B). These results indicate that IL-10 is capable of blocking NF- κ B activity by initially inhibiting IKK activity, I κ B α phosphorylation, and NF- κ B nuclear translocation, but that prolonged exposure of cells to TNF and IL-10 results in an inhibition of NF- κ B DNA binding through a yet unknown mechanism. We failed to detect nuclear accumulation of I κ B α , I κ B β , and I κ B ϵ following TNF and IL-10 treatment. This strongly suggests that these molecules do not play a role in the IL-10-mediated inhibition of NF- κ B DNA binding in the nucleus. Since it has been reported that binding of NF- κ B to DNA is controlled by the phosphorylation status of p65 (27, 46), it is possible that IL-10 may negatively regulate NF- κ B activity by modulating its phosphorylation status. Alternatively, IL-10 signaling could lead to the interaction of NF- κ B with a nuclear protein that is capable of blocking DNA recognition.

NF- κ B is known to positively regulate the promoter region of

many different proinflammatory cytokine genes, including TNF, IL-1 β , IL-8, and IL-6 (25, 42, 47). Moreover, exposure of cells to these cytokines in turn is known to stimulate NF- κ B transcriptional activity. Thus, the dysregulation of autocrine and paracrine modulating factors has been proposed to contribute to chronic NF- κ B activation, which is commonly associated with autoimmune disorders, rheumatoid arthritis, and inflammatory bowel disease (48–54). One of the body's natural defenses against chronic NF- κ B activation involves the production of anti-inflammatory cytokines, such as IL-10. Although IL-10 has been demonstrated to block NF- κ B activation, the molecular target for IL-10-induced inhibition of NF- κ B had not been established. In this study we provide evidence that IL-10 regulates NF- κ B by dual mechanisms. First, within 15 min of exposure to TNF, IL-10 inhibits TNF-induced activation of the IKK complex (Fig. 4, I). The ability of IL-10 to inhibit IKK activity is consistent with the observation that IL-10 delays TNF-mediated degradation of I κ B protein. Although IL-10 inhibits TNF-induced IKK activity, this effect accounts only for the immediate inhibitory action of IL-10 on NF- κ B activity. Interestingly, in agreement with previous reports (37, 40), under conditions of longer exposure of monocytic cells to TNF, IL-10 blocked TNF-induced NF- κ B DNA binding activity by an alternative mechanism which was not associated with the inhibition of IKK activity or the inhibition of NF- κ B nuclear translocation (Fig. 3, A and B, and Fig. 4, II). Therefore, in addition to blocking the activity of the IKK complex, IL-10 appears to have a secondary mechanism of inhibiting NF- κ B DNA binding activity. This dual type control would allow inhibition of NF- κ B nuclear translocation through the inhibition of IKK-dependent mechanisms, as well as blocking DNA binding of NF- κ B that has successfully translocated to the nucleus after longer exposure to TNF. Thus we provide evidence that IL-10 strongly blocks TNF-induced NF- κ B transcriptional activity up to 5 h post-TNF stimulation suggesting that both mechanisms, IL-10-mediated inhibition of IKK activity and inhibition of DNA-binding, contribute to the ability of IL-10 to block NF- κ B-dependent transcription. Our study has elucidated the anti-inflammatory mechanisms of IL-10 through inhibition of NF- κ B in monocytic and intestinal epithelial cell lines *in vitro*, which may show differences when compared with the multiple, complex biological interactions of IL-10 with interacting regulatory pathways *in vivo*. In our *in vitro* system single IL-10 treatment induced acute and time-limited responses. However, it would be predicted that the inhibitory action of this cytokine *in vivo* would be continuous due to constant exposure and may lead to prolonged anti-inflammatory effects by the repetitive IL-10-mediated inhibition of IKK and of NF- κ B DNA binding. Future experiments will further explore the signal transduction pathways required to inhibit the IKK complex. Moreover, additional experiments will elucidate the mechanisms by which IL-10 inhibits DNA binding of NF- κ B. Our data presented here underscores the importance of the inhibitory action of IL-10 on IKK activity making the I κ B kinase complex an attractive target for anti-inflammatory intervention.

Acknowledgments—We thank C. Y. Wang, D. Guttridge, and C. Jobin for critical comments. We gratefully acknowledge Dr. Frank Mercurio for providing the IKK antibody and for advice on the IKK assays and Allen Marshall for expert technical assistance. We thank Julie Vorobiov and the Immunotechnologies Core of the UNC Center for Gastrointestinal Biology and Disease for assistance with the IL-8 ELISA.

REFERENCES

- Fiorentino, D., Bond, M., and Mosman, T. (1989) *J. Exp. Med.* **170**, 2081–2095
- Del Prete, G., De Carli, M., Almerigogna, F., Giudizi, M., Bialotti, R., and Romagnani, S. (1993) *J. Immunol.* **150**, 353–360
- Bogdan, C., and Nathan, C. (1993) *Ann. N.Y. Acad. Sci.* **685**, 713–739
- Fiorentino, D., Zlotnik, A., Mosmann, T., Howard, M., and O'Garra, A. (1991) *J. Immunol.* **147**, 3815–3822
- de Waal Malefyt, R., Abrams, J., Bennett, B., Figdor, C. G., and de Vries, J. E. (1991) *J. Exp. Med.* **174**, 1209–1220
- Bogdan, C., Vodovotz, Y., and Nathan, C. (1991) *J. Exp. Med.* **174**, 1549–1555
- Wang, P., Wu, P., Anthes, J., Siegel, M., Egan, R., and Billah, M. (1994) *Blood* **83**, 2678–2683
- Wang, P., Wu, P., Siegel, M. I., Egan, R. W., and Billah, M. M. (1994) *J. Immunol.* **153**, 811–816
- Bogdan, C., Paik, J., Vodovotz, Y., and Nathan, C. (1992) *J. Biol. Chem.* **267**, 23301–23308
- Willems, F., Marchant, A., Delville, J.-P., Gerard, C., Delvaux, C., Velu, T., de Boer, M., and Goldman, M. (1994) *Eur. J. Immunol.* **24**, 1007–1009
- Moore, K., O'Garra, A., de Waal Malefyt, R., Vieira, P., and Mosmann, T. (1993) *Annu. Rev. Immunol.* **11**, 165–190
- Kühn, R., Löhler, J., Rennick, D., Rajewski, K., and Müller, W. (1993) *Cell* **75**, 263–274
- Powrie, F., Leach, M., Mauze, S., Caddle, L., and Coffman, R. (1993) *Int. Immunol.* **5**, 1461–1471
- Herfarth, H., Mohanty, S., Rath, H., Tonkonogy, S., and Sartor, R. (1996) *Gut* **39**, 836–845
- Herfarth, H. H., Bocker, U., Janardhanam, R., and Sartor, R. B. (1998) *Gastroenterology* **115**, 856–865
- Walmsley, M., Katsikis, P., Abney, E., Parry, S., Williams, R., Maini, R., and Feldmann, M. (1996) *Arthritis Rheum.* **39**, 495–503
- Rott, O., Fleischer, B., and Cash, E. (1994) *Eur. J. Immunol.* **24**, 1434–1440
- Van Laethem, J. L., Marchant, A., Delvaux, A., Goldman, M., Robbersrecht, P., Velu, T., and Deviere, J. (1995) *Gastroenterology* **108**, 1917–1922
- Pennline, K. J., Roque-Gaffney, E., and Monahan, M. (1994) *Clin. Immunol. Immunopathol.* **71**, 169–175
- Gerard, C., Bruyns, C., Marchant, A., Abramowicz, D., Vandenabeele, P., Delvaux, A., Fiers, W., Goldman, M., and Velu, T. (1993) *J. Exp. Med.* **177**, 547–550
- Schreiber, S., Heinig, T., Thiele, H.-G., and Raedler, A. (1995) *Gastroenterology* **108**, 1434–1444
- van Deventer, S., Elson, C., and Fedorak, R. (1997) *Gastroenterology* **113**, 383–389
- Geng, Y., Guibins, E., Altman, A., and Lotz, M. (1994) *Proc. Natl. Acad. Sci. U. S. A.* **91**, 8602–8606
- Poe, J. C., Wagner, D. H., Jr., Miller, R. W., Stout, R. D., and Suttles, J. (1997) *J. Immunol.* **159**, 846–852
- Baldwin, A. (1996) *Annu. Rev. Immunol.* **14**, 649–681
- Mori, N., and Prager, D. (1997) *Eur. J. Haematol.* **59**, 162–170
- Finco, T., and Baldwin, A. (1995) *Immunity* **3**, 263–272
- Schmitz, M., dos Santos Silva, M., and Baeuerle, P. (1995) *J. Biol. Chem.* **270**, 15576–15584
- DiDonato, J., Hayakawa, M., Rothwarf, D., Zandi, E., and Karin, M. (1996) *Nature* **388**, 548–554
- Brown, K., Gerstenberger, S., Carlson, L., Franzoso, G., and Siebenlist, U. (1995) *Science* **267**, 1485–1491
- Finco, T. S., Beg, A. A., and Baldwin, A. S., Jr. (1994) *Proc. Natl. Acad. Sci. U. S. A.* **91**, 11884–11888
- Rothwarf, D., Zandi, E., Natoli, G., and Karin, M. (1998) *Nature* **395**, 297–300
- Regnier, C. H., Song, H. Y., Gao, X., Goeddel, D. V., Cao, Z., and Rothe, M. (1997) *Cell* **90**, 373–383
- Zandi, E., Rothwarf, D. M., Delhase, M., Hayakawa, M., and Karin, M. (1997) *Cell* **91**, 243–252
- Woronicz, J. D., Gao, X., Cao, Z., Rothe, M., and Goeddel, D. V. (1997) *Science* **278**, 866–869
- Mercurio, F., Zhu, H., Murray, B. W., Shevchenko, A., Bennet, B. L., Li, J. W., Young, D. B., Barbosa, M., and Mann, M. (1997) *Science* **278**, 860–866
- Wang, P., Wu, P., Siegel, M. I., Egan, R. W., and Billah, M. M. (1995) *J. Biol. Chem.* **270**, 9558–9563
- Dokter, W., Koopmans, S., and Vellenga, E. (1996) *Leukemia* **10**, 1308–1316
- Romano, M. F., Lamberti, A., Petrella, A., Bisogni, R., Tassone, P. F., Formisano, S., Venuta, S., and Tursi, M. C. (1996) *J. Immunol.* **156**, 2119–2123
- Clarke, C. J. P., Hales, A., Hunt, A., and Foxwell, B. M. J. (1998) *Eur. J. Immunol.* **28**, 1719–1726
- Cheshire, J. L., and Baldwin, A. S., Jr. (1997) *Mol. Cell. Biol.* **17**, 6746–6754
- Stein, B., and Baldwin, A. S., Jr. (1993) *Mol. Cell. Biol.* **13**, 7191–7198
- Scherer, D. C., Brockman, J. A., Chen, Z., Maniatis, T., and Ballard, D. W. (1995) *Proc. Natl. Acad. Sci. U. S. A.* **92**, 11259–11263
- Lentseh, A. B., Shanley, T. P., Sarma, V., and Ward, P. A. (1997) *J. Clin. Invest.* **100**, 2443–2448
- Yin, M.-J., Yamamoto, Y., and Gaynor, R. B. (1998) *Nature* **396**, 77–80
- Naumann, M., and Scheidereit, C. (1994) *EMBO J.* **13**, 4597–4607
- Shirakawa, F., Saito, K., Bonagura, C. A., Galson, D. L., Fenton, M. J., Webb, A. C., and Auron, P. E. (1993) *Mol. Cell. Biol.* **13**, 1332–1344
- Barnes, P. J. (1997) *Int. J. Biochem. Cell Biol.* **29**, 867–870
- Handel, M. L., McMorrow, L. B., and Gravallesse, E. M. (1995) *Arthritis Rheum.* **38**, 1762–1770
- Burkhardt, H., and Kalden, J. R. (1997) *Rheumatol. Int.* **17**, 85–90
- Becker, H., Stengl, G., Stein, M., and Fedarlin, K. (1995) *Clin. Exp. Immunol.* **99**, 325–330
- Schreiber, S., Nikolaus, S., and Hampe, J. (1998) *Gut* **42**, 477–484
- Rogler, G., Brand, K., Vogl, D., Page, S., Hofmeister, R., Andus, T., Knuechel, R., Baeuerle, P., Scholmerich, J., and Gross, V. (1998) *Gastroenterology* **115**, 357–369
- Schottefuss, A., and Baldwin, A. S. (1999) *Int. J. Colorectal Dis.* **14**, 18–28
- Jobin, C., Hellerbrand, C., Licato, L. L., Brenner, D. A., and Sartor, R. B. (1998) *Gut* **42**, 779–787

ROC1, a Homolog of APC11, Represents a Family of Cullin Partners with an Associated Ubiquitin Ligase Activity

Tomohiko Ohta,*# Jennifer J. Michel,†
Arndt J. Schottelius,* and Yue Xiong*†‡§||
*Lineberger Comprehensive Cancer Center
†Curriculum in Genetics and Molecular Biology
‡Department of Biochemistry and Biophysics
§Program in Molecular Biology and Biotechnology
University of North Carolina at Chapel Hill
Chapel Hill, North Carolina 27599

Summary

We have identified two highly conserved RING finger proteins, ROC1 and ROC2, that are homologous to APC11, a subunit of the anaphase-promoting complex. ROC1 and ROC2 commonly interact with all cullins while APC11 specifically interacts with APC2, a cullin-related APC subunit. Yeast ROC1 encodes an essential gene whose reduced expression resulted in multiple, elongated buds and accumulation of Sic1p and Cln2p. ROC1 and APC11 immunocomplexes can catalyze isopeptide ligations to form polyubiquitin chains in an E1- and E2-dependent manner. ROC1 mutations completely abolished their ligase activity without noticeable changes in associated proteins. Ubiquitination of phosphorylated I κ B α can be catalyzed by the ROC1 immunocomplex *in vitro*. Hence, combinations of ROC/APC11 and cullin proteins potentially constitute a wide variety of ubiquitin ligases.

Introduction

Many regulatory proteins such as cyclins, CDK inhibitors, and transcription factors are regulated by the ubiquitin-dependent proteolytic pathway (Hochstrasser, 1996; King et al., 1996; Hershko, 1997). A cascade of enzymes, E1, E2, and E3, catalyze the attachment of ubiquitin (Ub) to substrates to form polyubiquitinated conjugates that are rapidly detected and degraded by the 26S proteasome. E1 and E2 both represent structurally related and well characterized enzymes that do not provide much substrate specificity. The E3 is ambiguously defined as a function containing two separate activities: an Ub ligase activity to catalyze isopeptide bond formation and a specific targeting activity to physically bring the ligase and substrate together. Elucidating the molecular nature and the regulation of E3s have become critical issues central to our understanding of regulated proteolysis.

Knowledge about E3 Ub ligases is very limited at present. The best characterized E3 ligase is the APC (anaphase-promoting complex or cyclosome), which plays a crucial role in regulating the passage of cells through anaphase (reviewed in King et al., 1996). Most proteins

known to be degraded by the APC contain a conserved 9-amino acid stretch, commonly known as the destruction box, that is necessary for their ubiquitination and degradation (Glotzer et al., 1991). Proteins that are degraded during G1 do not contain the conserved destruction box. Instead, substrate phosphorylation appears to play an important role in targeting their interaction with an E3 for ubiquitination. Genetic and biochemical analysis in yeast have identified an E3-like activity, the SCF, that plays a key role in regulating G1 progression. The SCF consists of at least three subunits, SKP1, CDC53/cullin, and an F box-containing protein, in which SKP1 functions as an adapter to connect CDC53 to the F box protein that binds directly to the substrate (reviewed in Hoyt, 1997).

Despite extensive investigations into the APC and SCF, the nature of E3 ligases still remains unclear. One inconsistency is that all *in vitro* reconstituted SCF ubiquitination reactions reported thus far have required the supplement of a cellular extract. This indicates that an essential protein component(s) or a critical modification was missing from the complexes assembled from isolated proteins. We report here the identification of a family of closely related RING finger proteins, ROC1, ROC2, and APC11. We present evidence that ROC1/APC11 are general cullin-binding proteins that have an associated ligase activity. Hence, ROC-cullins and APC11-APC2 may function as Ub ligases during interphase and mitosis, respectively.

Results

ROC1 Interacts Directly with All Cullins

In a yeast two-hybrid screen of a human HeLa pGAD-cDNA library using mouse cullin 4A as bait, we identified a gene encoding a RING finger protein, named ROC1 (regulator of cullins). ROC1 can also interact with cullins 1, 2, and 5 (Figure 1A). We then demonstrated that ROC1 interacts with the COOH-terminal 527 amino acid residues of CUL1, but not the NH₂-terminal 249 residues (Figure 1B). In contrast, SKP1 binds to the NH₂-terminal domain of CUL1. These results indicate that CUL1 contains at least two distinct domains, a NH₂-terminal SKP1-binding domain and a central/COOH-terminal ROC1-binding domain. Such structural separation suggests that it is unlikely that ROC1 competes with SKP1 for CUL1. Supporting this idea, we have detected ROC1 in the α -SKP1 immunocomplex, and SKP1 was reciprocally detected in the α -Roc1 immunocomplex when cells were cotransfected with ROC1, CUL1, and SKP1 (data not shown). Hence, ROC1 and SKP1 may coexist in the same protein complex with CUL1 to perform different functions.

To confirm the interaction between ROC1 and cullin proteins, Saos-2 cells were transfected with plasmids directing the expression of HA-tagged human ROC1 (HA-ROC1) together with CUL1 or other myc-epitope tagged cullins. Transfected cells were metabolically labeled with [³⁵S]methionine, and cell lysates were reciprocally immunoprecipitated with either α -HA, α -CUL1, or

|| To whom correspondence should be addressed (e-mail: yxiong@email.unc.edu).

Permanent address: First Department of Surgery, St. Marianna University School of Medicine, Kawasaki, 216 Japan.

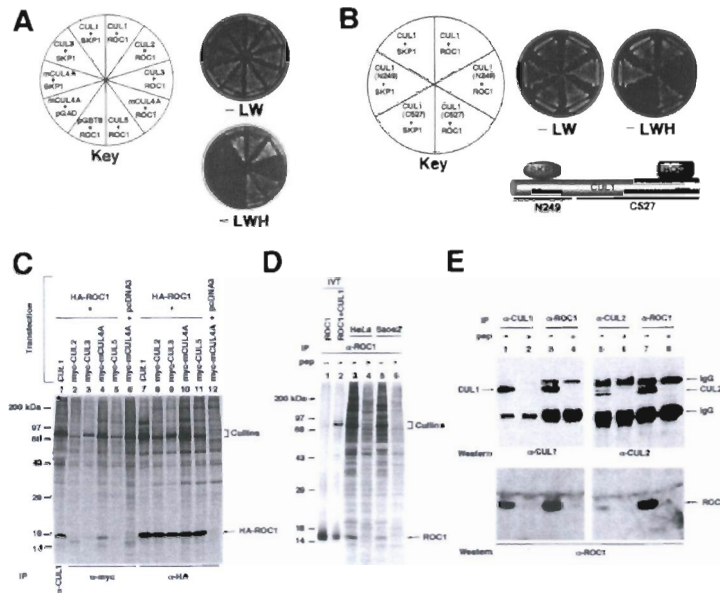


Figure 1. ROC1 Interacts with Members of the Cullin Family

(A) Yeast HF7c cells were cotransformed with plasmids expressing indicated proteins (key) and plated onto media lacking leucine and tryptophan (–LW) to verify the presence of both bait (Leu⁻) and prey (Trp⁻) plasmids; or onto media lacking leucine, tryptophan, and histidine (–LWH) to assay for interactions between bait and prey proteins.

(B) ROC1 interacts with the C-terminal portion of CUL1. HF7c yeast cells were cotransformed with plasmids expressing indicated proteins. Protein–protein interaction was assayed as described in (A).

(C–E) In vivo association of ROC1 with cullins. (C) ³⁵S-methionine-labeled lysates prepared from HeLa cells transfected with indicated plasmids.

(D) ³⁵S-methionine-labeled, in vitro translated ROC1 and CUL1, or cell lysates from HeLa and Saos-2 cells were immunoprecipitated with indicated antibodies and resolved by SDS-PAGE.

(E) Lysates prepared from HeLa cells were immunoprecipitated with indicated antibodies with (+) or without (–) competing antigen peptide. Proteins were resolved by SDS-PAGE and analyzed by Western analysis using indicated antibodies.

α -myc antibody. All five cullins coprecipitated with ROC1 by the α -HA antibody (Figure 1C; lanes 7–11). Reciprocally, HA-ROC1 was detected in α -CUL1 and α -myc-mCUL4A immunoprecipitations (lanes 1 and 4). The association between ROC1 and cullin 1 was not disrupted by buffer containing 0.1% SDS (data not shown), indicating that the ROC1–cullins association is very stable.

To obtain evidence for in vivo ROC1–cullins association under physiological conditions, we raised rabbit polyclonal antibodies specific to ROC1. This antibody is capable of precipitating both ROC1 and the ROC1–CUL1 complex as determined by the use of in vitro translated proteins (Figure 1D; lanes 1 and 2). From metabolically labeled HeLa and Saos-2 cells, the α -ROC1 antibody precipitated a protein of approximately 14 kDa (lanes 3 and 5). This protein corresponds to ROC1 as judged by its comigration with in vitro produced ROC1 and by competition using the antigen peptide (lanes 4 and 6). Several proteins that migrated in the 90 kDa range (indicated as “cullins” in Figure 1D) were also specifically competed by the antigen peptide. We immunopurified these proteins and determined their sequences by protein microsequencing. At least four cullin proteins (CUL1, CUL2, CUL3, and CUL4A or 4B) have been identified from this analysis thus far. HeLa cell lysate was then immunoprecipitated with antibodies to ROC1, CUL1, and CUL2, and precipitates were analyzed by Western blotting. As shown in Figure 1E, both CUL1 (lane 3) and CUL2 (lane 7) were readily detected in the ROC1 immunocomplexes and were specifically competed by ROC1 antigen peptide. Reciprocally, ROC1 was detected in both CUL1 (lane 1) and CUL2 (lane 5) complexes (lower panel, Figure 1E). Thus, ROC1 is a general cullin-interacting protein.

ROC1 Represents a Family of RING Finger Proteins Related to APC11

ROC1 encodes a 108-amino acid residue protein with a predicted molecular weight of 12265 D (Figure 2A). Database searches identified ROC1 as a highly evolutionarily conserved gene whose *S. cerevisiae* (ROC1-Sc), *S. pombe* (ROC1-Sp), and plant (ROC1-At) homologs share 67%, 88%, and remarkably 98% protein sequence identity with human ROC1, respectively, over the 82-amino acid region compared (Figure 2C). Database searches have also identified two additional genes, ROC2 in higher eukaryotes and APC11 in all eukaryotic species (Figures 2B and 2C), that are closely related to ROC1. ROC1 and ROC2 share an overall protein sequence identity of 51% with each other and 38% and 35% identity with APC11, respectively. Both ROC2 and APC11 are also highly evolutionarily conserved. Therefore, ROC1/ROC2/APC11 define a new family of proteins that are likely to carry out important cellular functions.

ROC/APC11 proteins contain two characteristic features: a RING finger and richness in tryptophan residues. The RING finger domain has been found in many eukaryotic proteins with diverse functions and is thought to mediate protein–protein interactions (Borden and Freemont, 1996). Three of the six highly conserved tryptophan residues in ROC1 are followed by an acidic amino acid residue (Asn, Glu, or Asp) that resembles the WD repeat indicating that they may be involved in mediating protein–protein interactions.

Selective Interaction between ROC2, APC11, and Cullin Family Proteins

We next determined whether ROC2 and APC11 also interact with cullins. Almost identical to ROC1, ROC2 interacted strongly with cullins 1, 2, 4A, and 5 (Figure

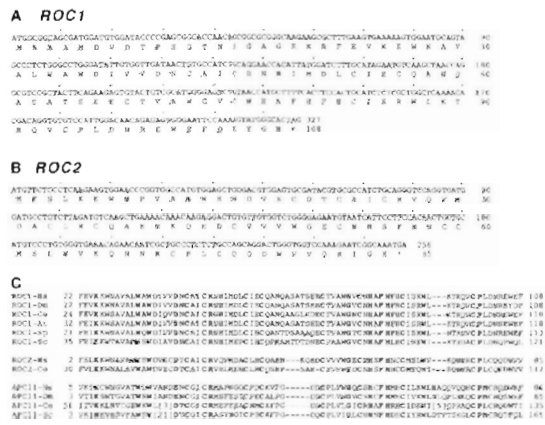


Figure 2. ROC1 Represents a Family of RING Finger Proteins Including APC11
(A) Nucleotide and amino acid sequences of human ROC1.
(B) Nucleotide and amino acid sequences of human ROC2.
(C) Sequence comparison of the ROC/APC11 family of proteins from representative organisms: human (Hs), fruit fly (Dm), nematodes (Ce), mouse ear cross (At), fission yeast (Sp), and budding yeast (Sc). Only residues that are identical to all sequences are in bold. The number in the bracket of certain sequences indicates the length of insertion omitted. The number preceding and following each sequence indicates the position of the first amino acid residue in each gene and the total length of each protein, respectively.

3A). In contrast, APC11 only interacted with cullin 5, but not other cullins (Figure 3B). Saos-2 cells were then transfected with HA-ROC2 and untagged CUL1 or myc-tagged cullins followed by [³⁵S]IP. All five cullins were coprecipitated with ROC2 by the HA antibody (Figure 3C; lanes 6–10). Reciprocally, ROC2 (preferentially the faster migrating form) was detected in cullin 2, 3, and 4 immunocomplexes (lanes 2–4). In contrast and with the exception of cullin 5, APC11 and cullins were not detected to interact with each other (Figure 3D; lanes 1–10). Cullin 5 was weakly but reproducibly detected in the APC11 immunocomplex (lane 10). Of all six mammalian cullins, CUL5 is the most divergent member of the cullin family and contains the highest sequence similarity to APC2. When tested by the two-hybrid assay, APC11, but not ROC1 or ROC2, interacted with mouse APC2 (Figure 3E). Consistent with this data, APC2 and APC11 were reciprocally detected in APC11 and APC2 immunocomplexes, respectively, in Saos-2 cells detected by [³⁵S]IP following transfection (data not shown, and see below; Figure 5B).

Yeast Roc1p Interacts with the Yeast CDC53/Cullin Family
The yeast genome contains a single ROC gene, ScROC1 (ORF YOL133w), providing a simpler system to determine the in vivo function of ROC family proteins. We determined whether the yeast ROC/APC11 family also could directly interact with the yeast cullin/CDC53 family proteins by the yeast two-hybrid assay. The yeast genome contains four cullin members, CDC53, CUL-B (ORF YGR003w), CUL-C (ORF YJL047c), and APC2. ScROC1 interacted with all four yeast cullin genes including the most distantly related APC2. In contrast,

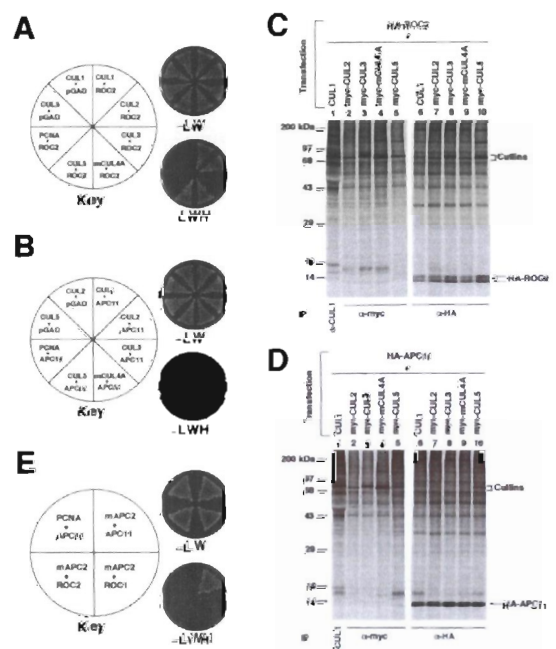


Figure 3. ROC2 and APC11 Selectively Interact with Cullins and APC2
(A and B) HF7c yeast cells were cotransformed with plasmids expressing human ROC2 or human APC11 and various cullins. pGBT8-PCNA and pGAD vector plasmid were included as negative controls. Protein-protein interactions were determined by the yeast two-hybrid assay as described in Figure 1A.
(C and D) Interaction between ROC2, APC11, and cullin family proteins in mammalian cells. Transfection followed by [³⁵S]IP was performed as described in Figure 1C.
(E) Selective interaction between APC2 and ROC or APC11. HF7c yeast cells were cotransformed with plasmids expressing indicated proteins (key). Protein-protein interaction was determined by the yeast two-hybrid assay using selective medium lacking histidine (-LWH) supplemented with 5 mM 3-AT to suppress the low transactivating activity of GAL4⁶⁰-APC2 fusion protein.

ScAPC11 only interacted weakly with CUL-C, but not CDC53 or CUL-B (Figure 4A). Interaction of ScAPC11 with ScAPC2 could not be tested because both are self-activating as baits. Hence, like human ROC proteins, yeast ROC1 also commonly interacts with all cullins.

Decrease of Roc1 Protein Causes a *cdc53-*, *cdc34-*, and *cdc4*-like Phenotype
We determined the consequence of deleting the ScROC1 gene by replacing it with a kanamycin resistance module by PCR homologous recombination. A 2:2 segregation was observed in 19/20 tetrads dissected on complete medium, and all of the viable colonies were kanamycin sensitive when replica plated onto selective medium. Upon microscopic inspection of the inviable spores, germination and a limited number of cell divisions to form microcolonies were observed reflecting a "maternal" supply of Roc1p (data not shown). Hence, ScROC1 is an essential gene for yeast viability.

We next created a conditional yeast strain in which

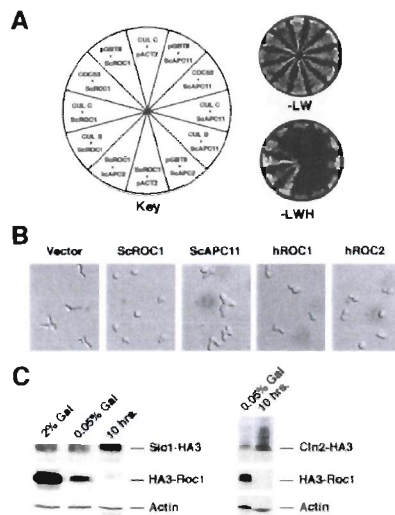


Figure 4. Function of ROC1 in Yeast

(A) ScRoc1p interacts with all yeast cullins. HF7c cells were cotransformed with plasmids expressing indicated proteins (Key). Protein-protein interactions were determined by the yeast two-hybrid assay as described in Figure 1(A).

(B) Human ROC1 and ROC2 can rescue the multibudded phenotype resulting from ScRoc1p depletion. His3MX6:P_{GAL}-HA3-ROC1 haploids were transformed with pADH-414 vector, pADH-ScROC1, pADH-ScAPC11, pADH-hROC1, or pADH-hROC2. Transformants were streaked onto selective plates containing 2% glucose and grown for 24 hr. Yeasts were formaldehyde fixed and sonicated before photography.

(C) Sic1p and Cln2p accumulate in yeast depleted of ScRoc1p. Haploid His3MX6:P_{GAL}-HA3-ROC1 SIC1-HA3:TRP1 and His3MX6:P_{GAL}-HA3-ROC1 CLN2-HA3:TRP1 yeast were grown in either 2% or 0.05% galactose plus 2% raffinose, or 2% glucose for 10 hr. Cell lysates were resolved on an SDS-PAGE gel, transferred to nitrocellulose, and blotted with anti-HA antibody to detect Sic1p-HA3, Cln2p-HA3, and HA3-Roc1p and with anti-actin antibody to verify equal protein loading.

ScROC1 was under the control of the galactose-inducible, glucose-repressible GAL1 promoter. Repression of ScROC1 by exposure to glucose caused the yeast to begin exhibiting a mutant phenotype at 9 hr and resulted in the accumulation of a multiply elongated budded yeast population with a single nucleus by 24 hr (Figure 4B and data not shown). This Roc1p depletion-induced phenotype is indistinguishable from those caused by temperature-sensitive mutations in the CDC53, CDC4, and CDC34 genes (Mathias et al., 1996). Taking advantage of this conditional phenotype, we determined the functional conservation and specificity of ROC family proteins. The multibudded phenotype incurred by Roc1p depletion can be completely rescued by the expression of yeast ROC1, but not vector control (Figure 4B), confirming that the level of Roc1p was the rate-limiting factor causing the multibudded phenotype. Ectopic expression of both human ROC1 and ROC2 also rescued the phenotype of ScRoc1p depletion. This indicates a functional conservation of the ROC gene family. Ectopic expression of yeast APC11, however, did not rescue the phenotype (Figure 4B) demonstrating a functional specificity between members of the ROC/APC11 family.

Roc1p Is Required for Sic1p and Cln2p Degradation

Phenotypic similarity between Roc1p depleted and cdc53 mutant cells and the interaction of ScROC1 with CDC53 prompted us to determine whether ScROC1 played a role in regulating protein degradation. Two critical substrates of the CDC53/SCF pathway are the G1 CDK inhibitor p40^{Sic1p} and the G1 cyclin Cln2p (Feldman et al., 1997; Skowyra et al., 1997). As such, we asked whether Sic1p and Cln2p were stabilized in yeast depleted of ScRoc1p as determined by Western blot analysis. We created two yeast strains in which either the SIC1 gene or the CLN2 gene was HA3 epitope tagged in a GAL-HA3-ScROC1 background. Yeast cells grown in a low concentration of galactose (0.05% plus 2% raffinose) expressed a reduced level of Roc1p but still exhibited a wild-type phenotype. After 10 hr of culturing in the presence of 2% glucose to deplete ScRoc1p, Sic1p and Cln2p accumulated (Figure 4C). Protein accumulation closely correlated with the appearance of multiple elongated buds. These results provide *in vivo* evidence that ROC1 functions in Ub-mediated proteolysis.

ROC1 and APC11 Complexes Contain Ub Ligase Activity

To test whether ROC1 immunocomplexes can function as Ub ligases, we immunoprecipitated ROC1 and CUL1 complexes from either 293T or HeLa cells and assayed for their ability to catalyze substrate independent Ub-Ub ligations (described in detail in Tan et al., 1999 [this issue of *Molecular Cell*]; Figure 5A). The ROC1 immunocomplex derived from both HeLa (lane 3) and 293T cells (lane 7) catalyzed the incorporation of ³²P-labeled Ub into a high molecular weight smear characteristic of an incremental Ub ladder in an E1- (lane 1) and E2- (lane 2) dependent manner. Inclusion of ROC1 antigen peptide in the ROC1 immunoprecipitation effectively blocked the ligase activity (lane 4), indicating that the polyubiquitination is catalyzed by the ROC1 immunocomplex. Similarly, the CUL1 complex also exhibited the Ub ligase activity (lane 6). Substitution of E2/CDC34 with E2/UbcH5c also supported ROC1-catalyzed Ub-Ub ligation (data not shown) and Ub-substrate ligation (see below), indicating that the ROC1 complex is capable of utilizing more than one E2 enzyme.

In contrast to ROC1, the anti-APC11 complex exhibited only background levels of ligase activity when similarly incubated with E1 and E2/CDC34 (Figure 5A, lane 5). A possible explanation is that ROC1 and APC11 selectively utilizes different E2s. To test this possibility, we substituted E2/CDC34 with UbcH5c, an isoform of E2/Ubc4 (97% identity), which was previously shown to be involved in ubiquitination of mitotic cyclin B by the APC (King et al., 1995). E2-UbcH5C supported Ub ligase activity of the α -APC11 immunocomplex (Figure 5B, lane 3). α -HA immunocomplexes derived from cells transfected with HA-APC11 and myc-APC2 (lane 6), but not with empty vector and myc-APC2 (lane 5), also exhibited high levels of Ub ligase activity. The immunocomplexes associated with the ligase activity predominantly contain HA-APC11 and myc-APC2 (compare lanes 7 and 8). These results demonstrate that ROC1/APC11 proteins play a role in the activity capable of linking together two Ub molecules by an isopeptide bond to form polyubiquitin chains.

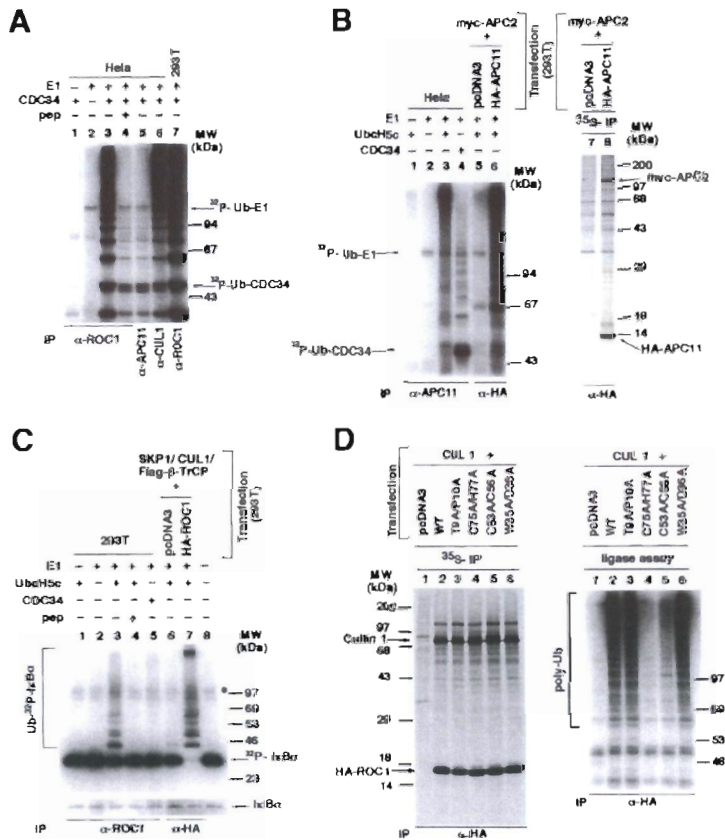


Figure 5. ROC1 and APC11 Constitute Ub Ligases with Cullin 1 and APC2

(A) Ub ligase activity of ROC1. Lysates (2 mg) from HeLa or 293T cells were immunoprecipitated with 2 μ g of antibodies to either ROC1, APC11, or CUL1 as indicated. Immunocomplexes immobilized on the beads were washed and then mixed with purified E1, E2/CDC34 (unless otherwise indicated), 32 P-labeled Ub, and ATP. After incubation, the reactions were terminated by boiling the sample in Laemmli loading buffer and resolved by SDS-PAGE.

(B) Ub ligase activity of APC11. Lysates from untransfected HeLa or transfected 293T cells were immunoprecipitated with indicated antibodies. Ub ligase activity was assayed with either E2/CDC34 or E2/UbcH5C as described in (A). In vivo association of transfected APC11 and APC2 was confirmed by [35 S]IP (lanes 7 and 8).

(C) In vitro ubiquitination of I κ B α by ROC1 ligase. Purified I κ B α was phosphorylated with IKK β and incubated with ROC1 immunocomplexes derived from untransfected or transfected 293T cells as indicated. Lane 8 represents a total input of the phosphorylated substrate I κ B α used in each reaction. The faint band (denoted by an asterisk) may correspond to the autophosphorylated form of IKK β . After autoradiography, the gel was stained with Coomassie blue to visualize I κ B α (bottom panel).

(D) Protein complex formation and ligase activity of mutant ROC1. Two sets of 293T cells were cotransfected in parallel with a CUL1 expressing plasmid with either vector control or a plasmid expressing wild-type or mutant ROC1 as indicated. Thirty-six hours after

transfection, one set of cells was pulse labeled with [35 S]Met for 2 hr, lysed, and immunoprecipitated with HA antibody, and resolved by SDS-PAGE. The second set of transfected cells were lysed and immunoprecipitated with HA antibody under the same lysis and wash conditions and subjected to the Ub ligase activity assay.

Discovery of the Ub-Ub ligation catalyzed by α -Roc1 and α -APC11 immunocomplexes prompted us to determine whether they can also catalyze Ub-substrate ligations. We chose I κ B α , an inhibitor of the NF- κ B transcription factor, for this study, as it was recently reported that signal-induced phosphorylation of I κ B α targets it for ubiquitination by cullin 1, SKP1, and the F box protein, β -TrCP (Yaron et al., 1998; Spencer et al., 1999; Winston et al., 1999). Incubation of the ROC1 complex immunoprecipitated from 293T cells with IKK β -phosphorylated, 32 P-labeled I κ B α resulted in an evident accumulation of a high molecular weight species (Figure 5C). Addition of a competing ROC1 antigen peptide reduced the I κ B α ubiquitination to background levels (lane 4), confirming that I κ B α ubiquitination is ROC1 dependent. Ubiquitination of I κ B α by ROC1 is dependent on E1 (lane 1) and E2/UbcH5C (lane 2), and substitution of UbcH5C with CDC34 failed to catalyze I κ B α ubiquitination (lane 5). Compared with ROC1 complexes derived from untransfected cells (lane 3), a much higher level of ligase activity toward I κ B α was obtained with HA immunocomplexes derived from HA-ROC1/CUL1/SKP1/ β -TrCP transfected cells (lane 7). Note that all of the phosphorylated I κ B α was converted into a high molecular weight ubiquitinated form. Coomassie blue staining of the gel after

autoradiography showed that equal amounts of I κ B α protein remained ubiquitinated after incubation with the ROC1 complex (Figure 5C, lane 7, bottom). This indicates that only the phosphorylated form of I κ B α was ubiquitinated by the ROC1 complex.

ROC1 Is an Essential Subunit for Ligase Activity

Demonstration of ROC1-, CUL1-, and APC11-associated Ub ligase activities led us to seek direct evidence that ROC1 is an essential subunit for ligation. We mutated several amino acid residues that are highly conserved between members of the ROC family from different species (Figure 2C). HA-tagged wild-type or mutant ROC1 was cotransfected in parallel with a CUL1 into two sets of 293T cells. While one set was employed for [35 S]IP analysis, the other set was analyzed for Ub ligase activity (Figure 5D). There is no detectable difference in the ROC1-CUL1 associated proteins between wild-type and the four mutant ROC1 complexes (Figure 5D, left panel). While double mutations of T9A/P10A (Figure 5D, right panel, lane 3) and W35A/D36A (lane 6) had no detectable effect on the ligase activity of ROC1, mutation of C53A/C56A dramatically reduced ROC1-associated ligase activity (lane 5), and mutation of C75A/H77A reduced the associated ligase activity to background levels (lane 4).

These results demonstrate that ROC1 is an essential subunit for the observed ligase activity.

Discussion

We have described an E3 ligase activity associated with a novel family of RING finger proteins, ROC/APC11, which complex with cullins to potentially constitute a large number of E3 Ub ligases. The detailed biochemical role the ROC/APC11 family plays in ubiquitination remains to be determined. Nonetheless, the presented experimental evidence supports the notion that ROC family proteins function as essential subunits of the ligase by forming heterodimers with cullins. ROC1 was shown to be an essential gene in yeast whose protein depletion caused an elongated, multibudded phenotype and concomitant accumulation of Sic1p and Cln2p (Figure 4). More convincingly, mutations in ROC1 completely abolished the associated ligase activity without a detectable alteration in the composition of ROC1-CUL1-associated proteins (Figure 5). Thus, strong evidence demonstrates that ROC1 is an essential subunit of the ligase. Though we have not definitively proven a cullin dependency for ROC1 associated ligase activity, it is likely that the cullin subunit is an obligate partner. We have demonstrated that ROC1 and ROC2 interact directly with cullins with a very high affinity, for both mammalian and yeast counterparts (Figures 1 and 4). Reinforcing this direct interaction is the *in vivo* association of a cullin-related protein, APC2, and a ROC protein, APC11 (Zachariae et al., 1998; Yu et al., 1998) (Figures 1 and 5B). Furthermore, in coupled transfection/ligase assays, CUL1 and ROC1 are the two predominant polypeptides in the ROC1 ligase complex. A critical issue that remains to be determined is whether the heterodimeric ROC/APC11-cullin complexes themselves contain intrinsic ubiquitin ligase activity or whether ROC/APC11 proteins act to bring the E2 and the cullins into close proximity for E2-mediated Ub-substrates ligations.

Discovery of ROC1 and APC11 as essential subunits for Ub ligation provides a clearer view of the ubiquitination pathway. In the case of the APC, identification of APC11 as a potential ligase subunit should help to determine how it is activated, inhibited, and targeted by other APC subunits. For the SCF complex, which consists of SKP1, CDC53/cullin 1, and an F box protein, it is now clear that SKP1 and the F box proteins are involved in substrate targeting. It should be pointed out that whether the SCF model can be generally applied to other cullins remains to be determined. Only cullin 1 interacts with SKP1 to be targeted by an F box protein to the substrate (Michel and Xiong, 1998), and whether higher eukaryotes contain additional SKP1-like cullin-interacting molecules is not clear. Conversely, cullin 1 and ROC1 are most likely required for ligase activity. Unlike SKP1, ROC1 and ROC2 interact commonly with all cullins that we have examined in both mammalian and yeast cells (Figures 1, 3, and 4). Hence, ROC1 and ROC2 are not just components of the SCF but essential subunits of all cullin-associated ubiquitination activities. Finally, both ROC/APC11 and cullin/APC2 represent multigene families. Among more than a dozen subunits identified, ROC/APC11 and cullin/APC2 are the only two

proteins common to both the APC and the SCF complexes. The variety of combinations that the ROC/APC11 family can form with different cullins point to a potentially large number of Ub ligases, and each may be involved in a specific cellular pathway as exemplified by the function of APC11-APC2 in mitosis, ROC1-CDC53 in yeast G1 control and ROC1-cullin 1 in NF- κ B/I κ B α -mediated transcriptional regulation.

Experimental Procedures

Plasmids Constructs

Mouse cullin 4A cDNA was described (Michel and Xiong, 1998). Human ROC2 and APC11 cDNAs were isolated by PCR amplification from a HeLa cDNA library and confirmed by DNA sequencing. The mouse APC2 EST cDNA clone (W13204) was used. ROC1 mutations were introduced by site-directed mutagenesis using Quick-Change kit (Stratagene) and verified by DNA sequencing.

Yeast cDNA sequences were amplified by PCR using lyticase-treated YEF473 genomic DNA and verified by DNA sequencing. CUL B, CUL C, and ScAPC2 were PCR amplified using the long template Expand kit (Boehringer Mannheim) following manufacturer's instructions. p414-ADH vector (CEN) was used for yeast rescue experiments. pcDNA3 (Invitrogen) was used for expression in mammalian cells. pGBT8, pGAD-GH, and pACT2 vectors were used for the yeast two-hybrid experiments.

Cell Culture

HeLa, Saos-2, and 293T were cultured in DMEM (10% FBS) in a 37 C incubator with 5% CO₂. Cell transfections were carried out using the LipofectAMINE reagent according to the manufacturer's instructions (GIBCO-BRL) or calcium-phosphate buffer (for 293T cells). For each transfection, 5 or 15 μ g of total plasmid DNA were used for each 60 mm or 100 mm dish.

Antibodies

Procedures for [³⁵S]methionine metabolic labeling, immunoprecipitation, and immunoblotting have been described previously (Jenkins and Xiong, 1995). The sequence of synthetic peptides used in generating rabbit polyclonal antibodies are as follows: anti-human ROC1N (CMAAAMDVDTPSGTN, residues 1–14), anti-human ROC1C (CDNR EWEFQKYGH, residues 97–108), anti-human APC11 (CRQEWKFKF, residues 76–84), anti-human CUL2 (CRSQASADEYSYVA, residues 733–745). Antibodies to human CUL1 and SKP1 were previously described (Michel and Xiong, 1998). Monoclonal α -HA (12CA5, Boehringer-Mannheim) and α -myc (9E10, NeoMarker) antibodies were purchased commercially. Antibody to yeast actin was provided by Dr. J. Pringle. Coupled *in vitro* transcription and translation reactions were performed using the TNT kit following the manufacturer's instructions (Promega).

Yeast

All *S. cerevisiae* strains were derived from YEF473 (*a/* α *ura3-52/ura3-52 his3 Δ -200/his3 Δ -200 trp1 Δ -63/trp1 Δ -63 leu2 Δ -1/leu2 Δ -1 lys2-801/lys2-801*). Yeast were cultured per standard protocol (Guthrie and Fink, 1991). The procedure followed for lysing and immunoblotting has been described previously (Lamb et al., 1994). Yeast were fixed in 3.7% formaldehyde for 1 hr at 30°C, sonicated, and washed in 1 \times PBS.

Yeast strains were constructed using PCR-based gene deletion and modification by homologous recombination (Longtine et al., 1998). Primers for PCR products contained 40 bp of sequence homologous to the gene-specific sequence and 20 bp homologous to the vector template. PCR was performed using the Expand Long Template PCR System (Boehringer Mannheim) as described (Longtine et al., 1998). PCR products were transformed into diploid YEF473 yeast (to construct strains JM1 and JM5, see below) or into the haploid strain JM5 (to construct strain JM7 and JM8, see below)

using a standard protocol. To identify transformants that had integrated by homologous recombination, PCR was performed on genomic DNA. JM1: ROC1/roc1:kanMX6; JM5: ROC1/His3MX6:P_{-GAL}-HA3-ROC1; JM7: MATa His3MX6:P_{-GAL}-HA3-ROC1 SIC1-HA3:TRP1; JM8: MATa His3MX6:P_{-GAL}-HA3-ROC1 CLN2-HA3:TRP1.

Ub Ligase Activity Assay

Human E1 was purified from HeLa cells as described (Hershko et al., 1983). Mouse E2/CDC34 was purified from insect cells infected with a mouse CDC34 expressing baculovirus, and human E2/UbcH5C were expressed in bacteria and purified using nickel beads (QIAGEN). Ub was prepared by subcloning full-length Ub as a fusion protein with a protein kinase C recognition site (LRRASV) and purified with nickel beads. Purified Ub was labeled with [³²P] by incubating with [^γ-³²P]ATP and cAMP kinase (Sigma) at 37°C for 30 min. For ubiquitination assays, immunocomplexes immobilized on protein A agarose beads were washed and added to an Ub ligation reaction mixture (30 μl) that contained 50 mM Tris-HCl (pH 7.4), 5 mM MgCl₂, 2 mM NaF, 10 mM Okadaic Acid, 2 mM ATP, 0.6 mM DTT, 0.75 μg [³²P]Ub, 60 ng E1, and 300 ng E2 protein. Reactions were incubated at 37°C for 60 min. For the IκBα ubiquitination assay, 8 μg of purified GST-IκBα (residues 1–54) were phosphorylated with 0.05 μg of IKKβ in the presence of 4 μCi of [^γ-³²P]ATP by incubating the reaction at 30°C for 30 min in a total volume of 40 μl of kinase buffer (20 mM HEPES [pH 7.7], 2 mM MgCl₂, 2 mM MnCl₂, 10 μM ATP, 10 mM β-glycerophosphate, 10 mM NaF, 10 mM PNPP, 300 μM Na₂VO₄, and 1 mM DTT). Ubiquitination of ³²P-labeled GST-IκBα was performed as described above, except that 1 μg of ³²P-labeled GST-IκBα and 12 μg of unlabeled purified bovine Ub (Sigma) were used in place of [³²P]Ub.

Acknowledgments

We are grateful to John Pringle and Mark Longtine for help with the yeast studies, Yiron Ben-Neriah for providing the mouse β-TrCP cDNA, Bob Duronio for critical reading of the manuscript, Mike Tyers and Wade Harper for providing reagents, and Zhen-Qiang Pan for advice on the ubiquitination assay and discussion throughout this study. T. O. is supported in part by the First Department of Surgery, St. Marianna University School of Medicine. J. J. M. is supported by a United States Department of Defense predoctoral fellowship. A. J. S. is a recipient of a Research Fellowship Award of the Crohn's and Colitis Foundation of America. Y. X. is a recipient of American Cancer Society Junior Faculty Award and a Pew Scholar in Biomedical Science. This study was supported by Public Health Service grants CA65572 and CA68377 to Y. X.

Received September 18, 1998; revised March 26, 1999.

References

Borden, K.L., and Freemont, P.S. (1996). The RING finger domain: a recent example of a sequence-structure family. *Curr. Opin. Struct. Biol.* **6**, 395–401.

Feldman, R.M.R., Correll, C.C., Kaplan, K.B., and Deshaies, R.J. (1997). A complex of Cdc4p, Skp1p, and Cdc53p/cullin catalyzes ubiquitination of the phosphorylated CDK inhibitor Sic1p. *Cell* **91**, 221–230.

Glotzer, M., Murray, A.W., and Kirschner, M.W. (1991). Cyclin is degraded by the ubiquitin pathway. *Nature* **349**, 132–138.

Guthrie, C., and Fink, G.R., eds. (1991). *Methods in Enzymology*, Volume 194 (San Diego, CA: Academic Press, Inc.), pp. 273–281.

Hershko, A. (1997). Role of ubiquitin-mediated proteolysis in cell cycle control. *Curr. Opin. Cell Biol.* **9**, 788–799.

Hershko, A., Heller, H., Elias, S., and Ciechanover, A. (1983). Components of ubiquitin-protein ligase system. Resolution, affinity purification, and role in protein breakdown. *J. Biol. Chem.* **258**, 8206–8214.

Hochstrasser, M. (1996). Ubiquitin-dependent protein degradation. *Annu. Rev. Genet.* **30**, 405–439.

Hoyt, M.A. (1997). Eliminating all obstacles: regulated proteolysis in the eukaryotic cell cycle. *Cell* **91**, 149–151.

Jenkins, C.W., and Xiong, Y. (1995). Immunoprecipitation and immunoblotting in cell cycle studies. In *Cell Cycle: Materials and Methods*. M. Pagano, ed. (New York: Springer-Verlag), pp. 250–263.

King, R., Peters, J., Tugendreich, S., Rolfe, M., Hieter, P., and Kirschner, M. (1995). A 20S complex containing cdc27 and cdc16 catalyzes the mitosis-specific conjugation of ubiquitin to cyclin B. *Cell* **81**, 279–288.

King, R.W., Deshaies, R.J., Peters, J.-M., and Kirschner, M.W. (1996). How proteolysis drives the cell cycle. *Science* **274**, 1652–1659.

Lamb, J.R., Michaud, W.A., Sikorski, R.S., and Hieter, P.A. (1994). Cdc16p, Cdc23p and Cdc27p form a complex essential for mitosis. *EMBO J.* **13**, 4321–4328.

Longtine, M.S., McKenzie, A., DeMarini, D.J., Shah, N.G., Wach, A., Brachat, A., Philippsen, P., and Pringle, J.R. (1998). Additional modules for versatile and economical PCR-based gene deletion and modification in *Saccharomyces cerevisiae*. *Yeast* **14**, 953–961.

Mathias, N., Johnson, S.J., Winey, M., Adams, A.E.M., Goetsch, L., Pringle, J.R., Byers, B., and Gobel, M.G. (1996). Cdc53p acts in concert with cdc4p and cdc34p to control the G1-to-S phase transition and identifies a conserved family of proteins. *Mol. Cell Biol.* **16**, 6634–6643.

Michel, J., and Xiong, Y. (1998). Human CUL-1, but not other cullin family members, selectively interacts with SKP1 to form a complex with SKP2 and cyclin A. *Cell Growth Differ.* **9**, 439–445.

Skowyra, D., Craig, K., Tyers, M., Elledge, S.J., and Harper, J.W. (1997). F box proteins are receptors that recruit phosphorylated substrates to the SCF ubiquitin-ligase complex. *Cell* **91**, 209–219.

Spencer, E., Jiang, J., and Chen, Z.J. (1999). Signal-induced ubiquitination of IκBα by the F box protein Slimb/β-TrCP. *Genes Dev.* **13**, 284–294.

Tan, P., Fuchs, S.Y., Chen, A., Wu, K., Gomez, C., Ronai, Z., and Pan, Z.-Q. (1999). Recruitment of a ROC1–CUL1 ubiquitin ligase by Skp1 and HOS to catalyze the ubiquitination of IκBα. *Mol. Cell* **3**, this issue, 527–533.

Winston, J.T., Strack, P., Beer-Romero, P., Chu, C.Y., Elledge, S.J., and Harper, J.W. (1999). The SCF^{F^{TRCP}}-ubiquitin ligase complex associates specifically with phosphorylated destruction motifs in IκBα and β-catenin and stimulates IκBα ubiquitination in vitro. *Genes Dev.* **13**, 270–283.

Yaron, A., Hatzubai, A., Davis, M., Lavon, I., Amit, S., Manning, A.M., Andersen, J.S., Mann, M., Mercurio, F., and Ben-Neriah, Y. (1998). Identification of the receptor component of the IκBα-ubiquitin ligase. *Nature* **396**, 590–594.

Yu, H., Peters, J.-M., King, R.W., Page, A.M., Hieter, P., and Kirschner, M.W. (1998). Identification of a cullin homology region in a subunit of the anaphase-promoting complex. *Science* **279**, 1219–1222.

Zachariae, W., Shevchenko, A., Andrews, P.D., Ciosk, R., Galova, M., Stark, M.J.R., Mann, M., and Nasmyth, K. (1998). Mass spectrometric analysis of the anaphase-promoting complex from yeast: identification of a subunit related to cullins. *Science* **279**, 1216–1219.

GenBank Accession Numbers

ROC1 (AF142059) and ROC2 (AF142060) sequences have been deposited into the GenBank database.

Higher Expression of Glucocorticoid Receptor in Peripheral Mononuclear Cells in Inflammatory Bowel Disease

Arndt Schottelius, Dr. med., Susanne Wedel, Dr. med., Renita Weltrich, Wolfgang Rohde, Prof. Dr. med., Frank Buttgerit, Prof. Dr. med., Stefan Schreiber, Prof. Dr. med., and Herbert Lochs, Prof. Dr. med.

IV and III Medical Department of Medicine and Institute for Experimental Endocrinology, Charité University Medical Center, Berlin, Germany

OBJECTIVE: Glucocorticoids are widely used in the treatment of inflammatory bowel disease (IBD). Up- and down-regulated expression of glucocorticoid receptors (GR) has been reported for different chronic inflammatory diseases. The aim of this study was to investigate the expression of GR and their apparent dissociation constant (K_d) in patients with IBD.

METHODS: Thirty-nine patients with IBD (22 with ulcerative colitis, 17 with Crohn's disease) and 35 normal controls were studied. Twenty-five patients did not receive steroids, 14 patients were treated with steroids. Peripheral blood mononuclear cells from patients and controls were isolated using the Ficoll-Hypaque gradient and a whole cell [3 H]-dexamethasone binding assay and Scatchard plot analysis were performed to assess GR number and the apparent dissociation constant. Results were expressed as mean \pm standard deviation.

RESULTS: Normal controls showed an expression of 3969 ± 1555 GR per cell with an apparent dissociation constant of 6.16 ± 3.8 nmol/L. IBD patients without steroids had a significant increase both in the expression of GR per cell (6401 ± 2344 ; $p < 0.0001$; Wilcoxon-Mann-Whitney test) and in the apparent dissociation constant (11.02 ± 7.57 nmol/L; $p = 0.006$). Expression of GR in IBD patients was suppressed to normal levels under steroid treatment (4594 ± 2237 ; $p = 0.024$), but K_d remained elevated (13.56 ± 9.05 nmol/L). Plasma cortisol levels were not different between IBD patients and the control group.

CONCLUSIONS: Our data show a systemic increase in GR expression and a decrease in the affinity to the GR in IBD, in contrast to other inflammatory diseases such as rheumatoid arthritis and asthma. These changes point towards a systemic character of IBD, which might be considered in a decision between topical and systemic treatment. (Am J Gastroenterol 2000;95:1994–1999. © 2000 by Am. Coll. of Gastroenterology)

INTRODUCTION

Glucocorticoid receptors (GR) are ligand-dependent transcription factors that belong to a large family of related proteins (1). Glucocorticoid receptors can be localized in the cytoplasm of all body cells. The concentration of GR varies between different tissues and even within a given tissue; receptor levels may fluctuate with changes in the cell cycle (2), during aging (3), and in response to hormone exposure (4). It is well documented that a part of glucocorticoid action is mediated through high-affinity binding of steroids to the glucocorticoid receptor (5). Additionally, a non-receptor-mediated effect has been described. The magnitude of the biological effects of glucocorticoids is determined, among other factors, by the receptor density of the target cells and the receptor affinity of the glucocorticoid (6–11).

The expression of GR is regulated by endogenous as well as exogenous exposure to its cognate ligands (12–15). Homologous downregulation of GR has been described in inflammatory conditions as well as by chronic glucocorticoid stimulation *in vitro* (16–20). The ability of glucocorticoids to downregulate its own receptor has also been observed in *in vivo* studies on peripheral blood mononuclear cells (PBMC) (21). Interestingly, GR expression is also regulated by the presence of a variety of proinflammatory cytokines (22–25).

One of the main therapeutic effects of glucocorticoids is the downregulation of proinflammatory cytokines, which is mediated by several genomic mechanisms, involving the negative cross-talk to other transcription factors such as nuclear factor kappa B (NF- κ B) (26–33). As glucocorticoids are a major regulatory component of inflammation, the expression of GR plays a crucial role in the development and treatment of chronic inflammatory diseases. Consequently, several studies have elucidated the GR status in chronic inflammatory states such as rheumatoid arthritis (RA), asthma, and systemic lupus erythematosus (SLE). The PBMC of patients with RA have been shown to have markedly lower receptor density than those of healthy subjects (34). The mechanisms of GR downregulation, though, remain unclear and conflicting results exist in comparison to

other chronic inflammatory diseases such as asthma and SLE. Several studies have reported a decrease in GR number in steroid-resistant (SR) asthma without affecting receptor binding affinity (35–37), whereas other studies have found a significantly reduced GR affinity on PBMC from patients with SR asthma, which was associated with an increase in GR number when cells were incubated with a combination of IL-2 and IL-4 (22, 23). The importance of proinflammatory mediators and cytokines in the modulation of GR expression is backed up by *in vitro* studies that demonstrated an IL-1 β -, LPS-, and TNF- α -mediated increase of GR numbers with reduced binding affinity (K_d) (24, 25). In contrast to the observed GR downregulation in RA, studies in SLE have shown a significant upregulation of GR, with unchanged binding affinity (38).

Inflammatory bowel disease (IBD), in comparison to RA, asthma, or SLE is similarly characterized by chronic inflammation. The question has therefore been raised whether GR expression is also dysregulated in IBD. This would be of clinical importance, as glucocorticoids are the primary line of treatment in IBD and as a dysregulation of GR expression could interfere with sensitivity to steroid treatment. Although GR expression in IBD patients has been described earlier, results concerning the GR status from different groups have been variable. A recent study in a small number of patients with ulcerative colitis who had previously received steroid therapy demonstrated a significant increase in the number and affinity of GR in the steroid-resistant group of patients, whereas patients responding to steroid therapy had no change in their GR receptor status (39). In contrast, another study by Rogler *et al.* (40) described a lower systemic level of GR in corticosteroid-treated IBD patients compared to control subjects, whereas systemic levels in untreated IBD patients did not differ significantly from those in normal controls.

Moreover, a high percentage of Crohn's disease patients show steroid dependency and the underlying mechanisms have not been elucidated (41, 42). The aim of this study was therefore to investigate the GR expression in patients with IBD and to correlate GR expression with endogenous glucocorticoid levels. We further wanted to elucidate the effects of steroid treatment on GR expression in patients with IBD in comparison to healthy subjects.

MATERIALS AND METHODS

Patients and Control Subjects

Thirty-nine patients with IBD and 35 age-matched healthy controls were studied. Clinical data about the IBD patients is shown in Table 1. All patients had mildly to moderately active disease as indicated by a Crohn's Disease Activity Index (43) (CDAI) \geq 150 or by a Colitis Activity Index (44) (CAI) \geq 4. In 25 IBD patients measurements of GR expression were performed before the initiation of medical therapy. In the 14 patients receiving steroid treatment (10–60 mg prednisolone per day) measurements of GR

Table 1. Clinical Data of Patients*

	n	Steroids	
		Yes	No
Crohn's disease	17	7	10
Ulcerative colitis	22	7	15

* n = 39; m/f = 17/22.

were performed before daily steroid therapy. Blood samples were drawn between 8:00 and 12:00 AM after informed consent had been obtained. All experiments were performed in duplicate.

Preparation of PBMC

Peripheral blood mononuclear cells were prepared immediately after blood was obtained to avoid lymphocyte and receptor damage. PBMC were separated using the Ficoll-Hypaque centrifugation technique (45). In detail, 20 ml of blood was drawn into heparinized tubes. In LeucoSep tubes with a porous filter disc (Esquire, Zürich, Switzerland) the blood was diluted twofold with modified HBSS buffer (Hanks balanced salt solution [modified]; Sigma Diagnostics, St. Louis, MO; [pH 7.4], 0.04 mol/L HCl, 0.05 mol/L Tris-buffer, 0.27 mmol/L acetylsalicylic acid) and layered over Ficoll-Hypaque (Pharmacia, Uppsala, Sweden). Density gradient centrifugation was performed at 400 g for 20 min. The PBMC-enriched interphase was isolated and diluted with 30 ml of HBSS buffer. To remove endogenous cortisol, cells were incubated for 30 min at 37°C in a shaking waterbath, as previously described (2), and then centrifuged at 400 g for 8 min. The cell pellet was washed with 35 ml of HBSS buffer and the final pellet was resuspended in 3 ml HBSS buffer. The PBMC consisted of lymphocytes and between 5% and 20% monocytes, as determined by FACS analysis. Trypan blue staining revealed \geq 95% viable cells.

Determination of Receptor Density and Affinity

To 300 μ l of cell suspension containing approximately 1×10^6 PBMC, 200 μ l of 3 H-labeled dexamethasone (6.7 [3 H]; specific activity, 40–60 Ci/mmol; DuPont De Nemours, Brussels, Belgium), diluted in the same HBSS medium, was added. A Coulter counter was used in each experiment to determine exact cell numbers. Identical aliquots were incubated in the presence of 1000 times excess of unlabeled dexamethasone to determine nonspecific binding. Following an established procedure (2, 12, 15), five concentrations of tritiated dexamethasone (1.25–20 nmol/L) were used to achieve a complete binding curve. The incubations of all aliquots were performed at 37°C for 30 min, with continuous shaking. Incubations were stopped with 2 ml ice-cold phosphate-buffered saline (PBS). Samples were centrifuged at 800 g for 2 min and washed 3 times with 800 μ l PBS at 4°C. The final pellet was resuspended in 1.6 ml of PBS and transferred into 6 ml of liquid scintillation cocktail. All incubations were performed in duplicate. Radioactivity was measured for 3 min in a liquid scintillation counter (Model

Wallac 1410, Wallac Oy, Turku, Finland). The number of GR per cell was then calculated according to the method of Scatchard, using computer-assisted linear regression (46).

Cortisol Determination

The plasma cortisol concentrations were determined with commercially available ELISA kit (Synchron Enzyme Linked Immuno Sorbent Assay for Cortisol; elias Medizintechnik GmbH Freiburg, Germany). Plasma cortisol levels were compared to the normal plasma cortisol range of 140–665 nmol/L.

Statistical Analysis

The results of the GR number per cell and binding affinity are expressed as mean \pm SD. Statistical significance was assessed using the Wilcoxon-Mann-Whitney test (47). A $p < 0.05$ was considered statistically significant.

RESULTS

Glucocorticoid receptor numbers per cell of each patient or healthy control were determined in a whole-cell [^3H]-dexamethasone binding assay. We used five concentrations of triated dexamethasone to obtain a typical and complete binding curve for each normal control and IBD patient (Fig. 1). A single component of binding sites is indicated by the linearity of the Scatchard plot. To also determine the binding affinity of the glucocorticoid to its receptor, the apparent dissociation constant (K_d) was calculated for healthy controls and IBD patients.

The number of GR in PBMC of 35 healthy volunteers who served as normal controls was 3970 ± 1533 binding sites per cell. The apparent dissociation constant of the GR in the normal controls was 6.16 ± 3.8 nmol/L (Fig. 1). The 25 patients of the IBD group who were not taking exogenous steroids showed a significantly increased expression of 6401 ± 2344 GR per cell ($p < 0.0001$) and also had a significantly increased dissociation constant of 11.02 ± 7.57 nmol/L ($p = 0.006$), in comparison to controls (Fig. 2). This increased expression of GR in patients without steroid therapy in comparison to normal controls could be demonstrated in Crohn's disease ($n = 10$; 7409 ± 2766 ; $p = 0.0003$), as well as in ulcerative colitis ($n = 15$; 5729 ± 1657 ; $p = 0.0009$). There was no significant difference in GR numbers between untreated patients with Crohn's disease and ulcerative colitis ($p = 0.14$).

Because an increase in GR expression could also be caused by decreased plasma cortisol levels in an autoregulatory loop, we investigated endogenous plasma cortisol levels in patients who had not received exogenous steroids. Endogenous plasma cortisol levels were assessed in 22 IBD patients without steroid treatment and were not found to be decreased (Fig. 3). Whereas IBD patients showed a wide variation in their endogenous cortisol levels, all were within normal range (140–665 nmol/L). No correlation was seen

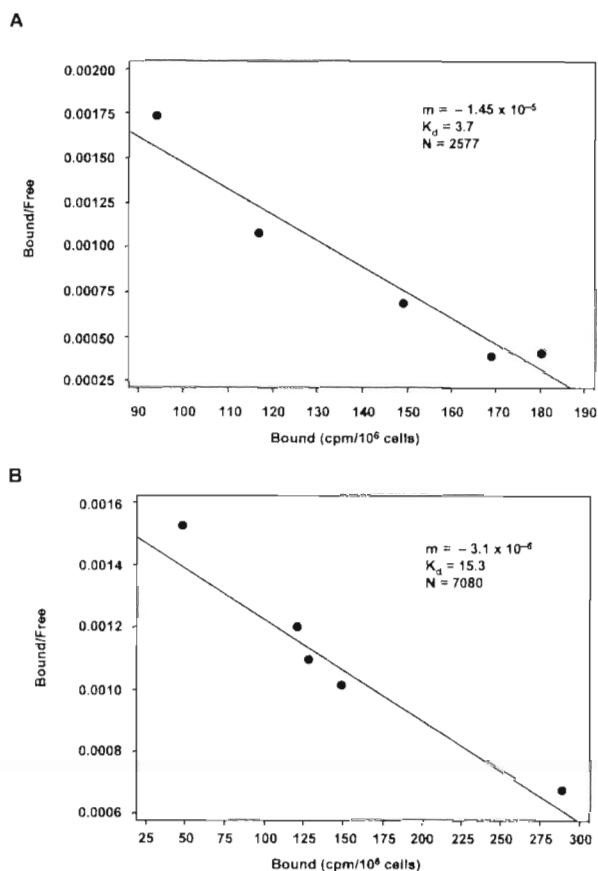


Figure 1. Scatchard analysis reveals specific binding of the glucocorticoid receptor. A single component of binding sites is indicated by the linearity of the Scatchard plot. Glucocorticoid receptor number per cell (N) is determined by the intercept of the x axis and is normalized for the number of cells. The dissociation constant (K_d) is determined by the reciprocal of the linear slope. (A) Scatchard plot of a binding assay performed with peripheral blood mononuclear cells of a normal control. (B) Scatchard plot of a binding assay performed with peripheral blood mononuclear cells of patient with Crohn's disease. m = slope; K_d = dissociation constant; N = number of binding sites per cell.

between glucocorticoid receptor number and plasma cortisol level (Fig. 3).

In comparison to nontreated patients, GR expression was significantly decreased ($n = 14$; 4594 ± 2237 ; $p = 0.024$) in the patients receiving steroid treatment (prednisolone 10–60 mg per day) (Fig. 1). In these patients GR levels were no longer different from those of normal controls ($p = 0.36$). In contrast, the apparent dissociation constant remained significantly raised in steroid-treated patients (13.56 ± 9.05 ; $p = 0.007$) when compared to normal controls.

A correlation between prednisolone dose and GR numbers could be detected in IBD patients taking steroid treatment (10 and 60 mg per day), with a decreasing expression of GR with higher doses of prednisolone (data not shown).

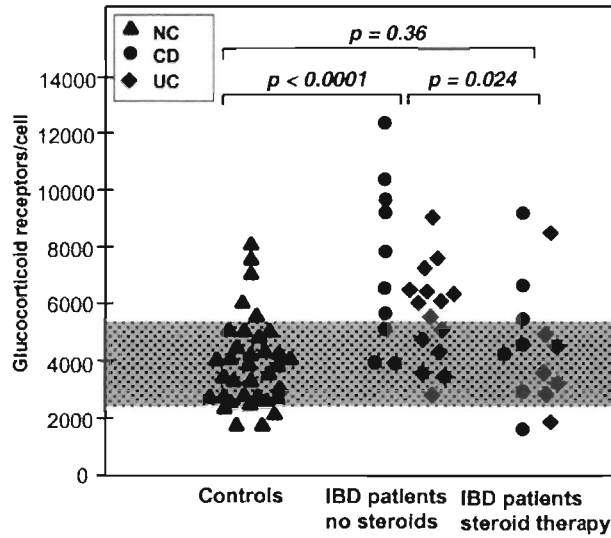


Figure 2. Number of glucocorticoid receptors (GR) per cell on peripheral mononuclear cells of patients with inflammatory bowel disease (IBD) without and with glucocorticoid therapy. The number of glucocorticoid receptors is significantly higher in IBD patients without steroid therapy, compared to control subjects ($p < 0.0001$). Expression of GR was suppressed to normal levels under steroid therapy ($p = 0.024$). The shaded area indicates normal levels of GR \pm SD as assessed in normal controls. (\blacktriangle = normal controls; \bullet = Crohn's disease; \blacklozenge = ulcerative colitis).

DISCUSSION

Our results clearly show an increased expression of GR in peripheral mononuclear cells of IBD patients with maintained regulation to steroid treatment. These findings support the view that IBD is a systemic disease with the involvement of peripheral immune cells (48). In the view of

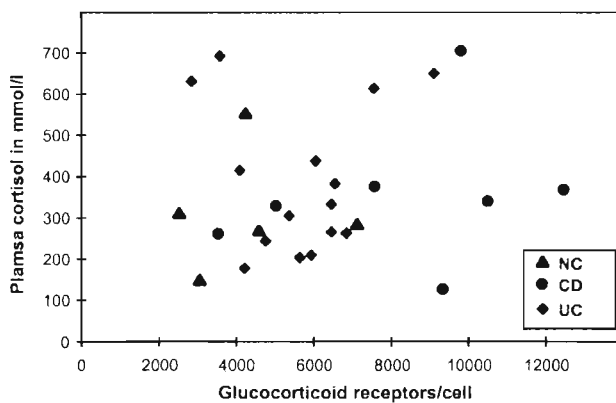


Figure 3. Levels of plasma cortisol measured in 22 patients with IBD without steroid therapy. Plasma cortisol levels were measured by ELISA. Cortisol levels were not found to be decreased as an explanation for the raised GR number per cell. Even though a wide variation between patients was found, all were within normal range (140–665 nmol/L). No correlation was seen between levels of plasma-cortisol and the number of glucocorticoid receptors per cell. (\blacktriangle = normal controls; \bullet = Crohn's disease; \blacklozenge = ulcerative colitis).

contradictory results concerning GR regulation in other chronic inflammatory diseases, the finding of the increased expression of GR needs to be discussed.

Increased production of proinflammatory cytokines including IL-1 β and TNF- α by mucosal lymphocytes and macrophages has been implicated in the pathogenesis of both Crohn's disease and ulcerative colitis (49–55). Recent studies have focused on the identification of signaling pathways and transcription factors that could control the enhanced proinflammatory cytokine gene transcription in IBD. New data suggest that the transcription factor NF- κ B plays a key role in the pathogenesis of chronic intestinal inflammation (56–59).

There is ample evidence for the mutual transrepression of the GR and NF- κ B by direct physical interaction between the GR and NF- κ B-p65 (26, 27). Moreover, inhibition of NF- κ B activity has been suggested to be a major component of the antiinflammatory properties of glucocorticoids by inducing transcription of the NF- κ B inhibitory molecule I κ B α (32, 33). As the negative cross-talk between NF- κ B and the GR is mutual (60), the status of GR expression may significantly alter NF- κ B activity and the NF- κ B status of a cell may significantly alter GR signaling and expression. It could be hypothesized that the increased expression of GR is a mechanism to counteract raised NF- κ B levels by enabling repression of NF- κ B through physical interaction of GR with NF- κ B-p65 and by mediating glucocorticoid-induced upregulation of the NF- κ B inhibitory molecule I κ B α .

Our findings are in concordance with reports of upregulated GR in systemic lupus erythematosus, and in inflammatory fibroblasts and PBMC of SR asthma patients when stimulated with proinflammatory cytokines (22–24, 38, 61). The contrast of our findings to reports of decreased GR numbers in RA and other studies with steroid-resistant asthma could be explained by distinct differences in the therapy of the patient groups (62, 63) or by different patterns of cytokines found in these diseases.

Furthermore, increased numbers of GR could also be explained by a decrease in endogenous glucocorticoid levels in patients with IBD. However, we could show that these levels were within the normal range and did not correlate with GR expression. Interestingly, the ability of exogenous steroids to decrease the numbers of GR was fully maintained in our patients and the extent of lowered GR numbers correlated well with the daily doses of prednisolone given.

An important finding was the increased K_d in IBD patients. As a high dissociation constant is a sign of low affinity of the glucocorticoid to its receptor, this could reflect reduced sensitivity of mononuclear cells to endogenous and exogenous steroids. The group of patients investigated were not corticosteroid resistant. However, our data are well in line with earlier results, demonstrating increased GR expression and increased dissociation constant in ulcerative colitis patients who were resistant to steroids (39). A high percentage of CD patients develop steroid dependency, which is of high clinical relevance (41, 42). Here we show

- receptors in peripheral leukocytes in asthmatic subjects. *Chung Hua Nei Ko Tsa Chih* 1994;33:150-3 (in Japanese).
38. Gladman DD, Urowitz MB, Doris F, et al. Glucocorticoid receptors in systemic lupus erythematosus. *J Rheumatol* 1991; 18:681-4.
 39. Shimada T, Hiwatashi N, Yamazaki H, et al. Relationship between glucocorticoid receptor and response to glucocorticoid therapy in ulcerative colitis. *Dis Colon Rectum* 1997; 40(suppl):S54-8.
 40. Rogler G, Meinel A, Lingauer A, et al. Glucocorticoid receptors are down-regulated in inflamed colonic mucosa but not in peripheral blood mononuclear cells from patients with inflammatory bowel disease. *Eur J Clin Invest* 1999;29:330-6.
 41. Munkholm P, Langholz E, Davidsen M, et al. Frequency of glucocorticoid resistance and dependency in Crohn's disease. *Gut* 1993;35:360-2.
 42. Reinisch W, Gasche C, Wyatt J, et al. Steroid dependency in Crohn's disease. *Lancet* 1995;345:859.
 43. Best W, Bechtel J, Singleton J, et al. Development of a Crohn's disease activity index. *Gastroenterology* 1976;70: 439-44.
 44. Rachmilewitz O. Coated mesosalazine versus sulphasalazine in the treatment of active ulcerative colitis: A randomized trial. *Br Med J* 1989;298:82-6.
 45. Boeyum A. Isolation of mononuclear cells and granulocytes from human blood. *Scand J Clin Lab Invest* 1968;(suppl 97):77-85.
 46. Scatchard G. The attractions of proteins by small molecules and ions. *Ann NY Acad Sci* 1949;51:660-72.
 47. Mann H, Whitney DR. On a test whether one of two random variables is stochastically larger than the other. *Ann Math Stat* 1947;18:50-60.
 48. Nikolaus S, Bauditz J, Gionchetti P, et al. Increased secretion of pro-inflammatory cytokines by circulating polymorphonuclear neutrophils and regulation by interleukin-10 during intestinal inflammation. *Gut* 1998;42:470-6.
 49. Strober W, Neurath M. Immunological diseases of the gastrointestinal tract. In: Rich R, ed. *Clinical immunology*. St. Louis: Mosby, 1995:28.
 50. Mahida Y, Wu K, Jewell D. Enhanced production of interleukin 1- β by mononuclear cells isolated from mucosa with active ulcerative colitis or Crohn's disease. *Gut* 1989;30: 835-8.
 51. Ligumsky M, Simon P, Karmeli F, et al. Role of interleukin 1 in inflammatory bowel disease: Enhanced production during active disease. *Gut* 1990;31:686-9.
 52. MacDonald T, Hutchings P, Choy M. Tumor necrosis factor alpha and interferon-gamma production measured at the single cell level in normal and inflamed human intestine. *Clin Exp Immunol* 1990;81:301-5.
 53. Stevens C, Walz G, Singaram C. Tumor necrosis factor- α , interleukin-1 β and interleukin 6 expression in inflammatory bowel disease. *Dig Dis Sci* 1992;37:818-26.
 54. Isaacs K, Sartor R, Haskill S. Cytokine messenger RNA profiles in inflammatory bowel disease mucosa detected by polymerase chain reaction amplification. *Gastroenterology* 1992; 103:1587-95.
 55. Reinecker H-C, Steffen M, Witthoef T. Enhanced secretion of tumor necrosis factor-alpha, IL-6, and IL-1 beta by isolated lamina propria mononuclear cells from patients with ulcerative colitis and Crohn's disease. *Clin Exp Immunol* 1993;94:174-81.
 56. Baldwin A. The NF- κ B and I κ B proteins: New discoveries and insights. *Annu Rev Immunol* 1996;14:649-81.
 57. Schreiber S, Nikolaus S, Hampe J. Activation of nuclear factor κ B in inflammatory bowel disease. *Gut* 1998;42:477-84.
 58. Neurath M, Peterson S, Meyer zum Büscherfelde K. Local administration of antisense phosphorothioate oligonucleotides to the p65 subunit of NF- κ B abrogates experimental colitis in mice. *Nat Med* 1996;2:998-1004.
 59. Schottelius AJG, Baldwin AS. A role for transcription factor NF- κ B in intestinal inflammation. *Int J Colorect Dis* 1999;14: 18-28.
 60. McKay LI, Cidlowski JA. Cross-talk between nuclear factor-kappa B and the steroid hormone receptors: Mechanisms of mutual antagonism. *Mol Endocrin* 1998;12:45-56.
 61. Damon M, Rabier M, Loubatiere J, et al. Glucocorticoid receptors in fibroblasts from synovial tissue. Changes during the inflammatory process. Preliminary results. *Agents Actions* 1986;17:478-83.
 62. Kopp E, Ghosh S. Inhibition of NF-kappa B by sodium salicylate and aspirin. *Science* 1994;265:956-9.
 63. Frantz B, O'Neill E. The effect of sodium salicylate and aspirin on NF-kappa B. *Science* 1995;270:2017-9.

that steroid treatment lowers GR expression in IBD with raised K_d levels remaining high as a sign of low affinity to the GR.

In summary, our data show changes in GR expression in IBD that are quite different from those in other chronic inflammatory diseases. The exact mechanisms involved in this GR dysregulation will have to be elucidated in future studies.

Reprint requests and correspondence: Arndt J. G. Schottelius, Dr. med., Schering AG, Müllerstrasse 178, D-13342 Berlin, Germany.

Received Oct. 22, 1999; accepted Feb. 22, 2000.

REFERENCES

- Evans RM. The steroid and thyroid hormone receptor superfamily. *Science* 1988;240:889-95.
- Cidlowski JA, Michaels GA. Alteration in glucocorticoid binding site number during the cell cycle in HeLa cells. *Nature* 1977;266:643-5.
- Chang WC, Roth GS. Changes in the mechanisms of steroid action during aging. *J Steroid Biochem* 1979;11:889-92.
- Cidlowski JA, Cidlowski NB. Glucocorticoid effects on HeLa S3 cell growth and thymidine incorporation. *Cancer Res* 1981; 41:2687-91.
- Barnes PJ, Adcock I. Anti-inflammatory actions of steroids: Molecular mechanisms. *Trends Pharmacol Sci* 1993;14:436-41.
- Pratt W. Glucocorticoid receptor and the initial events in signal transduction. In: Sato G, Stevens J, eds. *Molecular endocrinology and steroid hormone action*. New York: A.R. Liss, 1990:119.
- Truss M, Beato M. Steroid hormone receptors: Interaction with deoxyribonucleic acid and transcription factors. *Endocr Rev* 1993;14:459-79.
- Tsai BS, Watt G, Koesnadi K, et al. Lymphocyte glucocorticoid receptors in asthmatic and control subjects. *Clin Allergy* 1984;14:363-71.
- Bamberger C, Bamberger A, de Castro M, et al. Glucocorticoid receptor beta, a potential endogenous inhibitor of glucocorticoid action in humans. *J Clin Invest* 1995;95:2435-41.
- Müller M, Renkawitz R. The glucocorticoid receptor. *Biochem Biophys Acta* 1991;1088:171-8.
- Picard D, Yamamoto K. Two signals mediate hormone-dependent nuclear localization of the glucocorticoid receptor. *EMBO J* 1987;6:3333-40.
- Cidlowski JA, Cidlowski NB. Regulation of glucocorticoid receptors by glucocorticoids in cultured HeLa S3 cells. *Endocrinology* 1981;109:1975-82.
- Svec F, Rudis M. Glucocorticoids regulate the glucocorticoid receptor in the AtT20 cell. *J Biol Chem* 1981;256:5984-7.
- Danielsen M, Stallcup M. Down-regulation of the glucocorticoid receptor in mouse lymphoma cell variants. *Mol Cell Biol* 1984;4:449-53.
- Silva C, Powell-Oliver F, Cidlowski J. Regulation of the human glucocorticoid receptor by long-term and chronic treatment with glucocorticoids. *Steroids* 1994;59:436-42.
- Dong Y, Poellinger L, Gustafsson J, et al. Regulation of the glucocorticoid receptor expression: Evidence for transcriptional and posttranslational mechanisms. *Mol Endocrinol* 1988; 2:1256-64.
- Burnstein K, Jewell C, Cidlowski J. Human glucocorticoid receptor cDNA contains sequences sufficient for receptor down-regulation. *J Biol Chem* 1990;265:7284-91.
- Burnstein K, Bellingham D, Jewell C, et al. Autoregulation of glucocorticoid receptor gene expression. *Steroids* 1991;56: 52-8.
- Bellingham D, Sar M, Cidlowski J. Ligand-dependent down-regulation of stably transfected glucocorticoid receptors is associated with the loss of functional glucocorticoid responsiveness. *Mol Endocrinol* 1992;6:2090-102.
- Hoeck W, Rusconi S, Groner B. Down-regulation and phosphorylation of the glucocorticoid receptors in cultured cells. Investigations with a monospecific antiserum against a bacterially expressed receptor fragment. *J Biol Chem* 1989;264: 14396-402.
- Oshima H. Studies on the glucocorticoid receptor in human peripheral lymphocytes. II. Regulation by glucocorticoid. *Nippon Naibunpi Gakkai Zasshi* 1986;62:1298-305 (in Japanese).
- Kam J, Szeffler S, Surs W, et al. Combination IL-2 and IL-4 reduced glucocorticoid receptor-binding affinity and T cell response to glucocorticoids. *J Immunol* 1993;151:3460-6.
- Sher ER, Leung DY, Surs W, et al. Steroid-resistant asthma. Cellular mechanisms contributing to inadequate response to glucocorticoid therapy. *J Clin Invest* 1994;93:33-9.
- Verheggen M, van Hal P, Adriannsen-Soeting P, et al. Modulation of glucocorticoid receptor expression in human bronchial epithelial cell lines by IL-1 beta, TNF-alpha and LPS. *Eur Respir J* 1996;9:2036-43.
- Costas M, Kovalovsky D, Arzt E. Mechanisms of glucocorticoid sensitivity modulation by cytokines. *Medicina* 1997;57: 75-80.
- Drouin J, Sun YL, Chamberland M, et al. Novel glucocorticoid receptor complex with DNA element of the hormone-repressed POMC gene. *EMBO J* 1993;12:145-56.
- Scheinman RI, Gualberto A, Jewell CM, et al. Characterization of mechanisms involved in transrepression of NF-kappa B by activated glucocorticoid receptors. *Mol Cell Biol* 1995;15: 943-53.
- Schreck R, Baeuerle P. NF-kappa B as inducible transcriptional activator of the granulocyte-macrophage colony-stimulating factor gene. *Mol Cell Biol* 1990;10:1281-6.
- Shimizu H, Mitomo K, Watanabe T, et al. Involvement of NF-kappa B-like transcription factor in the activation of the interleukin-6 gene by inflammatory lymphokines. *Mol Cell Biol* 1990;10:561-8.
- Foletta VC, Segal DH, Cohen DR. Transcriptional regulation in the immune system: all roads lead to AP-1. *J Leukocyte Biol* 1998;63:139-52.
- Karin M, Liu Z, Zandi E. AP-1 function and regulation. *Curr Opin Cell Biol* 1997;9:240-6.
- Scheinman RI, Cogswell PC, Lofquist AK, et al. Role of transcriptional activation of I kappa B alpha in mediation of immunosuppression by glucocorticoids. *Science* 1995;270: 283-6.
- Auphan N, Di Donato J, Rosette C, et al. Immunosuppression by glucocorticoids: Inhibition of NF-kappa B activity through induction of I kappa B synthesis. *Science* 1995;270:286-90.
- Schlaghecke R, Kormely E, Wollenhaupt J, et al. Glucocorticoid receptors in rheumatoid arthritis. *Arthritis Rheum* 1992; 37:1127-31.
- Adcock IM, Lane SJ, Brown CR, et al. Abnormal glucocorticoid receptor-activator protein 1 interaction in steroid-resistant asthma. *J Exp Med* 1995;182:1951-8.
- Adcock IM, Lane SJ, Brown CR, et al. Differences in binding of glucocorticoid receptor to DNA in steroid-resistant asthma. *J Immunol* 1995;154:3500-5.
- Liu HG, Niu RJ, Hu DZ. The changes in glucocorticoid

Cellular Differentiation Causes a Selective Down-regulation of Interleukin (IL)-1 β -mediated NF- κ B Activation and IL-8 Gene Expression in Intestinal Epithelial Cells*

(Received for publication, April 12, 1999, and in revised form, December 16, 1999)

Ulrich Böcker \ddagger , Arndt Schottelius \S , Joanna M. Watson \S , Lisa Holt \ddagger , Laura L. Licato \ddagger , David A. Brenner \ddagger , R. Balfour Sartor \ddagger , and Christian Jobin \ddagger \parallel

From the \ddagger Center for Gastrointestinal Biology and Disease, Department of Medicine, \S Lineberger Comprehensive Cancer Center, University of North Carolina, Chapel Hill, North Carolina 27599-7080

Interleukin (IL)-1 β signals through various adapter proteins and kinases that lead to activation of numerous downstream targets, including the transcription factors including NF- κ B. In this study, we analyzed and characterized the effect of the differentiation of intestinal epithelial cells on IL-1 β -mediated NF- κ B activation and IL-8 gene expression. We report that IL-8 mRNA accumulation and protein secretion were down-regulated in IL-1 β - and lipopolysaccharide-stimulated differentiated HT-29 cells (HT-29/MTX, where MTX is methotrexate) compared with undifferentiated cells (HT-29/p), whereas no differential effects were found following tumor necrosis factor (TNF)- α or phorbol myristate acetate stimulation. Cross-linking and affinity binding studies reveal that IL-1 β exclusively binds the type I receptor (IL-1RI) and not IL-1RII in both HT-29/p and HT-29/MTX cells. IL-1 β -mediated I κ B kinase and c-Jun N-terminal kinase (JNK) activity were both diminished in differentiated HT-29 cells. DNA binding activity in differentiated HT-29 cells relative to HT-29/p cells was strongly reduced following IL-1 β exposure but not after TNF- α stimulation. The proximal IL-1 signaling molecule IL-1 receptor-associated kinase was not degraded in IL-1 β -stimulated HT-29 cells, in contrast to Caco-2 cells. κ B-luciferase reporter gene activity was 16-fold higher following TNF receptor-associated factor-6 transfection after IL-1 β stimulation in HT-29/MTX cells. We conclude that cellular differentiation of HT-29 cells selectively impairs the IL-1 β signaling pathway inhibiting both NF- κ B and JNK activity in response to IL-1 β . This relative unresponsiveness to IL-1 β may represent an important regulatory mechanism of differentiated intestinal epithelial cells.

The crypt-villus axis of the intestinal mucosa is composed of a dynamic cell population in perpetual transition from a proliferative, undifferentiated stage to mature surface villus epithelial cells. The migration from the crypt base to the surface of

the colon is accompanied by cellular differentiation that leads to important morphological and functional changes. Although several studies have shown that this process involves substantial changes of cellular morphology, growth, proliferation, and expression of biochemical markers (1, 2), little is known about the alteration of immunological functions during epithelial differentiation. It has been reported that spontaneous or sodium butyrate-induced epithelial cell differentiation inhibits IL-1 β -induced IL-8 gene expression in Caco-2 cells (3, 4). The molecular mechanism for this down-regulation is unclear. Moreover, the effect of epithelial cell differentiation on the NF- κ B signaling pathway is unknown. We have shown that cytokine-induced IL-8 gene expression in IEC requires activation of the transcription factor NF- κ B (5–8). Cytokine-induced NF- κ B activation is a complex phenomenon involving the participation of multiple coordinated kinases, some of them dedicated to a particular cytokine pathway. For example, following TNF- α stimulation, the TNF receptor-associated factor 2 (TRAF-2) and the adapter receptor-interacting protein are recruited to the cytoplasmic portion of TNF receptor 1 (TNFR-1) via the intermediate action of TNFR-1 receptor-associated death domain (9, 10). In contrast IL-1 β signaling requires coordinated participation of the IL-1 receptor accessory protein (IL-1RAcP), MyD88, and the IL-1 receptor-associated kinase (IRAK) which associates/activates TRAF-6 which in turn activates the TAK1 kinase (11–15). At this point both TRAF-2/receptor-interacting protein and TRAF-6/TAK1-transmitted signals converge upon either the NF- κ B-inducing kinase (NIK), which activates the IKK protein complex (16, 17) or the parallel stress-activated protein kinase/JNK pathway to activate the AP-1 transcription factor (18). NIK associates with TRAF-2 or TRAF-6 following TNF- α and IL-1 β stimulation, respectively, and is thought to be a cytokine-integrating signal dedicated to NF- κ B activation (18). NIK-activated IKK then phosphorylates I κ B α at serine residues 32 and 36 which triggers its ubiquitination/degradation with subsequent release of NF- κ B (19).

Exposure of HT-29 cells, which are transformed colonic epithelial cell line, to increasing doses of methotrexate results in the elimination of undifferentiated cells and favors the emergence of a stable differentiated epithelial cell population (20,

* This work was supported by a Career Development award (to C. J.), a Research Fellowship award (to A. S.) from the Crohn's and Colitis Foundation of America, National Institutes of Health ROI Grant DK 47700 (to R. B. S.), NIDDK Grant DK 34087 from the National Institutes of Health, and by the Deutsche Forschungsgemeinschaft Grants Bo 1340/1-1 and Bo 1340/2-1 (to U. B.). The costs of publication of this article were defrayed in part by the payment of page charges. This article must therefore be hereby marked "advertisement" in accordance with 18 U.S.C. Section 1734 solely to indicate this fact.

\parallel To whom correspondence should be addressed: Division of Digestive Diseases and Nutrition, 146 Glaxo Bldg., University of North Carolina, Chapel Hill, NC 27599-7080. Tel.: 919-966-7886; Fax: 919-966-7468; E-mail: Job@med.unc.edu.

¹ The abbreviations used are: IL, interleukin; IEC, intestinal epithelial cells; TNF, tumor necrosis factor; TRAF, TNF receptor-associated factor; TNFR, TNF receptor; IRAcP, IL-1 receptor accessory protein; icIL-1RA, intracellular IL-1R antagonist I; IRAK, IL-1 receptor-associated kinase; NIK, NF- κ B-inducing kinase; JNK, c-Jun N-terminal kinase; PMA, phorbol myristate acetate; LPS, lipopolysaccharide; GST, glutathione S-transferase; PAGE, polyacrylamide gel electrophoresis; PBS, phosphate-buffered saline; IKK, I κ B kinase; ELISA, enzyme-linked immunosorbent assays; MTX, methotrexate.

21). Many laboratories have used these cells to study the effect of cellular differentiation on epithelial cell gene regulation. In this study, we characterize the effect of cellular differentiation on the IL-1 β signaling pathway. We report that colonic cell differentiation is associated with a strong decrease of IL-1 β -mediated JNK and IKK activity that correlates with reduced NF- κ B DNA binding activity. However, TNF- α -mediated NF- κ B activity was unaffected by cellular differentiation. Similarly, IL-8 gene expression was strongly inhibited in IL-1 β - and LPS- but not in TNF- α - or PMA-stimulated differentiated cells, suggesting a selective effect of differentiation on IL-1 signaling pathway. The proximal IL-1 β kinase IRAK steady-state level was lower in differentiated compared with undifferentiated HT-29 cells and was not degraded following IL-1 β stimulation as opposed to the relatively undifferentiated Caco-2 cells. TRAF-6 overexpression triggered a strong increase in κ B-luciferase activity in HT-29/MTX. Therefore, IEC differentiation down-regulates the responsiveness of the IL-1 β signaling pathway downstream of IL-1R but upstream of NIK.

MATERIALS AND METHODS

Cell Culture and Treatment—The human colonic epithelial cells HT-29 (American Type Culture Collection, Manassas, VA; ATCC HTB 38), methotrexate-differentiated HT-29 cells (HT-29/MTX, provided by Dr. Lesuffleur, INSERM, Villejuif, France) (20), and Caco-2 cells were cultured as described previously (5). Cells were stimulated with human recombinant interleukin-1 β (R & D Systems, Minneapolis, MN), human recombinant TNF- α (R & D Systems), or phorbol myristate acetate (PMA; Sigma). Human recombinant intracellular IL-1R antagonist type I was a kind gift of Dr. S. Haskill (Lineberger Comprehensive Cancer Center, University of North Carolina, Chapel Hill). Polymorphonuclear cells were obtained and isolated from healthy volunteers as described previously (22). Polymorphonuclear and HT-29 cells were stimulated overnight with lipopolysaccharide (LPS; *Salmonella typhimurium* wild type, Ribi Immunochem, Hamilton, MT) at 100 ng/ml and 5 μ g/ml, respectively, or IL-1 β (2 ng/ml). For the IL-1 receptor type II (IL-1RII) blockade, cells were preincubated for 15 min with a monoclonal anti-IL-1RII antibody (10 μ g/ml; genzyme, Cambridge, MA). Cell viability before and after plating was >95% by trypan blue dye exclusion.

RNA Extraction and Northern Blot—RNA was isolated using Trizol® (Life Technologies, Inc.). Total RNA (5 μ g/lane) was electrophoresed through 1% agarose/formaldehyde gels and immobilized on Nytran nylon membrane (Schleicher & Schuell) by capillary action. Blots were prehybridized in 6 \times SSPE, 0.5% SDS, 5 \times Denhardt's solution, 200 μ g/ml single-stranded DNA, and 50% formamide at 42 $^{\circ}$ C for at least 2 h before the addition of the probe. cDNA probes for IL-8 and β -actin were radiolabeled with [³²P]dCTP by random priming as described previously (6). Blots were sequentially washed in 2 \times SSPE, 0.1% SDS for 30 min at room temperature and 42 $^{\circ}$ C and once in 0.2 \times SSPE, 0.1% SDS for 30 min at 56 $^{\circ}$ C. Blots were exposed to autoradiography film (XAR-5, Eastman Kodak, Co.) with intensifying screens at -70 $^{\circ}$ C for 1-5 days.

Nuclear Extracts and Electrophoretic Mobility Shift Assay—HT-29/MTX and HT-29 cells were stimulated for various times (0-90 min) with IL-1 β or TNF- α (both at 2 ng/ml), and then nuclear extracts were prepared as described previously (5). Extracts (5 μ g) were incubated with radiolabeled double-stranded class I major histocompatibility complex κ B sites (GGCTGGGATCCCCATCT), separated by nondenaturing electrophoresis and analyzed by autoradiography as described previously (5).

Whole Cell Extracts—Cells were plated (2 \times 10⁶ cells) in 100-mm dishes. At approximately 80% confluency, cells were stimulated with IL-1 β (2 ng/ml) for 0-20 min. The cells were scraped, washed with ice-cold PBS, and then lysed in Triton buffer (23) containing protease and phosphatase inhibitors (5). Lysates were rotated at 4 $^{\circ}$ C for 30 min and then cleared by centrifugation at 14,000 rpm, aliquoted, and stored at -80 $^{\circ}$ C. Protein concentrations were determined using the Bradford protein assay.

IKK Assay—IKK assay was performed as described previously (8). Briefly, the IKK complex was immunoprecipitated with a monoclonal anti-human IKK α antibody (PharMingen, San Diego, CA). Immunoprecipitates were incubated at 30 $^{\circ}$ C for 30 min in kinase reactions containing [γ -³²P]ATP (ICN Biochemicals, Inc., Costa Mesa, CA) and recombinant substrate GST-I κ B α (amino acid 1-54) immobilized on glutathione-agarose beads. Substrate protein was resolved by gel

electrophoresis, and phosphate incorporation was assessed by autoradiography and PhosphorImager analysis (Molecular Dynamics, Sunnyvale, CA).

JNK Assay—JNK activity was assessed in cells using an *in vitro* kinase assay as described previously (24). Recombinant GST-c-Jun protein (amino acids 1-79), containing the activation domain of c-Jun protein, was utilized as substrate. 25 μ g of whole cell extracts was incubated with 5 μ g of substrate protein linked to glutathione-Sepharose beads. After extensive washing of the complexes, the kinase reaction was performed with [γ -³²P]ATP (4500 Ci/mmol). The proteins were fractionated using 12.5% SDS-PAGE and visualized/quantitated by PhosphorImager analysis. Coomassie staining was used to demonstrate equal protein loading. A mutated GST-c-Jun (Ser-63 and Ser-73 substitution to Ala; GST-c-JunAA) was used as this substituted protein cannot be phosphorylated by colonic epithelial cells (25). Kinase assays were performed in duplicates using whole cell extracts from two independent experiments.

Western Blot Analysis—Cells were stimulated with IL-1 β (2 ng/ml) for 0-60 min. The cells were lysed in 1 \times Laemmli buffer, and 20 μ g of protein was electrophoresed on 10% SDS-polyacrylamide gels. Anti-IRAK (generous gift of Dr. D. K. Miller, Merck) diluted 1:5000, anti-IKK α (PharMingen) diluted 1:1000, or anti-I κ B α antibody (Santa Cruz Biotechnology; Santa Cruz, CA) were used to detect immunoreactive IRAK, IKK α or I κ B α , respectively, using the enhanced chemiluminescence light (ECL) detecting kit (Amersham Pharmacia Biotech) as described previously (5).

Transfections and Luciferase Reporter Assay—HT-29/MTX cells were transfected using LipofectAMINE Reagent (Life Technologies, Inc.) as described previously (5). The (κ B)₃-luciferase motif consists of three consensus NF- κ B sites linked to luciferase (26). Plasmids expressing TRAF-6 (2 μ g; generous gift of Dr. Jun-ichiro Inoue, University of Tokyo, Japan) or (κ B)₃-luciferase were transfected in combination or alone as described under "Results," and the total amount of DNA was equalized with empty vector. Transfected cells were incubated overnight after which the DNA/LipofectAMINE media were replaced with the serum-containing media and then the cells were incubated for an additional 12 h. Cells were treated with or without IL-1 β (2 ng/ml) for 12 h after which extracts were prepared using enhanced luciferase assay reagents (Analytical Luminescence, San Diego, CA). Luciferase assays were performed on a Monolight 2010 luminometer for 20 s (Analytical Luminescence, San Diego, CA), and results were normalized for extract protein concentrations measured with the Bio-Rad protein assay kit.

IL-1 Receptor-binding Assay—HT-29/p and HT-29/MTX cells were grown to confluency in 24-well plates. Cells were incubated with 10⁻¹¹ M [¹²⁵I]-IL-1 β (Amersham Pharmacia Biotech) alone or in the presence of a 500-1000-fold molar excess of unlabeled IL-1 β or TNF- α , respectively, for 3 h at 4 $^{\circ}$ C in CO₂-independent medium (Life Technologies, Inc.). Cells were washed three times in binding medium and once in 1 \times PBS, trypsinized, and then transferred to borosilicate tubes and counted for 1 min in a γ -counter. Cell viability and number was assessed by trypan blue staining.

Affinity Cross-linking—HT-29/p and HT-29/MTX cells were grown to confluency in 12-well plates. Cells were incubated with 10⁻¹⁰ M [¹²⁵I]-IL-1 β (Amersham Pharmacia Biotech) alone or in the presence of either 500-fold molar excess of unlabeled IL-1 β , 1000-fold molar excess anti-IL-1RI, or anti-IL-1RII antibodies for 4 h at room temperature in CO₂-independent medium (Life Technologies, Inc.) on an orbital shaker. Cells were washed three times with cold 1 \times PBS, and the cross-linking reagent bis(succinimidyl)suberate (1.3 mg/ml, Pierce) was added, and the cells were incubated for 1.5 h at room temperature as described above. The cells were washed twice with cold 1 \times PBS and then lysed in 1 \times Laemmli buffer. 40 μ g of protein was electrophoresed on 7% SDS-polyacrylamide gels and then visualized by autoradiography and by PhosphorImager analysis (Molecular Dynamics, Sunnyvale, CA).

IL-8 Enzyme-linked Immunosorbent Assay—Human IL-8 enzyme-linked immunosorbent assays (ELISA) of cell culture supernatants from HT-29 cells was performed in duplicate according to the manufacturer's specifications (R & D Systems).

RESULTS

Differentiation of Caco-2 cells has been reported to decrease IL-1 β -mediated IL-8 secretion (3, 4). We therefore investigated whether differentiation of HT-29 cells would lead to a similar alteration of IL-1 β responsiveness. The effect of cell differentiation on IL-8 gene expression was investigated using methotrexate-differentiated HT-29 cells (HT-29/MTX) and the undif-

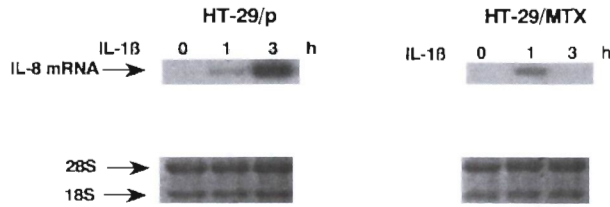


FIG. 1. Decreased IL-8 mRNA induction in IL-1 β -stimulated HT-29/MTX (differentiated) colonic epithelial cells compared with normal (HT-29/p) cells. HT-29/p and HT-29/MTX cells were stimulated with IL-1 β (2 ng/ml) for 0, 1, and 3 h. Total RNA was extracted and IL-8 expression analyzed by Northern blot as described under "Materials and Methods." Similar results were obtained in one other experiment.

differentiated parental HT-29 cells (HT-29/p) as contrasts. Cells were stimulated (1–3 h) with IL-1 β (2 ng/ml), and then IL-8 mRNA accumulation was determined by Northern blotting. As previously shown (5–8, 27), IL-1 β induced IL-8 mRNA accumulation in HT-29/p cells (Fig. 1). In contrast, this IL-1 β -mediated IL-8 induction was severely impaired in HT-29/MTX cells where maximal induction reached only 15% of the level found in HT-29/p and exhibited peak expression at 1 h rather than 3 h upon IL-1 β stimulation (Fig. 1). To define further the relative lack of IL-8 expression in differentiated cells, HT-29/p and HT-29/MTX cells were stimulated with various doses of IL-1 β (0.001–10 ng/ml), TNF- α (0.01–100 ng/ml), or PMA (0.01–100 ng/ml) for 12 h, then IL-8 concentration was assessed by ELISA in cell-free supernatants. TNF- α increased IL-8 secretion in both HT-29/MTX and HT-29/p cells in a dose-dependent manner with no marked difference in the response between the cell lines (Fig. 2A). IL-8 secretion was also stimulated by PMA in both HT-29/MTX and HT-29/p cells in a dose-dependent manner with a consistently higher response in HT-29/MTX cells at each dose of PMA (Fig. 2B). In accordance with the RNA results, IL-1 β -mediated IL-8 secretion was strongly reduced in HT-29/MTX compared with HT-29/p cells with a blunted dose response (Fig. 2C). These data demonstrate that HT-29/MTX cells have the capacity to produce high levels of IL-8 in response to certain stimuli. However, as described in Caco-2 cells (3, 4), cellular differentiation specifically inhibits IL-1 β -mediated IL-8 gene expression in HT-29 cells.

The IL-1 β signaling cascade is initiated by its binding to the IL-1 receptor type 1 (28). Both HT-29/p and HT-29/MTX cells express intracellular IL-1R antagonist I (icIL-1RA) protein that binds to the type I IL-1R with pure antagonistic activity (29, 30), with higher levels of icIL-1RA found in the differentiated compared with the parental cell line (29). We wanted to exclude the possibility that icIL-1RA I secreted into the supernatant caused the observed differences of IL-1 β -induced IL-8 secretion. Analysis of the cell-free supernatant after a culture period of 24 h revealed an icIL-1RA I concentration of less than 0.2 ng/ml for both cell lines (data not shown). However, IL-1 β -induced IL-8 secretion was inhibited (65%) only by much higher exogenous doses of icIL-1RA (10 ng/ml), with almost no inhibition by 1 ng/ml, which is over 5-fold more than measured levels of secreted icIL-1RA in our cells (Fig. 3). Furthermore, neutralization of IL-1RA by pretreatment of HT-29/p and HT-29/MTX cells with antiserum to IL-1RA did not enhance the IL-1 β -induced IL-8 secretion (data not shown). Finally, IL-1 β binding to its receptor was not blocked by cellular expression of icIL-1RA (see below).

Receptor-ligand interaction triggers the activation of various kinases that transmit cytokine-activated signals toward different effector molecules that ultimately modulate cellular gene expression. Because NF- κ B activation is critical in IL-1 β -mediated IL-8 expression in HT-29 cells (5–7, 31), we next deter-

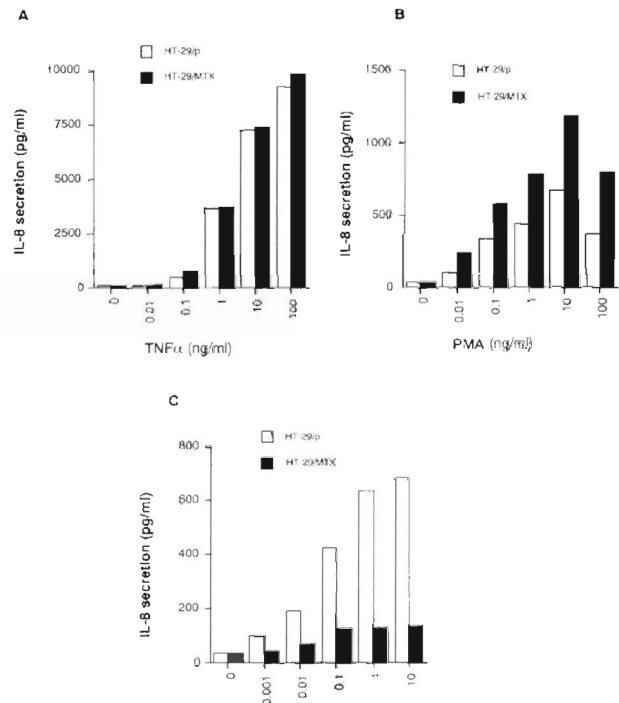


FIG. 2. Lack of IL-8 secretion in IL-1 β - but not PMA or TNF- α -stimulated HT-29/MTX cells. Undifferentiated parental HT-29 cells (HT-29/p) and methotrexate-differentiated HT-29 cells (HT-29/MTX 10^{-3}) were stimulated with various concentrations of TNF- α (A), PMA (B), or IL-1 β (C) for 12 h after which immunoreactive IL-8 concentrations were measured in cell supernatants using an ELISA technique. These results are expressed as means of triplicate determinations and are representative of three different experiments.

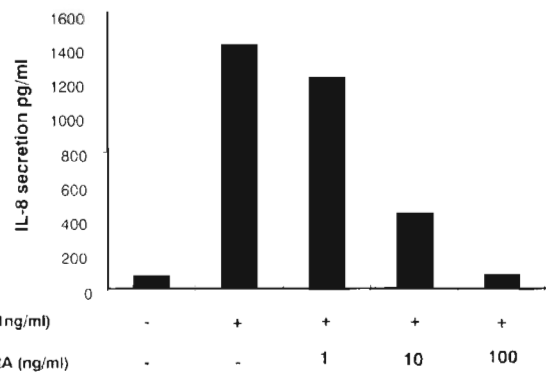


FIG. 3. IL-1 β stimulated IL-8 secretion of HT-29/p was dose-dependently inhibited by exogenous recombinant human intracellular IL-1 receptor antagonist (icIL-1RA). Increasing amounts of icIL-1RA (1, 10, and 100 ng/ml) were added to the cell media, and cells were stimulated with IL-1 β (2 ng/ml) for 12 h. Immunoreactive IL-8 concentrations were measured in cell supernatants using an ELISA technique. Data are presented as means of triplicate experiments. Two other experiments gave similar results.

mined the effect of cellular differentiation on the IL-1 β signaling cascade by dissecting the signaling cascade leading to NF- κ B activation. First, IL-1 β binding to its receptor was compared in differentiated and undifferentiated cells. Expression of IL-1 β receptors on the surface of HT-29/p and HT-29/MTX cells was demonstrated using a competitive ligand binding assay. Interestingly, 125 I-IL-1 β binding was higher in HT-29/MTX than HT-29/p (Fig. 4A), suggesting that impaired IL-8 secretion in HT-29/MTX was not due to absent or reduced IL-1 β binding. Binding of 125 I-IL-1 β was specific since a 1000-fold

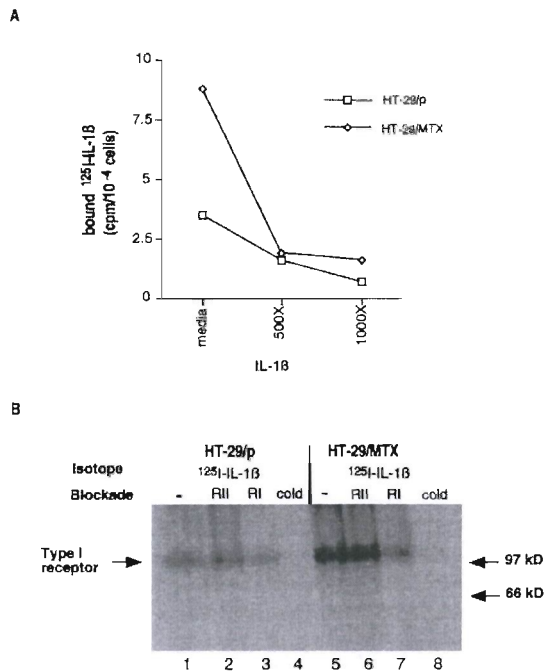


FIG. 4. A, IL-1 β binds to IL-1R in HT-29 cells. HT-29/p and HT-29/MTX cells were cultured to confluency and then incubated with ¹²⁵I-IL-1 β as described under "Materials and Methods." Specificity of IL-1R binding was confirmed by co-incubation with 500–1000-fold molar excess of unlabeled IL-1 β . Data are presented as means of triplicate experiments and are representative of two independent experiments. B, IL-1 β binds to the type I receptor in both HT-29/p and HT-29/MTX cells. Cells were cultured to confluency and then incubated with ¹²⁵I-IL-1 β (10⁻¹⁰ M) as described under "Materials and Methods." Specificity of IL-1R binding was confirmed by co-incubation with 500-fold molar excess of unlabeled IL-1 β (lanes 3 and 7) or 1000-fold molar excess of either anti-IL-1RI (lanes 3 and 7) or anti-IL-1RII (lanes 2 and 6) antibody. 20 μ g of protein were resolved on an 8% SDS-PAGE and exposed to a PhosphorImager screen.

excess of unlabeled IL-1 β reduced ¹²⁵I-IL-1 β binding by more than 80% in both cell lines (Fig. 4A). In contrast, unlabeled TNF- α did not significantly inhibit ¹²⁵I-IL-1 β binding in either cell line (data not shown).

IL-1RII has been shown to act as a decoy receptor for IL-1 cytokine (32–34) and could therefore be responsible for the decrease in HT-29/MTX IL-1 β responsiveness, despite the higher IL-1 β binding (Fig. 4A). However, an ¹²⁵I-IL-1 β cross-link affinity study revealed that IL-1 β exclusively binds the IL-1RI in both HT-29/p and HT-29/MTX cells (Fig. 4B, lanes 3 and 7). The binding of ¹²⁵I-IL-1 β was specific since either unlabeled IL-1 β or IL-1RI antibody reduced ¹²⁵I-IL-1 β binding in both cell lines with no effect of IL-1RII antibody (Fig. 4B, lanes 4 and 8). In addition, functional studies using a neutralizing monoclonal antibody against the IL-1RII demonstrated that IL-1 β -mediated IL-8 secretion is not augmented by IL-1R blockade in HT-29/MTX cells (Table I). In contrast, IL-8 secretion in response to IL-1 β , but not LPS, was increased 2-fold by blockade of IL-1RII in control PMN, a level similar to a previous report (34). IL-1 β -induced IL-8 secretion in HT-29/p also is unaffected by the blocking IL-1RII antibody (data not shown).

IRAK is a proximal kinase used by IL-1 β to transmit the signal to downstream targets. It has been shown that phosphorylated IRAK is rapidly degraded by the proteasome pathway following IL-1 β stimulation (35). We next compared IRAK steady-state levels in differentiated and undifferentiated cells following IL-1 β stimulation. HT-29/MTX, HT-29/p, and Caco-2 cells were stimulated with IL-1 β for 0–90 min, and IRAK

TABLE I

Blockade of IL-1RII by specific monoclonal antibody does not increase IL-1 β -stimulated IL-8 secretion in differentiated HT-29/MTX cells

Polymorphonuclear cells were used as a positive control for the IL-1RII blocking antibody. ND, not done. Data are expressed as mean \pm S.D.

Treatment	Cells	
	HT-29/MTX	Polymorphonuclear
Medium	399 (\pm 35)	1078 (\pm 43)
IL-1 β	608 (\pm 13)	3516 (\pm 241)
IL-1 β + blocking antibody	644 (\pm 54)	6966 (\pm 276) ^a
LPS	ND	20032 (\pm 706)
LPS + blocking antibody	ND	22600 (\pm 666)
Blocking antibody	395 (\pm 43)	1147 (\pm 16)

^a $p < 0.05$ versus IL-1 β alone.

steady-state levels were determined by Western blotting. The IRAK protein rapidly disappeared in IL-1 β -stimulated Caco-2 cells and was not resynthesized (Fig. 5A), suggesting that IL-1 β induced IRAK phosphorylation and degradation. Interestingly, IRAK was only partially degraded in either IL-1 β -stimulated HT-29/MTX (Fig. 5B) or HT-29/p (Fig. 5C) cells, and steady-state constitutive levels are lower in differentiated than in undifferentiated cells (Fig. 5D). These data demonstrate altered IRAK degradation in HT-29 cells, regardless of differentiation state and that differentiation decreases IRAK steady-state level.

The signal coming from IRAK/TRAF-6 diverges toward both the JNK and NF- κ B pathways. We next compared the kinase activities of JNK and IKK that are responsible for c-Jun and I κ B α phosphorylation, respectively, in the two cell lines. HT-29/MTX and HT-29/p cells were stimulated with IL-1 β for various times, and kinase activities were measured using a GST-c-Jun substrate for JNK and a GST-I κ B substrate for IKK. As presented in Fig. 6A, JNK activity was strongly induced in IL-1 β -stimulated HT-29/p cells but only marginally increased in HT-29/MTX cells exposed to identical IL-1 β concentration. Concurrently, IL-1 β -induced IKK activation increased in IL-1 β -stimulated HT-29/p but not in HT-29/MTX cells as measured by I κ B phosphorylation (Fig. 6B). IKK α steady-state levels are similar in HT-29/MTX and HT-29/p cells (Fig. 6C), indicating that the observed difference of I κ B phosphorylation was not due to an absence of IKK α protein but to less kinase activity. The data suggest that the IL-1 β signal leading to both JNK and IKK activation is significantly attenuated in differentiated HT-29 cells.

IL-1 β signals through the I κ B/NF- κ B pathway in HT-29 cells (5, 6, 8). The effect of cellular differentiation on I κ B α steady-state levels was investigated in HT-29/MTX and HT-29/p. Cells were stimulated with IL-1 β for 0–90 min, and cytoplasmic I κ B α levels were measured by Western blotting. Fig. 7A shows that I κ B α was not significantly degraded in either HT-29/MTX cells (upper panel) or HT-29/p cells (middle panel) following IL-1 β stimulation. To compare degrees of I κ B phosphorylation following cytokine stimulation, Caco-2, HT-29/p, and HT-29/MTX cells were pretreated with the proteasome inhibitor MG-132 for 45 min and then stimulated with IL-1 β for 0–15 min. Endogenous I κ B phosphorylation was determined using Western blotting with a specific I κ B phosphoserine antibody. Phosphorylated I κ B was detected in Caco-2 cells and to a much lesser extent in HT-29/p (Fig. 7A, lower panel) but not in HT-29/MTX cells (data not shown). This is in agreement with the lack of IKK activity in HT-29/MTX cells (Fig. 6B). We next compared NF- κ B DNA binding activity between the two cell lines. Cells were stimulated with IL-1 β or TNF- α for 0–90 min, and nuclear protein extracts were tested for NF- κ B DNA binding activity. IL-1 β and TNF- α induced a rapid and strong increase of NF- κ B DNA binding activity in HT-29/p cells (Fig.

FIG. 5. IRAK was rapidly degraded in IL-1 β -stimulated Caco-2 but not normal or differentiated HT-29 cells. A, Caco-2, HT-29/MTX (B) or HT-29/p cells (C) were stimulated with IL-1 β (2 ng/ml) for 0–90 min and IRAK steady-state level analyzed by Western blotting as described under “Materials and Methods.” D, IRAK steady-state level in unstimulated HT-29/p and HT-29/MTX cells. IRAK steady-state level was determined by Western blotting as described under “Materials and Methods.”

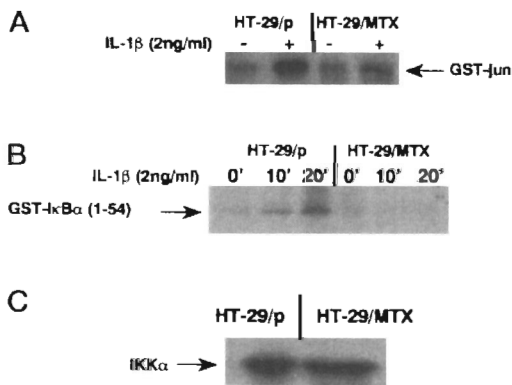
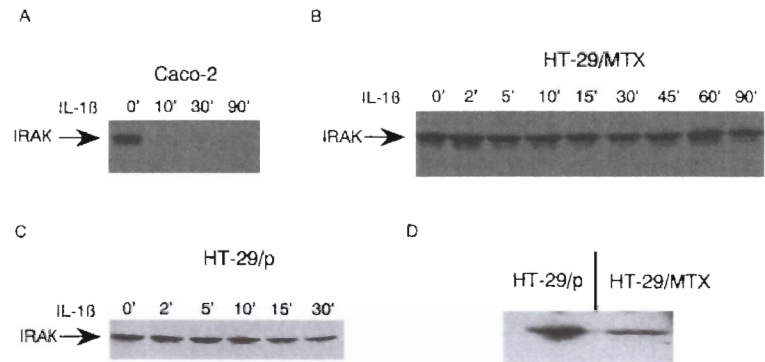


FIG. 6. Analysis of Jun and IKK α kinase activity in IL-1 β -stimulated HT-29/p and HT-29/MTX cells. A, cells were stimulated with IL-1 β (2 ng/ml) for 30 min, and phosphorylated GST-c-Jun was visualized after protein fractionation using 12.5% SDS-PAGE. B, cells were stimulated with IL-1 β (2 ng/ml) for 0, 10, and 20 min. Cells were lysed; IKK α was immunoprecipitated, and kinase activity was measured using a GST-I κ B(1–54) substrate as described under “Materials and Methods.” In both kinase assays, Coomassie staining was used to document equal protein loading. These two experiment results are representative of two independent determinations. C, IKK α steady-state level in unstimulated HT-29/p and HT-29/MTX cells. IKK α steady-state level was determined by Western blotting as described under “Materials and Methods.”

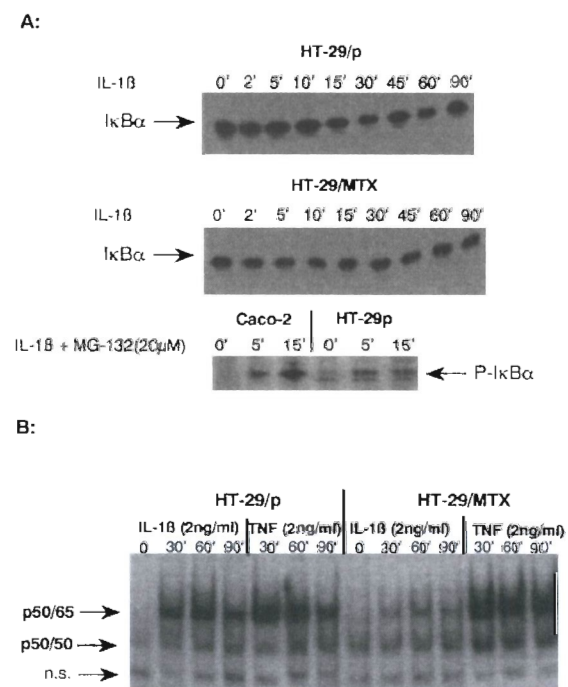


FIG. 7. Impaired I κ B α degradation (A) and NF- κ B DNA binding activity (B) in HT-29/MTX cells. A, HT-29/p and HT-29/MTX cells were stimulated with IL-1 β (2 ng/ml) for the indicated time. I κ B α steady-state level was assessed by Western blot analysis as described under “Materials and Methods.” B, cells were stimulated with IL-1 β (2 ng/ml) or TNF- α (2 ng/ml) for the indicated time points. NF- κ B DNA binding activity was measured in nuclear extracts as described under “Materials and Methods.” The arrows indicate various NF- κ B heterodimers. Two other experiments gave similar results. n.s., not specific.

7B) despite the apparent absence of complete I κ B α degradation (Fig. 7A). A similar lack of correlation between I κ B degradation and NF- κ B activation in HT-29 cells was previously reported (5, 36, 37). Interestingly, TNF- α , but not IL-1 β , strongly induced NF- κ B DNA binding activity in HT-29/MTX cells. IL-1 β induced only a slight increase in NF- κ B binding activity in the differentiated cells. This specific effect of cellular differentiation on IL-1 β signaling through NF- κ B is in agreement with the weak induction of IL-8 in HT-29/MTX cells (Figs. 1 and 2).

The relative lack of NF- κ B activation and IL-8 gene expression in response to IL-1 β but not TNF- α suggested that the defect in HT-29/MTX cells was upstream of the shared kinase NIK but downstream of IL-1R. We next investigated whether overexpression of TRAF-6, an IL-1 β adapter protein, would restore NF- κ B signaling in HT-29/MTX cells. The effect of TRAF-6 overexpression on a co-transfected luciferase reporter gene under the control of three upstream NF- κ B sites was investigated in HT-29/MTX cells. IL-1 β induced a modest 5-fold increase in luciferase activity, whereas TNF- α induced more than 60-fold activity in HT-29/MTX cells (Fig. 8). Interestingly, TRAF-6-transfected HT-29/MTX cells showed more than 90-fold induction of luciferase activity, which is 16-fold higher than IL-1 β -stimulated activity (Fig. 8). These results indicate that distal components of the signaling cascade in HT-29/MTX are capable of responding if TRAF-6 is appropriately activated.

It has been shown that LPS utilizes components of the IL-1 β signaling pathway to transmit its signal (38–40). We next investigated whether LPS-induced IL-8 secretion would also be affected by cellular differentiation. Fig. 9 shows that LPS induced IL-8 secretion by more than 10-fold in HT-29/p but only by 2-fold in HT-29/MTX cells. Therefore, similar to IL-1 β but in contrast to TNF- α or PMA, LPS signal transduction leading to IL-8 secretion is down-regulated by cellular differentiation. Altogether, our data demonstrate that cellular differentiation of HT-29 cells selectively impairs the IL-1 β signaling pathway abrogating NF- κ B activation and IL-8 gene expression upstream of NIK but downstream of IL-1R.

DISCUSSION

This study investigated the effect of cellular differentiation on the IL-1 β signaling pathway in IEC. By using permanently

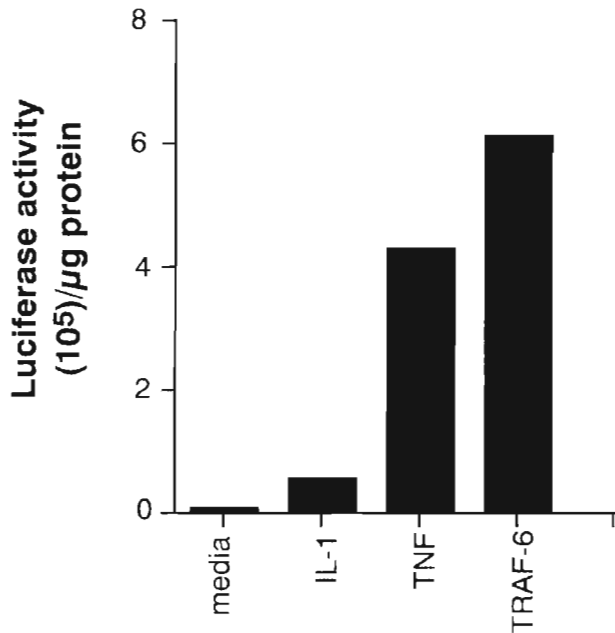


FIG. 8. TRAF-6 induced the transcription of a κ B-luciferase reporter gene transfected in HT-29/MTX cells. Cells were transfected with 1 μ g of κ B-luciferase plasmid alone or co-transfected with 2 μ g of TRAF-6 plasmids as described under "Materials and Methods." Cells 24 h post-transfection were stimulated with IL-1 β (2 ng/ml) or media alone for 12 h, and extracts were prepared for determination of luciferase activity. Results from one representative experiment performed in triplicate are shown. Similar results were obtained in two separate experiments.

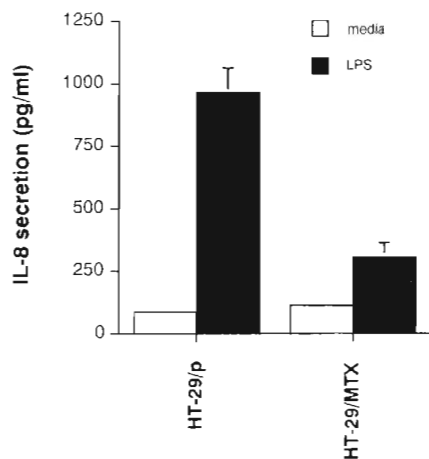


FIG. 9. LPS-induced IL-8 secretion is inhibited in HT-29/MTX compared with HT-29/p. Cells were stimulated with LPS (5 μ g/ml) overnight after which immunoreactive IL-8 concentrations were measured in cell supernatants using an ELISA technique. These results are expressed as means \pm S.D. of triplicate determinations.

differentiated HT-29/MTX cells, we report that IL-1 β -induced JNK, IKK activity, and NF- κ B activation are strongly reduced in differentiated cells compared with undifferentiated cells of the same lineage. As a consequence of impaired IL-1 β signaling in HT-29/MTX cells, inducible IL-8 gene expression, which is transcriptionally regulated by NF- κ B, is substantially diminished. IL-8 gene expression in response to TNF- α and PMA stimulation and IL-1 β receptor binding, however, remains normal in differentiated cells, suggesting a selective effect of cellular differentiation on IL-1 β signaling. Interestingly, TRAF-6 overexpression triggers a strong induction of a κ B-luciferase

reporter gene in HT-29/MTX cells, indicating that downstream components of the IL-1 β signaling cascade can be activated in differentiated cells if appropriately stimulated. In addition, LPS-induced IL-8 secretion was also impaired in differentiated cells. We therefore conclude that cellular differentiation specifically inhibits the IL-1 β signaling pathway upstream of NIK but downstream of IL-1R in HT-29 cells.

The observed selective decrease in responsiveness to IL-1 β in differentiated HT-29 cells is not merely a consequence of decreased IL-1R expression or competitive inhibition of IL-1 β binding by enhanced secretion of IL-1RA. Membrane binding of radiolabeled IL-1 β was increased in the differentiated cells, and measured secretion of immunoreactive IL-1RA, which did not differ between parental and HT-29/MTX cells, was at least 50-fold below concentrations necessary to inhibit IL-1 β -induced IL-8 expression. We have previously reported that icIL-1RA expression is increased in differentiated IEC with cytoplasmic protein only detectable within surface colonic epithelial cells (29). A yet to be characterized interaction of icIL-1RA with the IL-1 β signaling cascade remains a possible mechanism of diminished IL-1 β signal transduction in differentiated IEC.

One potential explanation of decreased IL-1 β responsiveness in HT-29/MTX cells is a result of an increased expression of the decoy IL-1RII, which does not transduce signals. Three experimental results argue against this possibility. First, a cross-link affinity study demonstrates that IL-1 β exclusively binds to the IL-1RI in both HT-29/p and HT-29/MTX cells. This is in agreement with previous findings showing that IL-1 β binds mostly to IL-1RI in IEC and that IL-1RII is not expressed by rat primary and IEC-6 lines (41, 42). Second, blocking IL-1RII with a specific neutralizing antibody failed to restore IL-1 β responsiveness in differentiated HT-29 cells. Finally, IL-8 secretion is also down-regulated in LPS-stimulated HT-29/MTX cells, an IL-1R (type I or II)-independent stimulus. Therefore, it is unlikely that the reduced IL-1 β signaling in HT-29/MTX cells is the result of a decoy receptor effect.

IL-1 binding to its receptors causes a cascade of signaling events that results in activation of JNK, p38 mitogen-activated protein kinases, and NF- κ B (38). Separate signals coming from IL-1 β or TNF- α converge on NIK and activate the IKK complex (37, 43, 44) which leads to phosphorylation, ubiquitination, and degradation of I κ B and subsequent NF- κ B activation. The finding that TNF- α -induced NF- κ B activity and IL-8 gene expression in HT-29/MTX cells is normal suggests that the NF- κ B signaling cascade pathway is functionally intact from the TNF- α receptor side. Therefore, the defect in IL-1 β signaling in HT-29/MTX cells is likely to be proximal to NIK, which is utilized by both TNF- α and IL-1 β . IRAK-1 has been implicated in both JNK and NF- κ B activation. The results obtained with TRAF-6 overexpression confirm that the IL-1 β signaling pathway is functional downstream of TRAF-6 in HT-29/MTX. Interestingly, IRAK, a kinase acting above TRAF-6, was rapidly degraded in Caco-2 cells but not in HT-29/MTX cells following IL-1 β stimulation. However, undifferentiated HT-29 cells also display an almost complete lack of IRAK degradation in response to IL-1 β stimulation, with no difference between IRAK degradation in differentiated and undifferentiated HT-29 cells. The lack of IRAK degradation in IL-1 β -stimulated HT-29 cells raised the possibility that another protein, such as IRAK-2, transmits the signal to downstream effector proteins. Of note, IRAK-1-deficient mice were still able to activate NF- κ B following IL-1 β stimulation, suggesting that an IRAK-1-independent route can be utilized by IL-1 β (45). Interestingly, LPS-induced IL-8 secretion was also impaired in differentiated cells. The LPS signal crosses the IL-1 pathway at a level lower than

IL-1RAcP and requires the participation of the cell-surface protein CD-14 and a Toll-like receptor (38, 46, 47). The precise junction point where the IL-1 β and LPS signal intersect is still unclear but may be at the level of MyD88 (40, 46, 47). Therefore, it is reasonable to speculate that MyD88 and/or TRAF-6 function is altered by cellular differentiation. Cellular differentiation could be an intrinsic regulation of IEC responses to inflammatory stimuli, and it remains to be seen whether a similar gradient of responsiveness exists along the crypt-villus axis *in vivo*. Of note, we found that Fas-mediated apoptosis is higher in differentiated than undifferentiated IEC both *in vivo* and *in vitro* (48).

An intriguing observation is the lack of effect of differentiation on the TNF- α signaling pathway. However, although HT-29 cells respond vigorously to TNF- α , many transformed and primary IEC are devoid of TNFR and hence are unresponsive to this cytokine (49). Therefore, the relevance of TNF- α on *in vivo* IEC activation remains unclear at this time.

Our demonstration that cellular differentiation modulates IEC responsiveness has important biologic and clinical implications. It is likely that differences in IEC immune responsiveness to IL-1 exist along the villus-crypt axis, since crypt cells are highly proliferative and undifferentiated, whereas cells at the villous tip are senescent and terminally differentiated (50). Crypt hyperplasia and relative undifferentiation of cells in the mid-crypt region are common features observed in the actively inflamed gut from patients with inflammatory bowel disease and *in vivo/in vitro* models of chronic immune mediated intestinal inflammation. The relative abundance of undifferentiated IEC in the inflamed mucosa may perpetuate the inflammatory process by enhancing cellular responses to IL-1 β . Several independent observations support the negative correlation between immune responsiveness and differentiation state of IEC demonstrated by our results. For example, immunohistochemistry performed on tissue sections derived from patients with active inflammatory bowel disease demonstrates the presence of activated NF- κ B in the crypt epithelial cells but not in the surface region (51). Differentiation of Caco-2 cells by exposure to sodium butyrate led to abrogation of IL-1-stimulated IL-8 expression (3, 4). Similarly cyclosporin A, which stimulates cell differentiation, inhibited IL-8 secretion in HT-29 cells (52, 53), and IL-1 β is produced only by undifferentiated, proliferating rat colonic crypt epithelial cells (54). In addition, IEC differentiation inhibits *Yersinia pseudotuberculosis* invasion of Caco-2 cells (55).

In summary, our data support a role for cellular differentiation in regulating the IL-1 β signaling pathway of IEC leading to activation of JNK, IKK, NF- κ B, and IL-8 gene expression. The physiological impact of IEC differentiation may include down-regulation of responsiveness to IL-1 β .

Acknowledgment—We thank Julie Vorobior from the Immunoassay Core of the Center for Gastrointestinal Biology and Disease for assistance in IL-8 ELISA and Dr. Richard B. Mailman for helpful advice on the cross-linking affinity study.

REFERENCES

- Louvard, D., Kedinger, M., and Hauri, H. P. (1992) *Annu. Rev. Cell Biol.* **8**, 157–195
- Zweibaum, A., Laburthe, M., Grasset, E., and Louvard, D. (1991) in *Handbook of Physiology: The Gastrointestinal System IV* (Fritzell, R. F. H., ed) pp. 223–255. Alan R. Liss, Inc., New York
- Huang, N., Katz, J. P., Martin, D. R., and Wu, G. D. (1997) *Cytokine* **9**, 27–36
- Huang, N., and Wu, G. D. (1997) *Adv. Exp. Med. Biol.* **427**, 145–153
- Jobin, C., Haskill, S., Mayer, L., Panja, A., and Sartor, R. B. (1997) *J. Immunol.* **158**, 226–234
- Jobin, C., Panja, A., Hellerbrand, C., Imuro, Y., Didonato, J., Brenner, D. A., and Sartor, R. B. (1993) *J. Immunol.* **160**, 410–418
- Jobin, C., Holt, L., Bradham, C. A., Street, K., Brenner, D. A., and Sartor, R. B. (1999) *J. Immunol.* **162**, 4447–4454
- Jobin, C., Bradham, C. A., Russo, M. P., Juma, B., Narula, A. S., Brenner, D. A., and Sartor, R. B. (1999) *J. Immunol.* **163**, 3474–3483
- Hsu, H., Shu, H.-B., Pan, M.-G., and Goeddel, D. V. (1996) *Cell* **84**, 299–308
- Hsu, H., Huang, J., Shu, H.-B., Baichwal, V., and Goeddel, D. V. (1996) *Immunity* **4**, 387–396
- Burns, K., Martinon, F., Esslinger, C., Pahl, H., Schneider, P., Bodmer, J.-L., Di Marco, F., Frech, L., and Tschopp, J. (1998) *J. Biol. Chem.* **273**, 12203–12209
- Cao, Z., Xiong, J., Takeuchi, M., Kurama, T., and Goeddel, D. V. (1996) *Nature* **383**, 443–446
- Cao, Z., Henzel, W. J., and Gao, X. (1996) *Science* **271**, 1128–1131
- Wesche, H., Henzel, W. J., Shillinglaw, W., Li, S., and Cao, Z. (1997) *Immunity* **7**, 837–847
- Ninomiya-Tsuji, J., Kishimoto, K., Hiyama, A., Inoue, J.-I., Cao, Z., and Matsumoto, K. (1999) *Nature* **398**, 252–256
- Lin, X., Mu, Y., Cunningham, E. T., Marcu, K. B., Gelezianus, R., and Greene, W. C. (1998) *Mol. Cell. Biol.* **18**, 5899–5907
- Ling, L., Cao, Z., and Goeddel, D. V. (1998) *Proc. Natl. Acad. Sci. U. S. A.* **95**, 3792–3797
- Natoli, G., Costanzo, A., Moretti, F., Fulco, M., Balsano, C., and Levrero, M. (1997) *J. Biol. Chem.* **272**, 26079–26082
- Verma, I. M., and Stevenson, J. (1997) *Proc. Natl. Acad. Sci. U. S. A.* **94**, 11758–11760
- Lesuffleur, T., Barbat, A., Dussaux, E., and Zweibaum, A. (1990) *Cancer Res.* **50**, 6334–6343
- Lesuffleur, T., Violette, S., Vasil-Pandrea, I., Dussaux, E., Barbat, A., Muleris, M., and Zweibaum, A. (1998) *Int. J. Cancer* **76**, 383–392
- Jobin, C., and Gauthier, J. (1997) *Inflammation* **21**, 235–250
- Raingaud, J., Gupta, S., Rogers, J. S., Dickens, M., Han, J., Ulevitch, R. J., and Davis, R. J. (1995) *J. Biol. Chem.* **270**, 7420–7426
- Jobin, C., Hellerbrand, C., Licato, L. L., Brenner, D. A., and Sartor, R. B. (1998) *Gut* **42**, 779–787
- Licato, L. L., and Brenner, D. A. (1998) *Dig. Dis. Sci.* **43**, 1454–1464
- Galang, C. K., Der, C. J., and Hauser, C. A. (1994) *Oncogene* **9**, 2913–2921
- Eckmann, L., Jung, H. J., Schürer-Maly, C., Panja, A., Morzycka-Wroblewska, E., and Kagnoff, M. J. (1993) *Gastroenterology* **105**, 1689–1697
- Ohno, Y., Lee, J., MacDermott, R. P., and Sanderson, I. R. (1997) *Proc. Natl. Acad. Sci. U. S. A.* **94**, 10279–10284
- Böcker, U., Damião, A., Holt, L., Han, D. S., Jobin, C., Panja, A., Mayer, L., and Sartor, R. B. (1998) *Gastroenterology* **115**, 1426–1438
- Bertini, R., Sironi, M., Martin-Padura, I., Colotta, F., Rambaldi, S., Bernasconi, S., Ghezzi, P., Haskill, S. J., Liu, D., and Mantovani, A. (1992) *Cytokine* **4**, 44–47
- Jobin, C., Morteau, O., Han, D.-S., and Sartor, R. B. (1998) *Immunology* **95**, 537–543
- Colotta, F., Re, F., Muzio, M., Bertini, R., Polentarutti, N., Sironi, M., Giri, J. G., Dower, S. K., Sims, J. E., and Mantovani, A. (1993) *Science* **261**, 472–475
- Rauschmayr, T., Groves, R. W., and Kupper, T. S. (1997) *Proc. Natl. Acad. Sci. U. S. A.* **94**, 5814–5819
- Sims, J. E., Gayle, M. A., Slack, J. L., Alderson, M. A., Bird, T. A., Giri, J. G., Colotta, F., Re, F., Mantovani, A., Shanebeck, K., Grabstein, K. H., and Dower, S. K. (1993) *Proc. Natl. Acad. Sci. U. S. A.* **90**, 6155–6159
- Yamin, T.-T., and Miller, D. K. (1997) *J. Biol. Chem.* **272**, 21540–21547
- Elewaut, D., Didonato, J. A., Kim, J. M., Truong, F., Eckmann, L., and Kagnoff, M. F. (1999) *J. Immunol.* **163**, 1457–1466
- Didonato, J. A., Hayakawa, M., Rothwarf, D., Zandi, E., and Karin, M. (1997) *Nature* **388**, 548–554
- O'Neill, L. A. J., and Greene, C. (1998) *J. Leukocyte Biol.* **63**, 650–657
- Zhang, F. X., Kirschning, C. J., Mancinelli, R., Xu, X.-P., Jin, Y., Faure, E., Mantovani, A., Rothe, M., Muzio, M., and Arditi, M. (1999) *J. Immunol.* **274**, 7611–7614
- Kawai, T., Adachi, O., Ogawa, T., Takeda, K., and Akira, S. (1999) *Immunity* **11**, 115–122
- McGee, D. W., Vitkus, S. J. D., and Lee, P. (1996) *Cell. Immunol.* **168**, 276–280
- Sutherland, D. B., Varilek, G. W., and Neil, G. A. (1994) *Am. J. Physiol.* **266**, C1198–C1203
- Mercurio, F., Zhu, H., Murray, B. W., Shevchenko, A., Bennett, B. L., Li, J. W., Young, D. B., Barbosa, M., Mann, M., Manning, A., and Rao, A. (1997) *Science* **278**, 860–866
- Zandi, E., Rothwarf, D. M., Belhase, M., Hayakawa, M., and Karin, M. (1997) *Cell* **91**, 243–252
- Kanakaraj, P., Schaffer, P. H., Cavender, D. E., Wu, Y., Ngo, K., Grealish, P. F., Wadsworth, S. A., Peterson, P. A., Siekierka, J. J., Harris, C. A., and Fung-Leung, W. P. (1998) *J. Exp. Med.* **187**, 2073–2079
- Wright, S. D. (1999) *J. Exp. Med.* **189**, 605–609
- Hoshino, K., Takeuchi, O., Kawai, T., Sanja, H., Ogawa, T., Takeda, Y., Takeda, K., and Akira, S. (1999) *J. Immunol.* **162**, 3749–3752
- Russo, M. P., Mehta, N. P., Keku, T. O., Sartor, R. B., and Jobin, C. (2000) *Gastroenterology* (abstr), in press
- Panja, A., Goldberg, S., Eckmann, L., Krishen, P., and Mayer, L. (1998) *J. Immunol.* **161**, 3675–3684
- Gordon, J. I. (1999) *Gastroenterology* **116**, 208–215
- Rogler, G., Brand, K., Vogl, D., Page, S., Hofmeister, R., Andus, T., Knuechel, R., Baeuerle, P. A., Scholrerich, J., and Gross, V. (1998) *Gastroenterology* **115**, 357–369
- Mengheri, E., Ciapponi, L., Vignolini, F., and Nobili, F. (1996) *Life Sci.* **59**, 1227–1236
- Saitoh, O., Matsuse, R., Sugi, K., Nakagawa, K., Uchida, K., Maemura, K., Kojima, K., Hirata, I., and Katsui, K. (1997) *J. Gastroenterol.* **32**, 605–610
- Radema, S. A., Van Deventer, S. J., and Cerami, A. (1991) *Gastroenterology* **100**, 1180–1186
- Cocconnier, M.-H., Bernet-Camard, M.-F., and Servin, A. L. (1994) *Differentiation* **58**, 87–94

Akt Suppresses Apoptosis by Stimulating the Transactivation Potential of the RelA/p65 Subunit of NF- κ B

LEE V. MADRID,^{1,2} CUN-YU WANG,³ DENIS C. GUTTRIDGE,¹ ARNDT J. G. SCHOTTELIUS,¹
ALBERT S. BALDWIN, JR.,^{1,2,4} AND MARTY W. MAYO^{1*}

Lineberger Comprehensive Cancer Center,¹ Curriculum in Genetics and Molecular Biology,² and Department of Biology,⁴ University of North Carolina, Chapel Hill, North Carolina 27599, and The Laboratory of Molecular Signaling, Department of Biologic and Material Science, School of Dentistry, University of Michigan, Ann Arbor, Michigan 48109³

Received 22 June 1999/Returned for modification 4 August 1999/Accepted 7 December 1999

It is well established that cell survival signals stimulated by growth factors, cytokines, and oncoproteins are initiated by phosphoinositide 3-kinase (PI3K)- and Akt-dependent signal transduction pathways. Oncogenic Ras, an upstream activator of Akt, requires NF- κ B to initiate transformation, at least partially through the ability of NF- κ B to suppress transformation-associated apoptosis. In this study, we show that oncogenic H-Ras requires PI3K and Akt to stimulate the transcriptional activity of NF- κ B. Activated forms of H-Ras and MEKK stimulate signals that result in nuclear translocation and DNA binding of NF- κ B as well as stimulation of the NF- κ B transactivation potential. In contrast, activated PI3K or Akt stimulates NF- κ B-dependent transcription by stimulating transactivation domain 1 of the p65 subunit rather than inducing NF- κ B nuclear translocation via I κ B degradation. Inhibition of I κ B kinase (IKK), using an IKK β dominant negative protein, demonstrated that activated Akt requires IKK to efficiently stimulate the transactivation domain of the p65 subunit of NF- κ B. Inhibition of endogenous Akt activity sensitized cells to H-Ras(V12)-induced apoptosis, which was associated with a loss of NF- κ B transcriptional activity. Finally, Akt-transformed cells were shown to require NF- κ B to suppress the ability of etoposide to induce apoptosis. Our work demonstrates that, unlike activated Ras, which can stimulate parallel pathways to activate both DNA binding and the transcriptional activity of NF- κ B, Akt stimulates NF- κ B predominantly by upregulating of the transactivation potential of p65.

Akt, also known as PKB (protein kinase B) (3, 13), is a serine/threonine protein kinase that has been shown to regulate cell survival signals in response to growth factors, cytokines, and oncogenic Ras (19, 23, 40). Akt becomes activated via the phosphoinositide-3-OH kinase (PI3K) pathway (18, 24, 29) and by other upstream kinases, including the recently identified Ca²⁺- and calmodulin-dependent kinase protein kinase (64). Akt inhibits cell death pathways by directly phosphorylating and inactivating proteins involved in apoptosis, including Bad, procaspase 9, and members of the Forkhead transcription factor family (7, 8, 15, 16, 36, 55). Phosphorylation of Bad by Akt at serine (Ser) residues 112 and 136 enables the 14-3-3 protein to interact with and sequester the inactivated Bad protein in the cytoplasm (15, 67). Akt also phosphorylates the procaspase 9 protease at Ser-196, which has been shown to contribute to the resistance of Ras-transformed cells to overcoming apoptotic agents (8). Finally, members of the Forkhead transcription factor family have been shown to be directly phosphorylated by Akt (7, 36, 55) and the inactivation of the Forkhead family member FKHL1 promotes cell survival (7). In addition to directly phosphorylating and inactivating proapoptotic protein targets, Akt can stimulate signaling pathways that upregulate the activity of the transcription factor NF- κ B (31, 44, 49, 52). Importantly, the antiapoptotic signals elicited by platelet-derived growth factor (PDGF) were shown to require Akt-induced NF- κ B transcriptional activity (49).

Classical NF- κ B, a heterodimer composed of p50 and p65

subunits, is a potent activator of gene expression from NF- κ B sites due to the presence of transactivating domains located in the C-terminal 120 amino acids of the p65 (also called RelA) protein (1, 21). Thus, NF- κ B is regulated through mechanisms that target the transcription function of NF- κ B (22, 47, 58, 68, 69). Additionally, NF- κ B activity is also regulated by the I κ B family of proteins that interact with and sequester the transcription factor in the cytoplasm. Following cellular stimulation, I κ B proteins become phosphorylated by the multisubunit I κ B kinase (IKK) complex, which subsequently targets I κ B for ubiquitination and degradation by the 26S proteasome (66). IKK-dependent degradation of I κ B liberates NF- κ B, allowing this transcription factor to translocate to the nucleus, where it upregulates transcription (1, 25). Thus, as is the case with several transcription factors, NF- κ B is regulated through signaling mechanisms that control nuclear translocation (such as IKK) and through mechanisms that are responsible for upregulating the transactivation function of NF- κ B.

We have previously demonstrated that oncogenic Ras stimulates NF- κ B-dependent transcription (20) and that NF- κ B is required for Ras-mediated transformation (22). Moreover, Ras activates NF- κ B to suppress oncogene-induced apoptosis (41). NF- κ B was originally found to be required to block apoptosis in response to tumor necrosis factor (TNF) (2, 37, 56, 57) and in response to genotoxic agents (57–59). Subsequently, it was shown that NF- κ B blocks TNF-induced apoptosis through the transcriptional activation of genes encoding antiapoptotic proteins (12, 26, 57, 58, 59a, 70). Although we have demonstrated that oncogenic Ras upregulates NF- κ B to suppress Ras-induced apoptosis, the signaling pathways utilized for NF- κ B-dependent cell survival under these conditions have not been elucidated. Because Akt provides a strong cell survival signal in response to activated Ras signaling (33, 34), we

* Corresponding author. Mailing address: Lineberger Comprehensive Cancer Center, Campus Box Number 7295, University of North Carolina, Chapel Hill, NC 27599. Phone: (919) 966-3884. Fax: (919) 966-0444.

asked whether H-Ras(V12) utilizes Akt to activate NF- κ B and to provide an antiapoptotic signal. Thus, we demonstrate that H-Ras(V12) stimulates NF- κ B-dependent transcription in a PI3K- and Akt-dependent manner. Recently, several groups have reported that PI3K and Akt are involved in the activation of NF- κ B in response to TNF, interleukin 1 β (IL-1 β), phorbol myristate acetate (PMA), pervanadate, and PDGF signaling (4, 5, 31, 44, 46, 49, 52). Several of these papers indicated that IKK activity is involved in the ability of Akt to stimulate NF- κ B transcriptional activity (30, 44, 49), presumably through direct mechanisms involving enhanced NF- κ B nuclear translocation. However, we found that constitutively activated forms of either PI3K or Akt stimulated NF- κ B transcriptional activity predominantly through signaling pathways that targeted the transactivation domain of the p65 subunit. Consistent with the importance of Akt in cell survival, we found that the inhibition of endogenous Akt activity resulted in a loss of NF- κ B transcriptional activity and sensitization of cells to H-Ras(V12)-induced apoptosis. Moreover, Akt-induced resistance to etoposide is mediated, in part, by the ability of this serine/threonine kinase to upregulate the transcriptional activity of NF- κ B. This study indicates that in addition to inhibiting preexisting proapoptotic proteins, like Bad, procaspase-9, and the Forkhead transcription factors, Akt provides long-term cell survival signals by activating pathways that target NF- κ B-dependent transcription.

MATERIALS AND METHODS

Cell culture and reagents. Murine NIH 3T3 fibroblasts were grown in Dulbecco modified Eagle medium (DMEM; Gibco/BRL) supplemented with 10% calf serum (Hyclone Laboratories, Logan, Utah) and penicillin-streptomycin unless otherwise indicated. Human 293T kidney and Rat-1 fibroblast cells were grown in DMEM supplemented with 10% fetal bovine serum (FBS; Hyclone Laboratories) and penicillin-streptomycin unless otherwise indicated in the figure legends. The H-Ras(V12)-inducible Rat1:Ras cell line has been described previously (42). Oncogenic Ras was induced by the addition of 5 mM isopropyl- β -D-thiogalactopyranoside (IPTG) to complete medium. Cells expressing dominant negative forms of Akt were generated by transfecting Akt K179A mutants into Rat-1:Ras cells. Stable transfectants were selected and subcloned in medium containing 1 μ g of puromycin (Sigma, St. Louis, Mo.) per ml. Clones were verified by Western blotting using an Akt-specific rabbit polyclonal antibody (New England Biolabs, Beverly, Mass.).

Plasmid constructs. 3 \times - κ B luciferase (3 \times - κ B-Luc) reporter constructs contain four κ B DNA binding consensus sites from the major histocompatibility complex class I promoter fused upstream to firefly luciferase. Mutant 3 \times - κ B-Luc reporter constructs contain two inactivating base pair mutations in each κ B site. The Gal4 luciferase (Gal4-Luc) constructs contain four Gal4 DNA consensus binding sites derived from the *Saccharomyces cerevisiae* GAL4 gene upstream of luciferase, and Gal4-p65 constructs have the yeast Gal4 DNA binding domain fused to the transactivation domain of p65 (50). Activated PI3K and Akt as well as dominant negative constructs have been described previously (34, 61).

Transfection and luciferase reporter assays. NIH 3T3 and 293T cells at 60 to 80% confluence were transiently transfected using the Superfect reagent (Qiagen, Valencia, Calif.) according to the manufacturer's instructions. Briefly, plasmid constructs (1 μ g of total DNA) were diluted in serum-free medium and mixed with the Superfect reagent. Complexes were allowed to form for 10 min before serum-containing medium was added to the mixture. The cells were washed once with 1 \times phosphate-buffered saline (PBS) and Superfect-DNA complexes were added to the cells and placed in a humidified incubator at 37°C with 5% CO₂. Three hours postaddition, cells were washed with 1 \times PBS and replenished with fresh serum-containing medium. Twenty-four hours posttransfection, cells were washed once with 1 \times PBS and lysed in Reporter Lysis Buffer (Promega, Madison, Wis.) for 10 min at room temperature. Extracts were collected and cleared by centrifugation at high speed. Rat-1:Ras cells expressing mutant Akt constructs were similarly transfected. However, cells were growth factor deprived in 0.5% serum for 12 to 18 h posttransfection and H-Ras(V12) was induced by the addition of IPTG for 12 h prior to cell harvest. Protein concentration was determined with the Bio-Rad (Hercules, Calif.) protein assay dye reagent. Luciferase assays were performed on equal amounts of protein (50 μ g/sample). D-Luciferin was used as a substrate, and relative light units were measured using an AutoLumat LB953 luminometer (Berthold Analytical Instruments). Results were normalized to those with an internal β -galactosidase (β -Gal)-expressing plasmid (pCMV-LacZ) by a β -Gal colorimetric assay followed by spectrophotometric quantitation (Promega). In addition, cells transfected with Akt or PI3K mutant constructs were cotransfected with pCMV-LacZ and

assayed for transfection efficiency and/or cell death by counting β -Gal-positive cells as previously described (41).

EMSA and Western blot analysis. Preparation of nuclear and cytoplasmic extracts and electrophoretic mobility shift assays (EMSAs) were performed as described previously (41). Briefly, nuclear extracts were prepared 48 h posttransfection and incubated with [α -³²P]dCTP-labeled, double-stranded probe containing a κ B consensus site from the class I major histocompatibility complex promoter. Labeled probe-nuclear extract complexes were incubated for 10 min at room temperature and separated on a 5% polyacrylamide gel. Subsequently, the gel was dried and exposed to X-ray film. Antibody supershift experiments were performed as previously described (41). Western blot analysis was performed by preparing whole-cell extracts in the presence of protease inhibitors. Total protein (50 μ g) was separated by sodium dodecyl sulfate (SDS)-polyacrylamide gel electrophoresis (PAGE) and transferred to nitrocellulose membranes. The indicated primary antibodies were incubated for 30 min, washed, and visualized by incubation with horseradish peroxidase (HRP)-conjugated secondary antibodies and enhanced chemiluminescence (ECL) reagents (Amersham, Piscataway, N.J.).

Apoptosis assays and adenovirus infections. Cell viability assays were performed using Rat-1:Ras cells expressing dominant negative forms of Akt [Akt (K179A)] and/or a vector control. Cells were split to subconfluence in medium containing 2% FBS for 24 to 36 h. Subsequently, supernatants containing apoptotic cells were centrifuged at low speed in a clinical centrifuge and washed gently with serum-free medium. Pellets were resuspended in 150 μ l of serum-free medium, and apoptotic cells were counted under light microscopy using a modified improved hemacytometer. Modified terminal deoxynucleotidyltransferase-mediated dUTP nicked-end labeling (TUNEL) assays were performed per the instructions of the manufacturer (Boehringer Mannheim, Indianapolis, Ind.). Adenovirus infections were performed as previously described (27). Briefly, Rat-1 or Rat-1:Ras cells were plated at a concentration of 5×10^5 cells/well in 2% FBS. Twelve to 18 h later, the medium was aspirated and replaced with 2% medium plus FBS containing adenovirus encoding the super repressor (SR) I κ B α (Ad-SRI κ B α) or adenovirus encoding the cytomegalovirus (CMV) promoter but not I κ B α (Ad-CMV) (control virus) at a concentration of 50 PFU/cell. Infection proceeded for 1 h, and then 2 ml of medium plus 2% FBS was added to the well with the addition of 5 mM IPTG, as indicated in the figures. Apoptotic cells were counted and assayed by TUNEL 48 h after the initial infection.

Kinase assays. Akt activity was measured by a phosphorylation assay using the Crosstide peptide (14) specific to the Akt phosphorylation sequence from GSK3 per the instructions of the manufacturer (Upstate Biotechnology, Lake Placid, N.Y.). Briefly, Rat-1:Ras cells were grown to subconfluence and pretreated with LY 294002 (10 μ M) for 1 h and 5 mM IPTG was added for 12 h prior to harvest. Immunoprecipitations were performed by combining 500 μ g of protein with 4 μ g of Akt monoclonal antibody (New England Biolabs) and incubating with protein A/E-agarose beads for 2 h at 4°C. Beads were washed and incubated with a PKA inhibitor peptide (17 μ M) and 100 μ Ci of [γ -³²P]dATP for 30 min at 30°C with constant agitation. Supernatants were spotted onto P81 phosphocellulose membranes, washed, and counted in a scintillation counter.

RESULTS

Activation of the PI3K pathway stimulates NF- κ B-dependent transcription. Ras directly interacts with effector targets, including the serine/threonine kinase Raf, PI3K, and the exchange factor Ral.GDS (63). Each of these targets is required for Ras-induced transformation (63). Since H-Ras(V12) is known to activate NF- κ B (9, 20, 22), it was important to elucidate which Ras effector pathways were being utilized to stimulate NF- κ B-dependent transcription. To address this question, NIH 3T3 cells were transiently cotransfected with an NF- κ B-responsive reporter (3 \times - κ B-Luc) and with either the empty vector control or plasmids bearing genes encoding various activated H-Ras effector mutants (63). As shown in Fig. 1, the H-Ras(V12, C40) effector mutant, which activates PI3K but not Raf or Ral.GDS, stimulated NF- κ B-dependent transcription as efficiently as activated H-Ras(V12) in NIH 3T3 cells. However, expression of either H-Ras(V12, S35) or H-Ras(V12, G37), which activates either the Raf kinase or the Ral.GDS exchange factor, respectively, was less effective at stimulating the transcriptional activity of NF- κ B (Fig. 1). Consistent with this data, our laboratory has recently demonstrated that the expression of the H-Ras(V12, C40) effector mutant effectively stimulates the transcriptional activity of NF- κ B (43). These results suggested that H-Ras(V12) can activate NF- κ B through signaling pathways involving PI3K.

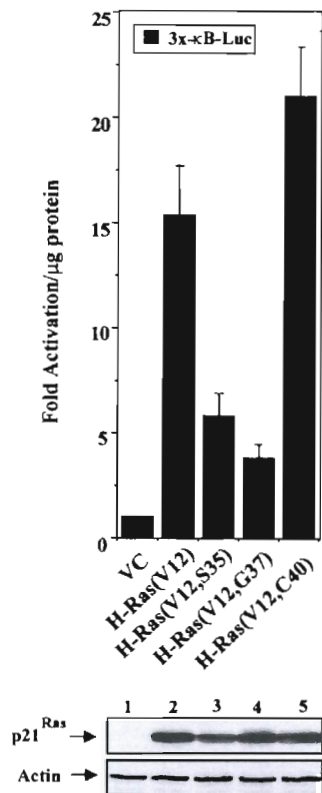


FIG. 1. Stimulation of NF- κ B-dependent transcription by the H-Ras(V12, C40) effector mutant. NIH 3T3 cells were transiently cotransfected with an NF- κ B-responsive reporter (3 \times - κ B-Luc, 0.5 μg) and with expression plasmids bearing the gene encoding H-Ras(V12), H-Ras effector mutants, or an empty vector control (VC) (1 μg each). Cell lysates were harvested 24 h posttransfection, and luciferase activity was assayed as described in Materials and Methods. Data are presented as multiples of the level of activation obtained for the vector control group, which was normalized to 1. Results are the means \pm standard deviations of results of three independent experiments. (Gel) Total protein was isolated from a representative transfection experiment, and immunoblot analysis was performed for transgene expression. Protein samples (50 μg per lane) were resolved on a 10% polyacrylamide gel, transferred to nitrocellulose, and probed for hemagglutinin-tagged p21^{Ras} proteins with a hemagglutinin-specific antibody (BABC0, Berkeley, Calif.). Immunoblot assays for actin expression confirmed that relatively equal amounts of proteins were loaded in each lane.

H-Ras(V12) requires PI3K and Akt to upregulate the transcriptional activity of NF- κ B. Activation of PI3K is known to stimulate at least two signal transduction pathways, one involving Rac and another involving Akt (28). Since we have recently demonstrated the requirement of Rac in H-Ras(V12)-induced activation of NF- κ B (43) and since Akt signaling has been clearly implicated in Ras-mediated cell survival (33, 34), we were interested in determining whether an activated form of either PI3K or Akt could stimulate the transcriptional activity of NF- κ B. NIH 3T3 cells were transiently transfected with an NF- κ B-responsive reporter and with expression constructs bearing genes encoding activated forms of H-Ras(V12), PI3K, or Akt. As shown in Fig. 2A, cells transfected with activated PI3K or Akt constructs demonstrated an increase in NF- κ B transcriptional activity. These results were similar to transcriptional levels observed in cells expressing H-Ras(V12) (Fig. 2A). The increases in 3 \times - κ B-Luc reporter activities observed following PI3K and Akt expression were not due to differences in transfection efficiencies, since all luciferase values were normalized to that of an internal β -Gal control. Moreover, cells transfected with wild-type forms of H-Ras, PI3K, or Akt dis-

played a ≤ 2 -fold increase in 3 \times - κ B luciferase activity relative to the level in vector control cells, indicating that the increase in NF- κ B transcriptional activity was associated with activated forms of these proteins (data not shown).

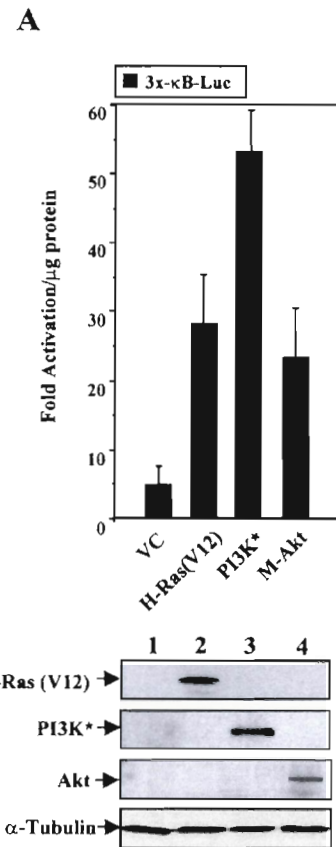


FIG. 2. H-Ras(V12) stimulates NF- κ B-dependent transcription through PI3K- and Akt-dependent pathways. (A) Activated forms of PI3K (PI3K*) and Akt stimulate the transcriptional activity of NF- κ B as effectively as H-Ras(V12). NIH 3T3 cells were cotransfected with the 3 \times - κ B-Luc reporter (0.5 μg), an internal control plasmid reporter (pCMV-LacZ, 1 μg), and various expression constructs (1 μg each). Luciferase and β -Gal activities were assayed 24 h posttransfection, and fold luciferase activity was determined by normalizing values to total protein levels and to β -Gal enzyme levels. Results are expressed as multiples of the level of activation obtained with the mutant 3 \times - κ B-Luc reporter, which contains mutated *cis* elements that are no longer capable of binding NF- κ B. Data are representative of results of at least three independent experiments, and the means \pm standard deviations are shown. (Gel) Immunoblot analysis demonstrates that transfected cells effectively express the various transgenes. (B) H-Ras(V12)-induced NF- κ B transcriptional activity requires PI3K- and Akt-dependent signaling pathways. NIH 3T3 cells were transiently transfected with the 3 \times - κ B-Luc reporter (0.5 μg), in either the absence (–) or presence (+) of H-Ras(V12) (1 μg). Additionally, cells were transfected with the empty vector control (VC) or with expression constructs bearing genes encoding dominant negative PI3K (Δ PI3K) or Akt (Akt T308A and Akt K179A, 1 μg each). Luciferase levels were measured 24 h posttransfection in order to avoid potential pitfalls associated with cell death. Data are multiples of the level of activation obtained with the mutant 3 \times - κ B-Luc control, as described above. Results are representative of at least three independent experiments and were normalized to an internal β -Gal-expressing plasmid. (Gel) Immunoblot analysis shows that transfected NIH 3T3 cells express the dominant negative PI3K (Δ PI3K) and Akt (DN Akt) constructs. (C) PI3K requires Akt to stimulate NF- κ B-dependent transcription. NIH 3T3 cells were transfected with the 3 \times - κ B-Luc reporter (0.5 μg), a vector control (VC), activated PI3K (PI3K*), or dominant negative Akt (Akt K179A) (1 μg each). Forty-eight h posttransfection whole-cell extracts were harvested and assayed for luciferase activity. Results are plotted as multiples of the level of activation of the vector control and are representative of three independent experiments. The means \pm standard deviations are shown.

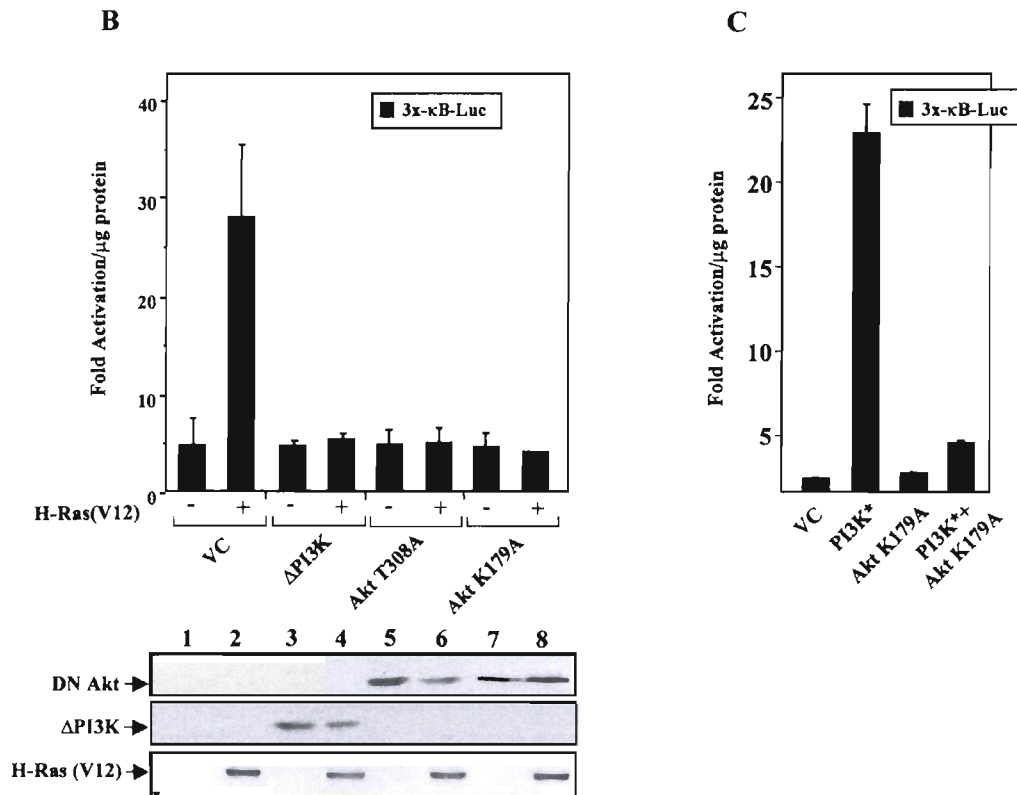


FIG. 2—Continued.

Based on these results, it was important to establish whether oncogenic Ras required PI3K and/or Akt activities to stimulate the transcriptional activity of NF- κ B. NIH 3T3 cells were co-transfected with the 3 \times - κ B-Luc reporter and with either the empty vector control or the plasmid bearing the gene encoding H-Ras(V12). In addition, some groups were also transfected with expression constructs bearing genes encoding dominant negative forms of either PI3K or Akt [Akt(T308A) or Akt(K179A)]. H-Ras(V12)-induced NF- κ B transcriptional activation was inhibited in NIH 3T3 cells coexpressing dominant negative forms of either PI3K or Akt (Fig. 2B). The ability of dominant negative PI3K and Akt constructs to block H-Ras(V12)-induced NF- κ B activity was not due to a suppression of the H-Ras(V12) expression vector, since cell extracts displayed similar levels of protein expression (Fig. 2B). These results indicate that H-Ras(V12) requires PI3K- and Akt-dependent signal transduction pathways to stimulate the transcriptional activity of NF- κ B.

To elucidate whether PI3K activates NF- κ B through an Akt-dependent manner, additional transfection experiments were performed. Consistent with previous results (Fig. 2A), expres-

sion of activated PI3K (PI3K*) upregulated the transcriptional activity of NF- κ B in NIH 3T3 cells (Fig. 2C). However, expression of the dominant negative Akt [Akt(K179A)] blocked PI3K*-induced activation of NF- κ B (Fig. 2C). Equal levels of activated PI3K protein were expressed in transfected cells, indicating that the inability of PI3K* to stimulate NF- κ B transcriptional activity was not due to suppression of the pCMV-PI3K* expression vector (data not shown). These results indicate that oncogenic H-Ras is capable of stimulating the transcriptional activity of NF- κ B through signaling pathways that involve PI3K and Akt.

PI3K and Akt stimulate NF- κ B by stimulating the transactivation domain 1 (TAD 1) of the p65 subunit. NF- κ B is regulated, in part, through a cellular process involving phosphorylation and degradation of its inhibitory protein I κ B, which allows NF- κ B to translocate to the nucleus and activate transcription (1, 25). Upon cellular stimulation, signal transduction pathways are activated and subsequently stimulate the activation of the IKK signalsome complex to phosphorylate the I κ B protein (66). To address whether PI3K or Akt could stimulate NF- κ B nuclear translocation and subsequent DNA binding, 293T cells were transiently transfected with expression constructs bearing genes encoding activated forms of H-Ras, MEKK-1, PI3K, or Akt (M-Akt). Since 293T cells demonstrate $\geq 70\%$ efficiency of transfection, we are able to transfect cells with plasmids bearing genes encoding the various transgenes, isolate nuclear proteins, and then analyze these extracts for nuclear NF- κ B activity by performing EMSAs. Nuclear extracts isolated from TNF-stimulated cells were used as a positive control for NF- κ B DNA binding activity. As shown in Fig. 3A, 293T cells expressing H-Ras(V12) or constitutively active

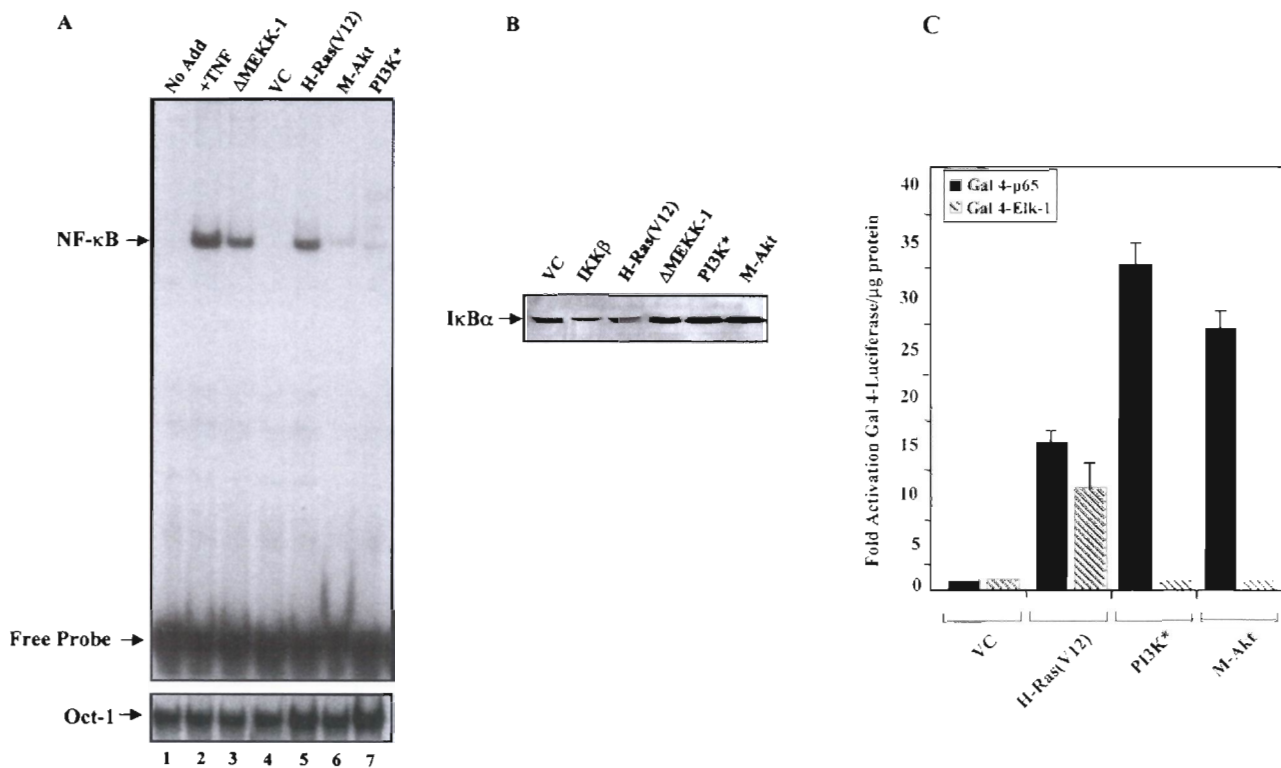


FIG. 3. PI3K and Akt activate NF- κ B by upregulating the transactivation potential of the p65 subunit. (A) Activated H-Ras(V12) and MEKK stimulate cellular pathways which result in nuclear translocation and increased DNA binding of NF- κ B. Human 293T cells were transiently transfected with the vector control (VC) or activated forms of MEKK, H-Ras, Akt, or PI3K (PI3K*) (3 μ g each). Nuclear extracts were prepared and EMSAs were performed to assess the presence of NF- κ B DNA binding activity. Nuclear extracts isolated from TNF-stimulated 293T cells (15 ng/ml for 15 min) served as a positive control for NF- κ B DNA binding activity. (Bottom) Nuclear extracts analyzed for NF- κ B DNA binding activity were reanalyzed using a 32 P-labeled Oct-1-specific double-stranded probe to confirm the quality of the nuclear proteins. Note that the Oct-1-specific DNA-protein complex but not the free probe is shown. No Add, no addition. (B) IKK β or H-Ras(V12) expression stimulates I κ B α degradation. NIH 3T3 cells were transfected with plasmids bearing the genes encoding wild-type IKK β or activated forms of H-Ras, MEKK, PI3K, or Akt (1 μ g each). Forty-eight hours posttransfection, cells were lysed and proteins (80 μ g per lane) were resolved by PAGE. Transfected I κ B α protein was detected using a Flag-specific antibody (M2; Sigma). Protein loading and transfection efficiencies were controlled by performing immunoblot analysis for His-tagged LacZ expression within each experimental group (data not shown). (C) Activated PI3K and Akt stimulate the transactivation domain of NF- κ B. NIH 3T3 cells were transiently transfected with the Gal4-luciferase reporter (100 ng) and with plasmids bearing the genes encoding either Gal4-p65 or Gal4-Elk-1 (100 ng each). Cells were also transfected with the empty vector control (VC) or activated H-Ras(V12), PI3K, or Akt. Luciferase levels were measured and expressed as multiples of the level of activation of the empty vector control. Data presented are the means \pm standard deviations of results of three independent experiments.

MEKK-1 (Δ MEKK-1) demonstrated an increase in the DNA binding activity of NF- κ B, compared to that of cells transfected with an empty vector control plasmid. This result is consistent with those of previous reports demonstrating that both H-Ras (V12) and Δ MEKK-1 can stimulate nuclear translocation and DNA binding of NF- κ B (41, 65). Expression of H-Ras(V12) and Δ MEKK-1 in 293T cells induced DNA-protein complexes which contained both p65 and p50, as detected by supershift analysis (data not shown). Interestingly, nuclear extracts from 293T cells expressing an activated form of either PI3K or Akt failed to demonstrate significant increases in NF- κ B DNA binding activity (Fig. 3A). Consistent with the inability of activated PI3K to stimulate nuclear translocation of NF- κ B, expression of plasmids bearing genes coding for H-Ras(V12, C40) in 293T cells also failed to increase the DNA binding activity of NF- κ B (data not shown). The inability of activated PI3K and Akt to stimulate NF- κ B DNA binding in 293T cells was not due to lack of protein expression (data not shown). This effect was also not caused by the quality of the nuclear extracts or the amount of proteins analyzed during EMSAs, since reanalysis of nuclear extracts isolated from transfected cells demonstrated similar levels of Oct-1 DNA-protein complexes (Fig. 3A, bottom gel). These results demonstrate that

unlike with activated H-Ras or Δ MEKK-1, the expression of an activated form of PI3K or Akt in 293T cells did not result in an increase in NF- κ B nuclear translocation and DNA binding activity. In support of our results, Kane et al. failed to detect nuclear translocation of NF- κ B following the expression of activated Akt in the absence of PMA induction (31).

Since the nuclear translocation of NF- κ B is controlled, at least in part, through IKK-dependent phosphorylation of I κ B, it was important to elucidate whether PI3K or Akt could stimulate signaling pathways that would phosphorylate and degrade I κ B α . This was an important issue to address in our cell model system, since recent reports indicate that Akt controls NF- κ B activity through mechanisms involving IKK-dependent phosphorylation and subsequent degradation of I κ B α (31, 44, 49). To explore this possibility, NIH 3T3 cells were cotransfected with plasmids bearing genes encoding Flag-tagged wild-type I κ B α and LacZ. Additionally, cells were cotransfected with either the empty vector control or plasmids bearing genes encoding H-Ras(V12), Δ MEKK-1, activated PI3K, or M-Akt. As shown in Fig. 3B, the expression of H-Ras(V12) in NIH 3T3 cells resulted in the degradation of the Flag-tagged I κ B α protein. However, cells expressing either activated PI3K or Akt failed to stimulate signaling pathways that were associated with

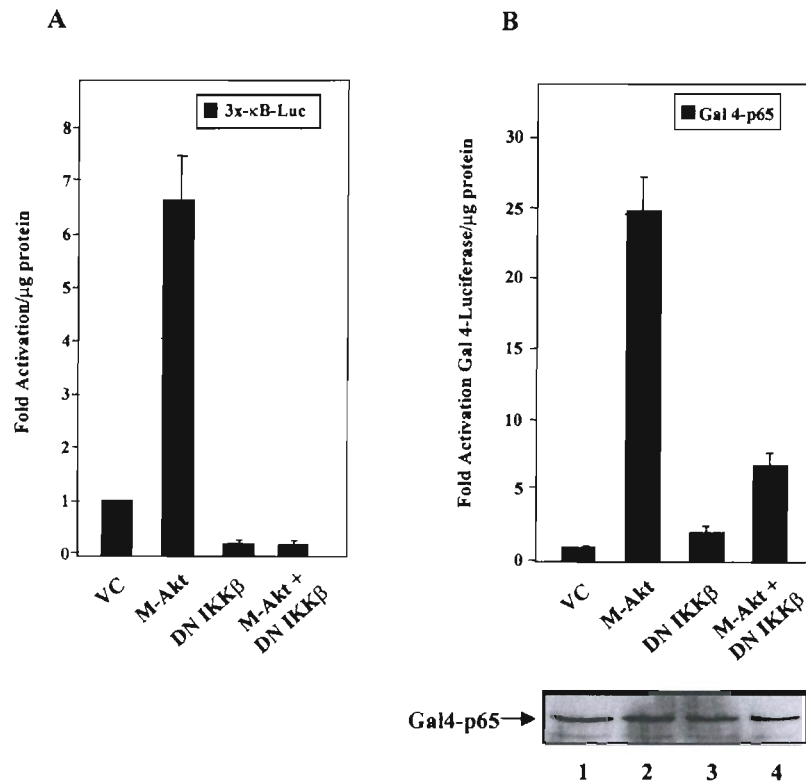


FIG. 4. Activated PI3K and Akt stimulate the p65 transactivation domain of NF- κ B in a manner dependent on I κ B kinase. (A) Akt requires IKK β to activate NF- κ B-dependent transcription. NIH 3T3 cells were transfected with the 3x- κ B-Luc reporter (0.5 μ g) and with the empty vector control (VC), M-Akt, or dominant negative IKK β (DN IKK β) alone or with M-Akt plus DN IKK β (1 μ g each). Forty-eight hours posttransfection, whole-cell extracts were harvested and assayed for luciferase activity. Results are plotted as multiples of the level of activation obtained with the vector control and are averages \pm standard deviations of results of three independent experiments. (B) Akt requires IKK to stimulate TAD 1 of the p65 subunit of NF- κ B. NIH 3T3 cells were transfected with the Gal4-luciferase reporter, Gal4-p65 (100 ng each), and the indicated constructs described above (1 μ g each). Results are expressed as multiples of the level of activation obtained with the vector control. The data are the means \pm standard deviations of results of three independent experiments. (Gel) Western blot analysis of transfected Gal4-p65. Whole-cell extracts of the transfections described above (25 μ g of protein each) were separated by SDS-10% PAGE, transferred to nitrocellulose, and assayed with an antibody specific for the Gal4 DNA binding domain (sc-510; Santa Cruz Biotech, Santa Cruz, Calif.). Primary antibodies were detected using an HRP-labeled secondary antibody and by performing ECL.

I κ B α degradation (Fig. 3B). Expression of IKK β served as positive control for inducing I κ B α degradation. The differences in Flag-tagged I κ B α protein levels observed in cells transfected with various expression constructs were not due to differences in plasmid transfection efficiencies, since cell extracts displayed similar levels of β -Gal protein (data not shown). These results are consistent with our observations that activated forms of PI3K or Akt alone are not capable of stimulating signaling pathways that lead to the phosphorylation and degradation of I κ B α as well as subsequent nuclear translocation and the DNA binding activity of NF- κ B (Fig. 3A and B). In support of our observations, we failed to detect significant activation of endogenous IKK activity in response to activated PI3K or AKT in 293T cells (data not shown). However, cells expressing H-Ras(V12) and Δ MEKK-1 proteins displayed increased IKK activity (data not shown). Thus, we found that activated forms of either PI3K or Akt when expressed alone do not induce signaling pathways that are capable of stimulating endogenous, I κ B α -specific IKK activity, I κ B α degradation, or nuclear translocation and DNA binding of NF- κ B.

Various cellular stimuli can activate NF- κ B-dependent transcription, at least in part, through mechanisms independent of signaling pathways which influence nuclear translocation. These signaling pathways stimulate the transactivation domain of the p65 subunit of NF- κ B, presumably by targeting basal or induced levels of NF- κ B in the nucleus (21, 47, 59a, 60, 68, 69).

Since activated forms of PI3K and Akt can increase the transcriptional activity of NF- κ B without stimulating nuclear translocation (Fig. 2A and 3A), we were interested in determining whether these signaling molecules could activate NF- κ B by targeting TAD 1 of the p65 subunit. To address this question, we used a plasmid bearing DNA encoding the Gal4-p65 fusion protein, where sequences encoding the DNA binding domain of Gal4 have been joined with sequences encoding TAD 1 of p65 (50). This plasmid, when cotransfected with a Gal4-Luc reporter, allowed us to determine whether cellular signals up-regulate gene expression by specifically targeting TAD 1 of the p65 subunit of NF- κ B. NIH 3T3 cells were cotransfected with a 4x-Gal4-Luc reporter, a Gal4-p65 expression construct, and plasmids bearing genes encoding activated H-Ras(V12), PI3K, or Akt. For control purposes, cells were also transfected under the same conditions, except expression constructs bearing genes encoding the Gal4-Elk-1 fusion protein were used instead of Gal4-p65. As shown in Fig. 3C, activated PI3K and Akt, as well as H-Ras(V12), stimulated TAD 1 of p65. Importantly, the ability of PI3K and Akt to activate TAD 1 of p65 was specific, since Gal4-Elk-1-mediated activity was stimulated by H-Ras(V12) but not by activated PI3K or Akt (Fig. 3C). These results indicate that PI3K and Akt, like H-Ras(V12), stimulate NF- κ B by targeting TAD 1 of the p65 subunit. However, unlike H-Ras(V12), which activates signal transduction pathways that increase NF- κ B transcriptional activity through both nuclear

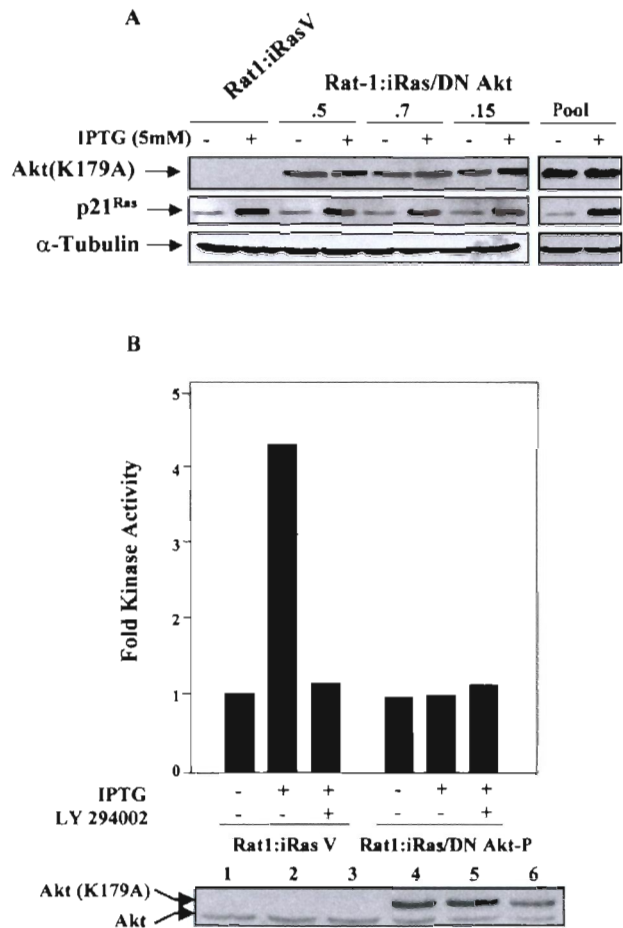


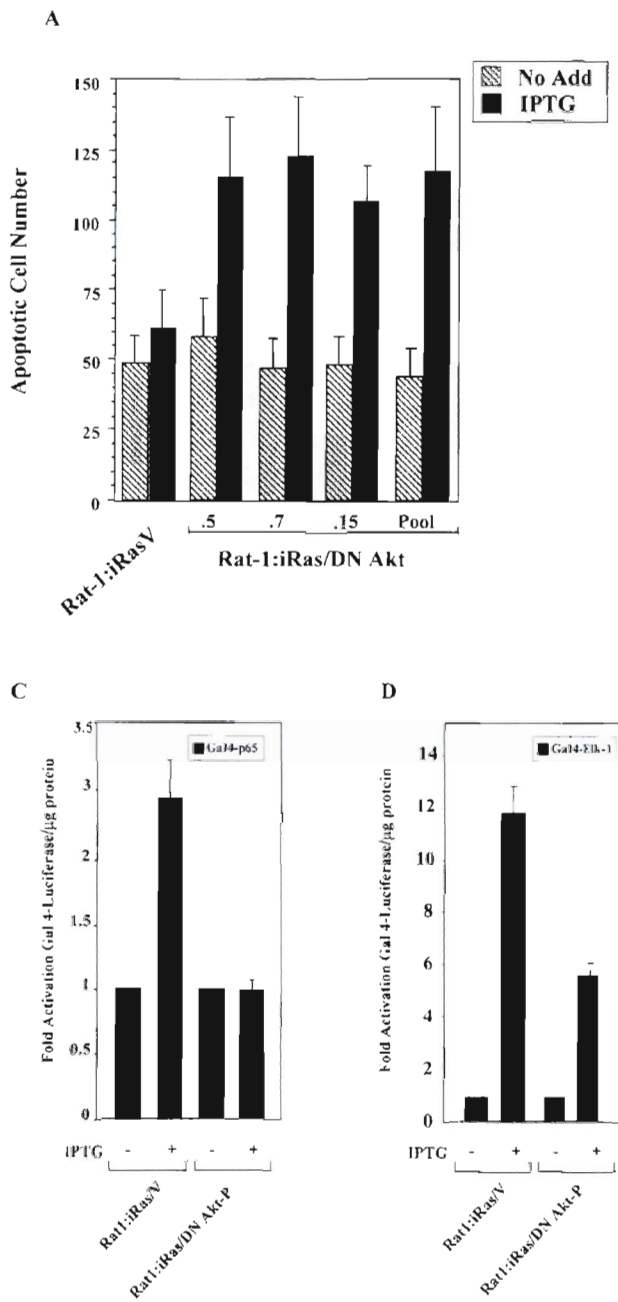
FIG. 5. Characterization of Rat-1:iRas cells expressing a dominant negative Akt protein. (A) Characterization of the Rat-1:iRas-dominant negative Akt cells. Rat-1:iRas cells ectopically expressing a plasmid bearing the gene encoding the dominant negative Akt(K179A) protein (DN Akt) or the vector control were generated, as described in the Materials and Methods. Total protein (50 μ g) was isolated from Rat-1:iRasV cells (vector control cells), three Rat-1:iRas-dominant negative Akt clones (.5, .7, and .15), and Rat-1:iRas-dominant negative Akt-P cells (Pool) in the absence or presence of IPTG (5 mM). Protein samples were resolved on an SDS-10% polyacrylamide gel, transferred to membrane, and analyzed for the presence of Akt, Ras, and α -tubulin. Akt(K179A) protein was detected using a hemagglutinin-specific antibody (BABCO). IPTG-induced p21^{Ras} expression was detected using a pan-Ras monoclonal antibody (Calbiochem, San Diego, Calif.). To ensure equal levels of protein loading, blots were reanalyzed with an α -tubulin-specific antibody (Sigma). Primary antibodies were detected using an HRP-labeled secondary antibody and by performing ECL. (B) Expression of the dominant negative Akt protein blocks H-Ras(V12)-induced endogenous Akt activity. Subconfluent Rat-1:iRasV and Rat-1:iRas-dominant negative Akt-P cells were grown overnight in medium containing 2% FBS. Eighteen hours later cells were washed and cultured for 4 h without serum and with or without IPTG (5 mM). Some groups received LY 294002 (10 μ M) 3 h after serum deprivation. Immunocomplex kinase assays for Akt were performed as described in Materials and Methods. The fold Akt activity was determined by obtaining values for Rat-1:iRasV and Rat-1:iRas-dominant negative Akt-P cells (grown in the absence of IPTG) and normalizing these numbers to 1. Data presented are representative of results of at least three different assays, which generated similar results. (Gel) Immunoblot analysis demonstrating that relatively equal amounts of total Akt protein were immunoprecipitated during the course of the experiment. Both endogenous Akt and hemagglutinin-tagged dominant negative Akt(K179A) proteins are shown.

translocation and an increased p65 transactivation potential, PI3K and Akt upregulate primarily the transactivation potential of the p65 subunit of NF- κ B. Consistent with this hypothesis, we detected basal levels of nuclear NF- κ B in proliferating

cells used in our experiments (data not shown). These findings suggest that PI3K and Akt stimulate the transcriptional activity of NF- κ B by targeting basal levels of nuclear NF- κ B and that these molecules effectively upregulate the transactivation potential of this transcription factor.

Activated Akt requires IKK to upregulate the transactivation domain of the p65 subunit of NF- κ B. In order to further explore a possible role of the IKK signalsome in Akt-induced activation of NF- κ B, we were interested in determining whether Akt required IKK to regulate NF- κ B transcriptional activity. To answer this question, NIH 3T3 cells were either transiently transfected with the 3 \times - κ B-Luc reporter or cotransfected with plasmids bearing genes encoding the Gal4-p65 and the Gal4-Luc reporters. In addition, cells were transfected with the vector control or with plasmids bearing the gene encoding M-Akt, dominant negative IKK β , or M-Akt plus dominant negative IKK β . Consistent with the ability of IKK to control NF- κ B nuclear translocation, NIH 3T3 cells expressing the dominant negative IKK β protein displayed reduced basal 3 \times - κ B luciferase activity (Fig. 4A). These results suggest that dominant negative IKK β blocked the accumulation of basal nuclear NF- κ B activity. However, as shown in Fig. 4A, the expression of dominant negative IKK β in NIH 3T3 cells blocked M-Akt-induced activation of NF- κ B, suggesting that M-Akt required endogenous IKK activity to regulate NF- κ B transcriptional activity. Since Akt did not induce nuclear localization of NF- κ B and since IKK activity has been implicated in controlling Akt activity (31, 44, 49), we were interested in determining whether IKK activity was required for Akt to stimulate TAD 1 of the p65 subunit of NF- κ B. As shown in Fig. 4B, expression of dominant negative IKK β blocked the ability of M-Akt to stimulate the transactivation potential of the Gal4-p65 protein. Importantly, expression of the dominant negative IKK β protein did not block expression of Gal4-p65 (Fig. 4B, gel). The ability of dominant negative IKK β to block Gal4-p65 activity was somewhat unexpected, because Gal4-p65 transcriptional activity is not under the control of I κ B-dependent phosphorylation and degradation events. The loss of Gal4-p65-induced luciferase activity in NIH 3T3 cells cotransfected with M-Akt and dominant negative IKK β was not due to the ability of dominant negative IKK β to inhibit pCMV-M-Akt expression, since relatively equal amounts of hemagglutinin-tagged Akt were observed (data not shown). Our results suggest that Akt activation alone does not induce NF- κ B through mechanisms involving I κ B degradation. Instead, our data indicate that Akt requires IKK to modulate TAD 1 of p65 through mechanisms independent of I κ B phosphorylation and degradation (see Discussion). These results may explain, at least to some degree, the observed dependence of IKK activity on Akt-dependent induction of NF- κ B activity (31, 49).

H-Ras(V12) requires Akt to stimulate the NF- κ B transactivation potential and to suppress oncogene-induced apoptosis. In order to investigate the physiological relevance of NF- κ B activation by Akt, it was important to inhibit endogenous Akt activities under conditions in which H-Ras(V12) was expressed. To experimentally address this point, we used the inducible Rat-1:iRas cell line, which contains stably integrated H-Ras(V12) under the control of an IPTG-responsive promoter (42). This cell line has been used previously to demonstrate that NF- κ B provides a cell survival role in H-Ras(V12) signaling (41). Rat-1:iRas cells were transfected with a plasmid bearing the gene encoding the dominant negative Akt(K179A) protein, and stable clones were generated. As shown in Fig. 5A, Rat-1:iRas-dominant negative Akt clones which expressed similar levels of the dominant negative Akt(K179A) protein were selected. Additionally, Rat-1:iRas-dominant negative



Akt stable clones displayed levels of IPTG-induced H-Ras expression similar to that of the vector control cells (Rat-1:iRasV) (Fig. 4A). Rat-1:iRas-dominant negative Akt clones (namely, .5, .7, and .15) were combined to create a pooled cell line (Rat-1:iRas-dominant negative Akt-P) (Fig. 5A).

To determine whether cells expressing the dominant negative Akt(K179A) protein displayed a reduction in H-Ras(V12)-induced Akt activity, immune complex kinase assays were performed using Crosstide as an Akt-specific peptide substrate (14). As shown in Fig. 5B, Rat-1:iRasV control cells demonstrated a fourfold increase in Akt activity following IPTG-induced H-Ras(V12) expression. In contrast, Rat-1:iRas-dominant negative Akt-P cells, constitutively expressing Akt

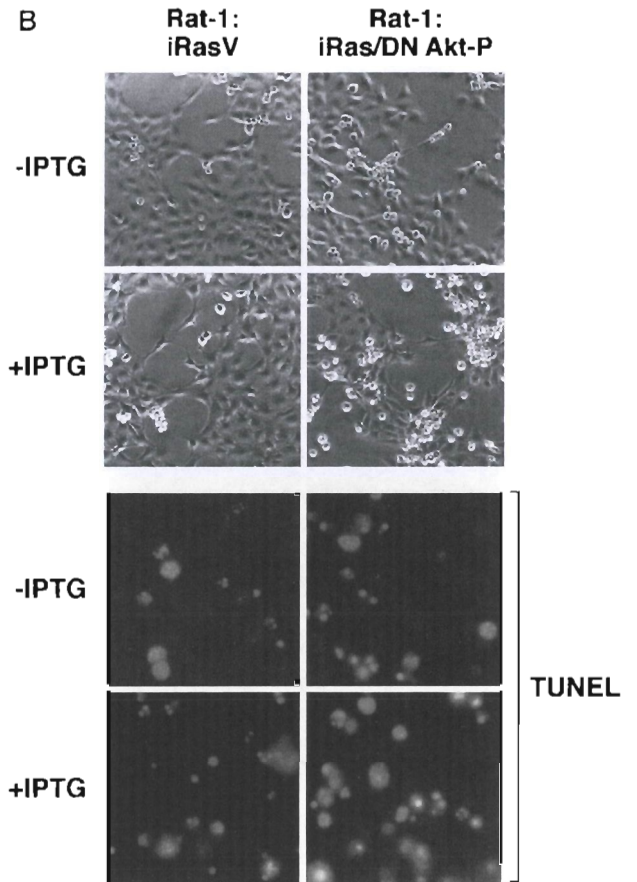


FIG. 6. The inhibition of endogenous Akt activity sensitizes cells to H-Ras (V12)-induced apoptosis. (A) Expression of H-Ras(V12) is associated with an increase in apoptosis in cells expressing the dominant negative Akt protein (DN Akt). Rat-1:iRasV, Rat-1:iRas-dominant negative Akt clones (.5, .7, and .15), and Rat-1:iRas-dominant negative Akt-P cells (pooled clone) were grown overnight in medium containing a reduced concentration of serum (2% FBS). Eighteen hours later, cells were treated in either the absence or presence of IPTG (5 mM). Apoptotic cells were harvested from the supernatants 48 h after IPTG addition, fixed in paraformaldehyde, and stained with Hoechst dye, and cells displaying nuclear fragmentation and condensation were counted, as described in Materials and Methods. Results are expressed as numbers of apoptotic cells (means \pm standard deviations). Assays were repeated at least three independent times. (B) Rat-1:iRasV and Rat-1:iRas-dominant negative Akt-P cells were cultured and stimulated with IPTG as described above. Cell morphologies were analyzed 48 h after IPTG addition. Paraformaldehyde-fixed cells were analyzed for apoptosis by performing TUNEL analysis (Boehringer Mannheim). The upper four images show phase-contrast microscopy (magnification, $\times 20$). The bottom four images show fluorescence microscopy of TUNEL-positive cells (magnification, $\times 40$). (C) H-Ras(V12) no longer stimulates the p65 transactivation domain in cells stably expressing the dominant negative Akt protein. Rat-1:iRasV and Rat-1:iRas-dominant negative Akt-P cells (pooled clone) were transfected with the Gal4-luciferase reporter (100 ng) and with constructs bearing the gene encoding the Gal4-p65 fusion protein (100 ng). Eighteen hours following transfections, cells were stimulated with IPTG (5 mM). Twenty-four hours following IPTG addition, cell extracts were isolated and luciferase activities were determined. Results are the averages \pm standard deviations from three independent experiments performed in triplicate. (D) H-Ras(V12) stimulates Gal4-Elk-1 in the vector control and cells expressing dominant negative Akt [Akt(K179A)]. Cells were transfected with Gal4-luciferase and Gal4-Elk-1 (100 ng each). Twenty-four hours posttransfection, cells were incubated in either DMEM containing 10% serum and IPTG (5 mM) or DMEM plus 10% serum alone for an additional 24 h. Whole-cell extracts were isolated and assayed for luciferase levels. Results are expressed as multiples of the level of activation obtained with the vector control or dominant negative Akt-P without IPTG incubation and are the averages \pm standard deviations of results of three independent experiments performed in triplicate.

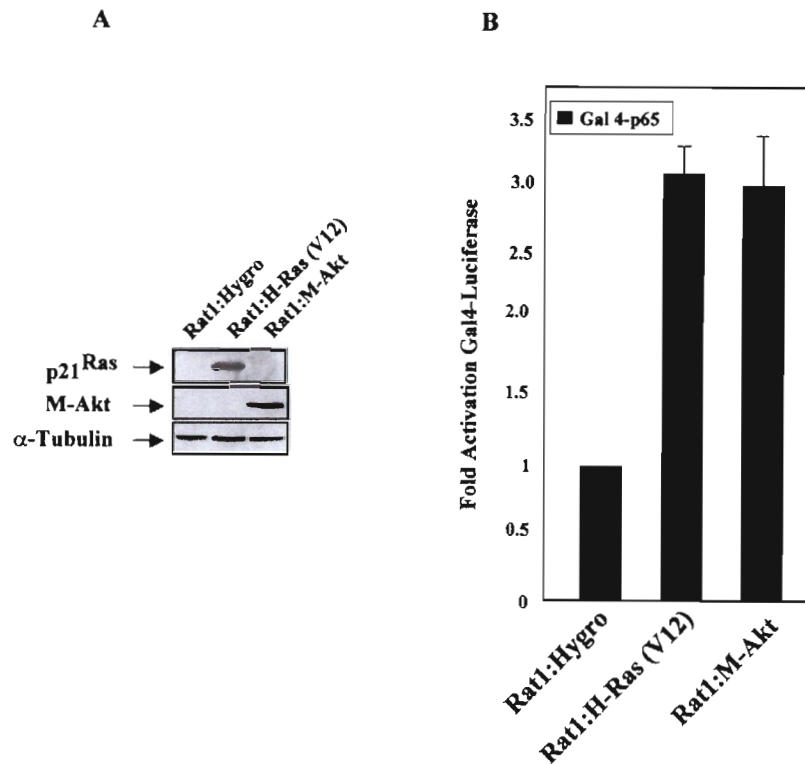


FIG. 7. M-Akt-transformed cells require NF- κ B to block etoposide-induced apoptosis. (A) Generation of H-Ras(V12)- and M-Akt-transformed Rat-1 cells. Rat-1 cells stably expressing activated H-Ras(V12) or M-Akt were generated as described in Materials and Methods. Total protein (50 μ g) was isolated from Rat-1:Hygro, Rat-1:H-Ras(V12), and Rat-1:M-Akt cells, resolved by performing PAGE, and transferred to nitrocellulose membrane. Immunoblot analysis was performed to detect transgenic expression of p21^{Ras} and M-Akt using the pan-Ras antibody or the hemagglutinin antibody, respectively. (B) The p65 transactivation domain is activated in Rat-1 cells transformed with either H-Ras(V12) or M-Akt. Rat-1:Hygro, Rat-1:H-Ras(V12), and Rat-1:M-Akt cells were transiently transfected with a Gal4-luciferase reporter (100 ng) and with constructs bearing the genes encoding Gal4-p65 (100 ng). Forty-eight hours following the start of transfection, cell extracts were harvested and luciferase activities were determined. Data are the averages \pm standard deviations of results of three experiments performed in triplicate. (C) Rat-1:M-Akt cells are resistant to apoptotic induction agents. Rat-1:Hygro and Rat-1:M-Akt cells were either left untreated (No Add) or given etoposide (15 μ M) or staurosporine (50 μ M). Apoptotic cell numbers were determined 18 h following the addition of either etoposide or staurosporine (Stauro). Results presented here are the means \pm standard deviations of results of two independent experiments performed in duplicate. (D) M-Akt requires NF- κ B to overcome etoposide-induced apoptosis. Rat-1:M-Akt cells were cultured overnight in medium containing 2% FBS, after which cells were infected with either Ad-CMV or Ad-SRI κ B α (50 PFU/cell). Six hours following adenovirus-mediated gene delivery, cells were either left untreated (No Add) or treated with either etoposide (5 μ M) or staurosporine (25 μ M). Apoptotic cell numbers were analyzed in etoposide-treated Rat-1:M-Akt cells over the time course indicated, while the apoptotic cell numbers detected for staurosporine were analyzed 60 h after the drug addition. Data presented are the averages \pm standard deviations of results of two different experiments where the numbers of apoptotic cells were counted in triplicate. (Gcl) Immunoblot analysis demonstrating that Ad-SRI κ B α is effectively expressed in the Rat-1 cell lines. κ B α proteins were detected using a rabbit polyclonal antibody (C-21; Santa Cruz Biotech). Protein samples analyzed in lanes 1, 3, 5, and 7 are from Rat-1:M-Akt cells infected with Ad-CMV, while those in lanes 2, 4, 6, and 8 are from cells infected with Ad-SRI κ B α .

(K179A) protein, failed to display increases in Akt kinase activity following IPTG addition (Fig. 5B). Phosphorylation of the crossside by endogenous Akt was specific to IPTG-induced H-Ras(V12) expression, and kinase activity was inhibited by the PI3K inhibitor LY 294002 (Fig. 5B). Differences in kinase activities between Rat-1:iRasV and Rat-1:iRas-dominant negative Akt-P cells were not due to unequal amounts of immunoprecipitated Akt, since analysis of input protein demonstrated that similar levels of protein were analyzed for the kinase activity (Fig. 5B, gel). These results indicate that the expression of the dominant negative Akt protein blocked the ability of H-Ras(V12) to stimulate endogenous Akt activity in Rat-1:iRas-dominant negative Akt-P cells.

To determine whether the loss of endogenous Akt activity would sensitize cells to H-Ras(V12)-induced apoptosis in our model system, Rat-1:iRasV and Rat-1:iRas-dominant negative Akt clones were grown in complete medium containing a reduced concentration of serum (2% FBS) in either the absence or presence of IPTG to induce H-Ras(V12) expression. Forty-eight hours after IPTG addition, cellular supernatants containing detached cells were harvested, fixed, and stained with

Hoechst dye and cells displaying fragmented nuclei were counted as described in Materials and Methods. As shown in Fig. 6A, both Rat-1:iRasV and Rat-1:iRas-dominant negative Akt clones displayed elevated basal apoptotic cell numbers (without IPTG) when cells were cultured with a reduced concentration of serum (2% FBS). However, this effect was not observed in cells cultured under normal conditions (10% FBS) (data not shown). Consistent with the antiapoptotic nature of Akt, we found that cells expressing the dominant negative Akt (K179A) protein were more susceptible to H-Ras(V12)-induced apoptosis than the control Rat-1:iRasV cells (Fig. 6A). Compared to vector control Rat-1:iRasV cells, IPTG-induced Rat-1:iRas-dominant negative Akt-P cells displayed enhanced morphological signs of apoptosis, including retraction of cellular processes, nuclear condensation, and loss of adherence (Fig. 6B, top). Moreover, IPTG-induced H-Ras(V12) expression stimulated apoptosis in Rat-1:iRas-dominant negative Akt-P cells, as detected by the appearance of TUNEL-positive cells (Fig. 6B, bottom). These results are consistent with reports indicating that Akt provides a cell survival signal downstream

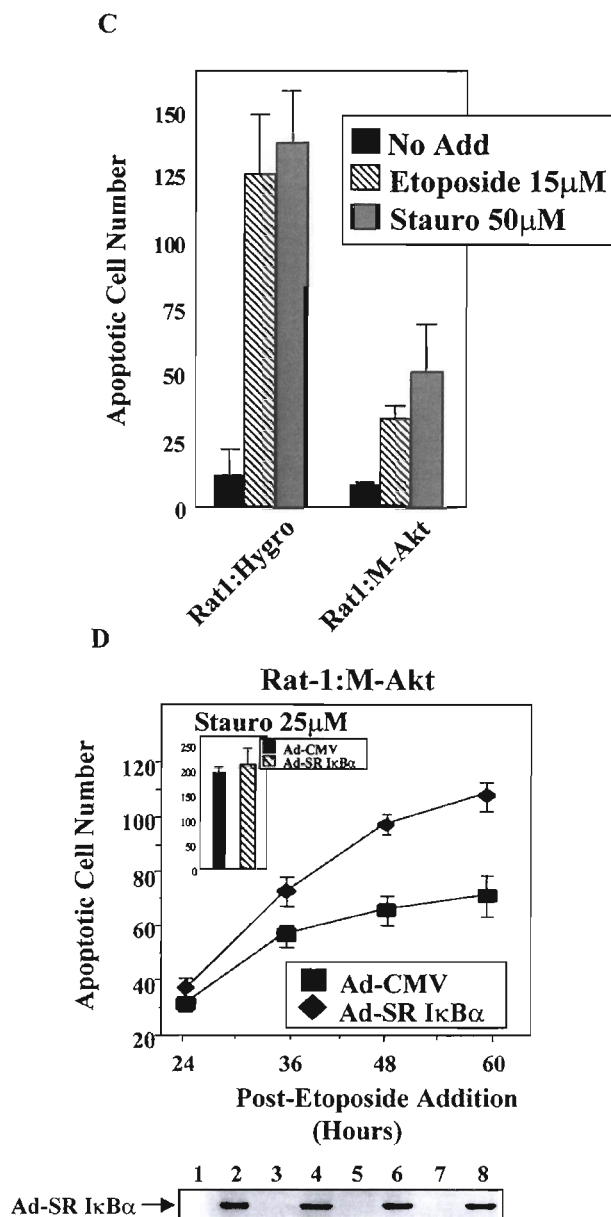


FIG. 7—Continued.

of activated H-Ras (33, 48) and indicate that Akt is one of the major antiapoptotic mediators of oncogenic Ras signaling.

To elucidate whether H-Ras(V12)-induced apoptosis, following the inhibition of Akt, was associated with a loss in NF- κ B transcriptional activity, transient-cotransfection assays were performed. As shown in Fig. 6C, the addition of IPTG to the control Rat-1:iRasV cells led to a subsequent increase in H-Ras(V12)-induced Gal4-p65 transcriptional activity. However, Rat-1:iRas-dominant negative Akt-P cells failed to show an increase in Gal4-p65 transcriptional activity following IPTG-induced H-Ras(V12) expression (Fig. 6C). To show that Akt-mediated signaling pathways defective in Rat-1:iRas-dominant negative Akt-P cells were specific for Gal4-p65, similar experiments were performed using Gal4-Elk-1. Rat-1:iRas-dominant negative Akt-P and vector control cells were capable of stimulating Gal4-Elk-1 activity following IPTG-induced

H-Ras(V12) expression (Fig. 6D). Thus, cells expressing the dominant negative Akt (K179A) still retain the ability to signal to other Ras effector pathways. Collectively, our results indicate that the inhibition of endogenous Akt activity is associated with a loss of H-Ras-induced NF- κ B-dependent transcription and enhanced susceptibility of these cells to apoptosis.

Akt-transformed Rat-1 cells require NF- κ B to suppress apoptosis induced by etoposide. Although our data implicate NF- κ B as a downstream mediator of the Akt cell survival response, we needed to determine whether the ability of Akt to transcriptionally upregulate NF- κ B contributes to the antiapoptotic function of this kinase. To address this point, we made stable cell lines which expressed activated forms of Ras [Rat-1: H-Ras(V12)] or Akt (Rat-1:M-Akt) or which contained the vector control plasmid (Rat-1:hygro [Hygro]). As shown in Fig. 7A, Rat-1 clones which express relatively equal levels of either H-Ras(V12) or M-Akt were selected. Unlike the Rat-1:Hygro control cells, both Rat-1:H-Ras(V12) and Rat-1:M-Akt cells displayed characteristics of transformed cells, as indicated by their abilities to form foci and to grow in soft agar (data not shown). Consistent with transient-transfection assays (Fig. 3C), we found that both Rat-1:H-Ras(V12) and Rat-1:M-Akt cells displayed elevated Gal4-p65 transcriptional activity, compared to that of the Rat-1:Hygro control cells (Fig. 7B). These results are consistent with the ability of H-Ras(V12) and M-Akt to stimulate NF- κ B by targeting TAD 1 of the p65 subunit.

To further confirm that NF- κ B is a downstream target of Akt, we took advantage of the fact that it has been recently demonstrated that Akt provides a cell survival signal that blocks apoptosis initiated by the PKC inhibitor, staurosporine, or by the topoisomerase II inhibitor, etoposide (8). Importantly, unlike staurosporine, which does not activate NF- κ B (58), etoposide is known to stimulate endogenous NF- κ B-responsive gene transcription (32, 59a). To determine whether M-Akt expression provides a cell survival function in response to proapoptotic agents, Rat-1:Hygro and Rat-1:M-Akt cells were treated in either the absence or presence of etoposide (15 μ M) or staurosporine (50 μ M) and apoptotic cell numbers were determined 18 h after drug addition. As shown in Fig. 7C, Rat-1:M-Akt cells were more resistant to etoposide- and staurosporine-induced apoptosis than the Rat-1:Hygro control cells. These results are consistent with previous findings demonstrating that activated Akt is capable of suppressing apoptosis by phosphorylating and inactivating procaspase-9 (8). The addition of etoposide to Rat-1:M-Akt cells stimulated NF- κ B-induced transcription in transient-transfection assays. However, staurosporine was unable to stimulate the transcriptional activity of NF- κ B in these cells (data not shown). Therefore, despite the ability of M-Akt to overcome apoptosis induced by etoposide and staurosporine, only etoposide-induced stress signals are capable of activating NF- κ B.

To determine whether M-Akt-transformed cells required NF- κ B to suppress apoptosis in response to etoposide, we used the SR I κ B α (6). This mutant I κ B α protein acts as a transdominant negative protein because it binds to NF- κ B and inhibits nuclear translocation and DNA binding (41, 47, 57). Importantly, expression of the SR I κ B α protein blocks the activation of NF- κ B-responsive genes (27, 58). Rat-1:M-Akt cells were infected with Ad-SRI κ B α or with Ad-CMV, and cells were treated with either etoposide or staurosporine. Adenovirus-mediated delivery of transgenes is extremely effective in Rat-1:M-Akt cells, where $\geq 95\%$ of cells effectively express transgenes 12 h following viral infection (Fig. 7D, gel, and data not shown). Rat-1:M-Akt cells were more susceptible to etoposide-induced apoptosis following the inhibition of NF- κ B by Ad-SRI κ B α than cells infected with Ad-CMV (control virus)

(Fig. 7D). However, compared to Rat-1:Hygro control cells, Rat-1:M-Akt cells were more resistant to apoptotic signals induced by etoposide even after the inhibition of NF- κ B transcriptional activity (data not shown). Although NF- κ B functions as a cell survival factor, these results suggest that other NF- κ B-independent pathways which provide strong antiapoptotic signals exist. Therefore, we presume that since Rat-1 cells express both Bad and caspase-9, these downstream targets are likely to be controlled by H-Ras(V12)-induced Akt activity in the absence of NF- κ B transcriptional activity. Although Rat-1:M-Akt cells were more resistant to apoptosis induced by staurosporine, the expression of SR-I κ B α did not sensitize staurosporine-treated cells to programmed cell death (Fig. 7D, inset). These results indicate that Rat-1:M-Akt cells require NF- κ B to overcome proapoptotic death pathways induced by etoposide but not signals stimulated by staurosporine. Thus, Akt is an important antiapoptotic signaling molecule that contributes to cell survival not only by directly phosphorylating proapoptotic targets but also by stimulating the transcriptional activity of NF- κ B.

DISCUSSION

The data presented here indicate that one mechanism whereby Akt-controlled signaling pathways inhibit apoptosis is through the activation of the transcription factor NF- κ B. Loss of endogenous Akt is associated with a downregulation in the transcriptional activity of NF- κ B and with H-Ras(V12)-induced apoptosis. Moreover, we find that activated Akt requires NF- κ B to partially suppress etoposide-induced apoptosis. Consistent with previous findings which demonstrate that Akt can inhibit multiple proapoptotic molecules through direct phosphorylation events (7, 8, 15, 16, 36), we found that the loss of NF- κ B transcriptional activity did not completely sensitize Akt-expressing cells to apoptosis in response to etoposide (Fig. 7D). Thus, our work and the work of others indicate that Akt mediates cell survival signals through immediate phosphorylation of proapoptotic proteins and through longer-term transcription-dependent mechanisms. These findings are consistent with extensive evidence for an antiapoptotic role for NF- κ B in blocking certain apoptotic stimuli and indicate that NF- κ B is a downstream target of Akt-induced cell survival signals.

We explored the potential involvement of Akt as a mediator in signaling between oncogenic Ras and NF- κ B. Oncogenic Ras has been demonstrated to induce both proapoptotic and antiapoptotic signals (40, 51), and we have shown previously that oncogenic Ras stimulates the transcriptional activity of NF- κ B to overcome H-Ras(V12)-induced apoptosis (41). Since both PI3K and Akt have been shown to provide an antiapoptotic signal in response to oncogenic Ras expression, we asked whether PI3K and Akt provide the link to NF- κ B activation. In this study, we have found that H-Ras(V12) requires the antiapoptotic pathways involving PI3K and Akt to stimulate the transcriptional activity of NF- κ B. Consistent with this, we demonstrate that inhibition of endogenous Akt kinase activity suppresses H-Ras(V12)-induced NF- κ B transcription and sensitizes cells to apoptosis. Although Akt was required to suppress apoptosis induced by H-Ras(V12), Ras is able to utilize additional signaling pathways to activate NF- κ B-dependent cell survival. This supposition is supported by our observations that inhibition of NF- κ B with the SR I κ B α further sensitized Rat-1:Ras-dominant negative Akt-P cells to Ras-mediated apoptosis (data not shown). Interestingly, unlike H-Ras(V12), M-Akt-transformed cells did not undergo apoptosis following the inactivation of NF- κ B with the SR I κ B α protein (data not shown). This observation suggests that, unlike H-Ras

(V12), activated Akt does not stimulate signaling pathways which induce cell death. An alternative possibility, however, is that the overexpression of M-Akt is such a powerful antiapoptotic factor that it overcomes programmed cell death signals following the inactivation of NF- κ B. Nevertheless, the evidence that Akt-induced activation of NF- κ B provides a cell survival function is shown by the ability of NF- κ B to protect Akt-expressing cells from etoposide-induced apoptosis (Fig. 7D).

The regulation of NF- κ B by Akt is likely to be important in cytokine and growth factor signaling, since many of the physiological inducers of Akt also stimulate the transcriptional activity of NF- κ B. Recently, physiological stimuli, including TNF- α , IL-1 β and PDGF, have been shown to activate NF- κ B in a PI3K- and Akt-dependent manner (31, 44, 49, 52). It is intriguing that the cell survival mechanisms and potentially the mitogenic pathways associated with growth factor signaling is controlled, at least partially, by NF- κ B-dependent mechanisms. Consistent with this point, we and others (27, 30) have recently shown that NF- κ B can promote cell growth by controlling the transcription of the cyclin D1 gene. It will be important to determine if Akt-derived mitogenic signals involve the transcription function of NF- κ B, possibly through the controlled upregulation of cyclin D1 or other functionally related proteins.

Previous work has indicated that PI3K and Akt are involved in NF- κ B activation. For example, it was shown (4) that activation of NF- κ B in response to the tyrosine phosphatase inhibitor pervanadate was blocked by the PI3K inhibitor wortmannin. It was proposed that tyrosine-phosphorylated I κ B α associated with the p85 subunit of PI3K, allowing nuclear translocation of NF- κ B. In that study, wortmannin did not block the ability of TNF to induce nuclear translocation of NF- κ B. Stark and colleagues have shown recently (52) that IL-1 β stimulates the association of the IL-1 receptor accessory protein with the p85 subunit of PI3K and that, consistent with our results, this leads to the stimulation of the transactivation potential of the p65 subunit of NF- κ B. Interestingly, it was shown that this response also leads to phosphorylation of the p65 subunit, but the site of this phosphorylation was not mapped. Additionally, Kane and colleagues (31) have shown that Akt expression augmented the ability of PMA to activate NF- κ B through enhanced I κ B α phosphorylation and degradation. The ability of Akt to synergize with PMA on the activation of an NF- κ B promoter was blocked by a kinase-inactive IKK. Interestingly, Akt was unable to activate NF- κ B nuclear translocation on its own, consistent with our data. More recently, two reports implicate Akt in NF- κ B activation induced by TNF (44) and by PDGF (49). Several such reports implicate IKK activity as being required for the Akt-controlled response.

Our data indicate that Akt activation alone is insufficient to activate endogenous IKK activity and NF- κ B nuclear translocation. However, our data demonstrate that Akt signals to a pathway that stimulates the transcriptional potential of the p65 subunit of NF- κ B through activation of TAD 1. Even though Akt is a serine/threonine kinase, it is unlikely that this protein directly phosphorylates p65 since the TAD 1 region does not contain consensus Akt phosphorylation sites. Moreover, we have been unsuccessful at detecting protein-protein interactions between p65 and Akt. (L. V. Madrid, A. S. Baldwin, Jr., and M. W. Mayo, unpublished observations). However, mutation of serine 529 in TAD 1 of p65, which is known to be phosphorylated in response to TNF signaling (60), inhibits the ability of Akt to activate p65 transcription. (Madrid et al., unpublished observations). As mentioned earlier, and in apparent contrast with reports which indicate that the role of Akt in inducing NF- κ B activity occurs through IKK-dependent

degradation of I κ B α (31, 44, 49), the overexpression of activated Akt is unable to stimulate endogenous IKK activity or I κ B α degradation (Fig. 3B and data not shown). In contrast, H-Ras(V12) expression in cells is able to stimulate endogenous IKK activity, induce degradation of I κ B α , and increase nuclear translocation and DNA binding of NF- κ B (Fig. 3A and B and data not shown). These results suggest that H-Ras(V12) regulates NF- κ B through two signals: one that leads to nuclear localization of NF- κ B and one that activates the transactivation function of the p65 subunit. Although M-Akt does not stimulate endogenous IKK activity directed towards I κ B α degradation, the IKK signalosome complex is still important in regulating the ability of Akt to stimulate NF- κ B. This hypothesis is supported by the observation that a dominant negative IKK β protein inhibited the ability of Akt to stimulate TAD 1 of p65 (Fig. 4B). These results suggest that IKK activity (possibly independent of I κ B α phosphorylation) or some structural aspect of IKK is required for the ability of Akt to stimulate NF- κ B transactivation function. The fact that Gal4-p65 is not regulated through an I κ B-dependent mechanism suggests that IKK is required for Akt to activate TAD 1 of p65, independent of nuclear translocation signals. Collectively, these results suggest that the IKK signalosome complex is capable of regulating NF- κ B through signaling events involved in nuclear translocation as well as Akt-induced transactivation pathways. Although our data indicate that Akt alone is unable to stimulate I κ B α degradation on its own, they do not rule out the possibility that Akt is required (but not sufficient) for activation of I κ B α phosphorylation and degradation in response to certain signal transduction cascades.

Our results demonstrating that H-Ras(V12) requires PI3K and Akt to stimulate NF- κ B-dependent transcription and cell survival are very likely to be important in cancer biology. Human tumors displaying upregulated endogenous Akt (10, 11, 23) or lacking tumor suppressor gene products which modulate PI3K activities, such as the PTEN phosphatidylinoside phosphatase (39, 53), may utilize elevated transcriptional activities of antiapoptotic and proliferative transcription factors, like NF- κ B, to enhance oncogenic potential. Therefore, loss of PTEN, which occurs in a variety of tumors (17, 37, 45, 54, 62), is predicted to lead to the upregulation of NF- κ B, providing signals potentially relevant to oncogenesis (27, 41).

The data provided here are consistent with those of other reports indicating that transforming events which upregulate Akt activity have profound effects not only on cell survival in terms of oncogenesis but also on chemoresistance. Along these lines, the activation of Akt in tumor cells may synergize with a chemotherapeutic response (such as that induced by etoposide) to provide an enhanced antiapoptotic function. Thus, the induction of NF- κ B nuclear translocation by etoposide plus an Akt signal to stimulate transactivation function may lead to a potent antiapoptotic response through enhanced regulation of antiapoptotic genes. In support of this point, we demonstrate that M-Akt provides resistance to the apoptotic agent etoposide and that M-Akt-mediated resistance to etoposide requires the transcriptional activity of NF- κ B. Since NF- κ B functions to positively upregulate gene products which are known to overcome chemotherapy-induced apoptosis, such as c-IAP1, c-IAP2, and A1 (12, 26, 58, 59a, 70), future experiments will determine whether constitutively active Akt potentiates chemoresistance by regulating expression of NF- κ B-controlled antiapoptotic gene products.

ACKNOWLEDGMENTS

We thank Channing Der (University of North Carolina) for kindly providing H-Ras(V12) and the activated Ras effector mutants, Phillip

Hawkins (The Babraham Institute, Cambridge, United Kingdom) for providing dominant negative Akt(T308A) constructs, and Anke Klippel (Chiron Corporation, Emeryville, Calif.) for providing the other PI3K and Akt constructs used in this study. We also thank Michael J. Weber and Sandy Westerheide for critical readings of the manuscript.

This research was supported by NIH grants awarded to M.W.M. (K01 78595), A.S.B. (CA72771), A.S.B. and M.W.M. (CA75080), and C.-Y.W. (DE/CA13196-01A1).

L. V. Madrid and M. W. Mayo contributed equally to the scientific merit and preparation of this paper.

REFERENCES

- Baldwin, A. S., Jr. 1996. The NF-kappa B and I kappa B proteins: new discoveries and insights. *Annu. Rev. Immunol.* **14**:649-683.
- Beg, A. A., and D. Baltimore. 1996. An essential role for NF-kappa B in preventing TNF-alpha-induced cell death. *Science* **274**:782-784.
- Bellacosa, A., J. R. Testa, S. P. Staal, and P. N. Tsichlis. 1991. A retroviral oncogene, akt, encoding a serine-threonine kinase containing an SH2-like region. *Science* **254**:274-277.
- Beraud, C., W. J. Henzel, and P. A. Baeuerle. 1999. Involvement of regulatory and catalytic subunits of phosphoinositide 3-kinase in NF-kappa B activation. *Proc. Natl. Acad. Sci. USA* **96**:429-434.
- Bird, T. A., K. Schooley, S. K. Dower, H. Hagen, and G. D. Virca. 1997. Activation of nuclear transcription factor NF-kappa B by interleukin-1 is accompanied by casein kinase II-mediated phosphorylation of the p65 subunit. *J. Biol. Chem.* **272**:32606-32612.
- Brockman, J. A., D. C. Scherer, T. A. McKinsey, S. M. Hall, X. Qi, W. Y. Lee, and D. W. Ballard. 1995. Coupling of a signal response domain in I κ B α to multiple pathways for NF- κ B activation. *Mol. Cell. Biol.* **15**:2809-2818.
- Brunet, A., A. Bonni, M. J. Zigmond, M. Z. Lin, P. Juo, E. S. Hu, M. J. Anderson, K. C. Arden, J. Blenis, and M. E. Greenberg. 1999. Akt promotes cell survival by phosphorylating and inhibiting a Forkhead transcription factor. *Cell* **96**:857-868.
- Cardone, M. H., N. Roy, H. R. Stennicke, G. S. Salvesen, T. F. Franke, E. Stanbridge, S. Frisch, and J. C. Reed. 1998. Regulation of cell death protease caspase-9 by phosphorylation. *Science* **282**:1318-1321.
- Chang, H. W., M. Aoki, D. Fruman, K. R. Auger, A. Bellacosa, P. N. Tsichlis, L. C. Cantley, T. M. Roberts, and P. K. Vogt. 1997. Transformation of chicken cells by the gene encoding the catalytic subunit of PI 3-kinase. *Science* **276**:1848-1850.
- Cheng, J. Q., D. A. Altomare, M. A. Klein, W. C. Lee, G. D. Kruh, N. A. Lissy, and J. R. Testa. 1997. Transforming activity and mitosis-related expression of the AKT2 oncogene: evidence suggesting a link between cell cycle regulation and oncogenesis. *Oncogene* **14**:2793-2801.
- Cheng, J. Q., B. Ruggeri, W. M. Klein, G. Sonoda, D. A. Altomare, D. K. Watson, and J. R. Testa. 1996. Amplification of AKT2 in human pancreatic cells and inhibition of AKT2 expression and tumorigenicity by antisense RNA. *Proc. Natl. Acad. Sci. USA* **93**:3636-3641.
- Chu, Z. L., T. A. McKinsey, L. Liu, J. J. Gentry, M. H. Malim, and D. W. Ballard. 1997. Suppression of tumor necrosis factor-induced cell death by inhibitor of apoptosis c-IAP2 is under NF-kappa B control. *Proc. Natl. Acad. Sci. USA* **94**:10057-10062.
- Coffer, P. J., and J. R. Woodgett. 1991. Molecular cloning and characterization of a novel putative protein-serine kinase related to the cAMP-dependent and protein kinase C families. *Eur. J. Biochem.* **201**:475-481.
- Cross, D. A., D. R. Alessi, P. Cohen, M. Andjelkovic, and B. A. Hemmings. 1995. Inhibition of glycogen synthase kinase-3 by insulin mediated by protein kinase B. *Nature* **378**:785-789.
- Datta, S. R., H. Dudek, X. Tao, S. Masters, H. Fu, Y. Gotoh, and M. E. Greenberg. 1997. Akt phosphorylation of BAD couples survival signals to the cell-intrinsic death machinery. *Cell* **91**:231-241.
- del Peso, L., M. Gonzalez-Garcia, C. Page, R. Herrera, and G. Nunez. 1997. Interleukin-3-induced phosphorylation of BAD through the protein kinase Akt. *Science* **278**:687-689.
- Di Cristofano, A., B. Pesce, C. Cordon-Cardo, and P. P. Pandolfi. 1998. Pten is essential for embryonic development and tumour suppression. *Nat. Genet.* **19**:348-355.
- Downward, J. 1998. Lipid-regulated kinases: some common themes at last. *Science* **279**:673-674.
- Downward, J. 1998. Ras signalling and apoptosis. *Curr. Opin. Genet. Dev.* **8**:49-54.
- Finco, T. S., and A. S. Baldwin, Jr. 1993. Kappa B site-dependent induction of gene expression by diverse inducers of nuclear factor kappa B requires Raf-1. *J. Biol. Chem.* **268**:17676-17679.
- Finco, T. S., and A. S. Baldwin. 1995. Mechanistic aspects of NF-kappa B regulation: the emerging role of phosphorylation and proteolysis. *Immunity* **3**:263-272.
- Finco, T. S., J. K. Westwick, J. L. Norris, A. A. Beg, C. J. Der, and A. S. Baldwin, Jr. 1997. Oncogenic Ha-Ras-induced signaling activates NF-kappa B transcriptional activity, which is required for cellular transformation. *J. Biol. Chem.* **272**:24113-24116.

23. Franke, T. F., D. R. Kaplan, and L. C. Cantley. 1997. PI3K: downstream AKTion blocks apoptosis. *Cell* **88**:435-437.
24. Fruman, D. A., R. E. Meyers, and L. C. Cantley. 1998. Phosphoinositide kinases. *Annu. Rev. Biochem.* **67**:481-507.
25. Ghosh, S., M. J. May, and E. B. Kopp. 1998. NF-kappa B and Rel proteins: evolutionarily conserved mediators of immune responses. *Annu. Rev. Immunol.* **16**:225-260.
26. Grumont, R. J., I. J. Rourke, and S. Gerondakis. 1999. Rel-dependent induction of A1 transcription is required to protect B cells from antigen receptor ligation-induced apoptosis. *Genes Dev.* **13**:400-411.
27. Guttridge, D. C., C. Albanese, J. Y. Reuther, R. G. Pestell, and A. S. Baldwin, Jr. 1999. NF-kappa B controls cell growth and differentiation through transcriptional regulation of cyclin D1. *Mol. Cell. Biol.* **19**:5785-5799.
28. Han, J., K. Luby-Phelps, B. Das, X. Shu, Y. Xia, R. D. Mosteller, U. M. Krishna, J. R. Falck, M. A. White, and D. Broek. 1998. Role of substrates and products of PI 3-kinase in regulating activation of Rac-related guanine triphosphatases by Vav. *Science* **279**:558-560.
29. Hawkins, P. T., H. Welch, A. McGregor, A. Eguinoa, S. Gobert, S. Krugmann, K. Anderson, D. Stokoe, and L. Stephens. 1997. Signalling via phosphoinositide 3OH kinases. *Biochem. Soc. Trans.* **25**:1147-1151.
30. Hinz, M., D. Krappmann, A. Eichten, A. Heder, C. Scheidereit, and M. Strauss. 1999. NF-kappa B function in growth control: regulation of cyclin D1 expression and G₀/G₁-to-S-phase transition. *Mol. Cell. Biol.* **19**:2690-2698.
31. Kane, L. P., V. S. Shapiro, D. Stokoe, and A. Weiss. 1999. Induction of NF-kappaB by the Akt/PKB kinase. *Curr. Biol.* **9**:601-604.
32. Kasibhatla, S., T. Brunner, L. Genestier, F. Echeverri, A. Mahboubi, and D. R. Green. 1998. DNA damaging agents induce expression of Fas ligand and subsequent apoptosis in T lymphocytes via the activation of NF-kappa B and AP-1. *Mol. Cell* **1**:543-551.
33. Kauffmann-Zeh, A., P. Rodriguez-Viciana, E. Ulrich, C. Gilbert, P. Coffey, J. Downward, and G. Evan. 1997. Suppression of c-Myc-induced apoptosis by Ras signalling through PI(3)K and PKB. *Nature* **385**:544-548.
34. Khwaja, A., P. Rodriguez-Viciana, S. Wennstrom, P. H. Warne, and J. Downward. 1997. Matrix adhesion and Ras transformation both activate a phosphoinositide 3-OH kinase and protein kinase B/Akt cellular survival pathway. *EMBO J.* **16**:2783-2793.
35. Klippel, A., W. M. Kavanaugh, D. Pot, and L. T. Williams. 1997. A specific product of phosphatidylinositol 3-kinase directly activates the protein kinase Akt through its pleckstrin homology domain. *Mol. Cell. Biol.* **17**:338-344.
36. Kops, G. J., N. D. de Ruiter, A. M. De Vries-Smits, D. R. Powell, J. L. Bos, and B. M. Burgering. 1999. Direct control of the Forkhead transcription factor AFX by protein kinase B. *Nature* **398**:630-634.
37. Li, J., C. Yen, D. Liaw, K. Podsypanina, S. Bose, S. I. Wang, J. Puc, C. Miliareis, L. Rodgers, R. McCombie, S. H. Bigner, B. C. Giovanella, M. Ittmann, B. Tycko, H. Hibshoosh, M. H. Wigler, and R. Parsons. 1997. PTEN, a putative protein tyrosine phosphatase gene mutated in human brain, breast, and prostate cancer. *Science* **275**:1943-1947.
38. Liu, Z. G., H. Hsu, D. V. Goeddel, and M. Karin. 1996. Dissection of TNF receptor 1 effector functions: JNK activation is not linked to apoptosis while NF-kappaB activation prevents cell death. *Cell* **87**:565-576.
39. Maehama, T., and J. E. Dixon. 1998. The tumor suppressor, PTEN/MMAC1, dephosphorylates the lipid second messenger, phosphatidylinositol 3,4,5-trisphosphate. *J. Biol. Chem.* **273**:13375-13378.
40. Marte, B. M., and J. Downward. 1997. PKB/Akt: connecting phosphoinositide 3-kinase to cell survival and beyond. *Trends Biochem. Sci.* **22**:355-358.
41. Mayo, M. W., C.-Y. Wang, P. C. Cogswell, K. S. Rogers-Graham, S. W. Lowe, C. J. Der, and A. S. Baldwin, Jr. 1997. Requirement of NF-kappaB activation to suppress p53-independent apoptosis induced by oncogenic Ras. *Science* **278**:1812-1815.
42. McCarthy, S. A., M. L. Samuels, C. A. Pritchard, J. A. Abraham, and M. McMahon. 1995. Rapid induction of heparin-binding epidermal growth factor/diphtheria toxin receptor expression by Raf and Ras oncogenes. *Genes Dev.* **9**:1953-1964.
43. Norris, J. L., and A. S. Baldwin, Jr. 1999. Oncogenic ras enhances NF-kappaB transcriptional activity through raf-dependent and raf-independent mitogen-activated protein kinase signaling pathways. *J. Biol. Chem.* **274**:13841-13846.
44. Ozes, O. N., L. D. Mayo, J. A. Gustin, S. R. Pfeffer, L. M. Pfeffer, and D. B. Donner. 1999. NF-kappaB activation by tumour necrosis factor requires the Akt serine-threonine kinase. *Nature* **401**:82-85.
45. Podsypanina, K., L. H. Ellenson, A. Nemes, J. Gu, M. Tamura, K. M. Yamada, C. Cordon-Cardo, G. Catoretti, P. E. Fisher, and R. Parsons. 1999. Mutation of Pten/Mmac1 in mice causes neoplasia in multiple organ systems. *Proc. Natl. Acad. Sci. USA* **96**:1563-1568.
46. Reddy, S. A., J. H. Huang, and W. S. Liao. 1997. Phosphatidylinositol 3-kinase in interleukin 1 signaling. Physical interaction with the interleukin 1 receptor and requirement in NFkappaB and AP-1 activation. *J. Biol. Chem.* **272**:29167-29173.
47. Reuther, J. Y., G. W. Reuther, D. Cortez, A. M. Pendergast, and A. S. Baldwin, Jr. 1998. A requirement for NF-kappaB activation in Bcr-Abl-mediated transformation. *Genes Dev.* **12**:968-981.
48. Rodriguez-Viciana, P., P. H. Warne, A. Khwaja, B. M. Marte, D. Pappin, P. Das, M. D. Waterfield, A. Ridley, and J. Downward. 1997. Role of phosphoinositide 3-OH kinase in cell transformation and control of the actin cytoskeleton by Ras. *Cell* **89**:457-467.
49. Romashkova, J. A., and S. S. Makarov. 1999. NF-kappaB is a target of AKT in anti-apoptotic PDGF signalling. *Nature* **401**:86-90.
50. Schmitz, M. L., and P. A. Baeuerle. 1991. The p65 subunit is responsible for the strong transcription activating potential of NF-kappa B. *EMBO J.* **10**:3805-3817.
51. Serrano, M., A. W. Lin, M. E. McCurrach, D. Beach, and S. W. Lowe. 1997. Oncogenic ras provokes premature cell senescence associated with accumulation of p53 and p16INK4a. *Cell* **88**:593-602.
52. Sizemore, N., S. Leung, and G. R. Stark. 1999. Activation of phosphatidylinositol 3-kinase in response to interleukin-1 leads to phosphorylation and activation of the NF-kappa B p65/RelA subunit. *Mol. Cell. Biol.* **19**:4798-4805.
53. Stambolic, V., A. Suzuki, J. L. de la Pompa, G. M. Brothers, C. Mirtsos, T. Sasaki, J. Ruland, J. M. Penninger, D. P. Siderovski, and T. W. Mak. 1998. Negative regulation of PKB/Akt-dependent cell survival by the tumor suppressor PTEN. *Cell* **95**:29-39.
54. Steck, P. A., M. A. Pershouse, S. A. Jasser, W. K. Yung, H. Lin, A. H. Ligon, L. A. Langford, M. L. Baumgard, T. Hattier, T. Davis, C. Frye, R. Hu, B. Swedlund, D. H. Teng, and S. V. Tavtigian. 1997. Identification of a candidate tumour suppressor gene, MMAC1, at chromosome 10q23.3 that is mutated in multiple advanced cancers. *Nat. Genet.* **15**:356-362.
55. Tang, E. D., G. Nuñez, F. G. Barr, and K. L. Guan. 1999. Negative regulation of the Forkhead transcription factor FKHR by Akt. *J. Biol. Chem.* **274**:16741-16746.
56. Van Antwerp, D. J., S. J. Martin, I. M. Verma, and D. R. Green. 1998. Inhibition of TNF-induced apoptosis by NF-kappa B. *Trends Cell Biol.* **8**:107-111.
57. Wang, C.-Y., M. W. Mayo, and A. S. Baldwin, Jr. 1996. TNF- and cancer therapy-induced apoptosis: potentiation by inhibition of NF-kappaB. *Science* **274**:784-787.
58. Wang, C.-Y., M. W. Mayo, R. G. Korneluk, D. V. Goeddel, and A. S. Baldwin, Jr. 1998. NF-kappaB antiapoptosis: induction of TRAF1 and TRAF2 and c-IAP1 and c-IAP2 to suppress caspase-8 activation. *Science* **281**:1680-1683.
59. Wang, C.-Y., J. C. Cusack, R. Liu, and A. S. Baldwin, Jr. 1999. Control of inducible chemoresistance: enhanced anti-tumor therapy through increased apoptosis by inhibition of NF-kappaB. *Nat. Med.* **5**:412-417.
- 59a. Wang, C.-Y., D. C. Guttridge, M. W. Mayo, and A. S. Baldwin, Jr. 1999. NF-kappaB induces expression of the Bcl-2 homologue A1/Bfl-1 to preferentially suppress chemotherapy-induced apoptosis. *Mol. Cell. Biol.* **19**:5923-5929.
60. Wang, D., and A. S. Baldwin, Jr. 1998. Activation of nuclear factor-kappaB-dependent transcription by tumor necrosis factor-alpha is mediated through phosphorylation of RelA/p65 on serine 529. *J. Biol. Chem.* **273**:29411-29416.
61. Welch, H., A. Eguinoa, L. R. Stephens, and P. T. Hawkins. 1998. Protein kinase B and rac are activated in parallel within a phosphatidylinositol 3OH-kinase-controlled signaling pathway. *J. Biol. Chem.* **273**:11248-11256.
62. Whang, Y. E., X. Wu, H. Suzuki, R. E. Reiter, C. Tran, R. L. Vessella, J. W. Said, W. B. Isaacs, and C. L. Sawyers. 1998. Inactivation of the tumor suppressor PTEN/MMAC1 in advanced human prostate cancer through loss of expression. *Proc. Natl. Acad. Sci. USA* **95**:5246-5250.
63. White, M. A., C. Nicolette, A. Minden, A. Polverino, L. Van Aelst, M. Karin, and M. H. Wigler. 1995. Multiple Ras functions can contribute to mammalian cell transformation. *Cell* **80**:533-541.
64. Yano, S., H. Tokumitsu, and T. R. Soderling. 1998. Calcium promotes cell survival through CaM-K kinase activation of the protein-kinase-B pathway. *Nature* **396**:584-587.
65. Yin, M. J., L. B. Christerson, Y. Yamamoto, Y. T. Kwak, S. Xu, F. Mercurio, M. Barbosa, M. H. Cobb, and R. B. Gaynor. 1998. HTLV-I Tax protein binds to MEKK1 to stimulate IkkappaB kinase activity and NF-kappaB activation. *Cell* **93**:875-884.
66. Zandi, E., and M. Karin. 1999. Bridging the gap: composition, regulation, and physiological function of the Ikb kinase complex. *Mol. Cell. Biol.* **19**:4547-4551.
67. Zha, J., H. Harada, E. Yang, J. Jockel, and S. J. Korsmeyer. 1996. Serine phosphorylation of death agonist BAD in response to survival factor results in binding to 14-3-3, not Bcl-X1. *Cell* **87**:619-628.
68. Zhong, H., H. SuYang, H. Erdjument-Bromage, P. Tempst, and S. Ghosh. 1997. The transcriptional activity of NF-kappaB is regulated by the IkkappaB-associated PKAc subunit through a cyclic AMP-independent mechanism. *Cell* **89**:413-424.
69. Zhong, H., R. E. Voll, and S. Ghosh. 1998. Phosphorylation of NF-kappa B p65 by PKA stimulates transcriptional activity by promoting a novel bivalent interaction with the coactivator CBP/p300. *Mol. Cell* **1**:661-671.
70. Zong, W. X., L. C. Edelstein, C. Chen, J. Bash, and C. Gelinas. 1999. The prosurvival Bcl-2 homolog Bfl-1/A1 is a direct transcriptional target of NF-kappaB that blocks TNFalpha-induced apoptosis. *Genes Dev.* **13**:382-387.

An Aspirin-Triggered Lipoxin A₄ Stable Analog Displays a Unique Topical Anti-Inflammatory Profile

Arndt J. Schottelius,* Claudia Giesen,* Khusru Asadullah,* Iolanda M. Fierro,^{1†}
Sean P. Colgan,[†] John Bauman,[‡] William Guilford,[‡] Hector D. Perez,[§] and John F. Parkinson^{2§}

Lipoxins and 15-epi-lipoxins are counter-regulatory lipid mediators that modulate leukocyte trafficking and promote the resolution of inflammation. To assess the potential of lipoxins as novel anti-inflammatory agents, a stable 15-epi-lipoxin A₄ analog, 15-epi-16-*p*-fluorophenoxy-lipoxin A₄ methyl ester (ATLa), was synthesized by total organic synthesis and examined for efficacy relative to a potent leukotriene B₄ (LTB₄) receptor antagonist (LTB₄R-Ant) and the clinically used topical glucocorticoid methylprednisolone aceponate. In vitro, ATLa was 100-fold more potent than LTB₄R-Ant for inhibiting neutrophil chemotaxis and *trans*-epithelial cell migration induced by fMLP, but was ~10-fold less potent than the LTB₄R-Ant in blocking responses to LTB₄. A broad panel of cutaneous inflammation models that display pathological aspects of psoriasis, atopic dermatitis, and allergic contact dermatitis was used to directly compare the topical efficacy of ATLa with that of LTB₄R-Ant and methylprednisolone aceponate. ATLa was efficacious in all models tested: LTB₄/Iloprost-, calcium ionophore-, croton oil-, and mezerein-induced inflammation and trimellitic anhydride-induced allergic delayed-type hypersensitivity. ATLa was efficacious in mouse and guinea pig skin inflammation models, exhibiting dose-dependent effects on edema, neutrophil or eosinophil infiltration, and epidermal hyperproliferation. We conclude that the LXA₄ and aspirin-triggered LXA₄ pathways play key anti-inflammatory roles in vivo. Moreover, these results suggest that ATLa and related LXA₄ analogs may have broad therapeutic potential in inflammatory disorders and could provide an alternative to corticosteroids in certain clinical settings. *The Journal of Immunology*, 2002, 169: 7063–7070.

Lipoxin A₄ (LXA₄)³ is a short-lived, tetraene eicosanoid with potent anti-inflammatory activities (Ref. 1 and references therein). LXA₄ is produced locally at sites of inflammation by transcellular biosynthesis via interaction of neutrophils with platelets or other leukocytes with epithelial cells. Endogenous LXA₄ synthesis in neutrophils is primed by cytokines (2) and elevated in neutrophils from asthmatic subjects (3–5). LXA₄ may exert its anti-inflammatory effects through signals generated by binding to a high affinity, G protein-coupled LXA₄ receptor, ALX-R (1). ALX-R is conserved in mammals; it is constitutively expressed on neutrophils, eosinophils, and monocytes and is induced on epithelium and vascular endothelium, thus being ideally localized to effect a counter-regulatory role in promoting the resolution of cell-mediated inflammatory responses. ALX-R expression on neutrophils and eosinophils correlates with the abil-

ity of lipoxins to potently inhibit chemotaxis and transcellular migration of these cells. Aspirin triggers 15-epi-LXA₄ formation both in vitro and in vivo via a mechanism involving cyclooxygenase-2 inhibition (6). Aspirin-triggered 15-epi-lipoxins (ATLs) retain the anti-inflammatory properties of LXA₄ and may mediate in part aspirin's therapeutic effects (7).

LXA₄ and ATLs undergo rapid metabolic inactivation by PG dehydrogenase-mediated oxidation and reduction (8, 9). These metabolites have reduced affinity for ALX-R and decreased anti-inflammatory potency. Chemical modifications to the C15-C20 region of LXA₄ and ATLs prevent metabolic inactivation, thus providing stable analogs with superior pharmaceutical characteristics (10). The stable lipoxin analogs inhibit neutrophil transcellular migration, pathogen- and TNF- α -induced epithelial cell IL-8 release, and vascular permeability of mouse ear skin exposed to inflammatory stimuli (Ref. 1 and references therein). In TNF- α -induced dorsal air pouch inflammation, stable LXA₄ analogs have potent local and systemic anti-inflammatory efficacy via down-regulation of proinflammatory cytokine and chemokine networks (11, 12). More specifically, lipoxins inhibit cytokine-stimulated IL-1 β , macrophage inflammatory protein-2, and superoxide production while stimulating the anti-inflammatory cytokine IL-4 in neutrophils (11). Eosinophil-driven allergic reactions are also inhibited by stable LXA₄ analogs (13, 14). Lipoxins inhibit eosinophil chemotaxis, and IL-5 and eotaxin secretion (13). Moreover, lipoxins inhibit mesangial cell proliferation (15). Finally, lipoxins have been shown to inhibit the transcription factor NF- κ B, which is a central regulator of inflammatory molecules and also is pivotal for proliferation and anti-apoptosis (16). Thus, an anti-proliferative effect can add to the anti-inflammatory mechanisms of lipoxins that interfere with the activation and migration of inflammatory cells.

*Research Business Area Dermatology, Research Laboratories, Schering AG, Berlin, Germany; [†]Center for Experimental Therapeutics and Reperfusion Injury, Brigham and Women's Hospital, Harvard Medical School, Boston, MA 02115; and Departments of [‡]Medicinal Chemistry and [§]Immunology, Berlex Biosciences, Richmond, CA 94804

Received for publication July 23, 2002. Accepted for publication October 15, 2002.

The costs of publication of this article were defrayed in part by the payment of page charges. This article must therefore be hereby marked *advertisement* in accordance with 18 U.S.C. Section 1734 solely to indicate this fact.

¹ Current address: Departamento de Farmacologia, Instituto de Biologia, Universidade do Estado do Rio de Janeiro, Avenue 28 de Setembro 87 fnds, 5o andar, sala 2, Rio de Janeiro RJ 20.560-001, Brazil.

² Address correspondence and reprint requests to Dr. John F. Parkinson, Department of Immunology, Berlex Biosciences, Richmond, CA 94804. E-mail address: john_parkinson@berlex.com

³ Abbreviations used in this paper: LXA₄, lipoxin A₄; ALX-R, LXA₄ receptor; AMC, 7-amino-4-methyl-coumarin; ATLa, 15-epi-16-*p*-fluorophenoxy-lipoxin A₄ methyl ester; DTH, delayed-type hypersensitivity; HTAB, hexadecyltrimethylammonium bromide; LTB₄, leukotriene B₄; LTB₄R-Ant, leukotriene B₄ receptor antagonist; MPA, methylprednisolone aceponate; TMA, trimellitic anhydride; TMB, tetramethylbenzidine.

Results to date suggest that the $LXA_4/ALX-R$ pathway promotes counter-regulatory signals to diverse proinflammatory mediators and that stable LXA_4 analogs may have therapeutic potential in inflammatory and autoimmune disease. Because of the limited amounts of synthetic LXA_4 analogs available, a role for $LXA_4/ALX-R$ in regulating cutaneous inflammation has not been studied systematically, and there is limited information on the efficacy profile of LXA_4 analogs in industry standard animal models that represent distinct mechanisms of clinically relevant cutaneous inflammation. Quantitative results comparing the potency and efficacy of a stable LXA_4 analog to other anti-inflammatory agents, including clinically relevant standards, such as glucocorticoids, is also lacking. To address these points, the topical efficacy of a stable ATL analog synthesized in bulk, namely 15-*epi*-16-*p*-fluorophenoxy-lipoxin A_4 methyl ester (ATLa; Fig. 1), was tested in a variety of skin inflammation models. The models were chosen to evaluate potential utility in distinct dermatoses, since they exhibit pathological features found in irritant contact dermatitis, psoriasis, allergic contact dermatitis, urticaria, and atopic dermatitis. Anti-inflammatory potency and efficacy were compared with those of a leukotriene B_4 (LTB_4) receptor antagonist (LTB_4-R -Ant) and methylprednisolone aceponate (MPA), a mid-potent glucocorticoid that is marketed in Europe and frequently used for topical treatment of atopic dermatitis in children. The present results indicate that ATLa displays broad topical efficacy in all models of skin inflammation examined and proved to be dose-dependent for inhibiting edema, leukocyte infiltration, and epidermal hyperproliferation. ATLa gives a unique anti-inflammatory profile, suggesting potential use in topical treatment of dermatoses.

Materials and Methods

The stable analog ATLa (Fig. 1) was synthesized using previously described methods (17). Material of >95% purity was qualified against a synthetic ATLa standard (provided by Dr. N. Petasis (University of Southern California, Los Angeles, CA) and Dr. C. N. Serhan (Brigham and Woman's Hospital, Harvard University, Boston, MA)) using 1H nuclear magnetic resonance, HPLC coinjection with photodiode array UV-visible detection (two methods), and liquid chromatography-mass spectrometry. The LTB_4 receptor antagonist ZK-158252 (18, 19) (LTB_4-R -Ant), lloprost, and LTB_4 for in vivo studies were synthesized at Schering AG (Berlin, Germany). LTB_4 for in vitro studies was purchased from Cayman (Ann Arbor, MI). Hexadecyltrimethylammonium bromide (HTAB), fMLP, calcium ionophore A-23187, croton oil, mezeirin, and trimellitic anhydride were obtained from Sigma (St. Louis, MO).

Human neutrophil chemotaxis and transcellular migration assays

Neutrophils from healthy volunteers were obtained as previously described (10) and suspended in RPMI 1640 (BioWhittaker, Walkersville, MD) at 1×10^6 cells/ml. fMLP (10 nM), 10 nM LTB_4 , or vehicle was added to the lower wells of a 48-well, 5- μ m pore size chemotaxis chamber (NeuroProbe, Cabin John, MD). Neutrophils (50 μ l) were placed in the upper wells, and the chamber was incubated (37°C, 5% CO_2) for 1 h. Following incubation, filters were removed, and cells were scraped from the upper

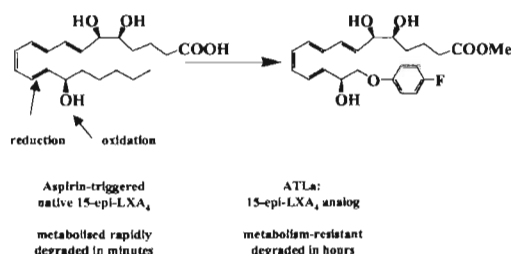


FIGURE 1. The figure shows the structure of ATLa, which is a metabolically stable analog of aspirin-triggered 15-epi-LXA₄.

surface. The filters were fixed and stained with Diff-Quik (Dade Behring, Newark, DE). For each incubation, performed in triplicate, cells that migrated across the filter toward the lower surface were enumerated by light microscopy. To assess inhibition of migration, neutrophils were suspended in RPMI medium with vehicle or increasing concentrations of the compounds (ATLa or LTB_4-R -Ant) and incubated for 30 min at 37°C before placement in the chamber. Human neutrophil transmigration across confluent monolayers of human T84 epithelial cells was performed as previously described (10).

Animal models

All animal studies were approved by the competent authority for labor protection, occupational health, and technical safety for the state and city of Berlin, Germany, and were performed in accordance with the ethical guidelines of Schering. Female NMRI mice (26–28 g) or pirbright white guinea pigs (Charles River, Wilmington, MA; 200–250 g) were housed according to institutional guidelines of the Schering animal facility. NMRI mice are outbred Swiss mice from Lynch to Pooley (National Institutes of Health, Bethesda, MD; albino, Aa, BB, cc, DD, histocompatibility H-2^d). Eight to 11 animals were randomly allocated to the different treatment groups.

Skin inflammation models

Because of the acute character of the models, ATLa, LTB_4-R -Ant, or MPA was applied topically at the same time as the elicitation of the inflammatory reaction. Tissue weight (ears or dorsal skin punch biopsies) served as a criterion for edema formation. Peroxidase activity in skin homogenates served as a measure of total granulocyte (neutrophil and eosinophil) infiltration, and elastase activity served as a specific measure of neutrophil infiltration.

LTB_4 /Iloprost-induced inflammation

The stable PGL_2 analog Iloprost enhances LTB_4 -induced ear inflammation, leading to edema and a neutrophilic infiltrate with a maximum reaction 24 h after elicitation (20). Ten microliters of 0.003% (w/v) LTB_4 and 0.003% (w/v) Iloprost in ethanol/isopropylmyristate (95/5), with or without the respective anti-inflammatory agent, were applied dorsally to mouse ears. Animals were euthanized with CO_2 24 h after application. Ears were cut off, weighed as an indicator for edema formation, and snap-frozen. Ears (area, ~1 cm²) were homogenized in 2 ml of buffer containing 0.5% HTAB and 10 mM MOPS (pH 7.0) in a Polytron(R) PT 3000 homogenizer (KINEMATICA, Lucerne, Switzerland) set at maximum speed (30,000 rpm). Samples were centrifuged, and 750 μ l of supernatants were transferred to 96-deep-well plates (Beckman, Palo Alto, CA). The supernatants were then used to determine peroxidase and elastase activity as a measure for infiltrating granulocytes (peroxidase) and neutrophils (elastase), as described below. Anti-inflammatory effects of a given compound were defined as the percent inhibition of edema formation and peroxidase and elastase activities.

Calcium ionophore-induced inflammation

The calcium ionophore A-23187, applied topically, induces acute inflammation with edema and granulocyte infiltration that peaks at ~24 h (21). Ten microliters of a 0.1% (w/v) solution of A-23187 in ethanol/isopropylmyristate (95/5), with or without the respective anti-inflammatory agent, were applied dorsally to mouse ears. Animals were euthanized 24 h later, and the ears were processed as described for the LTB_4 /Iloprost inflammation model.

Croton oil-induced inflammation

The nonspecific contact irritant croton oil leads to acute inflammation and is characterized by edema formation and a mainly granulocytic cell infiltration into the skin (22). Ten microliters of 1% (v/v) croton oil in ethanol/isopropylmyristate (95/5), with or without the respective anti-inflammatory agent, were applied dorsally to mouse ears. Animals were euthanized at 24 h, and ears were processed as described for the LTB_4 /Iloprost inflammation model.

Mezeirin-induced inflammation

Mezeirin causes acute inflammation, with edema formation and granulocyte infiltration within 24 h and epidermal hyperproliferation within ~72 h (23). Ten microliters of 0.03% (w/v) mezeirin in ethanol/isopropylmyristate (95/5) with or without the respective anti-inflammatory agent were applied dorsally to mouse ears. For inflammation end points, animals were euthanized at 24 h, and ears were processed as described for the LTB_4 /

Iloprost inflammation model. As an indication for hyperproliferation, epidermal thickness was determined morphometrically in Formalin-fixed, plastic-embedded, sectioned, and toluidine blue-stained specimens obtained from the ears of mice euthanized at 72 h.

Trimellitic anhydride-induced delayed-type hypersensitivity (DTH)

Sensitization with the occupational contact allergen trimellitic anhydride (TMA) induces a DTH reaction, with prominent eosinophil infiltration 24 h after challenge (24), which, in contrast to other types of acute contact dermatitis, is characterized by a mixed Th1/Th2 reaction. Mice were sensitized on days 0 and 1 by a single application of 50 μ l of 3% (w/v) TMA in acetone/isopropylmyristate (80/20) onto a shaven area of 2 \times 2 cm on the right flank. The DTH reaction was induced on day 5 by challenging the animals with a single application of 10 μ l of 3% (w/v) TMA in acetone/isopropylmyristate (80/20) with or without the respective anti-inflammatory substance onto the dorsal sides of both ears. Animals were euthanized 24 h after challenge, and ears were processed as described for the LTB₄/Iloprost inflammation model.

Peroxidase activity assay

Peroxidase activity as a measure of total granulocyte infiltration was measured as previously described (25). Briefly, tetramethylbenzidine (TMB) dihydrochloride was used as a sensitive chromogen substrate for peroxidase. To convert TMB into TMB dihydrochloride, 34 μ l of 3.7% hydrochloric acid (equimolar) was added to 5 mg of TMB. Then 1 ml of DMSO was added. This stock solution was slowly added to sodium acetate-citric acid buffer (0.1 mol/L, pH 6.0) in a ratio of 1:100. Two hundred microliters of this TMB solution, 40 μ l of the homogenized sample, and 25 μ l of 1 mM H₂O₂ were added to a microtiter plate to start the reaction. The reaction was stopped after 30 min with 45 μ l of 1 N H₂SO₄. Changes in OD were monitored at 450 nm at 25°C against the mixture of all solutions without the added sample homogenate. Absolute extinction numbers were used to express peroxidase activity.

Elastase activity assay

Elastase activity was measured by fluorescence of 7-amino-4-methylcoumarin (AMC) that is released from the substrate MeO-Succ-Ala-Ala-Pro-Val-AMC (Bachem, Torrance, CA). Homogenized samples in HTAB were diluted 1/10 in cetrimide buffer (0.3% cetrimide, 0.1 M Tris, and 1 M NaCl, pH 8.5). The substrate MeO-Succ-Ala-Ala-Pro-Val-AMC (300 mM in DMSO) was diluted 1/100 in cetrimide buffer to a working concentration of 3 mM. In cetrimide buffer, diluted samples were pipetted in multiwell plates, and the reaction was started by addition of the AMC substrate at 37°C. The reaction was stopped after 1 h with ice-cold 100 mM Na₂CO₃, and samples were measured in a Spectra Max Gemini (Molecular Devices, Menlo Park, CA) at 380 nm and compared against a standard curve with the AMC standard 7-amino-4-methylcoumarin (5 mM in ethanol).

Statistical analysis

For all animal models statistical analysis was performed with the so-called modified Hemm (inhibition) test, which was developed by Schering's Department of Biometrics based on the program SAS System for Windows 6.12 (SAS Institute, Cary, NC). To determine the inhibitory effect of anti-inflammatory compounds, the difference between the respective mean value of the positive controls and the mean value of the vehicle controls was set at 100%, and the percentile change by the test substance was estimated: % change = $\left[\frac{\text{mean value}_{\text{treated group}} - \text{mean value}_{\text{positive group}}}{\text{mean value}_{\text{positive group}} - \text{mean value}_{\text{control group}}} \right] \times 100$. To test whether the change caused by the treatment is different from zero, a 95% confidence interval was calculated under consideration of the variance of observations within the entire experiment. If the interval did not include zero, the hypothesis that there is no change was rejected at the level of $\alpha = 0.05$. For each experiment IC₅₀ values were determined graphically.

Results

Human neutrophil chemotaxis and transcellular migration

A hallmark of inflammation is the movement of circulating leukocytes into tissues via chemotaxis and transcellular migration across endothelial and epithelial cell barriers (26). Classical chemotactic mediators include the bacterially derived *N*-formylated peptide, fMLP, and the proinflammatory eicosanoid, LTB₄. Human neutrophil chemotaxis to fMLP (10 nM) was inhibited in a dose-dependent manner by ATLa with an IC₅₀ of \sim 0.1 nM and a

maximal effect at \sim 10 nM (data not shown). ATLa was \sim 100-fold more potent than the specific LTB₄ receptor antagonist (LTB₄R-Ant; IC₅₀ = \sim 10 nM). In contrast, LTB₄R-Ant inhibited neutrophil chemotaxis induced by LTB₄ (10 nM) more potently (IC₅₀ = \sim 1 nM) than ATLa (IC₅₀ = \sim 10 nM). In addition to chemotaxis, ATLa potently inhibited neutrophil transepithelial migration to 10 nM fMLP or 10 nM LTB₄ (Fig. 2). Inhibition was dose dependent, with an IC₅₀ of \sim 1 nM against fMLP and \sim 10 nM against LTB₄. As expected, LTB₄R-Ant inhibited LTB₄-induced transepithelial migration to LTB₄ (IC₅₀ = \sim 1 nM), but was virtually ineffective on transepithelial migration to fMLP (<20% inhibition at 1 μ M). Thus, in addition to potentially inhibiting human neutrophil chemotaxis, ATLa potently inhibits neutrophil transmigration through epithelial cell monolayers, a finding consistent with previous in vitro studies (10). The present results correlate with the finding that the receptor ALX-R is expressed on both human neutrophils and human epithelial cells and may mediate LXA₄-dependent effects in both cell types (1). Our results also suggest that ATLa might display broader anti-inflammatory potential than LTB₄R-Ant, since neutrophil responses to more than one mediator are potently attenuated.

Efficacy of ATLa in cutaneous inflammation models

To characterize its anti-inflammatory potential for human skin diseases, ATLa was examined in diverse models of skin inflammation. The models are based on cutaneous reactions to exogenous stimuli that provoke a variety of symptoms, including edema, neutrophil or eosinophil infiltration, and epidermal hyperproliferation.

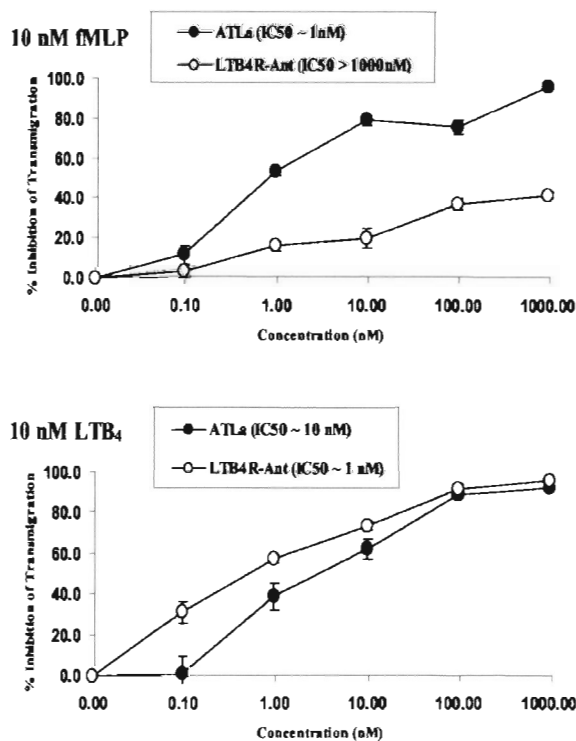


FIGURE 2. ATLa potently inhibits neutrophil transepithelial migration to fMLP and LTB₄. Transmigration of human neutrophils across human T-84 epithelial cell monolayers in response to 10 nM fMLP (top panel) or 10 nM LTB₄ (bottom panel) was performed as described (see Materials and Methods). The percent inhibition of transmigration by ATLa (●) and an LTB₄ receptor antagonist (○) was determined with increasing compound concentration. Data are expressed as the mean \pm SEM from three experiments, performed in triplicate.

The models encompass features of irritant dermatitis, allergic contact dermatitis, and some aspects of psoriasis and atopic dermatitis. A limitation of the models is their acute character, which does not allow for the assessment of therapeutic administration. Therefore, compounds were tested in a preventive manner by coapplication with the proinflammatory reagents. ATLa was compared with two reference compounds: LTB₄R-Ant and the topically active glucocorticoid, MPA. Comparative data for ATLa and LTB₄R-Ant in all models are summarized in Table I. Data for MPA are provided in the text and figures.

LTB₄/Iloprost-induced inflammation

As a direct correlate to antagonism of LTB₄ responses in vitro (see above), ATLa was characterized in an LTB₄-dependent model. Topical ATLa dose-dependently inhibited edema as well as neutrophil infiltration (Fig. 3). IC₅₀ values were ~40 μg/cm², and complete inhibition was achieved at 300 μg/cm² for both efficacy end points (mean of three independent experiments). The anti-inflammatory effects of ATLa in this model were comparable to the selective LTB₄R-Ant, which exhibited IC₅₀ in the range of 20–30 μg/cm² for all parameters tested. The results in this model are consistent with the potent in vitro functional antagonism of LTB₄-stimulated neutrophil responses by both ATLa and LTB₄R-Ant. Given their known anti-inflammatory mechanism of action (27), glucocorticoids such as MPA are not active in this direct model of LTB₄-induced inflammation and were not tested.

Calcium ionophore-induced inflammation

To examine the influence of ATLa on inflammation mediated by endogenous LTB₄ production, efficacy was tested in calcium ionophore-induced inflammation in mice (Table I). ATLa exerted dose-dependent efficacy on all end points in this model (IC₅₀ = <100–200 μg/cm²), with complete inhibition of cell infiltration and ~70% inhibition of edema at 1000 μg/cm². ATLa was equipotent to LTB₄R-Ant in this model, but was 100- to 1000-fold less potent than MPA (IC₅₀ = 0.1–10 μg/cm²). To demonstrate efficacy across species, ATLa effects were also tested in calcium iono-

phore-induced inflammation in the ears of guinea pigs (Table I). Inhibitory effects were similar in extent to LTB₄R-Ant. The data confirm that ATLa has anti-inflammatory efficacy in two species.

Croton oil- and mezerein-induced inflammation

Croton oil and mezerein are phorbol ester compounds that elicit an inflammatory reaction triggered by protein kinase C activation. This leads to the release of various proinflammatory mediators, which induce edema, cellular infiltration, and epidermal hyperproliferation. In the model of croton oil-induced inflammation, ATLa and LTB₄R-Ant inhibited edema formation and cell infiltration dose-dependently, with IC₅₀ values in the range of 200–600 μg/cm² (Table I). MPA inhibited these parameters with higher potency than both ATLa and LTB₄R-Ant (IC₅₀ = <0.2 μg/cm²). In the mezerein-induced inflammation model, IC₅₀ values for edema and cell infiltration measured at 24 h were ~100–150 μg/cm² for ATLa (Table I and Fig. 4). LTB₄R-Ant showed similar potency to ATLa, with IC₅₀ values from 100–260 μg/cm² for these end points. MPA was significantly more potent for all inflammatory parameters (IC₅₀ = <0.1–0.75 μg/cm²). Edema formation was inhibited by 70–80%, and cellular infiltration was completely inhibited at a dose of 1000 μg/cm² for the eicosanoids and at 10 μg/cm² for the glucocorticoid.

Mezerein induces a marked epidermal hyperproliferation: epidermal thickness at 72 h increased ~5-fold (see Fig. 5A, *i*, 11 μm; *ii*, 52 μm; and *iv*, 10 μm). ATLa caused a potent, dose-dependent inhibition of epidermal hyperproliferation (IC₅₀ = ~120 μg/cm²). Complete inhibition of hyperproliferation was achieved at the highest dose (1000 μg/cm²; Fig. 5A, *iii*, 10 μm; and *v*; and Fig. 5B), with near-complete inhibition observed at 300 μg/cm². ATLa was 3-fold more potent than LTB₄R-Ant (IC₅₀ = ~400 μg/cm²; Fig. 5B) on this end point. The potency of MPA on epidermal hyperproliferation was not directly compared with ATLa in these experiments, but is in the same same range as its anti-inflammatory effects (data not shown).

Table I. Summary of efficacy data for ATLa, LTB₄R-Ant, and MPA in skin inflammation models^a

Model and Species	Efficacy End Point	Potency	
		ATLa IC ₅₀ (μg/cm ²)	LTB ₄ R-Ant IC ₅₀ (μg/cm ²)
LTB ₄ /Iloprost, mouse	Edema	44 ± 34 ^b	32 ± 9 ^b
	Granulocytic infiltration	37 ± 33 ^b	21 ± 7 ^b
	Neutrophil infiltration	41 ± 10 ^b	27 ± 17 ^b
Calcium ionophore, mouse	Edema	200	300
	Granulocyte infiltration	180	190
	Neutrophil infiltration	<100 ^c	<100 ^c
Calcium ionophore, guinea pig	Edema	250	~100
	Granulocyte infiltration	200	<100 ^c
Mezerein, mouse	Edema	150	260
	Granulocyte infiltration	140	100
	Neutrophil infiltration	<100 ^c	100
	Epidermal hyperproliferation	120	400
Croton oil, mouse	Edema	390	550
	Granulocyte infiltration	600	310
	Neutrophil infiltration	500	200
Trimellitic anhydride (DTH), mouse	Edema	520	— ^d
	Granulocyte infiltration	420	— ^d
	Neutrophil infiltration	320	<100 ^c

^a The table summarizes the IC₅₀ for ATLa and LTB₄R-Ant for each efficacy end point tested in the cutaneous inflammation models.

^b Mean ± SEM from three independent experiments.

^c Estimated IC₅₀ outside of dose range tested.

^d Dose response not established.

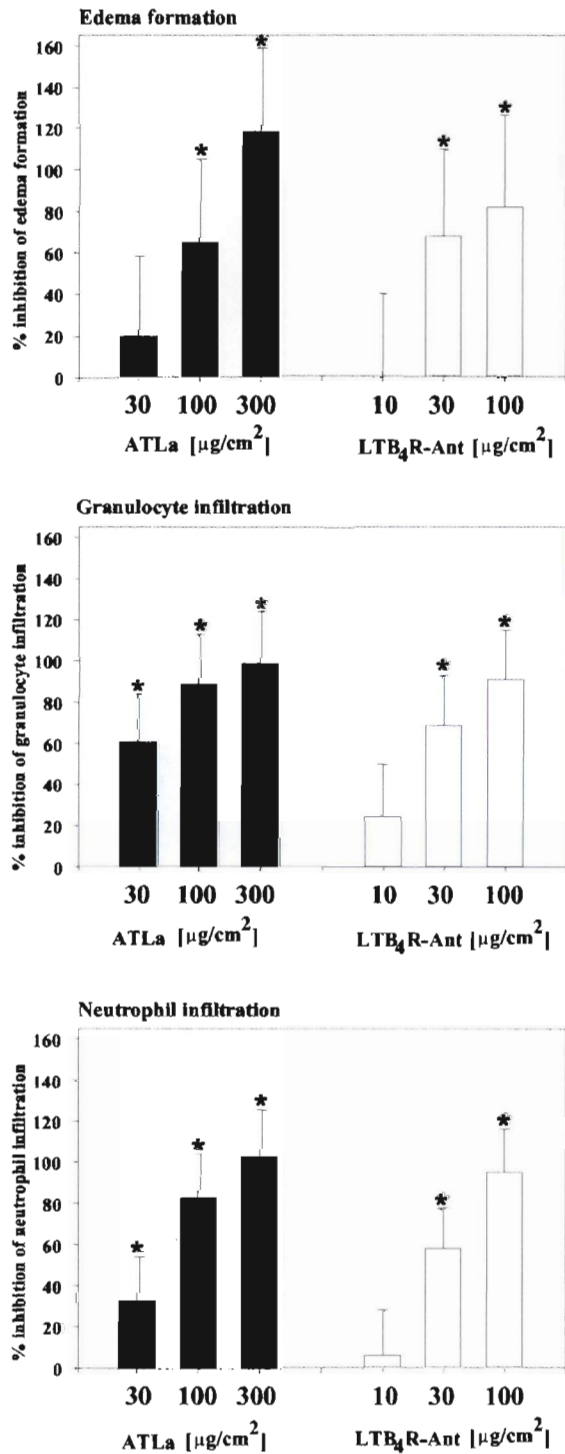


FIGURE 3. ATLa inhibits LTB₄/Iloprost-induced inflammation in the ears of mice. LTB₄/Iloprost-induced inflammation in mouse ears and measurement of edema, and granulocyte and neutrophil infiltration was measured at 24 h as described in *Materials and Methods*. Inhibitory effects of ATLa (■) were compared with those of LTB₄R-Ant (□), both of which were coapplied with LTB₄/Iloprost. Results are expressed as the mean \pm SEM of eight animals per group. *, $p < 0.05$ vs vehicle control.

Trimellitic anhydride-induced DTH

TMA stimulates a T cell-mediated inflammatory reaction with a characteristic of DTH. Application of TMA to sensitized animals evokes a mixed cellular infiltrate composed primarily of eosinophils, but with

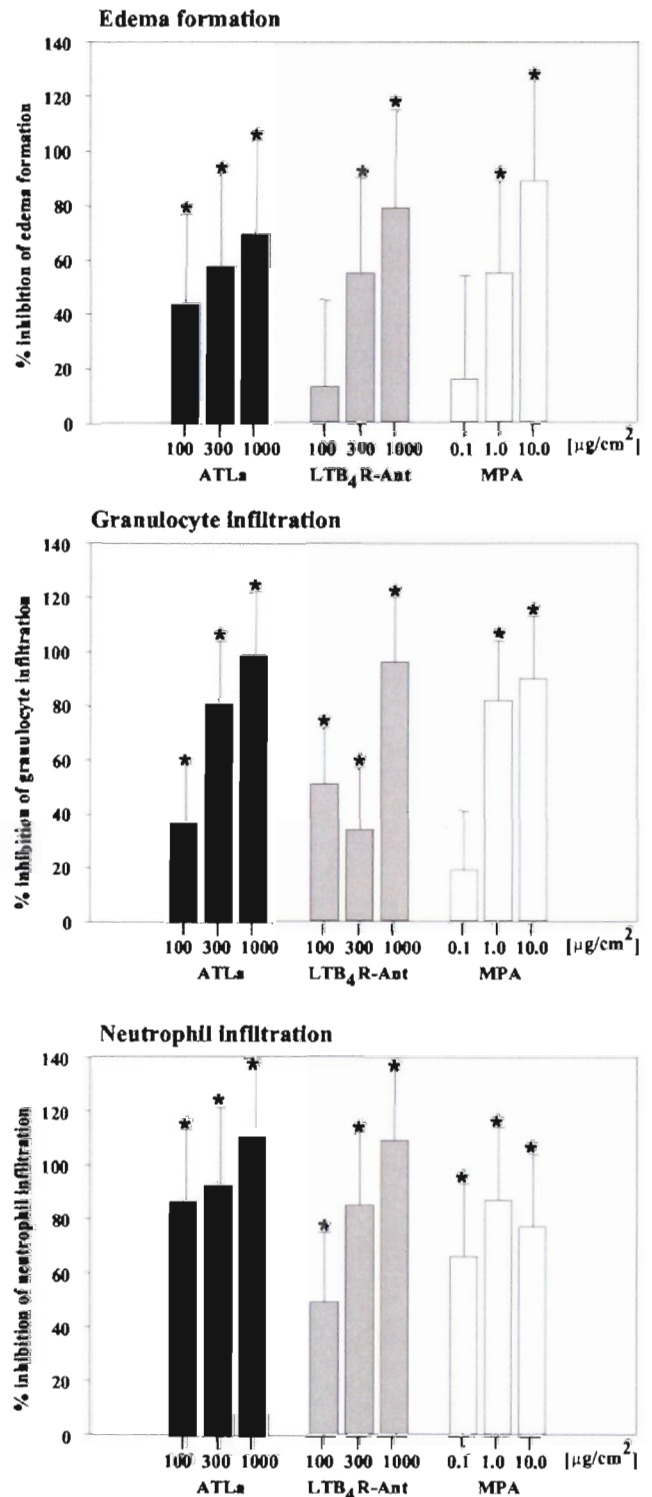
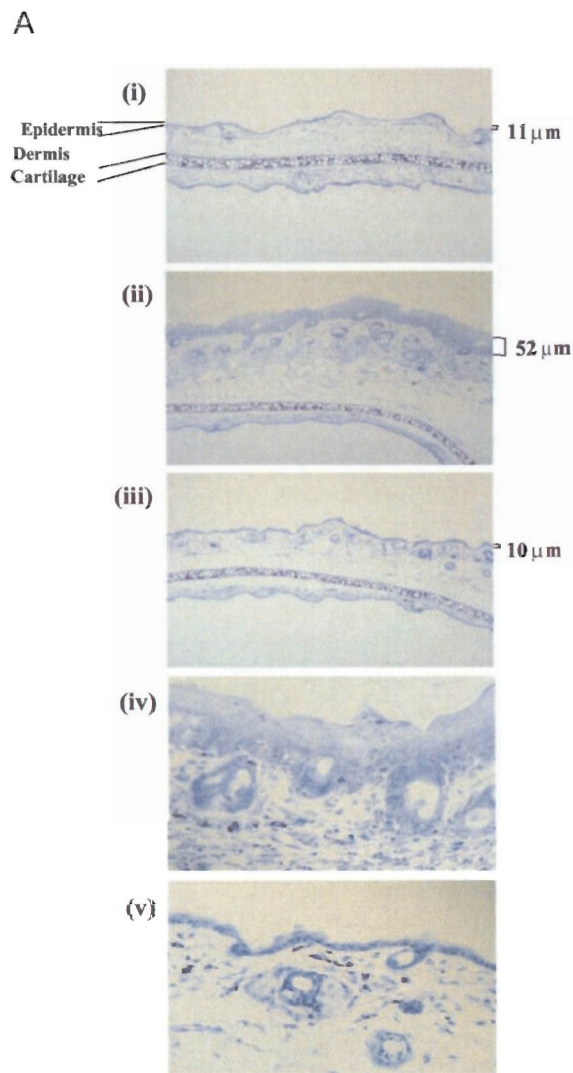


FIGURE 4. ATLa inhibits mezerein-induced ear inflammation. Mezerein-induced inflammation in mouse ears, edema, and granulocyte and neutrophil infiltration were measured at 24 h as described in *Materials and Methods*. The anti-inflammatory potency of ATLa (■) was compared with that of LTB₄R-Ant (□) and to the effects of MPA (□). All compounds were coapplied with mezerein. Results are expressed as the mean \pm SEM of 10 animals per group. *, $p < 0.05$ vs vehicle control.

some neutrophils. In this model MPA exerts very potent effects on edema formation and neutrophil infiltration ($IC_{50} = <0.2 \mu\text{g}/\text{cm}^2$), but weaker effects on eosinophil infiltration, as measured with the



B

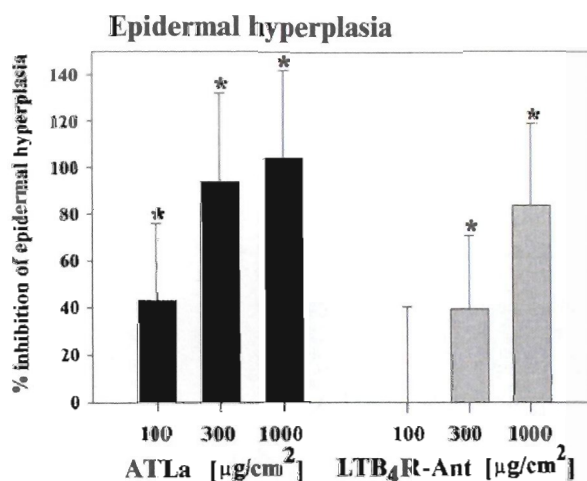


FIGURE 5. ATLa inhibits mezerein-induced epidermal hyperproliferation. *A*, Mezerein was applied, as described in Fig. 4, and epidermal hyperproliferation at 72 h was determined as described in *Materials and Methods*. Histological sections ($\times 25$ magnification) of mouse ear skin show the normal morphology of the vehicle control (*i*), with marked epidermal and dermal hyperproliferation induced by mezerein (*ii*), that was

peroxidase assay for total granulocytes ($\text{IC}_{50} = >10 \mu\text{g}/\text{cm}^2$). ATLa inhibited TMA-induced edema formation and cell infiltration, with IC_{50} values of $320\text{--}520 \mu\text{g}/\text{cm}^2$ (Fig. 6). Complete or almost complete inhibition for all parameters was achieved with $1000 \mu\text{g}/\text{cm}^2$. In contrast to the potent and dose-dependent effects of ATLa on eosinophil infiltration (parameter: granulocyte infiltration), the LTB₄R-Ant was only able to produce $\sim 40\%$ inhibition at the lowest dose tested and was completely ineffective at other dosages. The LTB₄R-Ant was able to potently inhibit neutrophil infiltration, as measured by the elastase assay. Together these results suggest a differential and superior effectiveness of ATLa compared with LTB₄R-Ant with respect to eosinophil infiltration in this allergic DTH reaction.

Discussion

Interaction of LXA₄ and aspirin-triggered 15-epi-LXA₄ with ALX-R has recently emerged as an endogenous signaling pathway for anti-inflammation (1). The field has developed substantially in recent years with the availability of metabolically stable LXA₄ analogs, such as ATLa, that facilitate pharmacological experimentation in vitro and in vivo. Despite these advances, the lack of substantial quantities of synthetic lipoxin analogs for detailed evaluation of the potency and efficacy vs benchmark research and clinical standards has not yet been possible. To this end we have synthesized and qualified the lipoxin analog ATLa, which showed intriguing biological properties in earlier studies (1) (see Fig. 1). Our present results establish the following. 1) ATLa potently inhibited neutrophil chemotaxis and transcellular migration, confirming earlier reports (10), and was a broader inhibitor of neutrophil responses than our own potent LTB₄ receptor antagonist. 2) Topically applied ATLa dose-dependently inhibited cutaneous inflammation evoked by diverse inflammatory mediators, with complete inhibition of several efficacy end points. 3) ATLa was efficacious in at least two species: mouse and guinea pig. 4) ATLa potency in vivo was at least equivalent to a potent LTB₄ receptor antagonist, but considerably less potent than MPA, a clinically used topical glucocorticoid standard. 5) ATLa was shown for the first time to block inflammation-dependent epidermal hyperproliferation and to inhibit a T cell-dependent allergic cutaneous reaction. These findings confirm the actions of ATLa and firmly establish that lipoxin analogs, such as ATLa, are a novel therapeutic class that may be considered for topical treatment of human dermatoses of diverse etiology.

ATLa inhibition of neutrophil chemotaxis and transcellular migration to both LTB₄ and fMLP in vitro demonstrates a broader influence for ATLa than LTB₄R-Ant. In addition to potent LTB₄ antagonism in vitro, ATLa exhibited dose-dependent topical efficacy in exogenous LTB₄/Iloprost-induced inflammation, with potency equivalent to LTB₄R-Ant. Earlier studies with lipoxin analogs in this model did not establish dose-dependence or potency relative to a direct LTB₄ antagonist (6). ATLa potency in this model was quite remarkable given that ATLa is not a direct LTB₄ receptor antagonist ($\text{IC}_{50} = >10 \mu\text{M}$) (28).

completely inhibited by $1000 \mu\text{g}/\text{cm}^2$ ATLa treatment (*iii*). The higher magnifications ($\times 100$) for mezerein (*iv*) and mezerein plus ATLa (*v*) treatments demonstrate a decrease in leukocyte infiltration. Big round structures in the dermis represent cross-sections of hair follicles. *B*, The bar graph shows the percent inhibition of mezerein-induced epidermal hyperproliferation by ATLa (■) compared with that by LTB₄ antagonist LTB₄R-Ant (□). Compounds were coapplied with mezerein. Results are expressed as the mean \pm SEM of animals per group experiments. *, $p < 0.05$ vs vehicle control.

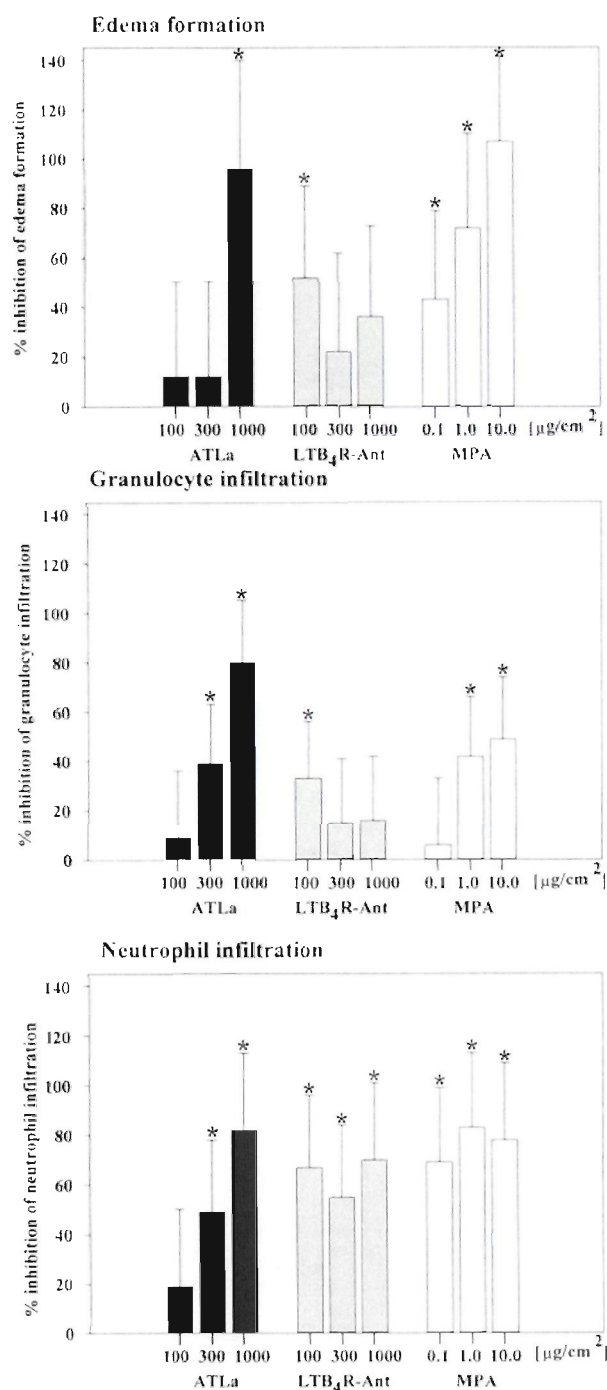


FIGURE 6. ATLa prevents trimellitic anhydride allergen-induced DTH in mice. Mice were sensitized and then challenged with TMA allergen as described in *Materials and Methods*. The inhibitory effects of ATLa (■) were compared with those of LTB₄R-Ant (▨) and MPA (□). All compounds were coapplied with TMA during challenge. Results are expressed as the mean ± SEM of 10 animals per group. *, $p < 0.05$ vs vehicle control.

To explore the broader effects of ATLa, efficacy was investigated in cutaneous reactions triggered by stimuli that induce endogenous release of various inflammatory mediators, including LTB₄. Calcium ionophore-induced inflammation is more prominent compared with the LTB₄/Iloprost model and is inhibited by LTB₄ receptor antagonists (29). As expected, ATLa exhibited

dose-dependent topical efficacy with similar potency to LTB₄R-Ant, but was less potent than MPA. Importantly, ATLa was shown to inhibit ionophore-induced inflammation in two species: mouse and guinea pig.

Croton oil is an irritant that stimulates keratinocytes *in vitro* and *in vivo* to release the inflammatory mediators IL-1 α , TNF- α , IL-8, and GM-CSF via protein kinase C stimulation (30, 31). As expected, MPA showed anti-inflammatory effects at low doses, whereas ATLa, although as efficacious as MPA, was ~1000-fold less potent. ATLa efficacy in this model is consistent with lipoxins inhibiting TNF- α -induced epithelial cell IL-8 release (32), and TNF- α -induced neutrophil infiltration and cytokine/chemokine networks in the mouse air pouch (11). Extensive ATLa inhibition of both inflammatory responses (24 h) and epidermal hyperproliferation (72 h) in the mezerein-induced model is particularly noteworthy. This is the first demonstration of an effect of lipoxins on epidermal hyperproliferation. Epidermal hyperproliferation is a frequent finding in some cutaneous disorders and is prominent in psoriasis. The enhanced epidermal growth not only contributes significantly to patient discomfort, but also complicates disease treatment (33, 34). The inhibitory effect on epidermal hyperproliferation might be a direct anti-proliferative effect on keratinocytes, since lipoxins have been shown to antagonize mitogenic effects and to be anti-proliferative (15). Moreover, keratinocyte hyperproliferation appears to be induced by IL-6 and IL-8, both of which are inhibited by lipoxins (1, 32, 33, 35, 36). The strong inhibitory effect of ATLa on epidermal hyperproliferation in combination with its ability to locally inhibit chemokine networks suggest that ATLa could be an effective topical treatment for psoriasis.

The occupational allergen TMA induces cutaneous and respiratory allergic reactions in man (37). TMA sensitizes and elicits a DTH reaction in animals, with a mixed Th1 and Th2 character (38). The pronounced efficacy of ATLa on edema formation as well as on neutrophil and eosinophil cell infiltration in this model is the first demonstration that lipoxin analogs can modulate a cutaneous, T cell-dependent allergic response. These results are consistent with earlier studies showing that lipoxin analogs inhibit eosinophil chemotaxis *in vitro* (39) and eosinophil-driven inflammation *in vivo* (13, 14). Taken together these findings suggest that ATLa could be explored for topical treatment of dermatoses with a prominent eosinophil component, such as allergic contact dermatitis or atopic dermatitis.

Lipoxins are produced in human asthmatics and potently attenuate human monocyte inflammatory responses (40). Moreover, ATLa potently attenuates airway hyper-reactivity and eosinophilia in murine allergic airway inflammation via multipronged suppression of inflammatory mediators (41). Such findings highlight the anti-inflammatory profile of lipoxins as being distinct from LTB₄ receptor antagonists. The latter have shown poor efficacy in murine allergic airway inflammation (42) and in human asthma clinical trials (43).

In summary, the *in vitro* and *in vivo* characterization of ATLa shows a unique anti-inflammatory profile and suggests its utility for the topical treatment of inflammatory reactions in skin. While less potent than the clinically used topical glucocorticoid MPA, topical ATLa showed equivalent efficacy on most end points measured. To date there is no evidence to suggest that lipoxins would be expected to cause skin atrophy or systemic endocrinological side effects, which limit the long term use of several topical steroids. ATLa and related lipoxins analogs might thus offer an alternative approach to chronic treatment of dermatoses or treatment of skin reactions that are steroid resistant. Based on the similarity of cutaneous inflammatory reactions and their underlying mechanisms to inflammation in other organs, the impressive therapeutic

effects of topically applied ATLa suggest potential utility in other inflammatory and autoimmune diseases. These include rheumatoid arthritis, multiple sclerosis, inflammatory bowel disease, acute respiratory distress syndrome, and ischemia/reperfusion injury. For these indications, further understanding of the systemic pharmacology, efficacy, and safety profile of ATLa and related lipoxin analogs is required.

Acknowledgments

We thank Eginhard Matzke (Research Business Area Dermatology, Schering AG) for excellent technical assistance. Drs. Nicos A. Petasis and Giovanni Bernasconi (Department of Chemistry, University of Southern California) provided synthetic samples of ATLa and general advice on the synthesis and handling of lipoxins.

References

- Serhan, C. N. 1997. Lipoxins and novel aspirin-triggered 15-epi-lipoxins (ATL): a jungle of cell-cell interactions or a therapeutic opportunity? *Prostaglandins* 53:107.
- Fiore, S., and C. N. Serhan. 1990. Formation of lipoxins and leukotrienes during receptor-mediated interactions of human platelets and recombinant human granulocyte/macrophage colony-stimulating factor-primed neutrophils. *J. Exp. Med.* 172:1451.
- Chavis, C., I. Vachier, P. Chanez, J. Bousquet, and P. Godard. 1996. 5(S),15(S)-dihydroxy-eicosatetraenoic acid and lipoxin generation in human polymorphonuclear cells: dual specificity of 5-lipoxygenase towards endogenous and exogenous precursors. *J. Exp. Med.* 183:1633.
- Sanak, M., B. D. Levy, C. B. Clish, N. Chiang, K. Gronert, L. Mastalerz, C. N. Serhan, and A. Szczeklik. 2000. Aspirin-tolerant asthmatics generate more lipoxins than aspirin-intolerant asthmatics. *Eur. Respir. J.* 16:44.
- Levy, B. D., J. M. Drazen, and C. N. Serhan. 1997. Agonist-induced lipoxin A₄ generation in vitro and in aspirin-sensitive asthmatics: detection by a novel lipoxin A₄-ELISA. *Adv. Exp. Med. Biol.* 400B:615.
- Takano, T., S. Fiore, J. F. Maddox, H. R. Brady, N. A. Petasis and C. N. Serhan. 1997. Aspirin-triggered 15-epi-lipoxin A₄ (LXA₄) and LXA₄ stable analogs are potent inhibitors of acute inflammation: evidence for anti-inflammatory receptors. *J. Exp. Med.* 185:1693.
- Takano, T., C. B. Clish, K. Gronert, N. Petasis, and C. N. Serhan. 1998. Neutrophil-mediated changes in vascular permeability are inhibited by topical application of aspirin-triggered 15-epi-lipoxin A₄ and novel lipoxin B₄ stable analogs. *J. Clin. Invest.* 101:819.
- Serhan, C. N., S. Fiore, D. A. Brezinski, and S. Lynch. 1993. Lipoxin A₄ metabolism by differentiated HL-60 cells and human monocytes: conversion to novel 15-oxo and dihydro products. *Biochemistry* 32:6313.
- Clish, C. B., B. D. Levy, N. Chiang, H. H. Tai and C. N. Serhan. 2000. Oxidoreductases in lipoxin A₄ metabolic inactivation: 15-oxoprostaglandin 13-reductase/leukotriene B₄ 12-hydroxy-dehydrogenase is a multifunctional eicosanoid oxidoreductase. *J. Biol. Chem.* 275:25372.
- Serhan, C. N., J. F. Maddox, N. A. Petasis, I. Akritopoulou-Zanze, A. Papayianni, H. R. Brady, S. P. Colgan, and J. L. Madara. 1995. Design of lipoxin A₄ stable analogs that block transmigration and adhesion of human neutrophils. *Biochemistry* 34:14609.
- Hachicha, M., M. Pouliot, N. A. Petasis, and C. N. Serhan. 1999. Lipoxin (LX)A₄ and aspirin-triggered 15-epi-LXA₄ inhibit tumor necrosis factor α -initiated neutrophil responses and trafficking: regulators of a cytokine-chemokine axis. *J. Exp. Med.* 189:1923.
- Clish, C. B., J. A. O'Brien, K. Gronert, G. L. Stahl, N. A. Petasis, and C. N. Serhan. 1999. Local and systemic delivery of a stable aspirin-triggered lipoxin prevents neutrophil recruitment in vivo. *Proc. Natl. Acad. Sci. USA* 96:8247.
- Bandeira-Melo, C., P. T. Bozza, B. L. Diaz, R. S. Cordeiro, P. J. Jose, M. A. Martins, and C. N. Serhan. 2000. Cutting edge: lipoxin (LX) A₄ and aspirin-triggered 15-epi-LXA₄ block allergen-induced eosinophil trafficking. *J. Immunol.* 164:2267.
- Bandeira-Melo, C., M. F. Serra, B. L. Diaz, R. S. Cordeiro, P. M. Silva, H. L. Lenzi, Y. S. Bakhle, C. N. Serhan, and M. A. Martins. 2000. Cyclooxygenase-2-derived prostaglandin E₂ and lipoxin A₄ accelerate resolution of allergic edema in *Angiostrongylus costaricensis*-infected rats: relationship with concurrent eosinophilia. *J. Immunol.* 164:1029.
- McMahon, B., C. Stenson, F. McPhillips, A. Fanning, H. R. Brady and C. Godson. 2000. Lipoxin A₄ antagonizes the mitogenic effects of leukotriene D₄ in human renal mesangial cells. *J. Biol. Chem.* 275:27566.
- Gewirtz, A. T., L. S. Collier-Hyams, A. N. Young, T. Kucharzik, W. J. Guildford, J. F. Parkinson, I. R. Williams, A. S. Neish and J. L. Madara. 2002. Lipoxin A₄ analogs attenuate induction of intestinal epithelial proinflammatory gene expression and reduce the severity of dextran sodium sulfate-induced colitis. *J. Immunol.* 168:5260.
- Nicolau, K. C., J. Y. Rampahl, N. A. Petasis, and C. N. Serhan. 1991. Lipoxins and related eicosanoids: biosynthesis, biological properties, and chemical synthesis. *Angew. Chem.* 30:1100.
- Devchand, P. R., A. K. Hiji, M. Perroud, W. D. Schlemmer, B. M. Spiegelman, and W. Wahli. 1999. Chemical probes that differentially modulate peroxisome proliferator-activated receptor α and BLTR, nuclear and cell surface receptors for leukotriene B₄. *J. Biol. Chem.* 274:23341.
- Yokomizo, T., K. Kato, H. Hagiya, T. Izumi, and T. Shimizu. 2001. Hydroxyeicosanoids bind to and activate the low affinity leukotriene B₄ receptor, BLT2. *J. Biol. Chem.* 276:12454.
- Ekerdt, R., and B. Müller. 1992. B. Role of prostanoids in the inflammatory reaction and their therapeutic potential in skin. *Arch. Dermatol. Res.* 284(Suppl. 1):S18.
- Marks, F., G. Furstenberger, and E. Kownatzki. 1981. Prostaglandin E-mediated mitogenic stimulation of mouse epidermis in vivo by divalent cation ionophore A23187 and by tumor promoter 12-O-tetradecanoylphorbol-13-acetate. *Cancer Res.* 41:696.
- Berg, D. J., M. W. Leach, R. Kuhn, K. Rajewsky, W. Muller, N. J. Davidson, and D. Rennick. 1995. Interleukin 10 but not interleukin 4 is a natural suppressant of cutaneous inflammatory responses. *J. Exp. Med.* 182:99.
- Mufson, R. A., S. M. Fischer, A. K. Verma, G. L. Gleason, T. J. Slaga, and R. K. Boutwell. 1979. Effects of 12-O-tetradecanoylphorbol-13-acetate and mezerein on epidermal ornithine decarboxylase activity, isoproterenol-stimulated levels of cyclic adenosine 3':5'-monophosphate, and induction of mouse skin. *Cancer Res.* 39:4791.
- Dearman, R. J., J. A. Mitchell, D. A. Basketter, and I. Kimber. 1992. Differential ability of occupational chemical contact and respiratory allergens to cause immediate and delayed dermal hypersensitivity reactions in mice. *Int. Arch. Allergy Immunol.* 97:315.
- Goka, J., and M. J. G. Farthing. 1987. The use of 3,3',5,5'-tetramethylbenzidine as a peroxidase substrate in microplate enzyme-linked immunosorbent assay. *J. Immunology* 8:29.
- Springer, T. A. 1995. Traffic signals on endothelium for lymphocyte recirculation and leukocyte emigration. *Annu. Rev. Physiol.* 57:827.
- Buttgereit, F. 2001. Mechanism of action and effects of glucocorticoids. *Z. Rheumatol.* 60:117.
- Gronert, K., T. Martinsson-Niskanen, S. Ravasi, N. Chiang, and C. N. Serhan. 2001. Selectivity of recombinant human leukotriene D₄, leukotriene B₄, and lipoxin A₄ receptors with aspirin-triggered 15-epi-LXA₄ and regulation of vascular and inflammatory responses. *Am. J. Pathol.* 158:3.
- Fretland, D. J., D. L. Widomski, J. M. Zemaitis, R. E. Walsh, S. Levin, S. W. Djuric, R. L. Shone, B. S. Tsai, and T. S. Gaginella. 1990. Inflammation of guinea pig dermis: effects of leukotriene B₄ receptor antagonist, SC-41930. *Inflammation* 14:727.
- Wilmer, J. L., F. G. Burleson, F. Kayama, J. Kanno, and M. I. Luster. 1994. Cytokine induction in human epidermal keratinocytes exposed to contact irritants and its relation to chemical-induced inflammation in mouse skin. *J. Invest. Dermatol.* 102:915.
- Haas, J., T. Lipkow, M. Mohammadzadeh, G. Kolde, and J. Knop. 1992. Induction of inflammatory cytokines in murine keratinocytes upon in vivo stimulation with contact sensitizers and tolerizing analogues. *Exp. Dermatol.* 1:76.
- Gronert, K., A. Gewirtz, J. L. Madara, and C. N. Serhan. 1998. Identification of a human enterocyte lipoxin A₄ receptor that is regulated by interleukin (IL)-13 and interferon γ and inhibits tumor necrosis factor α -induced IL-8 release. *J. Exp. Med.* 187:1285.
- Krueger, J. G., J. F. Krane, D. M. Carter, and A. B. Gottlieb. 1990. Role of growth factors, cytokines, and their receptors in the pathogenesis of psoriasis. *J. Invest. Dermatol.* 94:1355.
- Gottlieb, S. L., P. Gilletteau, R. Johnson, L. Estes, T. G. Woodworth, A. B. Gottlieb, and J. G. Krueger. 1995. Response to psoriasis to a lymphocyte-selective toxin (DAB389IL-2) suggests a primary immune, but not keratinocyte, pathogenic basis. *Nat. Med.* 1:442.
- Kulke, R., E. Bornscheuer, C. Schluter, J. Bartels, J. Rowert, M. Sticherling, and E. Christophers. 1998. The CXCR2 receptor 2 is overexpressed in psoriatic epidermis. *J. Invest. Dermatol.* 110:90.
- Grossman, R. M., J. Krueger, D. Yourish, A. Granelli-Piperno, D. P. Murphy, L. T. May, T. S. Kupper, P. B. Schgal, and A. B. Gottlieb. 1989. Interleukin-6 is expressed in high levels in psoriatic skin and stimulates proliferation of cultured human keratinocytes. *Proc. Natl. Acad. Sci. USA* 86:6367.
- Zeiss, C. R., J. H. Mitchell, P. F. Van Peenen, J. Harris, and D. Levitz. 1990. A twelve-year clinical and immunologic evaluation of workers involved in the manufacture of trimellitic anhydride (TMA). *Allergy Proc.* 11:71.
- Lauerma, A. I., B. Fenn, and H. I. Maibach. 1997. Trimellitic anhydride-sensitive mouse as an animal model for contact urticaria. *J. Appl. Toxicol.* 17:357.
- Soyombo, O., B. W. Spur, and T. H. Lee. 1994. Effects of lipoxin A₄ on chemotaxis and degranulation of human eosinophils stimulated by platelet-activating factor and N-formyl-L-methionyl-L-leucyl-L-phenylalanine. *Allergy* 49:230.
- Bonnans, C., I. Vachier, C. Chavis, P. Godard, J. Bousquet, and P. Chanez. 2002. Lipoxins are potential endogenous anti-inflammatory mediators in asthma. *Am. J. Respir. Crit. Care Med.* 165:1531.
- Levy, B. D., G. T. De Sanctis, P. R. Devchand, E. Kim, K. Ackerman, B. A. Schmidt, W. Szczeklik, J. M. Drazen, and C. N. Serhan. 2002. Multi-pronged inhibition of airway hyper-responsiveness and inflammation by lipoxin A₄. *Nat. Med.* 8:1018.
- Oliveira, S. H., C. M. Hogaboam, A. Berlin, and N. W. Lukacs. 2001. SCF-induced airway hyperreactivity is dependent on leukotriene production. *Am. J. Physiol.* 280:L1242.
- Evans, D. J., P. J. Barnes, S. M. Spathe, E. L. van Alstyne, M. I. Mitchell, and B. J. O'Connor. 1996. Effect of a leukotriene B₄ receptor antagonist, LY293111, on allergen induced responses in asthma. *Thorax* 51:1178.

INFLAMMATION AND INFLAMMATORY BOWEL DISEASE

Activation of signal transducer and activator of transcription (STAT) 1 in human chronic inflammatory bowel disease

S Schreiber, P Rosenstiel, J Hampe, S Nikolaus, B Groessner, A Schottelius, T Kühbacher, J Hämling, U R Fölsch, D Seegert

Gut 2002;51:379–385

See end of article for authors' affiliations

Correspondence to:
Dr S Schreiber, 1st
Medical Department,
Christian-Albrechts-University,
Schittenhelmstrasse 12,
24105 Kiel, Germany;
s.schreiber@mucosa.de

Accepted for publication
9 January 2001

Background: Increased expression of proinflammatory cytokines, including tumour necrosis factor α , interleukin 6, and interferon γ , as well as activation of proinflammatory signalling molecules such as nuclear factor kappa B, is characteristic of inflammatory bowel disease (IBD).

Aims: To investigate expression and activation of signal transducer and activator of transcription (STAT) 1 in patients with IBD.

Patients: Patients with active IBD (n=42), disease specificity controls (n=8), and normal controls (n=12) were investigated.

Methods: Expression and activation of STAT1 were assessed by western blotting and electrophoretic mobility shift assays in extracts of endoscopic colonic biopsies. Cellular localisation was determined by immunohistochemistry.

Results: Western blots and immunohistochemical staining revealed an increase in STAT1 expression and activation in mucosal samples from ulcerative colitis and to a lesser extent in Crohn's disease patients. High levels of suppressor of cytokine signalling (SOCS)-3 expression, an inhibitor of STAT activation, were observed in Crohn's disease patients and normal controls in western blot experiments whereas no differences were observed for SOCS-1 expression. Phosphorylated (p) STAT1 was mainly detected in monocytic cells and neutrophils in the inflamed mucosa. Induction of remission by systemic glucocorticoids led to a decrease in levels of pSTAT1. In vitro studies indicated a direct effect of steroid treatment on STAT1 activation.

Conclusions: Expression and activation of STAT1 are predominantly heightened in ulcerative colitis and may therefore play an important role in the pathophysiology of colonic inflammation.

Inflammatory bowel disease (IBD) is characterised by a dys-regulated mucosal immune response. The pathophysiology of this regulatory defect is reflected by a distorted balance of regulatory cytokines.^{1,2} In IBD as well as most animal models resembling IBD, enhanced secretion of proinflammatory cytokines is observed whereas contra-inflammatory cytokines may not be secreted in adequate amounts or their activity inhibited.³⁻⁷ The primary regulatory pathways for many of the functional and anatomical alterations found in IBD, which include increased permeability for macromolecules and tissue destruction, are unclear.^{7,8}

The IBD phenotype can be subclassified into Crohn's disease and ulcerative colitis using clinical, endoscopic, histological, and radiological characteristics.⁹ Given the substantial clinical differences between Crohn's disease and ulcerative colitis, the search for distinctive immunological characteristics in each of these subtypes is of interest. Patterns of cytokine secretion have been investigated for their potential to unveil specific immunological disturbances related to IBD subtypes. In mice, T helper cell type 1 (TH1) driven models of intestinal inflammation were generated which share similarities with human IBD.^{10,11} However, some investigators have found a preponderance of TH1 cytokine secretion in patients with Crohn's disease and of TH2 cytokine secretion in ulcerative colitis.¹²⁻¹⁴ Other data indicate increased production of the TH2 cytokine interleukin (IL)-4¹⁵ as a critical step in the development of early lesions of Crohn's disease. The TH1 cytokine interferon γ (IFN- γ) and cytokines with an IL-12-like activity may be major components of the pathophysiology of pouchitis and ulcerative colitis, respectively.^{14,15} Therefore, interpretation of

ex vivo cytokine assessments and of data from animal models of colitis with regard to human IBD appears to be difficult.

Most cytokines specifically activate transcription factors to regulate expression of specific genes. Whereas tumour necrosis factor α (TNF- α) and IL-1 β preferentially induce activation of the nuclear factor kappa B (NF κ B) system,^{16,17} many other growth factors and cytokines activate proteins of the signal transducer and activator of transcription (STAT) family.^{18,19} STAT proteins are dormant cytoplasmic transcription factors which become activated after phosphorylation by Janus kinases (JAK) or other kinases in response to binding of cytokine or growth factor receptors.^{20,21} The activated protein migrates into the nucleus and binds to specific promoter elements to regulate gene expression. STAT regulated genes include the Fc γ receptor,²² inducible nitric oxide synthetase,²³ major histocompatibility class II,²⁴ and intercellular adhesion molecule 1 (ICAM-1).²⁵ The phosphorylation of other STAT family molecules appears to be an important mechanism to confer the specificity of transcriptional regulation. In 1997, a new group of proteins was described which specifically inhibit activation of members of the STAT family.²⁶ These proteins are called

Abbreviations: IBD, inflammatory bowel disease; STAT, signal transducer and activator of transcription; SOCS, suppressor of cytokine signalling; IFN- γ , interferon γ ; TH1, TH2, T helper cell types 1 and 2; IL, interleukin; TNF- α , tumour necrosis factor α ; NF κ B, nuclear factor kappa B; JAK, Janus kinases; EMSA, electrophoretic mobility shift assay; PBS, phosphate buffered saline; AP-1, activator protein 1; ICAM-1, intercellular adhesion molecule 1.

suppressors of cytokine signalling (SOCS). SOCS-1 and -3 have been shown to inhibit phosphorylation of STAT1 and STAT3.^{27, 28}

Signal transduction abnormalities have been demonstrated previously in Crohn's disease and animal models of IBD—for example, for the NFκB system.^{29, 30} We have assessed activation of STAT1 in IBD because many immune regulatory genes contain STAT binding sites in their promoter regions. In addition, activation of STATs is important for signalling of many cytokine and growth factor receptors. The status of STAT activation and its expression were assessed in snap frozen tissue from diseased human intestine with different methodologies. The data presented here demonstrate the increased nuclear accumulation of STAT1 in IBD. A preponderance of STAT1 activation is seen in ulcerative colitis in comparison with Crohn's disease, indicating an important role for this protein and eventually TH1 driven immunity in the pathophysiology of colonic inflammation.

MATERIAL AND METHODS

Patients

A total of 14 patients with clinically active Crohn's disease and 28 patients with active ulcerative colitis participated in the study. Patients were recruited from the outpatient clinics of the Charité University Hospital, Berlin, the Tabea Hospital for Inflammatory Bowel Disease, Hamburg, and the Hospital of the Christian-Albrechts-University, Kiel, Germany. All patients were seen because of increased clinical activity. At the time mucosal biopsies were obtained, 8/14 patients with Crohn's disease and 24/28 patients with ulcerative colitis received treatment with oral salicylates (mesalazine—Salofalk, Claversal, or Pentasa; salazosulphapyridine—Azulfidine or Colopleon; olsalazine—Dipentum) in doses up to 4.5 g/day. None of the patients received steroids and/or cytotoxic drugs, immunosuppressives, or antibiotics. All IBD patients underwent sigmoidoscopy or colonoscopy for routine clinical evaluation. Diagnosis had been established by clinical, endoscopic, histological, and/or radiological criteria. The presence of infection or parasites was excluded by stool cultures, microscopic stool examination, and serology (*Yersinia*, *Campylobacter*). Nine patients with ulcerative colitis were followed until glucocorticoid induced remission. Normal controls (n=12) were age and sex matched healthy volunteers. Disease specificity controls included patients with diverticulitis, salmonellosis, and infectious enterocolitis. The study was approved by the institutional review board. Patients gave written informed consent 24 hours prior to the procedures.

Extracts

For electrophoretic mobility shift assays (EMSAs), snap frozen biopsies were pulverised in liquid nitrogen and nuclear and cytosolic extracts were prepared as previously described.²⁹ Protein concentration was assessed by a modified Bradford protein assay (Biorad, Hercules, California, USA) and all samples were adjusted to an equal protein concentration.

Isolation of peripheral blood monocytes

Peripheral blood monocytes were isolated as previously described.⁶ Briefly, 15 ml of Lymphoprep solution (Nycomed, Denmark) were placed into 50 ml Leucosep tubes (Greiner, Germany) and centrifuged for two minutes at 100 g until the entire solution was below the frit. Whole blood (30 ml) containing 1 mM EDTA as anticoagulant was directly poured onto the frit followed by centrifugation at 800 g for 15 minutes at room temperature. The resulting interphase was collected and washed twice with sterile phosphate buffered saline (PBS). The cells were counted, resuspended in RPMI with 10% fetal calf serum, plated on six well plates, and incubated for two hours at 37°C. Non-adherent cells were removed by washing with 2 ml of ice cold PBS and the remaining monocytes were overlaid with 2 ml of fresh medium (37°C). The viability of the cells was determined by trypan blue staining and

purity was examined by flow cytometry according to standard procedures and reached 80–90%.

Western blotting and quantification

Total protein (10 µg per lane) was separated on a 10% denaturing polyacrylamide gel and transferred to a polyvinylidene difluoride membrane (0.8 mA/cm², 75 minutes, transfer buffer: 25 mM Tris, 190 mM glycine, 20% MeOH, 0.5% sodium dodecyl sulphate) by semidry electroblotting (Biorad). The membrane was blocked for 60 minutes at room temperature with 5% non-fat dry milk in TTBS (10 mM Tris (7.5), 100 mM NaCl, 0.1% Tween-20). The primary antibody was diluted 1:250 to 1:1000 in blocking buffer and placed on the membrane for 60 minutes at room temperature. After washing with TTBS, the membrane was incubated with a peroxidase conjugated secondary antibody, which was diluted 1:1000 in blocking buffer for 20 minutes at room temperature. Detection was performed by incubation with ECL Plus (Amersham, Germany) and exposed to radio film. Bands were quantified by densitometry (ImageQuant; Molecular Dynamics, Sunnyvale, California, USA). Western blots were standardised by addition of geometrically diluted appropriate cell lysates. On the basis of these standards, the bands of the scanned films were normalised to an arbitrary intensity unit.

Electrophoretic mobility shift assay (EMSA)

Extract (2 µl=5 µg of protein) was incubated with 0.5 ng of ³²P-labelled GAS containing oligonucleotide (from the promoter of the human FcγRI gene: 5'-GTATTCCCAGAAAAGGAAC-3') in a total reaction volume of 10 µl supplemented with 2 µl of 5× Gelshift binding buffer (Promega, Madison, Wisconsin, USA) for 20 minutes at room temperature. After addition of 1 µl of 10× loading buffer the entire reaction mixture was run for 45 minutes on a 4% polyacrylamide gel with 0.5× TBE (1.8 mM Tris (8.3), 50 µM EDTA, 1.8 mM borate) at 300 V. The gel was dried, exposed overnight at room temperature to an imaging plate, and finally analysed with a Fuji FLA3700 phosphorimager. Supershift or competition experiments were performed by adding 1 µl of antibody or a 50-fold molar excess of unlabelled oligonucleotide (β-casein-gamma interferon activation site (GAS): AGATTCTAGGAATCAATC; NFκB: AGTTGAGGGGACTTCCAGGC; activator protein 1 (AP-1): CGCTTGATGAGTCAGCCGGAA) to the binding reaction.

Immunofluorescence and grading of histology

Biopsies were embedded in cryomatrix and snap frozen in liquid nitrogen. Cryostat sections (7 µm) were thaw mounted on Superfrost slides (Menzel/Merck Ltd, Poole, UK), postfixated for five minutes in acetone, air dried, and stored at -20°C before staining. Two slides of each biopsy were stained with haematoxylin-eosin for routine histopathology. On the other slides, tissue sections were made permeable with 0.1% Triton X-100 in 0.1 M PBS, washed three times in PBS, and blocked non-specifically with 0.75% bovine serum albumin in PBS. Subsequently, sections were incubated for 60 minutes with the appropriate antibody diluted 1:100 to 1:200 in 0.75% bovine serum albumin. After washing in PBS, tissue bound antibody was detected using biotinylated goat-antimouse IgG antibodies (Vector Laboratories, Burlingame, California, USA), followed by avidin-FITC (Vector Laboratories), both diluted at 1:100 in 5% human serum. Stainings with an irrelevant primary antibody, only with secondary antibody, and avidin-FITC served as controls. Nuclear counterstaining with bisbenzimidazole was performed. Fluorescence was visualised using an Axiophot microscope (Zeiss, Jena, Germany) with the appropriate filter systems, and photos were taken on Provia 1600 colour films (Fuji, Dusseldorf, Germany).

Inflammatory activity was graded as follows (haematoxylin-eosin stained slides): 0, no or non-significant

inflammatory activity; 1, significant inflammation present; and 2, severe changes. Parameters were intensity of the inflammatory infiltrate (neutrophils, mononuclear cells) and severity of destruction of the normal micro architecture. In order to be assigned to the "severe" category, a dense inflammatory infiltrate had to be present in conjunction with significant alterations of the micro architecture.

Other biochemicals

Fetal calf sera were purchased from Gibco (Grand Island, New York, USA) or Sigma (St Louis, Missouri, USA). All antibodies were purchased either from Santa Cruz Biotechnology (Santa Cruz, California, USA), BD Pharmingen (San Diego, California, USA), Dianova (Hamburg, Germany), or New England Biolabs (Beverly, Massachusetts, USA). All other chemicals were obtained from Sigma if not otherwise specified.

Expression of data

The symbol *n* refers to the number of experiments. All experiments were carried out three or more times. Normal distribution of the data was evaluated by calculating Lilliefors probabilities based on the Komolgorov-Smirnov test.^{31,32} Statistical significance of the differences for non-normally distributed data was tested using the Mann-Whitney U test or the Wilcoxon matched pairs test.³³ Results are expressed as mean (SD) if data followed a normal distribution or as median (interquartile range) if data were non-normally distributed.

RESULTS

Nuclear expression levels of STAT1 are increased in IBD and correlate with the endoscopic and histological activity of the disease

During activation, STAT proteins translocate into the nucleus. The amount of STAT1 in nuclear extracts of snap frozen colonic mucosal biopsy tissues was determined by western blot followed by densitometric measurement (fig 1A). Increased nuclear amounts of STAT1 (median 1.73 (interquartile range 1.4–2.8) arbitrary units, *n*=22) were detected in biopsies from patients with ulcerative colitis in comparison with both Crohn's disease patients (0.92 (0.45–1.21), *n*=10; *p*<0.01) and normal controls (0.20 (0.16–0.28), *n*=12; *p*<0.01). Nuclear levels of STAT1 in biopsies from inflamed mucosa were not different between similarly inflamed anatomical regions (for example, left sided colon versus right sided colon in ulcerative colitis; not shown). Patients with infectious colitis were examined to determine the specificity of our findings. In patients with non-IBD colonic inflammation, nuclear levels of STAT1 were increased (1.06 (0.6–1.6), *n*=8) in comparison with normal controls (*p*<0.01) although still considerably lower than in ulcerative colitis.

High total protein expression levels of STAT1 were found in unfractionated intestinal mucosal samples of patients with ulcerative colitis (2.19 (1.39–2.75), *n*=20) in comparison with patients suffering from Crohn's disease (0.95 (0.23–1.44), *n*=10; *p*<0.05) and normal controls (0.17 (0.05–0.23), *n*=12; *p*<0.001) (not shown). Total expression of STAT1 in Crohn's disease was statistically different from normal controls (*p*<0.005). Samples were obtained from the same anatomical sites as the biopsies used for nuclear extracts.

To examine whether nuclear levels of STAT1 correlate with disease activity, biopsies were obtained from patients with different degrees of endoscopic activity. Endoscopically non-involved mucosa from patients with ulcerative colitis showed increased levels of STAT1 in nuclear extracts (median 0.76 (interquartile range 0.53–1.13), *n*=9) in comparison with biopsies from normal controls (0.2 (0.16–0.28), *n*=12; *p*<0.05). Levels in endoscopically inflamed mucosa were considerably higher in comparison with samples from macroscopically non-inflamed tissue of the same patient (1.4 (0.73–2.3), *n*=9; *p*=0.011). Comparison of different degrees of histological activity is demonstrated in the western blot in fig 1B. This indicates

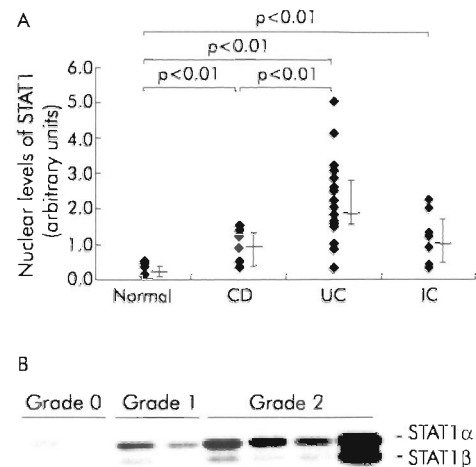


Figure 1 (A) Levels of signal transducer and activator of transcription 1 (STAT1) in the nuclear extracts of colonic biopsies. Extracts were examined by western blot with specific monoclonal antibodies. CD, Crohn's disease; UC, ulcerative colitis; IC, inflammatory controls. (B) Nuclear levels of STAT1 were determined by western blot in colonic mucosal biopsies from UC patients in relation to the histological degree of inflammation (grade 0, mild; grade 1, moderate; grade 2, severe). Representative of three experiments with identical findings.

that the degree of histological inflammation, as rated by an independent examiner, was related to nuclear accumulation of STAT1. The endoscopically "non-involved" mucosa, as described above, was associated with a histological degree of inflammation of 0 or 1 (on a scale of 0–2).

Phosphorylation and DNA binding activity of STAT1 is predominantly increased in ulcerative colitis

Activation of STAT1 as a regulator of transcription requires both phosphorylation and nuclear translocation of the factor, and leads to binding of specific DNA sites. To examine whether increased nuclear accumulation of STAT1 in IBD is associated with an increased level of activated (phosphorylated) STAT1, tyrosine phosphorylation of STAT1 was determined by western blot with a PY701-STAT1 specific antibody. All membranes were stripped and reprobbed with a STAT1 specific antibody. STAT1 phosphorylation was then expressed as the ratio between the amount of phosphorylated (*p*) STAT1 and the total amount of STAT1 in the biopsies (fig 2A). Patients with ulcerative colitis exhibited higher levels of tyrosine phosphorylated STAT1 in the intestinal mucosa (mean 1.73 (SD 0.75), *n*=7; *p*=0.0048) in comparison with normal controls (0.84 (0.45), *n*=7) or Crohn's disease (1.29 (0.4), *n*=7; *p*=0.0017). An example western blot of these sets of experiments is shown in fig 2B.

To assess the DNA binding activity of STAT1 in IBD, EMSAs were performed. Nuclear extracts from four different normal control biopsies or biopsies from ulcerative colitis (*n*=5) and Crohn's disease (*n*=4) patients were incubated with a ³²P-labelled oligonucleotide containing the GAS site from the FcγRI promoter, and DNA/protein complexes were separated on an acrylamide gel (see methods). Figure 3 shows a representative result obtained with one extract from each investigated group. A strong DNA binding complex was detected in ulcerative colitis homogenates but not (as shown), or to a significantly lesser degree, in Crohn's disease and normal control samples. STAT binding to the ³²P-labelled oligonucleotide was characterised by competition experiments with an excess of different unlabelled specific (FcγRI-GAS, β-casein-GAS) and unspecific (NFκB binding site, AP-1 binding site) oligonucleotides or coincubation with different specific anti-STAT antibodies, as outlined in the figure legend. The specificity of each antibody used has been reported previously. These experiments demonstrate that the DNA binding

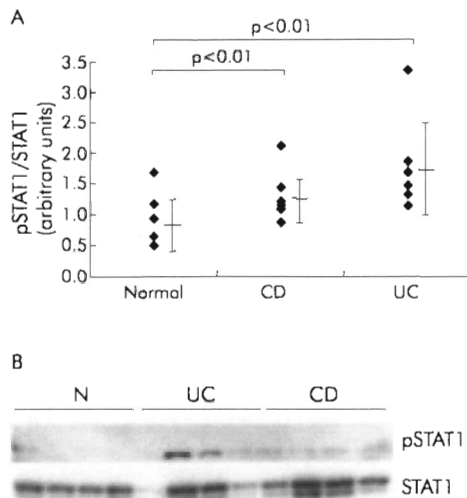


Figure 2 (A) Phosphorylation of signal transducer and activator of transcription 1 (pSTAT1) in the intestinal mucosa from patients with ulcerative colitis [UC] or Crohn's disease [CD] and normal controls (N). STAT1 phosphorylation was expressed as the ratio of pSTAT1 to total STAT1. Every membrane was probed with an anti-PY701-STAT1 antibody and afterwards reprobed with a STAT1 specific antibody (an example is shown in [B]).

complex detected in IBD mainly contains STAT1 but also lower amounts of STAT3.

Increased STAT1 expression in ulcerative colitis is mainly restricted to infiltrating neutrophils and monocytes in the lamina propria

To localise the anatomical site and type of cells in the lamina propria which contribute to the high expression and activation of STAT1, immunofluorescence studies were performed. Frozen sections from normal controls (n=5) and from patients with ulcerative colitis (n=6) and Crohn's disease (n=5), which were obtained in parallel from the same sites as the biopsies used for the cell biology studies, were stained with an anti-PY701-STAT1 antibody (fig 4A). Large numbers of cells were stained by the anti-pSTAT1 antibody in patients with ulcerative colitis but considerably less positive cells were detected in patients with Crohn's disease and only rarely in normal controls. Positive cells were exclusively found in the lamina propria. To investigate whether activation of STAT1 in ulcerative colitis is restricted to particular cell types, we used an anti-pSTAT1 antibody in combination with different cell type specific antibodies against neutrophils (human neutrophilic peptide), eosinophils (eosinophilic peroxidase), monocytes/macrophages (CD68), and T cells (CD3) (fig 4B). Detection of pSTAT1 was clearly associated with neutrophils and monocytic cells but not with eosinophils or T cells. The same results were obtained when the fluorescence dyes of the secondary antibodies were inverted, which demonstrated the specificity of our results.

Expression of the suppressor of cytokine signalling (SOCS)-3 in IBD

Altered levels of STAT1 activation could be based on different levels of SOCS-1 and SOCS-3 expression in ulcerative colitis and Crohn's disease. Therefore, levels of both proteins were examined by western blot in total extracts of biopsies from active IBD patients and compared with controls (example blot shown in fig 5). Colonic biopsies from patients with active ulcerative colitis showed lower protein levels of SOCS-3 protein expression (median 0.5 (interquartile range 0.3–0.9) arbitrary units, n=9) than active Crohn's disease patients (2.2 (1.2–3.1), n=9; p=0.004) or normal controls (2.0 (1.54–2.75), n=8; p=0.005). The same extracts were also investigated for SOCS-1 expression but all signals remained near or even less than the

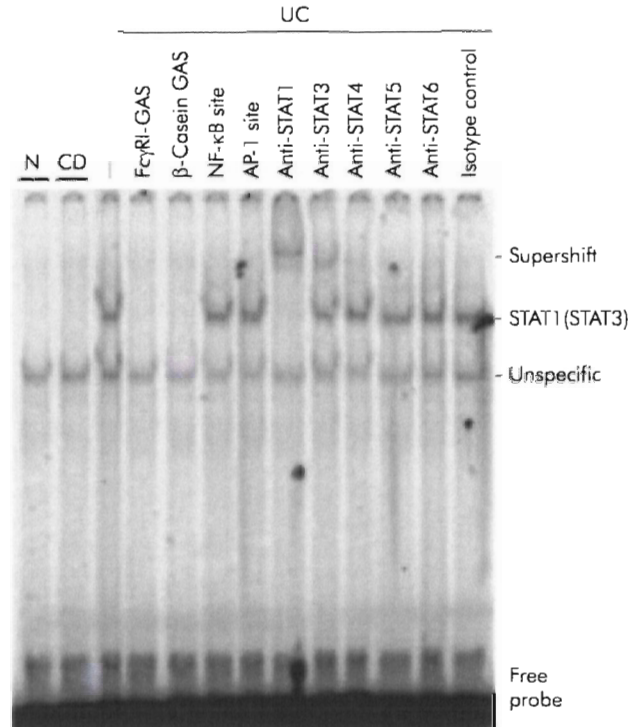


Figure 3 Representative electrophoretic mobility shift assay for assessment of signal transducer and activator of transcription (STAT)/DNA binding complexes in colonic mucosal biopsies from a control (N) subject, and two patients with ulcerative colitis (UC) or Crohn's disease (CD). The specificity of the complex was examined by cold competition with a 25-fold molar excess of unlabelled Fc γ RI-GAS (lane 4), β -casein-GAS (lane 5), nuclear factor kappa B [NF- κ B] binding (lane 6), or activator protein 1 [AP-1] binding (lane 7) oligonucleotides. The existence of STAT proteins in the DNA binding complex by parallel use of different anti-STAT antibodies (lanes 8–12). The last lane represents a control with an isotype specific control antibody.

detection levels of the antibodies used (not shown). SOCS-1 and SOCS-3 could not be detected by immunohistology.

STAT1 phosphorylation is decreased after glucocorticoid treatment

Biopsies from nine IBD patients were derived before and 2–4 weeks after beginning steroid therapy, and pSTAT1 levels were investigated by western blot. All patients received prednisolone (equivalent) in a dose of 60 mg for two weeks, which was then reduced to 40 mg (one week) and 30 mg (one week). Patients reached clinical remission after conclusion of the treatment. IBD patients before therapy (ratio between pSTAT1 and STAT1: mean 1.68 (SD 1.12)) showed significant downregulation of STAT1 phosphorylation after treatment (0.59 (0.3); p<0.05) (fig 6A). To examine whether downregulation of STAT1 phosphorylation is a direct effect induced by glucocorticoids or is secondary to the reduced level of inflammation, further in vitro assays were performed by treating isolated peripheral blood monocytes for different times with IFN- γ (1000 U/ml) and/or 10 μ M of prednisolone (fig 6B). These experiments indicated that glucocorticoids directly inhibited IFN- γ mediated STAT1 phosphorylation, as shown in the last lane (see fig 6B). Simultaneous stimulation of the cells with IFN- γ and prednisolone also resulted in marked loss of STAT1 phosphorylation (not shown). Similar results were obtained in additional experiments with monocytic THP-1 cells (not shown).

DISCUSSION

The normal non-inflamed mucosal immune system is characterised by a delicate balance between pro- and contra-inflammatory cytokines. The preponderance of proinflammatory cytokines, which is observed in IBD, has led to the

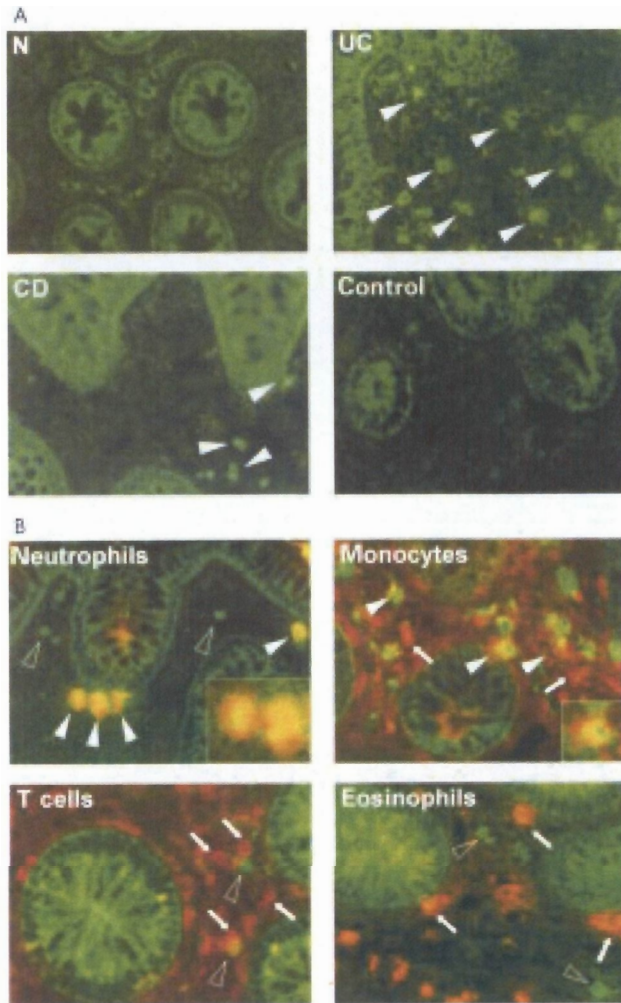


Figure 4 (A) Immunostaining for phosphorylated signal transducer and activator of transcription 1 (pSTAT1). Distinct staining with high numbers of positive cells were detected in ulcerative colitis (UC) in comparison with Crohn's disease (CD) or normal controls (N). The control shows a staining experiment with an irrelevant isotype antibody in a patient with ulcerative colitis. Arrowheads indicate the position of stained cells. (B) Double staining of UC biopsies with an anti-pSTAT1 antibody (green) and cell type specific antibodies (red) [open arrowheads, cells exclusively stained with the anti-pSTAT1 antibody; arrowheads: double stained cells; arrows, cells exclusively stained with cell type specific antibody].

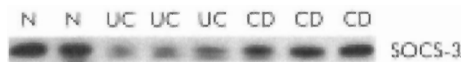


Figure 5 Example of a suppressor of cytokine signalling 3 (SOCS-3) specific western blot in extracts from mucosal biopsies from normal control colon (N) or inflamed colonic regions from patients with Crohn's disease (CD) or ulcerative colitis (UC).

development of therapeutic approaches that aim to readjust the balance (for example, the introduction of monoclonal antibodies directed against TNF- α ^{34,35} or systemic application of the contra-inflammatory cytokine IL-10^{36,37}). Analysis of cytokine dysregulation by assessment of cytokine secretion or expression in the mucosa may not completely represent the pathophysiological process. The biological activity of cytokines is dependent on interaction between mediators with their receptors and on the microenvironment of secretion.

Analysis of cytokine induced transcription factor activation may reveal additional insights into key steps of regulation of the complex cytokine network. Activation of the NF κ B system as a

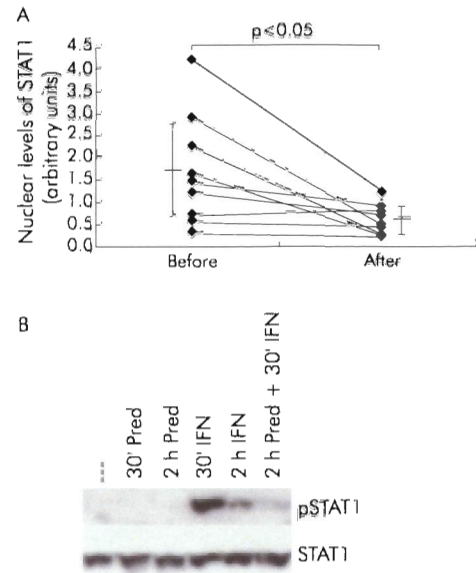


Figure 6 (A) Downregulation of signal transducer and activator of transcription 1 (STAT1) phosphorylation after therapy with glucocorticoids. Colonic mucosal STAT1 levels were examined before and 2–4 weeks after treatment of ulcerative colitis (UC) patients with systemic glucocorticoids (n=9) was initiated. Results were obtained by western blot and analysed densitometrically. (B) In vitro stimulation of isolated peripheral blood monocytes with interferon γ (IFN 1000 U/ml) and prednisolone (pred 10 μ M) for the indicated times (30 minutes and two hours). pSTAT1 (top panel) was detected by western blot and total amounts of STAT1 were examined by probing of the same membrane (bottom panel).

major cytokine signalling pathway has recently been described in different chronic inflammatory disorders, including Crohn's disease.^{29,37,38} However, activation of this system does not completely explain the nature of the inflammatory process. Many immunoregulatory genes contain multiple binding sites for transcription factors, including members of the STAT family. The mechanisms resulting in specificity of transcriptional regulation by STATs (in particular STAT1), which are involved in signalling of many cytokine receptors, are still unclear. Specificity may be reached through the sequential and cooperative binding of multiple transcription factors.³⁹

Specific activation of STAT1 was demonstrated previously in other chronic inflammatory diseases, including asthma and rheumatoid arthritis.^{40,41} In this study, we demonstrated that ulcerative colitis and Crohn's disease are characterised by increased expression and activation of STAT1 in the intestinal lamina propria. Activation of this transcription factor was found consistently using different assays targeting nuclear accumulation, phosphorylation, or functional activity of STAT1, respectively. The predominance of STAT1 activation in ulcerative colitis in comparison with Crohn's disease was not due to differences in inflammatory activity, as demonstrated by similar histological activity and by high levels of NF κ B p65 in Crohn's disease in the same set of nuclear extracts of biopsy tissue (data not shown). Most interestingly, STAT1 can also inhibit activation of NF κ B under certain conditions.⁴²

Immunohistology localised high levels of phosphorylated STAT1 to neutrophils and monocytic cells in the lamina propria. Increased infiltration with neutrophils and macrophages is a hallmark of the intestinal immunopathology of IBD. We therefore conclude that the observed elevation of STAT1 activation and expression in the intestinal mucosa is partially due to increased infiltration with STAT1 expressing cells. However, the heightened ratio between phosphorylated and total STAT1, as depicted in fig 2A, indicates an over proportional increase in STAT1 activation in ulcerative colitis. Therefore, both an increase in total levels but also a true activation are seen. We suggest that increased STAT1 activation in

ulcerative colitis and (to a lesser extent) in Crohn's disease may reflect an immunoregulatory difference of cytokine action in vivo. This would indicate that the animal model derived simplified hypothesis of a TH1 driven response in Crohn's disease and a TH2 driven immunity in ulcerative colitis does not reflect human pathophysiology.

Various cytokines can induce activation of STAT1. In addition to the interferons, these include epidermal growth factor, platelet derived growth factor, IL-6, or colony stimulating factor 1.^{23 43 44} The predominance of STAT1 activation seen in ulcerative colitis could be consistent with reports that have suggested that IFN- γ is an important mediator in both human IBD and in animal models of colitis.^{5 31 43-47} However, it should be noted that increased expression of IFN- γ has not been described consistently in human IBD. Although high levels of IFN- γ have been reported as a specific characteristic of Crohn's disease³ and in pouchitis,¹⁹ the IFN- γ gene does not appear to be a candidate for a primary genetic cause of IBD.⁴⁸ Therefore, it is unlikely that differences in the cytokine patterns are the only explanation for differences in STAT1 activation.

The surprising finding in this study that STAT1 appears to be mostly activated in ulcerative colitis and to a lesser degree in Crohn's disease has led to the question, which molecular mechanisms are responsible for this phenomenon in addition to cytokines? Downregulation of STAT activity is not caused primarily by degradation of signal transducers but is mostly due to active shutdown mechanisms, such as those mediated by phosphatases (that is, SHP-1).⁴⁹ Another recently described family of cytokine induced inhibitors of the JAK-STAT signal cascade are the SOCS.^{26 50 51} Western blot experiments revealed that SOCS-3 levels appeared to be higher in the majority of Crohn's disease and control samples in comparison with the ulcerative colitis samples (fig 5). However, SOCS-1 and SOCS-3 were not detectable by immunohistology. This is most likely due to technical reasons (that is, the monoclonal antibodies available do not work for this application or the concentration is below detection levels for this technique). Therefore, it is unclear whether SOCS-3 expression is increased in the same cells which show low STAT1 activity. SOCS-1 does not appear to be upregulated in the intestinal mucosa of patients with IBD (not shown). This is consistent with recently published findings from Suzuki *et al* demonstrating high expression of SOCS-3 but not SOCS-1 in IBD samples and also in murine colitis models.³²

Increased activation of STAT1 was recently shown to correlate with expression of ICAM-1.⁴⁰ In IBD, upregulated expression of ICAM-1 among other adhesion molecules is one of the hallmarks of inflammatory activity.³³ Increased expression of ICAM-1 is a pivotal factor for the homing of large numbers of activated phagocytes into intestinal lesions. Levels of STAT1 activation paralleled the endoscopic and histological presentation of inflammatory activity in patients with ulcerative colitis. Patients in remission showed nuclear levels of STAT1 which approached normal non-inflamed controls. STAT1 regulated genes such as major histocompatibility class II, Fc γ receptor, inducible nitric oxide synthase, or ICAM-1 also correspond in their expression to the overall inflammatory activity.³³⁻³⁷ Activation of STAT1 (in addition to the TNF/NF κ B system^{38 39}) may therefore contribute to many of the pathophysiological features observed in IBD.

This study also showed that glucocorticoids actively inhibit phosphorylation of STAT1. We found that prednisolone inhibited in vitro phosphorylation of STAT1 in isolated peripheral monocytes as well as in the THP-1 cell line. In addition, treatment of IBD patients with systemic glucocorticoids resulted in a decrease in pSTAT1 levels in the intestinal mucosa. While these experiments cannot prove a primary role for STAT1 activation in the inflammatory pathophysiology, they suggest that inhibition of the STAT system may be an important part of the anti-inflammatory efficacy of glucocorticoids. Patients with glucocorticoid induced remission had

lower nuclear levels of STAT1 (fig 6A). In addition, the action of glucocorticoids may explain the discrepancy between increased levels of STAT1 activation found in IBD in this study and the work by Suzuki *et al* who did not report increased phosphorylation of STAT1 in IBD.³² It should be pointed out that IBD patients in the study of Suzuki *et al* were pretreated with anti-inflammatory drugs and that only small numbers (two patients with ulcerative colitis, one patient with Crohn's disease) were investigated.

Microinvasion of *Escherichia coli* has been described as an important event in both IBD^{60 61} as well as colonic adenocarcinoma.⁶² The hypothesis has been raised that bacterial invasion into the mucosa may be an important early event in the onset of the inflammatory reaction. The heightened levels of nuclear accumulation of STAT1, which are seen in infectious colitis and diverticulitis, could point to a role for intestinal microorganisms in the mechanism of activation of this transcription factor. The role of microorganisms in the activation of STAT1 in ulcerative colitis is therefore under intense investigation. In this regard it will be important to evaluate genetic susceptibility as a potential permissive factor.⁶³⁻⁶⁵

In summary, we have shown that STAT1 expression and activation are significantly upregulated in the colonic mucosa of patients with active ulcerative colitis. Detection of phosphorylated STAT1 is mostly restricted to neutrophils and monocytes in the lamina propria and appears to be downregulated by glucocorticoids. Analysis of the intracellular signalling responses may reveal important novel aspects in complex inflammatory diseases such as human IBD. Activation of STAT1 and (as already demonstrated) other STAT family members could contribute to the pathophysiology of the disease. Further studies will demonstrate whether STATs are promising target molecules for future therapeutic interventions in colonic inflammation.

ACKNOWLEDGEMENTS

This work was supported by grants from the Deutsche Forschungsgemeinschaft (DFG), the BMBF competence network "Inflammatory Bowel Disease", as well as a training and mobility of researchers grant of the European Commission (ERBFMRXCT980240). The authors are grateful to J Sievers (Department of Anatomy, Christian-Albrechts-University, Kiel, Germany) for discussions and access to the immunofluorescence equipment. The contribution of the endoscopy staff at the Charité University Hospital, Tabea Centre for Inflammatory Bowel Diseases, and the Hospital of the Christian-Albrechts-University in obtaining colonic tissue as well as the excellent technical help of AM Wenner, S Eidner, and I Woywod are gratefully acknowledged.

Authors' affiliations

S Schreiber, J Hampe, S Nikolaus, J Hämling, U R Fölsch, D Seeger, 1st Department of Medicine, Christian-Albrechts-University, Schittenhelmstrasse 12, Kiel, Germany
B Groessner, Hospital for Conservative Dentistry and periodontology, Christian-Albrechts-University, Kiel, Germany
P Rosenstiel, Institute for Anatomy, Christian-Albrechts-University, Kiel, Germany
A Schottelius†, Charité University Hospital, 4th Medical Department, Humboldt University, Berlin, Germany
T Kühbacher, Clinica Media I, Policlinico S Orsola, University of Bologna, Italy

†Present address: Schering AG, Berlin, Germany

REFERENCES

- Hodgson HJ. Pathogenesis of Crohn's disease. *Baillieres Clin Gastroenterol* 1998;**12**:1-17.
- Abreu-Martin MT, Targan SR. Regulation of immune responses of the intestinal mucosa. *Crit Rev Immunol* 1996;**16**:277-309.
- MacDonald TT, Hutchings P, Choy MY, *et al*. Tumour necrosis factor-alpha and interferon-gamma production measured at the single cell level in normal and inflamed human intestine. *Clin Exp Immunol* 1990;**81**:301-5
- Kuhn R, Lohler J, Rennick D, *et al*. Interleukin-10-deficient mice develop chronic enterocolitis. *Cell* 1993;**75**:263-74

- 5 Powrie F, Leach MW, Mauze S, *et al*. Inhibition of Th1 responses prevents inflammatory bowel disease in scid mice reconstituted with CD45RBhi CD4+ T cells. *Immunity* 1994;1:553-62.
- 6 Schreiber S, Heinig T, Thiele HG, *et al*. Immunoregulatory role of interleukin 10 in patients with inflammatory bowel disease. *Gastroenterology* 1995;108:1434-44.
- 7 Wyatt J, Vogelsang H, Hubl W, *et al*. Intestinal permeability and the prediction of relapse in Crohn's disease. *Lancet* 1993;341:1437-9.
- 8 Pender SL, Breese EJ, Gunther U, *et al*. Suppression of T cell-mediated injury in human gut by interleukin 10: role of matrix metalloproteinases. *Gastroenterology* 1998;115:573-83.
- 9 Podolsky DK. Inflammatory bowel disease (1). *N Engl J Med* 1991;325:928-37.
- 10 Bregenholt S, Claesson MH. Increased intracellular Th1 cytokines in scid mice with inflammatory bowel disease. *Eur J Immunol* 1998;28:379-89.
- 11 Strober W, Ludviksson BR, Fuss IJ. The pathogenesis of mucosal inflammation in murine models of inflammatory bowel disease and Crohn disease. *Ann Intern Med* 1998;128:848-56.
- 12 Niessner M, Volk BA. Altered Th1/Th2 cytokine profiles in the intestinal mucosa of patients with inflammatory bowel disease as assessed by quantitative reversed transcribed polymerase chain reaction (RT-PCR). *Clin Exp Immunol* 1995;101:428-35.
- 13 Desreumaux P, Brandt E, Gambiez L, *et al*. Distinct cytokine patterns in early and chronic ileal lesions of Crohn's disease. *Gastroenterology* 1997;113:118-26.
- 14 Christ AD, Stevens AC, Koepfen H, *et al*. An interleukin 12-related cytokine is up-regulated in ulcerative colitis but not in Crohn's disease. *Gastroenterology* 1998;115:307-13.
- 15 Stallmach A, Schafer F, Hoffmann S, *et al*. Increased state of activation of CD4 positive T cells and elevated interferon gamma production in pouchitis. *Gut* 1998;43:499-505.
- 16 Baeuerle PA, Henkel T. Function and activation of NF-kappa B in the immune system. *Annu Rev Immunol* 1994;12:141-79.
- 17 Baldwin AS Jr. The NF-kappa B and I kappa B proteins: new discoveries and insights. *Annu Rev Immunol* 1996;14:649-83.
- 18 Shuai K, Schindler C, Prezioso VR, *et al*. Activation of transcription by IFN-gamma: tyrosine phosphorylation of a 91-kD DNA binding protein. *Science* 1992;258:1808-12.
- 19 Darnell JE Jr, Kerr IM, Stark GR. Jak-STAT pathways and transcriptional activation in response to IFNs and other extracellular signaling proteins. *Science* 1994;264:1415-21.
- 20 Sadowski HB, Shuai K, Darnell JE Jr, *et al*. A common nuclear signal transduction pathway activated by growth factor and cytokine receptors. *Science* 1993;261:1739-44.
- 21 Zhong Z, Wen Z, Darnell JE Jr. Stat3: a STAT family member activated by tyrosine phosphorylation in response to epidermal growth factor and interleukin-6. *Science* 1994;264:95-8.
- 22 Paquette RL, Minosa MR, Verma MC, *et al*. An interferon-gamma activation sequence mediates the transcriptional regulation of the IgG Fc receptor type IC gene by interferon-gamma. *Mol Immunol* 1995;32:841-51.
- 23 Singh K, Balligand JL, Fischer TA, *et al*. Regulation of cytokine-inducible nitric oxide synthase in cardiac myocytes and microvascular endothelial cells. Role of extracellular signal-regulated kinases 1 and 2 (ERK1/ERK2) and STAT1 alpha. *J Biol Chem* 1996;271:1111-17.
- 24 Lee YJ, Benveniste EN. Stat1 alpha expression is involved in IFN-gamma induction of the class II transactivator and class II MHC genes. *J Immunol* 1996;157:1559-68.
- 25 Jahnke A, Johnson JP. Intercellular adhesion molecule 1 (ICAM-1) is synergistically activated by TNF-alpha and IFN-gamma responsive sites. *Immunobiology* 1995;193:305-14.
- 26 Starr R, Willson TA, Viney EM, *et al*. A family of cytokine-inducible inhibitors of signalling. *Nature* 1997;387:917-21.
- 27 Ito S, Ansari P, Sakatsume M, *et al*. Interleukin-10 inhibits expression of both interferon alpha- and interferon gamma-induced genes by suppressing tyrosine phosphorylation of STAT1. *Blood* 1999;93:1456-63.
- 28 Sasaki A, Yasukawa H, Suzuki A, *et al*. Cytokine-inducible SH2 protein-3 (CIS3/SOCS3) inhibits Janus tyrosine kinase by binding through the N-terminal kinase inhibitory region as well as SH2 domain. *Genes Cells* 1999;4:339-51.
- 29 Schreiber S, Nikolaus S, Hampe J. Activation of nuclear factor kappa B in inflammatory bowel disease. *Gut* 1998;42:477-84.
- 30 Rogler G, Brand K, Vogl D, *et al*. Nuclear factor kappaB is activated in macrophages and epithelial cells of inflamed intestinal mucosa. *Gastroenterology* 1998;115:357-69.
- 31 Lilliefors HW. On the Kolmogorov-Smirnov test for normality with mean and variance unknown. *J Am Stat Assoc* 1967;64:399-402.
- 32 Sachs L. *Angewandte Statistik*. Heidelberg: Springer, 1992.
- 33 Mann HB, Whitney DR. On a test of whether one of two random variables is stochastically larger than the other. *Ann Math Statistics* 1947;18:50-60.
- 34 Targan SR, Hanauer SB, van Deventer, *et al*. A short-term study of chimeric monoclonal antibody cA2 to tumor necrosis factor alpha for Crohn's disease. Crohn's Disease cA2 Study Group. *N Engl J Med* 1997;337:1029-35.
- 35 Stack WA, Mann SD, Roy AJ, *et al*. Randomised controlled trial of CDP571 antibody to tumour necrosis factor-alpha in Crohn's disease. *Lancet* 1997;349:521-4.
- 36 Fedorak RN, Gangl A, Elson CO, *et al*. Recombinant human interleukin 10 in the treatment of patients with mild to moderately active Crohn's disease. The Interleukin 10 Inflammatory Bowel Disease Cooperative Study Group. *Gastroenterology* 2000;119:1473-82.
- 37 Schreiber S, Fedorak RN, Nielsen OH, *et al*. Safety and efficacy of recombinant human interleukin 10 in chronic active Crohn's disease. Crohn's Disease IL-10 Cooperative Study Group. *Gastroenterology* 2000;119:1461-72.
- 38 Nikolaus, Raedler A, Stikas N, *et al*. Mechanisms in failure of infliximab for Crohn's disease. *Lancet* 2000;356:1475-79.
- 39 Xu X, Sun YL, Hoey T. Cooperative DNA binding and sequence-selective recognition conferred by the STAT amino-terminal domain. *Science* 1996;273:794-7.
- 40 Sampath D, Castro M, Look DC, *et al*. Constitutive activation of an epithelial signal transducer and activator of transcription (STAT) pathway in asthma. *J Clin Invest* 1999;103:1353-61.
- 41 Yokota A, Narazaki M, Shima Y, *et al*. Preferential and persistent activation of the STAT1 pathway in rheumatoid synovial fluid cells. *J Rheumatol* 2001;28:1952-9.
- 42 Wang Y, Wu TR, Cai S, *et al*. Stat1 as a component of tumor necrosis factor alpha receptor 1-TRADD signaling complex to inhibit NF-kappaB activation. *Mol Cell Biol* 2000;20:4505-12.
- 43 Gerhartz C, Heesel B, Sasse J, *et al*. Differential activation of acute phase response factor/STAT3 and STAT1 via the cytoplasmic domain of the interleukin 6 signal transducer gp130. I. Definition of a novel phosphotyrosine motif mediating STAT1 activation. *J Biol Chem* 1996;271:12991-8.
- 44 Vignais ML, Sadowski HB, Walling D, *et al*. Platelet-derived growth factor induces phosphorylation of multiple JAK family kinases and STAT proteins. *Mol Cell Biol* 1996;16:1759-69.
- 45 Powrie F, Correa-Oliveira R, Mauze S, *et al*. Regulatory interactions between CD45RBhigh and CD45RBlow CD4+ T cells are important for the balance between protective and pathogenic cell-mediated immunity. *J Exp Med* 1994;179:589-600.
- 46 Rudolph U, Finegold MJ, Rich SS, *et al*. Gi2 alpha protein deficiency: a model of inflammatory bowel disease. *J Clin Immunol* 1995;15:101-55.
- 47 Berg DJ, Davidson N, Kuhn R, *et al*. Enterocolitis and colon cancer in interleukin-10-deficient mice are associated with aberrant cytokine production and CD4(+) TH1-like responses. *J Clin Invest* 1996;98:1010-20.
- 48 Hampe J, Hermann B, Bridger S, *et al*. The interferon-gamma gene as a positional and functional candidate gene for inflammatory bowel disease. *Int J Colorectal Dis* 1998;13:260-3.
- 49 Klingmuller U, Lorenz U, Cantley LC, *et al*. Specific recruitment of SH-PTP1 to the erythropoietin receptor causes inactivation of JAK2 and termination of proliferative signals. *Cell* 1995;80:729-38.
- 50 Naka T, Narazaki M, Hirata M, *et al*. Structure and function of a new STAT-induced STAT inhibitor. *Nature* 1997;387:924-9.
- 51 Endo TA, Masuhara M, Yokouchi M, *et al*. A new protein containing an SH2 domain that inhibits JAK kinases. *Nature* 1997;387:921-4.
- 52 Suzuki A, Hanada T, Mitsuyama K, *et al*. CIS3/SOCS3/SSI3 plays a negative regulatory role in STAT3 activation and intestinal inflammation. *J Exp Med* 2001;193:471-81.
- 53 Malizia G, Dino O, Pisa R, *et al*. Expression of leukocyte adhesion molecules in the liver of patients with chronic hepatitis B virus infection. *Gastroenterology* 1991;100:749-55.
- 54 Smolen JS, Gangl A, Pollerauer P, *et al*. HLA antigens in inflammatory bowel disease. *Gastroenterology* 1982;82:34-8.
- 55 Hommes DW, Meenan J, de Haas M, *et al*. Soluble Fc gamma receptor III (CD 16) and eicosanoid concentrations in gut lavage fluid from patients with inflammatory bowel disease: reflection of mucosal inflammation. *Gut* 1996;38:564-7.
- 56 Singer II, Kawka DW, Scott S, *et al*. Expression of inducible nitric oxide synthase and nitrotyrosine in colonic epithelium in inflammatory bowel disease. *Gastroenterology* 1996;111:871-85.
- 57 Nakamura S, Ohtani H, Watanabe Y, *et al*. In situ expression of the cell adhesion molecules in inflammatory bowel disease. Evidence of immunologic activation of vascular endothelial cells. *Lab Invest* 1993;69:77-85.
- 58 Schreiber S, Nikolaus S, Haupe J, *et al*. Tumor necrosis factor - alpha and interleukin - 1,3 in relapse of Crohn's disease. *Lancet* 1999;353:459-61.
- 59 Kullman F, Renmann H, Alt M, *et al*. Clinical and histopathological features of dextran sulfate sodium induced acute and chronic colitis associated with dysplasia in rats. *Int J Colorectal Dis* 2001;16:238-46.
- 60 Darfeuille-Michaud A, Neut C, Barnich N, *et al*. Presence of adherent Escherichia coli strains in ileal mucosa of patients with Crohn's disease. *Gastroenterology* 1998;115:1405-13.
- 61 Swidsinski A, Ladehoff A, Pernthaller A, *et al*. Mucosal flora in inflammatory bowel disease. *Gastroenterology* 2002; 122:44-54.
- 62 Swidsinski A, Khilkin M, Kerjaschki D, *et al*. Association between intraepithelial Escherichia coli and colorectal cancer. *Gastroenterology* 1998;115:281-6.
- 63 Hugot JP, Chamaillard M, Zouali H, *et al*. Association of NOD2 leucine-rich repeat variants with susceptibility to Crohn's disease. *Nature* 2001;411:599-602.
- 64 Ogura Y, Bonen DK, Inohara N. A frameshift mutation in NOD2 associated with susceptibility to Crohn's disease. *Nature* 2001;411:603-5.
- 65 Hampe J, Cuthbert A, Grouchu PJP, *et al*. An insertion mutation in the NOD2 gene predisposes to Crohn's disease in German and British populations. *Lancet* 2001;357:1925-8.

- teracting surface by site-directed mutagenesis. *J Biol Chem* 275:19041–19049
- Matiás PM, Donner P, Coelho R, Thomaz M, Peixoto C, Macedo S, Otto N, Joschko S, Scholz P, Wegg A, Basler S, Schafer M, Ruff M, Egner U, Carondo MA (2000) Structural evidence for ligand specificity in the binding domain of the human Androgen receptor: implications for pathogenic gene mutations. *J Biol Chem* 275:26164–26171
- McKay LJ, Cidlowski JA (1999) Molecular control of immune/inflammatory responses: interaction between nuclear receptor factor-Kappa B and steroid-receptor-signalling pathways. *Endocrine Rev* 4:435–459
- Moras D, Gronemeyer H (1998) The nuclear receptor ligand-binding domain: structure and function. *Curr Opin Cell Biol* 10:384–391
- Müller-Fahrnow A, Egner U (1999) Ligand-binding domain of estrogen receptors. *Curr Opin Biotechnol* 10:550–556
- Oakley RH, Jewell CM, Yudt MR, Bofetado DM, Cidlowski JA (1999) The dominant negative activity of the human glucocorticoid receptor b isoform. *J Biol Chem* 274:27857–27866
- Raynaud JP, Ojasoo T, Bouton MM, Philibert D (1997) Receptor binding as a tool in the development of new bioactive steroids. In: Ariens EJ (eds) *Drug Design*. Academic Press, New York, pp 169–214
- Reche-Rigon M, Gronemeyer H (1998) Therapeutic potential of selective modulators of nuclear receptor action. *Curr Opin Chem Biol* 2:701–507
- Sack JF, Kish KF, Wang C, Altar RM, Kiefer SE, An Y, Wu GY, Scheffler JE, Salvati ME, Krystek SR, Weinman R, Einspahr HM (2001) Crystallographic structures of the ligand-binding domains of the androgen receptor and its T877A mutant complexed with the natural agonist dihydrotestosterone. *Proc Natl Acad Sci* 98:4904–4909
- Teutsch G, Goubet F, Battman T, Bonfils A, Bouchoux F, Cerede E, Gofflo D, Gaillard-Kelly M, Philibert D (1994) Non-steroidal antiandrogens: synthesis and biological profile of high-affinity ligands for the androgen receptor. *J Steroid Biochem Mol Biol* 48:111–119
- Williams SP, Sigler PB (1998) Atomic structure of progesterone complexed with its receptor. *Nature* 393:392–396
- Wurtz JM, Bourguet W, Renaud JP, Vivat V, Chambon P, Moras D, Gronemeyer H (1996) A canonical structure for the ligand-binding domain of nuclear receptors [published erratum appears in *Nat Struct Biol* 1996 Feb3(2):206]. *Nat Struct Biol* 3:87–94

20 SEGRAs: A Novel Class of Anti-inflammatory Compounds

H. Schäcke, H. Hennekes, A. Schottellus, S. Jaroch, M. Lehmann, N. Schmees, H. Rehwinkel, K. Asadullah

20.1	Introduction	357
20.2	Hypothesis and Aims of the Project	362
20.3	Proof of Concept	362
20.4	Summary	368
	References	369

20.1 Introduction

Glucocorticoids (GCs) have been widely used in the treatment of acute and chronic inflammatory diseases for more than 50 years. They are very effective and represent standard therapies for many inflammatory conditions with immunologic or non-immunologic backgrounds. Unfortunately, the desired anti-inflammatory and immunosuppressant effects are often accompanied by severe and/or partially non-reversible side effects (Table 1). Beside unknown individual factors, dosage and duration of therapy are major contributors to the frequency and severity of these side effects. Thus, long-term and high-dose GC therapy is problematic and partially dangerous. However, no good alternative exists so far, as other anti-inflammatory therapies usually are either less effective (at least in certain indications) or display a high side-effect potential as well. Consequently, there is a strong medical need to develop substances with an anti-inflammatory potency similar to that of

Table 1. GC-mediated side effects appearing after systemic therapies (summarized by A. Cato from Piper et al. 1991 and Lukert and Raisz 1990)

Early in therapy
Insomnia
Emotional lability
Truncal obesity
Diabetes mellitus
Peptic ulcer
Acne
Anticipated with sustained treatment
Cushingoid habitus
Hypothalamic-pituitary-adrenal suppression
Infection diathesis
Osteonecrosis
Myopathy
Impaired wound healing
Delayed effects
Osteoporosis
Skin atrophy
Cataracts
Atherosclerosis
Growth retardation
Fatty liver
Rare and unpredictable effects
Psychosis
Pseudotumor cerebri
Glaucoma
Epidural lipomatosis
Pancreatitis
Hirsutism or Virilism
Convulsion
Hepatomegaly
Congestive heart failure

classical GCs but with reduced side effects. New insights into the molecular mechanisms of GC-mediated actions have revealed new opportunities to potentially find such substances with a better effect/side-effect profile.

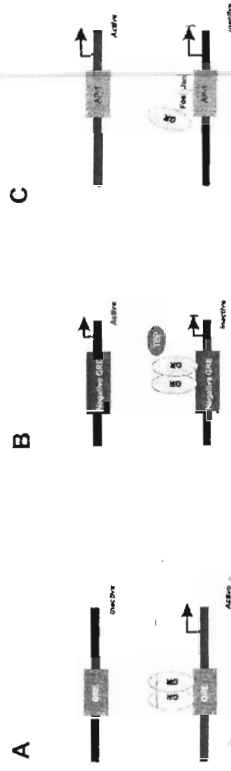


Fig. 1A–C. Molecular mechanisms of GC mediated effects. **A** Transactivation: the ligand-activated GR homodimer binds to GREs in promoter region of GC-sensitive genes, inducing gene transcription. **B** Transrepression: the ligand-activated GR homodimer binds to negative GREs in promoter region of GC-regulated genes (e.g., POMC promoter), thus inhibiting gene transcription. **C** Transrepression: ligand-activated GR monomer binds to a subunit of another transcription factor (e.g., c-Fos subunit of AP-1 or p65 subunit of NF-κB), thus inhibiting the induction of gene transcription by these factors

The effects of GCs are mediated by the specific glucocorticoid receptor (GR). After ligand binding, the cytoplasmic GR translocates into the nucleus and modulates gene transcription either by a positive (transactivation) or a negative (transrepression) mode of regulation. The positive regulation of target genes occurs by specific binding of the DNA-binding domain of the activated GR homodimer to GC response elements (GREs) in the promoter or enhancer region of responsive genes followed by an induction of gene transcription. While the transactivation is controlled by this protein–DNA interaction, the negative regulation by the GR may be exerted by protein–DNA as well as protein–protein interactions. In one case, the activated GR can bind to so-called negative GC response elements (nGREs) leading to a repression of gene transcription, via a protein–DNA interaction. Alternatively, in the more common way of transrepression, the GR may interact as a monomer via a protein–protein interaction with other transcription factors, e.g., AP-1, NF-κB, or STAT5, thus preventing activation of gene transcription (Fig. 1).

The crucial question is whether these different molecular mechanisms (transactivation/protein–DNA interaction on the one hand and transrepression/protein–protein interaction on the other hand) are responsible for distinct clinical effects and can be separated. For a few

Table 2. Summary of the important underlying molecular mechanisms of a number of GC side effects

Side effects are mediated predominantly via:
Transrepression
ACTH suppression
Disturbed wound healing
Infections
Osteoporosis
Transactivation
Diabetes mellitus
Glaucoma
Muscle atrophy/myopathy
Osteoporosis
Unknown mechanisms
Cataract
Peptic ulcer
Hypertension

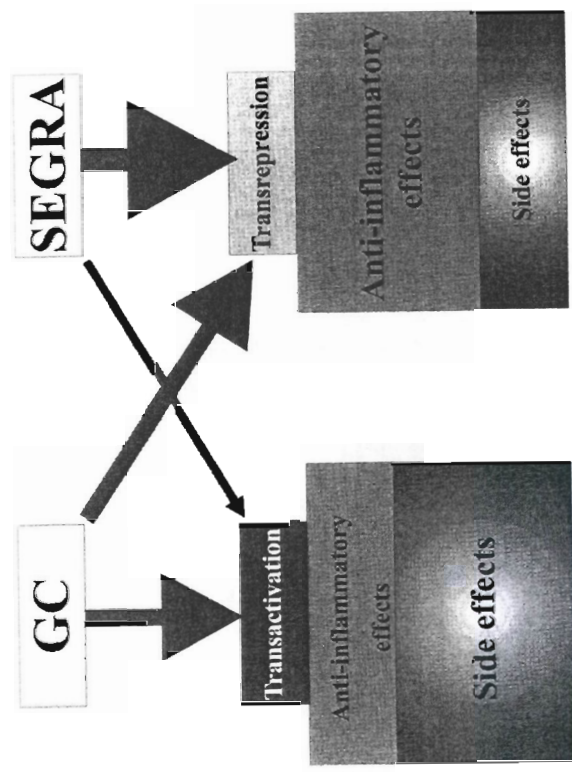


Fig. 2. Hypothesized profile for the induction of molecular mechanisms for classical GCs and dissociated GCs (SEGRAs)

duced glaucoma is caused by an increased synthesis of extracellular matrix proteins. Prolonged GC treatment leads to a major progressive induction of the 55-kDa TIGR/MYOC gene product in human trabecular meshwork cells (Lutjen-Drecoll et al. 1998). In contrast, an impaired wound healing caused by GCs depends on their anti-inflammatory and immunosuppressive activities via transrepression (Beer et al. 2000). Finally, in osteoporosis as a GC-induced side effect, transactivation as well as transrepression mechanisms are involved, besides a number of indirect effects (Weinstein et al. 1998; Silvestrini et al. 2000).

The differentiation of GR activity mediated via transrepression or transactivation into desired and undesired actions of GCs remains, therefore, a hypothesis, which is supported by some observations. However, the molecular mechanisms of all GR actions are still not completely understood, especially in the case of unwanted effects of GCs.

years, there has been growing evidence that certain side effects of glucocorticoids are mainly mediated by transactivation of genes, whereas anti-inflammatory effects predominantly result from transrepression (Belvisi et al. 2001) (Fig. 2). While this hypothesis provides a good general rule for GC action, some investigations showed that the induction of gene transcription of anti-inflammatory genes such as secretory leukocyte proteinase inhibitor (Sallenave et al. 1994), lipocortin-1 (Flower and Rothwell 1994), and interleukin (IL)-1 receptor antagonist (Levine et al. 1996) is also involved in anti-inflammatory responses of GCs. Similarly, not all side effects seem to be mediated exclusively by transactivation (Table 2). Steroid diabetes and steroid glaucoma seem to be induced mainly via the transactivation mechanism. The two most important enzymes of the gluconeogenesis, an essential pathway in the development of diabetes, the phosphoenolpyruvate carboxykinase (O'Brien et al. 1995; Crosson et al. 2000) and the glucose-6-phosphatase (Yoshiuchi 1998) are both induced by GCs. Steroid-in-

20.2 Hypothesis and Aims of the Project

Based on the new insight into the molecular mechanisms of GC-mediated action, we and others (e.g., Roussel-Uclaf, Michelle Resche-Rigon) hypothesized that activation of the GR with compounds inducing a predominant induction of transrepression over transactivation should lead to the majority of the anti-inflammatory effects of GCs with less side effects. Such selective GR agonists (SEGRAs) would represent a novel class of anti-inflammatory compounds with a favorable effect/side-effect profile (Fig. 2). For the identification of such compounds, it had to be demonstrated first as a precondition that transrepression alone is sufficient to mediate the anti-inflammatory action. Second, compounds with a dissociated profile *in vitro* had to be identified, and third, their superiority had to be demonstrated *in vivo*.

20.3 Proof of Concept

20.3.1 Efficacy of Classical GCs in GR^{dim/dim} Mice

Schütz and coworkers recently generated a transgenic mouse carrying a dimerization-incompetent GR (Reichardt et al. 1998). Due to this mutation, the GR could not bind to the DNA anymore, excluding any GC-induced transactivation of gene expression. Results obtained with these transgenic mice gave the strong suggestion that dimerization of the GR leading to transactivation of target genes is not required to ensure the fetal development and the survival, whereas in contrast, GR knockout mice are embryonally lethal. (Cole et al. 1995). Moreover, in the GR^{dim/dim} mice the induction of anti-inflammatory effects by classical GC treatment was observed (Reichardt et al. 2000; G. Schütz, personal communication). Thus, there is evidence that using only one of the two major GC-mediated molecular mechanisms (transrepression) is sufficient to reach anti-inflammatory effects.

20.3.2 Identification of Selective Glucocorticoid Receptor Agonists

In 1997 we started a research program aiming at the separation of different GR mechanisms by a new class of GR ligands. We are searching for compounds which bind to the GR and preferentially induce GR-protein interactions in the nucleus. Compounds are selected on the basis of their GR binding and dissociation between transrepression and transactivation. For determination of the transrepression and transactivation capacities we use reporter gene assays as well as the determination of the effects on endogenous tyrosine aminotransferase (TAT) production in a rat hepatoma cell line (transactivation) and IL-8 secretion in promyelocytic THP-1 cells (transrepression).

After screening of about 500,000 compounds and analyzing the effects of several hundred compounds with high GC-binding potential in more detail, we were able to identify numerous GC-binding compounds which show transrepression activities at least as good as dexamethasone. Further investigation of these mainly non-steroidal compounds led to the identification of three subgroups with regard to their transactivation profile: (1) agonists, (2) partial agonists, and (3) antagonists in transactivation. Moreover, some steroidal and non-steroidal compounds did show neither agonistic nor antagonistic effects on transactivation, while a transrepression was observed. The majority of compounds turned out to be agonists in transactivation. The subgroup of partial agonists in transactivation is significantly smaller. Only a few compounds were identified as being antagonists in transactivation, suggesting that this type of compound is more challenging to obtain.

One criterion for further compound selection was the degree of separation between transrepression and transactivation potencies. Interestingly, we found that prednisolone represents a slightly dissociated steroid (factor 7.6) better than dexamethasone (factor 5.4). Thus, the hurdle compounds had to take a dissociation better than found for prednisolone. Compounds with a dissociation factor higher than 10 were identified. However, one compound we investigated in more detail after topical application (see below) showed a dissociation factor comparable to that of prednisolone (factor 8), while being clearly more potent in transrepression.

Taken together, we demonstrated the existence of non-steroidal GR ligands which induce a predominant transrepression. Similar results

were recently reported from other groups (Vayssiere et al. 1997; Resche-Rigon and Gronemeyer 1998; Vanden Berghe et al. 1998; Belvisi et al. 2001).

20.3.3 Dissociation of Anti-inflammatory Effects from Side Effects by Use of SEGRAs in Animal Models

We have analyzed compounds with an *in vitro* dissociation between transactivation and transrepression in rodents. *In vivo* activities were examined first in the croton oil model of ear inflammation in mice and rats. Induction of TAT in the liver of mice and rats was used as a surrogate parameter for catabolic effects of GCs. The promoter of the TAT gene contains regulatory sequences enabling an activation of transcription by GCs (Hargrove and Granter 1987; Jantzen et al. 1987; Rigaud 1991). The standard GCs, dexamethasone (strong) and prednisolone (weak), were used as controls.

As a parameter for anti-inflammatory activity we measured the inhibition of ear edema. Both classical GCs as well as dissociated GCs were quite effective. Our compounds showed anti-inflammatory activity after systemic applications in the croton oil-induced ear inflammation model of mice and rats at least comparable to that of prednisolone. They reached a similar efficacy (80%–100%) compared to prednisolone (90%) after subcutaneous treatment of mice. Slight differences with regard to the potencies were observed in mice (ED₅₀ of prednisolone: ca. 5 mg/kg; compound A: ca 2 mg/kg and compound D: ca. 1 mg/kg). As a parameter for transactivation mediated side effects, we determined the induction of the TAT. If at all, a significant induction of TAT was only observed at the highest dosages for all tested novel compounds (at most a twofold increase), while for prednisolone an approximately sixfold increase of TAT activity was measured with the highest dosage of 30 mg/kg.

Thus, dissociated GCs show a good separation between inhibition of edema and TAT induction, which is in contrast to classical GCs. These *in vivo* data demonstrate that the translation from *in vitro* dissociation of transrepression and transactivation into *in vivo* separation of therapeutic efficacy and side effects is possible.

As a clinically more relevant parameter than the TAT induction we investigated the potential of increasing the blood glucose level in rats after systemic treatment. This is a particularly interesting parameter since it may serve as a surrogate parameter for the risk of diabetes induction, a frequent and dangerous side effect connected with the long-term use of GCs. Based on the knowledge of the underlying molecular mechanisms, dissociated GCs should not influence this parameter strongly. Furthermore, selected compounds were tested with regard to their effects on adrenocorticotropic hormone (ACTH) level. ACTH is a cleavage product of the pro-opiomelanocortin (POMC), whose transcription is negatively regulated by GCs. In the POMC promoter, the activated GRE-bound GR interferes with the binding of essential transcription factors, thus inhibiting the induction of gene transcription (Drouin et al. 1993). This negative regulation seems to be DNA-binding-dependent and should not be affected by dissociated GCs. However, ACTH secretion into the serum is underlying a DNA-binding-independent mechanism. The synthesis of the corticotropin-releasing hormone (CRH), responsible for ACTH release, is negatively regulated by the GR via a protein-protein interaction (Reichardt et al. 1998, 2000). Therefore, we did not expect an advantage of the SEGRAs compounds compared with standard GCs in *in vivo* experiments.

In contrast to classical GCs none of the tested dissociated compounds showed a significant increase in the blood glucose level after systemic treatment. While systemic prednisolone treatment induced the blood glucose dose dependently up to approximately 200% of the control with the highest dosage of 30 mg/kg, no increase was observed with compound D and only a 20% increase with all dosages of compound A. However, as expected, with regard to ACTH suppression, the compounds were as effective as prednisolone.

The idea to develop GCs with an improved effect/side-effect profile for systemic therapies is also attractive for other companies. Very recently, results were published by Belvisi and coworkers (2001) concluding that the *in vitro* separation of their compound was not confirmed *in vivo*. The investigators focused on a lung edema model in rats to demonstrate anti-inflammatory activity. Regarding side-effect induction, effects on bones, body weight, and thymus were analyzed. The *in vitro* dissociated compound was anti-inflammatory active *in vivo* showing a potency even better than budesonide and prednisolone. Unfortunately,

the compound was as effective as budesonide and prednisolone in induction of the measured side effects (serum marker of bone metabolism, femoral head histology, body weight, thymus involution), suggesting that *in vitro* dissociation does not always translate to an improved therapeutic ratio for GCs *in vivo* (Belvisi et al. 2001). Reasons for the obtained results could be that the authors did not distinguish between side effects regarding the underlying molecular mechanisms and, on the other hand, the compound might have been metabolized very rapidly to an active metabolite, which does not show such a dissociated profile. A separation of transactivation from transrepression activities *in vitro* should result in an *in vivo* separation of anti-inflammatory activity from e.g., diabetes induction measured by TAT induction in the liver or of glucose levels in serum of treated animals. Extensive pharmacokinetic characterization of the compound might help for a better understanding of the discrepancies between the obtained *in vitro* profile and the *in vivo* activity of the compound.

In addition, Coghlan and coworkers (2001) reported non-steroidal compounds that bind selective and with a high affinity to the GR. In an *in vivo* asthma model, one of the described compounds showed a functional profile similar to that of prednisolone, that means a good anti-inflammatory activity but no dissociation with regard to side effect induction.

Thus, the principle of identifying dissociated ligands of the GR, steroidal or non-steroidal, is still a very attractive one, and a few companies are on the way to developing such compounds with the expectation of an improved effect/side-effect profile in the therapy of chronic inflammatory diseases.

20.3.4 Introduction of a First Drug Candidate for Topical Application

GCs are the most widely used drugs in dermatology. The introduction of topical hydrocortisone and in particular of the first halogenated corticosteroid, triamcinolone acetonide, represented great advances compared to previously available therapies. However, adverse effects became apparent and the subsequent backlash of opinion against topical GCs has created confusion and prejudice against all steroid-containing prepara-

tions, in its extreme as "steroid phobia," which is still a considerable concern (see Sterry and Asadullah in this book). Importantly, not only cutaneous side effects like skin atrophy can occur during topical GC therapy but systemic side effects as well.

In order to get a first impression on the potential of SEGRAs, we therefore extensively investigated activity and side-effect induction after topical application of one of our early compounds. Interestingly, the compound was significantly active in the croton oil-induced ear inflammation model after subcutaneous application (80% inhibition of ear edema; ED₅₀: ca. 10 mg/kg). Moreover, after systemic application, if at all, the compound induced TAT only at the highest given dosage of 30 mg/kg (2.4-fold induction). It showed a slightly weaker potency (ED₅₀: ca. 0.01%) after topical administration, but it reached the full efficacy of the standard (prednisolone; ED₅₀: ca. 0.003%). However, after long-term topical treatment of rats, using 30 times the ED₅₀ (effective dosage) of both the compound and prednisolone, topical (skin thickness and breaking strength) and systemic side effects (reduction in body weight gain and reduction of adrenal weight) were clearly less pronounced in compound-treated than in prednisolone-treated rats. With regard to the topical side effects, the compound induced only 50% to 60% of the prednisolone effects. In addition the compound did not affect the adrenal weight and the body weight gain was only reduced by 20% (prednisolone reduced the body weight gain by 90%). Further on, the compound induced significantly less systemic immune deterioration (loss of thymus by 55% and spleen weight by 10%) than prednisolone (loss of thymus by 85% and spleen weight by 50%).

Here we show, that a compound with a dissociated *in vitro* profile with regard to transactivation and transrepression is effective in the treatment of acute inflammation while it induces less side effects. The compound displays potent anti-inflammatory activity after topical and systemic application and reaches an inhibition of the inflammatory response by 60%–80%. Importantly, the induction of side effects by this compound is clearly lower than by the weak GC prednisolone.

20.4 Summary

Dissociated GCs show a separation between anti-inflammatory effects and certain side effects. This renders them as attractive compounds with better effect/side-effect profile as promising drug candidates and tool compounds for analyzing the molecular mechanisms of single side effects.

A number of the GC-mediated side effects (e.g., osteoporosis, skin atrophy) are regulated in a very complex manner and use more than one molecular mechanism of the GR. Thus, theoretical predictions about the behavior of selective GR agonists regarding these effects are very difficult to make. Investigations of SEGRA compounds in relevant animal models will be the only way to get this important information. By availability of these tool compounds we now are in the advantageous situation to test them in vivo and to learn more about the possibilities and even the limitations of the selective GR agonists.

Considering that the compounds have a non-steroidal structure, i.e., totally unrelated to steroids or other hormones at all, displaying only partially the molecular effects of GCs and are dissociated in their clinical profile, they should not be considered as GCs. Therefore, we introduced the term selective glucocorticoid receptor agonists (SEGRAs).

These SEGRAs seem to represent a useful novel therapeutic modal-ity which may complement existing therapeutic principles for the topical and especially the systemic treatment of inflammatory diseases.

In summary, we and others are convinced that dissociated GCs are therapeutic compounds that exert many of the anti-inflammatory and immunosuppressive effects of standard GCs, while their potential to induce side effects is reduced. Whereas the in vitro dissociated profile of other compound classes (Belvisi et al. 2001) was not translated into a separation between anti-inflammatory activity and the induction of side effects in in vivo models, we could demonstrate this for the SEGRA compounds. Regarding the diversity of molecular mechanisms involved in mediating the complex side effects of GCs, it might be that only some of these unwanted effects can be reduced. However, as GCs are one of the most important anti-inflammatory therapeutics in the treatment of severe and chronic inflammatory diseases, even a partial reduction of side effect induction would be a great advantage for many patients.

Acknowledgements. The authors would like to thank Andrew Cato for providing Table 1 and Wolf-Dietrich Döcke and Ulrich Zügel for their helpful suggestions during the preparation of this manuscript.

References

- Beer H-D, Fässler R, Werner S (2000) Glucocorticoid-regulated gene expression during cutaneous wound repair. *Vitam Horm* 59:217–239
- Belvisi MG, Wicks SL, Battram CH, Bottoms SEW, Redford JE, Woodman P, Brown TJ, Webber SE, Foster ML (2000) Therapeutic benefit of a dissociated glucocorticoid and the relevance of in vitro separation of transrepression from transactivation activity. *J Immunol* 166:1975–1982
- Coghlan MJ, Kym PR, Elmore SW, Wang AX, Luly JR, Wilcox D, Stashko M, Lin C-W, Miner J, Tyree C, Nakane M, Jacobson P, Lane BC (2001) Synthesis and characterization of non-steroidal ligands for the glucocorticoid receptor: selective quinoline derivatives with prednisolone-equivalent functional activity. *J Med Chem* 44:2879–2885
- Cole TJ, Blency JA, Monaghan AP, Kriegstein K, Schmidt W, Aguzzi A, Fantuzzi G, Hummler I, Unsicker K, Schütz G (1995) Targeted disruption of the glucocorticoid receptor gene blocks adrenergic chromaffin cell development and severely retards lung maturation. *Genes Dev* 9:1608–1621
- Crosson SM, Roesler WJ (2000) Hormonal regulation of the phenolpyruvate carboxylase gene. *J Biol Chem* 275:5804–5809
- Drouin J, Sun YL, Chamberland M, Gauthier Y, De LA, Nemer M, Schmidt TJ (1993) Novel glucocorticoid receptor complex with DNA element of the hormone-repressed POMC gene *EMBO J* 12:145–156
- Flower RJ, Rothwell NJ (1994) Lipocortin-1: cellular mechanisms and clinical relevance. *Trends Pharmacol Sci* 15:71–76
- Hargrove JL, Granner DK (1987) Biosynthesis and intracellular processing of tyrosine aminotransferase. In: Christen P, Metzler DE (eds) *Transaminases*. John Wiley & Sons, New York, pp 511–532
- Jantzen H-M, Strähle U, Gloss B, Stewart F, Schmidt W, Boshart M, Miksick R, Schütz G (1987) Cooperativity of GC response elements located far upstream of the tyrosine aminotransferase gene. *Cell* 49:29–38
- Lavigne SJ, Benfield T, Shelhamer JH (1996) Corticosteroids induce intracellular interleukin-1 receptor antagonist type I expression by a human airway epithelial cell line. *Am J Respir Cell Mol Biol* 15:245–251
- Lukert BP, Raisz LG (1990) Glucocorticoid-induced osteoporosis: pathogenesis and management. *Ann Intern Med* 112:352–364

- Lutjen-Drecoll E, May CA, Polansky JR, Johnson DH, Bloemendal H, Nguyen TD (1998) Localization of the stress proteins alpha B-crystallin and trabecular meshwork inducible glucocorticoid response protein in normal and glaucomatous trabecular meshwork. *Invest Ophthalmol Vis Sci* 39:517-525
- O'Brien RM, Noisin EL, Suwanichkul A, Yamasaki T, Lucas PC, Wang J-C, Powell DR, Granner DK (1995) Hepatic nuclear factor 3- and hormone-regulated expression of the phosphoenolpyruvate carboxykinase and insulin-like growth factor-binding protein-1 genes. *Mol Cell Biol* 15:1747-1758
- Piper JM, Ray WA, Daugherty JR, Griffin MR (1991) Corticosteroid use and peptic ulcer disease: role of nonsteroidal anti-inflammatory drugs. *Ann Intern Med* 114:735-740
- Reichardt HM, Kaestner KH, Tuckermann J, Kretz O, Wessely O, Bock R, Gass P, Schmidt W, Herrlich P, Angel P, Schütz G (1998) DNA binding of the glucocorticoid receptor is not essential for survival. *Cell* 93:531-541
- Reichardt HM, Tronche F, Bauer A, Schütz G (2000) Molecular genetic analysis of glucocorticoid signaling using the Cre/loxP system. *Biol Chem* 381:961-964
- Resche-Rigon M, Gronemeyer H (1998) Therapeutic potential of selective modulators of nuclear receptor action. *Curr Opin Chem Biol* 4:501-507
- Rigaud G, Roux J, Pictet R, Grange T (1991) In vivo footprinting of rat TAT gene: dynamic interplay between the GC receptor and a liver-specific factor. *Cell* 67:977-986
- Sallenne JM, Shulmann J, Crossley J, Jordana M, Gaudi J (1994) Regulation of secretory leukocyte proteinase inhibitor (SLPI) and elastase-specific inhibitor (ESI/elafin) in human airway epithelial cells by cytokines and neutrophilic enzymes. *Am J Respir Cell Mol Biol* 11:733-741
- Silverstrim G, Ballanti P, Patacchioli FR, Mocetti P, Di Grezia R, Martin Wedard B, Angelucci L, Bonucci E (2000) Evaluation of apoptosis and the GC receptor in the cartilage growth plate and metaphyseal bone cells of rats after high-dose treatment with corticosterone. *Bone* 26:33-42
- Vanden Berghe W, Francesconi E, De Bosscher K, Resche-Rigon M, Haeghe-man G (1998) Dissociated glucocorticoids with anti-inflammatory potential repress interleukin-6 gene expression by a nuclear factor- κ B-dependent mechanism. *Mol Pharm* 56:797-806
- Vaysiere BM, Dupont S, Choquet A, Petit F, Garcia T, Marchandeu C, Gronemeyer H, Resche-Rigon M (1997) Synthetic glucocorticoids that dissociate transactivation and AP-1 transrepression exhibit antiinflammatory activity in vivo. *Mol Endocrinol* 11:1245-1255
- Weinstein RS, Jilka RL, Parfitt AM, Manolagas SC (1998) Inhibition of osteoblastogenesis and promotion of apoptosis of osteoblasts and osteocytes by GCs. Potential mechanisms of their deleterious effects on bone. *J Clin Invest* 102:274-282

- Yoshiuchi I, Shingu R, Nakajima H, Hamaguchi T, Horikawa Y, Yamasaki T, Oue T, Ono A, Miyagawa JI, Namba M, Hanfusa T, Matsuzawa Y (1998) Mutation/polymorphism scanning of glucose-6-phosphatase gene promoter in noninsulin-dependent diabetes mellitus patients. *J Clin Metab* 83:1016-1019

Molecular mechanisms of interleukin-10-mediated inhibition of NF- κ B activity: a role for p50

F. DRIESSLER*, K. VENSTROM†, R. SABAT*, K. ASADULLAH* & A. J. SCHOTTELIUS* *Research Business Area Dermatology, Research Laboratories of Schering AG, Berlin, Germany and †Research Business Area Dermatology USA, Richmond, CA, USA

(Accepted for publication 28 October 2003)

SUMMARY

Nuclear factor kappa B (NF- κ B) is a transcription factor pivotal for the development of inflammation. A dysregulation of NF- κ B has been shown to play an important role in many chronic inflammatory diseases including rheumatoid arthritis, inflammatory bowel disease and psoriasis. Although classical NF- κ B, a heterodimer composed of the p50 and p65 subunits, has been well studied, little is known about gene regulation by other hetero- and homodimeric forms of NF- κ B. While p65 possesses a transactivation domain, p50 does not. Indeed, p50/p50 homodimers have been shown to inhibit transcriptional activity. We have recently shown that Interleukin-10 exerts its anti-inflammatory activity in part through the inhibition of NF- κ B by blocking I κ B kinase activity and by inhibiting NF- κ B already found in the nucleus. Since the inhibition of nuclear NF- κ B could not be explained by an increase of nuclear I κ B, we sought to further investigate the mechanisms involved in the inhibition of NF- κ B by IL-10. We show here that IL-10 selectively induced nuclear translocation and DNA-binding of p50/p50 homodimers in human monocytic cells. TNF- α treatment led to a strong translocation of p65 and p50, whereas pre-treatment with IL-10 followed by TNF- α blocked p65 translocation but did not alter the strong translocation of p50. Furthermore, macrophages of p105/p50-deficient mice exhibited a significantly decreased constitutive production of MIP-2 α and IL-6 in comparison to wild type controls. Surprisingly, IL-10 inhibited high constitutive levels of these cytokines in wt macrophages but not in p105/p50 deficient cells. Our findings suggest that the selective induction of nuclear translocation and DNA-binding of the repressive p50/p50 homodimer is an important anti-inflammatory mechanism utilized by IL-10 to repress inflammatory gene transcription.

Keywords Interleukin-10 NF- κ B signal transduction inflammation monocytes macrophages

INTRODUCTION

Interleukin-10 (IL-10) is a pleiotropic cytokine produced by many cell types including monocytes/macrophages, cells that play a critical role in the inflammatory process [reviewed in 1]. IL-10 exerts its anti-inflammatory effects by suppressing the production of macrophage inflammatory proteins such as MIP-2 α , IL-1 β , IL-6, IL-8, IL-12, TNF- α , GM-CSF and G-CSF. Additionally, it inhibits the expression of MHC class II molecules, B7 and intercellular adhesion molecule-1 on antigen presenting cells and diminishes Th1 cell activity by suppressing secretion of IL-2 and IFN- γ in T-cells [reviewed in 1]. The fact that IL-10 deficient mice develop

chronic enterocolitis with similarities to inflammatory bowel disease (IBD) is strong evidence for the *in vivo* role of IL-10 as an important immunoregulator with potent anti-inflammatory and immunosuppressive activities [2]. Treatment with IL-10 is beneficial in models of induced colitis [3–5] and arthritis [4,6], as well as in models of experimental autoimmune encephalomyelitis, pancreatitis, diabetes mellitus and experimental endotoxemia *in vivo* [7–10]. Moreover, patients suffering from Crohn's disease [11,12] and psoriasis [13] display clinical improvement following IL-10 treatment.

Many of the pro-inflammatory cytokines and costimulatory proteins demonstrated to be suppressed by IL-10 are known to be regulated by the transcription factor NF- κ B [14]. Dysregulation of NF- κ B has been implicated in the pathogenesis of a variety of chronic inflammatory diseases including rheumatoid arthritis [15], IBD [16] and psoriasis [17]. Blockade of NF- κ B has thus shown beneficial effects in animal models for these chronic inflammatory diseases [18,19]. In mammals the NF- κ B family

Correspondence: Arndt J. Schottelius, Research Business Area Dermatology, U.S.A., Berlex BioSciences, 2600 Hilltop Drive, Richmond, CA 94804-0099, U.S.A.

E-mail: arndtschottelius@schering.de

consists of several proteins including NF- κ B1 (p50), NF- κ B2 (p52), RelA (p65), c-Rel (Rel), and RelB which share the so-called Rel homology domain. The p50 and p52 subunits, which lack transactivation domains, are produced by processing of precursor molecules of 105 kDa and 100 kDa, respectively. p50 may also be processed cotranslationally with p105 [20]. The classical NF- κ B heterodimer composed of p50 and p65 subunits is a potent activator of gene expression [21,22]. While p65 possesses a transactivation domain, p50 does not [22]. The classical p65/p50 heterodimer is sequestered in the cytoplasm as an inactive complex bound to its inhibitor protein I κ B [21]. In response to a variety of extracellular stimuli, such as IL-1 β , TNF- α , lipopolysaccharide (LPS) or phorbol esters, I κ B proteins are rapidly phosphorylated by the I κ B kinase (IKK) complex. Phosphorylation targets these inhibitory proteins for rapid polyubiquitination and degradation through the 26S proteasome [23]. Degradation of the inhibitor results in liberation of the classical NF- κ B heterodimer p65/p50 from I κ B and subsequent translocation of NF- κ B to the nucleus where it regulates gene transcription. In contrast, p50/p50 homodimers inhibit transcriptional activation [24]. However, little is known regarding their regulation.

Several mechanisms are currently being discussed for IL-10 mediated cytokine suppression. In human monocytes and neutrophils IL-10 induces the expression of suppressor of cytokine signalling 3 (SOCS-3) [25] which inhibits LPS-induced macrophage activation [26]. Moreover, IL-10 has been shown to inhibit the expression of both interferon alpha- and interferon gamma-induced genes by suppressing tyrosine phosphorylation of STAT1 [27]. While the ability of IL-10 to suppress cytokine synthesis apparently does not depend on p38 mitogen-activated protein kinase [28] the involvement of NF- κ B in this important anti-inflammatory mechanism has been controversial [29–32]. We have recently demonstrated that the blockade of IKK activation and direct inhibition of DNA-binding of the nuclear p65/p50 heterodimer are targets of IL-10 in the suppression of NF- κ B activity [33]. This, however, could not fully explain the inhibitory effects of IL-10 suggesting the existence of further mechanisms. In particular, the mechanisms underlying the ability of IL-10 to inhibit nuclear NF- κ B remained unclear. Our data presented here provide evidence that in addition to the inhibition of p65/p50 nuclear translocation, the selective induction and translocation of p50/p50 homodimers is an important mechanism by which IL-10 inhibits NF- κ B activity.

MATERIALS AND METHODS

Preparation of PBMC and cell culture

Human PBMC from various healthy donors were isolated from citrated venous blood by density gradient centrifugation using Ficoll-Paque (Pharmacia, Freiburg, Germany). For inhibiting monocyte adherence, culture vessels were coated with poly(2)-hydroxyethylmethacrylate (ICN Biomedicals, Eschwege, Germany) [34]. The human monocytic cell line U937 (CRL-1593) was obtained from the American Type Culture Collection.

Recombinant human (rh)TNF- α was purchased from R & D Systems (Minneapolis, MN, USA). LPS (from *E. coli* Serotype 055:B5) was purchased from Sigma Chemical Co. (St. Louis, MO, USA) and recombinant human (rh)IL-10 was purchased from R & D Systems.

Western blot analysis

Cytoplasmic (C) and nuclear (N) extracts were prepared as previously described [33]. Cytosolic and nuclear proteins (20–25 μ g) were resolved over sodiumdodecyl sulphate-polyacrylamide gel electrophoresis (SDS-PAGE). SDS-PAGE were performed according to standard protocols [33]. Equal amounts of extracts were subjected to SDS-PAGE electrophoresis and transferred to nitrocellulose membranes. Specific proteins were visualized by ECL (enhanced chemiluminescence) (Amersham Pharmacia Biotech, Freiburg, Germany). Antibodies (Ab) for p50 (H-119) and p65 (C-20) were obtained from Santa Cruz Biotechnology (Santa Cruz, CA, USA). The antibodies for p65 (N67620) and I κ B α (158220) were obtained from Transduction Laboratories (BD Biosciences Pharmingen, Franklin Lakes, NJ, USA). The antibody α -Tubulin (T5168) was obtained from Sigma (Sigma Aldrich, Seelze, Germany).

Nuclear extraction for EMSA

Nuclear extracts (N) were prepared as follows: 1×10^6 cells were treated with 500 μ l of lysis buffer (50 mM KCl, 0.5% Nonidet P-40, 25 mM HEPES, 1 mM phenylmethylsulphonylfluoride (PMSF), 10 μ g/ml leupeptin, 20 μ g/ml aprotinin, 100 μ M dithiothreitol (DTT)) and kept on ice for 4 min. Nuclei were pelleted by centrifugation at 25 000 g for 1 min, and supernatants were discarded.

The nuclei were washed one time with lysis buffer not containing Nonidet P-40, and the nuclei were extracted in 300 μ l of extraction buffer (500 mM KCl, 10% glycerol, 25 mM Hepes, 1 mM PMSF, 10 μ g/ml leupeptin, 20 μ g/ml aprotinin, and 100 μ M DTT). After centrifugation at 25 000 g for 5 min, the supernatants were harvested. The protein concentration of the resulting nuclear protein extract was determined by the method of Bradford using a Protein Assay Kit (Bio-Rad), and the samples were diluted to 1 μ g per μ l with extraction buffer.

Electrophoretic mobility shift assays (EMSA)

8 mg of extract were incubated for 20 min in a total of 20 μ l containing 1 mg of poly (dI-dC) with $4\text{--}6 \times 10^4$ cpm of a 32 P-labelled oligonucleotide probe containing a κ B site from the human class I MHC promoter [5'-CAG GGC TGG GGA TTC CCC ATC TCC ACA GTT TCA CTT C-3' (UV 21)] which binds both p65/p50 heterodimers and p50/p50 homodimers [33] and a κ B site from the human TNF- α promoter; 5'-GAT CCA CAG GGG GCT TTC CCT CCA-3' (κ B 3) [24]. The final buffer concentration was 10 mM Tris-HCl pH 7.7, 50 mM NaCl, 0.5 mM EDTA, 1 mM DTT, 10% glycerol. Complexes were resolved on a 5% polyacrylamide gel. Dried gels were exposed on film for 15–48 h. For supershift analysis, antibodies against specific NF- κ B subunits were added to the nuclear extract and incubated for 15 min prior to the addition of poly (dI-dC) and labelled oligonucleotide probe. The following antibodies were used for supershift analysis: p65 (Rockland, Boyertown, PA, USA), p50 (H-119 from Santa Cruz Biotechnology, CA, USA).

Purification and stimulation of murine peritoneal macrophages and spleen cells

p105/p50 $-/-$ mice (B6; 129P-Nf κ b1^{tm1Ba}), aged 8–13 weeks and wild type controls with the same genetic background (B6; 129PF2/J, age 8–13 weeks) were purchased from Jackson Laboratories (Bar Harbor, ME, USA). All animal studies were approved by the competent authority for labour protection, occupational

health and technical safety for the state and city of Berlin, Germany and performed in accordance with Schering AG ethical guidelines. The generation of the p105/p50 $-/-$ mice have been described elsewhere [34]. Peritoneal macrophages were obtained by injection and withdrawal of 7 ml of cold PBS *w/o* Mg⁺⁺, Ca⁺⁺ (Gibco BRL). After plating, the nonadherent cells were removed by washing 3 h later. Spleens were removed and cell suspensions were prepared by homogenization in a tissue grinder. The erythrocytes were lysed by brief incubation in RBC-Lysing-Buffer. The cells were maintained in RPMI 1640 supplemented with 2 mM L-Glutamine, 50 U/ml penicillin, 50 µg/ml streptomycin, and 5% heat inactivated FCS (all from Gibco BRL). The cells were stimulated with recombinant murine (rm)TNF- α (R & D Systems) in the presence or absence of recombinant murine (rm)IL-10 (R & D Systems). Supernatants were collected after incubation for 8–17 h, at 1×10^6 cells per ml.

Cytokine quantification assays

Detection of mL-6 and mMIP-2 α concentrations in murine macrophage and spleen cell culture supernatants was performed by the commercially available Enzyme-linked immunosorbent assay (ELISA) kits from R & D Systems.

Statistics

For the analysis of the inhibitory potency of IL-10 in the *ex vivo* studies, the so-called 'modified Hemm' (inhibition) test, which was developed by Schering's Department of Biometrics based on the programme SAS System for Windows 6-12 (SAS Institute Inc., NC, USA), was employed. To determine the inhibitory effect of an anti-inflammatory compound such as IL-10, the difference between the respective mean value of the positive controls and the mean value of the vehicle controls was set to 100% and the percentile change by the test substance was estimated:

$$\% \text{ change} = \frac{mv_{\text{treated group}} - mv_{\text{positive group}}}{mv_{\text{positive group}} - mv_{\text{control group}}} \times 100$$

(where mv is mean value)

In order to test whether the change caused by the treatment is different from zero a 95% confidence interval was calculated under consideration of the variance of observations within the entire experiment. If the interval did not include zero, the hypothesis that there is no change was rejected at the level of $\alpha = 0.05$.

For the analysis of statistical differences for cytokine secretion levels between the genotypes, the Dunnett Test was used. All data are derived from at least three independent experiments and are expressed as mean + SD.

RESULTS

IL-10 blocks nuclear translocation of p65 but induces nuclear translocation of p50

One of the main points of control for NF- κ B activity is the interaction with its inhibitor I κ B α , which keeps NF- κ B in an inactive state by sequestering it in the cytoplasm. To experimentally address the question whether IL-10 inhibits nuclear translocation of NF- κ B by modulating the degradation status of I κ B α in U937 cells and PMBC, cells were stimulated with TNF- α or LPS in either the absence or presence of human recombinant IL-10. Cytoplasmic and nuclear proteins were extracted, and Western blot analysis was performed to

determine whether addition of IL-10 effected degradation of I κ B α and the subcellular localization of the NF- κ B subunits p50 and p65. Immunoblot analysis for I κ B α demonstrated that this inhibitor protein in comparison to untreated cells (Figs 1a & 2a, panel 3, lane 1) was unaffected in PMBC and U937 cells treated with IL-10 alone, regardless of variations in dose and duration of IL-10 treatment (Figs 1a & 2a, panel 3, lanes 2 and 3). Stimulation with TNF- α resulted in the almost complete degradation of I κ B α (Figs 1 & 2a, panel 3, lane 4). However, pretreatment of cells with IL-10 followed by stimulation with a low dose of TNF- α (10 ng/ml, 15 min) delayed degradation of I κ B α to some extent (Fig. 1a, panel 3, lane 5). In contrast, IL-10 pretreatment did not visibly delay I κ B α degradation when followed by a longer and higher dose of TNF- α stimulation (20 ng/ml, 30 min) (Fig. 2a, panel 3, lane 6). I κ B α was not detected in nuclear extracts of cells that were left untreated or had been treated with IL-10 in the absence or presence of TNF- α (Figs 1b & 2b, panel 3, lanes 1–5). Treatment of PMBC with LPS (80 ng/ml, 60 min) resulted in clear degradation of I κ B α (Fig. 2a, panel 3, lanes 5 and 7), which was not visibly affected by prior IL-10 treatment. These results confirm earlier results [33] indicating that a single dose of IL-10 pretreatment can at least partially inhibit degradation of I κ B α induced by low-dose TNF- α .

To elucidate whether IL-10 affected the subcellular distribution of NF- κ B subunits, Western blot analysis was performed with cytoplasmic and nuclear extracts of U937 cells and PMBCs that had been treated with IL-10 in the absence or presence of TNF- α or LPS. In untreated cells, p65 was predominantly localized in the cytoplasm (Figs 1a & 2a, panel 2, lane 1 and Figs 1b & 2b, panel 2, lane 1). Cells stimulated with TNF- α (15 and 30 min, respectively) demonstrated an increase in nuclear translocation of p65 and p50 (Fig. 1a & 2a, panel 1 and 2, lane 4 and Figs 1b & 2b, panel 1 and 2, lane 4). In contrast, while LPS (80 ng/ml, 60 min) alone and in combination with IL-10 clearly augmented nuclear p50, it did not visibly induce nuclear translocation of p65, even though degradation of I κ B α had been observed. IL-10 treatment alone did not alter the subcellular distribution of p65 in these cells (Fig. 1a & 2a, panel 2, lanes 2 and 3 and Figs 1b & 2b, panel 2, lanes 2 and 3). In contrast, treatment with IL-10 alone clearly induced nuclear translocation of p50 in U937 cells and PMBC (Fig. 1a and 2a, panel 1, lanes 2 and 3 and Figs 1b & 2b, panel 1, lanes 2 and 3). The expression of cytoplasmic p105 and p50 was not visibly affected by IL-10, TNF- α or LPS alone or in combination with IL-10 (Figs 1a & 2a, panel 1). (Note that the nuclear increase of NF- κ B is not necessarily accompanied by a visible decrease of cytoplasmic NF- κ B, as the translocated protein visualized by Western blot from concentrated nuclear extracts might represent an only small part of the large pool of cytoplasmic NF- κ B [33]) Importantly, pretreatment of IL-10 clearly blocked TNF- α -induced nuclear translocation of p65 (Fig. 1a, panel 2, lane 5 and Fig. 2a, panel 2, lane 6 and Fig. 1b, panel 2, lane 5 and Fig. 2b, panel 2, lane 6, respectively), whereas high levels of nuclear p50 remained stable (Fig. 1a, panel 1, lane 5, Fig. 2a, panel 1, lane 6, Fig. 1b, panel 1, lane 5 & Fig. 2b, panel 1, lane 6, respectively). Immunoblotting with α -Tubulin demonstrated equal protein loading of the gels (Fig. 1a, panel 4 & Fig. 2a, panel 4). These data show that IL-10 blocks TNF- α -induced nuclear translocation of p65 while inducing the nuclear accumulation of p50.

Treatment with IL-10 induces the expression of p105 and p50 in the presence of LPS

Since we had observed that IL-10 induced nuclear translocation of p50 but did not alter the expression of p50 and p105 in the presence of TNF- α , we wanted to further elucidate if treatment with IL-10 would change the synthesis of the p50 and p105 proteins in the presence of a broader, but equally potent stimulus. To address this question, U937 cells were treated with IL-10 in the presence or absence of LPS, and cytoplasmic and nuclear proteins were isolated and subjected to Western blot analysis. Immunoblotting for p105 and p50 demonstrated an approximately 2-fold increase of cytoplasmic protein levels of p105 and p50 upon treatment with a high dose of IL-10 (100 ng/ml) over 120 min (Fig. 3, lane 3). LPS-treatment alone did not visibly change the expression of p105 or p50 (Fig. 3, lane 5). However, in the presence of LPS, IL-10 induced the expression of both p105 and p50 in a dose-dependent fashion (Fig. 3, lanes 7, 9 and 11). Levels of p105 and p50 protein were increased at least 3-fold by high doses of IL-10 (100 ng/ml) in the presence of LPS (Fig. 3, lane 11). In contrast, protein levels of p65 were not affected by

IL-10 treatment in the presence or absence of LPS (data not shown).

IL-10 inhibits DNA-binding of the classical p65/p50 heterodimer but induces DNA-binding of the repressive p50/p50 homodimer

To assess whether IL-10 inhibited NF- κ B-dependent transcription through the suppression of DNA-binding of this transcription factor, EMSAs were performed. For these assays we used UV21, an oligonucleotide probe with binding sites that bind both p65/p50 heterodimers and p50/p50 homodimers [33], and κ B3, an oligonucleotide probe with marked preference and high affinity for p50/p50 homodimers compared to p65/p50 [24]. Nuclear extracts were prepared from untreated cells or from cells treated with IL-10 alone, or treated with TNF- α in the presence or absence of an IL-10 pretreatment and nuclear proteins were analysed for the ability to recognize the ³²P-labelled UV21 or κ B3 probe with an NF- κ B consensus site. Gelshift analysis with nuclear extracts of U937 cells using specific DNA-probes for either the p65/p50 heterodimers or the p50/p50 homodimers supported the Western blot analysis data.

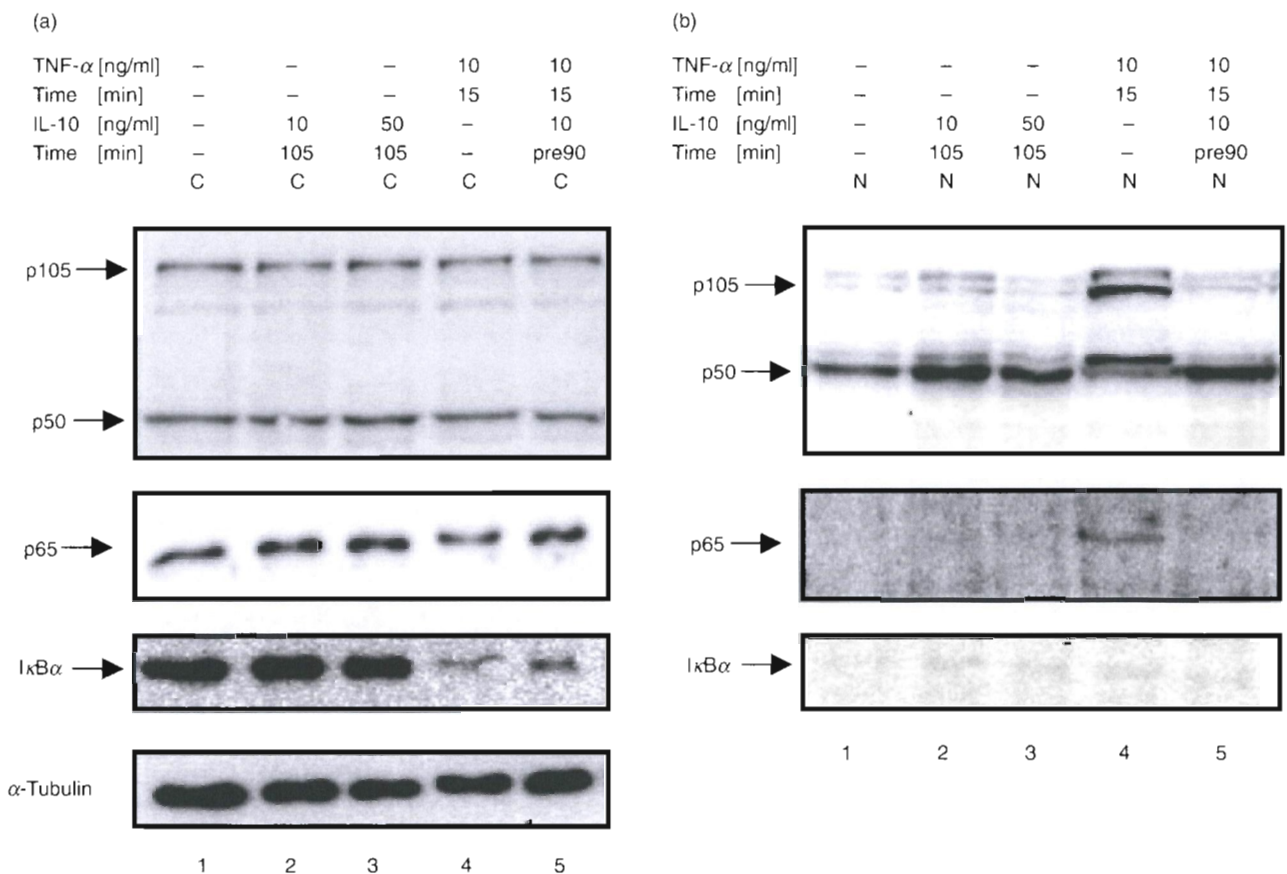


Fig. 1. IL-10 blocks nuclear translocation of p65 but induces nuclear translocation of p50 in monocytic U937 cells. U937 cells were left untreated (lane 1) or were treated with different doses of IL-10 alone (lane 2, 10 ng/ml, 105 min; lane 3, 50 ng/ml, 105 min), or treated with TNF- α in the absence (lane 4, 10 ng/ml, 15 min) or presence of increasing doses of IL-10 (lane 5, 10 ng/ml, lane 6, 50 ng/ml; 90 min pretreatment). (a) Cytoplasmic extracts (C) and (b) nuclear extracts (N) were analysed by Western blot using antibodies against p105/p50 (panel 1), p65 (panel 2) and I κ B α (panel 3) and were compared for I κ B α degradation and p65 and p50 nuclear translocation. Western blotting for α -Tubulin was performed as a loading control (panel 4). One representative of at least three independent experiments with similar results is shown.

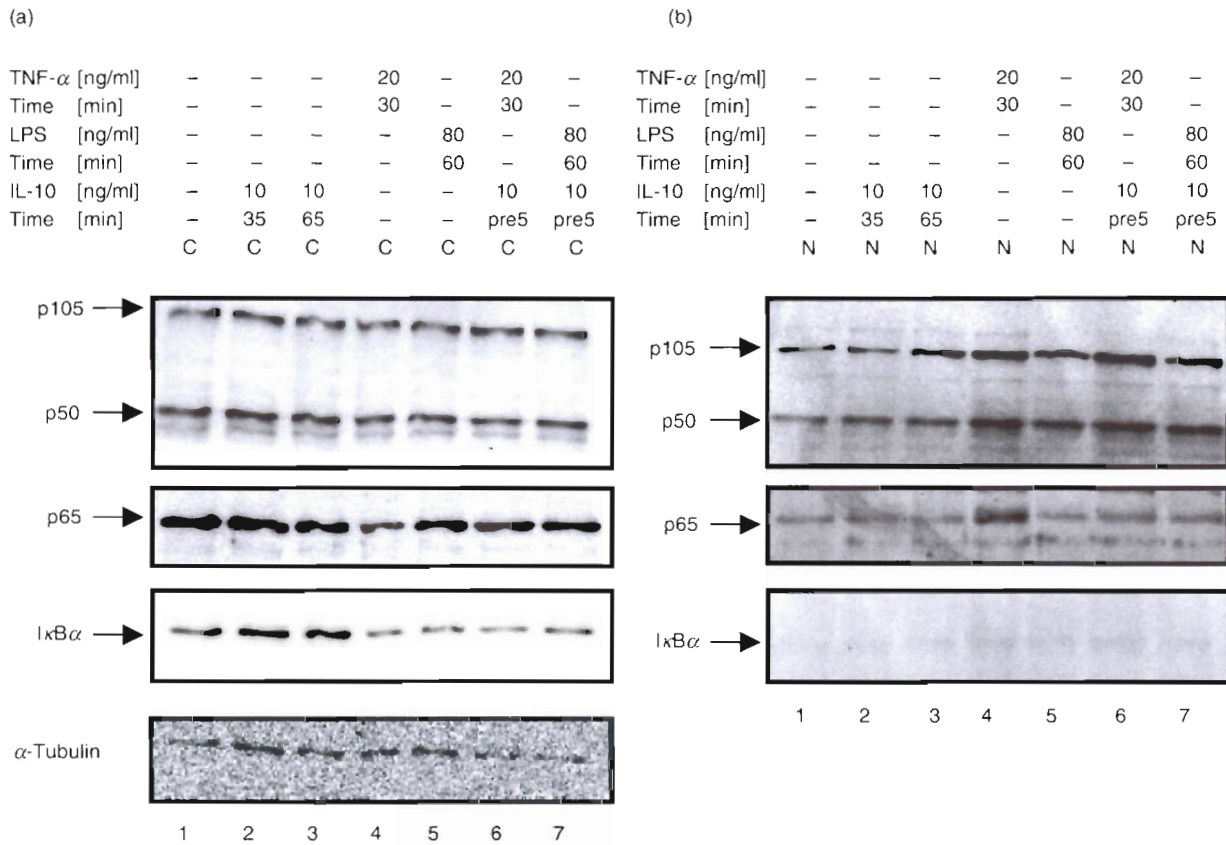


Fig. 2. IL-10 blocks nuclear translocation of p65 but induces nuclear translocation of p50 in human PBMC. Human PBMC were left untreated (lane 1), were treated with IL-10 alone (lane 2: 10 ng/ml, 35 min; lane 3: 10 ng/ml, 65 min), or treated with TNF- α in the absence (lane 4: 20 ng/ml, 30 min) or presence of IL-10 (lane 5: 10 ng/ml, 5 min pretreatment). (a) Cytosolic extracts (C) and (b) nuclear extracts (N) were extracted and subjected to Western blot analysis and probed for p105/p50 (panel 1), p65 (panel 2), and I κ B α (panel 3) and were compared for I κ B α degradation and p65 and p50 nuclear translocation. Western blotting for α -Tubulin was performed as a loading control (panel 5). One representative of at least three independent experiments with similar results is shown.

Constitutive binding of NF- κ B complexes was seen in untreated cells for p50/p50 homodimers and weakly for p65/p50 heterodimers (Fig. 4a,b lane 1). IL-10 treatment alone inhibited constitutive NF- κ B DNA-binding activity of p65/p50 heterodimers (Fig. 4a, lane 2), but induced NF- κ B DNA-binding activity of p50/p50 homodimers (Fig. 4b, lane 2). Stimulation with TNF- α (30 min) strongly induced nuclear translocation and DNA-binding of the classical p65/p50 heterodimer (Fig. 4a, lane 3), while binding of the p50/p50 homodimer was similar to constitutive levels. However, pretreatment with IL-10 followed by TNF- α stimulation significantly inhibited TNF- α -induced DNA-binding of p65/p50 heterodimers (Fig. 4a, lane 4 and 5), whereas DNA-binding activity of p50/p50 homodimers remained at constitutive levels (Fig. 4b, lane 4 and 5). Specificity of binding for NF- κ B complexes was demonstrated by competition with 100-fold excess of unlabelled UV21 probe (Fig. 4a, lane 6 and 7). Supershift experiments showed the subunit composition of the p65/p50 heterodimer (Fig. 4a, lanes 9 & 10) and the p50/p50 homodimer.

Similar effects of IL-10 treatment were observed in human PBMC (data not shown).

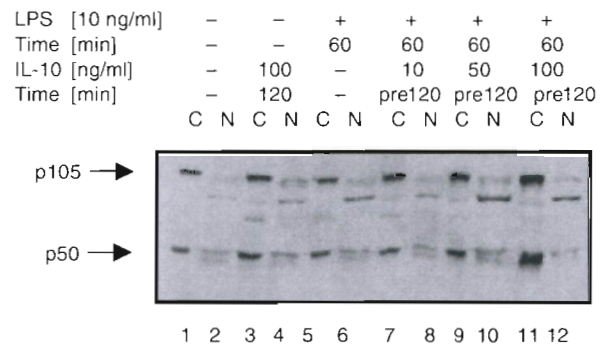


Fig. 3. Treatment with IL-10 induces the expression of p105 and p50 in the presence of LPS in monocytic U937 cells. U937 cells were left untreated (lane 1), were treated with IL-10 alone (lane 3 & 4; 100 ng/ml, 120 min), or treated with LPS in the absence (lane 5 & 6; 10 ng/ml, 60 min) or the presence of increasing doses of IL-10 (lane 7 & 8; 10 ng/ml; lane 9 & 10; 50 ng/ml; lane 11 & 12: 100 ng/ml; 120 min pretreatment). (a) Cytoplasmic extracts (C) and (b) nuclear extracts (N) were analysed by Western blot using antibodies against p105/p50 and were compared for p105 and p50 expression levels. Western blotting for α -Tubulin was performed as a loading control (not shown). One experiment of three independent with similar results is shown.

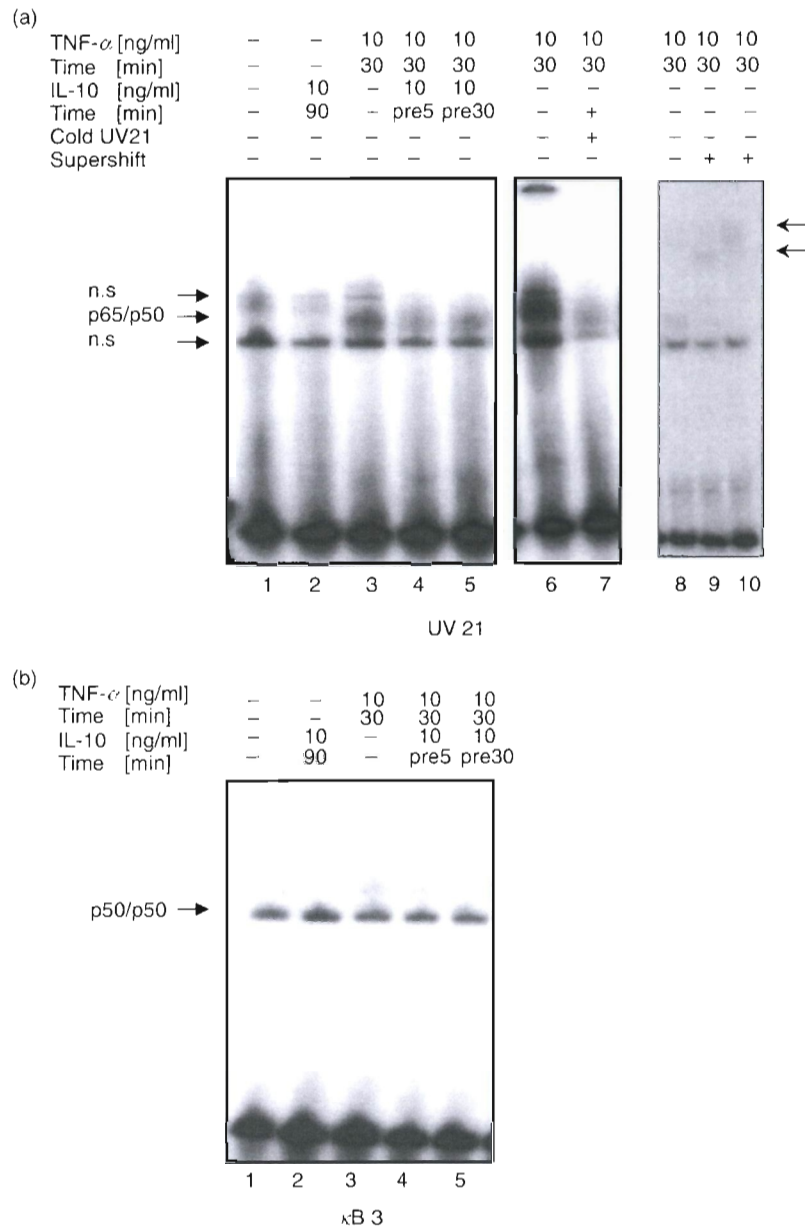


Fig. 4. Inhibition of DNA-binding of the classical p65/p50 heterodimer but induction of DNA-binding of the repressive p50/p50 homodimer by IL-10 in U937 cells. U937 cells were left untreated (lane 1), were treated with IL-10 alone (lane 2: 10 ng/ml, 90 min) or were stimulated with TNF-α (10 ng/ml, 30 min) in the absence (lane 3 and 8) or presence of IL-10 (lane 4 & 5, 10 ng/ml, 5 and 30 min pretreatment, respectively). Nuclear extracts were prepared and subjected to EMSA. Supershift experiments used antibodies to p50 (lane 9) and to both p50 and p65 (lane 10). (a) DNA-binding activity of nuclear extracts were analysed by using the UV21 oligonucleotide specific for p65/p50 complexes or (b) the κB3 oligonucleotide which is specific for p50-p50 complexes. Specificity for NF-κB binding was shown with cold competition of 100-fold excess of unlabelled UV21 oligonucleotide probe (a, lane 6 & 7). One representative of three independent experiments with similar results is shown.

Cells deficient of p105/p50 exhibit very low constitutive and induced inflammatory cytokine/chemokine secretion levels – IL-10 loses its ability to inhibit constitutive cytokine/chemokine secretion in these cells

Since our results from the Western blot and gelshift analyses with U937 cells and PBMC were pointing towards a role for p50 in the IL-10-mediated inhibition of NF-κB, we further wanted to

elucidate the *ex vivo* effects of IL-10 and TNF-α on the expression and secretion of IL-6 and MIP-2α, cytokines/chemokines that are central in the inflammatory response and tightly regulated by NF-κB [35,36], in the presence or absence of p50 expression. In order to experimentally address this question, macrophages and spleen cells isolated from p105/p50 sufficient or deficient mice were treated with TNF-α in the absence or

presence of IL-10, and supernatants were analysed for the secretion of the inflammatory cytokine/chemokine IL-6 and MIP-2 α by ELISA.

Unstimulated macrophages isolated from p105/p50 sufficient mice showed considerable constitutive secretion levels for IL-6 and MIP-2 α (Fig. 5a,b, left panel, group a). IL-10 (10 ng/ml, 8 h) treatment alone inhibited these constitutive IL-6 and MIP-2 α levels by 38% and 42%, respectively (Fig. 5a,b, left panel, group b). TNF- α (20 ng/ml, 8 h) treatment in the absence of IL-10 increased IL-6 and MIP-2 α levels by 31% and 24%, respectively (Fig. 5a,b, left panel, group c). Importantly, IL-10 treatment (10 ng/ml, 8 h) followed by immediate stimulation with TNF- α (20 ng/ml, 8 h) significantly inhibited IL-6 and MIP-2 α levels with a maximum of

40% and 42%, respectively (Fig. 5a,b, left panel, groups d-f). However, no dose-dependency of the inhibitory effect on IL-6 and MIP-2 α secretion could be demonstrated with increasing doses of IL-10 (Fig. 5a,b, left panel). Maximal inhibition was already reached with the lowest dose of this anti-inflammatory cytokine (Fig. 5a,b, left panel, group d).

Remarkably, unstimulated macrophages of p105/p50-deficient mice exhibited a significantly decreased constitutive production of IL-6 and MIP-2 α (11- and 8-fold decrease, respectively) in comparison to wt controls (Fig. 5a,b, right panel, group a). Importantly, IL-10 treatment alone (10 ng/ml, 8 h) did not further inhibit these low constitutive levels of both inflammatory proteins (Fig. 5a,b, right panel, group b).

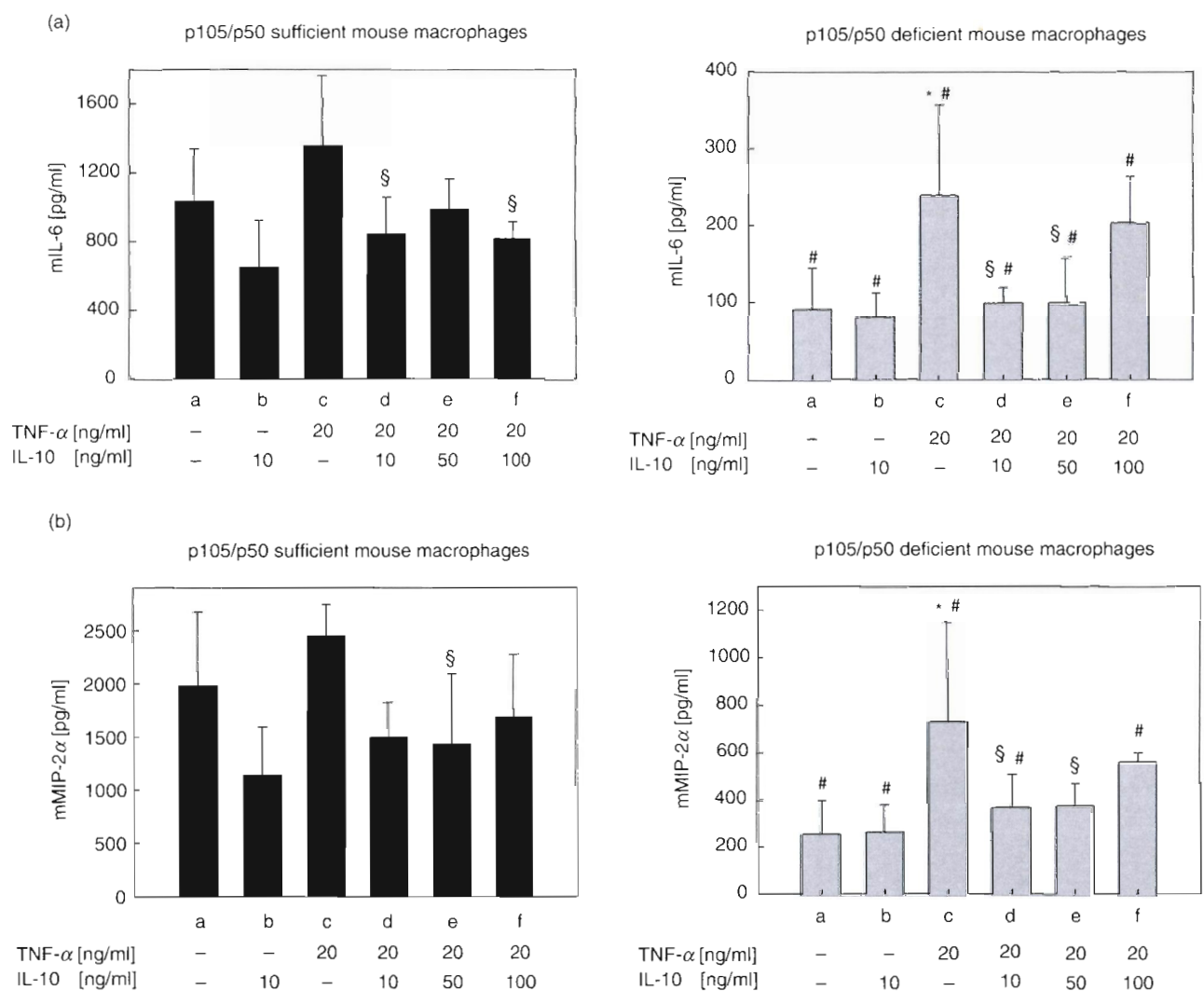


Fig. 5. IL-10 mediated effects on NF- κ B-regulated inflammatory cytokine secretion in p105/p50 sufficient and deficient mouse macrophages. Peritoneal macrophages were isolated from (a) p105/p50 sufficient mice or (b) p105/p50 deficient mice as described in Materials and Methods. Cells were incubated with medium alone or were incubated with TNF- α in the absence or presence of IL-10 and supernatants were assayed for mIL-6 and mMIP-1 α secretion by ELISA as described in Materials and Methods: (a) culture medium only; (b) IL-10 only (10 ng/ml, 8 h); (c) TNF- α only (20 ng/ml, 8 h); (d) IL-10 (10 ng/ml, 8 h) + TNF- α (20 ng/ml, 8 h); (e) IL-10 (50 ng/ml, 8 h) + TNF- α (20 ng/ml, 8 h); (f) IL-10 (100 ng/ml, 8 h) + TNF- α (20 ng/ml, 8 h). * P < 0.05 versus control (a); \$ P < 0.05 versus TNF- α (c); # P < 0.05 versus p105/p50 sufficient cells. Results represent the mean values of three independent experiments; standard deviations are indicated by error bars.

TNF- α -stimulated IL-6 and MIP-2 α secretion in p105/p50 deficient cells was significantly lower in p105/p50 deficient macrophages in comparison to p105/p50 sufficient macrophages, although in p105/p50 deficient cells the relative increase compared to unstimulated cells was about 2-fold higher (Fig. 5a,b, right panel, group c). Importantly, IL-10 (10–100 ng/ml) inhibited TNF- α -induced IL-6 and MIP-2 α production in p105/p50 deficient macrophages with a maximum of 59% and 50%, respectively (Fig. 5a,b, right panel, groups d–f). However, as for the p105/p50 sufficient cells, no dose-dependency was seen for IL-10-mediated inhibition of TNF- α -induced inflammatory cytokine secretion in p105/p50 deficient cells. In contrast, the inhibitory effect was partially lost with a high-dose of IL-10 (Fig. 5a,b, right panel, group f). Remarkably, the inhibitory effect of IL-10-mediated suppression of TNF- α -induced IL-6 and MIP-2 α secretion was even more pronounced in p105/p50 deficient cells in comparison to p105/p50 sufficient cells (Fig. 5a,b, groups d–f). Similar data was obtained with p105/p50 sufficient and deficient spleen cells (data not shown). These results indicate that while IL-10 loses its ability to inhibit constitutive inflammatory cytokine secretion in the absence of p50, inducibility of NF- κ B-regulated cytokine secretion by stimuli like TNF- α is fully maintained or even increased. Moreover, IL-10 fully maintains its ability to inhibit TNF- α -induced cytokines in the absence of p105/p50.

DISCUSSION

It is well established that IL-10 controls inflammatory processes by suppressing the expression of pro-inflammatory cytokines, chemokines, adhesion molecules, as well as antigen-presenting and costimulatory molecules in monocytes/macrophages, neutrophils and T-cells [reviewed in 1]. Different mechanisms have been discussed that mediate IL-10's cytokine inhibiting function. These mechanisms include the up-regulation of SOCS3 [25,26], the inhibition of tyrosine phosphorylation of STAT1 [27] but apparently do not involve the p38 pathway [28]. Since an abundance of the inflammatory proteins suppressed by IL-10 are transcriptionally controlled by NF- κ B it was suggested that IL-10 may exert a significant part of its anti-inflammatory properties through inhibiting this transcription factor. We have recently shown that IL-10 inhibits NF- κ B activity by dual mechanisms. Since the inhibition of nuclear NF- κ B could not be explained by an increase of nuclear levels of its inhibitor I κ B [33] we sought to further investigate the mechanisms underlying this observation.

We show here for the first time that IL-10 selectively induced p50/p50 homodimer translocation into the nucleus and that IL-10 pretreatment followed by TNF- α stimulation blocked the nuclear translocation of the p65 subunit without affecting the nuclear translocation of p50.

We further demonstrate that high doses of IL-10 significantly increased both p105 and p50 protein levels in the absence or presence of low-dose LPS stimulation in monocytic cells (Fig. 3). This observation is supported by reports of p105/p50 up-regulation in the presence of LPS tolerance that can only be induced with low-dose LPS [37]. Since we observed differential effects of IL-10 on p105 and p50, possible mechanisms of interference with p105/p50 generation have to be considered. Two different models of p105/p50 generation are presently discussed. The model proposed by

Heissmeyer *et al.* [38] describes the inducible phosphorylation by IKK α and IKK β and the subsequent degradation of p105 leading to the liberation of sequestered subunits including the processing product p50. The other model proposed by Lin *et al.* [20] describes cotranslational processing which allows the production of both p50 and p105 from one single mRNA. The fact that TNF- α -induced activity of the IKK complex can be inhibited by IL-10 [33] suggests that IL-10 treatment in our cell models inhibited the IKK-dependent post-translational processing of p105.

Interestingly, increased expression of p105 has also been described in LPS-tolerant cells [37] and IL-10 itself has been implicated to play a role in the process of LPS tolerance induction [39]. Both observations, the IL-10-induced expression of p105/p50 and the selective nuclear translocation of p50, could be explained by a putative IL-10-mediated induction of the cotranslational processing of p105 and p50 that would substitute for the putatively blocked post-translational processing of p105. Furthermore, several studies have provided evidence indicating that the C-terminal region of p105 has a functional role similar to the I κ B protein, as p105 can form heterodimers and sequester the p50 subunit or other Rel proteins in the cytoplasm [40–45]. Considering the I κ B-like function of p105, it might also bind p65 to sequester this subunit in the cytoplasm. IL-10-mediated up-regulation of p105 may thus additionally contribute to the inhibition of TNF- α -induced nuclear translocation of p65.

Importantly, IL-10 treatment alone inhibited high constitutive secretion levels of IL-6 and of MIP-2 α in p105/p50 sufficient but not in deficient macrophages. NF- κ B is the exclusive transcription factor for induction of IL-6 in response to TNF- α [35] and also MIP-2 α is tightly regulated by NF- κ B activity [36]. Based on our *in vitro* experiments, this inhibition of constitutive cytokine/chemokine secretion in cells expressing p105/p50 could thus be explained by the selective induction of nuclear translocation of repressive p50/p50 homodimers that would bind to DNA and inhibit NF- κ B activity.

IL-10 inhibited TNF- α -induced IL-6 and MIP-2 α secretion both in p105/p50 sufficient and deficient murine macrophages and spleen cells (Fig. 5 and data not shown). Importantly, constitutive secretion levels of the NF- κ B-controlled cytokines IL-6 and MIP-2 α were significantly decreased in p105/p50 deficient when compared to p105/p50 sufficient macrophages. These results suggest that p50 is required in a complex with p65 for the transcriptional activation of constitutive cytokine/chemokine synthesis. In summary, we demonstrate here that IL-10, selectively induced the expression of p105/p50 as well as the nuclear translocation and DNA-binding of the repressive p50/p50 homodimer (Fig. 6). Furthermore, pretreatment with IL-10 followed by TNF- α inhibited nuclear translocation of the p65/p50 heterodimer without affecting strong translocation of p50. Additionally, IL-10 lost its ability to inhibit constitutive cytokine/chemokine secretion in p105/p50 deficient cells suggesting that the selective induction of p50/p50 homodimer nuclear translocation is an important mechanism employed by IL-10 to mainly inhibit constitutive NF- κ B activity in immune cells. Thus, by specifically inducing nuclear translocation of the repressive p50/p50 homodimer while inhibiting translocation of the classical p65/p50 heterodimer, IL-10 exerts a dual inhibitory function in the NF- κ B pathway. This study broadens our understanding of the mechanisms used by IL-10 to control inflammatory processes and might thus contribute to the development of new therapeutic avenues in the management of chronic inflammatory diseases.

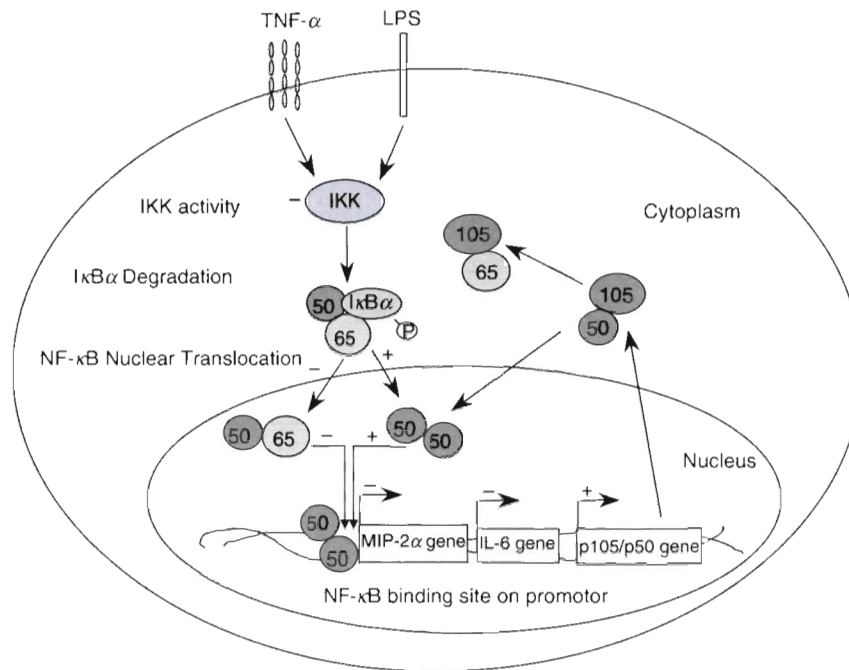


Fig. 6. Scheme representing the molecular mechanisms employed by IL-10 to inhibit NF- κ B activity. In the absence of an activating stimulus such as TNF- α , IL-10 specifically induces the nuclear translocation of repressive p50/p50 homodimers, which compete with pro-inflammatory p65/p50 heterodimers for DNA-binding to NF- κ B promoter sites on inflammatory genes such as IL-6 or MIP-2 α . In the presence of a stimulus such as TNF- α , IL-10 can suppress nuclear translocation and DNA-binding of p65/p50 heterodimers by inhibiting IKK activity and thus delaying degradation of I κ B α . Conserved levels of I κ B α will sequester p65 in the cytoplasm, while p105/p50 expression is up-regulated and p50 free to translocate to the nucleus to form homodimers. Up-regulated p105 may also additionally sequester p65 in the cytoplasm. In the absence of the p105/p50 gene, IL-10 loses its ability to suppress constitutive NF- κ B activity. Upon activation of p105/p50 deficient cells, p65 may recruit a different Rel protein to form transcriptionally active heterodimers, which can still be inhibited by IL-10.

ACKNOWLEDGEMENTS

The authors wish to thank Sandy Westerheide, Chapel Hill for critical reading of the manuscript and Detlef Opitz, Berlin for his help in performing statistics.

REFERENCES

- Moore KW, de Waal Malefyt R, Coffman RL *et al.* Interleukin-10 and the interleukin-10 receptor. *Annu Rev Immunol* 2001; **19**:683–65.
- Kuhn R, Lohler J, Rennick D *et al.* Interleukin-10-deficient mice develop chronic enterocolitis. *Cell* 1993; **75**:263–74.
- Powrie F, Leach M, Mauze S *et al.* Phenotypically distinct subsets of CD4⁺ T cells induce or protect from chronic intestinal inflammation in C. B-17 scid mice. *Int Immunol* 1993; **5**:1461–71.
- Herfarth H, Mohanty S, Rath H *et al.* Interleukin-10 suppresses experimental chronic, granulomatous inflammation induced by bacterial cell wall polymers. *Gut* 1996; **39**:836–45.
- Herfarth H, Bocker U, Janardhanam R *et al.* Subtherapeutic corticosteroids potentiate the ability of interleukin-10 to prevent chronic inflammation in rats. *Gastroenterology* 1998; **115**:856–65.
- Walmsley M, Katsikis P, Abney E *et al.* Interleukin-10 inhibition of the progression of established collagen-induced arthritis. *Arthritis Rheum* 1996; **39**:495–3.
- Rott O, Fleischer B, Cash E. Interleukin-10 prevents experimental allergic encephalomyelitis in rats. *Eur J Immunol* 1994; **24**:1434–40.
- Van Laethem JL, Marchant A, Delvaux A *et al.* Interleukin-10 prevents necrosis in murine experimental acute pancreatitis. *Gastroenterology* 1995; **108**:1917–22.
- Pennline KJ, Roque-Gaffney E, Monahan M. Recombinant human IL-10 prevents the onset of diabetes in the nonobese diabetic mouse. *Clin Immunol Immunopathol* 1994; **71**:169–75.
- Gerard C, Bruyns C, Marchant A *et al.* Interleukin-10 reduces the release of tumor necrosis factor and prevents lethality in experimental endotoxemia. *J Exp Med* 1993; **177**:547–50.
- Schreiber S, Heinig T, Thiele HG *et al.* Immunoregulatory role of interleukin-10 in patients with inflammatory bowel disease. *Gastroenterology* 1995; **108**:1434–44.
- van Deventer S, Elson C, Fedorak R. Multiple doses of intravenous interleukin-10 in steroid-refractory Crohn's disease. *Crohn's Dis Study Group Gastroenterol* 1997; **113**:383–9.
- Asadullah K, Sterry W, Stephanek K *et al.* IL-10 is a key cytokine in psoriasis. Proof of principle by IL-10 therapy: a new therapeutic approach. *J Clin Invest* 1998; **101**:783–94.
- Baldwin A. The NF-kappa B and I kappa B proteins: new discoveries and insights. *Annu Rev Immunol* 1996; **14**:649–83.
- Makarov SS. NF-kappa B in rheumatoid arthritis: a pivotal regulator of inflammation, hyperplasia, and tissue destruction. *Arthritis Res* 2001; **3**:200–6.
- Schottelius AJ, Baldwin A. A role for transcription factor NF-kB in intestinal inflammation. *Int J Colorect Dis* 1999; **14**:18–28.
- Robert C, Kupper TS. Inflammatory skin diseases, T cells, and immune surveillance. *New Engl J Med* 1999; **341**:1817–28.

- 18 Foxwell B, Browne K, Bondeson J, Clarke C, de Martin R, Brennan F, Feldmann M. Efficient adenoviral infection with IkappaB alpha reveals that macrophage tumor necrosis factor alpha production in rheumatoid arthritis is NF-kappaB dependent. *Proc Natl Acad Sci USA* 1998; **95**:8211–5.
- 19 Yamamoto Y, Gaynor RB. Therapeutic potential of NF-kappaB pathway in the treatment of inflammation and cancer. *J Clin Invest* 2001; **107**:135–42.
- 20 Lin L, DeMartino GN, Greene WC. Cotranslational dimerization of the Rel homology domain of NF-kappaB1 generates p50-p105 heterodimers and is required for effective p50 production. *EMBO J* 2000; **19**:4712–22.
- 21 Finco T, Baldwin A. Mechanistic aspects of NF-kappa B regulation. The emerging role of phosphorylation and proteolysis. *Immunity* 1995; **3**:263–72.
- 22 Schmitz M, dos Santos Silva MA, Baeuerle PA. Transactivation domain 2 (TA2) of p65 NF-kappa B. Similarity to TA1 and phorbol ester-stimulated activity and phosphorylation in intact cells. *J Biol Chem* 1995; **270**:15576–84.
- 23 Finco TS, Beg AA, Baldwin AS Jr. Inducible phosphorylation of I kappa B alpha is not sufficient for its dissociation from NF-kappa B and is inhibited by protease inhibitors. *Proc Natl Acad Sci USA* 1994; **91**:11884–8.
- 24 Baer M, Dillner A, Schwartz RC *et al*. Tumor necrosis factor alpha transcription in macrophages is attenuated by an autocrine factor that preferentially induces NF-kappa B p50. *Mol Cell Biol* 1998; **18**:5678–89.
- 25 Cassatella MA, Gasperini S, Bovolenta C *et al*. Interleukin-10 (IL-10) selectively enhances CIS3/SOCS3 mRNA expression in human neutrophils: evidence for an IL-10-induced pathway that is independent of STAT protein activation. *Blood* 1999; **94**:2880–9.
- 26 Berlato C, Cassatella MA, Kinjyo I, Gatto L, Yoshimura A, Bazzoni F. Involvement of suppressor of cytokine signaling-3 as a mediator of the inhibitory effects of IL-10 on lipopolysaccharide-induced macrophage activation. *J Immunol* 2002; **168**:6404–11.
- 27 Ito S, Ansari P, Sakatsume M, Dickensheets H, Vazquez N, Donnelly RP, Larner AC, Finbloom DS. Interleukin-10 inhibits expression of both interferon alpha- and interferon gamma-induced genes by suppressing tyrosine phosphorylation of STAT1. *Blood* 1999; **93**:1456–63.
- 28 Denys A, Udalova I, Smith C, Williams LM, Ciesielski CJ, Campbell J, Andrews C, Kwaitkowski D, Foxwell BMJ. Evidence for a dual mechanism for IL-10 suppression of TNF- α production that does not involve inhibition of p38 mitogen-activated protein kinase or NF- κ B in primary human macrophages. *J Immunol* 2002; **168**:4837–45.
- 29 Wang P, Wu P, Siegel MJ *et al*. Interleukin (IL) -10 inhibits nuclear factor kappa B (NF kappa B) activation in human monocytes. IL-10 and IL-4 suppress cytokine synthesis by different mechanisms. *J Biol Chem* 1995; **270**:9558–63.
- 30 Dokter W, Koopmans S, Vellenga E. Effects of IL-10 and IL-4 on LPS-induced transcription factors (AP-1, NF-IL6 and NF-kappa B) which are involved in IL-6 regulation. *Leukemia* 1996; **10**:1308–16.
- 31 Romano MF, Lamberti A, Petrella A *et al*. IL-10 inhibits nuclear factor-kappa B/Rel nuclear activity in CD3-stimulated human peripheral T lymphocytes. *J Immunol* 1996; **156**:2119–23.
- 32 Clarke CJP, Hales A, Hunt A *et al*. IL-10-mediated suppression of TNF-alpha production is independent of its ability to inhibit NF kappa B activity. *Eur J Immunol* 1998; **28**:1719–26.
- 33 Schottelius AJ, Mayo MW, Sartor RB *et al*. Interleukin-10 signaling blocks inhibitor of kappaB kinase activity and nuclear factor kappaB DNA binding. *J Biol Chem* 1999; **274**:31868–74.
- 34 Sha WC, Liou HC, Tuomanen EL *et al*. Targeted disruption of the p50 subunit of NF-kappa B leads to multifocal defects in immune responses. *Cell* 1999; **80**:321–30.
- 35 Vanden Berghe W, Vermeulen L, De Wilde G *et al*. Signal transduction by tumor necrosis factor and gene regulation of the inflammatory cytokine interleukin-6. *Biochem Pharmacol* 2000; **60**:1185–95.
- 36 Shi MM, Chong I, Godleski J *et al*. Regulation of macrophage inflammatory protein-2 gene expression by oxidative stress in rat alveolar macrophages. *Immunology* 1999; **97**:309–15.
- 37 Ziegler-Heitbrock HWL, Petersmann I, Frankenberger M. p50 (NF-kappa B1) is upregulated in LPS tolerant P388D1 murine macrophages. *Immunobiology* 1997; **198**:73–80.
- 38 Heissmeyer V, Krappmann D, Wulczyn FG *et al*. NF-kappa B p105 is a target of IkappaB kinases and controls signal induction of Bcl-3-p50 complexes. *EMBO J* 1999; **18**:4766–78.
- 39 Randow F, Syrbe U, Meisel C *et al*. Mechanism of endotoxin desensitization: involvement of interleukin-10 and transforming growth factor beta. *J Exp Med* 1995; **181**:1887–92.
- 40 Blank V, Kourilsky P, Israel A. Cytoplasmic retention, DNA-binding and processing of the NF-kappaB p50 precursor are controlled by a small region in its C-terminus. *EMBO J* 1991; **10**:4159–67.
- 41 Henkel T, Zabel U, van Zee JM *et al*. Intramolecular masking of the nuclear location signal and dimerization domain in the precursor for the p50 NF-kappa B subunit. *Cell* 1992; **68**:1121–33.
- 42 Rice NR, Mackichan ML, Israel A. The precursor of NF-kappa B p50 has I kappa B-like functions. *Cell* 1992; **78**:243–53.
- 43 Hatada EN, Naumann M, Scheidereit C. Common structural constituents confer I kappa B activity to NF-kappa B p105 and I kappa B/MAD-3. *EMBO J* 1993; **12**:2781–8.
- 44 Mercurio F, DiDonato JA, Rosette C *et al*. p105 and p98 precursor proteins play an active role in NF-kappa B-mediated signal transduction. *Genes Dev* 1993; **7**:705–18.
- 45 Naumann M, Wulczyn FG, Scheidereit C. The NF-kappa B precursor p105 and the proto-oncogene product Bcl-3 are I kappa B molecules and control nuclear translocation of NF-kappaB. *EMBO J* 1993; **12**:213–22.

Differential regulation of P-selectin ligand expression in naive versus memory CD4⁺ T cells: evidence for epigenetic regulation of involved glycosyltransferase genes

Uta Syrbe, Silke Jennrich, Arndt Schottelius, Anne Richter, Andreas Radbruch, and Alf Hamann

Lymphocytes are targeted to inflamed sites by specific "homing" and chemokine receptors. Most of them, including ligands for P- and E-selectin, are absent from naive CD4⁺ T cells and become induced after activation and differentiation in effector/memory cells. Polarized effector cells are characterized by the rapid production of distinct cytokines upon restimulation. Their cytokine memory is in part controlled by epigenetic imprinting during differentiation. Here we ask whether a similar mecha-

nism could regulate selectin ligand expression, mediating entry into inflamed sites, notably within the skin. We report that acquisition of selectin ligands by naive but not memory CD4⁺ cells depends on progression through the G₁/S phase of the cell cycle—a phase susceptible to modification of the chromatin structure. Cell-cycle arrest prevented transcriptional activation of glycosyltransferases involved in the generation of selectin ligands, suggesting that progression through the cell cycle is required to

unlock their genes. Artificial DNA demethylation strongly increased the frequency of selectin ligand-expressing cells, suggesting that DNA methylation keeps transferase genes inaccessible in naive T cells. Due to these findings we propose that selectin-dependent inflammation-seeking properties are imprinted by epigenetic modifications upon T-cell differentiation into effector cells. (Blood. 2004;104:3243-3248)

© 2004 by The American Society of Hematology

Introduction

Activation of naive T lymphocytes by specific antigen under appropriate conditions leads to functional differentiation into subsets of effector cells.¹ This differentiation is accompanied by changes in homing receptor expression resulting in memory subsets displaying distinct homing properties. While naive T cells recirculate between lymphoid organs, fractions of effector/memory T cells gain access to peripheral inflamed sites.^{2,3} In contrast to naive T cells, these effector cells express receptors for inflammatory chemokines and ligands for E- and P-selectin but lack L-selectin expression.⁴⁻⁷

E- and P-selectin ligands are fucosylated oligosaccharides decorating distinct carrier proteins such as P-selectin glycoprotein binding protein-1 (PSGL-1) and enable trafficking of leukocytes and T cells into inflamed areas, particularly within the skin.⁸⁻¹⁰ The oligosaccharide epitopes become induced upon differentiation into effector/memory cells on a fraction of cells.^{6,11} A related E-selectin binding epitope involved in skin-specific homing of T cells has been termed "cutaneous lymphocyte antigen" (CLA).¹²

The generation of selectin ligands depends on the coordinated action of a set of glycosyltransferases, which determines both tissue-specific and differentiation-dependent generation of selectin-binding epitopes.⁸ Particularly in T lymphocytes, expression of fucosyltransferase (FucT) VII and core-2 glycosaminyltransferase (C2 GlcNAcT) appears to correlate with the expression of selectin

ligands, and deletion of these enzymes abrogates the inducible expression on T cells.^{13,14}

Secondary immune responses are more efficient than primary responses due to the presence of effector cells, which can rapidly recall their effector functions. Those cells evolved from naive T cells, which after activation by an appropriate peptide-major histocompatibility complex (peptide-MHC) underwent clonal expansion and programmed differentiation. This differentiation is associated with the commitment to produce particular effector cytokines such as interferon- γ (IFN- γ) ("Th1" cells) or interleukin-4 (IL-4) ("Th2" cells), which are recalled upon subsequent stimulation.^{15,16}

Permanent differentiation of cell lineages is often associated with chromatin modification controlling gene expression in a heritable, clonal manner. Key mediators of epigenetic changes are postsynthetic modifications of DNA itself or of proteins, which are closely attached to the DNA.^{17,18}

Changes in the pattern of DNA methylation and histone acetylation of regulatory regions of the IL-4 and IFN- γ gene suggest that similar mechanisms are involved in the stabilization of the functional polarization of effector lymphocytes.¹⁹⁻²¹ The cell cycle, providing a window for chromatin remodeling, is a major checkpoint for the acquisition of effector functions. Thus, arrest of naive T cells after T-cell receptor (TCR) engagement prevented

From Experimentelle Rheumatologie, Medizinische Klinik, Charité Universitätsmedizin Berlin, Campus Mitte, Berlin, Germany; Research Business Area Dermatology, Research Laboratories, Schering, Berlin, Germany; Deutsches Rheumaforschungszentrum, Berlin, Germany; and Charité, Campus Benjamin Franklin, Medizinische Klinik I, Berlin, Germany.

Submitted September 5, 2003; accepted May 17, 2004. Prepublished online as *Blood* First Edition Paper, August 5, 2004; DOI 10.1182/blood-2003-09-3047.

Supported by the Deutsche Forschungsgemeinschaft (SFB 366).

U.S. and S.J. contributed equally to this study.

Reprints: Alf Hamann, Experimentelle Rheumatologie c/o DRFZ, 10117 Berlin, Germany; e-mail: hamann@drfz.de.

The publication costs of this article were defrayed in part by page charge payment. Therefore, and solely to indicate this fact, this article is hereby marked "advertisement" in accordance with 18 U.S.C. section 1734.

© 2004 by The American Society of Hematology

functional differentiation without affecting the levels of lineage-determining transcription factors.²²⁻²⁴ As a result, the model emerged that master transcription factors interfere with the action of specific DNA methyltransferases like DNA methyltransferase 1, which are recruited to replication forks at S phase where they establish symmetric CpG methylation of hemimethylated substrates, effectively duplicating the DNA methylation pattern on newly synthesized DNA strands.²⁵

The rapid recruitment of effector/memory cells to sites of inflammation is a prerequisite for an effective immune response. It implies that subsets of effector/memory cells retain inflammation-seeking homing properties for longer times or rapidly recall this property. We hypothesized that epigenetic mechanisms regulating gene accessibility could be involved in the fixation of such an inflammation-seeking homing pattern. Therefore, we determined whether induction of selectin ligands after activation of naive T cells is controlled by the cell cycle, and show that their up-regulation and induction of the involved glycosyltransferases are indeed strictly dependent on entry into the cell cycle in naive but not memory T cells. This indicates that the respective gene loci are closed in naive T cells and become permanently accessible after priming in a part of T cells. DNA methylation appears to be involved in the control of accessibility of the genes, because expression of the selectin ligands is strongly enhanced by treatment with methylation inhibitors. These findings provide first evidence for the involvement of epigenetic mechanisms resulting in a stable imprinting of homing properties on effector T cells.

Materials and methods

Mice

DO11.10 mice (a kind gift from D. Y. Loh, Washington University School of Medicine, St Louis, MO) carrying a transgenic TCR specific for the ovalbumine (OVA)-peptide 323-339 and BALB/c mice were bred under specific pathogen-free conditions in the Bundesinstitut für Risikobewertung, Berlin, Germany. All animal experiments were performed in accordance with institutional, state, and federal guidelines.

Isolation and cell purification

CD4⁺ T cells were purified from pooled peripheral and mesenteric lymph nodes of DO11.10 mice either by panning using anti-CD8 (53-672), anti-CD25 (PC/6), anti-Mac-1 (M1/70), and anti-FcR II/III (2.4G2) antibodies or by direct isolation of CD4⁺ cells by anti-CD4-fluorescein isothiocyanate (anti-CD4-FITC) (GK1.5) and anti-FITC multisort-magnetic cell separation (MACS) beads (Miltenyi Biotec, Bergisch Gladbach, Germany) to a purity of at least 98%. Naive CD4⁺ CD62L⁺ cells were positively selected with anti-CD62L microbeads (Miltenyi Biotec) to a purity of at least 98%. Antigen-presenting cells (APCs) were prepared by depletion of CD90⁺ cells from spleen cells or purified CD4 negative fraction using anti-CD90 MACS microbeads (Miltenyi Biotec). APCs were irradiated (30 Gy) before culture. For cultures containing naive and

memory cells, CD4⁺ cells were isolated from peripheral lymph nodes with anti-CD4 (L3T4) microbeads (Miltenyi Biotec).

CFSE labeling

Labeling of naive CD4⁺ CD62L⁺ cells with 5-(and 6-)carboxyfluorescein diacetate succinimidyl ester (CFSE; Molecular Probes, Eugene, OR) was performed as described.²² In brief, washed cells were resuspended at 1×10^7 /mL in phosphate-buffered saline (PBS), CFSE (5 μ M final concentration) was added, and cells were incubated for 3 minutes at room temperature. The reaction was stopped by washing with RPMI 1640 containing 10% fetal calf serum (FCS).

Cell culture

Cell culture was set up with 2×10^6 cells per milliliter in complete RPMI 1640 containing 10% FCS and 10 μ M 2-mercaptoethanol (2-ME) (Life Technologies, Bethesda, MD). CD4⁺ CD62L⁺ T cells from OVA TCR transgenic mice and APCs were cultured at a ratio of 1:4 in the presence of OVA₃₂₃₋₃₃₉ peptide (Biochemistry Department, Charité Universitätsmedizin Berlin, Germany) at 0.5 μ M. Cell cultures containing total CD4⁺ cells were stimulated with 0.1 μ M OVA₃₂₃₋₃₃₉ peptide, supporting better survival of memory cells. Cell cultures were supplemented with recombinant murine IL-12 (R&D Systems, Minneapolis, MN) at 5 ng/mL, IFN- γ (R&D Systems) at 20 ng/mL, and neutralizing anti-IL-4 antibodies at 5.5 μ g/mL (11B11) as indicated. For mRNA detection, 1×10^6 /mL naive T cells were activated with plate-bound anti-CD3 (1 μ g/mL) and soluble anti-CD28 (1 μ g/mL).

Inhibitors

Progression of cells through the cell cycle was inhibited by addition of either 300 μ M L-mimosine (ICN, Santa Ana, CA), 2 μ g/mL aphidicolin (Sigma Chemical, St Louis, MO), 200 nM paclitaxel (ICN), or mycophenolic acid at 1 μ M (Sigma Chemical) to the cell culture.

To study the possible role of DNA methylation, 5-aza-2-deoxycytidine (Sigma Chemical), as an inhibitor of cytosine methylation, was added to the cell culture at concentrations of 5 μ M for 48 hours.

Cytometric analysis and cell sorting

For cytometric analysis dead cells were excluded by staining with 4,6-diamidino-2-phenylindole (Sigma Chemical). OVA TCR transgenic T cells were identified by the clonotype-specific monoclonal antibody KJ1-26.1. P-selectin binding ligands were detected by P-selectin-human immunoglobulin G (IgG) chimeric protein (provided by Dr D. Vestweber, Max-Planck-Institut für Vaskuläre Biologie, Münster, Germany) and phycoerythrin (PE)-conjugated anti-human IgG antibody F(ab')₂ (Dianova, Hamburg, Germany) as secondary reagent, as previously described.¹¹ Naive and effector/memory cells were identified by the expression of CD45RB (clone 16A, Pharmingen, San Diego, CA). The state of activation was determined by fluorochrome-conjugated monoclonal antibody to CD25 (Pharmingen). Cytometric analysis was performed using an LSR or FACSCalibur and CellQuest research software (BD Biosciences). Cell sorting was done using a MoFlo fluorescence-activated cell sorter (FACS; Cytomation, Fort Collins, CO).

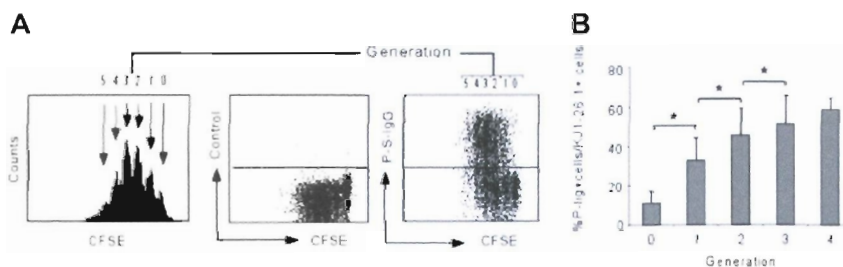


Figure 1. Proliferation enhances P-lig expression on activated CD4⁺ lymphocytes. Naive CD4⁺ T cells from DO11.10 mice were CFSE labeled and stimulated with OVA₃₂₃₋₃₃₉ peptide and APCs plus IL-12, IFN- γ , and α IL-4. On day 3, individual generations (arrows, nos.) of undivided and divided KJ1-26.1⁺ cells were identified by loss of CFSE staining. (A) An example of control and P-lig staining in combination with CFSE. (B) The frequency of P-lig⁺ cells within indicated generations of KJ1-26.1⁺ cells is summarized from 7 independent experiments (* $P < .05$).

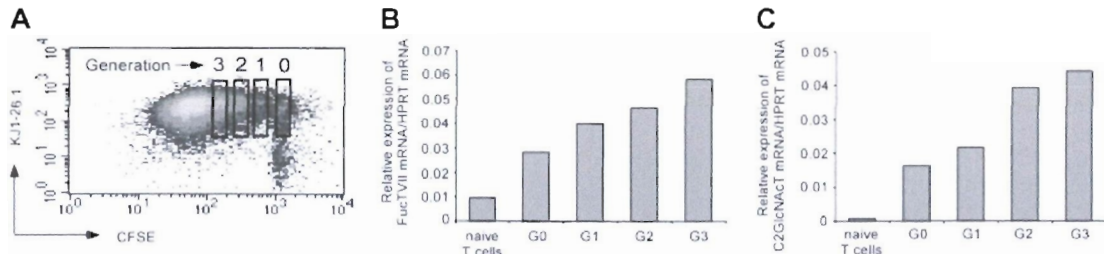


Figure 2. Proliferation enhances FucT VII and C2 GlcNAcT mRNA expression in activated CD4⁺ lymphocytes. On day 3 after activation as in Figure 1, transgenic KJ1-26.1⁺ T cells were sorted according to the CFSE stain into individual generations (G0 to G3) (A). FucT VII mRNA and C2 GlcNAcT mRNA expression in relation to HPRT as a housekeeping gene was determined by quantitative PCR within these sorted fractions and in naive T cells (B-C). One representative of 2 experiments is shown.

RNA isolation and real-time PCR analysis

For determination of mRNA expression, about 1 × 10⁶ cells were lysed and RNA was isolated using the RNeasy Mini kit (Qiagen, Hilden, Germany). After DNase treatment RNA was reverse transcribed by Moloney murine leukemia virus reverse transcriptase (M-MLV-RT) (Gibco, Carlsbad, CA) using oligo(dT) primer (Amersham Pharmacia Biotech, Piscataway, NJ). For quantitative PCR the following primer (TIB-Molbiol, Berlin, Germany) and probes (Metabion, Planegg-Martinsried, Germany) were used. Primer: hypoxanthine phosphoribosyl transferase (HPRT) reverse: 5'-TTG AGC ACA CAG AGG GCC A; HPRT forward: 5'-ATC ATT ATG CCG AGG ATT TGG AA; FucT VII reverse: 5'-CAG ATG CAC CCT CTA GTA CTC TGG; FucT VII forward: 5'-TGC ACT GTC CTT CCA CAA CC; C2 GlcNAcT reverse: 5'-TGC CAG TTT ATC AGC GGG AC; C2 GlcNAcT forward: 5'-CAG GAG TCA GAG CCT CAA CAG A. Probes: HPRT: 5'-FAM-TGG ACA GGA CTG AAA GAC TTG CTC GAG ATG-TAMRA; FucT VII: 5'-FAM-CCT GCG CCC AGT GTA CAG TCT GCA-TAMRA; C2 GlcNAcT: 5'-FAM-TCA GGC TGC CTG TGA TTC TAA ACG TGA TAT C-TAMRA.

Quantitative PCR was done in a GeneAmp 5700 Sequence Detection System (Applied Biosystems, Weiterstadt, Germany) using 10 to 100 ng cDNA and qPCR mastermix (Eurogentec, Seraing, Belgium) with the respective primers (900 nM) and probes (250 nM).

Results

Proliferation enhances P-lig expression on CD4⁺ lymphocytes

In vivo studies have shown that after activation of naive T cells the frequency of cells expressing P-selectin ligands (P-lig) increases with proliferation.²⁶ We found similar results after activation of naive CD4⁺ cells in vitro under appropriate conditions^{11,27}—that is, in the presence of IL-12, IFN-γ, and

anti-IL-4: among T cells that had not divided, only 5% to 15% expressed P-lig while completion of the first mitosis and further divisions significantly increased the likelihood of P-lig expression on day 3 after activation (Figure 1).

Proliferation enhances mRNA expression of FucT VII and C2 GlcNAcT

To verify if glycosyltransferases involved in the generation of selectin ligands are the target of cell-cycle-dependent regulation, we analyzed mRNA expression of FucT VII and C2 GlcNAcT. Therefore, we activated CFSE-labeled naive T cells from OVA TCR transgenic D011.10 mice for 3 days by OVA₃₂₃₋₃₃₉ peptide and APCs in the presence of IL-12, IFN-γ, and αIL-4. Then, transgenic T cells were stained by the clonotype-specific antibody KJ1-26.1 and sorted into different generations according to their CFSE content (Figure 2A). Expression of FucT VII and C2 GlcNAcT mRNA was determined by quantitative PCR. Cells that had undergone one or more divisions showed a dramatically increased FucT VII mRNA and C2 GlcNAcT mRNA expression compared with naive T cells and, to a lesser degree, with cells from the same culture that had not divided yet (Figure 2B-C).

Arresting the cells in G₁/S phase of the cell cycle abrogates P-lig induction, which is accompanied by inhibition of FucT VII and C2 GlcNAcT mRNA induction

A small but significant fraction of nondivided cells expressed P-lig; these cells might have entered but not yet completed the cell cycle. To clarify this, cell-cycle inhibitors were used to stop mitosis at different phases of the cell cycle. The presence of inhibitors during

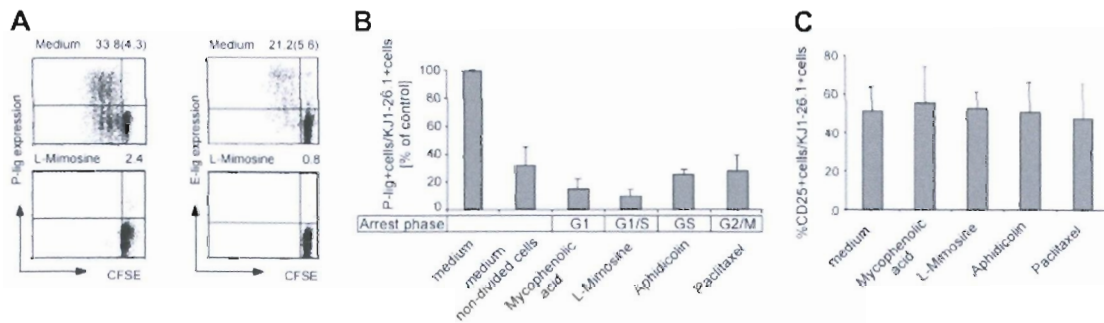


Figure 3. Inhibitors of the cell cycle suppress expression of P-lig but not other activation-induced molecules. Naive CD4⁺ T cells were stimulated as in Figure 1 in the absence or presence of the indicated drugs arresting the T cells in different phases of the cell cycle. The percentage of selectin lig-positive cells within CD4⁺ KJ1-26.1⁺ cells was determined on day 3. (A) A representative dot plot of P-lig and E-lig expression among total KJ1-26.1⁺. The percentages of selectin lig-positive cells among all and among undivided (in parentheses) cells is given. (B) Four separate experiments are summarized, and the mean + SD is given. To compare these experiments, the frequency of P-lig-positive cells induced in the absence of cell-cycle inhibitors is set to 100% for each experiment, and the relative frequency within undivided and inhibitor-treated cultures was determined. (C) CD25 expression on KJ1-26.1⁺ cells at day 1 after activation. The mean + SD from 3 separate experiments is given.

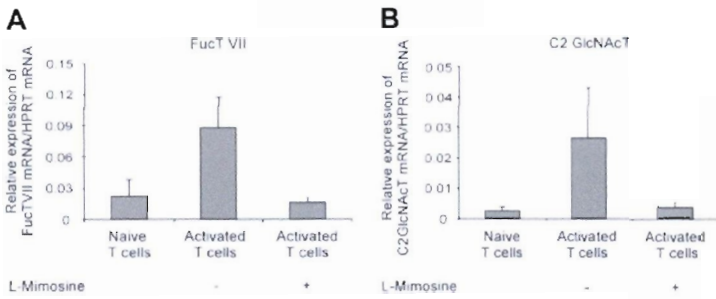


Figure 4. Cell-cycle arrest prevents up-regulation of FucT VII and C2 GlcNAcT mRNA expression. A total of 1×10^6 naive T cells were activated by plate-bound anti-CD3 and soluble anti-CD28 plus IL-12, IFN- γ , and anti-IL-4 for 3 days. The relative expression of FucT VII (A) and C2 GlcNAcT (B) mRNA to housekeeping gene HPRT was determined for naive T cells and cells activated in the presence or absence of L-mimosine. The mean (\pm SD) from 4 individual experiments is shown.

activation strongly suppressed the induction of P-lig as shown in Figure 3A-B. Arrest in an early phase of the cell cycle (G_1 phase by mycophenolic acid and G_1/S phase by L-mimosine) almost completely abrogated the induction of P-lig in naive cells (2% to 4% P-lig-positive cells, Figure 3A), and arrest in later phases (S or G_2/M phase) by aphidicolin or paclitaxel allowed P-lig expression at levels comparable to untreated cells that had not completed cell division (Figure 3B). Furthermore, we confirmed the absence of functional P-selectin ligands on L-mimosine-treated cells in a nonstatic adhesion assay and found that adhesion of G_1/S -arrested T cells to P-selectin was reduced to only 5% (\pm 0.75%) of that of untreated Th1 cells (data not shown).

Induction of E-selectin ligands appears to be regulated in parallel as shown in Figure 3A: undivided T cells showed a low frequency of E-lig-positive cells, and L-mimosine treatment abrogated induction of E-lig.

Therefore, entry into the S phase seems to be indeed a critical determinant in the regulation of the relevant genes. In contrast, expression of activation markers such as CD25 is observed rapidly after activation and is not blocked by inhibition of mitosis (Figure 3C). The same applies to CD69, L-selectin down-regulation, and IL-2 secretion 1 or 2 days after stimulation.²² This confirms unimpaired activation in the inhibitor-treated cultures and the peculiar type of gene regulation involved in P-lig induction.

The impact of the cell cycle on the mRNA expression of fucosyltransferase VII (FucT VII) and core-2 glycosaminyltransferase (C2 GlcNAcT) was determined 3 days after activation of naive T cells in the presence or absence of L-mimosine. Naive T cells were activated by plate-bound α CD3 and soluble α CD28 to avoid contamination by mRNA from APCs. In line with its effects on P-lig expression, L-mimosine treatment prevented the up-regulation of mRNA expression for FucT VII and C2 GlcNAcT seen in untreated cultures (Figure 4). This indicated that, in contrast to most molecules induced after activation, transcription of both FucT VII and C2 GlcNAcT genes not only requires activating signals but also entry into the cell cycle. The strict link between expression and mitosis points to the involvement of chromatin remodeling.

Most memory/effector cells can express P-selectin ligands independent of cell cycling

If imprinting by chromatin remodeling is involved in glycosyltransferase regulation, at least subfractions of memory cells primed under P-lig-permissive conditions should carry the ligand-generating genes either permanently active or in an accessible, cell cycle-independent state. To investigate this prediction, CFSE-labeled CD4⁺ T cells isolated from peripheral lymph nodes of DO11.10 mice were activated in the presence or absence of L-mimosine, arresting the cells in G_1/S phase of the cell cycle. For identification of naive and effector/memory cells, we used a combination of CFSE labeling and CD45RB staining, which traces the proliferation-associated down-regulation of CD45RB and allows discrimination of naive and effector/memory cells for up to 3 days after activation (Figure 5A). In line with previous observations, only negligible numbers of naive, CD45RB^{high} cells expressed P-lig when arrested in G_1/S phase on day 3 after activation (Figure 5B). In contrast, memory cells contained about 10% P-lig-expressing cells after isolation *ex vivo*, and an additional fraction of 20% to 35% up-regulated the ligands independent of cell cycling. To exclude the possibility that selective survival of P-lig-positive memory/effector cells results in enhanced frequencies of P-lig-positive cells under these conditions, we sorted P-lig-positive and P-lig-negative CD45RB^{low} CD4⁺ cells and activated the cells as described in "Materials and methods."²⁷ Comparable survival rates of 20% and 25% at day 3, respectively, excluded a preferential enrichment of P-lig-positive compared with P-lig-negative memory T cells (data not shown).

Thus, more than 50% of memory cells able to express P-lig, according to nontreated culture, did so independent of cell cycling, indicating that they carry the P-lig-generating loci in an open conformation.

Artificial demethylation enhances induction of selectin ligands

The above data do not provide clues as to the mechanisms that stabilize accessibility of the transferase genes. Demethylation of

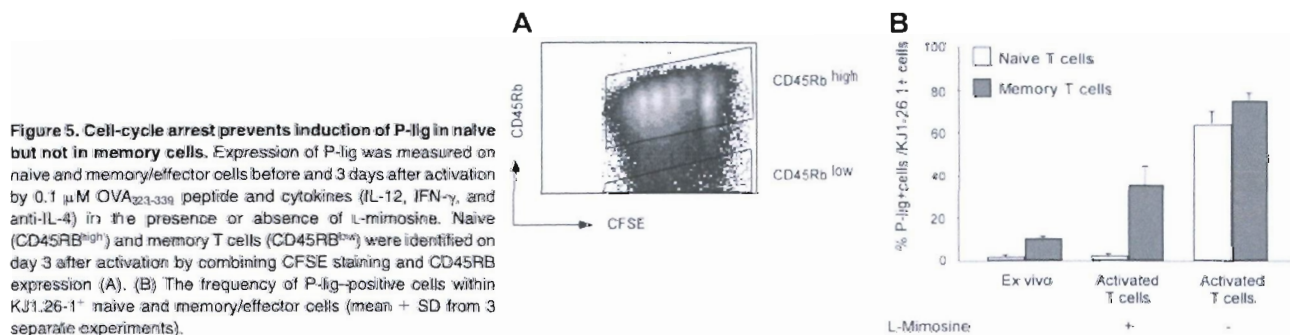


Figure 5. Cell-cycle arrest prevents induction of P-lig in naive but not in memory cells. Expression of P-lig was measured on naive and memory/effector cells before and 3 days after activation by 0.1 μ M OVA₂₂₃₋₃₃₉ peptide and cytokines (IL-12, IFN- γ , and anti-IL-4) in the presence or absence of L-mimosine. Naive (CD45RB^{high}) and memory T cells (CD45RB^{low}) were identified on day 3 after activation by combining CFSE staining and CD45RB expression (A). (B) The frequency of P-lig-positive cells within KJ1.26-1⁺ naive and memory/effector cells (mean \pm SD from 3 separate experiments).

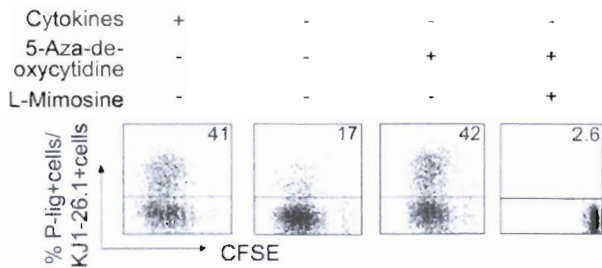


Figure 6. Artificial DNA demethylation up-regulates P-lig expression on effector T cells. Naive transgenic CD4⁺ cells were activated with OVA₃₂₃₋₃₃₉ peptide and APCs either with or without cytokine supplement (IL-12, IFN- γ , and α IL-4) as indicated and in the presence or absence of the DNA methylation inhibitor 5-aza-2-deoxycytidine (5 μ M) and cell-cycle inhibitor L-mimosine. Data from 1 of 4 similar experiments are shown. Numbers in top right corners indicate the percentage of P-lig-positive cells in culture.

DNA is a key mechanism in epigenetic regulation of gene expression. To elucidate a possible role in the regulation of P-selectin ligand expression, naive T cells were exposed to 5-aza-2-deoxycytidine, a cytosine methylation inhibitor, during activation under the least permissive conditions for P-lig induction—that is, in the absence of IL-12 (Figure 6). Indeed, artificial DNA demethylation was accompanied by induction of a high frequency of P-lig-expressing cells similar to what is observed under optimal in vitro conditions containing IL-12. If cell cycling was simultaneously blocked by L-mimosine treatment, no significant induction of P-lig was seen, excluding unspecific effects. This indicates that methylation keeps P-lig-generating genes inaccessible in naive cells and that chromatin remodeling has to occur with primary induction of selectin ligands under permissive conditions.

Discussion

Expression of appropriate homing receptors on effector cells allows their accumulation at the site of infection, which, in concert with the polarized effector functions, ensures a rapid and efficient immune response during secondary infection. Here, we provide first evidence that an inflammation-seeking homing potential might be imprinted by epigenetic gene modification, a mechanism shown to be involved in the fixation of functional differentiation of effector cells.

First, we demonstrate that the cell cycle is a major checkpoint for the regulation of P-lig expression in lymphocytes. In general, proliferation enhances the frequency of cells expressing P-selectin ligands as shown here and upon in vivo activation.²⁶ This also applies to mRNA expression of FucT VII and C2 GlcNAc, which were induced only in activated T cells progressing through the cell cycle. Arrest of the cells in early phases of the cell cycle completely prevented acquisition of P-selectin ligands as well as E-selectin ligands and up-regulation of fucosyltransferase VII and core-2 glycosaminyltransferase, showing that mRNA expression of both enzymes is sensitive to cell cycling.

References

- Mosmann TR, Sad S. The expanding universe of T-cell subsets: Th1, Th2 and more. *Immunol Today*. 1996;17:138-146.
- Reinhardt RL, Khoruts A, Merica R, Zell T, Jenkins MK. Visualizing the generation of memory CD4 T cells in the whole body. *Nature*. 2001;410:101-105.
- Reinhardt RL, Bullard DC, Weaver CT, Jenkins MK. Preferential accumulation of antigen-specific effector CD4 T cells at an antigen injection site involves CD62E-dependent migration but not local proliferation. *J Exp Med*. 2003;197:751-762.
- Sallusto F, Kremmer E, Palermo B, et al. Switch in chemokine receptor expression upon TCR stimulation reveals novel homing potential for recently activated T cells. *Eur J Immunol*. 1999;29:2037-2045.
- Sallusto F, Lenig D, Mackay CR, Lanzavecchia A. Flexible programs of chemokine receptor expression on human polarized T helper 1 and 2 lymphocytes. *J Exp Med*. 1998;187:875-883.
- Xie H, Lim YC, Lusinskas FW, Lichtman AH. Acquisition of selectin binding and peripheral homing properties by CD4(+) and CD8(-) T cells. *J Exp Med*. 1999;189:1765-1776.
- Roman E, Miller E, Harmsen A, et al. CD4 effector T cell subsets in the response to influenza: heterogeneity, migration, and function. *J Exp Med*. 2002;196:957-968.

Secondly, artificial demethylation by 5-aza-2-deoxycytidine, a cytosine methylation inhibitor, enhances the induction of selectin ligands under the least permissive in vitro conditions to levels observed under optimal inductive conditions. This effect of DNA demethylation and the requirement to complete early phases of the cell cycle that are vulnerable to chromatin remodeling strongly suggest that induction of selectin ligands is epigenetically modulated in lymphocytes during differentiation. Therefore, our data indicate that methylation keeps P-lig-generating genes inaccessible in naive cells and that chromatin remodeling has to occur with primary induction of selectin ligands under permissive conditions and might be involved in keeping the genes permanently accessible. The cell-cycle-linked expression of FucT VII and C2 GlcNAc mRNA suggests that epigenetic regulation occurs in the regulatory regions of these genes; however, not entirely excluded at present is an indirect mechanism where imprinting resides on the level of a proximal regulatory element such as an undetermined transcription factor.

The above model let us predict that effector/memory cells primed in vivo under P-lig-permissive conditions carry the ligand-generating genes permanently accessible, resulting either in constitutive expression or cell cycle-independent re-expression. Indeed, whereas the frequency of cells constitutively expressing selectin ligands is low among resting memory cells, more than 40% expressed the ligands independently from the cell cycle. This suggests that the transferase genes are not switched on permanently but remain accessible. Whether this state results in distinct, possibly less stringent requirements for transcriptional activation is presently under investigation.

The observed frequency of memory cells expressing P-lig without the need for mitosis resembles that among CD4⁺ effector cells found in vivo during acute inflammation²⁸ and most likely represents the fraction of memory cells initially primed to express P-lig.

In conclusion, the findings of this study reveal a striking similarity between induction of the cytokine memory and generation of effector cell subsets displaying selective, inflammation-seeking trafficking properties. Dependency on cell cycling, a role of DNA methylation, and the capacity to recall a functionally polarized state are hallmarks of epigenetic imprinting. Thus, epigenetic modifications might provide the basis for a long-term inflammation-seeking homing pattern of effector/memory cells, ensuring a rapid secondary immune response within peripheral extralymphoid sites.

Acknowledgments

We thank D. Vestweber for providing the P-selectin-IgG chimera, M. Loehning for helpful discussions and comments on the manuscript, and P. Bertram for excellent performance of quantitative PCR analysis.

8. Lowe JB. Glycosylation in the control of selectin counter-receptor structure and function. *Immunol Rev.* 2002;186:19-36.
9. Fuhlbrigge RC, Kieffer JD, Armerding D, Kupper TS. Cutaneous lymphocyte antigen is a specialized form of PSGL-1 expressed on skin homing T cells. *Nature.* 1997;389:978-981.
10. Tietz W, Allemand Y, Borges E, et al. CD4+ T-cells only migrate into inflamed skin if they express ligands for E- and P-selectin. *J Immunol.* 1998;161:963-970.
11. Austrup F, Vestweber D, Borges E, et al. P- and E-selectin mediate recruitment of T-helper-1 but not T-helper-2 cells into inflamed tissues. *Nature.* 1997;385:81-83.
12. Picker LJ, Michie SA, Rott LS, Butcher EC. A unique phenotype of skin-associated lymphocytes in humans: preferential expression of the HECA-452 epitope by benign and malignant T cells at cutaneous sites. *Am J Pathol.* 1990;136:1053-1068.
13. Smithson G, Rogers CE, Smith PL, et al. Fuc-TVII is required for T helper 1 and T cytotoxic 1 lymphocyte selectin ligand expression and recruitment in inflammation, and together with Fuc-TIV regulates naive T cell trafficking to lymph nodes. *J Exp Med.* 2001;194:601-614.
14. Sperandio M, Thatte A, Foy D, Ellies LG, Marth JD, Ley K. Severe impairment of leukocyte rolling in venules of core 2 glucosaminyltransferase-deficient mice. *Blood.* 2001;97:3812-3819.
15. Murphy KM, Reiner SL. The lineage decisions of helper T cells. *Nat Rev Immunol.* 2002;2:933-944.
16. Ansel KM, Lee DU, Rao A. An epigenetic view of helper T cell differentiation. *Nat Immunol.* 2003;4:616-623.
17. Jaenisch R, Bird A. Epigenetic regulation of gene expression: how the genome integrates intrinsic and environmental signals. *Nat Genet.* 2003;33(suppl):245-254.
18. Jones PA, Takai D. The role of DNA methylation in mammalian epigenetics. *Science.* 2001;293:1068-1070.
19. Lee DU, Agarwal S, Rao A. Th2 lineage commitment and efficient IL-4 production involves extended demethylation of the IL-4 gene. *Immunity.* 2002;16:649-660.
20. Agarwal S, Rao A. Modulation of chromatin structure regulates cytokine gene expression during T cell differentiation. *Immunity.* 1998;9:765-775.
21. Avni O, Lee D, Macian F, Szabo SJ, Glimcher LH, Rao A. T(H) cell differentiation is accompanied by dynamic changes in histone acetylation of cytokine genes. *Nat Immunol.* 2002;3:643-651.
22. Richter A, Löhning M, Radbruch A. Instruction for cytokine expression in T helper lymphocytes in relation to proliferation and cell cycle progression. *J Exp Med.* 1999;190:1439-1450.
23. Bird JJ, Brown DR, Mullen AC, et al. Helper T cell differentiation is controlled by the cell cycle. *Immunity.* 1998;9:229-237.
24. Mullen AC, Hutchins AS, Villarino AV, et al. Cell cycle controlling the silencing and functioning of mammalian activators. *Curr Biol.* 2001;11:1695-1699.
25. Leonhardt H, Page AW, Weier HU, Bestor TH. A targeting sequence directs DNA methyltransferase to sites of DNA replication in mammalian nuclei. *Cell.* 1992;71:865-873.
26. Campbell DJ, Butcher EC. Rapid acquisition of tissue-specific homing phenotypes by CD4+ T cells activated in cutaneous or mucosal lymphoid tissues. *J Exp Med.* 2002;195:135-141.
27. Knibbs RN, Craig RA, Maly P, et al. Alpha(1,3)-fucosyltransferase VII-dependent synthesis of P- and E-selectin ligands on cultured T lymphoblasts. *J Immunol.* 1998;161:6305-6315.
28. Kretschmer U, Bonhagen K, Debes GF, et al. Expression of selectin ligands on murine effector and IL-10-producing CD4+ T cells from non-infected and infected tissues. *Eur J Immunol.* In press.

Dissociation of transactivation from transrepression by a selective glucocorticoid receptor agonist leads to separation of therapeutic effects from side effects

Heike Schäcke*[†], Arndt Schottelius*, Wolf-Dietrich Döcke*, Peter Strehle[‡], Stefan Jaroch[‡], Norbert Schmees[‡], Hartmut Rehwinkel[‡], Hartwig Hennekes[§], and Khusru Asadullah*

*Corporate Research Business Area Dermatology, [§]Corporate Project Management Strategic Business Unit Specialized Therapeutics, and [†]Medicinal Chemistry, Schering AG, Berlin, D-13342 Berlin, Germany

Edited by Etienne-Emile Baulieu, Collège de France, Le Kremlin-Bicêtre Cedex, France, and approved November 13, 2003 (received for review March 4, 2003)

Glucocorticoids (GCs) are the most commonly used antiinflammatory and immunosuppressive drugs. Their outstanding therapeutic effects, however, are often accompanied by severe and sometimes irreversible side effects. For this reason, one goal of research in the GC field is the development of new drugs, which show a reduced side-effect profile while maintaining the antiinflammatory and immunosuppressive properties of classical GCs. GCs affect gene expression by both transactivation and transrepression mechanisms. The antiinflammatory effects are mediated to a major extent via transrepression, while many side effects are due to transactivation. Our aim has been to identify ligands of the GC receptor (GR), which preferentially induce transrepression with little or no transactivating activity. Here we describe a nonsteroidal selective GR-agonist, ZK 216348, which shows a significant dissociation between transrepression and transactivation both *in vitro* and *in vivo*. In a murine model of skin inflammation, ZK 216348 showed antiinflammatory activity comparable to prednisolone for both systemic and topical application. A markedly superior side-effect profile was found with regard to increases in blood glucose, spleen involution, and, to a lesser extent, skin atrophy; however, adrenocorticotropic hormone suppression was similar for both compounds. Based on these findings, ZK 216348 should have a lower risk, e.g., for induction of diabetes mellitus. The selective GR agonists therefore represent a promising previously undescribed class of drug candidates with an improved therapeutic index compared to classical GCs. Moreover, they are useful tool compounds for further investigating the mechanisms of GR-mediated effects.

inflammation | nuclear receptor | dissociated glucocorticoid receptor ligand

Glucocorticoids (GCs) have been widely and successfully used in the treatment of acute and chronic inflammatory diseases for >50 yr. They exert their effects by different mechanisms interfering with most inflammatory pathways. Unfortunately, the desired antiinflammatory and immunosuppressant effects are often accompanied by severe and/or partially non-reversible side effects (e.g., diabetes mellitus, peptic ulcer, Cushing's syndrome, osteoporosis, skin atrophy, psychosis, glaucoma, and many others). The use of GCs is limited by these side effects, and there is a major need for the development of compounds with the antiinflammatory potency of standard GCs but with reduced side effects (1–3).

New insights into the molecular mechanisms of GC-mediated actions have provided opportunities for identification of substances with a better therapeutic index (4–9). After entry into target cells, GCs bind to the GC receptor (GR), which then translocates into the nucleus to regulate gene transcription directly or indirectly. The ligand-activated GR binds as a homodimer to consensus sequences, termed GC response elements, in the promoter region of GC-sensitive genes to induce transcription (transactivation) of genes such as tyrosine amino-

transferase (TAT) (10, 11). An indirect negative regulation of gene expression (transrepression) is achieved by GR-protein interaction. The ligand activated receptor binds as a monomer to transcription factors, such as NF- κ B, activator protein-1, and others (1) to inhibit the activity of many proinflammatory transcription factors. This transrepression is considered the key mechanism for the antiinflammatory activity of GCs. Indeed, this assumption has been confirmed by investigations with transgenic mice expressing a dimerization-deficient GR (GR^{dim/dim}). Although transactivation is suppressed in these mice, the transrepression function is intact and GCs inhibit edema in a croton oil-induced ear inflammation test as effectively as in wild-type animals (12).

In contrast, several side effects are thought to be predominantly mediated via transactivation. Thus, ligands that preferentially induce the transrepression and not transactivation function of the GR should be as effective as standard GCs but with fewer undesirable effects (1). Although the molecular mechanisms of GC-induced side effects are complex and often not yet well understood, it appears justified to assume that some of these undesired effects, such as steroid diabetes, require GR-DNA interaction and transactivation. For example, the two most important enzymes of gluconeogenesis, an essential pathway in the development of diabetes, phosphoenolpyruvate carboxylase (13, 14) and glucose-6-phosphatase (15), are both induced by GCs. In contrast, a key mechanism for suppression of the hypothalamo-pituitary-adrenal axis, the decreased release of adrenocorticotropic hormone (ACTH) by corticotrophin-releasing hormone, is mediated by the GR via a transrepression mechanism (8). Other GC-mediated side effects (e.g., osteoporosis, skin atrophy, growth retardation, Cushing's syndrome) are subject to complex regulation involving a variety of mechanisms. However, a transactivation mechanism seems to be at least partially involved in the regulation also of these side effects (16).

To prove the concept that ligand-activated GRs predominantly mediate their antiinflammatory effects via transrepression and side effects predominantly via transactivation, we aimed to identify GR agonists with a dissociated profile. To identify such compounds, we have assessed several hundred compounds with regard to their binding to the GR and to other nuclear receptors [progesterone (PR) and mineralocorticoid receptors (MR)] and their activity in transactivation (induction of TAT) and transrepression (inhibition of IL-8 production) assays. Here we describe a nonsteroidal selective GR agonist (SEGRA). This

This paper was submitted directly (Track II) to the PNAS office.

Abbreviations: ACTH, adrenocorticotropic hormone; DEX, dexamethasone; GC, glucocorticoid; GR, GC receptor; MR, mineralocorticoid receptor; PR, progesterone receptor; PRED, prednisolone; SEGRA, selective GR agonist; TAT, tyrosine aminotransferase; LPS, lipopolysaccharide; TNF- α , tumor necrosis factor α .

[†]To whom correspondence should be addressed. E-mail: heike.schaecke@schering.de.

© 2003 by The National Academy of Sciences of the USA

compound, ZK 216348, has antiinflammatory activity similar to prednisolone (PRED) in rodents and induces less transactivation-mediated side effects. However, one side effect induced mainly by transrepression, the suppression of the hypothalamo-pituitary-adrenal axis, was also seen with ZK 216348 after systemic treatment of rats. ZK 216348 represents a previously undescribed class of nonsteroidal GR ligands that preferentially induce transrepression, resulting in an improved therapeutic index *in vivo*.

Materials and Methods

Receptor-Binding Assays. Cytosol preparations of Sf9 cells, infected with recombinant baculovirus coding for the human GR, MR, or PR, were used for the binding assays. After centrifugation (15 min, 600 × *g*) Sf9 pellets were resuspended in 1/20 volume of 20 mM Tris-HCl, pH 7.5/0.5 mM EDTA/2 mM DTT/20% glycerol/400 mM KCl/20 mM sodium molybdate/0.3 μM aprotinin/1 μM pepstatin/10 μM leupeptin and shock frozen in liquid nitrogen. After three freeze-thaw cycles, the homogenate was centrifuged for 1 h at 100,000 × *g*. Protein concentration of the resulting supernatant was between 10 and 15 mg/ml. Aliquots were stored at -40°C.

For the binding assays for GR, MR, and PR, [³H]dexamethasone (DEX) (≈20 nM), [³H]aldosterone or [³H]progesterone, SF9 cytosol (100–500 μg protein), test compound, and binding buffer (10 mM Tris-HCl, pH 7.4/1.5 mM EDTA/10% glycerol) were mixed in a total volume of 50 μl and incubated for 1 h at room temperature. Specific binding was defined as the difference between binding of [³H]DEX, [³H]aldosterone, and [³H]progesterone in the absence and presence of 10 μM unlabeled DEX, aldosterone, and progesterone. After incubation, 50 μl of cold charcoal suspension was added for 5 min, and the mixtures were transferred to microtiter filtration plates. The mixtures were filtered into Picoplates (Canberra Packard, Dreieich, Germany) and mixed with 200 μl of Microsint-40 (Canberra Packard). The bound radioactivity was determined with a Packard Top Count plate reader. The concentration of test compound giving 50% inhibition of specific binding (IC₅₀) was determined from Hill analysis of the binding curves.

Induction of TAT. Induction of TAT by test compounds was determined *in vitro* in the rat liver hepatoma cell line H4-II-E-C3. Cells were grown in MEM (Life Technologies, Karlsruhe, Germany) supplemented with 10% FBS (Life Technologies), 2 mM L-glutamine (Life Technologies), and 1% NEAA (nonessential amino acids) (Life Technologies). For compound testing, cells were seeded in 96-well plates (2 × 10⁴ cells per well) and incubated with test compounds or DEX for 20 h. Cells were then lysed and TAT activity assayed as described below for hepatic TAT induction *in vivo*.

Inhibition of IL-8 Production. IL-8 synthesis was induced by stimulation of the human promyelocytic cell line THP-1 with lipopolysaccharide (LPS, *Escherichia coli* serotype 0127:B8; Sigma). Cells (2.5 × 10⁴ cells per well) were treated with 10 μg/ml LPS in the absence or presence of test compounds or DEX for 18 h. IL-8 concentration was determined in the supernatant by an IL-8 specific ELISA (Beckman Coulter).

Inhibition of Monokine Secretion. Monocytic secretion of tumor necrosis factor α (TNF-α) and IL-12 p70 was determined after stimulation of peripheral blood mononuclear cells from healthy donors with 1 μg/ml LPS (*E. coli* serotype 0127:B8; Sigma) and 10 ng/ml IFN-γ 1b (Imukin, Boehringer Ingelheim).

After 24-h stimulation at 37°C, 5% CO₂, in the absence or presence of different concentrations of the compounds, concentrations of IL-12 p70 and TNF-α in culture supernatants were

determined by using commercial ELISA kits from R & D Systems (IL-12 HS Immunoassays, Nivelles, Belgium) and BioSource International (TNF-α EASIA, Wiesbaden, Germany). The calculated IC₅₀ value represents the concentration of compound giving 50% inhibition of the maximal TNF-α and IL-12 p70 production.

Animal Models. *Animals.* NMRI mice (26–28 g) and Shoe:Wistar rats (140–160 g) were housed according to institutional guidelines with access to food and water *ad libitum*. Eight to 11 animals were randomly allocated to the different treatment groups.

Croton oil-induced ear inflammation. Topical application of the nonspecific contact irritant croton oil, a mixture of several phorbol esters, leads to acute inflammation characterized by edema and a mainly granulocytic cell infiltration into the skin (17). Experiments were performed as recently described in detail (18). Briefly, for topical application, compounds were dissolved in the same vehicle as used for croton oil and were coapplied. Systemic application of compounds (s.c.) was performed 2 h before croton oil application. At the maximum of the inflammatory reaction, animals were killed, and ears (mice, area ≈1 cm²) or a punch biopsy (rats, 10-mm diameter) were weighed as an indicator of edema formation, then snap-frozen in liquid nitrogen in polypropylene tubes and kept at -20°C for up to 24 h. **Peroxidase activity assay.** Peroxidase activity, as a measure for total granulocyte infiltration, was assayed by using a modification of a previously described method (19), as described by Schottelius *et al.* (18).

Induction of TAT *in vivo*. TAT induction was evaluated 6 h after compound administration (s.c.) to juvenile rats by determination of TAT activity in liver homogenates. Animals were killed, and biopsies (10-mm diameter) were taken from the liver and snap frozen. Biopsies were homogenized in 2 ml of homogenizing buffer (140 mM KCl in 20 mM KPO₄ buffer, pH 7.6) and centrifuged at 24,000 × *g* for 20 min at 4°C. Supernatants were assayed for protein content by the BCA (bicinchoninic acid) Protein Assay Kit from Pierce (20). Twenty microliters of supernatant diluted 1:50 in PBS was incubated for 30 min at 37°C with 200 μl of TAT-reaction buffer (tyrosine 1.2 mg/ml or 6.6 mM/45 mM KH₂PO₄/0.06 mM pyridoxal-5'-phosphate/12 mM oxoglutaric acid, adjusted to pH 7.6 with KOH). After stopping the reaction with 10 M KOH and further incubation for 30 min, extinction was measured at 340 nm, and TAT activity was calculated in relation to 500 μg/ml total protein content.

TAT induction was defined as *x*-fold increase in TAT activity measured as OD at 340 nm in comparison to the TAT activity in vehicle-treated animals.

ACTH suppression in rats. Animals were isolated before the study to avoid stress. Six hours after application of compounds, animals were killed, and EDTA-anticoagulated blood was collected from abdominal aorta. Plasma content of ACTH was determined by using the ACTH ¹²⁵I-assay system (ImmuChem Double Antibody hACTH) following the instructions of the vendor (ICN).

Increased blood glucose in rats. Animals were isolated before the study to avoid stress and fasted for 16 h. Six hours after application of compounds, animals were killed, and EDTA blood was collected from abdominal aorta.

Glucose in plasma was measured by colorimetric serum glucose determination by using hexokinase and glucose-6-phosphate dehydrogenase (21) with a Hitachi 904 automatic analyzer (Roche Diagnostics).

Skin atrophy. To assess the atrophic potential, ZK 216348 or the reference compound PRED (75 μl on a marked area of 9 cm² in 95% ethanol/5% isopropyl myristate) was applied daily for 19 days to the dorsal skin of nude rats (strain *hr-hr*, 120–140 g, Iffa-Credo). Animals were killed on day 20. Skin thickness was determined by using a specifically designed dial thickness gauge (Schering). Mean values were derived by measuring two adjacent

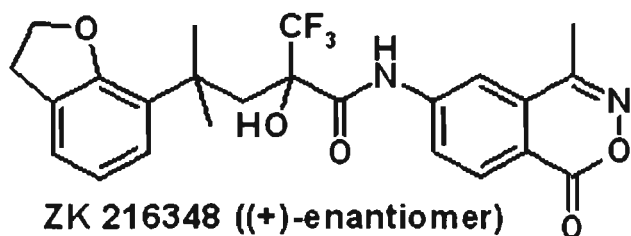


Fig. 1. Structure of ZK 216348. ZK 216348 [(+)-enantiomer] was synthesized by standard methods starting with the commercially available dihydrobenzofurane.

treated skin areas. To determine skin-breaking strength of treated skin, a dorsal skin patch (5 × 5 cm) was removed. The skin patch was placed on filter paper, and two double-T-piece skin strips (50 mm long, 4 mm wide at the narrowest point) were punched in a caudal–cranial direction out of the patch. The skin strips were covered with moistened filter paper to avoid drying and were fixed with the wider ends into an apparatus developed in-house to measure skin-breaking strength. At a constant rate of stretch (200 mm/min), the force necessary to tear the skin strip was determined with a pressure sensor and was expressed as the skin-breaking strength (in N).

Thymus, spleen, adrenal, and body weight. To determine effects on body weight, animals were weighed before and after completion of treatment. Thymus, spleen, and adrenal glands were removed from animals killed after systemical or topical treatment and weighed. Organ weights were expressed as absolute values or in percent inhibition when compared with untreated animals.

Statistical analysis. For all animal models, statistical analysis was performed with the “modified Hemm” (inhibition) test developed by Schering based on the program SAS SYSTEM FOR WINDOWS 6.12 (SAS Institute, Cary, NC) (18). Statistical significance in TAT, glucose induction, and ACTH suppression was assessed by using Dunnett’s test. Differences between ZK 216348 and the corresponding PRED group were assessed by using the Mann–Whitney test.

Results

In Vitro Investigations. Receptor binding, IL-8 suppression, and TAT induction in cell lines. In the GR-binding screen, we first identified the racemic compound ZK 209614 with a high binding affinity to the GR. Although the (–)-enantiomer (ZK 216347) did not show any binding to the GR, the (+)-enantiomer (ZK 216348) (Fig. 1) bound to the GR with a similar affinity as DEX and with an ≈3-fold higher affinity than PRED (Table 1). ZK 216348 also binds to the PR and MR.

To determine whether this ligand exhibits dissociation between transactivation and transrepression on binding to the GR,

Table 1. Binding affinities to nuclear receptors

	Binding IC ₅₀ , nM		
	GR	PR	MR
Dexamethasone	14 ± 6	>1,000	>1,000
PRED	68 ± 30	>1,000	>1,000
ZK 216347 (–)	>1,000	>1,000	>1,000
ZK 216348 (+)	20.3 ± 2.6	20.4 ± 1.3	79.9 ± 1.3

Binding to the recombinant human GR, PR, and MR was determined in comparison to dexamethasone, progesterone, and aldosterone, respectively. IC₅₀ values represent the concentration of compounds that inhibited 50% of specific binding of [³H]dexamethasone, [³H]progesterone, and [³H]aldosterone. Mean ± SD of three to five separate experiments are shown.

Table 2. Effect on IL-8 secretion and TAT activity in cell lines

	IL-8 inhibition	IL-8 inhibition	TAT induction	TAT induction
	IC ₅₀ , nM	efficacy, %	EC ₅₀ , nM	efficacy, %
DEX.	2.6 ± 1	100	0.3	100
PRED	18 ± 12	92 ± 8	1.5	100
ZK 216348	35 ± 10	52 ± 15	95	88

Inhibition of IL-8 secretion in monocytic THP-1 cells as a parameter for transrepression and induction of TAT in hepatic H4-II-E-C3 cells as a transactivation parameter were determined for ZK 216348 in comparison to standard GCs. Efficacy is expressed relative to the maximal response to DEX. For IL-8 inhibition, mean ± SD values of three to five separate experiments are shown, whereas single values are given for TAT induction.

the inhibition of IL-8 synthesis in THP-1 cells (transrepression) and the induction of TAT in liver hepatoma cells (transactivation) were investigated. Compared with PRED, ZK 216348 inhibited IL-8 secretion with only a 2-fold lower potency and a lower efficacy (Table 2). Importantly, this compound is ≈60-fold less potent than PRED with regard to TAT induction. In comparison to DEX, ZK 216348 was ≈14-fold less potent in the IL-8 assay, whereas DEX was >300-fold more potent in induction of TAT. Consequently, ZK 216348 induces significantly less transactivation compared to standard GCs in this assay and shows a clear selectivity for transrepression. Therefore, this compound is considered as a SEGRA.

Antiinflammatory effects in human peripheral blood mononuclear cells (PBMCs). Additionally, we investigated whether the compound is active in inhibiting TNF-α and IL-12 production in LPS-stimulated PBMCs. Similar to the results obtained in THP-1 cells, DEX and PRED were more potent than ZK 216348. However, the compound inhibited TNF-α and IL-12 with an efficacy similar to the standards (Table 3).

In Vivo Activity. In the *in vivo* studies, the SEGRA compound was compared with the classical GC PRED.

Antiinflammatory activity. The SEGRA compound ZK 216348 was tested in the croton oil model of ear inflammation in rodents. After topical application, the antiinflammatory effect of ZK 216348 in mice was similar to that of PRED (Fig. 2). ZK 216348 had comparable potency regarding the inhibition of ear edema (ED₅₀: 0.02 μg/cm² SEGRA, 0.03 μg/cm² PRED) and granulocyte infiltration as assessed by peroxidase activity (ED₅₀: 0.03 μg/cm² SEGRA, 0.04 μg/cm² PRED). In this experiment, PRED was tested only up to 100 μg/cm², although the highest dose of ZK 216348 was 300 μg/cm². We know from previous experiments that the concentration used here gives the maximal antiinflammatory effect of PRED.

In rats, the compound is significantly less active than PRED after topical application (Fig. 2). Given s.c., ZK 216348 inhibited ear edema similarly to PRED in both mice (ED₅₀: 2 mg/kg SEGRA, 9 mg/kg PRED) and rats (ED₅₀: 2 mg/kg SEGRA, 3.5 mg/kg PRED) (Fig. 3).

Table 3. Effect on monokine production in human PBMC

	IL-12 p70	IL-12 p70	TNF-α	TNF-α
	IC ₅₀ , nM	efficacy, %	IC ₅₀ , nM	efficacy, %
DEX	3.2	89	3.1	97
PRED	7.9	84	11	93
ZK 216348	52	89	89	63

The effect of ZK 216348 on secretion of IL-12 p70 and TNF-α 24 h after LPS stimulation of human peripheral blood mononuclear cells was determined in comparison to the effect of standard GCs. Efficacy is expressed as absolute maximal inhibition of LPS-induced increase in cytokine release. Single values are shown.

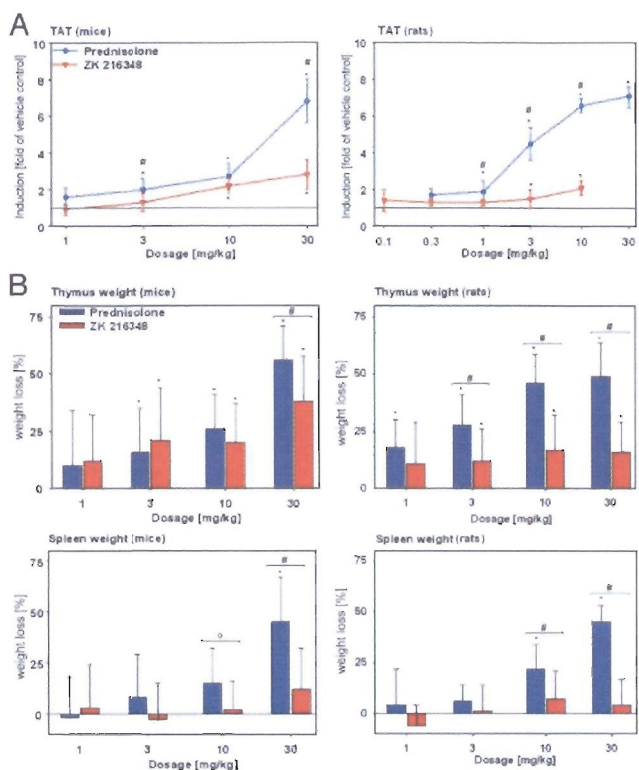


Fig. 5. Effect on hepatic TAT activity and thymus and spleen weights after s.c. application in mice and rats. (A) Induction of TAT 6 h after s.c. treatment was determined in mice and rats and is shown as x-fold induction (mean \pm SD; mice $n = 10$, rats $n = 5$) compared to vehicle control. *, $P < 0.05$ vs. vehicle group in Dunnett's test. #, $P < 0.05$ vs. PRED in the Mann-Whitney test. (B) Thymus and spleen weights 24 h after s.c. treatment were determined in mice and rats. The reduction in organ weight is shown as percent weight loss (mean \pm SD, $n = 10$) compared to vehicle control. *, $P < 0.05$ vs. vehicle group in the modified Hemm test. #, $P < 0.05$; °, $P = 0.052$ vs. PRED in the Mann-Whitney test.

The transactivation-mediated increase in blood glucose concentration by GCs reflects the risk for induction of diabetes mellitus. After s.c. treatment in rats, PRED triggered a dose-dependent increase in blood glucose. In contrast, the SEGRA compound ZK 216348 did not lead to a significant increase in blood glucose even at the highest dose of 30 mg/kg (Fig. 6).

Regarding ACTH suppression, an advantage of SEGRAs over classical GCs was not expected, because transrepression seems to be the key mechanism underlying this effect. Indeed, ZK 216348 suppressed ACTH plasma concentrations in rats as effectively as PRED (Fig. 6). Although there is a significant difference between PRED and ZK 216348 at a dose of 3 mg/kg, the effects of both compounds are similar at higher doses.

Taken together, the separation of transactivation from transrepression demonstrated *in vitro* is reflected *in vivo* by a similar antiinflammatory activity but reduced transactivation-mediated side effects.

Discussion

Recent studies have provided new insights into the molecular mechanisms of GR-mediated effects and have led to the hypothesis that therapeutic effects are mediated to a major extent via a transrepression process, whereas side effects are predominantly mediated by transactivation (12). Using a screen discriminating between these mechanisms, we have identified the nonsteroidal SEGRA compound ZK 216348 that binds to the

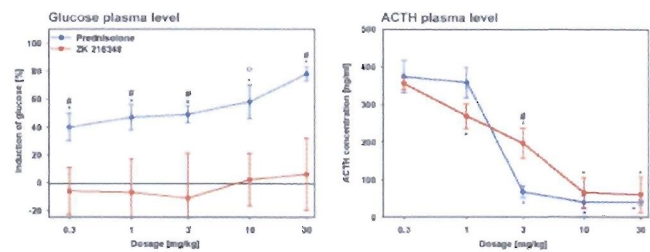


Fig. 6. Effect on blood glucose and ACTH concentrations after s.c. application in rats. Blood glucose concentration was determined 6 h after s.c. treatment of rats that were fasted 16 h before treatment. ACTH plasma concentrations were determined 6 h after s.c. treatment of rats that had been isolated to avoid stress. Data are given as mean \pm SD of five animals per group. *, $P < 0.05$ vs. vehicle group in Dunnett's test. #, $P < 0.05$; °, $P = 0.056$ vs. PRED in the Mann-Whitney test.

GR with high affinity and preferentially induces the transrepression function of the GR. Binding of ZK 216348 to the PR and MR leads to a predominantly antagonistic activity at the PR (50% efficacy) and a fully antagonistic activity at the MR (100% efficacy) (data not shown). Although ZK 216348 binds to the GR with an affinity similar to DEX, it is less active in all cellular *in vitro* assays. Possible explanations for this discrepancy might be that the chemical structure of ZK 216348 results in different physicochemical properties and cellular uptake behavior and/or the ligand does not induce a receptor conformation required for full repression effects.

We demonstrated, however, that the antiinflammatory activity of the SEGRA compound ZK 216348 is comparable to that of PRED. A somewhat lower activity of ZK 216348 in rats in comparison to mice might be caused by a different metabolism. Taken together, our data strongly suggest that selective transrepression is sufficient for antiinflammatory activity *in vivo* and are in line with the observations by Schütz and coworkers in GR^{dim/dim} mice (12).

Moreover, we have shown that the dissociation between transrepression and transactivation observed with ZK 216348 *in vitro* is reflected by an improved therapeutic index *in vivo* after both topical and systemic administration. The compound induces significantly fewer transactivation-mediated side effects, such as increased blood glucose and induction of hepatic TAT in rats. Therefore, we believe that the risk of diabetes induction with ZK 216348 should be clearly lower than that for PRED. The reduction of lymphoid organ weights was also diminished after systemic and long-term topical administration of ZK 216348 in comparison to PRED. In contrast, no clear differences were observed regarding the suppression of the hypothalamo-pituitary-adrenal axis. Because the secretion of ACTH to corticotrophin-releasing hormone (CRH) stimulation is affected by a GR-protein interaction via the transrepression mechanism of CRH itself (22, 23), we do not expect an advantage of this compound class in comparison to standard GCs here. Although species-specific differences in activity have been observed for ZK 216348, the compound shows a better therapeutic index in comparison to PRED in both mice and rats. It has to be determined in clinical studies whether this effect translates into a similar dissociation in humans.

Our results regarding a reduced activity of the SEGRA compound with regard to induction of TAT and increased blood glucose but a sustained ACTH suppression correspond to the current knowledge of the underlying mechanisms of GC-mediated side effects. The precise mechanisms of many other GC effects, however, are not yet well understood. Moreover, many of the side effects (e.g., skin atrophy, osteoporosis, Cushing's syndrome) seem to use more than one mechanism (24–26).

Thus, it is difficult to predict the behavior of SEGRA compounds with regard to these effects. Investigations using ZK 216348 as a tool compound or GC treatment in GR^{dim/dim} mice will help to determine the molecular mechanisms involved in these GC side effects. For example, the less-pronounced loss of skin thickness and skin-breaking strength observed after long-term topical treatment with ZK 216348 in comparison to PRED might suggest that transactivation is involved in skin atrophy.

In the past, optimization of pharmacokinetic properties was used to improve the therapeutic index of GR ligands. Deflazacort, a prodrug derivative of PRED, has been shown clinically to induce fewer side effects than PRED while having only slightly less antiinflammatory activity (27).

Currently the development of steroidal and nonsteroidal GC ligands that induce an altered GR activation profile has moved into the focus of several groups. Representatives of this new generation of GR ligands are the RU compounds 40066, 24782, and 24858 (3). These compounds show a high affinity to the GR and repress activator protein-1 very efficiently. Regarding transactivation, they reach only 8–35% of DEX efficacy. Unfortunately, this dissociated *in vitro* profile was not reflected *in vivo*; therefore, RU 24858 had antiinflammatory activity *in vivo* comparable to PRED but failed to show any reduction in systemic side effects (osteoporosis or reduction of body and thymus weights) (28). Another group described that RU 24858 showed stronger transactivation activity *in vivo* than *in vitro* (29). We agree with the conclusion drawn by the authors that these results, rather than disproving the concept, represent a problem of this particular compound.

This assumption is supported by other new GR ligands such as ZK 216348 and AL-438 (30). AL-438 was shown to be more

efficacious in transrepression than in transactivation *in vitro*. It was antiinflammatory active *in vivo* and showed less increase in blood glucose than PRED. Additionally, Coghlan *et al.* (31) reported a lesser osteoporotic potential for AL-438 in rats compared to PRED. Therefore, although the antiinflammatory activity of AL-438 was weaker than PRED in the reported models, the compound showed a dissociated profile not only *in vitro* but also *in vivo*.

In this respect, AL-438 behaves similarly to the SEGRA compound ZK 216348, which we found to be equipotent in antiinflammation to PRED in our murine model. ZK 216348 demonstrates that the principle of an improved therapeutic index by the separation of the molecular mechanisms of the GR regarding therapeutic effect and side effects is possible.

In summary, ZK 216348 is a previously undescribed SEGRA, representing a compound class with an improved therapeutic index compared to classical GCs. Because these compounds have a reduced risk of developing certain side effects, such as diabetes mellitus, they are representatives of a generation of GR ligands with a high clinical value. Moreover, the compound will serve as a tool to further investigate the molecular basis of GC side effects.

We thank Andrew Cato (Forschungszentrum Karlsruhe, Karlsruhe, Germany) for helpful discussions, Steven Katz (National Institutes of Health, Bethesda), and Fiona McDonald (Schering AG, Berlin) for the critical reading of the manuscript. We specifically thank M. Backhus, D. Schröder, H.-U. Klein, R. Schmidt, D. Gerhard, E. Matzke, D. Opitz, B. Schulz, and S. Schoepe (Schering AG, Berlin) for excellent technical assistance.

- Barnes, P. J. (1998) *Clin. Sci.* **94**, 557–572.
- Resche-Rigon, M. & Gronemeyer, H. (1998) *Curr. Opin. Chem. Biol.* **4**, 501–507.
- Vayssiere, B. M., Dupont, S., Choquart, A., Petit, F., Garcia, T., Marchandeu, C., Gronemeyer, C. & Resche-Rigon, M. (1997) *Mol. Endocrinol.* **11**, 1245–1255.
- Yamamoto, K. R. (1985) *Annu. Rev. Genet.* **19**, 209–252.
- Heck, S., Kullmann, M., Gast, A., Ponta, H., Rahmsdorf, H. J., Herrlich, P. & Cato, A. C. (1994) *EMBO J.* **13**, 4087–4095.
- Beato, M., Herrlich, P. & Schütz, G. (1994) *Cell* **83**, 851–857.
- Cole, T. J., Blendy, J. A., Monaghan, A. P., Krieglstein, K., Schmidt, W., Aguzzi, A., Fantuzzi, G., Hummler, E., Unsicker, K. & Schütz, G. (1995) *Genes Dev.* **9**, 1608–1621.
- Reichardt, H. M., Kaestner, K. H., Tuckermann, J., Kretz, O., Wessely, O., Bock, R., Gass, P., Schmidt, W., Herrlich, P., Angel, P. & Schütz, G. (1998) *Cell* **93**, 531–541.
- Kassel, O., Sancono, A., Krätzschmar, J., Krcft, B., Stassen, M. & Cato, A. C. (2001) *EMBO J.* **20**, 7108–7116.
- Jantzen, H.-M., Strähle, U., Gloss, B., Stewart, F., Schmidt, W., Boshart, M., Miksicek, R. & Schütz, G. (1987) *Cell* **49**, 29–38.
- Rigaud, G., Roux, J., Pictet, R. & Grange, T. (1991) *Cell* **67**, 977–986.
- Reichardt, H. M., Tuckermann, J. P., Göttlicher, M., Vujic, M., Weih, F., Angel, P., Herrlich, P. & Schütz, G. (2001) *EMBO J.* **20**, 7168–7173.
- O'Brien, R. M., Noisin, E. L., Suwanichkul, A., Yamasaki, T., Lucas, P. C., Wang, J.-C., Powell, D. R. & Granner, D. K. (1995) *Mol. Cell. Biol.* **15**, 1747–1758.
- Crosson, S. M. & Roesler, W. J. (2000) *J. Biol. Chem.* **275**, 5804–5809.
- Yoshinuchi, I., Shingu, R., Nakajima, H., Hamaguchi, T., Horikawa, Y., Yamasaki, T., Oue, T., Ono, A., Miyagawa, J. I., Namba, M., *et al.* (1998) *J. Clin. Metab.* **83**, 1016–1019.
- Schäcke, H., Döcke, W.-D. & Asadullah, K. (2002) *Pharmacol. Ther.* **96**, 23–43.
- Berg, D. J., Leach, M. W., Kuhn, R., Rajewski, K., Muller, W., Davidson, N. J. & Rennick, D. (1995) *J. Exp. Med.* **182**, 99–108.
- Schottelius, A. J., Giesen, C., Asadullah, K., Fierro, I. M., Colgan, S. P., Bauman, J., Guilford, W., Perez, H. D. & Parkinson, J. F. (2002) *J. Immunol.* **169**, 7063–7070.
- Goka, J. & Farthing, M. J. G. (1987) *J. Immunoassay* **8**, 29–41.
- Smith, P. K., Krohn, R. I., Hermanson, G. T., Mallia, A. K., Gartner, F. H., Provenzano, M. D., Fujimoto, E. K., Goeke, N. M., Olson, B. J. & Klenk, D. C. (1985) *Anal. Biochem.* **150**, 76–85.
- Carroll, J. J., Smith, N. & Babson, A. L. (1971) *Biochem. Med.* **2**, 171–180.
- Reichardt, H. M. & Schütz, G. (1998) *Mol. Cell. Endocrinol.* **146**, 1–6.
- Reichardt, H. M., Tronche, F., Bauer, A. & Schütz, G. (2000) *Biol. Chem.* **381**, 961–964.
- Ziegler, R. & Kasperk, C. (1998) *Steroids* **63**, 344–348.
- Manelli, F. & Giustina, A. (2000) *Trends Endocrinol. Metab.* **11**, 79–85.
- Patschan, D., Loddenkemper, K. & Buttgerit, F. (2001) *Bone* **6**, 498–505.
- Anonymous (1999) *Drug Ther. Bull.* **3**, 57–58.
- Belvisi, M. G., Wicks, S. L., Battram, C. H., Bottoms, S. E. W., Redford, J. E., Woodman, P., Brown, T. J., Webber, S. E. & Foster, M. L. (2001) *J. Immunol.* **166**, 1975–1982.
- Tanigawa, K., Tanaka, K., Nagase, H., Miyake, H., Kiniwa, M. & Ikizawa, K. (2002) *Biol. Pharm. Bull.* **25**, 1619–1622.
- Miner, J. N. (2002) *Biochem. Pharmacol.* **64**, 355–361.
- Coghlan, M. J., Jacobson, P. B., Lane, B., Nakane, M., Lin, C. W., Elmore, S. W., Kym, P. R., Luly, J. R., Carter, G. W., Turner, R., *et al.* (2003) *Mol. Endocrinol.* **17**, 860–869.

Novel 3-Oxa Lipoxin A₄ Analogues with Enhanced Chemical and Metabolic Stability Have Anti-inflammatory Activity in Vivo

William J. Guilford,^{*,†} John G. Bauman,[†] Werner Skuballa,[‡] Shawn Bauer,[†] Guo Ping Wei,[†] David Davey,[†] Caralee Schaefer,[§] Cornell Mallari,[§] Jennifer Terkelsen,[§] Jih-Lie Tseng,[#] Jun Shen,[#] Babu Subramanyam,[#] Arndt J. Schottelius,^{||} and John F. Parkinson[‡]

Departments of Medicinal Chemistry, Immunology, Animal Pharmacology, and Pharmacokinetics and Drug Metabolism, Berlex Biosciences, 2600 Hilltop Drive, Richmond, California 94804, and Research Business Area Dermatology and Medicinal Chemistry, Schering AG, Berlin, Germany

Received November 11, 2003

Lipoxin A₄ (LXA₄) is a structurally and functionally distinct natural product called an eicosanoid, which displays immunomodulatory and anti-inflammatory activity but is rapidly metabolized to inactive catabolites in vivo. A previously described analogue of LXA₄, methyl (5*R*,6*R*,7*E*,9*E*,11*Z*,13*E*,15*S*)-16-(4-fluorophenoxy)-5,6,15-trihydroxy-7,9,11,13-hexadecatetraenoate (**2**, ATLa), was shown to have a poor pharmacokinetic profile after both oral and intravenous administration, as well as sensitivity to acid and light. The chemical stability of the corresponding *E,E,E*-trien-11-yne analogue, **3**, was improved over **2** without loss of efficacy in the mouse air pouch model of inflammation. Careful analysis of the plasma samples from the pharmacokinetic assays for both **2** and **3** identified a previously undetected metabolite, which is consistent with metabolism by β -oxidation. The formation of the oxidative metabolites was eliminated with the corresponding 3-oxatetraene, **4**, and the 3-oxatrien-11-yne, **5**, analogues of **2**. Evaluation of 3-oxa analogues **4** and **5** in calcium ionophore-induced acute skin inflammation model demonstrated similar topical potency and efficacy compared to **2**. The 3-oxatrien-11-yne analogue, **5**, is equipotent to **2** in an animal model of inflammation but has enhanced metabolic and chemical stability and a greatly improved pharmacokinetic profile.

Introduction

Lipoxins are a structurally and functionally distinct class of natural products called eicosanoids, which play a key role in inflammation. Arachidonate-derived lipid mediators such as prostaglandins or leukotrienes are involved in the initiation and maintenance of inflammatory responses and are proinflammatory; however, lipoxins are involved in the regulation and resolution of inflammation and are anti-inflammatory.¹ Since lipoxin A₄ (**1**, LXA₄, Figure 1) was reported in 1984,² the trihydroxytetraene structure has attracted the attention of synthetic chemists, as seen in a number of reported syntheses.^{3–6} The potent anti-inflammatory and immunomodulatory activity of LXA₄ has attracted the attention of researchers for use as a treatment of allergic asthma,⁷ T cell-mediated dermatoses, and inflammatory bowel diseases and as a gastroprotective agent.⁸ Development of LXA₄, however, has been limited by its metabolic and chemical instability.

The metabolic instability of the natural product, LXA₄, is the result of a series of steps initiated by the rapid oxidation of the 15(*S*) alcohol by prostaglandin dehydrogenase (PGDH) to form inactive catabolites, as 15-oxo-LXA₄ and 13,14-dihydro-LXA₄.⁹ The initial de-

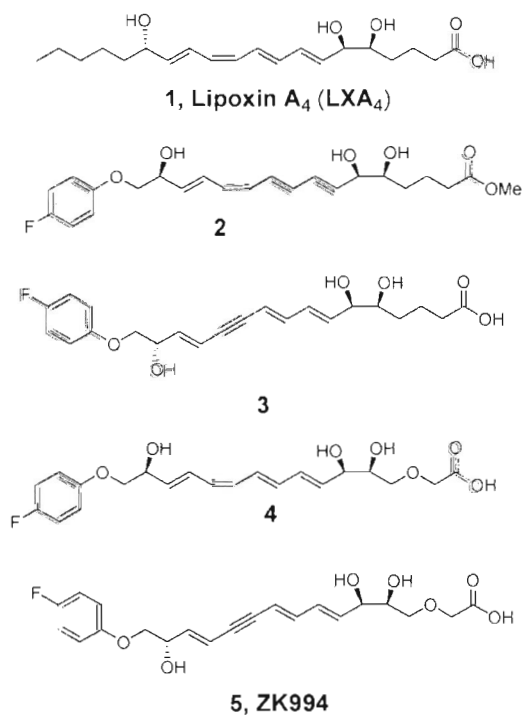


Figure 1. Lipoxin A₄ and analogues.

sign of metabolically stable LXA₄ analogues focused on identifying poor substrates for PGDH,¹⁰ which maintained potency in in vitro assays. The discovery that 15-epi-LXA₄, or aspirin-triggered LXA₄, was equipotent in

* To whom correspondence should be addressed. Phone: 510 669 4065. Fax: 510 669 4310. E-mail: william_guilford@berlex.com.

[†] Department of Medicinal Chemistry, Berlex Biosciences.

[‡] Medicinal Chemistry, Schering AG.

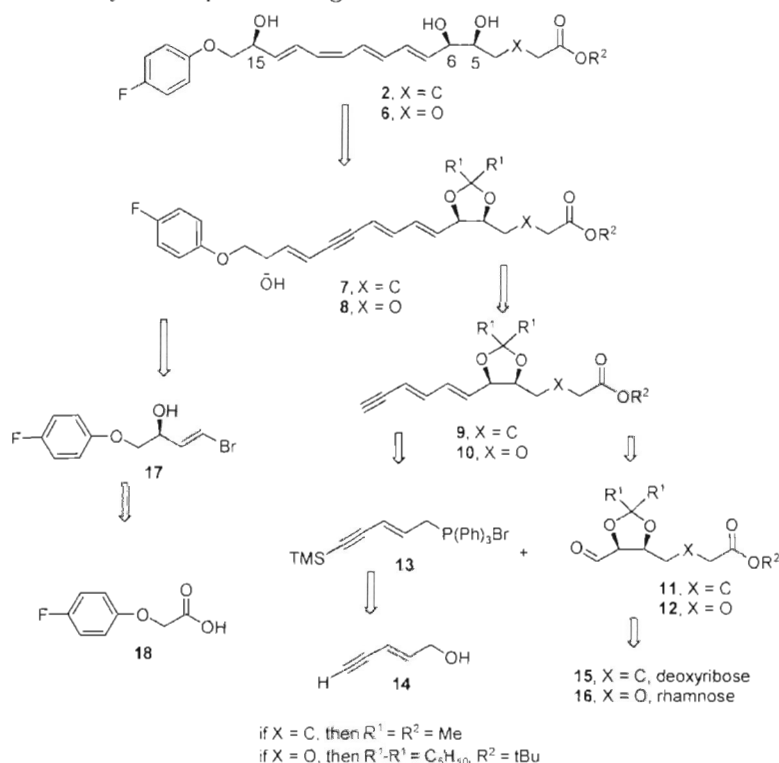
[§] Department of Animal Pharmacology, Berlex Biosciences.

[#] Department of Pharmacokinetics and Drug Metabolism, Berlex Biosciences.

^{||} Research Business Area Dermatology, Schering AG.

[‡] Department of Immunology, Berlex Biosciences.

Scheme 1. Retrosynthetic Analysis of Lipoxin Analogues



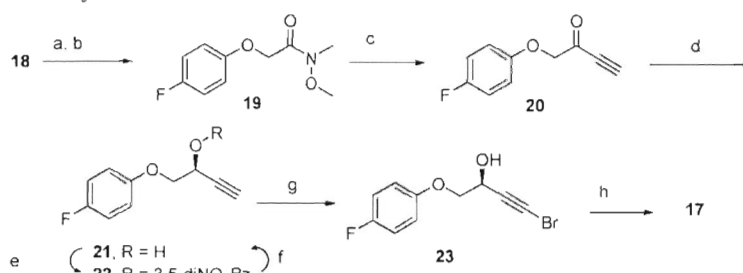
in vitro assays to LXA₄ but was a poorer substrate for PGDH provided support for the potential novel analogue design. Several structural elements were combined in **2**, methyl (5*R*,6*R*,7*E*,9*E*,11*Z*,13*E*,15*S*)-16-(4-fluorophenoxy)-5,6,15-trihydroxy-7,9,11,13-hexadecatetraenoate (15-epi-16-(*p*-fluoro)phenoxy-LXA₄, ATLa, ATLa2), which has enhanced metabolic stability and was selected for scale-up and further testing. The potent anti-inflammatory and immunomodulatory properties of **2** were demonstrated in a series of in vivo models, including an allergic airway inflammation model,¹¹ a T-cell dependent skin inflammation model,¹² a dextran sulfate (DSS) induced colitis model,¹³ and an adaptive immunity model with 5-LO knockout mice.¹⁴ Taken together, these studies provide evidence that **2** can directly or indirectly modulate T cell effector function in the setting of Th₁- and Th₂-dependent inflammation and adaptive immunity.

Although **2** has enhanced metabolic stability over LXA₄ in vivo, **2** is reported to be cleared within 15 min after intravenous injection in the mouse.¹⁵ In addition, **2** shares the same trihydroxytetraene structure with LXA₄ and, therefore, has the same chemical stability issues, light and acid sensitivity. LXA₄ isomerizes to a mixture of double bond isomers including the corresponding *E,E,E,E*- or 11-*trans*-LXA₄ in the presence of light and decomposes to a mixture of products in the presence of strong acid. To circumvent the metabolic and chemical stability issues, we explored simple replacements for the *E,E,Z,E*-tetraene unit that would maintain potency. Herein, we describe the results of our effort to identify analogues of **2** that have increased metabolic and chemical stability, improved pharmacokinetics, and anti-inflammatory activity in vivo, which led to the discovery of **5**.

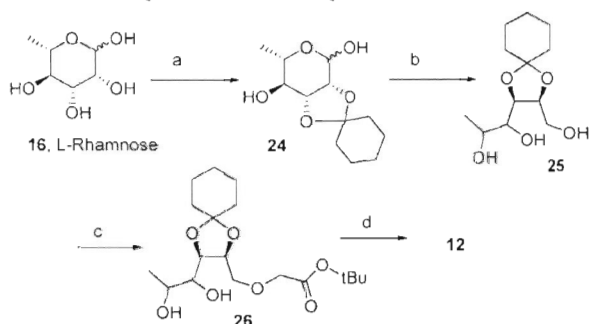
Chemistry

The structure of **2** and **3** can be characterized as a linear chain of 16 carbons in which all but three carbon atoms are either unsaturated or substituted with oxygen. The 3-oxa analogues **4** and **5** differ in that all of the carbon atoms in the chain are either unsaturated or substituted with oxygen. As in the reported synthesis of **2**,¹⁶ the retrosynthetic analysis of the lipoxin analogues is based on the Nicolaou synthesis of lipoxin A₄ (**1**) and is shown in Scheme 1.¹⁷ This convergent approach divides the molecule into three parts: an enyne Wittig reagent (**13**),¹⁸ an aldehyde (**11** or **12**), and a vinyl bromide unit (**17**). The stereochemistry at C5 and C6 is set with the starting sugar, **15** or **16**, and the stereochemistry at C15 is set by a chiral reduction. The geometry of the C9–C10 double bond is established with starting *E*-pentenynol, **14**. The geometry of the C13–C14 double bond is set by reduction of an acetylenic alcohol (Scheme 2). The geometry of the C7–C8 and C11–C12 double bonds is set during the synthesis.

Preparation of the vinyl bromide intermediate is shown in Scheme 2. Weinreb amide **19** was prepared from 4-fluorophenoxyacetic acid, **18**, through the corresponding acid chloride. Treatment of amide **19** with lithium acetylide gave ketone **20**, which was reduced with the chiral reducing agent *R*-Alpine-Borane.¹⁹ Although the enantiomeric excess of **21** was typically in the 60–70% range, material having >98% ee was obtained by recrystallization of the corresponding dinitrobenzoyl derivative (**22**). Hydrolysis of the dinitrobenzoyl ester followed by bromination of the acetylene with *N*-bromosuccinimide and silver nitrate gave the acetylenic bromide **23**.²⁰ Reduction of the acetylenic bromide

Scheme 2. Preparation of Vinyl Bromide **17**^a

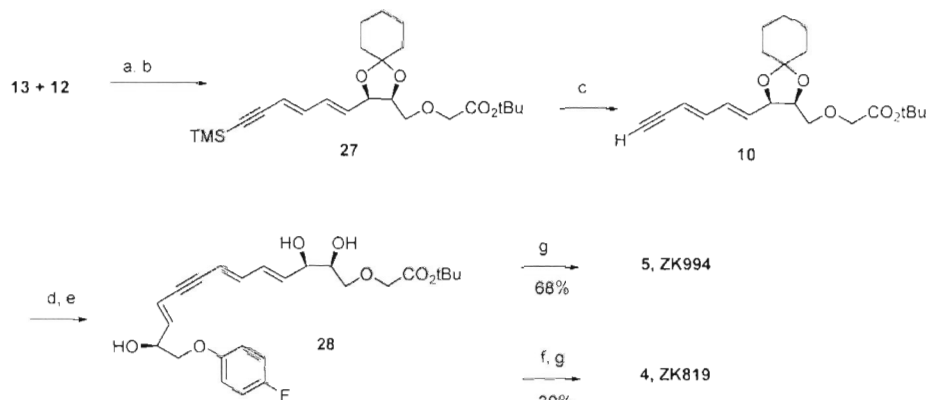
^a (a) (COCl)₂, DMF, ether; (b) MeON(H)Me·HCl, sat. K₂CO_{3(aq)}, EtOAc, 0 °C, 73% from **18**; (c) HCCMgBr, THF, 40 min, 91%; (d) *R*-Alpine-Borane, 97% (e) 3,5-dinitrobenzoyl chloride, TEA, DMAP, CH₂Cl₂, 0 °C, 1–2 h, followed by recrystallization, 54%; (f) K₂CO₃, MeOH, THF, 3.5 h, 80%; (g) NBS, AgNO₃, acetone, 99%; (h) AlCl₃, LiAlH₄, ether, 81%.

Scheme 3. Synthesis of Aldehyde **12** from Rhamnose^a

^a (a) H₂SO₄, Cu(II)SO₄, cyclohexanone, room temp, 16 h, 57%; (b) NaBH₄, MeOH, 3 h, room temp, 88%; (c) toluene, 25% NaOH_(aq), Bu₄N, HSO₄, *t*Bu bromoacetate, 44%; (d) H₂O, acetone, NaIO₄, 92%.

with a lithium aluminum hydride/aluminum chloride mixture gave the desired *E*-vinyl bromide **17**.²¹

Lipoxin analogues **2** and **3** were prepared from deoxyribose **15** via dienyne **9** using a procedure described earlier¹⁶ (Scheme 1). Sonogashira coupling of dienyne **9** and vinyl bromide **17** gave the complete carbon skeleton as the trienyne **7**.¹⁷ Hydrolysis of the isopropylidene ketal under acidic conditions and methyl ester under basic conditions gave **3**. The relatively good acid stability of the trien-11-yne unit was demonstrated by the treatment of **7** with 1 N HCl needed to cleave the ketal protecting group in good yield. Treatment of deketalized **7** with activated zinc using the Boland procedure²² gave **2**.

Scheme 4. Synthesis of 3-oxa-lipoxin Analogues^a

^a (a) BuLi, THF, 30–0 °C, 3 h; (b) I₂, CH₂Cl₂, 1 h, 49% from **12**; (c) TBAF, THF, 99%; (d) (Ph₃P)₄, Et₂NH, CuI, THF, **17**, 50%; (e) AcOH, H₂O, EtOAc, 58%; (f) Zn, AgNO₃, Cu(II)(OAc)₂, MeOH, H₂O; (g) NaOH, H₂O, MeOH.

Introduction of the 3-oxa group into the dienyne unit, **10**, was accomplished as outlined in Scheme 3. Cyclohexylidene ketal, **24**, prepared from rhamnose, **16**,²³ was reduced with sodium borohydride to triol **25**. Selective O-alkylation of the primary hydroxyl group using phase-transfer conditions and *tert*-butyl bromoacetate gave ether **26**. The desired aldehyde, **12**, was prepared by oxidative cleavage of **26** using sodium metaperiodate. Coupling of **12** and **13** yielded dienyne, **27**, as a mixture of *E,E* and *E,Z* isomers (Scheme 4). Iodine-catalyzed isomerization to the *E,E*-dienyne **27** and removal of the trimethylsilyl protecting group gave intermediate **10**. Palladium-catalyzed Sonogashira coupling of **10** and **17** followed by hydrolysis of the cyclohexylidene ketal gave the corresponding *tert*-butyl ester **28**. As in the case of esters of **3**, the trienyne unit was stable to acid over a 24 h period required to cleave the ketal. Base-catalyzed ester hydrolysis gave **5**. Reduction of **28** with activated zinc²² gave the *E,E,Z,E*-tetraene and subsequent ester hydrolysis yielded **4**.

Identification of Metabolite

Since the report¹⁵ that **2** is cleared from the mouse within 15 min after intravenous injection, using a dose of 2 μg per mouse, the pharmacokinetic parameters of **2** and related analogues were evaluated in the rat at a dose of 5 mg/kg (about 1 mg per rat). The results are shown in Table 1. Evaluation of the pharmacokinetic parameters of **2** in the rat was complicated by the rapid hydrolysis of the methyl ester in rat plasma to the corresponding carboxylic acid, **29** (see Figure 2). The

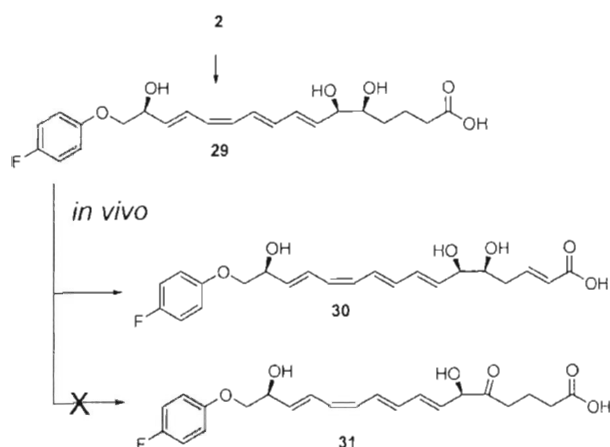


Figure 2. Proposed metabolites of **2**.

Table 1. Pharmacokinetic Data in the Rat after iv ($n = 3$, 3 mg/kg) and po ($n = 3$, 5 mg/kg) Dosing

compd	iv				po			
	$T_{1/2}$, h	Cl, (mL/mg)/kg	AUC _{all} , (h· μ g)/mL	$T_{1/2}$, h	C_{max}	T_{max} , h	F , %	
2	0.3	51	1.0	0.5	0.2	0.5	12	
29	0.2	28	1.8	1.1	0.3	1.0	13	
3	0.1	58	0.9	1.8	0.2	0.5	28	
4	1.3	50	1.0	1.1	0.04	0.5	4	
5	2.3	7	7.0	2.2	0.4	1.3	14	

calculated pharmacokinetic parameters for **2** listed in Table 1 were obtained by dosing **2** but analyzing the plasma samples for **29**. The half-life of **2** and **29** were about 15 min, in agreement with the data reported in mice.¹⁵ Careful analysis of the plasma samples indicated the presence of a metabolite, which had a molecular weight 2 mass units lower than that of **29**. Since compound **2** was designed to minimize all the known major metabolic routes, the identification of a new metabolite by LC/MS-MS was unexpected. The UV spectra of both **29** and the metabolite were identical, which is consistent with an intact *E,E,Z,E*-tetraene chromophore⁹ and minimal structural modification. Two structures were consistent with the data: **30** and **31** (see Figure 2). Since the metabolite was stable to treatment with sodium borodeuteride in methanol, the 5-oxo structure, **31**, could be ruled out and the structure of the metabolite was assigned as the 2,3-dehydro analogue **30**. Attempts to isolate **30** from in vitro metabolism studies, such as liver microsomes, for a more complete structural determination were unsuccessful. By analogy to lipid metabolism in the prostaglandin^{24,25} and leukotriene²⁶ fields, we propose that **30** would be formed as the first step in the β -oxidation of **2**. Consistent with the proposal, the corresponding 2-mass-unit-lower metabolite was observed during a pharmacokinetic assay of **3** in rats but not in 3-oxa analogues **4** and **5**, which were designed to eliminate this pathway.²⁷

The pharmacokinetic parameters for tetraene analogue **2** is characterized by rapid clearance and relatively short half-lives after both oral gavage (po) and intravenous injection (iv). The corresponding trienylene analogue, **3**, had similar properties after iv administration but a significantly better effective half-life after oral administration. The elimination of the β -oxidation pathway had a minimal impact on the pharmacokinetic profile

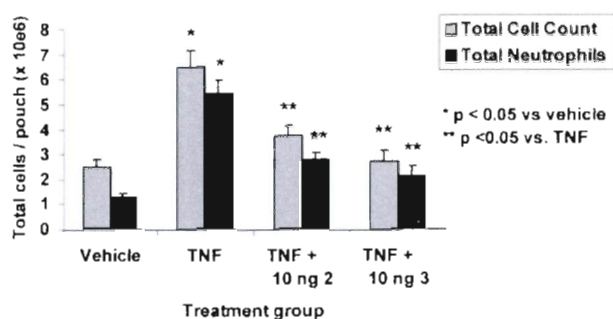


Figure 3. Tetraene and trienylene lipoxin analogues are both anti-inflammatory in vivo. Analogues **2** and **3** were tested for local anti-inflammatory effects in the murine dorsal air pouch model of TNF-induced inflammation, as described in "Experimental Section" and ref 29. The figure shows the effect of 10 ng of locally delivered analogues on total leukocyte (grey bars) and neutrophil (black bars) cell counts in the pouch exudate 4 h following TNF administration. A robust and similar inhibitory effect (~50%) on TNF-induced leukocyte trafficking into the pouch was observed for **2** and **3**. Data are the mean \pm SEM from $N = 20$ mice: (*) $p < 0.05$ versus vehicle; (**) $p < 0.05$ versus TNF.

of **4** compared with **2**, **29**, or **3**. In contrast, trienylene **5** had a significantly improved half-life and a significantly reduced clearance after both po and iv dosing in the rat. The similar F values in the rat for **2** and **5** hide the improved pharmacokinetic parameters of **5** as determined by the area under the curve value, AUC_{all} after iv dosing. Comparison of the corresponding pharmacokinetic parameters for **2** and **5** in the dog after iv dosing (2 mg/kg) are complicated by the incomplete ester hydrolysis of **2**. Comparison of the pharmacokinetic parameters for **5** in the dog versus the rat shows a slight increase in the iv half-life from 2.3 to 2.7 h (2 mg/kg) and a slight increase in the po half-life from 2.2 to 3.2 h (2 mg/kg). Similar improvements in C_{max} and T_{max} values after oral dosing increased the F value for **5** in the dog to 40.

In Vivo Models of Inflammation. Analogue **2** has been shown to be efficacious in the TNF α -induced murine dorsal air pouch model, which is an acute experimental model of inflammation.²⁸⁻³⁰ The model is characterized by cellular infiltration into a localized area, i.e., air pouches raised on the dorsal area of mice. Once the air pouch is established and stabilized, an injection of TNF α induces a temporal infiltration of inflammatory cells into the air pouch. The infiltrate is predominantly composed of proinflammatory neutrophils but also contains eosinophils and smaller numbers of mononuclear cells (monocytes and T- and B-lymphocytes). Four hours after injection of the compound and TNF α , the cells were harvested from the air pouch for enumeration and differential count analysis. As seen in Figure 3, compounds **2** and **3** showed a significant decrease in the total number of cells and neutrophils infiltrating into the air pouches at similar doses of 10 ng/pouch compared with vehicle-treated mice.

Topical efficacy for native LXA₄, **1**, and **2** has been demonstrated in several models of skin inflammation.¹² The calcium ionophore model was chosen to compare 3-oxa analogues **4** and **5** with **2**. In this model, calcium ionophore A-23187 with or without anti-inflammatory agents is applied topically to the ears of a mouse, which induces acute inflammation with edema and granulocyte

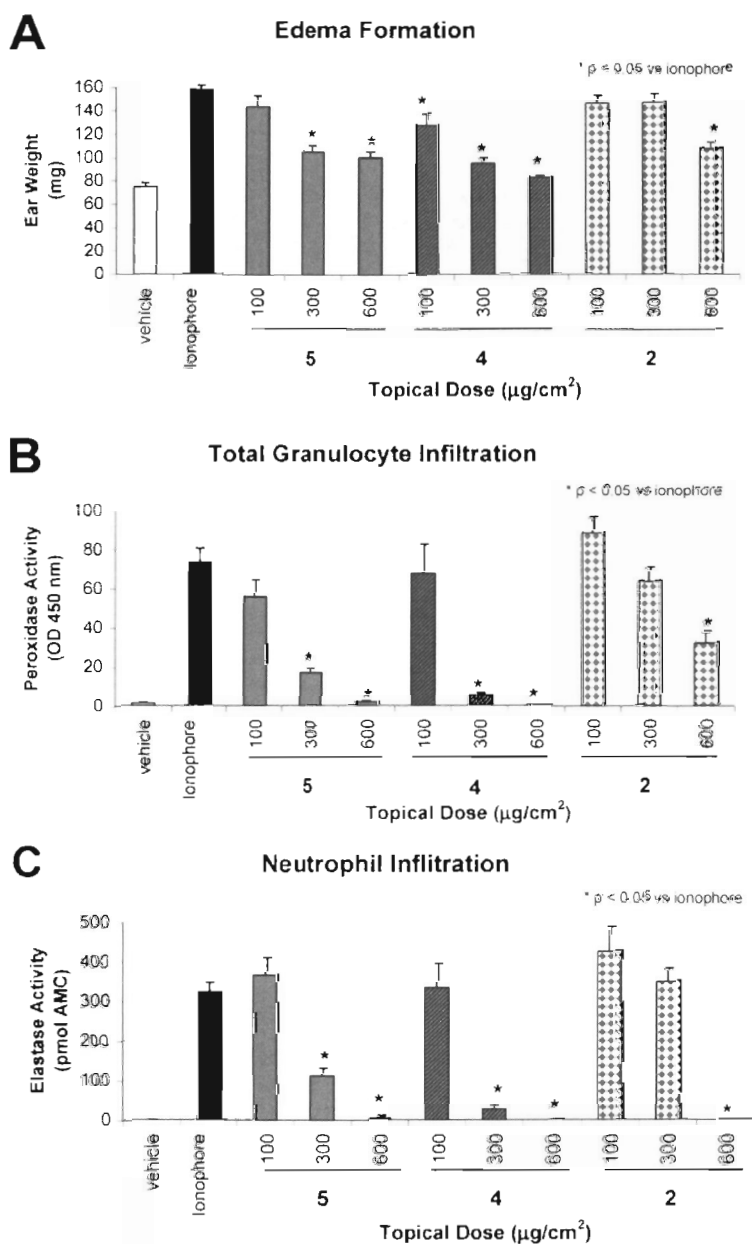


Figure 4. 3-Oxa-lipoxin analogues are potent topical anti-inflammatory agents. Acute mouse ear skin inflammation was induced by topical application of 0.1% w/v calcium ionophore in isopropylmyristate, as described in "Experimental Section" and ref 12. Inflammation was measured after 24 h. Data for vehicle control (open bars), ionophore control (black bars), and treatment by topical coapplication of **5** (gray bars), **4** (gray hashed bars), and the positive control **2** (stippled bars) are shown at doses of 100, 300, and 600 µg/cm². Dose-dependent anti-inflammatory effects were observed on edema (ear weight, panel A), total leukocyte infiltration (peroxidase activity, panel B), and neutrophil infiltration (elastase activity, panel C). ED₅₀ was <300 µg/cm² for **5** and **4** on all endpoints. Data are the mean ± SEM with *N* = 8–to 10 mice for all groups, except *N* = 5 for 600 µg/cm² dose of **2**: (*) *p* < 0.05 versus ionophore control.

cyte infiltration that peaks at approximately 24 h. The extent of granulocyte infiltration was determined using the peroxidase assay. Elastase activity was used as a measure of neutrophil infiltration. Anti-inflammatory effects of a given compound were defined as inhibition of edema formation (Figure 4A), peroxidase activity (Figure 4B), and elastase activity (Figure 4C). The data shown in Figure 4 clearly show that **2**, **4**, and **5** inhibited edema formation and neutrophil and granulocyte infiltration in a dose-dependent manner. In addition, neutrophil and granulocyte infiltration was completely

inhibited at the highest dose tested (600 µg/cm²). The IC₅₀ for **4** and **5** on all three topical efficacy parameters was <300 µg/cm².

Conclusion

The natural product, lipoxin A₄, has immunomodulatory and anti-inflammatory activity but is rapidly metabolized to inactive catabolites in vivo. Chemically and metabolically stable LXA₄ analogues of **2**, which are equipotent in animal models of inflammation, have been reported. The synthesis of the trienene and tetraene

analogues is described in both the carbon and 3-oxa series. In the carbon series, we demonstrated that the tetraene unit is not needed for efficacy in the air pouch model of inflammation. On the basis of the identification of a new metabolic route for **2**, the β -oxidation-resistant 3-oxa series was developed (trienyne, **5**, and tetraene, **4**) with anti-inflammatory activity comparable to that of **2** in cutaneous inflammation. On the basis of the increased acid, metabolic, and UV stability, equivalent anti-inflammatory activity, improved pharmacokinetic parameters, and ease of synthesis, **5** has pharmaceutical properties suitable for clinical development. Taken together, the results provide new insights on the in vivo catabolism of lipoxins and structure–activity relationships essential for in vivo actions. The 3-oxa-based lipoxin A₄ analogues provide superior pharmacophores with which to explore preclinical and clinical concepts in immunomodulation.

Experimental Section

All starting materials not described below were purchased from commercial sources. All reagents and solvents were used as received from commercial sources without additional purification. Elemental analyses were performed by Robertson Microlit Laboratories (Madison, NJ), and results were within $\pm 0.4\%$ of the calculated values. Proton NMR spectra were recorded with a Varian XL-300 spectrometer at 400 MHz proton and were consistent with the assigned structures. Carbon-13 NMR spectra at 100 and 125 MHz were obtained on a Varian XL-300 spectrometer and the Bruker Avance 500 spectrometer. HPLC was performed with a Rainin SD-1 Dynamax system and a C-18 reverse-phase Dynamax 60A column using a gradient of methanol (0.1% TFA) or acetonitrile (0.1% TFA) in water (0.1% TFA). The enantiomeric excess of **21** was determined by HPLC analysis on the corresponding dinitrobenzoate, **22**, using a Diacel Chiralpak AD (4.6 mm \times 250 mm, 60% 2-propanol/hexane, 1 mL/min), which separates the (*R*) (11.5 min) and the (*S*) (19.3 min) enantiomers.

Identification of the Metabolite of 2. Since **2** is rapidly metabolized in plasma to the corresponding acid **29**, the standard analytical protocol for analysis of **2** in biological samples was developed for **29**. Analytical quantification was carried out using LXA₄ as an internal standard using a C18 column (Waters XTerra RP18, 5 μ m, 2.1 mm \times 50 mm) and a 10–80% "A" in "B" gradient over 2 min (6 min total run time). Solvent "A" was water with 0.1% formic acid, and solvent "B" was acetonitrile with 0.1% formic acid. The MS–MS method monitored the *m/e* = 403–111 (negative ionization conditions).

***N*-Methoxy-*N*-methyl-2-(4-fluorophenoxy)ethanamide (19).** Oxalyl chloride (60 mL, 686 mmol) and a catalytic amount of dimethylformamide were added to a stirred suspension of 2-(4-fluorophenoxy)ethanoic acid (**18**, 97.3 g, 572 mmol) in dichloromethane (500 mL). After 22 h, the mixture was concentrated under vacuum to obtain 108 g of the corresponding acid chloride as a yellow oil in quantitative yield: ¹H NMR (CDCl₃) δ 4.90 (s, 2H), 6.84 (m, 2H), 6.99 (m, 2H) ppm. The residue was added slowly to a stirred suspension of *N,O*-dimethylhydroxylamine hydrochloride (55.80 g, 572 mmol) in saturated potassium carbonate and ethyl acetate (375 mL). A moderately exothermic reaction occurred. After 20 min, the reaction mixture was partitioned between water and ether. The ether layer was washed with 1 M hydrochloric acid and saturated sodium chloride, dried over magnesium sulfate, and concentrated under vacuum to give **19** as an off-white crystalline solid, 113.05 g (73% yield from starting acid): ¹H NMR (CDCl₃, 400 MHz) δ 3.21 (s, 3H), 3.73 (s, 3H), 4.75 (s, 2H), 6.87 (m, 2H), 6.95 (m, 2H) ppm.

4-(4-Fluorophenoxy)-1-butyn-3-one (20). A solution of **19** (20.00 g, 74 mmol) in THF (100 mL) was cooled in an ice bath as a solution of ethynylmagnesium bromide (0.5 M in THF, 508 mL, 254 mmol) was added. After an additional 30 min at 0 °C, the reaction mixture was poured into a vigorously stirred mixture of 1 M NaH₂SO₄ (1700 mL) and ether (1 L). The layers were separated, and the aqueous layer was then extracted with ether (700 mL). The combined organic phases were washed with brine and dried over MgSO₄, filtered, and concentrated under vacuum. The residue was purified by eluting through a plug of silica gel (10 cm \times 3 cm) with 1:4 ether/petroleum ether to afford 27.65 g (91% yield) as a low-melting solid: ¹H NMR (CDCl₃) δ 3.40 (s, 1H), 4.70 (s, 2H), 6.85 (m, 2H), 7.0 (t, 2H) ppm.

(3*S*)-4-(4-Fluorophenoxy)-3-hydroxy-1-butyne (21). A solution of *R*-Alpine-Borane (0.5 M in THF, 930 mL, 465 mmol) was evaporated to dryness under vacuum to give about 150 g of a thick syrup. Neat **20** (27.6 g, 155 mmol) was added, and the reaction mixture was stirred for 2 days. The reaction mixture was cooled to 0 °C, and acetaldehyde (26 mL, 465 mmol) was added to quench the excess reagent. After being stirred at ambient temperature for 2 h, the reaction mixture was placed under vacuum and stirred first at 0 °C for 1 h, then at 65 °C for 2 h. The reaction mixture was cooled to ambient temperature, and ether (300 mL) was added under nitrogen. Ethanolamine (30 mL, 465 mmol) was added dropwise at 0 °C, and the resulting reaction mixture was stored in the freezer overnight. The resulting precipitate was removed by filtration and washed with cold ether. The combined filtrates were concentrated under vacuum. Purification by flash chromatography on a 2.5 L column using a 10–25% gradient of ethyl acetate in hexane gave 27 g (97%): ¹H NMR (CDCl₃) δ 2.56 (s, 1H), 4.10 (m, 2H), 4.78 (m, 1H), 6.85 (m, 2H), 7.0 (m, 2H). This material was determined to be about 64% ee based on chiral HPLC of its 3,5-dinitrobenzoyl ester. To a solution of **21** (about 490 mmol) in methylene chloride (1 L) was added, between –5 and 0 °C, 3,5-dinitrobenzoyl chloride (125 g, 539 mmol), followed by slow addition of triethylamine (10.8 mL, 77 mmol) and a catalytic amount of (dimethylamino)pyridine (20 mg). After being stirred for 40 min, the reaction mixture was cautiously partitioned between methylene chloride and aqueous sodium bicarbonate. The aqueous layer was extracted with dichloromethane. The combined organic layers were washed with water and brine, dried over Na₂SO₄, filtered through a pad of silica gel, and concentrated to give a tan solid. Rapid recrystallization from a 99:1 mixture of methanol/acetic acid (5 L) gave 101 g (54%) of the enantiomerically enriched product as fluffy white needles. This material was determined to have >98% ee by HPLC: ¹H NMR (CDCl₃) δ 2.65 (s, 1H), 4.40 (m, 2H), 6.05 (m, 1H), 6.90 (m, 2H), 7.0 (t, 2H), 9.15 (s, 2H), 9.25 (s, 1H) ppm. To a solution of **22** (10.35 g, 98% ee, 27.6 mmol) in THF (115 mL), was added methanol (115 mL) and potassium carbonate (0.58 g). After being stirred for 3.5 h, the reaction mixture was quenched with acetic acid (2 mL). The solvents were evaporated. The resulting slurry was filtered, and the solid was washed with ether. The filtrate was concentrated, and the filtration/ether wash sequence was repeated to give 4.02 g (80%): ¹H NMR (CDCl₃) δ 2.56 (s, 1H), 4.10 (m, 2H), 4.78 (m, 1H), 6.85 (m, 2H), 7.0 (m, 2H).

(3*S*)-1-Bromo-4-(4-fluorophenoxy)-3-hydroxy-1-butyne (23). A mixture of **21** (2.5 g, 14 mmol), *N*-bromosuccinimide (2.74 g, 15.4 mmol), and silver nitrate (0.12 g, 0.7 mmol) in acetone (70 mL) was stirred at ambient temperature. The pale solution became cloudy over 30 min. The mixture was concentrated. Filtration through a plug of silica gel, eluting with 20% ethyl acetate in hexane, gave 3.6 g (99%) of a pale-yellow oil: ¹H NMR (CDCl₃) δ 3.95–4.15 (m, 2H), 4.75 (m, 1H), 6.86 (m, 2H), 6.97 (m, 2H) ppm.

(1*E*,3*S*)-1-Bromo-4-(4-fluorophenoxy)-3-hydroxy-1-butene (17). Aluminum chloride (2.79 g, 21 mmol) was added in portions to a mixture of lithium aluminum hydride (1.06 g, 28 mmol) in ether (70 mL). A solution of **23** (3.6 g) in ether (10 mL) was added cautiously. A vigorous reaction with evolution of hydrogen gas was observed. The mixture was

warmed to reflux in a water bath for 30 min. The reaction mixture was cooled to 0 °C and treated sequentially with 2.8 mL of water, 2.8 mL of 15% NaOH, and 8.4 mL of water. The resulting suspension was stirred for 10 min and filtered, and the solids were washed with THF and ether. The filtrate was concentrated to afford 2.94 g (81%): ¹H NMR (CDCl₃) δ 2.41 (t, 1H), 3.85 (dd, 1H), 3.99 (dd, 1H), 4.50 (m, 1H), 6.31 (dd, 1H), 6.52 (dd, 1H), 6.83 (m, 2H), 6.97 (t, 2H) ppm.

(2R,3R)-3-(1,2-Dihydroxypropyl)-1,4-dioxaspiro[4,5]-decane-2-carboxaldehyde (24). Rhamnose hydrate (100 g, 0.55 mol) was converted into 92.3 g (0.31 mol, 57%) of cyclohexylidene ketal as described earlier:²³ [α]_D +0.46 (10.49 mg/cc, MeOH); ¹H NMR (CDCl₃) δ 1.34 (d, 3H), 1.40 (m, 2H), 1.6 (m, 8H), 2.78 (d, 1H), 3.0 (s, 1H), 3.9 (m, 1H), 4.07 (m, 1H), 4.6 (d, 1H), 4.9 (m, 1H), 5.4 (s, 1H) ppm. Anal. (C₁₂H₂₀O₅·0.5C₆H₁₀O) C, H.

(2R,3S)-α²-(1-Hydroxyethyl)-1,4-dioxaspiro[4,5]decane-2,3-dimethanol (25). A slurry of sodium borohydride (34.2 g, 0.9 mol) in methanol (400 mL) was cooled in an ice bath and treated with a solution of **24** (92 g, 0.27 mol) in methanol (200 mL). The reaction mixture was stirred for about 4 h before the addition of acetic acid to adjust the pH to about 6 (about 120 mL). The reaction mixture was filtered. The filtrate was concentrated to give a slightly yellow viscous oil. Treatment of an ether solution with hexane gave 81.2 g (88%) of an off-white solid after drying: ¹H NMR (CD₃OD) δ 1.28 (d, 3H), 1.43 (m, 2H), 1.7 (m, 8H), 3.42 (dd, 1H), 3.7 (m, 3H), 4.25 (m, 1H), 4.42 (dd, 1H) ppm.

1,1-Dimethylethyl [(2S,3R)-3-(1,3-Dihydroxypropyl)-1,4-dioxaspiro[4,5]dec-2-yl]methoxy]acetate (26). A mixture of **25** (81 g, 0.32 mol) and *tert*-butyl bromoacetate (77 g, 0.39 mol, 1.2 equiv) in 1 L of toluene and 80 mL of aqueous sodium hydroxide (25 wt %) was stirred as tetrabutylammonium sulfate (7.8 g, 23 mmol, 0.07 equiv) was added. After about 16 h, the reaction mixture was diluted with ethyl acetate and saturated aqueous monobasic potassium phosphate. The combined organic layers were dried and concentrated to give a clear oil. Purification on silica gel using a step gradient of ether in hexane (20–50%) gave 50.8 g (44%) of an oil: [α]_D +8.59 (10.30 mg/cc, MeOH); ¹H NMR (CDCl₃) δ 1.24 (d, 3H), 1.35 (m, 2H), 1.47 (s, 9H), 1.6 (m, 8H), 3.6 (m, 2H), 3.8 (m, 2H), 3.95 (m, 2H), 4.32 (m, 1H), 4.4 (m, 1H) ppm. Anal. (C₁₈H₃₂O₇·0.2H₂O) C, H.

1,1-Dimethylethyl [(2S,3S)-3-Formyl-1,4-dioxaspiro[4,5]dec-2-yl]methoxy]acetate (12). A solution of **26** (50 g, 138 mmol) in acetone (350 mL) was treated with a solution of periodate (50 g, 235 mmol, 1.7 equiv) in water (1.2 L). After about 4 h, solvent was removed by distillation and the residue was extracted with ethyl acetate (3 × 500 mL). The combined organic layers were dried and concentrated under reduced pressure without heating to give 40 g (92%) of a clear oil: [α]_D -1.14 (10.15 mg/cc, MeOH); ¹H NMR (CDCl₃) δ 1.38 (m, 2H), 1.42 (s, 9H), 1.61 (m, 8H), 1.73 (m, 2H), 3.52 (dd, 1H), 3.72 (dd, 1H), 3.88 (s, 2H), 4.38 (dd, 1H), 4.52 (m, 1H), 9.62 (s, 1H) ppm. Anal. (C₁₆H₂₆O₆) C, H.

1,1-Dimethylethyl [(2S,3R)-3-[(1E,3E)-6-(Trimethylsilyl)-1,3-hexadien-5-ynyl]-1,4-dioxaspiro[4,5]dec-2-yl]methoxy]ethanoate (27). A slurry of phosphonium salt (**13**, 67.1 g, 0.14 mol) in THF (875 mL) was stirred under nitrogen, cooled in a dry ice acetonitrile bath (-30 °C internal), and treated with a solution of ⁿBuLi (66.5 mL, 0.133 mol, 2 M in hexane) via dropwise addition. The reaction mixture was allowed to warm to about 0 °C, then cooled back to about -30 °C. The reaction mixture was treated with a solution of **12** (40 g, 0.127 mol) in 125 mL of THF. After 1 h, the reaction was diluted with saturated potassium phosphate (pH 5). The aqueous layer was washed with ether (3×). The combined organic layers were washed with water and brine, dried, and concentrated. Impurities were precipitated from an ether solution with hexane. The concentration of the filtrate gave 50.29 g of a 2:1 mixture of *E,Z* to *E,E* isomers by NMR analysis. *Z,E* isomer: ¹H NMR (CDCl₃) δ 0.15 (s, 9H), 1.3 (m, 2H), 1.4 (s, 9H), 1.6 (m, 8H), 3.45 (m, 2H), 3.92 (m, 2H), 4.34

(m, 1H), 5.02 (m, 1H), 5.48 (dd, 1H), 5.6 (d, 1H), 6.16 (dd, 1H), 6.82 (dd, 1H) ppm. The residue was dissolved in methylene chloride (400 mL) and was treated with iodine until a red color persisted. After about 1 h, the reaction mixture was treated with an aqueous solution of sodium hydrosulfite, dried, filtered, and concentrated. Purification by chromatography on silica gel using a gradient of ether in hexane gave 27.8 g (49%) of the desired product: [α]_D -19.10 (10.88 mg/cc, MeOH); ¹H NMR (CDCl₃) δ 0.15 (s, 9H), 1.3 (m, 2H), 1.4 (s, 9H), 1.6 (m, 8H), 3.45 (m, 2H), 3.92 (m, 2H), 4.34 (m, 1H), 4.62 (m, 1H), 5.54 (d, 1H), 5.72 (dd, 1H), 6.26 (dd, 1H), 6.56 (dd, 1H) ppm. Anal. (C₂₄H₃₈SiO₅·0.4H₂O) C, H.

1,1-Dimethylethyl [(2S,3R)-3-[(1E,3E)-1,3-Hexadien-5-ynyl]-1,4-dioxaspiro[4,5]dec-2-yl]methoxy]ethanoate (10). A solution of **27** (27.8 g, 63 mmol) in THF (25 mL) was cooled in an ice bath and treated with a solution of tetrabutylammonium fluoride in THF (71 mL, 71 mmol, 1 M in THF). After about 1 h, the reaction mixture was diluted with saturated aqueous monobasic potassium phosphate and ether. The aqueous layer was washed with ether (2×). The combined organic layers were washed with saturated aqueous monobasic potassium phosphate solution and brine solution, dried, and concentrated to give 23.4 g (99%) of an oil: ¹H NMR (CDCl₃) δ 1.3 (m, 2H), 1.4 (s, 9H), 1.6 (m, 8H), 3.02 (s, 1H), 3.5 (m, 2H), 3.96 (m, 2H), 4.38 (q, 1H), 4.66 (t, 1H), 5.54 (dd, 1H), 5.78 (dd, 1H), 6.33 (dd, 1H), 6.65 (dd, 1H) ppm.

1,1-Dimethylethyl [(2S,3R)-3-[(1E,3E,7E,9S)-10-(4-Fluorophenoxy)-9-hydroxyl-1,3,7-decatrien-5-ynyl]-1,4-dioxaspiro[4,5]dec-2-yl]methoxy]ethanoate (8). A solution of **17** (16.6 g, 63 mmol), solid tetrakis(triphenylphosphine)Pd(0) (3.67 g, 3 mmol), and Cu(I) iodide (1.2 g, 6.3 mmol) in diethylamine (50 mL) and THF (800 mL) was stirred and deoxygenated by bubbling argon through the mixture for 90 min. An argon deoxygenated solution of **10** (23 g, 63 mmol) in 200 mL of THF was added dropwise. After 2 h, the reaction mixture was diluted with hexane (about 400 mL), treated with silica gel (about 40 g), and filtered. The solid was washed with a 1:1 solution of ether and hexane. The filtrate was concentrated to give 36.8 g of an oil. Purification by chromatography on silica gel using a 15–50% gradient of ether in hexane gave 16.9 g (50%) as an oil: [α]_D -21.17 (10.16 mg/cc, MeOH); ¹H NMR (CDCl₃) δ 1.3 (m, 2H), 1.4 (s, 9H), 1.6 (m, 8H), 2.42 (s, 1H), 3.5 (d, 2H), 3.96 (m, 4H), 4.38 (q, 1H), 4.58 (m, 1H), 4.66 (t, 1H), 5.72 (m, 1H), 5.78 (dd, 1H), 6.03 (m, 1H), 6.16 (dd, 1H), 6.33 (dd, 1H), 6.58 (dd, 1H), 6.88 (m, 4H) ppm. Anal. (C₃₁H₃₈FO₇) C, H, F.

(5R,6R,7E,9E,13E,15S)-16-(4-Fluorophenoxy)-3-oxa-5,6,15-trihydroxy-7,9,13-hexadecatrien-11-ynoic Acid (5). A solution of **8** (1 g, 1.8 mmol) in acetic acid (50 mL) was diluted with ethyl acetate (50 mL) and placed in a 55 °C oil bath for 20 h. The reaction was complete by TLC analysis. Acetic acid and ethyl acetate were removed by distillation under high vacuum. The residue was diluted with water and extracted with ethyl acetate (3×). The combined organic layers were washed with water, saturated aqueous sodium carbonate, water, and brine solution, dried, and concentrated to give 0.9 g of an oil. Chromatography on an HP-20 column, eluting with a gradient of methanol in water, gave 0.5 g (58%) of **28** upon concentration. The combined fractions were treated with 1 N sodium hydroxide solution (2 mL) and concentrated. The reaction was complete by TLC after about 1 h and the mixture was placed on a column of CHP20P resin (75–150 μm, Mitsubishi Chemical Corp.) and eluted using a gradient of methanol in water to give 0.3 g (68%) of the desired product that solidified upon standing: ¹H NMR (CD₃OD) δ 3.63 (m, 1H), 3.67 (m, 2H), 3.86 (dd, *J* = 9.9, 6.7 Hz, 1H), 3.94 (dd, *J* = 9.7, 4.5 Hz, 1H), 4.11 (s, 2H), 4.15 (t, *J* = 6.1, 1H), 4.50 (dd, *J* = 5.4, 1.5 Hz, 1H), 5.76 (dd, *J* = 15.3, 2 Hz, 1H), 5.95 (dd, *J* = 15.6 Hz, 1H), 6.00 (dt, *J* = 17.2 Hz, 1H), 6.20 (dd, *J* = 15.8, 5.5 Hz, 1H), 6.38 (dd, *J* = 15.8, 10.8 Hz, 1H), 6.60 (dd, *J* = 15.8, 10.8 Hz, 1H), 6.95 (m, 4H) ppm; ¹³C NMR (100 MHz, CD₃OD) δ 69.1, 71.2, 73.2, 73.5, 73.9, 74.7, 90.7, 91.0, 112.2, 112.4, 116.7, 116.9, 116.9, 131.9, 137.1, 142.4, 142.8, 156.5, 158.8, 174.5 ppm. Anal. (C₂₁H₂₃FO₇·0.2H₂O) C, H, F.

(5R,6R,7E,9E,11Z,13E,15S)-16-(4-Fluorophenoxy)-3-oxa-5,6,15-trihydroxy-7,9,11,13-hexadecatetraenoic Acid (4). Activated zinc was prepared from 10 g of zinc using the Boland procedure.²² A solution of ester (0.25 g, 0.5 mmol) in methanol (5 mL) was added to a slurry of activated zinc in a 1:1 mixture of methanol to water (45 mL). The flask was stirred vigorously under nitrogen for 24 h. The mixture was filtered through a pad of non-acid-washed Celite 545, and the pad was rinsed with methanol (3 × 25 mL). The fractions were combined, condensed, and placed on a column of CHP20P resin. The tetraene ester was eluted with a gradient of methanol in water (20–100%) and treated with 1 N aqueous sodium hydroxide (2 mL). After about 1 h, the reaction mixture was placed on an CHP20P column and the product was eluted with a gradient of methanol in water (20–100%) to afforded 65 mg (30%) of the sodium salt, which solidified after concentration. Since coupling constants could not be obtained on the sample in methanol-*d*₄, DMSO-*d*₆ was used: ¹H NMR (DMSO-*d*₆) δ 3.20 (m, 1H), 3.48 (m, 2H), 3.5 (q, *J* = 15.9 Hz, 1H), 3.88 (dq, *J* = 14.8, 4.8 Hz, 2H), 3.97 (m, 1H), 4.42 (m, 1H), 5.28 (d, *J* = 4.9 Hz, 1H), 5.82 (dd, *J* = 14, 5.6 Hz, 1H), 6.00 (m, 3H), 6.32 (m, 2H), 6.55 (br s, 1H), 6.7 (dd, *J* = 14, 9.9 Hz, 1H), 6.85 (dd, *J* = 15, 9.9 Hz, 1H), 6.94 (m, 2H), 7.09 (m, 2H); ¹³C NMR (125 MHz, CD₃OD) δ 72.1, 72.2, 73.9, 74.2, 74.3, 75.3, 117.0, 117.2, 117.5, 117.5, 128.7, 129.5, 130.3, 131.6, 133.0, 133.3, 134.7, 135.4, 136.0, 157.1, 158.3, 160.2, 178.9. Anal. (C₂₁H₂₄FO₇Na·0.8H₂O) C, H, F, Na.

Cutaneous Model of Inflammation. The calcium ionophore induced model of acute inflammation was used as described.¹² Briefly, calcium ionophore A-23187 (10 μL, 0.1% w/v), with or without the anti-inflammatory agent, was applied topically to the dorsal surface of mouse ears, using isopropylmyristate as the vehicle. The animals were euthanized after 24 h. Ear weight was used as an indicator of edema. The extent of granulocyte and neutrophil infiltration was determined on the basis of the measurement of peroxidase and elastase activity, respectively, in mouse ear homogenates.

Air Pouch Model of Inflammation. The mice used in the study were age-matched male Balb/c, 6–8 weeks old [purchased from Sprague-Dawley] and were in groups of 20. On day 0, all mice were anesthetized with 3% isoflurane. Dorsal areas were shaved, cleaned with alcohol swabs, and injected subcutaneously with sterile air (3 mL, passed through 20 μm filter) near the tail. On day 3, all mice were injected with 3 mL of sterile air. On day 6, the air pouches of anesthetized mice were injected sequentially with 900 μL of either 2 or 3 in 0.1% ethanol/PBS or vehicle and with 100 000 units of recombinant mouse TNF-α (0.1 mL PBS; Boehringer Mannheim). Four hours after TNF injection, mice were euthanized with carbon dioxide. Air pouches were lavaged three times with 3 mL of sterile PBS. The cellular exudates were centrifuged for 15 min at 2000 rpm, and the resulting cell pellets were resuspended in 1 mL of sterile PBS/10% BSA. The total number of leukocytes, collected from the pouches, was counted using a Coulter Z1 counter. Total neutrophils were enumerated by differential cell counts on stained slides.

Acknowledgment. The authors thank Eginhard Matzke and Detlef Opitz (Research Business Area Dermatology, Schering AG) and Jerry Dallas (Biophysics, Berlex Biosciences) for excellent technical assistance. We acknowledge the support of Drs. H. Daniel Perez, Khusru Asadullah, and Gary B. Phillips for this work.

References

- Serhan, C. N. Lipoxins and aspirin-triggered 15-epi-lipoxin biosynthesis: an update and role in anti-inflammation and pro-resolution. *Prostaglandins Other Lipid Mediators* **2002**, *68–69*, 433–455.
- Serhan, C. N.; Hamberg, M.; Samuelsson, B. Trihydroxytetraenes: a novel series of compounds formed from arachidonic acid in human leukocytes. *Biochem. Biophys. Res. Comm.* **1984**, *118*, 943–949.
- Adams, J.; Fitzsimmons, B. J.; Rokach, J. Synthesis of Lipoxins: Total Synthesis of Conjugated Trihydroxy Eicosatetraenoic Acids. *Tetrahedron Lett.* **1984**, *25*, 4713–4716.
- Corey, E. J.; Su, W. G. Simple Synthesis and Assignment of Stereochemistry of Lipoxin A. *Tetrahedron Lett.* **1985**, *26*, 281–284.
- Nicolaou, K. C.; Webber, S. E. A General Strategy for the Total Synthesis of the Presumed Lipoxin Structures. *J. Chem. Soc., Chem. Commun.* **1985**, 297–298.
- Rodriguez, A. R.; Spur, B. W. Total Synthesis of aspirin-triggered 15-epi-lipoxin A4. *Tetrahedron Lett.* **2001**, *42*, 6057–6060.
- Levy, B. D.; Serhan, C. N. Exploring new approaches to the treatment of asthma: potential roles for lipoxins and aspirin-triggered lipid mediators. *Drugs Future* **2003**, *39*, 373–384.
- Wallace, J. L.; Fiorucci, S. A Magic Bullet for Mucosal Protection ... and Aspirin Is the Trigger! *Trends Pharmacol. Sci.* **2003**, *24*, 323–326.
- Clish, C. B.; Levy, B. D.; Chiang, N.; Tai, H. H.; Serhan, C. N. Oxidoreductases in lipoxin A4 metabolic inactivation: A novel role for 15-oxoprostaglandin 13-reductase/leukotriene B4 12-hydroxydehydrogenase in inflammation. *J. Biol. Chem.* **2000**, *33*, 25372–25380.
- Serhan, C. N.; Maddox, J. F.; Petasis, N. A.; Akritopoulou-Zanze, I.; Papayianni, A.; Brady, H. R.; Colgan, S. P.; Madara, J. L. Design of Lipoxin A4 Stable Analogs That Block Transmigration and Adhesion of Human Neutrophils. *Biochemistry* **1995**, *34*, 14609–14615.
- Levy, B. D.; De Sanctis, G. T.; Devchand, P. R.; Kim, E.; Ackerman, K.; Schmidt, B. A.; Szczeklik, W.; Drazen, J. M.; Serhan, C. N. Multi-pronged inhibition of airway hyper-responsiveness and inflammation by lipoxin A₄. *Nat. Med.* **2002**, *8*, 1018–1023.
- Schottelius, A. J.; Giesen, C.; Asadullah, K.; Fierro, I. M.; Colgan, S. P.; Bauman, J.; Guilford, W. J.; Perez, H. D.; Parkinson, J. F. An aspirin-triggered lipoxin A4 stable analog displays a unique topical anti-inflammatory profile. *J. Immunol.* **2002**, *168*, 7064–7070.
- Gewirtz, A. T.; Collier-Hyams, L. S.; Young, A. N.; Kucharzik, T.; Guilford, W. J.; Parkinson, J. F.; Williams, I. R.; Neish, A. S.; Madara, J. L. Lipoxin A4 analogs attenuate induction of intestinal epithelial proinflammatory gene expression and reduce the severity of dextran sodium sulfate-induced colitis. *J. Immunol.* **2002**, *168*, 5260–5267.
- Aliberti, J.; Serhan, C. N.; Sher, A. Parasite-induced lipoxin A4 is an endogenous regulator of IL-12 production and immunopathology in *Toxoplasma gondii* infection. *J. Exp. Med.* **2002**, *196*, 1253–1262.
- Clish, C. B.; O'Brien, J. A.; Gronert, K.; Stahl, G. L.; Petasis, N. A.; Serhan, C. N. Local and systemic delivery of a stable aspirin-triggered lipoxin prevents neutrophil recruitment in vivo. *Proc. Natl. Acad. Sci. U.S.A.* **1999**, *96*, 8247–8252.
- Phillips, E. D.; Chang, H.-F.; Holmquist, C. R.; McCauley, J. P. Synthesis of methyl (5R,6R,7E,9E,11Z,13E,15S)-16-(4-fluorophenoxy)-5,6,15-trihydroxy-7,9,11,13-hexadecatetraenoate, an analogue of 15R-lipoxin A4. *Bioorg. Med. Chem. Lett.* **2003**, *13*, 3223–3226.
- Nicolaou, K. C.; Veale, C. A.; Webber, S. E.; Katerinopoulos, H. Stereocontrolled Total Synthesis of Lipoxins A. *J. Am. Chem. Soc.* **1985**, *107*, 7515–7518.
- Robinson, R. S.; Clark, J. S.; Holmes, A. B. The Synthesis of (+)-Laurencin. *J. Am. Chem. Soc.* **1993**, *115*, 10400–10401.
- Gooding, O. W.; Beard, C. C.; Cooper, C. F.; Jackson, D. Y. Triply Convergent Synthesis of 15-(Phenoxyethyl) and 4,5-Allenyl Prostaglandins. Preparation of an Individual Isomer of Enprostil. *J. Org. Chem.* **1993**, *58*, 3681–3686.
- Hofmeister, H.; Annen, K.; Laurent, H.; Wiechert, R. A Novel Entry to 17α-Bromo- and 17α-Iodoethyl Steroids. *Angew. Chem., Int. Ed. Engl.* **1984**, *23*, 727–729.
- Bohlmann, F.; Rotard, W. Synthese von (2E,4Z)-2,4,11-Dodecatrien-1-al, einem Abbauprodukt der Linolensäure (Synthesis of (2E,4Z)-2,4,11-Dodecatrien-1-al, a Degradation Product of Linolenic Acid. *Liebigs Ann. Chem.* **1982**, 1216–1219.
- Boland, W.; Schroer, N.; Sieler, C.; Feigl, M. 96. Sterospecific Syntheses and Spectroscopic Properties of Isomeric 2,4,6,8-Undecatetraenes. New Hydrocarbons from the Marine Brown Alga *Giffordia mitchellae* *Helv. Chim. Acta* **1987**, *70*, 1025–1040.
- Wheatley, J. R.; Beacham, A. R.; Lilley, P. M. deQ.; Watkin, D. J.; Fleet, G. W. J. Ketals of L-Rhamnoheptonolactones: Potential Mimics of L-Rhamnose. *Tetrahedron: Asymmetry* **1994**, *5*, 2523–2534.
- Ellis, C. K.; Smigel, M. D.; Oates, J. A.; Oelz, O.; Sweetman, B. J. Metabolism of prostaglandin D2 in the monkey. *J. Biol. Chem.* **1979**, *254*, 4152–4163.
- Sturzebecher, S.; Haberey, M.; Muller, B.; Schillinger, E.; Schroder, G.; Skuballa, W.; Stock, G.; Vorbruggen, H.; Witt, W. Pharmacological profile of a novel carbacyclin derivative with high metabolic stability and oral activity in the rat. *Prostaglandins* **1986**, *31*, 95–109.

- (26) Guindon, Y.; Delorme, D.; Lau, C. K.; Zamboni, R. Total Synthesis of LTB₄ and Analogues. *J. Org. Chem.* **1988**, *53*, 267–275.
- (27) Skuballa, W.; Schillinger, E.; Stuerzebecher, C. St.; Vorbrueggen, H. Synthesis of a New Chemically and Metabolically Stable Prostacyclin Analogue with High and Long-Lasting Oral Activity. *J. Med. Chem.* **1986**, *29*, 313–315.
- (28) Takano, T.; Clish, C. B.; Gronert, K.; Petasis, N.; Serhan, C. N. Neutrophil-Mediated Changes in Vascular Permeability Are Inhibited by Topical Application of Aspirin-Triggered 15-Epi-lipoxin A₄ and Novel Lipoxin B₄. *J. Clin. Invest.* **1998**, *101*, 819–826.

- (29) Hachicha, M.; Pouliot, M.; Petasis, N. A.; Serhan, C. N. Lipoxin (LX) A₄ and aspirin-triggered 15-epi-LXA₄ inhibit tumor necrosis factor 1 α -initiated neutrophil responses and trafficking: regulators of a cytokine-chemokine axis. *J. Exp. Med.* **1999**, *189*, 1923–1930.
- (30) Serhan, C. N.; Takano, T.; Clish, C. B.; Gronert, K.; Petasis, N. Aspirin-triggered 15-epi-lipoxin A₄ and novel lipoxin B₄ stable analogues inhibit neutrophil-mediated changes in vascular permeability. *Adv. Exp. Med. Biol.* **1999**, *469*, 287–293.

JM030569L



A miniaturized high-throughput screening assay for fucosyltransferase VII

Oliver von Ahsen^{a,*}, Ulrike Voigtmann^a, Monika Klotz^a, Nikolay Nifantiev^b,
Arndt Schottelius^{a,1}, Alexander Ernst^{a,2}, Beate Müller-Tiemann^a, Karsten Parczyk^a

^a Bayer Schering Pharma AG, Müllerstraße 178, 13342 Berlin, Germany

^b GlycoSense AG, Winzerlaer Str. 2a, 07745 Jena, Germany

Received 20 June 2007

Available online 28 August 2007

Abstract

Fucosyltransferase VII (FucTVII) is a very promising drug target for treatment of inflammatory skin diseases. Its activity is required for synthesis of the sialyl-Lewis X glycoepitopes on the E- and P-selectin ligands, necessary for lymphocyte migration into the skin. High-throughput screening (HTS) of large chemical libraries has become the main source of novel chemical entities for the pharmaceutical industry. The screening of very large compound collections requires the use of specialized assay techniques that minimize time and costs. We describe the development of a miniaturized scintillation proximity assay for human FucTVII based on a oligosaccharide acceptor substrate that is identical to the glycosylation of the physiological substrate. In addition to assay development, the assay performance in a HTS campaign is shown. We screened 798,131 compounds from the Schering AG HTS library and identified 233 IC₅₀ hits; 229 hits were FucTVII specific in so far as they did not inhibit either α -fucosidase or galactosyltransferase. In addition to screening a drug-like small-molecule collection, we worked on rational approaches to develop inhibitors or glycosidic decoys based on oligosaccharide-substrate analogues. The structure–activity relationship observed thereby is very narrow and shows strict requirements that are consistent with the described substrate specificity of FucTVII.

© 2007 Elsevier Inc. All rights reserved.

Keywords: Assay techniques; High-throughput screening; Scintillation proximity assay; Fucosyltransferase; Inhibitor; Glycosidic decoy

Migration of T cells plays a crucial role in the pathogenesis of inflammatory skin diseases such as psoriasis, atopic dermatitis, and allergic dermatitis and these conditions are now classified as T-cell-mediated dermatoses. Thus the mechanism of T-cell-recruitment into the skin is of interest for development of antiinflammatory drugs. The processes of lymphocyte recirculation and skin homing have been reviewed [1–3].

Binding of T cells to E-selectin and P-selectin expressed on the surface of endothelial cells is crucial for migration of T cells from the bloodstream into the skin. Naive T cells weakly express selectin ligands, whereas selectin ligand positive cells are found with higher frequencies among activated memory and effector cells, since expression of selectin ligands increases during inflammatory responses [4,5]. Inflammatory events are also accompanied by strong transcriptional upregulation of selectins and integrin ligands on the endothelial cells. These surface markers are expressed in response to inflammatory cytokines such as IL-1 β and TNF α [6]. Selectin-based leukocyte trafficking has been identified as a promising field of pharmaceutical research and selectins as target have been addressed with antiselectin antibodies, recombinant ligands, and low-molecular-weight glycomimetics as recently reviewed [7].

* Corresponding author.

E-mail address: oliver.vonahsen@bayerhealthcare.de (O. von Ahsen).

¹ Current address: Genentech Inc., 1 DNA Way, South San Francisco, CA-94080, USA.

² Current address: Dottikon Exclusive Synthesis AG., Hembrunnstr. 17, CH-5605, Dottikon, Switzerland.

Key to the interaction of T cells with P-selectin and E-selectin are the selectin ligand proteins PSGL-1 and ESL-1 expressed on the lymphocyte surface. Especially important is their modification with the sialyl-Lewis X (sLex)³ epitope. The carbohydrate antigen sLex {Neu5Ac α -(2 \rightarrow 3)-Gal β -(1 \rightarrow 4)-[Fuc α -(1 \rightarrow 3)]-GlcNAc β -R} is synthesized by a series of glycosyltransferases. The last step in sLex epitope formation is catalyzed by α (1 \rightarrow 3)-fucosyltransferase VII (FucTVII), which transfers a fucosyl moiety from GDP-fucose to the core oligosaccharide structures. Therefore, FucTVII is the key to lymphocyte localization and a very attractive target for treatment of inflammatory skin diseases [8–11].

The validity of FucTVII as drug target is supported by the findings that Th1 cells from FucTVII-deficient mice display reduced rolling on endothelial surfaces [12] and are not able to migrate into areas of skin inflammation [13]. Also it was reported that blocking selectins with antibodies and using FucTVII-deficient T cells resulted in nearly complete abrogation of homing into inflamed joints in arthritis models [14].

High-throughput screening (HTS) of large chemical libraries is the main source of potential new small-molecule drugs. Assays that are used in HTS should be miniaturized to very small volumes in 384- or 1536-well microtiter plates to save reagent costs and should avoid time-consuming separation steps. The traditional assay formats for glycosyltransferase activity, based on scintillation counting of radiolabeled sugars transferred to the acceptor molecule after ion-exchange [15], are not suited to HTS. The same holds true for use of carbohydrate microarrays in microtiter plates [16] or membrane-bound acceptor substrates [17] because both assays required washing steps. Glycosyltransferase assays suitable for high-throughput-screening have been published, though not in a miniaturized format [18,19]. They use the scintillation proximity assay (SPA) principle to detect the transfer of a radiolabeled sugar moiety to a protein acceptor coated on scintillant-impregnated microspheres. This allows for easy mix and measure assays, avoiding time-consuming washing and separation steps. Published fucosyltransferase assays use GDP-[³H]fucose as donor and fetuin or asialofetuin as acceptor substrates. A limitation of this approach using a protein acceptor is the limited binding capacity of the SPA beads for protein. This requires high bead concentrations which cause a cost issue for screening large libraries. Also, fetuin and asialofetuin are not the substrates of FucTVII that are involved in selectin ligand formation.

Our aim was to use well-defined, specific oligosaccharide acceptors to ensure high specificity of the assays and optimal biochemical reaction conditions. Furthermore, substrates as natural as possible should be used for inhibitor

screening, so that the enzyme adopts a regular conformation allowing also for identification of uncompetitive inhibitors that bind to an enzyme–substrate complex. As substrates, small oligosaccharide acceptors are best for handling and specificity.

Since natural acceptors of FucTVII are 6-sulfated 3'-sialyllactosamine [6-*O*-sulfo-SLN] residues on the E-selectin and P-selectin ligand molecules ESL-1 and PSGL-1 [20], our strategy for assay development was to test whether these kinds of carbohydrate epitopes with a biotin tag are suitable *in vitro* substrates for FucTVII.

Following assay development and validation, we used this assay in a lead discovery program. In addition to screening the Schering AG compound library, we tested a set of rationally designed acceptor analogues. Depending on structural design, these glycosidic acceptor analogues may act as inhibitors or decoys of FucTVII and might serve as a starting point in the development of more drug-like inhibitors. Taking into account that issues with regard to pharmacokinetic and metabolic properties have to be solved for these acceptor analogues, they will be advantageous with regard to selectivity in comparison to donor analogues.

Materials and methods

Materials

Scintillation proximity beads precoated with streptavidine were purchased from Amersham, UK. White small-volume 384-well microtiter plates were obtained from Greiner, Frickenhausen, Germany. GDP-fucose and fetuin were purchased from Sigma: GDP-[³H]fucose (55 Ci/mmol) was from Amersham, UK. 3'-SLN-BSA was obtained from Dextra Laboratories, Reading, UK. "Complete" (EDTA free), a premixed protease inhibitor cocktail, was purchased from Roche Diagnostics, Mannheim, Germany. NP-40 was bought from Fluka. All other reagents were purchased from Sigma. Biotinylated small oligosaccharide derivatives that were used in the optimization of the SPA-based FucTVII assay and the 3'-sialyllactosamine (3'-SLN) derivatives tested as potential FucTVII inhibitors were purchased from GlycoSense AG, Jena, Germany.

Expression and purification of fucosyltransferase VII

The FucTVII catalytic domain was expressed in HEK cells as a secreted fusion protein with the N-terminal amino acids 1–63 from FucTVI as described [20].

Biotinylation of FucTVII substrate proteins

3'-SLN-BSA (2 mg) was biotinylated in 1 ml PBS using a 20-fold molar excess of Sulfo-NHS-LC-biotin (Pierce) for 2 h on ice. Excess labeling reagent was then quenched by addition of Tris buffer and removed *via* size exclusion chromatography on a NAP-5 column (Amersham, UK). Fetuin (10 mg) was labeled using a 12-fold molar excess of

³ Abbreviations used: sLex, sialyl-Lewis X; HTS, high-throughput screening; SPA, scintillation proximity assay; BSA, bovine serum albumin; NP-40, Nonidet-P40; PBS, phosphate-buffered saline; NHS, *N*-hydroxy succinimidyl; RT, room temperature; DMSO, dimethyl sulfoxide.

Sulfo-NHS-LC-biotin for 2 h on ice in 1 ml PBS. Excess labeling reagent was removed as described above.

Miniaturized scintillation proximity assay

FucTVII activity was assayed in a final volume of 15 μ l in assay buffer consisting of 50 mM Hepes, pH 7.4, 10 mM $MnCl_2$, 10% glycerol, 0.04% NP-40, and 'Complete, EDTA free' as protease inhibitor. We used 1.4 μ M 6-*O*-sulfo-sialyllactosamine, 0.25 μ M GDP-fucose, and 50 nCi GDP- 3H fucose per well as substrates and recombinant FucTVII from HEK293 cell supernatants in a final dilution of 1:15. Microtiter plates were incubated in a wet chamber for 20 h and the reaction was stopped by addition of 5 μ l stop solution (0.05 M H_2SO_4) containing 70 μ g streptavidine SPA beads. The resulting pH shift completely inactivates FucTVII. Plates were sealed and incubated for 60 min at room temperature (RT). After 15 min centrifugation at 1500 rpm, plates were measured in a topcount plate reader. Read-out time was 1 min per well.

High-throughput screening for FucTVII inhibitors

High-throughput screening was performed as usual in lead discovery programs at Schering AG before the middle of 2006. Compounds were screened in pools of 10. Briefly, each compound is placed in two independent sets of 10 compounds by use of an orthogonal matrix pooling strategy. In this approach, every compound is tested twice but in two different sets of pooled compounds. Active compounds are found after electronic deconvolution of the raw data. The pooling and deconvolution strategy has been published [21]. The 384-well ready-to-use assay plates were prepared by transferring 750-nl compound pools from mother plates with a CyBiwell pipettor (CyBio, Germany) (200 μ M each in 30% DMSO). These ready-to-use assay plates are currently being stored for up to 6 months at $-20^\circ C$ without loss of quality as determined by reproducibility of IC₅₀ values.

For screening, assay plates were thawed, brought to RT, and filled with 7.5 μ l enzyme in assay buffer. After 20 min preincubation at RT, to ensure even binding of slow-binding compounds to the enzyme, 7.5 μ l solution containing the substrates was added. The reaction was stopped by addition of streptavidine SPA beads in stop solution. After incubation for developing detection signals, plates were read in a topcount plate reader (Perkin-Elmer).

Active compounds were identified by electronic deconvolution using Schering's in-house HTS software. Compounds that caused an average inhibition above 50% with a difference between the data from two pools below 30% were picked from the Schering compound depository and submitted for retesting as single compounds. Retest reactions were done independently in triplicates and compounds with a median of inhibition above 50% were submitted for determination of IC₅₀ values using concentrations between 0.3 nM and 30 μ M.

Results and discussion

Assay development

The traditional assay format for glycosyltransferase activity is based on the selective removal of unreacted GDP- 3H fucose by ion-exchangers in batch mode and subsequent scintillation counting of 3H fucose transferred to the acceptor molecule [15]. This procedure is not suitable for HTS. Jobron and colleagues [17] developed a method based on glycosylation of *N*-acetyllactosamine immobilized on cellulose membranes, but this technique is too laborious and slow for HTS because membranes have to be washed and subjected to scintillation counting. The same holds true for use of microtiter-plate-based carbohydrate microarrays, where fucosylation was detected with a peroxidase-labeled lectin [16]. Although very elegant, this approach is not practical for screening of large libraries because it also requires washing steps.

Hood and colleagues [18] first used the HTS-compatible scintillation proximity principle for an $\alpha(1-3)$ -fucosyltransferase activity assay. In this assay, scintillant-impregnated microspheres emit light by scintillation only if the 3H fucose is in close proximity to the bead, which is the case when the acceptor is fucosylated. In the work of Hood and colleagues, SPA beads were coated with suitable glycoprotein acceptors such as fetuin, and GDP- 3H fucose and FucTVI were then added to start the reaction. The transfer of 3H fucose to the glycoprotein results in light emission, whereas the unreacted GDP- 3H fucose that remains in the mixture is not close enough to the beads to generate a signal.

The SPA assay format was also applied for FucTVII by De Vries and colleagues [20] and more recently by Miyashiro and colleagues [19]. Both groups used glycoprotein substrates such as fetuin or asialofetuin that were bound to WGA-coated SPA beads *via* the lectin. With these substrates, 1 mg SPA beads had to be used per well to generate a sufficiently strong signal in these studies. For large HTS campaigns this generates a cost issue.

We always try to use substrates as natural and specific as possible for drug discovery purposes to ensure that the enzyme is in the most natural conformation with bound substrate. Because physiological substrates are thought to be best to find all types of inhibitors, we used defined, small oligosaccharides close to the cellular substrate of FucTVII. The resulting strategy for substrate finding was to test the fucosyltransferase activity toward small oligosaccharides that mimic the PSGL-1 and ESL-1 glycosyl decoration (Table 1). According to the physiological role of FucTVII, we tested type II lactosamine-based biotinylated substrates and compared them to biotinylated fetuin which was already described as a potential acceptor in FucTVII assay. All acceptors were used in biotinylated form to make possible their use in combination with streptavidine-coated SPA beads for detection of 3H fucose transfer. The use of the streptavidine biotin system should allow a high

Table 1
Acceptor substrates

Short name	Composition
Fetuin	Fetuin-Biotin
3'SLN-BSA	Neu5Ac α -(2-3)-Gal β -(1-4)-GlcNAc β -O-BSA-Biotin
3'SLN	Neu5Ac α -(2-3)-Gal β -(1-4)-GlcNAc β -O-C ₃ H ₆ -Biotin
3'SLNL	Neu5Ac α -(2-3)-Gal β -(1-4)-GlcNAc β -(1-3)-Gal β -(1-4)-Glc β -O-C ₃ H ₆ -Biotin
6-sulfo-3'SLN	Neu5Ac α -(2-3)-Gal β -(1-4)-6-O-sulfo-GlcNAc β -O-C ₃ H ₆ -Biotin

binding (100 pmol/mg bead) and thus high signal to background ratios at low costs. The complete composition of the substrates including spacers and biotin is given in Table 1 together with the short names that will be used in the text in the following. For brevity, we will not use the complete names with spacer and biotin.

The results of the substrate comparison (shown in Fig. 1) show that small oligosaccharides are indeed very good substrates for screening purposes. Signals were increased twofold by use of 3'SLN compared to 3'SLN-BSA. The addition of a lactose residue to 3'SLN (3'SLNL) resulted in a lower signal, although closer to the natural substrate on selectin ligands. The addition of a sulfate moiety to the glucosamine unit of 3'SLN resulted in a strong increase of the signal. The traditionally applied fetuin used as a standard in our study was only half as good as the 6-*O*-sulfo-3'SLN. This result is in agreement with reports that sialation and 6-*O*-sulfation precede the fucosylation of selectin ligands [22–27]. Also, the findings of Hiraoka and colleagues [28], that the content of 6-*O*-sulfo-*N*-acetylglucosamines is increased in FucTVII knockout mice, show again that 6-*O*-sulfation is an early event that precedes the fucosylation.

Since the 6-*O*-sulfo-3'SLN gave the highest signal and is most physiological, further assay development was based on this acceptor substrate. Then, reaction conditions were optimized in order to maximize the sensitivity of the assay. The basic reaction conditions, mainly a broad pH maxi-

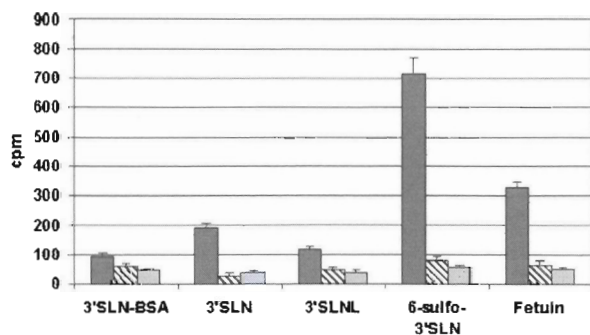


Fig. 1. [³H]fucose transfer to different acceptor substrates. All substrates were used in biotinylated form at a final concentration of 1.4 μ M. Fucose transfer was measured by SPA. Control reactions were performed without enzyme (hatched) and with enzyme inhibited by addition of stop buffer before addition of substrates (light gray). The error bars show the standard deviation obtained from triplicate measurements.

imum ranging 7–10, a sensitivity against salt, and a preference for manganese as bivalent cation described by De Vries et al. [20] could be confirmed (data not shown). The final buffer conditions are specified under Materials and methods.

Screening for inhibitors should be done at substrate concentrations around the respective K_m value to be sensitive against all kind of inhibitors [29]. Therefore, we next determined K_m values for the substrates used. First, we determined the K_m value for 6-*O*-sulfo-3'SLN (Fig. 2), which is 50 μ M. The published K_m for 3'SLN [30] was 1.6 mM. We think that we obtained a much lower K_m value for the 6-*O*-sulfo-3'SLN because it resembles the *in vivo* substrate and should bind with higher affinity than SLN.

We then determined the K_m value for GDP-fucose to be 0.12 μ M. For the published value of 6.2 μ M [20] it was unclear whether this experiment was done in presence of fetuin or 3'SLN. Britten and colleagues [30] published a very similar K_m value for GDP-fucose of 8 μ M. These authors used 3'SLN. Probably, the affinity for GDP-fucose is higher when 6-*O*-sulfo-3'SLN is bound to the enzyme compared to 3'SLN.

During further assay development we used 1.4 μ M 6-*O*-sulfo-3'SLN because the concentration of the biotinylated acceptor substrate is limited by the available binding sites on the streptavidine SPA beads. An excess of biotinylated acceptor over the binding sites on the SPA beads would even limit the signal. GDP-fucose was used at 0.25 μ M (twofold K_m) to have an efficient reaction while ensuring sensitivity toward GDP-fucose competitive inhibitors. This was important for the HTS approach because the GDP-fucose binding site is predicted to be the most drugable site, especially for the lead-like small molecules in a typical HTS library.

To ensure sensitivity to inhibition, it is mandatory to stay in the linear range of enzyme concentration and reaction time. Fig. 3A shows the enzyme titration at a 24-h reaction time. We observed linearity up to 1 μ l FucTVII preparation per 15 μ l reaction volume. For the HTS assay, a FucTVII dilution of 1:15 was chosen to stay in the linear range. Then, the linearity of the time course was tested under these conditions. The reaction is linear up to 25 h (Fig. 3B). Obviously, the recombinant FucTVII is very stable at room temperature. For practical reasons, a 20-h overnight incubation time was chosen. This is in agreement with data from Hood and colleagues [18] who used a 16-h incubation at 22 $^{\circ}$ C for their FucTVII and FucTIII assays.

Keeping the enzyme and substrate concentrations and the reaction time of 20 h, SPA beads were titrated to maximize the signal to background ratio. The signal reached a maximum at 130 μ g per well but the background significantly increased with bead concentration (Fig. 4). The signal to background ratio showed an optimum >20 between 50 and 100 μ g beads/well. The screening assay was then set to 70 μ g SPA beads per well in consideration of signal and assay costs. Compared to the published assays [18–20], this is a factor 14 reduction in bead costs. A signal to back-

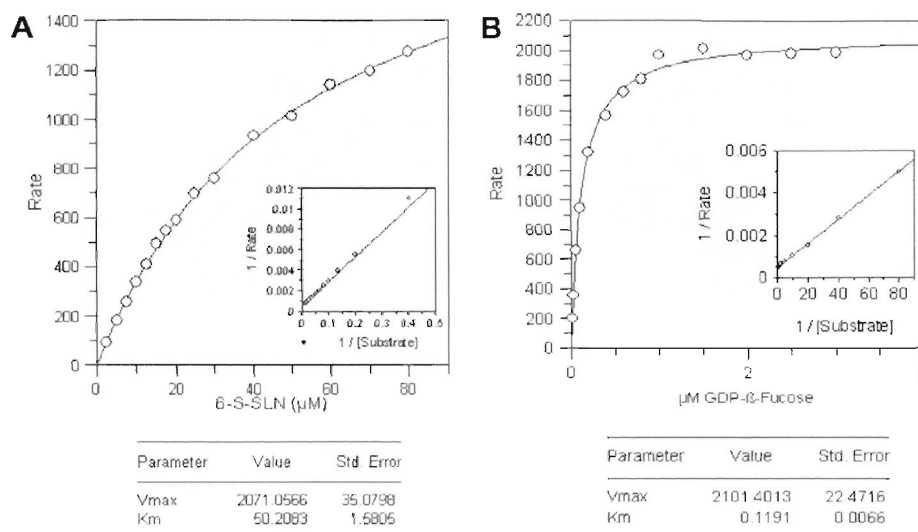


Fig. 2. (A) K_m values for 6-*O*-sulfo-3'SLN, (B) K_m values for GDP-fucose. The K_m values were determined by plotting initial rates in cpm per minute versus substrate concentration. Every time point at every substrate concentration was measured in quadruplicates (variance around 5%). Graft software was used for linear regression of the initial rates and for the Michaelis–Menten plot. Lineweaver–Burk plots are shown as insets.

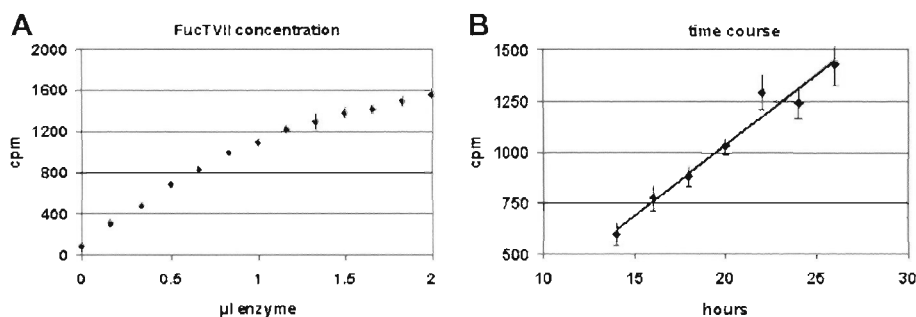


Fig. 3. Reaction kinetics and dependence on enzyme concentration. (A) Titration of FucTVII (μ l per 15 μ l assay volume); 1.4 μ M 6-*O*-sulfo-3'SLN and 0.25 μ M GDP-fucose were used. The reaction was run for 24 h, stopped, and incubated with SPA beads (100 μ g/well) for 1 h before measuring. (B) Time course of the reaction with 1 μ l FucTVII in 15 μ l final assay volume containing 1.4 μ M 6-*O*-sulfo-3'SLN and 0.25 μ M GDP-fucose. The error bars show the standard deviation obtained from triplicate measurements.

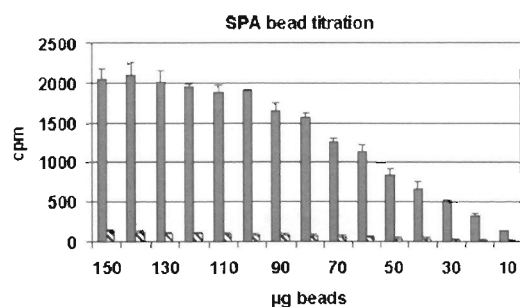


Fig. 4. Titration of SPA beads. PVT SPA beads were titrated over the usual range used in our laboratory. Signals are shown in gray; the background values without FucTVII enzyme are shown as hatched columns. The error bars show the standard deviation obtained from triplicate measurements.

ground ratio >20 was reached with 1.85 kBq GDP-fucose, which is in the range that Hood et al. [18] (1.66 kBq) and Miyashiro et al. [19] (5 kBq) also used.

FucTVII proved to be very stable against freeze/thaw cycles as shown in Fig. 5A. Up to five freeze/thaw cycles are tolerated without loss of activity.

The sensitivity of enzymes toward DMSO is often a critical parameter in assay development. Therefore, we checked whether FucTVII may be inhibited by DMSO in the concentrations typically applied during screening. Fig. 5B shows that recombinant FucTVII is not influenced by DMSO in concentrations up to 5%. This is far more than our final DMSO concentration of 1.5% that results from addition of screening library compounds.

Finally, the validity of the FucTVII assay was tested using 6-F-GDP-fucose as reference inhibitor [31] (Fig. 6). 6-F-GDP-fucose is able to block FucTVII activity to 100%. Its IC_{50} value was determined to be 0.64 μ M, which corresponds to a K_i value of 0.2 μ M. Thus, the assay is sensitive to specific inhibitors and suitable for screening. When the dilutions of 6-F-GDP-fucose were performed in 0.04% NP-40 in water or pure water instead of 30% DMSO in

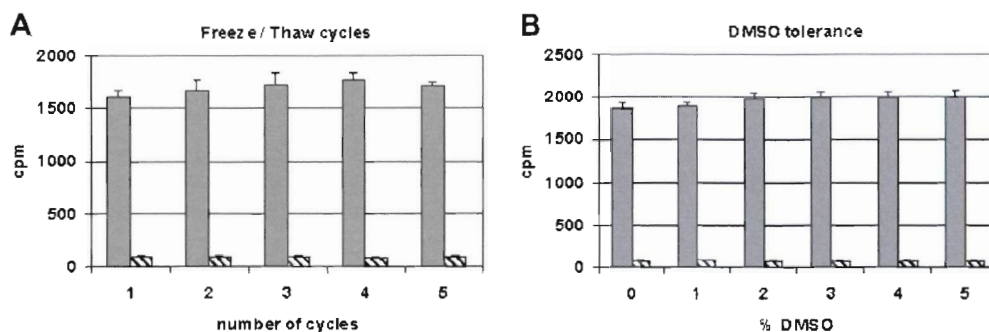
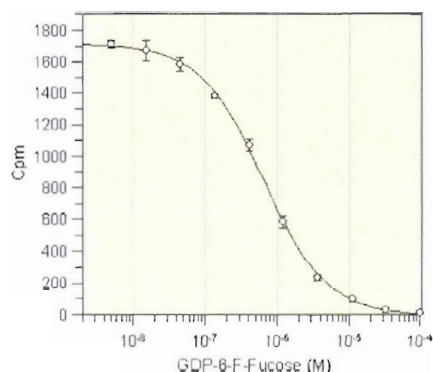


Fig. 5. Freeze/thaw tolerance and DMSO tolerance of recombinant FucTVII. (A) The enzyme was subjected to the indicated number of freeze/thaw cycles in liquid nitrogen before starting the reaction by addition of substrates. (B) Sensitivity toward DMSO was tested by running the reaction in presence of DMSO as indicated. Signals are shown in gray, the background values without FucTVII enzyme are shown as hatched columns. The error bars show the standard deviation obtained from triplicate measurements.



Parameter	Value	Std. Error
Y Range	1722.0211	25.0751
IC 50	6.43259e-007	2.82423e-008
Slope factor	0.9843	0.0404
Background	-7.1406	15.2204

Fig. 6. IC₅₀ of the tool compound 6-F-GDP-fucose. The inhibitor was titrated from 5 nM to 100 μ M final concentration and the assay performed as described under Materials and methods. Average cpm values after background subtraction (reaction without enzyme) are displayed. All samples were tested in triplicates; the standard deviations are shown as error bars. GraFit software was used to plot signal versus inhibitor concentration.

water, the IC₅₀s were 0.77 or 0.63 μ M, respectively. So the IC₅₀ value of 6-F-GDP-Fucose was nicely reproducible and independent of the solvents used for dilution.

The assay quality is very high. The assay window (signal to background ratio) between control and inhibitor control (100 μ M 6-F-GDP-fucose) was above 20. The z' factor [32] was around 0.8, which indicates a very high statistical resolution of the assay. Previous studies reported signal to background ratios between 5 and 10 only.

Assay performance in high-throughput screening

The assay proved to be very robust and suitable for high-throughput screening. In total 480 microtiter plates (384-well plates) containing 798,131 compounds were measured in 7 days of primary screening.

Assay quality was continuously monitored during screening (Fig. 7). The z' values were stable around 0.8, indicating an excellent statistical resolution. The signal to background ratio started at 20 as during assay development and increased later, beginning with plate number 316 due to the use of a new batch of GDP-[³H]fucose with higher specific activity and a new batch of recombinant FucTVII during the second part of the screening campaign.

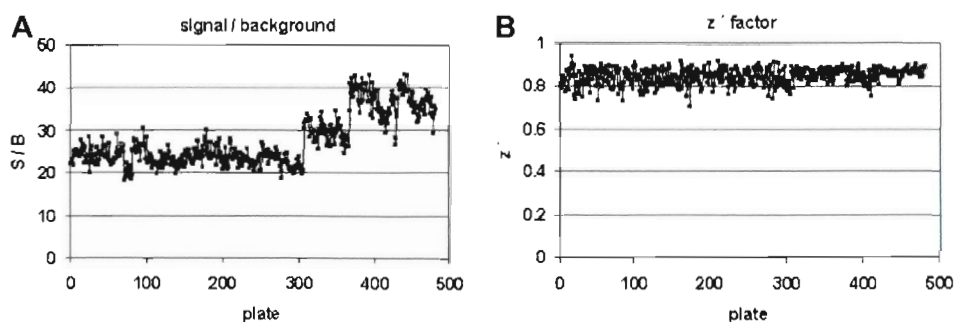


Fig. 7. Assay performance during HTS. (A) The signal to background ratios were calculated platewise using the 12 neutral controls and 6 inhibitor controls (100 μ M 6-F-GDP-fucose) that were included on every assay plate during the HTS run. (B) The z' value as measure of statistical quality was calculated according to Zhang et al. [32] using the control wells as described in (A).

This batch gave initially high signal to background values up to 40 but was apparently not as stable as the first batch since the S/B slightly decreased during a HTS run as seen in Fig. 7A. This did not significantly affect the statistical quality of the assay expressed as z' value (Fig. 7B).

Following the primary screening, 1959 compounds that caused more than 50% inhibition of FucTVII activity were retested; 557 of these primary hits were confirmed by single retests. The confirmation rate of 28% is rather typical for a screening approach that uses pools of 10 compounds in the primary screen. In pool screening many positional false positive hits can result from electronic deconvolution if the hit rate is high [21]. IC₅₀ determinations for the confirmed hits resulted in 223 hits with IC₅₀s below 30 μ M. These hits were then tested for selectivity against α -fucosidase and galactosyltransferase. Only 4 hits inhibited galactosyltransferase (data not shown). So the HTS assay for FucTVII identified specific inhibitors. Since the galactosyltransferase assay was also based on the scintillation proximity assay, it ensured that the vast majority of the FucTVII hits were not interfering with the detection system ("assay interference").

Results from rational design of acceptor analogues

In addition to high-throughput screening of the Schering compound library for small-molecule inhibitors we tried to identify inhibitors of FucTVII by rational design based on the knowledge from the literature and that gained during our assay development. Up to now, several inhibitors of FucTs in general have been published. They are already quite potent but based mainly on donor analogues, i.e., GDP-fucose, and therefore not selective toward a specific fucosyltransferase isoform [31,33–35]. Acceptor or bisubstrate analogues have also been synthesized but have displayed rather weak inhibitory properties so far [35–37].

We decided to concentrate our approach on acceptor analogues. This might give us the chance to obtain selective derivatives by taking advantage of the acceptor specificities between the different fucosyltransferases [26,38,39].

It has been reported that FucTVII is able to fucosylate only α -(2→3)-sialylated, small *N*-acetylglucosamine type 2 structures and is inactive with asialo acceptors [30,40,41]. Changes were therefore introduced in the fucosylation site, the 3-position on the glucosamine of sialyllactosamine. We planned to investigate whether unreactive in the broader sense bioisosteric residues such as OMe (**5a**), H (**5b**), F (**5c**), NH₂ (**5d**), NHCOCH₃ (**5e**), NHCOCF₃ (**5f**), or NHCONHCH₃ (**5g**) can be utilized instead of OH to generate acceptor analogues that are recognized by FucTVII and cause inhibition. As it is also described and confirmed by us that sulfated sialyllactosamines are the best substrates for FucTVII, a sulfate residue at O-6 of glucosamine (**5h**) was introduced to increase the affinity of a potential inhibitor with C-3 OMe (Table 2).

Unfortunately, none of the 3-dehydroxy sialyllactosamine derivatives tested showed any inhibition of the

enzyme. It seems that the hydroxy group is strictly required for binding. No changes, not even methylation, were tolerated. Obviously, the 3-hydroxy group not only is the site of fucosylation but also is essential for the conformation of the trisaccharide and the substrate recognition by FucTVII.

Metabolic inhibition by acceptor substrates provides another promising way to interfere with glycoconjugate biosynthesis [42–44]. Carbohydrate moieties of naturally occurring glycoproteins can compete with them as substrates for glycosyltransferases, diverting oligosaccharide biosynthesis from endogenous glycoconjugates to these synthetic carbohydrates. It has been shown that treatment of cancer cells with a *N*-acetylglucosamine (LacNAc) decoy could interfere with metastasis [45]. Acceptor analogues as precursors of sLex derivatives might also act as selectin blockers, if they are secreted from the cells and maintain affinity to the selectins. Such soluble sLex derivatives could protect against inflammatory cell migration as described [46]. The use of soluble sLex mimetics has been reviewed by Kaila & Thomas [47].

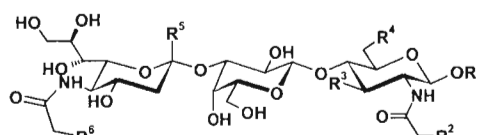
LacNAc is, however, a substrate for a wide range of glycosyltransferases. Therefore it is our aim to develop oligosaccharide decoys that would specifically target FucTVII. On the other hand, the hydrophilic nature of sugars prevents these acceptor-based decoys from permeating the cell membrane. To solve this problem, the partial methylation, acetylation, or acetyloxymethylation of hydroxyl groups has been shown to be effective [48–50].

We started with the identification of functional groups that are essential for recognition and others that can be modified to enhance the affinity of the acceptor. A maximal simplification of the structure in addition to peracetylation has to be achieved to receive metabolically stable and bioavailable decoys. For metabolic stability, the introduction of S- or C-glycosides, carbosugars, or fluorine residues may be necessary later.

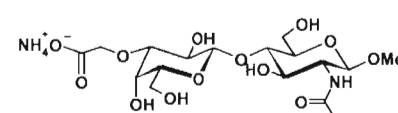
Sialic acid is necessary for recognition of the substrate by FucTVII but sialic acid bears several additional functional groups, especially the charged carboxylate. The attempt to replace the carboxylate by an amide (**5r**) or hydroxymethyl group (**5s**) and the substitution of sialic acid by acetic acid (**5t**) resulted in complete loss of affinity. Therefore, it is not just simply replaceable by the presence of a negative charge as attempted with the substitution by acetic acid. These findings are in agreement with the observations by Britten et al. [36] who found that the fucosylation by FucTVI is reduced to 9% if sialic acid is substituted by a sulfate.

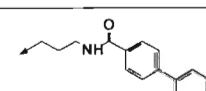
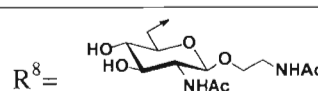
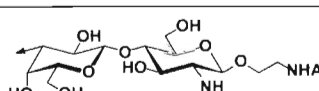
It has also been demonstrated that hydrophobic aglycons and per-O-acetylation enable the cell and Golgi uptake of disaccharides leading to the downregulation of sLex ligand expression [51]. Additionally, those acceptor analogues showed enhanced enzyme-binding affinity toward FucTIV and FucTVI with greater hydrophobicity of the aglycon moiety.

Table 2
Fucosyl acceptor analogues of 3'SLN as potential inhibitors or decoys of FTVII



No.	R ¹	R ²	R ³	R ⁴	R ⁵	R ⁶	IC ₅₀ μM
5a	CH ₃	H	CH ₃ O	OH	CO ₂ ⁻ NH ₄ ⁺	H	> 300
5b	CH ₃	H	H	OH	CO ₂ ⁻ NH ₄ ⁺	H	> 300
5c	CH ₃	H	F	OH	CO ₂ ⁻ NH ₄ ⁺	H	> 300
5d	CH ₃	H	H ₂ N	OH	CO ₂ ⁻ NH ₄ ⁺	H	> 300
5e	CH ₃	H	CH ₃ CONH	OH	CO ₂ ⁻ NH ₄ ⁺	H	> 300
5f	CH ₃	H	CF ₃ CONH	OH	CO ₂ ⁻ NH ₄ ⁺	H	> 300
5g	CH ₃	H	CH ₃ NHCONH	OH	CO ₂ ⁻ NH ₄ ⁺	H	> 300
5h	CH ₃	H	CH ₃ O	OSO ₃ ⁻ NH ₄ ⁺	CO ₂ ⁻ NH ₄ ⁺	H	> 300
5i	CH ₃	H	HO	OH	CO ₂ ⁻ NH ₄ ⁺	H	51.6
5j	CH ₃	H	HO	OSO ₃ ⁻ NH ₄ ⁺	CO ₂ ⁻ NH ₄ ⁺	H	10.4
5k	CH ₃	H	HO	H	CO ₂ ⁻ NH ₄ ⁺	H	27.9
5l	CH ₃	OH	HO	OH	CO ₂ ⁻ NH ₄ ⁺	H	> 300
5m	(CH ₂) ₃ NH ₂	H	HO	OH	CO ₂ ⁻ NH ₄ ⁺	OH	35.0
5n	(CH ₂) ₃ NH ₂	H	HO	OH	CO ₂ ⁻ NH ₄ ⁺	H	227
5o	R ⁷	H	HO	OH	CO ₂ ⁻ NH ₄ ⁺	H	14.3
5p	R ⁸	H	HO	OH	CO ₂ ⁻ NH ₄ ⁺	H	34.7
5q	R ⁹	H	HO	OH	CO ₂ ⁻ NH ₄ ⁺	H	83.8
5r	CH ₃	H	HO	OH	CO ₂ NH ₂	H	> 300
5s	CH ₃	H	HO	OH	CH ₂ OH	H	> 300

5t		> 300
----	---	-------

R ⁷ =		R ⁸ =		R ⁹ =	
------------------	---	------------------	---	------------------	---

The natural substrate of FucTVII is a glycoprotein carrying 3'SLN-terminated polygalactosamine chains. Therefore, we compared the influence of different aglycons (R¹) for affinity to FucTVII, e.g., O-Me (5i), propyl amine (5n), biphenyl-4-carboxylic acid propyl amide (5o), GalNAc (5p), and LacNAc (5q). The highest affinity was achieved with the most hydrophobic aglycon biphenyl-4-carboxylic acid propyl amide (5o, IC₅₀ = 14 μM) which is advantageous with regard to drug likeness.

It is beyond dispute that an acceptor analogue with a 6-O-sulfated glucosamine most closely resembles the natural substrate. As expected, the corresponding derivative (5j) showed the highest affinity (IC₅₀ = 10 μM), but the more favorable 6-deoxy derivative (5k) also showed an acceptable affinity toward FucTVII (IC₅₀ = 28 μM).

Our results during search for an assay substrate and the results for the acceptor analogues show that the 6-O-sulfo-GlcNAc modification is required for 3'SLN to bind efficiently to FucTVII. However, the 6-deoxy derivative is also accepted as a glycosidic decoy. A combination with a hydrophobic biphenyl or similar aglycon will probably result in enhanced affinity.

Conclusions

Different assay formats have been used for detection of glycosyltransferase activity. The traditional approaches such as ion exchange, hydrophobic chromatography, gel filtration, TLC, or microtiter-plate-based microarray approaches that require washing steps are not HTS compatible. We have developed a miniaturized high-throughput assay for FucTVII based on the scintillation proximity principle. By using the natural oligosaccharide acceptor substrate, we reached a very high signal to background ratio of 20 that allowed us to miniaturize the assay to 15 μl reaction volume in 384-well plates. We were able to reduce the bead concentration and thus costs to less than 10% of previously reported values while increasing the assay quality. Using this assay we ran a HTS campaign with very good quality ($z' > 0.7$) at affordable costs of 16 cents per well. This HTS campaign identified 229 selective IC₅₀ hits that did not inhibit galactosyltransferase and α-fucosidase nor interfered with the detection system.

Our results during search for an acceptor oligosaccharide and the results for the acceptor analogues show that

substrate analogues have to be similar to the natural substrate to work as decoys for FucTVII. The development of metabolically stable and bioavailable decoys by simplification of the complex saccharide structure seems extremely challenging. Further candidates have to combine the hydrophobic biphenyl aglycon and the 6-deoxy residue where we expect an increase in affinity. However, due to the very narrow Structure–activity relation and the long way from glycosidic inhibitors to drug-like molecules, we think that the probability of success for this approach is relatively low. Therefore, future efforts in search for FucT-VII inhibitors should rather focus on in-depth characterization and optimization of hits identified in the HTS campaign but this will not be pursued due to patent constraints.

Acknowledgments

We thank Ulrich Zügel and Christian Bergsdorf for critical reading of the manuscript and very productive discussions and Bärbel Bennua-Skalmowski for synthesis of 6F-GDP-fucose. We are also grateful to Jorg Kroll and colleagues from the Compound Logistics Laboratory for supply of test compounds.

References

- [1] T.A. Springer, Traffic signals for lymphocyte recirculation and leukocyte emigration: the multistep paradigm, *Cell* 76 (1994) 301–314.
- [2] M.P. Schon, T.M. Zollner, W.H. Boehncke, The molecular basis of lymphocyte recruitment to the skin: clues for pathogenesis and selective therapies of inflammatory disorders, *J. Invest. Dermatol.* 121 (2003) 951–962.
- [3] K. Ley, The role of selectins in inflammation and disease, *Trends Mol. Med.* 9 (2003) 263–268.
- [4] S. Thoma, K. Bonhagen, D. Vestweber, A. Hamann, J. Reimann, Expression of selectin-binding epitopes and cytokines by CD4+ T cells repopulating scid mice with colitis, *Eur. J. Immunol.* 28 (1998) 1785–1797.
- [5] W. Tietz, Y. Allemand, E. Borges, D. von Laer, R. Hallmann, D. Vestweber, A. Hamann, CD4+ T cells migrate into inflamed skin only if they express ligands for E- and P-selectin, *J. Immunol.* 161 (1998) 963–970.
- [6] T. Collins, M.A. Read, A.S. Neish, M.Z. Whitley, D. Thanos, T. Maniatis, Transcriptional regulation of endothelial cell adhesion molecules: NF- κ B and cytokine-inducible enhancers, *FASEB J.* 9 (1995) 899–909.
- [7] C. Kneuer, C. Ehrhardt, M.W. Radomski, U. Bakowsky, Selectins – potential pharmaceutical targets? *Drug Discov. Today* 11 (2006) 1034–1040.
- [8] J.B. Lowe, Glycosylation in the control of selectin counter-receptor structure and function, *Immunol. Rev.* 186 (2002) 19–36.
- [9] A.J. Schottelius, A. Hamann, K. Asadullah, Role of fucosyltransferases in leukocyte trafficking: major impact for cutaneous immunity, *Trends Immunol.* 24 (2003) 101–104.
- [10] T.M. Zollner, K. Asadullah, Selectin and selectin ligand binding: a bittersweet attraction, *J. Clin. Invest.* 112 (2003) 980–983.
- [11] K. Ley, G.S. Kansas, Selectins in T-cell recruitment to non-lymphoid tissues and sites of inflammation, *Nat. Rev. Immunol.* 4 (2004) 325–335.
- [12] W. Wening, L.H. Ulfman, G. Cheng, N. Souchkova, E.J. Quackenbush, J.B. Lowe, U.H. von Andrian, Specialized contributions by alpha(1,3)-fucosyltransferase-IV and FucT-VII during leukocyte rolling in dermal microvessels, *Immunity* 12 (2000) 665–676.
- [13] I. Erdmann, E.P. Scheidegger, F.K. Koch, L. Heinzerling, B. Odermatt, G. Burg, J.B. Lowe, T.M. Kundig, Fucosyltransferase VII-deficient mice with defective E-, P-, and L-selectin ligands show impaired CD4+ and CD8+ T cell migration into the skin, but normal extravasation into visceral organs, *J. Immunol.* 168 (2002) 2139–2146.
- [14] F. Austrup, D. Vestweber, E. Borges, M. Lohning, R. Brauer, U. Herz, H. Renz, R. Hallmann, A. Scheffold, A. Radbruch, A. Hamann, P- and E-selectin mediate recruitment of T-helper-1 but not T-helper-2 cells into inflamed tissues, *Nature* 385 (1997) 81–83.
- [15] J.P. Prieels, D. Monnom, M. Dolmans, T.A. Beyer, R.L. Hill, Copurification of the Lewis blood group N-acetylglucosaminide α 1-4 fucosyltransferase and an N-acetylglucosaminide α 1-3 fucosyltransferase from human milk, *J. Biol. Chem.* 256 (1981) 10456–10463.
- [16] M.C. Bryan, L.V. Lee, C.H. Wong, High-throughput identification of fucosyltransferase inhibitors using carbohydrate microarrays, *Bioorg. Med. Chem. Lett.* 14 (2004) 3185–3188.
- [17] L. Jobron, K. Sujino, G. Hummel, M.M. Palcic, Glycosyltransferase assays utilizing N-acetylglucosamine acceptor immobilized on a cellulose membrane, *Anal. Biochem.* 323 (2003) 1–6.
- [18] C.M. Hood, V.A. Kelly, M.I. Bird, C.J. Britten, Measurement of α -(1-3) fucosyltransferase activity using scintillation proximity, *Anal. Biochem.* 255 (1998) 8–12.
- [19] M. Miyashiro, S. Furuya, T. Sugita, A high-throughput screening system for α 1-3 fucosyltransferase-VII inhibitor utilizing scintillation proximity assay, *Anal. Biochem.* 338 (2005) 168–170.
- [20] T. de Vries, J. Storm, F. Rotteveel, G. Verdonk, M. van Duin, D.H. van den Eijnden, D.H. Joziassse, H. Bunschoten, Production of soluble human α 3-fucosyltransferase (FucT VII) by membrane targeting and in vivo proteolysis, *Glycobiology* 11 (2001) 711–717.
- [21] J.J. Devlin, A. Liang, L. Trinh, M.A. Polokoff, D. Senator, W. Zheng, J. Kondracki, P.J. Kretschmer, J. Morser, S.E. Lipsen, R. Spann, J.A. Loughlin, K.V. Dunn, M.M. Morrissey, High capacity screening of pooled compounds: Identification of the active compound without re-assay of pool members, *Drug Dev. Res.* 37 (1996) 80–85.
- [22] D. Crommie, S.D. Rosen, Biosynthesis of GlyCAM-1, a mucin-like ligand for L-selectin, *J. Biol. Chem.* 270 (1995) 22614–22624.
- [23] E.V. Chandrasekaran, R.K. Jain, R.D. Larsen, K. Wlasicuk, K.L. Matta, Selectin ligands and tumor-associated carbohydrate structures: specificities of α -2,3-sialyltransferases in the assembly of 3'-sialyl-6-sialyl/sulfo Lewis x and x, 3'-sialyl-6'-sulfo Lewis x, and 3'-sialyl-6-sialyl/sulfo blood group T-hapten, *Biochemistry* 34 (1995) 2925–2936.
- [24] R.G. Spiro, V.D. Bhojroo, Characterization of a spleen sulphotransferase responsible for the 6-O-sulphation of the galactose residue in sialyl-N-acetyl-lactosamine sequences, *Biochem. J.* 331 (1998) 265–271.
- [25] N. Kimura, C. Mitsuoka, A. Kanamori, N. Hiraiwa, K. Uchimura, T. Muramatsu, T. Tamatani, G.S. Kansas, R. Kannagi, Reconstitution of functional L-selectin ligands on a cultured human endothelial cell line by cotransfection of α 1 \rightarrow 3 fucosyltransferase VII and newly cloned GlcNAc β :6-O-sulfotransferase cDNA, *Proc. Natl. Acad. Sci. USA* 96 (1999) 4530–4535.
- [26] K. Fukunaga, K. Shinoda, H. Ishida, M. Kiso, Systematic synthesis of sulphated sialyl-a-(2,3)-neolactotetraose derivatives and their acceptor specificity for an α -(1,3)-fucosyltransferase(Fuc-TVII) involved in the biosynthesis of L-selectin ligand, *Carbohydrate Research* 328 (2000) 85–94.
- [27] K. Honke, N. Ikeda, N. Taniguchi, Differences in recognition of sulfated and sialylated carbohydrate chains, *Methods Enzymol.* 363 (2003) 222–229.
- [28] N. Hiraoka, B. Petryniak, H. Kawashima, J. Mitoma, T.O. Akama, M.N. Fukuda, J.B. Lowe, M. Fukuda, Significant decrease of $\{\alpha\}$ 1,3-linked fucose is associated with increase in 6-sulfated N-acetylglucosamine in peripheral node addressin of FucT-VII deficient mice exhibiting diminished lymphocyte homing, *Glycobiology* 17 (2007) 277–293.

- [29] R.A. Copeland, Mechanistic considerations in high-throughput screening, *Anal. Biochem.* 320 (2003) 1–12.
- [30] C.J. Britten, D.H. van den Eijnden, W. McDowell, V.A. Kelly, S.J. Witham, M.R. Edbrooke, M.I. Bird, T. de Vries, N. Smithers, Acceptor specificity of the human leukocyte α (1-3) fucosyltransferase: role of FucT-VII in the generation of selectin ligands, *Glycobiology* 8 (1998) 321–327.
- [31] M.D. Burkart, S.P. Vincent, A. Duffels, B.W. Murray, S.V. Ley, C.H. Wong, Chemo-Enzymatic Synthesis of Fluorinated Sugar Nucleotide: Useful Mechanistic Probes for Glycosyltransferases, *Bioorg. Med. Chem.* 8 (2000) 1937–1946.
- [32] J.H. Zhang, T.D. Chung, K.R. Oldenburg, A Simple Statistical Parameter for Use in Evaluation and Validation of High Throughput Screening Assays, *J. Biomol. Screen.* 4 (1999) 67–73.
- [33] L.V. Lee, M.L. Mitchell, S.J. Huang, V.V. Fokin, K.B. Sharpless, C.H. Wong, A Potent and Highly Selective Inhibitor of Human α -1,3-Fucosyltransferase via Click Chemistry, *J. Am. Chem. Soc.* 125 (2003) 9588–9589.
- [34] M.L. Mitchell, F. Tian, L.V. Lee, C.H. Wong, Synthesis and Evaluation of Transition-State Analogue Inhibitors of α -1,3-Fucosyltransferase, *Angew. Chem. Int. Ed.* 16 (2002) 3041–3044.
- [35] V. Filippov, H. van den Elst, M. Tromp, G.A. van der Marel, C.A.A. van Boeckel, H.S. Overkleef, J.H. van Boom, Parallel Solid Phase Synthesis of Tricomponent Bisubstrate Analogues as Potential Fucosyltransferase Inhibitors, *Synlett* 5 (2004) 773–778.
- [36] B.R. Bowen, I. Jefferies, Synthesis of inhibitors of α -1,3-fucosyltransferase, *Bioorg. Med. Chem. Lett.* 7 (1997) 1171–1174.
- [37] P. Compain, O.R. Martin, Design Synthesis and Biological Evaluation of Iminosugar-Based Glycosyltransferase Inhibitors, *Curr. Topics Med. Chem.* 3 (2003) 541–560.
- [38] K. Shinoda, E. Tanahashi, K. Fukunaga, H. Ishida, M. Kiso, Detailed acceptor specificities of human α 1,3-fucosyltransferases, Fuc-TVII and Fuc-TVI, *Glycoconjugate J.* 15 (1998) 969–974.
- [39] E. Grabenhorst, M. Nímtz, J. Costa, H.S. Conradt, *In Vivo* Specificity of Human α 1,3/4-Fucosyltransferases III-VII in the Biosynthesis of LewisX and Sialyl LewisX Motifs on Complex-type N -Glycans, *J. Biol. Chem.* 273 (1998) 30985–30994.
- [40] K. Sasaki, K. Kurata, K. Funayama, M. Nagata, E. Watanabe, S. Ohta, N. Hanai, T. Nishi, Expression cloning of a novel α 1,3-fucosyltransferase that is involved in biosynthesis of the sialyl Lewis x carbohydrate determinants in leukocytes, *J. Biol. Chem.* 269 (1994) 14730–14737.
- [41] S. Natsuka, K.M. Gersten, K. Zenita, R. Kannagi, J.B. Lowe, Molecular cloning of a cDNA encoding a novel human leukocyte α -1,3-fucosyltransferase capable of synthesizing the sialyl Lewis x determinant, *J. Biol. Chem.* 269 (1994) 16789–16794.
- [42] J.R. Brown, M.M. Fuster, J.D. Esko, Glycoside Decoys of Glycosylation, *Trends Glycosci. Glycotechnol.* 13 (2001) 335–343.
- [43] J.R. Brown, M.M. Fuster, T. Whisenant, J.D. Esko, Expression Patterns of 2,3-Sialyltransferases and 1,3-Fucosyltransferases Determine the Mode of Sialyl Lewis X Inhibition by Disaccharide Decoys, *J. Biol. Chem.* 278 (2003) 23352–23359.
- [44] M.C. Galan, C.S. Dodson, A.P. Venot, G.J. Boons, Glycosyltransferase activity can be selectively modulated by chemical modifications of acceptor substrates, *Bioorg. Med. Chem. Lett.* 14 (2004) 2205–2208.
- [45] M.M. Fuster, J.R. Brown, L. Wang, J.D. Esko, A Disaccharide Precursor of Sialyl Lewis X Inhibits Metastatic Potential of Tumor Cells, *Cancer Res.* 63 (2003) 2775–2781.
- [46] M.S. Mulligan, J.B. Lowe, R.D. Larsen, J. Paulsen, Z.L. Zheng, S. DeFrees, K. Maemura, M. Fukuda, P.A. Ward, Protective Effects of sialylated Oligosaccharides in Immune Complex-induced Acute Lung Injury, *J. Exp. Med.* 178 (1993) 623–631.
- [47] N. Kaila, B.E. Thomas, Design and Synthesis of Sialyl LewisX Mimetics as E- and P-Selectin Inhibitors, *Med. Res. Rev.* 22 (2002) 566–601.
- [48] A.K. Sarkar, T.A. Fritz, W.H. Taylor, J.D. Esko, Disaccharide uptake and priming in animal cells: inhibition of sialyl Lewis X by acetylated Gal beta 1→4GlcNAc beta-O-naphthalenemethanol, *Proc. Natl. Acad. Sci. USA* 92 (1995) 3323–3327.
- [49] A.K. Sarkar, K.S. Rostand, R.K. Jain, K.L. Matta, J.D. Esko, Fucosylation of Disaccharide Precursors of Sialyl LewisX Inhibit Selectin-mediated Cell Adhesion, *J. Biol. Chem.* 272 (1997) 25608–25616.
- [50] A.K. Sarkar, J.R. Brown, J.D. Esko, Synthesis and glycan priming activity of acetylated, *Carbohydr. Res.* 329 (2000) 287–300.
- [51] T.K.-K. Mong, L.V. Lee, J.R. Brown, J.D. Esko, C.-H. Wong, Synthesis of N-Acetylactosamine Derivatives with Variation in the Aglycon Moiety for the Study of Inhibition of Sialyl Lewis x Expression, *Chem. Bio. Chem.* 4 (2003) 835–840.

The Role of Mitogen-Activated Protein Kinase-Activated Protein Kinase 2 in the p38/TNF- α Pathway of Systemic and Cutaneous Inflammation

Arndt J. Schottelius¹, Ulrich Zügel², Wolf-Dietrich Döcke³, Thomas M. Zollner³, Lars Röse³, Anne Mengel⁴, Bernd Buchmann⁴, Andreas Becker⁵, Gerald Grütz⁶, Sandra Naundorf⁶, Anke Friedrich⁶, Matthias Gaestel⁷ and Khusru Asadullah³

Mitogen-activated protein kinase-activated protein kinase 2 (MK2) is a downstream molecule of p38, involved in the production of TNF- α , a key cytokine, and an established drug target for many inflammatory diseases. We investigated the role of MK2 in skin inflammation to determine its drug target potential. MK2 deficiency significantly decreased plasma TNF- α levels after systemic endotoxin application. Deficient mice showed decreased skin edema formation in chronic 2-*O*-tetradecanoylphorbol-13-acetate (TPA)-induced irritative dermatitis and in subacute 2,4-dinitrofluorobenzene (DNFB)-induced contact hypersensitivity. Surprisingly, MK2 deficiency did not inhibit edema formation in subacute 2,4-dinitrochlorobenzene (DNCB)-induced contact allergy and even increased TNF- α and IL-1 β levels as well as granulocyte infiltration in diseased ears. Ear inflammation in this model, however, was inhibited by TNF- α neutralization as it was in the subacute DNFB model. MK2 deficiency also did not show anti-inflammatory effects in acute DNFB-induced contact hypersensitivity, whereas the p38 inhibitor, SB203580, ameliorated skin inflammation supporting a pathophysiological role of p38. When evaluating possible mechanisms, we found that TNF- α production in MK2-deficient spleen cells was strongly diminished after TLR stimulation but less affected after T-cell receptor stimulation. Our data suggest that MK2, in contrast to its downstream effector molecule, TNF- α , has a rather elusive role in T-cell-dependent cutaneous inflammation.

Journal of Investigative Dermatology (2010) **130**, 481–491; doi:10.1038/jid.2009.218; published online 6 August 2009

INTRODUCTION

Mitogen-activated protein kinase (MAPK)-activated protein kinase 2 (MK2) is one of several kinases that are regulated exclusively through direct phosphorylation by p38 MAP kinase in response to stress stimuli (Gaestel, 2006). The role of the stress-activated p38 MAPK protein kinase cascade in

inflammation was defined several years ago by the anti-inflammatory effect of the p38 inhibitor, SB203580, and related compounds (Lee *et al.*, 1994; Jackson *et al.*, 1998). Accordingly, it was expected that several components of this kinase cascade may have been essential for early signaling in the inflammatory response and therefore yielded targets for anti-inflammatory therapy. Targeted disruption of p38 in mice results in embryonic lethality and impaired interleukin (IL)-1 signaling (Allen *et al.*, 2000). Deletion of one of the two known specific upstream activators of p38, the dual-specific MAPK kinase 3 (MKK3), leads to a reduction in IL-12 production (Lu *et al.*, 1999) and impaired tumor necrosis factor (TNF)- α -induced cytokine expression (Wysk *et al.*, 1999), and heterozygosity for p38 α reduces ear swelling and cell infiltration in acute DNFB-induced contact allergy (Takanami-Ohnishi *et al.*, 2002).

Mice deficient in MK2 showed a reduction in bacterial lipopolysaccharide (LPS)-induced biosynthesis of TNF- α , interferon (IFN)- γ , IL-1 β , IL-6, and nitric oxide, suggesting a critical role of MK2 in inflammatory cytokine production and inflammation (Kotlyarov *et al.*, 1999). It was later shown that MK2 regulates biosynthesis of IL-6 at the levels of mRNA stability and of TNF- α mainly through an AU-rich element-dependent translational control (Neininger *et al.*, 2002). The

¹MorphoSys AG, Martinsried, Germany; ²Common Mechanism Research Early Projects, Global Drug Discovery, Bayer Schering Pharma AG, Berlin, Germany; ³Target Discovery, Global Drug Discovery, Bayer Schering Pharma AG, Berlin, Germany; ⁴Medicinal Chemistry, Global Drug Discovery, Bayer Schering Pharma AG, Berlin, Germany; ⁵Protein Supply, Global Drug Discovery, Bayer Schering Pharma AG, Berlin, Germany; ⁶Institute of Medical Immunology, Charité University Medicine, Berlin, Germany and ⁷Center for Biochemistry/Institute of Biochemistry, Medical School of Hannover, Hannover, Germany

Correspondence: Dr Arndt J. Schottelius, MorphoSys AG, D-82152 Planegg/Martinsried, Germany. E-mail: arndt.schottelius@morphosys.com

Abbreviations: DNCB, 2,4-dinitrochlorobenzene; DNFB, 2,4-dinitrofluorobenzene; IFN, interferon; IL, interleukin; LPS, lipopolysaccharide; MAPK, mitogen-activated protein kinase; MAPKAP, mitogen-activated protein kinase-activated protein; MK2, mitogen-activated protein kinase-activated protein kinase 2; TCR, T-cell receptor; TLR, toll-like receptor; TNF, tumor necrosis factor; TPA, 12-*O*-tetradecanoylphorbol-13-acetate

Received 8 August 2008; revised 29 May 2009; accepted 14 June 2009; published online 6 August 2009

crucial role for MK2 in regulating TNF- α and IL-6 production was also shown in a mouse arthritis model. MK2-deficient mice had significantly lower LPS-induced TNF- α and IL-6 serum levels when compared with wild-type controls and were resistant to induction of collagen-induced arthritis (Hegen *et al.*, 2006). Moreover, deficiency of MK2 has been shown to markedly reduce infarct size following cerebral ischemic injury in mice. This protective effect was attributed to significantly lower expression of IL-1 β , but not TNF- α mRNA (Wang *et al.*, 2002).

A series of pyridinyl imidazole compounds, exemplified by SB203580, have been developed as specific p38 inhibitors (Badger *et al.*, 1996). *In vivo* studies using some of these compounds have suggested that they might be useful in the treatment of several inflammatory conditions including immunologically driven and irritant-associated airway inflammation, rheumatoid arthritis, and psoriasis (Badger *et al.*, 1996; Jackson *et al.*, 1998). However, the preclinical efficacy of SB203580 has been associated with potential adverse events (Rogers and Giembycz, 1998; Dambach, 2005), and targeting p38 directly might thus have liabilities for drug development. Although p38-deficient mice are lethal, MK2 knockout mice are viable and show a normal phenotype (Allen *et al.*, 2000).

Taken together, targeting MK2 as a downstream kinase in the p38 pathway might have advantages over targeting p38 directly. Moreover, in contrast for example to TNF- α , MK2 as a kinase is considered as a molecular target druggable by small molecules (Gaestel *et al.*, 2007), an attractive characteristic that is also reflected by the fact that a number of pharmaceutical companies are pursuing drug discovery and development programs with MK2 (Anderson *et al.*, 2007; Gaestel *et al.*, 2007).

The aim of this study was (i) to determine the biological role of MK2 in skin inflammation models mainly by comprehensively comparing wild-type *versus* knockout mice responses in several models of cutaneous and systemic inflammation and (ii) to determine whether MK2 represents a promising drug target for the treatment of inflammatory skin diseases.

RESULTS

MK2 is involved in acute, systemic inflammation after endotoxin challenge in mice

As TNF- α is a key mediator of inflammation and a well-established drug target in skin inflammation (Schottelius *et al.*, 2004), we wanted to test the effect of MK2 deficiency on plasma levels of TNF- α in the model of LPS-induced systemic inflammation. As expected, homozygous MK2 deficiency resulted in significantly reduced TNF- α serum levels following a systemic LPS challenge in comparison with wild-type mice ($P < 0.05$) (Figure 1). Partial deficiency of MK2 (MK2 heterozygous mice) also strongly reduced TNF- α serum levels, but the reduction did not reach statistical significance. These data confirm a report published earlier (Kotlyarov *et al.*, 1999) and show that the MK2-deficient mice we used for our studies displayed a similar phenotype as described.

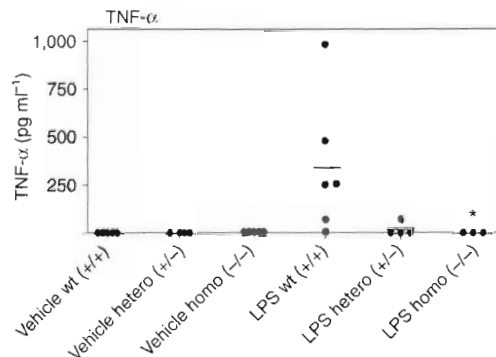


Figure 1. MK2 deficiency results in suppression of TNF- α production after systemic LPS exposure. Wild-type, MK2-heterozygous, and MK2-deficient mice were left untreated (NaCl control) or intraperitoneally challenged with LPS from *E. coli* (5 mg kg⁻¹). TNF- α serum levels as determined by Luminex measurement were strongly and significantly elevated at 1.5 hours after LPS challenge in wild-type mice ($n = 6$), but were completely suppressed in mice heterozygous for MK2 ($n = 4$) and in MK2-deficient mice ($n = 3$; $P < 0.05$, Mann-Whitney *U*-test).

To investigate the pathophysiological role of MK2 in skin disease, we tested MK2-deficient and wild-type mice in models of skin inflammation, which display characteristics of chronic, subacute, and acute skin inflammation.

Impact of MK2 deficiency on the chronic TPA-induced skin inflammation model in mice

MK2 knockout mice and wild-type controls were subjected to chronic 12-*O*-tetradecanoylphorbol-13-acetate (TPA)-induced irritative skin inflammation. Inflammatory edema formation after repeated TPA exposure was significantly decreased in MK2-deficient mice on days 5 ($P < 0.001$) and 10 ($P < 0.05$) (Figure 2a). Moreover, a significant reduction of neutrophil infiltration, as assessed by neutrophil elastase activity in skin homogenates, could be observed in MK2 knockout *versus* wild-type mice ($P < 0.05$) (Figure 2c). Overall granulocyte infiltration, as assessed by peroxidase activity, however, was not different in MK2 knockout mice *versus* wild-type controls (Figure 2b).

Impact of MK2 deficiency on subacute DNFB- and DNCB-induced contact allergy models in mice

On repeated challenges with contact allergy-inducing haptens, DNFB (dinitrofluorobenzene)- or DNCB (dinitrochlorobenzene)-sensitized mice develop a T-cell-dependent skin inflammation of a pronounced Th1 phenotype. Owing to the subacute regimen with repeated challenges, these models may be particularly relevant for inflammatory skin diseases, such as psoriasis (Zollner *et al.*, 2004) in which TNF- α protein expression in lesional skin is suggested to be post-transcriptionally regulated by activated MK2 (Johansen *et al.*, 2006).

First, we tested MK2 knockout mice in a subacute model of DNFB-induced contact allergy. A significant reduction of ear edema formation was observed for MK2-deficient mice compared with the respective wild-type controls with the strongest reduction seen on day 8 (day 7 $P < 0.05$; day 8

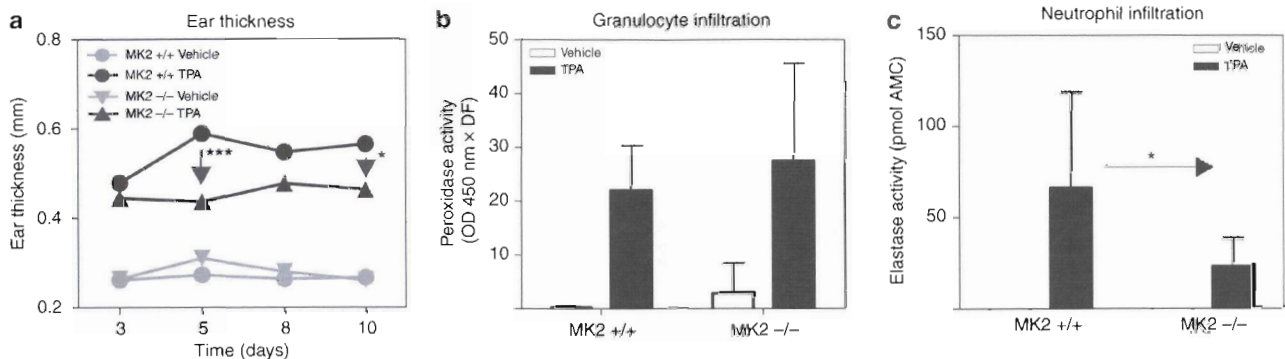


Figure 2. Skin inflammation is reduced in MK2-deficient mice in the chronic TPA-induced irritative dermatitis model. MK2-deficient and wild-type mice ($n = 10$ per group) were subjected to TPA-induced skin inflammation. Mice ears were treated with TPA on days 1, 3, 5, 8, and 10 and killed on day 10 at 6 hours after the last TPA application. (a) The kinetics of ear thickness was assessed with a caliper. Skin inflammation was significantly decreased on days 5 and 10 in MK2-deficient mice compared with wild-type mice ($***P < 0.001$ day 5, $*P < 0.05$ day 10, Mann-Whitney U -test) after sensitization with TPA, whereas skin inflammation was not significantly decreased on days 3 and 8 in MK2-deficient mice. Moreover, although there was a significant reduction of neutrophil infiltration as assessed by elastase activity in ear homogenates on day 10 ($*P < 0.05$) (c), peroxidase activity as a parameter for overall granulocyte infiltration was not significantly different in MK2 knockout mice compared with wild-type controls. (b) DF, dilution factor.

$P < 0.001$) (Figure 3a). Interestingly, as in TPA-induced chronic skin inflammation, the reduction of edema formation was not accompanied by a consistent reduction in cutaneous granulocyte infiltration. Peroxidase activity in skin homogenates, as a parameter for overall granulocyte infiltration, was even significantly increased ($P < 0.05$, Figure 3b), whereas neutrophil elastase activity, as a parameter for neutrophil infiltration, was significantly decreased ($P < 0.05$, Figure 3c) in MK2-deficient animals compared with wild-type controls.

To elucidate whether inflammation in the subacute DNFB model is driven by TNF- α , we tested TNF- α expression at the mRNA and protein levels and the effect of neutralization with an anti-TNF- α antibody. The TNF- α mRNA levels were significantly upregulated following repeated challenges with DNFB in this model peaking at day 8 ($P < 0.05$ day 8 vs day 5) (Figure 3d, left panel). IL-1 β mRNA levels also increased steadily up to day 8, but the increase was not statistically significant (Figure 3d, right panel). Neutralization of TNF- α with two different anti-TNF- α antibodies significantly reduced ear edema in this model ($P < 0.05$ for hamster anti-mouse TNF- α versus hamster control on day 8; $P < 0.05$ for rabbit anti-mouse TNF- α versus rabbit control on days 7 and 8) (Figure 3e) and also strongly and significantly suppressed protein levels of TNF- α and IL-1 β ($P < 0.01$ versus control for both) (Figure 3f). These data suggest that the pathophysiology of the subacute DNFB contact allergy model is mainly driven by the inflammatory effects of TNF- α and that MK2-deficiency leads to a significant reduction in ear inflammation, potentially through TNF- α suppression in this model.

In contrast, the formation of ear edema 8 or 9 days post challenge was not reduced when MK2 knockout mice were tested in the subacute DNCB-induced contact allergy model (Figure 4a). Surprisingly, in this model, the infiltration of inflammatory cells was even strongly and significantly

increased in MK2-deficient mice compared with wild-type controls ($P < 0.001$ for cutaneous peroxidase and elastase activity) (Figure 4b and c). To further investigate whether the increase of cellular infiltration in MK2-deficient mice in DNCB-induced contact allergy was accompanied by changes in cutaneous cytokine production, we analyzed ear homogenates of DNCB-challenged mice for the presence of inflammatory cytokines. TNF- α and IL-1 β levels were increased at 24 hours after the last DNCB challenge in both MK2 wild-type and deficient mice compared with unchallenged mice (Figure 4d). However, MK2 knockout mice produced significantly higher levels of TNF- α and IL-1 β after repeated challenges with DNCB when compared with wild-type controls ($P < 0.05$ for TNF- α , $P < 0.001$ for IL-1 β). Increased infiltration of inflammatory cells in MK2 knockout mice in DNCB-induced contact allergy was thus accompanied by a higher production of TNF- α and IL-1 β .

As MK2 deficiency caused different effects on skin inflammation in DNFB- versus DNCB-induced contact allergy, we further wanted to elucidate whether TNF- α also has a pathophysiological role in the subacute DNCB-induced contact allergy model, that is, whether TNF- α levels are incrementally increased and whether neutralization of TNF- α would reduce inflammation equally in this model. In line with the results from the subacute DNFB model, we observed increasing TNF- α and IL-1 β mRNA expression in the subacute DNCB model ($P < 0.05$ for TNF- α for days 7 and 9 vs day 6 and for IL-1 β for day 9 vs day 6) (Figure 4e). Most importantly, neutralization of TNF- α with an anti-TNF- α antibody reduced ear thickness significantly and with comparable efficacy as in subacute DNFB-induced contact allergy (Figure 3e) in the subacute DNCB-induced contact allergy ($P < 0.05$ for days 7, 8, and 9) (Figure 4f). Also, in the DNCB-induced contact allergy model, neutralization of TNF- α strongly and significantly suppressed protein levels of TNF- α and IL-1 β ($P < 0.01$ for TNF- α and $P < 0.05$ for IL-1 β) (Figure 4g).

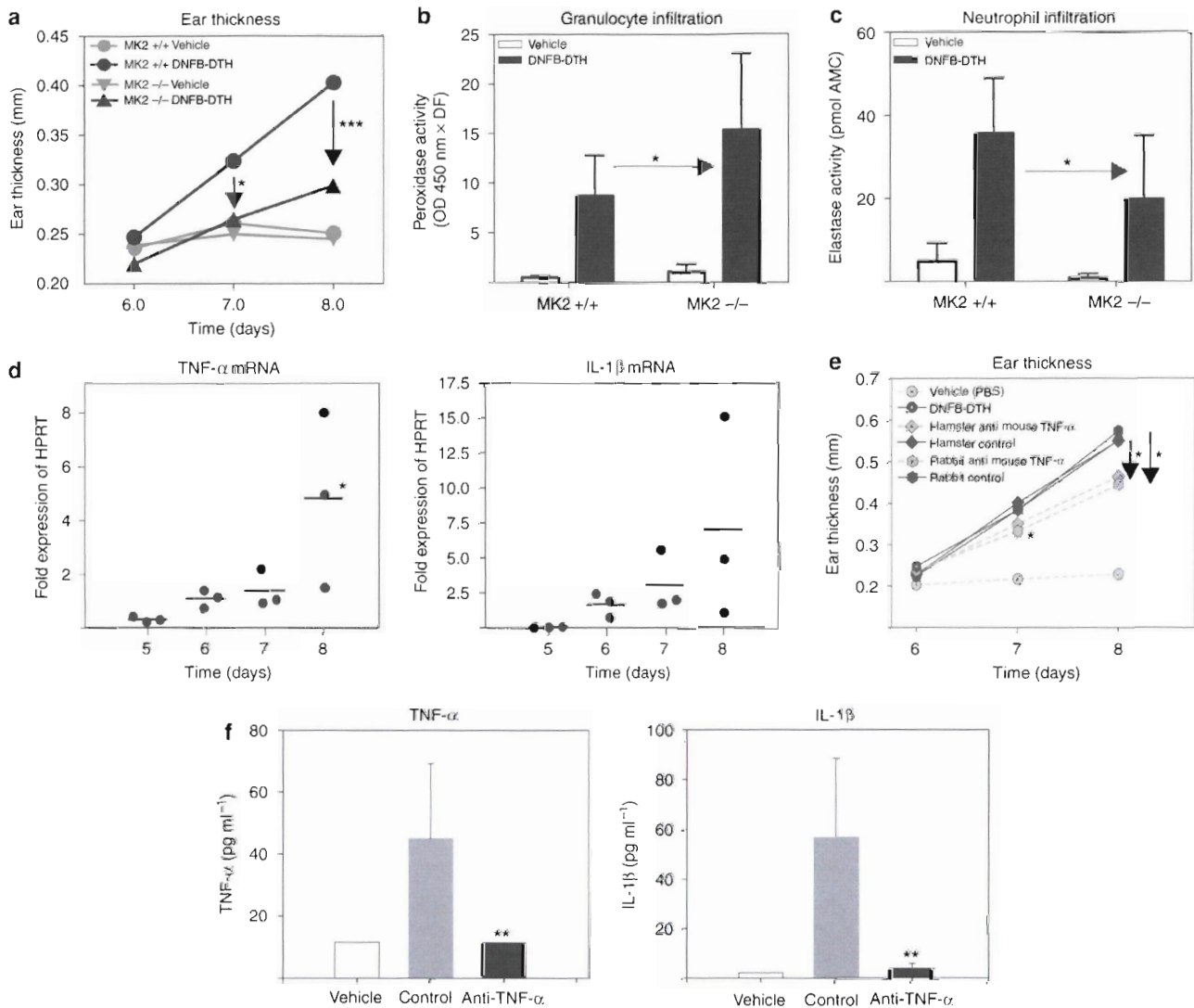


Figure 3. MK2-deficient mice show decreased skin inflammation in the subacute model of DNFB-induced contact allergy. MK2-deficient and wild-type mice ($n = 10$ per group) were challenged on the ears with DNFB on days 5, 6, and 7 after sensitization. (a) Ear thickness was measured with a caliper on days 6, 7, and 8 after DNFB sensitization. MK2-deficient mice developed significantly less ear edema when compared with wild-type controls ($*P < 0.05$ day 7; $***P < 0.001$ day 8, Mann-Whitney U -test). (b, c) Ears were homogenized on day 8 after sensitization and assayed for peroxidase activity as a parameter for granulocyte infiltration (b) and elastase activity for neutrophil infiltration (c). Both parameters were significantly increased after challenge with DNFB. Although granulocyte infiltration was significantly increased ($*P < 0.05$), neutrophil infiltration was significantly decreased in MK2-deficient versus wild-type mice ($*P < 0.05$, Mann-Whitney U -test). The subacute model of DNFB-induced contact allergy is mainly driven by TNF- α . (d) Wild-type mice were challenged with DNFB on days 5, 6, and 7 after DNFB sensitization. mRNA was extracted from ear homogenates of mice killed on days 5, 6, 7, and 8 after sensitization ($n = 3$ for each time point). TNF- α and IL-1 β mRNA levels steadily increased up to day 8 ($*P < 0.05$ day 8 vs day 5 for TNF- α , Mann-Whitney U -test). (e, f) Treatment with either hamster or rabbit anti-mouse TNF- α antibodies before challenges (day 5) significantly reduced ear inflammation in subacute DNFB-induced contact allergy in C57Bl/6 wild-type mice ($n = 7$ for anti-TNF- α antibodies; $n = 10$ for control IgGs). (e) TNF neutralization significantly diminished ear thickness on day 7 ($*P < 0.05$ for rabbit anti-mouse TNF- α versus rabbit control, Mann-Whitney U -test) and on day 8 after sensitization ($*P < 0.05$ for hamster anti-mouse TNF- α versus hamster control and for rabbit anti-mouse TNF- α versus rabbit control, Mann-Whitney U -test). (f) Neutralization of TNF- α by hamster anti-mouse TNF- α significantly reduced protein levels of TNF- α and IL-1 β ($**P < 0.01$ versus hamster control IgG, Mann-Whitney U -test) in ear homogenates on day 8 after DNFB sensitization. DF, dilution factor.

Taken together, our data establish the central role of TNF- α in the pathogenesis of both the subacute DNFB- and DNCB-induced contact allergy models and further show that the differential functional effects of MK2-deficiency in these models cannot be explained by the lack of a role for TNF- α in inducing inflammation in one model versus the other.

Differing effect of MK2 deficiency and p38 inhibition on the acute DNFB-induced contact allergy model in mice

As MK2 knockout mice showed the most prominent and significantly reduced ear edema formation in the subacute DNFB contact allergy model, we wanted to investigate whether this anti-inflammatory effect of MK2-deficiency

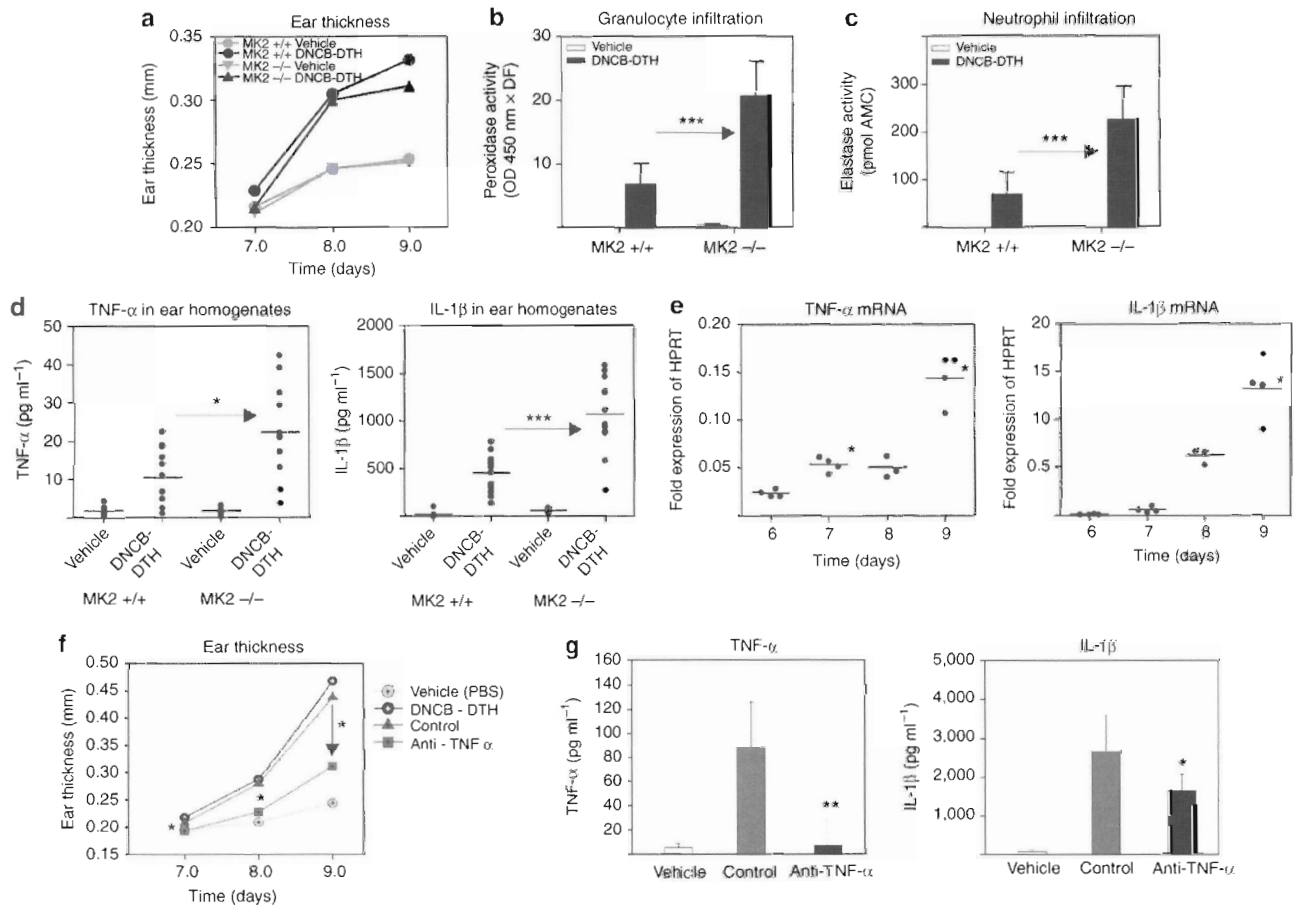


Figure 4. Skin inflammation is not reduced in MK2-deficient mice in the subacute DNCB-induced contact allergy model. MK2-deficient and wild-type mice ($n = 10$ per group) were challenged with DNCB on days 6, 7, and 8 after sensitization. (a) Ear thickness was measured with a caliper on days 7, 8, and 9 after DNCB sensitization. No significant differences in ear thickness were detected between MK2-deficient and wild-type mice. (b, c) Ears were homogenized on day 9 after sensitization and assayed for peroxidase activity as a parameter for granulocyte infiltration (b) and elastase activity for neutrophil infiltration (c). Both parameters were significantly strongly increased in MK2-deficient compared with wild-type mice ($***P < 0.001$ for granulocyte and neutrophil infiltration, Mann-Whitney U -test). (d) TNF- α and IL-1 β protein levels in ear homogenates were determined on day 9 after sensitization ($n = 6$ –12 for each group). Both TNF- α and IL-1 β were significantly increased in MK2-deficient compared with wild-type mice ($*P < 0.05$ for TNF- α , $***P < 0.001$ for IL1 β). The subacute model of DNCB-induced contact allergy is driven by TNF- α . (e) Wild-type mice were challenged with DNCB on days 6, 7, and 8 after DNCB sensitization. mRNA was extracted from ear homogenates of mice killed on days 6, 7, 8, and 9 after sensitization ($n = 4$ for each time point). TNF- α and IL-1 β mRNA levels steadily increased up to day 9 ($*P < 0.05$ days 7 and 9 vs day 6 for TNF- α and day 9 vs day 6 for IL-1 β , Mann-Whitney U -test). (f, g) C57Bl/6 wild-type mice ($n = 10$ for rabbit anti-TNF- α and $n = 8$ for rabbit IgG controls) were challenged with DNCB on days 6, 7, and 8 after sensitization. Treatment with rabbit anti-mouse TNF- α antibodies was performed before the challenges (day 6). (f) TNF- α neutralization significantly reduced ear inflammation as assessed by ear thickness ($*P < 0.05$ versus rabbit IgG control on days 7, 8, and 9, Mann-Whitney U -test). (g) TNF- α neutralization significantly reduced protein levels of TNF- α and IL-1 β ($**P < 0.01$ and $*P < 0.05$ versus rabbit IgG control, respectively, Mann-Whitney U -test) in ear homogenates on day 9 after sensitization. DF, dilution factor.

could also be observed in the acute model of DNFB-induced contact allergy using a single challenge of the same hapten in sensitized mice. In contrast to the effects seen in the subacute DNFB-induced contact allergy model after 3 DNFB challenges, no significant anti-inflammatory effect was seen in MK2 knockout mice in the acute DNFB contact allergy model compared with controls (Figure 5a–c). Comparable induction of ear edema formation (Figure 5a) and granulocyte (Figure 5b) as well as neutrophil infiltration (Figure 5c) was seen in MK2 knockout and wild-type mice in this model.

To further explore whether the p38 axis has any role in the pathophysiology of this acute contact allergy model, we

tested the effects of the potent p38 inhibitor, SB203580, in MK2 wild-type mice compared with the potent glucocorticoid, dexamethasone, as a positive control. The pharmacological inhibition of p38 strongly and dose-dependently decreased skin inflammation and blocked ear edema formation and cell infiltration as potently as dexamethasone ($P < 0.01$ for 0.3 and 1 mg kg⁻¹ dexamethasone and for 3 and 10 mg kg⁻¹ SB203580; inhibition of granulocyte infiltration: $P < 0.01$ for 1 mg kg⁻¹ dexamethasone and for 3 and 10 mg kg⁻¹ SB203580; inhibition of neutrophil infiltration: $P < 0.05$ for 1 mg kg⁻¹ dexamethasone and $P < 0.01$ for 3 and 10 mg kg⁻¹ SB 203580) (Figure 6a–c), showing that the p38

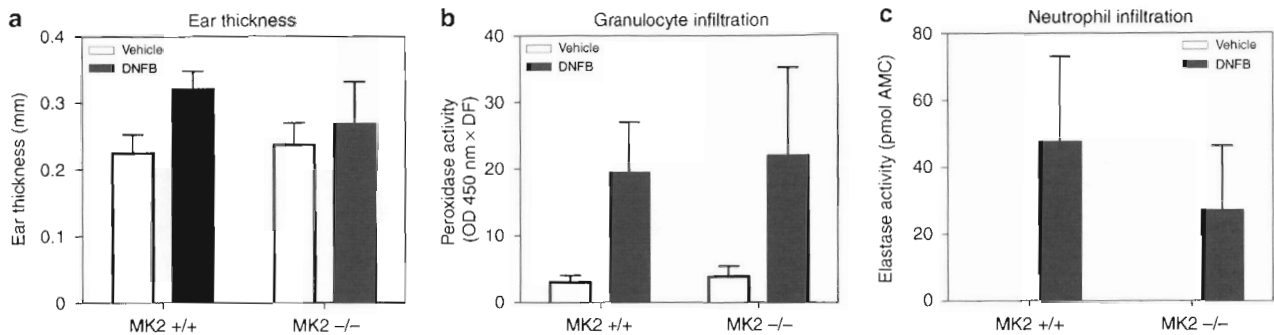


Figure 5. Skin inflammation is not reduced in MK2-deficient mice in the acute model of DNFB-induced contact allergy. MK2-deficient mice (vehicle $n = 6$, DNFB $n = 6$) and wild-type mice (vehicle $n = 10$, DNFB $n = 11$) were challenged on the ears with DNFB on day 5 after sensitization and killed on day 6. (a) As assessed by the ear thickness measurements with a caliper, MK2-deficient and wild-type mice developed similar degrees of ear edema. Moreover, cell infiltration was not different between MK2-deficient and wild-type mice as determined by peroxidase (b) and elastase (c) activities in ear homogenates as parameters for granulocyte and neutrophil infiltration, respectively. DF, dilution factor.

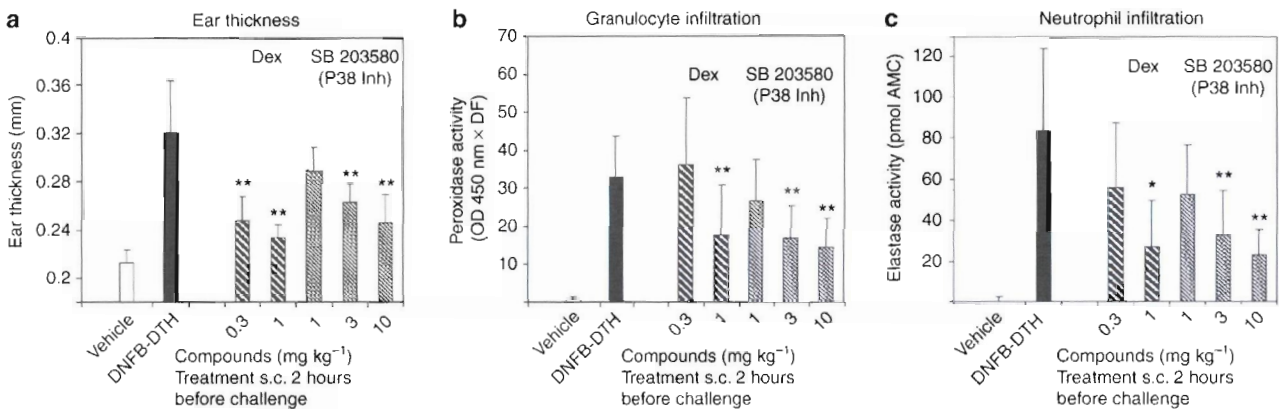


Figure 6. Pharmacological inhibition of p38 strongly and dose-dependently inhibits skin inflammation in the acute DNFB-induced contact allergy model in wild-type mice. DNFB-sensitized female NMRI mice ($n = 10$ per group) were s.c. treated with different dosages of the p38 inhibitor, SB 203580, or vehicle at 2 hours before DNFB challenge on both ears at day 5 after sensitization and killed on day 6. Treatment with the glucocorticoid dexamethasone (Dex) served as positive control. Both compounds, SB 203580 and dexamethasone, significantly and dose-dependently inhibited (a) ear edema formation as determined by caliper measurement on day 6 after DNFB sensitization (** $P < 0.01$ for 0.3 & 1 mg kg⁻¹ dexamethasone and for 3 and 10 mg kg⁻¹ SB203580, Mann-Whitney U -test) as well as (b) granulocyte infiltration (peroxidase activity) (** $P < 0.01$ for 1 mg kg⁻¹ dexamethasone and for 3 and 10 mg kg⁻¹ SB203580, Mann-Whitney U -test) and (c) neutrophil infiltration (elastase activity in ear homogenates) (* $P < 0.05$ for 1 mg kg⁻¹ dexamethasone and ** $P < 0.01$ for 3 and 10 mg kg⁻¹ SB 203580, Mann-Whitney U -test). DF, dilution factor.

axis needs to be intact for inflammation to develop in acute DNFB-induced contact allergy.

Collectively, these data show that specific MK2 deficiency does not exert a significant anti-inflammatory effect in this model of DNFB-induced acute skin inflammation, whereas the upstream regulatory molecule p38 is clearly involved, showing the relevance of the p38 pathway in this acute contact allergy model.

The TNF- α regulatory role of MK2 is consistent for TLR stimulation but may be restricted in T-cell stimulation

For a better mechanistic understanding of the observed differential *in vivo* effects, we further wanted to elucidate the role of MK2 signaling for the production of TNF- α in the most prominent pathways in relevant immune cells

ex vivo/in vitro. Stimulation of different toll-like receptors (TLRs) in splenocytes with their respective ligands led to a strong induction of TNF- α , which was consistently and significantly reduced in the absence of MK2 ($P < 0.01$ for LPS, $P < 0.05$ for zymosan and imiquimod) (Figure 7a). The LPS *in vitro* data are consistent with our results observed in the model of LPS-induced systemic inflammation (Figure 1). Moreover, *in vitro* TNF- α production was comparably inhibited after the pharmacological blockade of p38 in wild-type splenocytes as in MK2-deficient splenocytes.

Remarkably, a quite similar inhibition of TNF- α production was seen in splenocytes stimulated with LPS alone or in combination with IFN- γ or anti-CD40 co-stimulation ($P < 0.05$ for all stimuli) (Figure 7b, left panel) showing the robustness of the effects. However, in isolated splenic CD4⁺

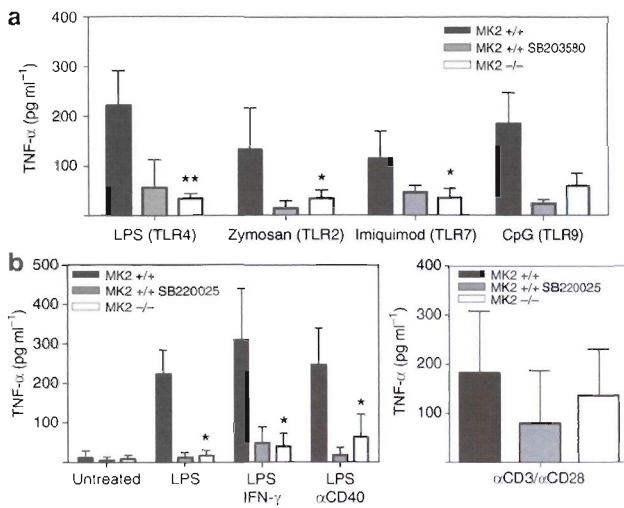


Figure 7. (a) TNF- α secretion after stimulation with different TLR stimuli is MK2-dependent. Spleen cells ($5 \times 10^6 \text{ ml}^{-1}$) from C57Bl/6 mice (wt; dark gray bars) or MK2-deficient mice (white bars) were stimulated for 4 hours with several TLR stimuli (LPS at $5 \mu\text{g ml}^{-1}$, zymosan at $10 \mu\text{g ml}^{-1}$, imiquimod at $1 \mu\text{g ml}^{-1}$, or CpG ODNs at $10 \mu\text{g ml}^{-1}$) as indicated. As a control, wild-type spleen cells were also stimulated in the presence of the p38 MAP kinase inhibitor, SB203580, at $10 \mu\text{M}$ (light gray bars). TNF- α content in supernatants was determined by ELISA. Absolute values are depicted from two (CpG) or 3–6 (all others) mice as means with error bars indicating SD. Significant differences between cell cultures from wild-type and MK2-deficient mice were determined by the Mann–Whitney U -test ($*P < 0.05$, $**P < 0.01$). (b) MK2 deficiency significantly diminishes TNF- α secretion after LPS stimulation with and without co-stimuli, but not after TCR stimulation. Splenocytes from C57Bl/6 (dark gray bars) and MK2-deficient mice (white bars) were left untreated or activated with LPS alone or in combination with co-stimulation (IFN- γ or anti-CD40) for 4 hours (left panel). As a control, wild-type spleen cells were also stimulated in the presence of the p38 MAP kinase inhibitor, SB220025, at $10 \mu\text{M}$ (light gray bars). TNF- α levels in supernatants were analyzed by ELISA, and the results are shown as the means from four mice (\pm SD). CD4 $^+$ T cells separated from the spleens of either C57Bl/6- (dark gray bars) or MK2-deficient mice (white bars) were activated with plate-bound anti-CD3 and anti-CD28 antibodies for 72 hours (right panel). As a control, wild-type CD4 $^+$ T cells were also stimulated in the presence of the p38 MAP kinase inhibitor, SB220025, at $10 \mu\text{M}$ (light gray bars). TNF- α levels in supernatants were analyzed by ELISA. Results are shown as the means from four mice (\pm SD). Significant differences between cell cultures from wild-type and MK2-deficient mice were determined by Mann–Whitney U -test ($*P < 0.05$).

T cells stimulated with anti-CD3/anti-CD28 antibodies, MK2 deficiency did not significantly alter the production of TNF- α (Figure 7b, right panel).

In summary, these *in vitro* data show that the p38/MK2 axis has a pivotal role in TLR-stimulated production of TNF- α in splenocytes, whereas anti-CD3/anti-CD28-driven TNF- α production in splenic T cells appears to be less dependent on MK2 signaling.

DISCUSSION

The p38 MAP kinase pathway has been shown to be a central regulator of inflammation (Lee *et al.*, 1994). MK2 is exclusively regulated by p38 and controls key inflammatory

cytokines such as TNF- α and IL-6 (Kotlyarov *et al.*, 1999; Neiningner *et al.*, 2002) as well as chemokines and adhesion molecules (Gorska *et al.*, 2007). Both kinases have thus been identified as potentially promising drug targets and have become the focus of several drug discovery programs (Gaestel, 2006; Duraisamy *et al.*, 2008). Targeting MK2 as a downstream kinase in the p38 pathway might have advantages over targeting p38 directly, because pharmacological inhibition of p38 was implicated with potential adverse events (Dambach, 2005). The relevance of MK2 as a drug target was elucidated for certain inflammatory diseases such as rheumatoid arthritis in relevant animal models (Hegen *et al.*, 2006); however, its target relevance in inflammatory skin disease has remained elusive. Although a recent report shows a role of MK2 in the oxazolone-induced contact allergy model (Funding *et al.* 2009), here, we provide a comprehensive characterization of the pathophysiological role of MK2 in a broad panel of murine models of skin inflammation, contributing to its evaluation as a drug target in inflammatory skin disease.

Here, we show that MK2 deficiency exerts anti-inflammatory effects in chronic TPA-induced irritative skin inflammation and in the subacute model of DNFB-induced contact allergy leading to a significant reduction in the development of ear edema (Figures 2a and 3a). However, the reduction in edema formation was accompanied by an only partial reduction of inflammatory cell infiltration parameters in these models. Although neutrophil infiltration, assessed by elastase activity, was significantly reduced in MK2-deficient mice (Figures 2c and 3c), general granulocyte infiltration, as assessed by cutaneous peroxidase activity, was in tendency or significantly enhanced (Figures 2b and 3b, respectively). Moreover, we did not observe any inhibitory effect of MK2 deficiency on inflammation in the subacute DNCB contact allergy model. Here, a lack of significant inhibition of ear edema formation was accompanied by even significantly increased cell infiltration parameters (Figure 4a–c). It is noted that this increase in cutaneous cell infiltration in MK2 knockout mice was also accompanied by a significant increase in TNF- α and IL-1 β production in the inflammatory skin lesions of MK2-deficient mice compared with wild-type controls (Figure 4d). This result was surprising, because experiments with MK2 knockout mice used in our studies were able to confirm that LPS-induced plasma levels of TNF- α were drastically reduced as reported earlier (Figure 1) (Kotlyarov *et al.*, 1999).

Remarkably, the differential effects of MK2 deficiency in the subacute DNFB- versus the subacute DNCB-induced contact allergy model cannot be explained by a different role for TNF- α in the pathogenesis of these models, because in both models cutaneous TNF- α expression significantly increased with inflammation (Figures 3d and 4e) and neutralization of TNF- α exerted a potent and comparable anti-inflammatory effect (Figures 3e and 4f). Although both DNFB and DNCB are considered Th1-inducing haptens, a variety of studies have shown a number of differences in the cellular and molecular mechanisms elicited by these compounds, all of which may have contributed to the

differential effects observed in contact allergy in mice in the absence of MK2, namely the different effects on CD86 and HLA-DR expression in dendritic cells (Manome *et al.*, 1999) indicating a more potent role of DNCB over DNFB in dendritic cells and the distinct ability of DNFB to induce IL-10-producing mast cells and NK cell-mediated memory responses (O'Leary *et al.*, 2006; Grimbaldston *et al.*, 2007) where the p38/MK2 pathway may have a differential role *versus* contact allergy elicited by DNCB.

When tested in the acute model of DNFB-induced contact allergy, MK2 knockout mice did not develop significantly less skin inflammation than their wild-type controls (Figure 5a–c). In contrast, the pharmacological inhibition of p38 potently and dose-dependently abrogated both edema formation and infiltration of inflammatory cells in acute DNFB-induced contact allergy (Figure 6a–c). These results confirm the reported role of p38 MAP kinase in the pathophysiology of acute DNFB-induced contact hypersensitivity (Takanami-Ohnishi *et al.*, 2002). The lack of a significant anti-inflammatory effect by MK2 deficiency in acute DNFB-induced contact allergy thus cannot be attributed to a lesser pathophysiological role of the p38 pathway in this skin inflammation model. The p38 kinase has also been shown to be activated in lesional psoriatic skin (Johansen *et al.*, 2005), supporting its relevance in human inflammatory skin disease.

One possible explanation for the inconsistent impact of MK2 deficiency in T-cell-dependent contact allergy models might be provided by the results of our mechanistic studies in mouse splenocytes. We show that, as *in vivo*, MK2 has a pivotal role in TLR-triggered TNF- α production in splenocytes. In contrast, however, the CD3/CD28-mediated TNF- α production in splenic T cells appears to be less dependent on MK2 signaling.

The fact that TLR-dependent, but not TCR-dependent, TNF production is significantly decreased in MK2-deficient and SB22025-treated splenocytes is in agreement with the established role of the p38/MK2 module in signal transduction located directly downstream to the canonical TLR4/IRAK4/TAK1/MKK3/6 pathway (summarized in Gaestel, Kotlyarov, and Kracht, 2009). In contrast, stimulation of TNF- α production in response to TCR stimulation could proceed in a non-canonical manner through non-receptor protein tyrosine kinases, such as Lck (Salvador *et al.*, 2005), Itk, or Syk, in a more p38/MK2-independent manner. This non-canonical stimulation of TNF- α generation downstream of TCR stimulation could in turn explain that the pharmacological blockade of p38 by the compound SB22025 and MK2 deficiency shows much lesser effects on TNF production in splenocytes on anti-CD3/anti-CD28 stimulation.

One could further hypothesize that the autoimmune suppressor Gadd45a may have some function in the differentiated role of TCR-mediated TNF production in splenocytes. Gadd45a can inhibit p38 Tyr323 phosphorylation, which is specific for the non-canonical or alternative pathway of p38 activation in T cells (Salvador *et al.*, 2005).

Taken together, our results confirm the crucial function of MK2 in LPS-induced TNF- α production in systemic inflam-

mation and further support the observation that this axis has distinct roles for different inflammatory pathways in different cell types and target organs.

Here, we show that MK2 deficiency exerts limited anti-inflammatory effects or can even enhance inflammation in specific, more chronic mouse models of skin inflammation in which TNF- α has a central role in the development of disease, and, in contrast to p38 inhibition, did not exert inhibitory effects in an acute T-cell-dependent DNFB-induced contact allergy model. These results may indicate that MK2 is bypassed in skin inflammation or that MK2 function is compensated for by a different kinase. One such kinase candidate may be MK3, another MAPKAP kinase downstream of p38, which has been described to be also involved in TNF- α production and which might compensate for the function of MK2 (Hegen *et al.*, 2006; Ronkina *et al.*, 2007).

Our results are in partial contrast to other reports that concluded a general potent anti-inflammatory effect of MK2 inhibition, based on MK2 deficiency in other cytokine-driven diseases such as LPS-induced systemic inflammation or mouse arthritis models (Kotlyarov *et al.*, 1999; Hegen *et al.*, 2006) and also on a recent report showing that MK2 deficiency diminishes inflammation in an oxazolone-induced acute allergic contact dermatitis model (Funding *et al.* 2009). Interestingly, MK2 deficiency has been shown to exacerbate TNF-dependent inflammatory bowel disease in the mouse (Kontoyiannis *et al.*, 2002). The observed differences may be based on the distinct role for the p38/MK2/TNF- α axis in the pathogenesis of these different inflammation models in different target organs.

From a methodological point of view, our data show that drawing general conclusions from a single skin inflammation model alone may not be reliable. The data we obtained in the subacute DNFB-induced contact allergy (and also the chronic TPA-induced irritative skin inflammation model), suggesting an impact of MK2 in skin inflammation, were neither confirmed in a different subacute contact allergy model nor in the acute DNFB model, when the hapten was applied in a more acute setting. Therefore, both the kinetics of the model (acute *versus* subacute) and the resulting dominating stimulatory pathways (for example, TCR stimulation *versus* cytokine stimulation) as well as the choice of hapten (DNFB *versus* DCNB) appear to have an impact on the biological role of MK2 in skin inflammation and its downstream effects on TNF- α . Investigating the effects of compounds or genetic alterations in several different contact allergy models comprehensively may thus be required before general conclusions can be drawn from a data set.

In conclusion, our studies confirm the role of MK2 in an acute TLR-driven systemic inflammation, whereas MK2 seems to have at least a less prominent and more complex role in skin inflammation. However, the entire role of MK2 in chronic relapsing T-cell-dependent skin diseases in man is still not fully understood and awaits further analysis. As expression analysis of MK2 in human lesional skin from patients with chronic plaque-type psoriasis revealed an activation of MK2 protein in inflamed psoriatic skin (Johansen

et al., 2006), the role of MK2, for example, in psoriasis, is still subject to further investigations.

As neutralization or inhibition of TNF- α has been validated as a potent therapy for rheumatoid arthritis, inflammatory bowel disease, and psoriasis in the clinic (Schottelius et al., 2004), disruption or dampening of TNF- α production would be expected to yield good therapeutic effects. It would thus seem conceivable that MK2 is an attractive target for a pharmacological inhibition in treating a variety of inflammatory diseases. With the data available to date, including our findings reported here, this approach might yield more therapeutic promise in rheumatoid arthritis than in inflammatory skin diseases such as psoriasis or atopic dermatitis. Future studies with MK2-deficient mice in other animal models of disease may be able to further elucidate the role of MK2 for other inflammatory conditions such as Crohn's disease or ulcerative colitis.

MATERIALS AND METHODS

Mice

C57Bl/6 mice (purchased from Charles River, Sulzfeld, Germany), NMRI female mice (from "Schoenwalde NMRI colonies" exclusively bred for Bayer Schering Pharma AG at Charles River, Germany), and MK2 knockout mice (provided from Hannover Medical School, Hannover, Germany) in the age group of 8–12 weeks were housed in the animal facility at the Bayer Schering Pharma AG. All animal studies were approved by the competent authority for labor protection, occupational health, and technical safety for the state and city of Berlin, Germany, and were performed in accordance with the ethical guidelines of Bayer Schering Pharma AG.

Systemic endotoxin-induced inflammation in mice

C57Bl/6 wild-type, MK2-heterozygous, and MK2-deficient mice were treated by intraperitoneal injection with 5 mg kg⁻¹ LPS (*E. coli* 0111:B4; Sigma L-4391, Steinheim, Germany) or NaCl control. At 1.5 hours after LPS challenge, the mice were killed, and the serum levels of TNF- α were determined by Luminex assay (Biorad, Munich, Germany).

Acute DNFB-induced contact allergy model

For sensitization, female WT and MK2-deficient mice were topically treated on day 0 and day 1 with 25 μ l of 0.5% (w/v) 2,4-dinitrofluorobenzene (DNFB) (Sigma) in acetone/olive oil 4:1 (v/v) on the shaved abdomen. After 5 days, groups of 10 mice were challenged by the topical application of 20 μ l of 0.3% (w/v) DNFB in acetone/olive oil 4:1 (v/v) on both sides of one ear. Small molecule inhibitors were applied subcutaneously (s.c.) in a volume of 0.1 ml per 20 g body weight in 0.9% NaCl solution containing 0.085% Myrj 53 (ICI, UK) and 5% ethanol 2 hours before DNFB challenge of the animals on day 5. On day 6 (24 hours after challenging animals), the thickness of the inflamed ears were determined, and myeloperoxidase (for granulocyte infiltration) and granulocyte elastase activities (a parameter for neutrophil infiltration) were measured in homogenates of inflamed ears as described earlier (Schottelius et al., 2002; Zugel et al., 2002).

Subacute DNFB- and DNCB-induced contact allergy models

To examine the role of MK2 in the subacute DNFB model, female and male WT and MK2 knockout mice were topically sensitized on

day 0 and day 1 with 25 μ l of a 0.5% (w/v) DNFB (Sigma) solution in acetone/olive oil 4:1 (w/v) on the shaved abdomen. On days 5, 6, and 7, contact allergy was induced by repeated challenge of the ears with topically applied DNFB (10 μ l of a 0.15% [w/v] DNFB solution in acetone/olive oil 4:1 [w/v]). Ear thickness was monitored during the study as follows: day 0, day 5 (before challenge), day 6 (24 hours after first challenge), day 7 (24 hours after second challenge), and day 8 (24 hours after third challenge). In the subacute DNCB model, female and male WT and MK2 knockout mice were topically sensitized on day 0 with 25 μ l of a 0.5% (w/v) 2,4-dinitrochlorobenzene (DNCB) (Merck, Darmstadt, Germany) in acetone/olive oil 4:1 (w/v) on the shaved abdomen. On days 6, 7, and 8, contact allergy was induced by repeated challenge of the ears with topically applied DNCB (10 μ l of a 0.15% [w/v] DNCB solution in acetone/olive oil 4:1 [w/v]). Ear thickness was monitored during the study as follows: day 0, day 6 (before challenge), day 7 (24 hours after first challenge), day 8 (24 hours after second challenge), and day 9 (24 hours after third challenge). On day 8 (DNFB) or day 9 (DNCB), animals were killed, and peroxidase activity (for granulocyte infiltration) and elastase activity (a parameter for neutrophil infiltration) were measured in homogenates of inflamed ears as described earlier (Schottelius et al., 2002; Zugel et al., 2002). Genders have been combined in all figures as no significant gender differences have been observed for any of the skin inflammation models investigated.

TNF- α neutralization in subacute DNFB- and DNCB-induced contact allergy

Female C57Bl/6 mice were sensitized with 25 μ l of 1% DNCB in acetone/olive oil (4:1) on the shaved flank skin on day 0. Challenges with 10 μ l 1% DNCB in acetone/olive oil (1:9) on the dorsum of both ears were performed on days 6, 7, and 8. As treatment in both contact allergy models purified rabbit polyclonal anti-mouse-TNF- α antibodies (endogen) and in an additional treatment group in the subacute DNFB model purified hamster polyclonal anti-mouse TNF- α (Abcam Cambridge, UK) and as isotype controls purified rabbit and purified hamster IgG (AbD Serotec, Munich, Germany) was used.

The proteins were prepared for *in vivo* use with SLIDE-A-LYZER dialysis cassettes (Serotec). Treatment was applied 1 hour before the first challenge i.p. Ear thickness was determined over the time course with a custom-built automated caliper/micrometer (Bayer Schering Pharma AG, Berlin, Germany). At day 9, animals were killed and the ears were cut, weighed, and mechanically homogenized in 2 ml homogenization buffer (hexadecyltrimethyl ammonium bromide/morpholinopropan sulfonic acid (Sigma)), centrifuged at 25,000 g for 20 minutes at 12°C, and the supernatant was used for determination of immune mediators. Cutaneous granulocyte infiltration was assessed by myeloperoxidase activity assay in ear homogenates as described earlier (Schottelius et al., 2002). Cytokine levels in ear homogenates were measured using MSD 96-Well MULTI-ARRAY and MULTI-SPOT technology (Meso Scale Discovery, Gaithersburg, MD) according to the manufacturer's instructions.

Chronic TPA-induced skin inflammation model

Ten microliters of the phorbol ester TPA (0.01 w/v) were applied to the inner and outer surfaces of each mouse ear using a micropipette. TPA was applied over a 10-day course on alternate days (days 1, 3, 5, 8, and 10). Ear thickness was assessed with a caliper starting

6 hours after TPA application (Alford *et al.*, 1992). Animals were killed on day 10 at 6 hours after last TPA application, and their ears were cut off, snap frozen, and later analyzed for peroxidase and elastase activity as described above.

Determination of elastase and peroxidase activities in ear homogenates

Peroxidase activity assay. Peroxidase activity as a measure of total granulocyte infiltration was measured as described earlier (Schottelius *et al.*, 2002). Briefly, tetramethylbenzidine (TMB) dihydrochloride was used as a sensitive chromogenic substrate for peroxidase. To convert TMB into TMB dihydrochloride, 34 μl of 3.7% hydrochloric acid (equimolar) was added to 5 mg of TMB. Then, 1 ml of DMSO was added. This stock solution was slowly added to sodium acetate-citric acid buffer (0.1 mol l⁻¹, pH 6.0) in a ratio of 1:100. Two hundred microliters of this TMB solution, 40 μl of the homogenized sample, and 25 μl of 1 mM H₂O₂ were added to a microtiter plate to start the reaction. The reaction was stopped after 30 minutes with 45 μl of 1 N H₂SO₄. Changes in OD were monitored at 450 nm at 25°C against the mixture of all solutions without the added sample homogenate. Absolute extinction numbers multiplied by respective dilution factors were used to express peroxidase activity.

Elastase activity assay. Elastase activity was measured by fluorescence of 7-amino-4-methyl-coumarin (AMC) that is released from the substrate MeO-Succ-Ala-Ala-Pro-Val-AMC (Bachem, Torrance, CA). Homogenized samples in HTAB were diluted 1/10 in cetrimide buffer (0.3% cetrimide, 0.1 M Tris, and 1 M NaCl, pH 8.5). The substrate MeO-Succ-Ala-Ala-Pro-Val-AMC (300 mM in DMSO) was diluted 1/100 in cetrimide buffer to a working concentration of 3 mM. In cetrimide buffer, diluted samples were pipetted in multiwell plates, and the reaction was started by addition of the AMC substrate at 37°C. The reaction was stopped after 1 hour with ice-cold 100 mM Na₂CO₃, and samples were measured in a Spectra Max Gemini (Molecular Devices, Menlo Park, CA) at 380 nm and compared against a standard curve with the AMC standard 7-amino-4-methylcoumarin (5 mM in ethanol).

Cytokine analyses in serum from LPS-triggered systemic inflammation model and in ear homogenates from skin inflammation models

Inflamed ears from mouse skin inflammation models were mechanically homogenized in 2 ml homogenization buffer (hexadecyltrimethyl ammonium bromide/morpholinopropan sulfonic acid, Sigma, Deisenhofen, Germany), centrifuged at 25,000 g for 20 minutes at 12°C, and supernatants were used for determination of immune mediators. Cytokine levels in ear homogenates were determined using a multiplex chemiluminescence method and MesoScale SI 6000 equipment (MesoScale Discovery, Gaithersburg, MD).

Gene expression analyses in mouse skin

For purification of RNA from mouse skin, ears were homogenized in 800 μl lysis buffer and digested with 2 mg ml⁻¹ Proteinase K (BD Biosciences, Erembodegem, Belgium) for 1 hour. Purified RNA from mouse skin was qualified with the Agilent Bioanalyzer 2100 system with RNA 6000 Nano Assay Kit (Agilent Technologies, Santa Clara, CA). cDNA was synthesized using Reverse Transcription Reagents

and GeneAmp PCR System 9700 (Applied Biosystems, Foster City, CA). RT-PCR was performed in 12.5 μl using a universal PCR Master Mix without UNG (Eurogentec, Cologne, Germany) on a 7900 HT Sequence Detection System (Applied Biosystems) under thermal conditions: 40 cycles at 95°C for 10 minutes, 95°C for 15 seconds, and 60°C for 1 minute. Expression of target genes was quantified as the fold expression of the housekeeping gene, hypoxanthine phosphoribosyltransferase (HPRT). The expression of the following mouse genes was determined in triplicated analyses using Assays on demand from Applied Biosystems: IL-1 β (Mm 00434228_m1) and TNF- α (Mm 00443258_m1).

Cell culture

Spleen cells from C57Bl/6 wild-type or Mapkapk2^{tm1Mgl} (C57Bl/6) mice were brought into suspension after squeezing through a cell strainer in RPMI-1640 and supplemented with 10% FCS, 1 mM L-glutamine, 100 U ml⁻¹ penicillin, and 100 μg ml⁻¹ streptomycin at a density of 5 \times 10⁶ cells per ml. For TLR stimulation, cells were then directly stimulated for 4 hours with either 5 μg ml⁻¹ LPS (TLR4 grade, Alexis, Lörrach, Germany) alone or in combination with co-stimulation: either 10 ng ml⁻¹ of IFN- γ (R&D Systems, Wiesbaden, Germany) or activating anti-CD40 antibody (clone 3/23, 1 μg ml⁻¹; BD Bioscience, Heidelberg, Germany). Furthermore, splenocytes were stimulated for 4 hours with other TLR stimuli such as 10 μg ml⁻¹ zymosan (Sigma, Steinheim, Germany), 1 μg ml⁻¹ imiquimod (Sequoia Research Product, Reading, UK), or 10 μg ml⁻¹ CpG ODN (R&D Systems, Germany). As a control, wild-type spleen cells were treated additionally with p38 MAP kinase inhibitors SB203580 (10 μM ; Merck Biosciences, Darmstadt, Germany) or SB220025 (10 μM ; Axxora, Lörrach, Germany), respectively.

For TCR stimulation, CD4⁺ T cells were positively separated from splenocytes by using anti-CD4 (L3T4)-coated magnetic MACS beads (Miltenyi Biotech, Bergisch Gladbach, Germany) following the manufacturer's protocol. T cells were cultured at a density of 2 \times 10⁶ cells per ml in RPMI-1640 medium supplemented with FCS (10% v/v), L-glutamine (2 mM), and penicillin/streptomycin (each at 10,000 U ml⁻¹) (all Biochrom KG, Berlin, Germany) and stimulated with plate-bound anti-CD3 (clone 17A2, 10 μg ml⁻¹; BD Bioscience) and anti-CD28 (clone 37.51, 10 μg ml⁻¹; BD Bioscience). As a control, wild-type spleen cells were treated additionally with SB203580 (Merck Biosciences) at a concentration of 10 μM .

Supernatants were collected after stimulation of the respective cells and cytokine concentrations were determined with TNF- α ELISA (OptEIA set; BD Biosciences) according to the manufacturer's description.

Statistical methods

Statistical methods used for murine skin inflammation models (comparison of groups in kinetic measurements of skin thickness) were the Kruskal-Wallis and Mann-Whitney *U*-tests by SPSS software (SPSS). Statistics for end point parameters were collected by Fieller's test using a program from Bayer Schering Pharma AG based on the SAS System for Windows 6.12 (SAS Institute) (Schottelius *et al.*, 2002). Statistical methods used for *ex vivo* and *in vitro* investigations were the Mann-Whitney *U*-test and Wilcoxon's matched-pairs signed-ranks test, respectively, using SPSS software. If not otherwise indicated, mean values \pm SD are shown. Statistical significances at $P < 0.05$, < 0.01 , and < 0.001 are indicated by one, two, and three asterisks, respectively.

CONFLICT OF INTEREST

The authors UZ, WDD, TMZ, LR, AM, BB, AB, and KA are employees and shareholders of Bayer Schering AG. Bayer Schering Pharma AG is not actively pursuing MK2.

ACKNOWLEDGMENTS

We thank Detlef Opitz, Christian Okon, Michaela Nieter, and Antje HaeuBler-Quade for excellent technical assistance. All data for this publication have been generated at Bayer Schering Pharma AG.

REFERENCES

- Alford JG, Stanley PL, Todderud G, Trampusch KM (1992) Temporal infiltration of leukocyte subsets into mouse skin inflamed with phorbol ester. *Agents Actions* 37:260-7
- Allen M, Svensson L, Roach M, Hambor J, McNeish J, Gabel CA (2000) Deficiency of the stress kinase p38alpha results in embryonic lethality: characterization of the kinase dependence of stress responses of enzyme-deficient embryonic stem cells. *J Exp Med* 191:859-70
- Anderson DR, Meyers MJ, Vernier WF, Mahoney MW, Kurumbail RG, Caspers N et al. (2007) Pyrrolopyridine inhibitors of mitogen-activated protein kinase-activated protein kinase 2 (MK-2). *J Med Chem* 50:2647-54
- Badger AM, Bradbeer JN, Votta B, Lee JC, Adams JL, Griswold DE (1996) Pharmacological profile of SB 203580, a selective inhibitor of cytokine suppressive binding protein/p38 kinase, in animal models of arthritis, bone resorption, endotoxin shock and immune function. *J Pharmacol Exp Ther* 279:1453-61
- Dambach DM (2005) Potential adverse effects associated with inhibition of p38alpha/beta MAP kinases. *Curr Top Med Chem* 5:929-39
- Duraisamy S, Bajpai M, Bughani U, Dastidar SG, Ray A, Chopra P (2008) MK2: a novel molecular target for anti-inflammatory therapy. *Expert Opin Ther Targets* 12:921-36
- Funding AT, Johansen C, Gaestel M, Bibby BM, Lilleholt LL, Kragballe K et al. (2009) Reduced oxazolone-induced skin inflammation in MAPKAP kinase 2 knockout mice. *J Invest Dermatol* 129:891-8
- Gaestel M (2006) MAPKAP kinases - MKs - two's company, three's a crowd. *Nat Rev Mol Cell Biol* 7:120-30
- Gaestel M, Mengel A, Bothe U, Asadullah K (2007) Protein kinases as small molecule inhibitor targets in inflammation. *Curr Med Chem* 14:2214-34
- Gaestel M, Kotlyarov A, Kracht M (2009) Targeting innate immunity protein kinase signaling in inflammation. *Nat Rev Drug Discov* 8:480-99
- Gorska MM, Liang Q, Stafford S, Goplen N, Dharajiya N, Guo L et al. (2007) MK2 controls the level of negative feedback in the NF-kappaB pathway and is essential for vascular permeability and airway inflammation. *J Exp Med* 204:1637-52
- Grimbaldeston MA, Nakae S, Kalesnikoff J, Tsai M, Galli SJ (2007) Mast cell-derived interleukin 10 limits skin pathology in contact dermatitis and chronic irradiation with ultraviolet B. *Nat Immunol* 8:1095-104
- Hegen M, Gaestel M, Nickerson-Nutter CL, Lin LL, Telliez JB (2006) MAPKAP kinase 2-deficient mice are resistant to collagen-induced arthritis. *J Immunol* 177:1913-7
- Jackson JR, Bolognese B, Hillegass L, Kassis S, Adams J, Griswold DE et al. (1998) Pharmacological effects of SB 22025, a selective inhibitor of P38 mitogen-activated protein kinase, in angiogenesis and chronic inflammatory disease models. *J Pharmacol Exp Ther* 284:687-92
- Johansen C, Funding AT, Otkjaer K, Kragballe K, Jensen UB, Madsen M et al. (2006) Protein expression of TNF-alpha in psoriatic skin is regulated at a posttranscriptional level by MAPK-activated protein kinase 2. *J Immunol* 176:1431-8
- Johansen C, Kragballe K, Westergaard M, Henningsen J, Kristiansen K, Iversen L (2005) The mitogen-activated protein kinases p38 and ERK1/2 are increased in lesional psoriatic skin. *Br J Dermatol* 152:37-42
- Kontoyiannis D, Boulougouris G, Manoloukos M, Armaka M, Apostolaki M, Pizarro T et al. (2002) Genetic dissection of the cellular pathways and signaling mechanisms in modeled tumor necrosis factor-induced Crohn's like inflammatory bowel disease. *J Exp Med* 196:1563-74
- Kotlyarov A, Neining A, Schubert C, Eckert R, Birchmeier C, Volk HD et al. (1999) MAPKAP kinase 2 is essential for LPS-induced TNF-alpha biosynthesis. *Nat Cell Biol* 1:94-7
- Lee JC, Laydon JT, McDonnell PC, Gallagher TF, Kumar S, Green D et al. (1994) A protein kinase involved in the regulation of inflammatory cytokine biosynthesis. *Nature* 372:739-46
- Lu HT, Yang DD, Wysk M, Gatti E, Mellman I, Davis RJ et al. (1999) Defective IL-12 production in mitogen-activated protein (MAP) kinase kinase 3 (Mkk3)-deficient mice. *EMBO J* 18:1845-57
- Manome H, Aiba S, Tagami H (1999) Simple chemicals can induce maturation and apoptosis of dendritic cells. *Immunology* 98:481-90
- Neining A, Kontoyiannis D, Kotlyarov A, Winzen R, Eckert R, Volk HD et al. (2002) MK2 targets AU-rich elements and regulates biosynthesis of tumor necrosis factor and interleukin-6 independently at different post-transcriptional levels. *J Biol Chem* 277:3065-8
- O'Leary JG, Goodarzi M, Drayton DL, von Andrian UH (2006) T cell- and B cell-independent adaptive immunity mediated by natural killer cells. *Nat Immunol* 7:507-16
- Rogers DF, Giembycz MA (1998) Asthma therapy for the 21st century. *Trends Pharmacol Sci* 19:160-4
- Ronkina N, Kotlyarov A, Dittrich-Breiholz O, Kracht M, Hitti E, Milarski K et al. (2007) The mitogen-activated protein kinase (MAPK)-activated protein kinases MK2 and MK3 cooperate in stimulation of tumor necrosis factor biosynthesis and stabilization of p38 MAPK. *Mol Cell Biol* 27:170-81
- Salvador JM, Mittelstadt PR, Guszczynski T, Copeland TD, Yamaguchi H, Appella E et al. (2005) Alternative p38 activation pathway mediated by T cell receptor-proximal tyrosine kinases. *Nat Immunol* 6:390-95
- Schottelius AJ, Giesen C, Asadullah K, Fierro IM, Colgan SP, Bauman J et al. (2002) An aspirin-triggered lipoxin A4 stable analog displays a unique topical anti-inflammatory profile. *J Immunol* 169:7063-70
- Schottelius AJ, Moldawer LL, Dinarello CA, Asadullah K, Sterry W, Edwards CK III (2004) Biology of tumor necrosis factor-alpha- implications for psoriasis. *Exp Dermatol* 13:193-222
- Takanami-Ohnishi Y, Amano S, Kimura S, Asada S, Utani A, Maruyama M et al. (2002) Essential role of p38 mitogen-activated protein kinase in contact hypersensitivity. *J Biol Chem* 277:37896-903
- Wang X, Xu L, Wang H, Young PR, Gaestel M, Feuerstein GZ (2002) Mitogen-activated protein kinase-activated protein (MAPKAP) kinase 2 deficiency protects brain from ischemic injury in mice. *J Biol Chem* 277:43968-72
- Wysk M, Yang DD, Lu HT, Flavell RA, Davis RJ (1999) Requirement of mitogen-activated protein kinase kinase 3 (MKK3) for tumor necrosis factor-induced cytokine expression. *Proc Natl Acad Sci USA* 96:3763-8
- Zollner T, Igney FH, Asadullah K (2004) Acute and chronic models of allergic contact dermatitis: advantages and limitations. In: *Animal Models of T Cell-Mediated Skin Diseases*. (Zollner T, Renz H, Asadullah K, eds). Springer Berlin, Heidelberg, New York, ISBN: 3-540-21067-9, 255-75
- Zugel U, Steinmeyer A, Giesen C, Asadullah K (2002) A novel immunosuppressive 1alpha,25-dihydroxyvitamin D3 analog with reduced hypercalcemic activity. *J Invest Dermatol* 119:1434-42



Published in final edited form as:

Br J Dermatol. 2010 March ; 162(3): 487–496. doi:10.1111/j.1365-2133.2009.09552.x.

Visualizing CD4 T-cell migration into inflamed skin and its inhibition by CCR4/CCR10 blockades using *in vivo* imaging model

X. Wang^{*}, M. Fujita[†], R. Prado[†], A. Tousson[‡], H-C. Hsu^{*}, A. Schottelius[§], D.R. Kelly[¶], P.A. Yang^{*}, Q. Wu^{*}, J. Chen^{*}, H. Xu^{**}, C.A. Elmetz^{**}, J.D. Mountz^{*,††}, and C.K. Edwards III[†]

^{*}Department of Medicine, Division of Clinical Immunology and Rheumatology, University of Alabama at Birmingham, Birmingham, AL 35294, USA

[‡]High Resolution Imaging Facility and Department of Cell Biology, University of Alabama at Birmingham, Birmingham, AL 35294, USA

[¶]Department of Pathology, Children's Hospital, University of Alabama at Birmingham, Birmingham, AL 35294, USA

^{**}Department of Dermatology, University of Alabama at Birmingham, Birmingham, AL 35294, USA

[†]Department of Dermatology, University of Colorado Denver, Aurora, CO 80045, USA

[§]Department of Development, Genentech, South San Francisco, CA 94080-4990, USA (currently at MorphoSys AG, Martinsried, Germany)

^{††}Veterans Affairs Medical Center, Birmingham, AL 35233, USA

Summary

Background—Chemokines are critical mediators of T-cell homing into inflamed skin. The complex nature of this multicellular response makes it difficult to analyse mechanisms mediating the early responses *in vivo*.

Objectives—To directly visualize T-cell homing into inflamed skin and its inhibition by blockades using a unique noninvasive confocal microscopy.

Materials and methods—A mouse model of allergic contact dermatitis was used. T cells from oxazolone-sensitized and -challenged Balb/c mice were first analysed phenotypically *in vitro*. CD4 T cells were then labelled with a tracker dye and transferred into Balb/c-SCID mice. The recipient mice were challenged with oxazolone and CD4 T-cell homing into inflamed skin was visualized.

Results—T cells with the skin homing receptors CCR4 and CCR10 were increased in the affected skin and draining lymph nodes, and effectively attracted by their specific chemokines CCL17, CCL22 and CCL27 *in vitro*. Using *in vivo* imaging, T-cell migration into the inflamed skin was observed at 2 h after application, peaking at 12 h and continuing for 48 h. Simultaneous systemic administration of neutralizing antibodies against CCR4 ligands (CCL17 and CCL 22) and CCR10 ligand (CCL27) led to a significant suppression of T-cell migration and skin inflammation.

Correspondence Mayumi Fujita, mayumi.fujita@ucdenver.edu.

Conflicts of interest

None declared.

This article contains online supplementary material.

Conclusions—Our data indicate that these tissue-selective adhesion molecules and chemokine/receptor pathways act in concert to attract specialized T-cell populations to mediate cutaneous inflammation. The *in vivo* imaging technique can be applicable to other models of cutaneous diseases to help with better understanding of the pathogenesis and monitoring the therapeutic effects.

Keywords

cell trafficking; chemokines; skin homing; T cells

Expression of specific chemokine receptors and adhesion molecules on T-cell subsets accounts for selective recruitment of effector T cells to sites of inflammation.¹ Identification of chemokine ligand–receptor interactions that mediate the earliest events in the recruitment of T cells to the allergen-impregnated skin could potentially have broad implications for the development of therapeutic strategies.

Two chemokine receptors, CCR4 and CCR10, have been proposed to be important for homing of skin-specific T lymphocytes in humans.^{2–6} CCR4 has two known ligands: CCL17 (thymus and activation-regulated chemokine) and CCL22 (macrophage-derived chemokine). Both are expressed abundantly by dendritic cells and facilitate the recruitment of activated T cells into inflamed skin.^{7,8} CCR10 ligand, CCL27 (cutaneous T cell-attracting chemokine), is expressed by skin keratinocytes.^{2,9–10}

The role of CCR4 and CCR10 for T-cell trafficking into inflamed skin is a topic of extensive research. However, experimental data for the requirement and redundancy of individual receptors in T-cell homing and the resulting skin inflammation is controversial. Homey *et al.* demonstrated marked reduction of dinitrofluorobenzene (DNFB)-induced allergic contact dermatitis (ACD) with neutralization of CCL27–CCR10 interactions in Balb/c mice.⁵ Alferink *et al.* reported the reduction of DNFB- and fluorescein–isothiocyanate (FITC)-induced ACD in CCL17-deficient mice.¹¹ On the other hand, Reiss *et al.* concluded that simultaneous inhibition of CCR4 and CCR10 is required to block lymphocyte recruitment by showing the necessity of anti-CCL27 to reduce DNFB-induced ACD in CCR4 knockout B57Bl/6 mice.² Similarly, Mirshahpajah *et al.* demonstrated that only combination therapy of neutralizing antibodies to CCL17, CCL22 and CCL27 resulted in oedema inhibition using three different ACD models.⁶

Different models and experiment designs in these studies may in part explain the controversial results. For example, the effect of blocking chemokine ligands or receptors may not be well represented in studies using knockout mice, because immune system and compensatory mechanisms may be developmentally altered in these animals. Given that tissue microenvironment strongly influences chemokine expression and T-cell migration, a functional assay using intact tissue where the physiological context is preserved may be important to properly assess the dynamic migration of specific T-cell subpopulations and address the role of chemokine ligand–receptor interactions *in vivo* and *ex vivo*.¹²

Here we developed a unique *in vivo* imaging technique that allowed direct and real-time visualization of T-cell migration and its response to chemokines in the inflamed skin. We demonstrate that CCL17, CCL22 and CCL27 play important roles in attracting skin-homing memory T cells into the inflamed skin of oxazolone-induced ACD, and that simultaneous blockade of these interactions is required to efficiently attenuate T-cell migration and inflammation.

Materials and methods

Animals

Female Balb/c and Balb/c-SCID mice (6–8-weeks old) were obtained from The Jackson Laboratory (Bar Harbor, ME, U.S.A.) and were kept under specific pathogen-free conditions. Experiment protocols were approved by the Institutional Animal Care and Use Committee of University of Alabama at Birmingham. Animal studies were performed in accordance with National Institutes of Health Animal Care and Use guidelines.

Mouse model of allergic contact dermatitis and antichemokine treatment

The protocol for inducing ACD is illustrated in Figure 1. Balb/c mice were sensitized on day 0 by applying 150 μ L of 3% oxazolone (4-ethoxymethylene-2-oxazolin-5-one; Sigma-Aldrich, St Louis, MO, U.S.A.) in acetone : olive oil (4 : 1) on the shaved abdomen. Mice were challenged on day 6 by epicutaneous application of 1% oxazolone (20 μ L) on the right ear. Left ears were treated with vehicle alone. Mice were sacrificed 24 h later and lymphocytes from skin-draining lymph nodes (LNs) (cervical, axillary and brachial) were prepared using a 70- μ m nylon cell strainer (BD Falcon, San Jose, CA, U.S.A.). Skin-infiltrating T cells were released from the dermis after separating the epidermal sheets as described.¹³ Lymphocytes from bilateral LNs and ears were collected separately and used for phenotypic and functional characterization.

Lymphocytes from right-side draining LNs were purified with CD4 selection columns (R&D Systems, Inc., Minneapolis, MN, U.S.A.). The column-purified CD4⁺ T cells were labelled *in vitro* with 10 μ mol L⁻¹ carboxyfluorescein succinimidyl ester (CFSE; Molecular Probes, Eugene, OR, U.S.A.) according to the manufacturer's instructions. CFSE-labelled T cells (5×10^7) suspended in 200 μ L of phosphate-buffered saline (PBS) were injected via the tail vein into unprimed congenic Balb/c-SCID recipients. Immediately after the adoptive transfer, 1% oxazolone (20 μ L) was applied to the right ears of the recipients while left ears were treated with vehicle only. Both ears were imaged in the confocal microscope.

For antichemokine experiments, 6 h and 2 h prior to the adoptive transfer, Balb/c-SCID mice received intravenously either 100 μ g neutralizing antichemokine antibodies (rat antimouse CCL17, goat antimouse CCL22, rat antimouse CCL27; R&D Systems) in PBS (200 μ L), or the same volume of IgG isotype control antibodies (rat IgG2A, goat IgG and rat IgG2B, respectively). Ear thickness was measured in a blinded fashion using Mitutoyo Dial Thickness Gage (APIS Inc., Middleburg Heights, OH, U.S.A.) at 0, 2, 12 and 48 h.

Flow cytometry analysis

Single-cell suspensions from bilateral LNs and skin were stained with goat FITC-conjugated anti-CD4, Cy5-conjugated anti-CD8, phycoerythrin (PE)-conjugated anti-CD62L, APC-conjugated anti-CD44 and APC-conjugated anti-CD3 (BD-Pharmingen, San Diego, CA, U.S.A.). They were also stained with goat anti-CCR4 (Abcam, Cambridge, MA, U.S.A.) and anti-CCR10 (Capralogics Inc., Hardwick, MA, U.S.A.), followed by cychrome-conjugated or biotinylated polyclonal antigoat IgG (Abcam). Cutaneous lymphocyte-associated antigen (CLA)-expressing cells were identified by flow cytometry using a recombinant mouse E-Selectin/Fc chimera (R&D Systems, Inc)14:15 followed by PE-conjugated goat antihuman IgG (Jackson Immunoresearch, Inc., West Grove, PA, U.S.A.).

Immunohistochemistry

Cryosections (6- μ m) of mouse ear skin and LNs were fixed in Fix-Frozen cocktail solutions (University of Alabama at Birmingham Center for Immunohistochemistry, Birmingham, AL, U.S.A.) for 20 min, and treated with avidin-biotin block solutions (Biogenex, San

Ramon, CA, U.S.A.) and FcR block (Innovex Biosciences, Richmond, CA, U.S.A.) consecutively for 10 min each at room temperature. Sections were incubated overnight at 4 °C with primary antibodies (rabbit antimouse CCR4 or goat antimouse CCR10; Alexis Biochemicals, San Diego, CA, U.S.A.) or isotype control antibodies. To block endogenous peroxidase activity, 3% aqueous hydrogen peroxide (Sigma-Aldrich) was used for 15 min at room temperature. Biotinylated goat antirabbit IgG or mouse antigoat IgG (Biocare Medical, Walnut Creek, CA, U.S.A.) were incubated for 40 min at room temperature, followed by horseradish peroxidase-conjugated streptavidin. Slides were developed using diaminobenzidine tetrachloride substrate, counterstained with haematoxylin and analysed using light microscopy.

Chemotaxis assay

Single-cell suspensions were prepared from draining LNs as above. Standard transmigration assays using 3- μ m pore Millipore Multiscreen MIC (Millipore, Billerica, MA, U.S.A.) were performed. CCL17, CCL22 or CCL27 (100 nmol L⁻¹; R&D Systems, Inc.) or the combination of three chemokines was added to the 96-well feeder tray (lower chamber). Recombinant murine CCL21 (secondary lymphoid tissue chemoattractant, SLC; PeproTech, Rocky Hill, NJ, U.S.A.) was used as a positive control. Donor mouse CD3⁺ T cells (1×10^6) or purified CD4⁺ T cells (> 95% pure) were suspended in 100 μ L chemotaxis buffer (1 \times Hank's balanced saline solution with 20 mmol L⁻¹ HEPES, pH 7.4 and 0.5% bovine serum albumin) and placed into the upper chamber. After 3-h incubation at 37 °C and 5% CO₂, 16 μ L of 6.25 μ g mL⁻¹ Calcein AM (Molecular Probes) was added into each well and incubated for 45 min at 37 °C in the dark. Migration of T cells to chemoattractants was measured using a Fusion™ Universal microplate analyser (Packard Bioscience, Boston, MA, U.S.A.) at excitation : emission wavelengths of 585 : 530 nm. The percentage migration was calculated by dividing the number of migrated T cells by the number of input cells multiplied by 100.

In vivo imaging

The hair on the ear of Balb/c-SCID mice was removed using 'Nair® lotion' 48 h before imaging. Ears of recipient mice were positioned on a glass transparent microscope cover slip and imaged after the adoptive transfer. During imaging, mice were maintained under anaesthesia with 200 mg kg⁻¹ pentobarbital sodium by intraperitoneal injection with constant heart rate and body temperature monitoring. Imaging was performed using a Leica DMIRBE inverted epifluorescence/Nomarski microscope outfitted with Leica TCS NT Laser Confocal optics (Leica, Inc., Exton, PA, U.S.A.). Excitation of CFSE was provided with an Argon neon laser using the 488 nm line and 553 nm for blood vessels. Precise control of fluorochrome excitation and emission was afforded by an acoustooptical tunable filter and TCS SP prism spectrophotometer (Leica, Inc.), respectively. Streaming video wide-field fluorescence microscopy was performed using a digital Canon camera attached on the ocular head of the Leica DM IRBE microscope. In this case, fluorescence excitation of the CFSE label was provided by a Mercury vapour lamp.

Statistical analysis

Data were analysed using standard statistical analysis (analysis of variance and Student's *t*-test). Data are presented as mean \pm SEM and differences were considered significant if *P* < 0.05.

Results

Allergic contact dermatitis to oxazolone induces increased number of CCR4 and CCR10 positive cells in the skin and draining lymph nodes

Induction of ACD was confirmed by oedema and marked infiltration of neutrophils, lymphocytes and plasma cells histologically (Fig. S1a,b). Immunohistochemical staining revealed CCR4⁺ cells and CCR10⁺ cells in oxazolone-treated but not vehicle-treated skin and LNs (Fig. S1c–j).

As expression of CCR4 and CCR10 has been well characterized in CD4⁺ T cells,^{10,16} their expression in skin and draining LNs was further analysed for the presence of CLA on the CD4⁺CD62L^{lo}CD44^{hi} memory subpopulation (Fig. 2a).¹⁷ CLA⁺ memory CD4⁺ T cells were increased in draining LNs of oxazolone-treated skin compared with controls (Fig. 2b). CD4⁺CD62L^{lo}CD44^{hi}CLA⁺ T cells expressing CCR4 and CCR10 were significantly increased in oxazolone-challenged ear and LNs, compared with those of controls (Fig. 2c). These findings confirm that oxazolone-induced ACD results in upregulation of CCR4 and CCR10 on CD4⁺CD62L^{lo}CD44^{hi}CLA⁺ T cells in the LNs, leading to the selective recruitment and enrichment of T cells expressing these chemokine receptors in the oxazolone-treated ear skin.

CCL17, CCL22 and CCL27 chemoattract skin-homing CD4⁺ T cells

We next determined if the expression of CCR4 or CCR10 induced by oxazolone sensitization correlates with their functional response to the ligands CCL17, CCL22 and CCL27 in a chemotaxis assay.¹⁸ After 3-h incubation with either CCL17, CCL22 or CCL27 alone, or all three in combination, CD4⁺ T cells from draining LNs migrated efficiently towards the individual or the combined chemokines (Fig. 3). Interestingly, migration to the combined chemokines was not greater than migration to the individual chemokines. Unfractionated CD3⁺ T cells exhibited lower migration responses to these ligands, but migrated equally well to a positive control chemokine, SLC2.¹⁴ These results indicate that CD4⁺ T cells from oxazolone-treated draining LNs respond effectively to CCR4 ligands (CCL17, CCL22) or CCR10 ligand (CCL27). There appear to be little additive or synergistic effect of these chemokines for effective T-cell recruitment to skin *in vitro*.

Oxazolone-induced allergic contact dermatitis increases migration and extravasation of sensitized T cells in skin

To enable *in vivo* imaging of T cells, we applied a two-step T-cell migration model as shown in Figure 1. Oxazolone-sensitive donor CD4⁺ T cells were labelled *in vitro* with CFSE (Fig. 4a), and injected intravenously in unprimed recipient Balb/c-SCID mice. Balb/c-SCID mice were used as recipients, due to their lack of lymphocytes, allowing clear evaluation of migration of donor lymphocytes without the effects from the recipient's immune system. Ears of recipient mice were challenged, and migration of the adoptively transferred donor T cells was analysed by time-lapse confocal microscopy (Fig. 4b,c) or streaming video wide-field fluorescence microscopy (Fig. 5) when cell movement was observed. When cell movement was markedly decreased, migration of T cells was analysed by static wide-field fluorescence microscopy (Fig. 4d–g). Together, these microscopy methods provided information in X-Y-Z-T dimensions. Wide-field fluorescence microscopy was also helpful in acquiring images of T cells when fluorescence intensity of the labelled T cells was weak or when a higher background fluorescence of the tissue was needed to trace the path of the T cells through the dark, fluorescent-negative blood vessels.

Immediately after adoptive transfer, circulating CFSE⁺ cells were visible within blood vessels of both oxazolone-treated and vehicle-treated ears. From 0 h up to 2 h post-transfer,

no difference in the number of circulating T cells was noted between oxazolone-treated and vehicle-treated ears (Fig. 4b,c), although capillaries were enlarged in the oxazolone-treated ears. Shortly after 2-h post-transfer, transmigration of intravascular CFSE⁺ cells to the tissue was noted in the oxazolone-treated ears but not vehicle-treated ears. This extravasation of T cells peaked at 12 h (Fig. 4d,e), and continued until 48 h after the application of oxazolone (Fig. 4f,g). Detailed evaluation of individual extravasating T cells was performed using streaming-video still frames, which allowed the documentation of the entire process, including the intravascular movement of the T cell (Fig. 5a–d), reduction of intravascular cell velocity and rolling, with subsequent adherence to the endothelium (Fig. 5e,f), crossing of the vessel wall (Fig. 5f,g) and migration into the skin tissue (Fig. 5h,i). It was noted that cells remained adherent to the endothelium for at least 20 s prior to transmigration.

Neutralization of CCL17, CCL22 and CCL27 impairs lymphocyte recruitment to the inflamed ear skin

To determine the effects of CCR4 and CCR10 ligands on the recruitment of T cells into the skin, recipient mice were administered anti-CCL17, anti-CCL22 and anti-CCL27 neutralizing antibodies 6 h and 2 h before adoptive transfer (Fig. 1). Isotype control antibodies were used in control mice. Extravasated T cells were observed in oxazolone-treated ears but not vehicle-treated ears after 2 h (Fig. 6a,b). Blocking CCR4 (with a combination of anti-CCL17 and anti-CCL22) or CCR10 (with anti-CCL27) did not reduce the recruitment of CD4⁺ cells into the inflammation sites (data not shown). However, simultaneous administration of all three neutralizing antibodies led to a marked decrease in trafficking of CD4⁺ cells at 12 h and 48 h compared with the administration of isotype control antibodies (Fig. 6b,d). As expected, vehicle-treated ears demonstrated only a small number of CD4⁺ cells, which was not changed with administration of neutralizing antibodies (Fig. 6a,c). Videos are available as online supplementary material.

Cryostat sections of ear tissues demonstrated reduction of green fluorescing CFSE⁺ skin-infiltrating T cells after administration of all three neutralizing antibodies compared with those after isotype control treatment (Fig. 6e,f).

Quantitative analysis of the *in vivo* migration was performed by counting the number of extravasated CFSE⁺ T cells in 10 nonconsecutive microscopic images of each ear at each time point, in a blinded fashion. As shown in Figure 6g, administering three neutralizing antibodies led to a significant decrease in trafficking of CD4⁺ cells into oxazolone-treated ear compared with treatment with control antibodies at 12 h and 48 h of inflammation.

Inhibition of CCR4 and CCR10 chemokines *in vivo* impairs ear swelling responses

To determine if inhibiting T-cell migration into the ear by antichemokine antibodies is associated with a reduction in the inflammatory cascades that lead to ear swelling, measurement of ear thickness was performed. Mice not receiving donor cells did not exhibit significant ear swelling after vehicle or oxazolone application (Fig. 7, left group, 1st and 2nd columns). Ear swelling was observed in mice that had received donor T cells and were applied with oxazolone (left group, 4th column), but not in those applied with vehicle (left group, 3rd column). Mice that had been pretreated with either anti-CCL17 plus anti-CCL22 or anti-CCL27 exhibited increased ear swelling comparable to that of the mice that were left untreated or treated with isotype controls (middle two groups of columns). In contrast, simultaneous administration of all three antichemokine neutralizing antibodies led to a significant reduction in skin swelling in the oxazolone-treated ears (right group columns).

Discussion

T cells are essential participants in pathological cutaneous inflammatory reactions. Using an oxazolone ACD mouse model,¹⁹ we demonstrated that T cells with the skin homing receptors CCR4 and CCR10 are increased in the affected skin and draining LNs, and that these cells are effectively attracted by their specific chemokines CCL17, CCL22 and CCL27 *in vitro*. Using *in vivo* confocal and wide-field fluorescence microscopy, we demonstrated that oxazolone exposure increases migration and extravasation of sensitized T cells in skin, and that this can be blocked by simultaneous neutralization of CCL17, CCL22 and CCL27. These results were supported by the impaired *in vivo* ear swelling through simultaneous inhibition of CCR4 ligands (CCL17 and CCL22) and CCR10 ligand (CCL27). Neutralization of CCR4 ligands or CCR10 ligand alone was not sufficient to block the transmigration of T cells into the tissue, indicating a redundant and compensatory mechanism. The results suggest that these tissue-selective adhesion molecules and chemokine-receptor pathways may act in concert to attract specialized subpopulations of T cells to mediate cutaneous inflammation. Although the reduction in T-cell transmigration was statistically significant, it was not completely blocked when both CCR4 and CCR10 ligands were neutralized. This can be explained by incomplete neutralization of CCL17/22/27 by antibodies *in vivo*, the presence of other chemokines reacting to CCR4 and/or CCR10, the presence of other chemokine receptors in skin homing or complexity of extravasation steps.

Recruitment of T cells into an inflammatory site is crucial in the pathogenesis of skin disorders. It is mediated by a multistep process involving activation through chemoattractant-receptor interactions, as well as attachment and rolling through selectin-carbohydrate interactions.²⁰ Analysis of T-cell migration *in vivo* enables direct visualization of migrating T cells and evaluation of these complex interactive effects of several chemokines in the tissue microenvironment. The unique intravital confocal microscopy technique described here provides the means to image the behaviour of effector T cells in response to subsequent stimuli or inhibitors in its microenvironment, and was used for the evaluation of selectin-dependent T-cell migration in an ACD mouse model.²¹

In vivo imaging has not only been proven to be an important technique in basic science research, but has recently been explored as a potentially powerful tool in the clinical setting,²² especially to assist differentiating allergic from irritant contact dermatitis.²³⁻²⁵ Reflectance confocal microscopy used in patients with various cutaneous conditions may provide tissue resolution comparable to that of standard histology and allows repeated monitoring of the dynamic cell changes, demonstrating useful translation of scientific research into clinical applications.

Another important clinical application of modern technology in basic science research is the use of biological blocking agents. Blocking cytokines or inflammatory receptors has shown significant therapeutic potential in a number of inflammatory diseases such as psoriasis, rheumatoid arthritis and cancer.²⁶ Dual CCR4 and CCR10 antibody blockage could potentially be used in cutaneous diseases where memory T-cell trafficking plays a major role in the pathogenesis. The relative requirement (or redundancy) of CCR4 and CCR10 during skin lymphocyte homing may vary under different circumstances and requires further investigation to optimize the therapeutic potentials.

Although we propose that *in vivo* results from the oxazolone-treated animal model are more informative than *in vitro* studies, caution should be exercised in attempting any extrapolation of the findings to human diseases. Animal models of cutaneous diseases may not precisely mimic skin diseases observed in humans,²⁷ and T-cell skin homing receptors may have

different roles in different species. The exact role of these chemokine receptors in T-cell homing to the skin and the translation of current animal studies into human therapeutic drugs awaits further elucidation.

In summary, our results using a unique *in vivo* imaging technique demonstrate that simultaneous inhibition of both CCR4 and CCR10 effectively blocks lymphocyte recruitment, supporting the concept of redundant and overlapping roles of CCR4 and CCR10 in the T-cell recruitment into the inflamed skin in mice. Further investigation will be needed to determine if, under different physiological conditions, CCR4 and/or CCR10 receptors and their respective chemokines exert separate or additive biological effects. We believe the unique *in vivo* imaging technique can be applicable to other models of cutaneous diseases to help with better understanding of pathogenesis in a living system.

Supplementary Material

Refer to Web version on PubMed Central for supplementary material.

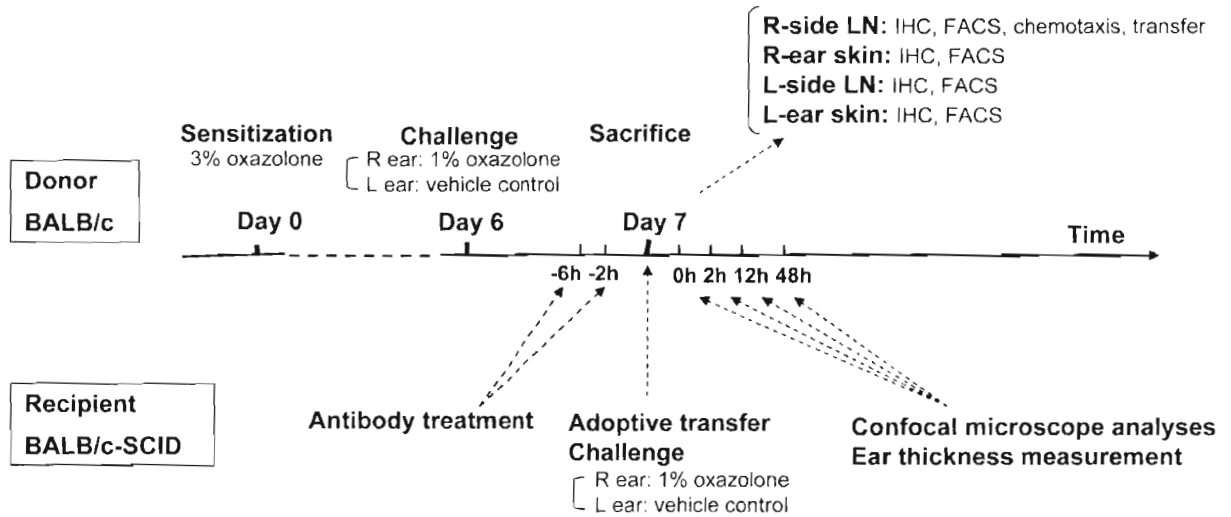
Acknowledgments

We thank Ms Lualhati Harkins for expert technical assistance with immunohistochemistry staining, and Ms Carol Humber, Evelyn Rogers and Nancy Gunzner for excellent secretarial assistance. This work is supported by NIH grants R01AI046990-05 and P30 AR50948, a University of Alabama at Birmingham HSF-GEF grant, a National Psoriasis Foundation Grant and a Birmingham VAMC Merit Review Grant.

References

1. Santamaria LF, Perez Soler MT, Hauser C, et al. Allergen specificity and endothelial transmigration of T cells in allergic contact dermatitis and atopic dermatitis are associated with the cutaneous lymphocyte antigen. *Int Arch Allergy Immunol.* 1995; 107:359–362. [PubMed: 7613172]
2. Reiss Y, Proudfoot AE, Power CA, et al. CC chemokine receptor (CCR)4 and the CCR10 ligand cutaneous T cell-attracting chemokine (CTACK) in lymphocyte trafficking to inflamed skin. *J Exp Med.* 2001; 194:1541–1547. [PubMed: 11714760]
3. Soler D, Humphreys TL, Spinola SM, et al. CCR4 versus CCR10 in human cutaneous TH lymphocyte trafficking. *Blood.* 2003; 101:1677–1682. [PubMed: 12406880]
4. Kunkel EJ, Kim CH, Lazarus NH, et al. CCR10 expression is a common feature of circulating and mucosal epithelial tissue IgA Ab-secreting cells. *J Clin Invest.* 2003; 111:1001–1010. [PubMed: 12671049]
5. Homey B, Alenius H, Muller A, et al. CCL27-CCR10 interactions regulate T cell-mediated skin inflammation. *Nat Med.* 2002; 8:157–165. [PubMed: 11821900]
6. Mirshahpanah P, Li YY, Burkhardt N, et al. CCR4 and CCR10 ligands play additive roles in mouse contact hypersensitivity. *Exp Dermatol.* 2008; 17:30–34. [PubMed: 18095942]
7. Hammad H, Smits HH, Ratajczak C, et al. Monocyte-derived dendritic cells exposed to Der p 1 allergen enhance the recruitment of Th2 cells: major involvement of the chemokines TARC/CCL17 and MDC/CCL22. *Eur Cytokine Netw.* 2003; 14:219–228. [PubMed: 14715413]
8. Lieberam I, Forster I. The murine beta-chemokine TARC is expressed by subsets of dendritic cells and attracts primed CD4+ T cells. *Eur J Immunol.* 1999; 29:2684–2694. [PubMed: 10508243]
9. Morales J, Homey B, Vicari AP, et al. CTACK, a skin-associated chemokine that preferentially attracts skin-homing memory T cells. *Proc Natl Acad Sci U S A.* 1999; 96:14470–14475. [PubMed: 10588729]
10. Moed H, Boersma DM, Tensen CP, et al. Increased CCL27-CCR10 expression in allergic contact dermatitis: implications for local skin memory. *J Pathol.* 2004; 204:39–46. [PubMed: 15307136]
11. Alferink J, Lieberam I, Reindl W, et al. Compartmentalized production of CCL17 *in vivo*: strong inducibility in peripheral dendritic cells contrasts selective absence from the spleen. *J Exp Med.* 2003; 197:585–599. [PubMed: 12615900]

12. Edinger M, Hoffmann P, Contag CH, et al. Evaluation of effector cell fate and function by *in vivo* bioluminescence imaging. *Methods*. 2003; 31:172–179. [PubMed: 12957575]
13. Kunkel EJ, Campbell JJ, Haraldsen G, et al. Lymphocyte CC chemokine receptor 9 and epithelial thymus-expressed chemokine (TECK) expression distinguish the small intestinal immune compartment: epithelial expression of tissue-specific chemokines as an organizing principle in regional immunity. *J Exp Med*. 2000; 192:761–768. [PubMed: 10974041]
14. Campbell JJ, Bowman EP, Murphy K, et al. 6-C-kine (SLC), a lymphocyte adhesion-triggering chemokine expressed by high endothelium, is an agonist for the MIP-3beta receptor CCR7. *J Cell Biol*. 1998; 141:1053–1059. [PubMed: 9585422]
15. Zanardo RC, Bonder CS, Hwang JM, et al. A down-regulatable E-selectin ligand is functionally important for PSGL-1-independent leukocyte-endothelial cell interactions. *Blood*. 2004; 104:3766–3773. [PubMed: 15304396]
16. Andrew DP, Ruffing N, Kim CH, et al. C-C chemokine receptor 4 expression defines a major subset of circulating nonintestinal memory T cells of both Th1 and Th2 potential. *J Immunol*. 2001; 166:103–111. [PubMed: 11123282]
17. Seddon B, Tomlinson P, Zamoyska R. Interleukin 7 and T cell receptor signals regulate homeostasis of CD4 memory cells. *Nat Immunol*. 2003; 4:680–686. [PubMed: 12808452]
18. Campbell JJ, Haraldsen G, Pan J, et al. The chemokine receptor CCR4 in vascular recognition by cutaneous but not intestinal memory T cells. *Nature*. 1999; 400:776–780. [PubMed: 10466728]
19. Xu H, DiIulio NA, Fairchild RL. T cell populations primed by hapten sensitization in contact sensitivity are distinguished by polarized patterns of cytokine production: interferon gamma-producing (Tc1) effector CD8+ T cells and interleukin (Il) 4/Il-10-producing (Th2) negative regulatory CD4+ T cells. *J Exp Med*. 1996; 183:1001–1012. [PubMed: 8642241]
20. Carballido JM, Biedermann T, Schwarzler C, et al. The SCID-hu skin mouse as a model to investigate selective chemokine mediated homing of human T-lymphocytes to the skin *in vivo*. *J Immunol Methods*. 2003; 273:125–135. [PubMed: 12535803]
21. Hwang JM, Yamanouchi J, Santamaria P, et al. A critical temporal window for selectin-dependent CD4+ lymphocyte homing and initiation of late-phase inflammation in contact sensitivity. *J Exp Med*. 2004; 199:1223–1234. [PubMed: 15117973]
22. Gerger A, Hofmann-Wellenhof R, Samonigg H, et al. *In vivo* confocal laser scanning microscopy in the diagnosis of melanocytic skin tumours. *Br J Dermatol*. 2009; 160:475–481. [PubMed: 19183178]
23. Swindells K, Burnett N, Rius-Diaz F, et al. Reflectance confocal microscopy may differentiate acute allergic and irritant contact dermatitis *in vivo*. *J Am Acad Dermatol*. 2004; 50:220–228. [PubMed: 14726876]
24. Astner S, Gonzalez E, Cheung AC, et al. Non-invasive evaluation of the kinetics of allergic and irritant contact dermatitis. *J Invest Dermatol*. 2005; 124:351–359. [PubMed: 15675954]
25. Gonzalez S, Gonzalez E, White WM, et al. Allergic contact dermatitis: correlation of *in vivo* confocal imaging to routine histology. *J Am Acad Dermatol*. 1999; 40:708–713. [PubMed: 10321598]
26. Haringman JJ, Tak PP. Chemokine blockade: a new era in the treatment of rheumatoid arthritis? *Arthritis Res Ther*. 2004; 6:93–97. [PubMed: 15142257]
27. Zollner, TM.; Igney, FH.; Asadullah, K. Acute and chronic models of allergic contact dermatitis: advantages and limitations. In: Zollner, TM.; Renz, H.; Asadullah, K., editors. *Animal Models of T Cell Mediated Skin Diseases*; Ernst Schering Foundation Symposium Proceedings; Berlin, Heidelberg. Springer, 2005. p. 255-275.

**Fig. 1.**

Schematic diagram of the induction of oxazolone-induced allergic contact dermatitis mouse model and the T-cell adoptive transfer for *in vivo* imaging of T-cell migration. Balb/c female donor mice were sensitized with 3% oxazolone on the shaved abdomen on day 0 and were challenged with 1% oxazolone on the R ear on day 6, while the L ears were treated with vehicle alone. On day 7, LNs and ear skin were harvested for histological analysis and phenotypic analysis of lymphocytes by FACS. In addition, lymphocytes from R-side skin-draining LNs were used for *in vitro* chemotaxis analysis. CD4⁺ T cells purified from R-side skin-draining LNs were labelled with carboxyfluorescein succinimidyl ester ($10 \mu\text{mol L}^{-1}$) *in vitro*, and injected intravenously into unprimed recipient Balb/c-SCID mice. Immediately after the adoptive transfer, recipient mice were challenged with oxazolone or vehicle control on the R or L ear, respectively. Both ears of the anaesthetized recipients were then analysed by confocal microscopy at 0, 2, 12 and 48 h after the challenge. At each time point, ear thickness was also measured. In some experiments, the recipients received antichemokine antibodies (anti-CCL17, anti-CCL22 and anti-CCL27) or isotype control antibodies by intravenous injection 6 h and 2 h prior to donor cell transfer and challenge. FACS, fluorescence-activated cell sorting; IHC, immunohistochemistry; L, left; LN, lymph node; R, right

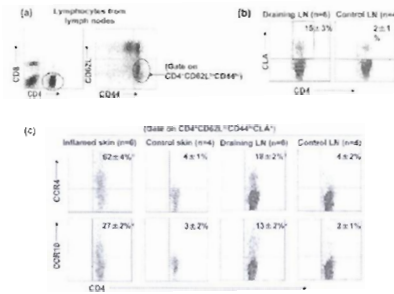


Fig. 2.

Cutaneous oxazolone challenge induces CD4⁺CD62L^{lo}CD44^{hi}CLA⁺ effector T cells and CCR4/CCR10 expression. Single-cell preparations of lymphocytes from draining LNs and the ear skin of the donor Balb/C mice were stained with anti-CD4, anti-CD8, anti-CD62L, anti-CD44, anti-CD3, and anti-CCR4 or anti-CCR10 and subjected to fluorescence-activated cell sorting analysis. Cells were gated on the T-cell memory phenotype (CD4⁺, CD62L^{lo} and CD44^{hi}), and CLA-expressing cells within this population were characterized by their staining with recombinant mouse E-Selectin/Fc chimera. The addition of ethylenediamine tetraacetic acid abolished binding of this chimera to the cells and served as a negative control (not shown). (a) Flow cytometry plots showing gated lymphocytes CD4⁺ and CD4⁺ memory population (CD4⁺CD62L^{lo}CD44^{hi}) from donor LNs. (b) Dot plots showing CLA vs. CD4 in the gated T-cell memory population CD4⁺CD62L^{lo}CD44^{hi}CLA⁺ from involved draining LNs or control LNs. (c) Dot plots showing CD4 vs. CCR4 (upper plot, CD4⁺CD62L^{lo}CD44^{hi}CLA⁺CCR4) or CD4 vs. CCR10 (lower plot, CD4⁺CD62L^{lo}CD44^{hi}CLA⁺CCR10) in the gated T-cell effector population from inflamed ear skin and control skin (left two panels) involved draining LNs and control LNs (right two panels). The differences in CCR4 and CCR10 expression observed in both skin and LN between treated and control animals were statistically significant (**P* < 0.05). LN, lymph node; CLA, cutaneous lymphocyte-associated antigen

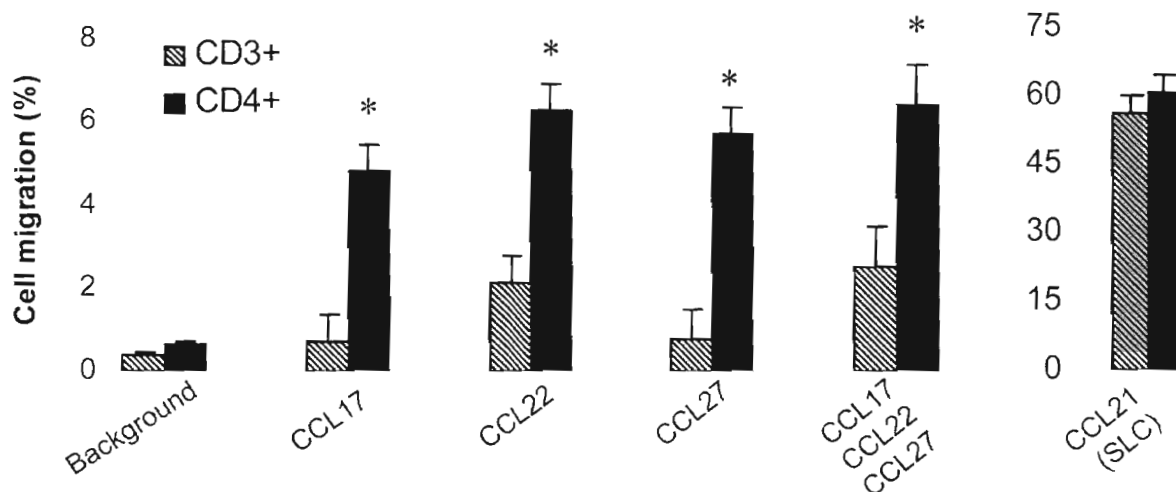
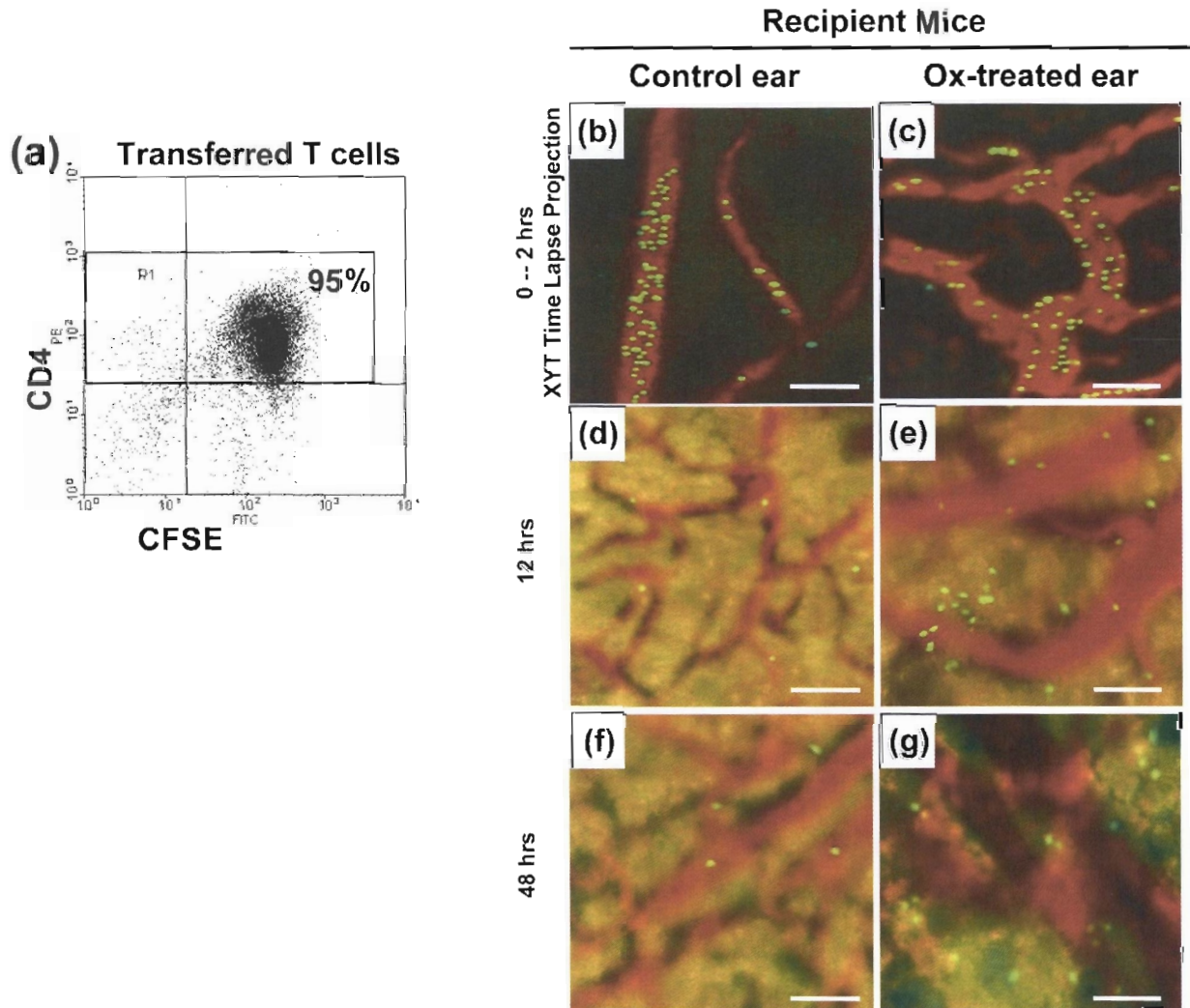


Fig. 3.

CD4⁺ T cells in oxazolone-induced ACD effectively migrate to CCL17, CCL22 and CCL27. Migration of purified CD4⁺ T lymphocytes obtained from skin draining LNs of donor mice compared with the migration of pan CD3⁺ T cells obtained from the same mice in response to optimal concentrations (100 nmol L⁻¹) of CCL17, CCL22 and CCL27 or the combination of all three through 3- μ m pores. Migration to CCL21 (SLC) served as a positive control. Migration was indicated as percentage of migrated T cells from upper chamber to bottom chamber. Background represents cell migration in response to the medium alone. The values represent the mean \pm SEM. These results are representative of three independent experiments. The data were obtained from eight different mice in each group. * $P < 0.05$. ACD, allergic contact dermatitis; SLC, secondary lymphoid tissue chemoattractant

**Fig. 4.**

In vivo confocal microscopy allows real-time evaluation of T-cell migration in an ACD mouse model. CD4⁺ T cells (5×10^7) from donor mice were labelled with CFSE *in vitro* (a) and injected intravenously into recipient Balb/c-SCID mice. Both ears of the living recipients were imaged after donor cell transfer and ear painting with oxazolone or vehicle. Immediately after transfer, a 2-h time lapse series of single-plane, 0.3- μ m thick, confocal images taken 2 min apart, showed circulating CFSE-labelled T cells (green) in the blood vessels of the vehicle control ear (b) and of the oxazolone-treated ear (c). The natural autofluorescence of haemoglobin in the blood vessels was imaged in the red channel and merged with the green channel to show the path of T cells through the vessels. The resultant X-Y-T image series were respectively flattened into a single projection to show the total path of migrating T cells through the blood vessels with respect to time. This migration was not merely peripheral or tangential to the vessels, as the T cells were both in the very same confocal plane of the vessels and corresponded spatially to the path of the vessels. Very few cells were seen incongruous to or outside of the vessels. After 12–48-h post-adoptive

transfer, composite bright-field/wide-field fluorescence images, approximately 15- μm thick, which show both green T cells and red blood vessels, exhibited higher numbers of extravasated T cells in the oxazolone-treated ear (e,g) in comparison to the vehicle control ear (d,f). Bar, 100 μm . ACD, allergic contact dermatitis; CFSE, carboxyfluorescein succinimidyl ester

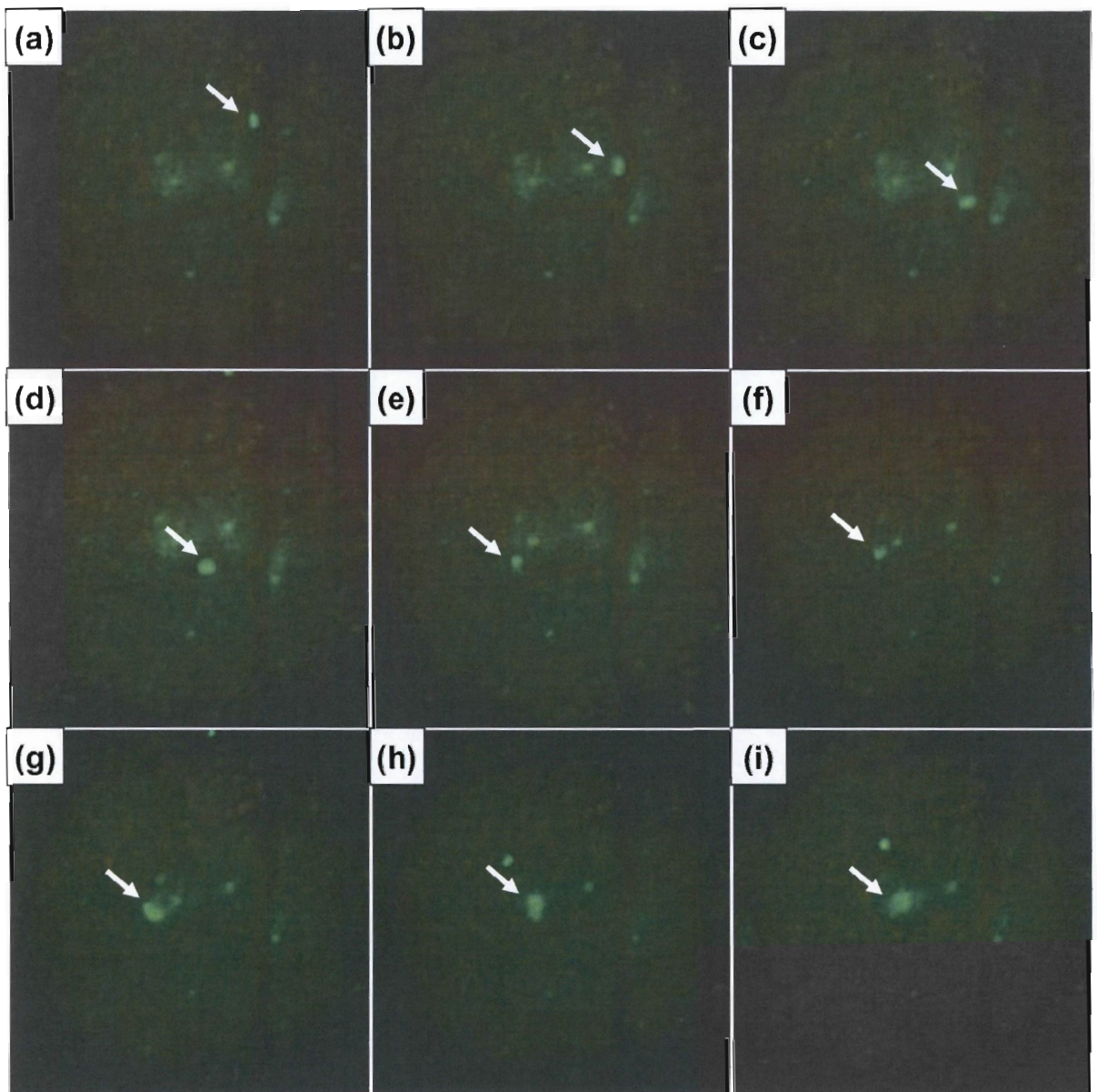
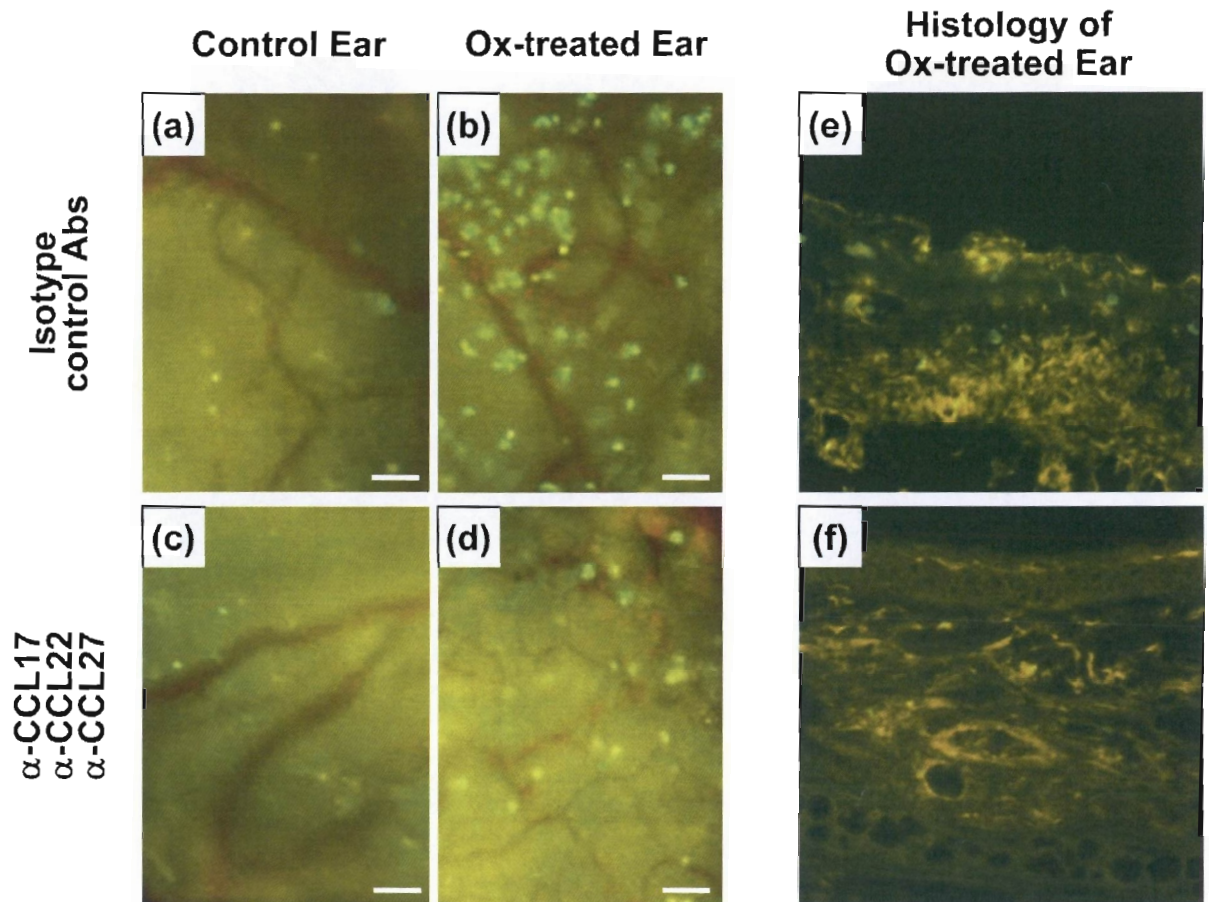


Fig. 5.

In vivo confocal microscopy allows real-time evaluation of T-cell attachment to blood vessels, rolling and extravasation into the skin in an allergic contact dermatitis mouse model. Still frames from a streaming video clip were imaged with wide-field fluorescence optics in the green channel, allowing visualization of CFSE⁺ T cells (arrows). Blood vessels are seen as dark, fluorescent negative channels. In these images, a T cell is seen initially moving within a blood vessel (a–d). Subsequently, the movement was progressively halted, and the T cell remained adherent to the endothelium for at least 20 s (e,f). It finally crossed the vessel wall (f,g), and was seen in the skin tissue (h,i). Acquisition rate of 30 frames per second was used. CFSE, carboxyfluorescein succinimidyl ester

Recipient mice (12 hrs after adoptive transfer and Ox challenge)



(g)

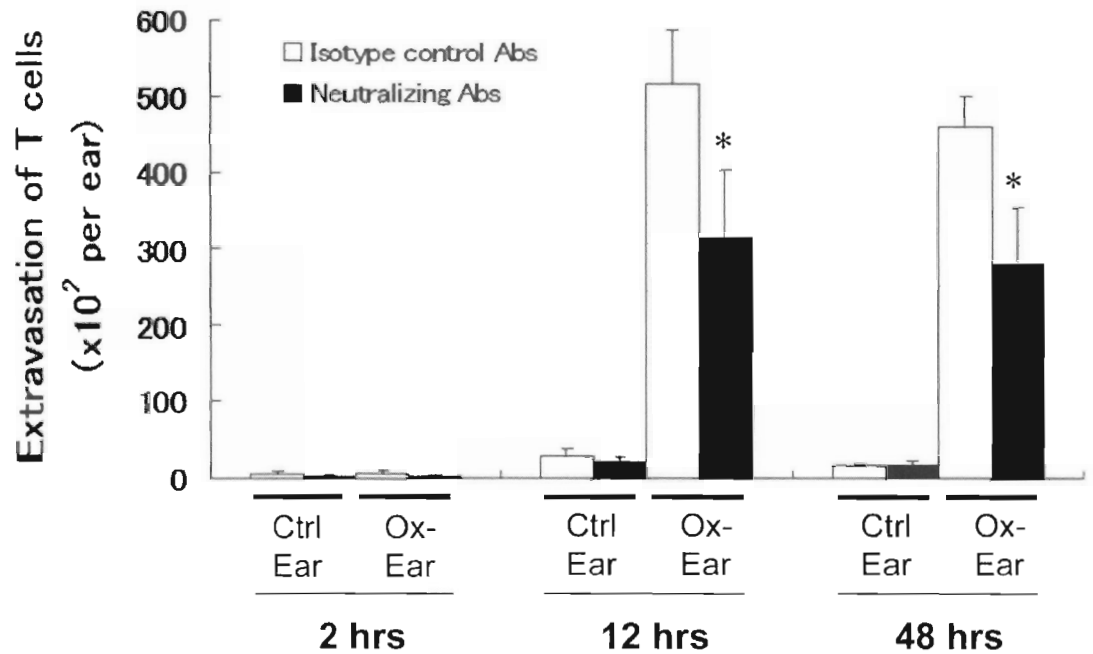


Fig. 6.

Neutralization of CCL17, CCL22 and CCL27 impairs lymphocyte recruitment to the inflamed ear skin. Neutralizing antibodies against CCL17, CCL22 and CCL27 were injected into recipient mice 6 h and 2 h before adoptive transfer of donor CFSE-labelled T cells and oxazolone challenge. Subsequent T-cell migration was assessed by fluorescence microscopy at 0, 2, 12 and 48 h after application of oxazolone to right ears. Cryostat sections of the ears were also processed for analysis CFSE⁺ T cells after being counterstained with Hoechst. Representative micrographs are shown from different skin areas of different mice. Wide-field fluorescence micrograph representing fields approximately 15- μ m thick was imaged in both green and red channels to show T cells and corresponding blood vessels. (a,b) Control ear and oxazolone-treated ear from mice were given relevant isotype control antibodies at 12 h after adoptive transfer and oxazolone challenge. Bar, 100 μ m. (c,d) Fluorescence images of control ear and oxazolone-treated ear from mice given neutralizing antibodies (anti-CCL17, anti-CCL22 and anti-CCL27). Bar, 100 μ m. (e) Cryostat section of oxazolone-treated ear from mice given isotype control antibodies. (f) Cryostat section of oxazolone-treated ear from mice given neutralizing antibodies. (g) Quantitative analysis of T-cell extravasation. At all time points (2h, 12h and 48h after oxazolone challenge), the entire recipient mouse ear was viewed by wide-field fluorescence microscopy, 10 nonconsecutive images were obtained, and the numbers of extravasated CFSE⁺ T cells in each field were counted in a blind fashion. The absolute number of total T cells in the whole ear was calculated. The data were obtained from four different mice in each group. Bars represent mean \pm SEM; **P* < 0.05. CFSE, carboxyfluorescein succinimidyl ester, Ctrl, control; Ox, oxazolone

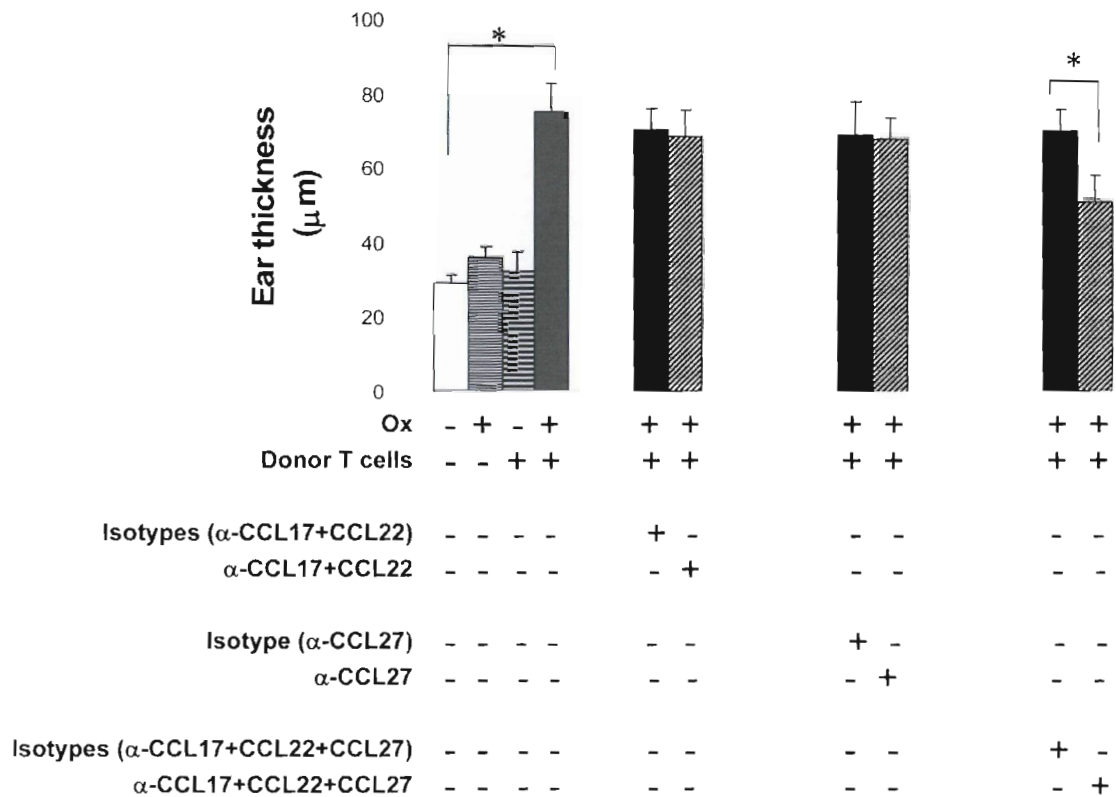


Fig. 7.

Inhibition of CCR4 and CCR10 *in vivo* impairs swelling of the oxazolone-challenged ears in recipient mice that received sensitized T cells. Antibodies against chemokine receptor ligands for either CCR4 or CCR10 individually or combined were injected 6 h and 2 h before adoptive transfer and oxazolone challenge. Ear thickness was measured 2, 12 and 48 h after the challenge. Ear thickness at 12-h post-challenge is presented. Vehicle application and/or no donor cell transfer or appropriate isotype control antibody treatments were used as controls. The data were obtained from 12 different mice in each group. Mean \pm SEM, * $P < 0.01$.



OPEN ACCESS

EXTENDED REPORT

MOR103, a human monoclonal antibody to granulocyte–macrophage colony-stimulating factor, in the treatment of patients with moderate rheumatoid arthritis: results of a phase Ib/IIa randomised, double-blind, placebo-controlled, dose-escalation trial

Frank Behrens,^{1,2} Paul P Tak,^{3,4,5} Mikkel Østergaard,⁶ Rumen Stoilov,⁷ Piotr Wiland,⁸ Thomas W Huizinga,⁹ Vadym Y Berenfus,¹⁰ Stoyanka Vladeva,¹¹ Juergen Rech,¹² Andrea Rubbert-Roth,¹³ Mariusz Korkosz,¹⁴ Dmitriy Rekalov,¹⁵ Igor A Zupanets,¹⁶ Bo J Ejbjerg,¹⁷ Jens Geiseler,¹⁸ Julia Fresenius,¹⁸ Roman P Korolkiewicz,¹⁹ Arndt J Schottelius,¹⁹ Harald Burkhardt^{1,2}

Handling editor Tore K Kvien

► Additional material is published online only. To view please visit the journal online (<http://dx.doi.org/10.1136/annrheumdis-2013-204816>).

For numbered affiliations see end of article.

Correspondence to

Professor Dr Harald Burkhardt, Division of Rheumatology/CIRI, Johann Wolfgang Goethe University, Theodor-Stern-Kai 7, Frankfurt/Main D 60590, Germany; Harald.Burkhardt@kgu.de

AJS and HB contributed equally.

Received 24 October 2013

Revised 9 January 2014

Accepted 24 January 2014

ABSTRACT

Objectives To determine the safety, tolerability and signs of efficacy of MOR103, a human monoclonal antibody to granulocyte–macrophage colony-stimulating factor (GM-CSF), in patients with rheumatoid arthritis (RA).

Methods Patients with active, moderate RA were enrolled in a randomised, multicentre, double-blind, placebo-controlled, dose-escalation trial of intravenous MOR103 (0.3, 1.0 or 1.5 mg/kg) once a week for 4 weeks, with follow-up to 16 weeks. The primary outcome was safety.

Results Of the 96 randomised and treated subjects, 85 completed the trial (n=27, 24, 22 and 23 for pooled placebo and MOR103 0.3, 1.0 and 1.5 mg/kg, respectively). Treatment emergent adverse events (AEs) in the MOR103 groups were mild or moderate in intensity and generally reported at frequencies similar to those in the placebo group. The most common AE was nasopharyngitis. In two cases, AEs were classified as serious because of hospitalisation: paronychia in a placebo subject and pleurisy in a MOR103 0.3 mg/kg subject. Both patients recovered fully. In exploratory efficacy analyses, subjects in the MOR103 1.0 and 1.5 mg/kg groups showed significant improvements in Disease Activity Score-28 scores and joint counts and significantly higher European League Against Rheumatism response rates than subjects receiving placebo. MOR103 1.0 mg/kg was associated with the largest reductions in disease activity parameters.

Conclusions MOR103 was well tolerated and showed preliminary evidence of efficacy in patients with active RA. The data support further investigation of this monoclonal antibody to GM-CSF in RA patients and potentially in those with other immune-mediated inflammatory diseases.

Trial registration number NCT01023256

INTRODUCTION

Despite major advances in the treatment of rheumatoid arthritis (RA), many patients are unable

to achieve treatment goals.^{1–2} There is thus a continuing need for the exploration and development of therapeutic strategies with novel mechanisms of action.

One molecule that may play a critical role in inflammatory arthritis is granulocyte–macrophage colony-stimulating factor (GM-CSF). Although originally characterised by its ability to promote myeloid haematopoiesis, GM-CSF is associated with a multitude of additional effects on mature myeloid cells, including stimulation of the production of inflammatory mediators by neutrophils and macrophages^{3–4} and promotion of the differentiation and pathogenicity of proinflammatory T-helper 17 cells.^{5–6}

Several lines of data suggest that GM-CSF strongly influences the development and pathogenesis of RA.⁷ Animal models support a key role for this molecule in both initiating and exacerbating inflammatory arthritis.^{8–11} In humans, GM-CSF is found at elevated levels in the synovial tissue and fluid of patients with RA.^{12–14} Exacerbation of established RA has been reported in patients who received GM-CSF as supportive therapy.^{14–15} More recently, clinical trials have found that GM-CSF receptor- α blockade reduced disease activity in patients with RA.^{16–17}

Targeting the cytokine directly by means of a monoclonal antibody to GM-CSF provides an alternative means of blocking GM-CSF. MOR103 is a high-affinity recombinant human IgG1 antibody that binds to a GM-CSF epitope, thereby blocking cytokine–receptor interaction and receptor activation.¹⁸ Although GM-CSF receptor blockade and direct GM-CSF targeting are both expected to block GM-CSF-mediated signalling, the targeting of receptor versus cytokine could potentially result in different target-mediated drug disposition. In addition, since MOR103 targets the soluble cytokine, no antibody- or complement-dependent cytotoxicity is anticipated. We report the results of the first in patient study with MOR103 in patients with RA.

To cite: Behrens F, Tak PP, Østergaard M, et al. *Ann Rheum Dis* Published Online First: [please include Day Month Year] doi:10.1136/annrheumdis-2013-204816

Clinical and epidemiological research

METHODS

Trial design and treatment

This trial (NCT01023256) was a randomised, double-blind, placebo-controlled, multidose, dose-escalation trial of three MOR103 doses (0.3, 1.0 and 1.5 mg/kg). These doses were chosen on the basis of a previous safety study in healthy human subjects and pharmacokinetic modelling of trough levels required for GM-CSF inhibition in synovial tissue. Additional information on the study drug manufacturer and intravenous administration can be found in the online supplementary text.

Subject eligibility was determined at the screening visit (up to 35 days before treatment initiation) and confirmed at baseline before the first dose on day 1. Eligible subjects were enrolled into three cohorts according to a randomisation schedule through an interactive web response system. All investigators and participants were blinded to the study randomisation scheme.

Each subject received a total of four doses, one per week at baseline and days 8 (week 1), 15 (week 2) and 22 (week 3). Subjects made follow-up visits to the trial centre at weeks 4, 5, 6, 8, 10, 13 and 16. An independent Data Safety Monitoring Board (DSMB) reviewed an interim safety report with data from at least 20 subjects in each of the first two cohorts (0.3 and 1.0 mg/kg). DSMB approval was required before the study was allowed to proceed to the next higher dose. A second safety review was performed when all subjects in these cohorts had completed their week 5 visit.

The trial was initiated on 19 January 2010 and the last visit was on 14 June 2012. Subjects were treated in 26 centres in Europe (see online supplementary table S1 for participating countries). The trial protocol was approved by the institutional review boards or independent ethics committees at the participating sites and was conducted in accordance with the Declaration of Helsinki (revised edition, Seoul 2008) and the International Conference on Harmonisation Guidelines for Good Clinical Practice. Patients provided written informed consent for the trial before undergoing screening procedures. Authors had full access to data and certify the accuracy and completeness of data analysis.

Subjects

Men or women 18 years of age or older with active RA according to the revised 1987 criteria of the American College of Rheumatology (ACR)¹⁹ and a body mass index between 19.0 and 35.0 kg/m² (inclusive) were eligible for this trial. Subjects were required to have: (1) at least three swollen and three tender joints using the Disease Activity Score-28 joints (DAS28) joint count, with at least one swollen joint in the wrist or hand excluding the proximal interphalangeal joints; (2) C-reactive protein (CRP) levels >5 mg/L if seronegative for rheumatoid factor and anti-cyclic citrullinated peptide antibody, or >2 mg/L if seropositive for either marker; (3) DAS28 ≤5.1; and (4) ACR functional class of I, II or III.²⁰ Patients with high disease activity (DAS28 >5.1) were excluded as the efficacy of MOR103 was unknown. Subjects had to be willing to use effective contraception, be surgically sterile or at least 2 years postmenopausal. Previous treatment with biological/immunosuppressive therapies other than cell-depleting agents was allowed with an adequate washout period. Stable concomitant treatment with non-biological disease-modifying antirheumatic drugs or low doses of oral corticosteroids was allowed. Exclusion criteria were presence or history of major chronic inflammatory autoimmune disease, clinically significant abnormalities in haematology

parameters, liver enzymes or pulmonary function tests (PFTs), and significant systemic illness or malignancy.

Safety and tolerability assessments

The primary end point was the evaluation of safety and tolerability. Data on adverse events (AEs; MedDRA V.13.0), vital signs, serum chemistry, haematology and urinalysis were collected at each visit. Additional evaluations included coagulation parameters, whole blood flow cytometry, and ECG. Samples for laboratory analyses were collected before dosing. Laboratory analyses were performed at a central laboratory (Eurofins Medinet BV, Breda, The Netherlands).

Because high levels of GM-CSF autoantibodies have been associated with idiopathic pulmonary alveolar proteinosis,^{21 22} serum surfactant D levels were measured at all visits except the screening visit, and PFTs, including forced expiratory volume in the first second (FEV₁), vital capacity, forced vital capacity and diffusing capacity of the lung for carbon monoxide (D_LCO), were performed at screening and weeks 2, 4, 10 and 16. Decreased D_LCO was reported as an AE only if judged to be potentially clinically relevant by the treating physician. An additional evaluation of patients experiencing a ≥20% decrease in D_LCO compared with screening was also conducted.

Serum levels of proinflammatory cytokines, including tumour necrosis factor (TNF), interleukin (IL)-1β, IL-6, IL-8, IL-10, interferon (IFN)-γ and GM-CSF (free cytokine only, not MOR103-bound GM-CSF), were measured at baseline, weeks 1–4 and week 16 by use of the Cytokine Multiplex Kit (Life Technologies GmbH, Darmstadt, Germany) and a Luminex reader. A validated direct ELISA was used to test patient serum samples for MOR103 antibodies at screening and weeks 10, 13 and 16. Bound drug antibodies were detected using anti-IgG- or anti-IgM-specific secondary antibodies.

Clinical assessments

The primary exploratory efficacy outcome was change from baseline in DAS28 calculated using the erythrocyte sedimentation rate as the acute phase reactant.²³ Other exploratory efficacy assessments included the proportions of patients achieving European League Against Rheumatism (EULAR) response²⁴ and ACR improvement criteria²⁵ and changes in DAS28 and ACR core measures, including tender joint count (TJC; 69 joints), swollen joint count (SJC; 66 joints), patient's self-assessment of pain (measured on a 100 mm visual analogue scale) and the Health Assessment Questionnaire-Disability Index (HAQ-DI).²⁶ Fatigue was measured at baseline and weeks 4, 8 and 16 by the Functional Assessment of Chronic Illness Therapy (FACIT)-fatigue self-assessment scale, which has been validated in RA.²⁷ MRI of the wrist and hand was performed at screening, week 4 and week 8. The side with a swollen wrist or the most swollen joints within the 2nd to 5th metacarpophalangeal (if neither or both wrists were swollen) was selected for imaging; the right side was chosen if swollen joints were equivalent. Two independent experts blinded to patient data and image chronology scored the images in a single reading campaign using the Outcome Measures in Rheumatology (OMERACT) RA MRI Studies (RAMRIS) scoring system.^{28 29} Central medical imaging services were provided by BioClinica (Newton, Pennsylvania, USA) and its affiliates.

Statistical methods

Data were analysed by descriptive statistics using SAS for Windows, Release V9.3. The Cochran–Mantel–Haenszel test and Fisher's exact test were used to determine p values for

EULAR and ACR response rates, respectively. *p* Values for other efficacy measures were derived from pairwise comparisons between each dosage group and the pooled placebo group based on an analysis of covariance (ANCOVA) model including fixed-effect terms for dose and the covariate CRP level at baseline. *p* Values were calculated on outcome parameters from weeks 4 through 16 but not at earlier visits, as the efficacy outcome of greatest interest was response after completion of treatment. Post hoc analyses of differences in baseline demographic characteristics among groups used the Kruskal-Wallis test. $p < 0.05$ indicated significance.

To minimise the risk of exposing a large number of subjects without evidence of clinical benefit, sample size calculations were based on the primary exploratory efficacy outcome, change in DAS28. Assuming a statistical power of 80%, an α of 0.05 (two-sided test), a common SD of 1.0, and a discontinuation rate of 15%, we estimated that 21 subjects were required for each MOR103 treatment group and seven subjects for each placebo group (pooled placebo group of 21) to demonstrate a difference of 1.0 point in mean DAS28 change from baseline in the active group compared with placebo. This treatment difference was based on the DAS28 difference between active and placebo treatments of 1.3–1.6 observed over 12 weeks with adalimumab,³⁰ adjusted for length of exposure.

RESULTS

Subjects

Of the 288 subjects who were screened, 98 were randomised, 96 received treatment at 26 trial centres in Europe, and 85 (86.7%) completed the study (figure 1; see online supplementary table S1 for distribution by country). Two randomised patients did not receive treatment and were excluded from all analyses. All patients who received treatment ($N=96$; full analysis set) were included in outcome assessments.

Baseline demographic and clinical characteristics were generally comparable among treatment groups, although post hoc analyses revealed differences in mean CRP levels and TJC that reached the level of significance (table 1).

Safety and tolerability

A total of 144 treatment-emergent AEs were reported in 54 (56.3%) subjects (42 subjects (60.9%) in the MOR103 groups (see online supplementary table S2) and 12 (44.4%) in the pooled placebo group). The most common treatment-emergent AE by preferred term in the active and placebo groups was nasopharyngitis (table 2). The incidences of fatigue, cough and AEs related to RA (worsening or flares) in the MOR103 group were >4% higher than in the placebo group. In eight of the nine MOR103 subjects who reported RA exacerbations, this AE occurred after the last dose of MOR103 (10 days to >12 weeks), suggesting that disease flares were related to withdrawal of active treatment. No cases of infusion reaction were reported, but temporal correlations suggest that one case of rash (MOR103 0.3 mg/kg) and one of fatigue (MOR103 1.0 mg/kg) may have been related to MOR103 infusion. Nasopharyngitis, fatigue, RA exacerbations, rhinitis and oropharyngeal pain occurred at higher incidences (>4% higher) in the MOR103 1.0 mg/kg group than in other active treatment groups or the pooled placebo group. These differences should be interpreted with caution as they are based on small subject numbers.

None of the AEs were considered to be probably or definitely related to treatment. AEs possibly related to treatment were reported in seven placebo (14 AEs) and 10 MOR103 subjects (19 AEs; table 3). Only three AEs (fatigue, anaemia and decreased D_LCO) were considered possibly related to treatment in more than one subject.

All AEs were judged to be of mild or moderate intensity except for one severe AE of hospitalisation due to paronychia in the placebo group. The patient recovered fully. There were two serious treatment-emergent AEs during the study: the aforementioned case of paronychia (placebo group) and pleurisy of moderate intensity (MOR103 0.3 mg/kg group), both of which resulted in hospitalisation. In the MOR103 subject, pleurisy was detected 5 days after the last dose of the trial. The patient was treated with antibiotics and recovered fully. One treatment-emergent AE in a placebo patient, decreased D_LCO , resulted in treatment discontinuation. There were no deaths in the trial.

Additional evaluations of subjects with a $\geq 20\%$ decrease in D_LCO or alterations in PFTs did not reveal any patterns of

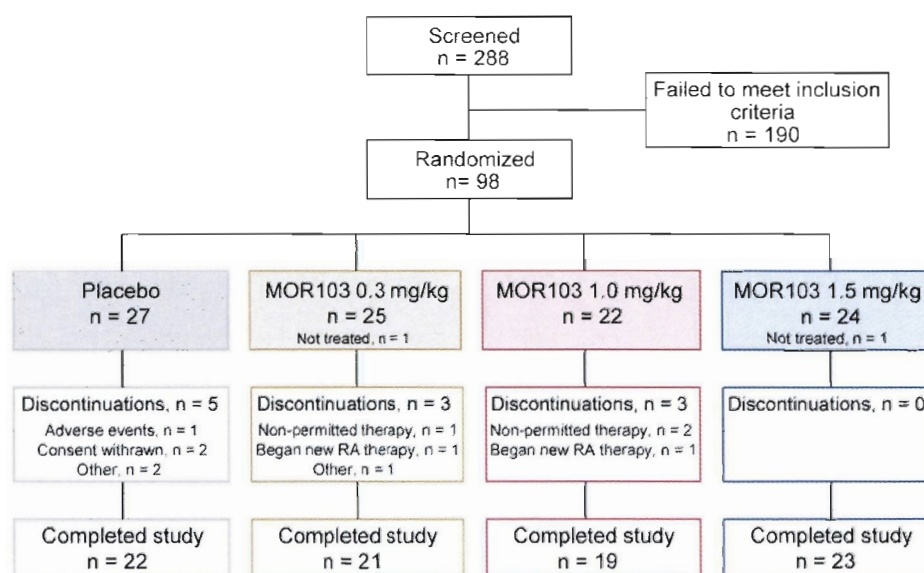


Figure 1 Disposition of patients with rheumatoid arthritis randomised to receive placebo or MOR103 in the full analysis set.

Clinical and epidemiological research

Table 1 Baseline demographic and clinical characteristics

Characteristic	Pooled placebo (N=27)	MOR103		
		0.3 mg/kg (N=24)	1.0 mg/kg (N=22)	1.5 mg/kg (N=23)
Age (years)	53.8 (12.7)	57.4 (8.3)	49.0 (12.7)	53.0 (9.9)
Body mass index (kg/m ²)	26.3 (3.5)	26.3 (3.6)	26.1 (4.6)	25.7 (4.7)
Female, n (%)	19 (70.4)	21 (87.5)	17 (77.3)	18 (78.3)
Caucasian, n (%)	27 (100)	24 (100)	22 (100)	23 (100)
DAS28-ESR	4.88 (0.41)	4.88 (0.54)	4.78 (0.66)*	4.87 (0.38)
CRP (mg/L)†	18.2 (20.0)	23.1 (20.8)	11.7 (12.6)	18.0 (30.1)
ESR (mm/h)	28.7 (14.8)	28.1 (12.2)	21.9 (12.0)	24.9 (14.4)
Swollen joints	6.3 (3.2)	5.5 (2.3)	7.3 (4.7)	6.7 (2.5)
Tender joints‡	9.4 (7.0)	8.0 (4.7)	12.3 (7.6)	11.3 (5.8)
RF positive,‡ n/N (%)	25/26 (96.2)	21/24 (87.5)	19/21 (90.5)	19/23 (82.6)
Anti-CCP positive,§ n/N (%)	17/25 (68.0)	16/21 (76.2)	16/21 (76.2)	16/22 (72.7)
Prior medication,¶ n (%)				
Systemic corticosteroids	18 (66.7)	21 (87.5)	13 (59.1)	16 (69.6)
DMARD**	21 (77.8)	18 (75.0)	15 (68.2)	20 (87.0)
TNF inhibitor	2 (7.4)	1 (4.2)	0 (0.0)	0 (0.0)
Concomitant medication at baseline, n (%)				
Systemic corticosteroids	19 (70.4)	20 (83.3)	13 (59.1)	15 (65.2)
DMARD**	26 (96.3)	22 (91.7)	17 (77.3)	21 (91.3)
MTX	21 (77.8)	18 (75.0)	14 (63.6)	19 (82.6)

Data are presented as mean (SD) unless otherwise indicated. For RF and anti-CCP positive, percentages were calculated on the number of patients with data, not on the full cohort size.

*One patient had missing data.

†p<0.05 for differences in mean values between groups by Kruskal–Wallis test.

‡Defined as >13.9 IU/mL.

§Defined as >5 U/mL.

¶Medication in the 3 months prior to screening.

**Conventional (non-biological) DMARDs.

CCP, cyclic citrullinated peptide; CRP, C-reactive protein; DAS, Disease Activity Score; DMARD, disease-modifying antirheumatic drug; ESR, erythrocyte sedimentation rate; MTX, methotrexate; RF, rheumatoid factor; TNF, tumour necrosis factor.

concern in MOR103-treated patients (see online supplementary text). There were no clinically important changes in surfactant D levels, vital signs, ECG, whole blood flow cytometry or urine, haematology or serum chemistry parameters during treatment and no clinically important differences between active treatment and placebo in these measures.

None of the peripheral blood cytokines evaluated in this trial showed notable or consistent changes related to MOR103 infusions (data not shown). The levels of GM-CSF and certain other cytokines, including IFN γ , TNF and IL-10, remained at or near the lower limit of quantification throughout the trial.

Serum samples were tested for anti-MOR103 IgG and IgM antibodies. Only sporadic positives were detected (see online supplementary text), and there was no evidence that antibodies to MOR103 affected serum MOR103 concentrations or clinical outcomes.

Efficacy

In exploratory investigations, the two higher doses of MOR103 were associated with significant reductions in disease activity. Compared with the pooled placebo group, significantly greater changes from baseline in DAS28 scores (the primary efficacy outcome according to study protocol) were observed in the MOR103 1.0 mg/kg group from weeks 4 through 10 and in the

Table 2 Incidence of treatment-emergent adverse events occurring in >2 subjects in any treatment group

Adverse event	Placebo (N=27)	MOR103			Pooled active (N=69)
		0.3 mg/kg (N=24)	1.0 mg/kg (N=22)	1.5 mg/kg (N=23)	
Subjects with any treatment-emergent AE	12 (44.4)	13 (54.2)	14 (63.6)	15 (65.2)	42 (60.9)
Nasopharyngitis	3 (11.1)	1 (4.2)	7 (31.8)	1 (4.3)	9 (13.0)
RA*	0 (0.0)	3 (12.5)	4 (18.2)	2 (8.7)	9 (13.0)
Fatigue	1 (3.7)	1 (4.2)	4 (18.2)	1 (4.3)	6 (8.7)
Hypertension	1 (3.7)	1 (4.2)	2 (9.1)	2 (8.7)	5 (7.2)
Headache	1 (3.7)	1 (4.2)	0 (0.0)	2 (8.7)	3 (4.3)
Cough	0 (0.0)	1 (4.2)	0 (0.0)	2 (9.7)	3 (4.3)
Anaemia	0 (0.0)	0 (0.0)	0 (0.0)	2 (8.7)	2 (2.9)
Decreased D _L co	2 (7.4)	2 (8.3)	0 (0.0)	0 (0.0)	2 (2.9)
Oropharyngeal pain	1 (3.7)	0 (0.0)	2 (9.1)	0 (0.0)	2 (2.9)
Rhinitis	0 (0.0)	0 (0.0)	2 (9.1)	0 (0.0)	2 (2.9)
Rhinorrhoea	0 (0.0)	0 (0.0)	0 (0.0)	2 (8.7)	2 (2.9)
Viral respiratory tract infection	0 (0.0)	0 (0.0)	0 (0.0)	2 (8.7)	2 (2.9)
Peripheral oedema	2 (7.4)	0 (0.0)	1 (4.5)	0 (0.0)	1 (1.4)
Rash	3 (11.1)	1 (4.2)	0 (0.0)	0 (0.0)	1 (1.4)
Upper respiratory tract infection	2 (7.4)	0 (0.0)	0 (0.0)	0 (0.0)	0 (0.0)
Urinary tract infection	3 (11.1)	0 (0.0)	0 (0.0)	0 (0.0)	0 (0.0)

Values shown are number (%) of subjects with events.

*Worsening or exacerbation of existing RA (flares). Except for one patient in the MOR103 0.3 mg/kg group (date of flare not reported), all events occurred from 10 days to >12 weeks following the last dose of active treatment.

AE, adverse event; D_Lco, diffusing capacity of the lung for carbon monoxide; RA, rheumatoid arthritis.

MOR103 1.5 mg/kg group from weeks 4 through 6 (figure 2; see online supplementary figure S1 for mean DAS28 scores during treatment). There were no significant differences in DAS28 changes between placebo and MOR 103 0.3 mg/kg. In the MOR103 1.0 and 1.5 mg/kg groups, improvements in DAS28 scores were observed at the earliest post-treatment visit (week 1). By week 16, mean DAS28 scores were at or above baseline in all groups except MOR103 1.0 mg/kg, which continued to maintain DAS28 scores at levels well below baseline. As with DAS28, the MOR103 1.0 mg/kg group showed the most pronounced effects in additional efficacy outcomes (highest response rates and largest reductions in disease activity parameters; table 4).

MRIs were evaluated for synovitis, bone oedema and erosions at weeks 4 and 8 by the OMERACT RAMRIS scoring system. No statistically significant differences between the pooled placebo group and any of the MOR103 groups were observed (data not shown). The largest difference between active treatment and placebo was for the MOR103 1.0 mg/kg synovitis score at week 4 (−0.84 vs placebo; p=0.35).

DISCUSSION

A growing body of literature has documented the potential role of GM-CSF in the pathogenesis of RA. Here we present the first in patient data on the effects of GM-CSF blockade by means of a fully-human antibody to GM-CSF, MOR103, in patients with RA. Although the primary objective of this trial was to determine the safety and tolerability of multiple doses of MOR103,

Table 3 Incidence of possibly treatment-related AEs by preferred term for AEs occurring in one or more MOR103-treated subjects

Adverse event	MOR103				Pooled active (N=69)
	Placebo (N=27)	0.3 mg/kg (N=24)	1.0 mg/kg (N=22)	1.5 mg/kg (N=23)	
Subjects with at least 1 possibly treatment-related AE*	7 (25.9)	3 (12.5)	3 (13.6)	4 (17.4)	10 (14.5)
Fatigue	0 (0.0)	1 (4.2)	1 (4.5)	1 (4.3)	3 (4.3)
Anaemia	0 (0.0)	0 (0.0)	0 (0.0)	2 (8.7)	2 (2.9)
Decreased D _{LCO}	1 (3.7)	2 (8.3)	0 (0.0)	0 (0.0)	2 (2.9)
Nasopharyngitis	2 (7.4)	1 (4.2)	0 (0.0)	0 (0.0)	1 (1.4)
Rash	2 (7.4)	1 (4.2)	0 (0.0)	0 (0.0)	1 (1.4)
Decreased FEV ₁	0 (0.0)	1 (4.2)	0 (0.0)	0 (0.0)	1 (1.4)
Sinus tachycardia	0 (0.0)	1 (4.2)	0 (0.0)	0 (0.0)	1 (1.4)
RA flare	0 (0.0)	0 (0.0)	1 (4.5)	0 (0.0)	1 (1.4)
Nausea	0 (0.0)	0 (0.0)	1 (4.5)	0 (0.0)	1 (1.4)
Oedema	0 (0.0)	0 (0.0)	1 (4.5)	0 (0.0)	1 (1.4)
Hypertension	0 (0.0)	0 (0.0)	1 (4.5)	0 (0.0)	1 (1.4)
Dermatitis	0 (0.0)	0 (0.0)	1 (4.5)	0 (0.0)	1 (1.4)
Oral herpes	0 (0.0)	0 (0.0)	0 (0.0)	1 (4.3)	1 (1.4)
Rales	0 (0.0)	0 (0.0)	0 (0.0)	1 (4.3)	1 (1.4)
Presyncope	0 (0.0)	0 (0.0)	0 (0.0)	1 (4.3)	1 (1.4)

Subjects could have more than one AE. Values shown are number (%) of subjects with events.

*14 AEs in placebo group; 7 in MOR103 0.3 mg/kg; 6 in MOR103 1.0 mg/kg; 6 in MOR103 1.5 mg/kg. Additional AEs in the placebo group that did not occur in a MOR103 subject and are not shown in the table were increased liver function tests (n=2) and one case each of pharyngitis, upper respiratory tract infection, urinary tract infection, flank pain, oropharyngeal pain, exertional dyspnoea and haematoma. AE, adverse event; D_{LCO}, diffusing capacity of the lung for carbon monoxide; FEV₁, forced expiratory volume in the first second; RA, rheumatoid arthritis.

exploratory analyses provided suggestive evidence for the efficacy of this agent.

In this phase Ib/IIa clinical trial, MOR103 was well tolerated and associated with a satisfactory safety profile in patients with active moderate RA who received up to four doses at weekly intervals. Although overall rates of treatment-emergent AEs

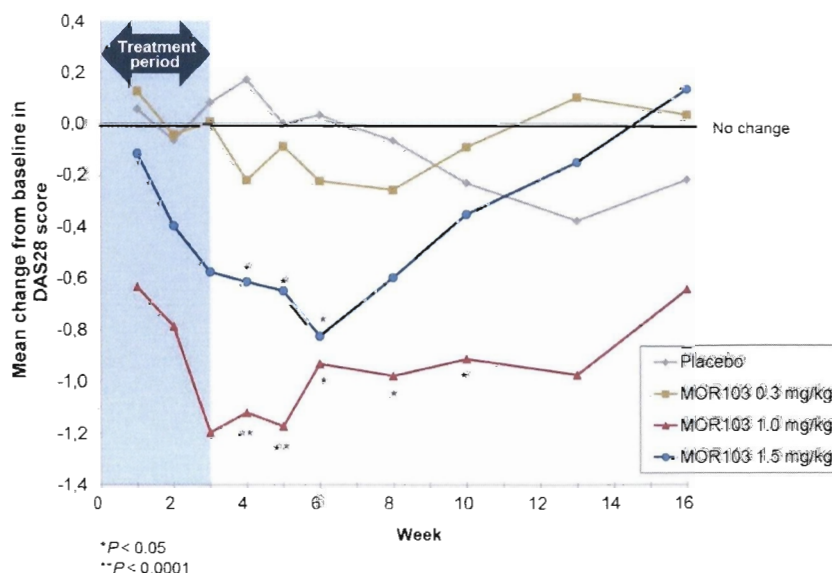
were higher in the MOR103 groups (60.0%) compared with placebo (44.4%), most treatment-emergent AEs occurred at similar incidences. Fatigue, cough and RA worsening/flare (primarily occurring after the end of active treatment) were reported more frequently by MOR103 subjects than placebo subjects. All treatment-emergent AEs in the MOR103 groups were of mild or moderate intensity. One serious AE, pleurisy of moderate intensity, occurred in a MOR103 subject (0.3 mg/kg) and resolved on antibiotic treatment.

Because of the association between GM-CSF autoantibodies and idiopathic pulmonary alveolar proteinosis,^{21 22} surfactant D levels and PFTs were closely monitored. Decreased D_{LCO} was observed in some subjects, but there were no obvious differences between placebo and active treatment groups. Surfactant D levels remained normal and there was no overall pattern of PFT alterations in MOR103-treated subjects. Similar findings on the lung safety of anti-GM-CSF receptor therapy were reported in the phase II mavrilimumab trial.¹⁷ Cytokine release was not observed in MOR103-treated subjects. Anti-MOR103 antibody testing detected only sporadic positives, and there was no clear association between assay results and clinical outcomes.

In exploratory efficacy analyses, MOR103 resulted in significant improvements relative to placebo in several outcome measures. The most pronounced effects were observed with MOR103 1.0 mg/kg. The effect of this dose on disease activity was robust for all major efficacy variables and over time, and did not appear to be driven by geographical imbalance, individual centres, concomitant medications, or outliers. Subjects treated with MOR103 1.5 mg/kg also showed significant improvements in certain efficacy parameters, but the changes were not as pronounced or as sustained as for MOR103 1.0 mg/kg. A rapid onset of action was observed at both of the higher MOR103 doses. MOR103 0.3 mg/kg resulted in significant improvements over placebo in SJC at week 4, but did not affect other measures of disease activity.

It seems unlikely that the discrepancy in clinical activity between the 1.0 and 1.5 mg/kg doses reflects a true difference in clinical efficacy, as the difference in dose is relatively small and we are not aware of other studies of cytokine inhibition with a bell-shaped optimum response curve. As for other phase I/II clinical trials, limitations of this study include its small

Figure 2 Mean change from baseline in DAS28 scores. Statistical significance was not evaluated before the week 4 visit as specified in the study protocol. DAS28, Disease Activity Score-28 joints.



Clinical and epidemiological research

Table 4 Efficacy outcomes at weeks 4 and 8

Outcome	Pooled placebo (N=27)		MOR103		1.0 mg/kg (N=22)		1.5 mg/kg (N=23)	
	Week 4	Week 8	Week 4	Week 8	Week 4	Week 8	Week 4	Week 8
<i>Response assessments, n (%)</i>								
EULAR								
Good	1 (3.7)	1 (3.7)	3 (12.5)	1 (4.2)	5 (22.7)	7 (31.8)	1 (4.3)	2 (8.7)
Moderate	1 (3.7)	6 (22.2)	6 (25.0)	7 (29.2)	10 (45.5)	6 (27.3)	15 (65.2)	11 (47.8)
None	20 (74.1)	15 (55.6)	14 (58.3)	13 (54.2)	6 (27.3)	6 (27.3)	7 (30.4)	10 (43.5)
Missing	5 (18.5)	5 (18.5)	1 (4.2)	3 (12.5)	1 (4.5)	3 (13.6)	0 (0.0)	0 (0.0)
p Value*	–	–	0.06	0.91	0.0002	0.019	0.0001	0.2565
ACR								
ACR20	2 (7.4)	5 (18.5)	6 (25.0)	3 (12.5)	15 (68.2)†	7 (31.8)	7 (30.4)	6 (26.1)
ACR50	1 (3.7)	2 (7.4)	1 (4.2)	0 (0.0)	5 (22.7)	4 (18.2)	2 (8.7)	0 (0.0)
ACR70	0 (0.0)	0 (0.0)	1 (4.2)	0 (0.0)	1 (4.5)	2 (9.1)	0 (0.0)	0 (0.0)
Missing	5 (18.5)	5 (18.5)	1 (4.2)	3 (12.5)	1 (4.5)	2 (9.1)	0 (0.0)	0 (0.0)
<i>Additional efficacy assessments, change from baseline in mean values (SD)</i>								
DAS28	0.2 (0.8)	−0.1 (0.9)	−0.2 (1.1)	−0.3 (0.9)	−1.1 (0.9)†	−1.0 (1.3)‡	−0.6 (0.7)‡	−0.6 (0.9)
Swollen joints	0.1 (3.5)	−0.8 (3.6)	−1.7 (2.4)‡	−1.9 (2.2)	−3.5 (5.1)‡	−4.1 (4.4)‡	−3.3 (3.2)‡	−3.3 (3.1)‡
Tender joints	2.0 (6.4)	2.1 (8.0)	0.1 (7.1)	0.3 (5.0)	−4.8 (3.2)§	−6.8 (4.1)†	−3.7 (6.2)‡	−4.0 (5.3)§
ESR (mm/h)	2.8 (12.5)	0.9 (13.1)	8.8 (24.5)	2.0 (16.6)	−6.3 (12.5)	−0.7 (17.4)	−2.5 (17.7)	−0.6 (14.3)
Pain	−3.3 (16.5)	−8.0 (16.1)	−8.6 (22.8)	−4.1 (23.1)	−17.4 (17.2)‡	−13.4 (20.9)	−11.4 (11.5)	−9.5 (11.9)
HAQ-DI	−0.45 (0.54)	−0.44 (0.54)	−0.21 (0.41)‡	−0.21 (0.56)	−0.53 (0.52)	−0.51 (0.56)	−0.31 (0.24)	−0.25 (0.22)
Physician GA	−3.0 (15.7)	−3.5 (16.3)	−0.6 (19.7)	−4.7 (20.0)	−18.0 (19.6)‡	−18.1 (22.6)‡	−7.8 (10.8)	−6.5 (13.4)
Patient GA	−3.0 (16.1)	−8.2 (17.5)	−2.7 (20.5)	−4.5 (21.9)	−16.6 (15.6)‡	−13.3 (24.7)	−6.0 (17.7)	−4.0 (18.3)
FACIT fatigue scores	3.0 (8.1)	4.3 (9.1)	2.7 (9.2)	2.1 (5.6)	9.1 (10.2)‡	9.4 (12.6)	3.1 (6.0)	4.7 (7.1)

*p Values for pairwise comparisons with pooled placebo group determined by Cochran–Mantel–Haenszel test (missing values not included).

†p<0.0001 for pairwise comparisons with pooled placebo group. Fisher's exact test was used for ACR response (missing values not included) and ANCOVA was used for additional efficacy assessments.

‡p<0.05 for pairwise comparisons with placebo group by ANCOVA.

§p<0.001 for pairwise comparisons with placebo group by ANCOVA.

ACR, American College of Rheumatology; ANCOVA, analysis of covariance; DAS28, Disease Activity Score-28 joints; ESR, erythrocyte sedimentation rate; EULAR, European League Against Rheumatism; FACIT, Functional Assessment of Chronic Illness Therapy; GA, global assessment of disease activity; HAQ-DI, Health Assessment Questionnaire-Disability Index.

sample size, limited duration, and exclusion of patients with severe RA. Larger clinical trials are needed to define the optimal MOR103 dosage.

It is too early to comment on possible differences in clinical profiles between MOR103 and mavrimumab, an antibody to GM-CSF receptor.^{16 17} Because of the different targets of these two agents (soluble cytokine vs membrane-bound receptor), there may be differences in tolerability and spectrum of activity. Further studies will be required to explore these issues.

The data presented here establish proof of concept for the use of antibodies to GM-CSF in the treatment of RA and support the initiation of larger clinical trials to confirm the safety and efficacy of MOR103. Our findings suggest that MOR103 has the potential to become a novel and valuable therapeutic option for RA.

Author affiliations

¹CIRI/Division of Rheumatology, Johann Wolfgang Goethe-University, Frankfurt am Main, Germany

²Department of Translational Medicine and Pharmacology, Fraunhofer Institute IME, Frankfurt am Main, Germany

³Academic Medical Center/University of Amsterdam, Amsterdam, The Netherlands

⁴GlaxoSmithKline, Stevenage, UK

⁵University of Cambridge, Cambridge, UK

⁶Copenhagen Center for Arthritis Research, Center for Rheumatology and Spinal Diseases, Copenhagen University Hospital Glostrup, Glostrup, Denmark

⁷University Hospital (MHAT) St Ivan Rilski, Sofia, Bulgaria

⁸Department of Rheumatology and Internal Medicine, Wrocław Medical University, Wrocław, Poland

⁹Department of Rheumatology, Leiden University Medical Center, Leiden, The Netherlands

¹⁰Regional Clinical Hospital, Donetsk, Ukraine

¹¹Second Internal Clinic UMHAT Stara Zagora, Stara Zagora, Bulgaria

¹²University of Erlangen-Nuremberg, Erlangen, Germany

¹³Med Clinic I, University of Cologne, Cologne, Germany

¹⁴Malopolskie Centrum Medyczne, Krakow, Poland

¹⁵Zaporizhzhia Regional Hospital, Zaporozhe, Ukraine

¹⁶National University of Pharmacy, Kharkiv, Ukraine

¹⁷Department of Rheumatology, Hospital at Slagelse, Slagelse, Denmark

¹⁸Asklepios Clinic Munich-Gauting, Gauting, Germany

¹⁹MorphoSys AG, Martinsried/Planegg, Germany

Acknowledgements We thank all of the patients and investigators who participated in this trial. We also thank Samson Fung (Fung Consulting, Eching, Germany) and Dominika Weinelt (MorphoSys AG, Martinsried/Planegg, Germany) for contributing to data analysis and interpretation, Steffen Stürzebecher (MorphoSys AG, Martinsried/Planegg, Germany) for reviewing the manuscript, and Sharon L Cross, PhD (Mission Viejo, CA) for providing medical writing services on behalf of MorphoSys AG.

Contributors All authors were involved in drafting the article or revising it critically for important intellectual content, and all authors approved the final version. FB, PPT, MØ, TWH, AJS and HB were involved in the study conception and design, FB, PPT, MØ, BJE, RS, PW, TWH, VYB, SV, JR, AR-R, MK, DR, IAZ, BOE, JG, JF and HB were responsible for data acquisition, and FB, PPT, MØ, RPK, AJS and HB were involved in analysis and interpretation of data.

Funding The study was supported by MorphoSys AG, which provided funding for the trial, data analyses, and medical writing services.

Competing interests FB, PPT, MØ, RS, PW, TWH, VYB, SV, JR, AR-R, MK, DR, IAZ and HB have received investigator grants and/or advisory fees from MorphoSys AG, the sponsor of this study. MØ, BJE, JG and JF received compensation from MorphoSys for their work as central readers for MRI or pulmonary function tests during the trial. RPK and AJS are employees of MorphoSys AG.

Patient consent Obtained.

Ethics approval Institutional review boards or independent ethics committees at the participating sites (26 centres in Europe).

Provenance and peer review Not commissioned; externally peer reviewed.

Open Access This is an Open Access article distributed in accordance with the Creative Commons Attribution Non Commercial (CC BY-NC 3.0) license, which permits others to distribute, remix, adapt, build upon this work non-commercially, and license their derivative works on different terms, provided the original work is properly cited and the use is non-commercial. See: <http://creativecommons.org/licenses/by-nc/3.0/>

REFERENCES

- Furst DE, Pangan AL, Harrold LR, *et al*. Greater likelihood of remission in rheumatoid arthritis patients treated earlier in the disease course: results from the Consortium of Rheumatology Researchers of North America registry. *Arthritis Care Res (Hoboken)* 2011;63:856–64.
- Hetland ML, Christensen IJ, Tarp U, *et al*. Direct comparison of treatment responses, remission rates, and drug adherence in patients with rheumatoid arthritis treated with adalimumab, etanercept, or infliximab. *Arthritis Rheum* 2010;62:22–32.
- Hamilton JA. Colony-stimulating factors in inflammation and autoimmunity. *Nat Rev Immunol* 2008;8:533–44.
- Cornish AL, Campbell IK, McKenzie BS, *et al*. G-CSF and GM-CSF as therapeutic targets in rheumatoid arthritis. *Nat Rev Rheumatol* 2009;5:554–9.
- Sonderegger I, Iezzi G, Maier R, *et al*. GM-CSF mediates autoimmunity by enhancing IL-6-dependent Th17 cell development and survival. *J Exp Med* 2008;205:2281–94.
- El-Behi M, Ciric B, Dai H, *et al*. The encephalitogenicity of Th17 cells is dependent on IL-1- and IL-23-induced production of the cytokine GM-CSF. *Nat Immunol* 2011;12:568–75.
- Hamilton JA, Tak PP. The dynamics of macrophage lineage populations in inflammatory and autoimmune diseases. *Arthritis Rheum* 2009;60:1210–21.
- Cook AD, Braine EL, Campbell IK, *et al*. Blockade of collagen-induced arthritis post-onset by antibody to granulocyte-macrophage colony-stimulating factor (GM-CSF): requirement for GM-CSF in the effector phase of disease. *Arthritis Res* 2001;3:293–8.
- Plater-Zyberk C, Joosten LA, Helsen MM, *et al*. GM-CSF neutralisation suppresses inflammation and protects cartilage in acute streptococcal cell wall arthritis of mice. *Ann Rheum Dis* 2007;66:452–7.
- Cook AD, Turner AL, Braine EL, *et al*. Regulation of systemic and local myeloid cell subpopulations by bone marrow cell-derived granulocyte-macrophage colony-stimulating factor in experimental inflammatory arthritis. *Arthritis Rheum* 2011;63:2340–51.
- Cook AD, Pobjoy J, Sarros S, *et al*. Granulocyte-macrophage colony-stimulating factor is a key mediator in inflammatory and arthritic pain. *Ann Rheum Dis* 2013;72:265–70.
- Alvaro-Gracia JM, Zvaifler NJ, Brown CB, *et al*. Cytokines in chronic inflammatory arthritis. VI. Analysis of the synovial cells involved in granulocyte-macrophage colony-stimulating factor production and gene expression in rheumatoid arthritis and its regulation by IL-1 and tumor necrosis factor- α . *J Immunol* 1991;146:3365–71.
- Wright HL, Bucknall RC, Moots RJ, *et al*. Analysis of SF and plasma cytokines provides insights into the mechanisms of inflammatory arthritis and may predict response to therapy. *Rheumatology* 2012;51:451–9.
- de Vries EG, Willemse PH, Biesma B, *et al*. Flare-up of rheumatoid arthritis during GM-CSF treatment after chemotherapy. *Lancet* 1991;338:517–18.
- Hazenberg BP, Van Leeuwen MA, Van Rijswijk MH, *et al*. Correction of granulocytopenia in Felty's syndrome by granulocyte-macrophage colony-stimulating factor. Simultaneous induction of interleukin-6 release and flare-up of the arthritis. *Blood* 1989;74:2769–70.
- Burmester GR, Feist E, Sleeman MA, *et al*. Mavrilimumab, a human monoclonal antibody targeting GM-CSF receptor- α , in subjects with rheumatoid arthritis: a randomised, double-blind, placebo-controlled, phase I, first-in-human study. *Ann Rheum Dis* 2011;70:1542–49.
- Burmester GR, Weinblatt ME, McInnes IB, *et al*. Efficacy and safety of mavrilimumab in subjects with rheumatoid arthritis. *Ann Rheum Dis* 2013;72:1445–52.
- Steidl S, Ratsch O, Brocks B, *et al*. *In vitro* affinity maturation of human GM-CSF antibodies by targeted CDR-diversification. *Mol Immunol* 2008;46:135–44.
- Arnett FC, Edworthy SM, Bloch DA, *et al*. The American Rheumatism Association 1987 revised criteria for the classification of rheumatoid arthritis. *Arthritis Rheum* 1988;31:315–24.
- Hochberg MC, Chang RW, Dvosh I, *et al*. The American College of Rheumatology 1991 revised criteria for the classification of global functional status in rheumatoid arthritis. *Arthritis Rheum* 1992;35:498–502.
- Kitamura T, Tanaka N, Watanabe J, *et al*. Idiopathic pulmonary alveolar proteinosis as an autoimmune disease with neutralizing antibody against granulocyte/macrophage colony-stimulating factor. *J Exp Med* 1999;190:875–80.
- Bonfield TL, Russell D, Burgess S, *et al*. Autoantibodies against granulocyte macrophage colony-stimulating factor are diagnostic for pulmonary alveolar proteinosis. *Am J Respir Cell Mol Biol* 2002;27:481–6.
- Prevoo ML, van 't Hof MA, Kuper HH, *et al*. Modified disease activity scores that include twenty-eight-joint counts. Development and validation in a prospective longitudinal study of patients with rheumatoid arthritis. *Arthritis Rheum* 1995;38:44–8.
- van Gestel AM, Prevoo MLL, van't Hof MA, *et al*. Development and validation of the European League Against Rheumatism response criteria for rheumatoid arthritis. Comparison with the preliminary American College of Rheumatology and the World Health Organization/International League Against Rheumatism criteria. *Arthritis Rheum* 1996;39:34–40.
- Felson DT, Anderson JJ, Boers M, *et al*. American College of Rheumatology preliminary definition of improvement in rheumatoid arthritis. *Arthritis Rheum* 1995;38:727–35.
- Fries JF, Spitz P, Kraines RG, *et al*. Measurement of patient outcome in arthritis. *Arthritis Rheum* 1980;23:137–45.
- Cella D, Yount S, Sorensen M, *et al*. Validation of the functional assessment of chronic illness therapy fatigue scale relative to other instrumentation in patients with rheumatoid arthritis. *J Rheumatol* 2005;32:811–19.
- Østergaard M, Peterfy C, Conaghan P, *et al*. OMERACT Rheumatoid Arthritis Magnetic Resonance Imaging Studies. Core set of MRI acquisitions, joint pathology definitions, and the OMERACT RA-MRI scoring system. *J Rheumatol* 2003;30:1385–6.
- Conaghan P, Bird P, Ejbjerg B, *et al*. The EULAR-OMERACT rheumatoid arthritis MRI reference image atlas: the metacarpophalangeal joints. *Ann Rheum Dis* 2005;64(Suppl 1):11–21.
- van de Putte LBA, Rau R, Breedveld FC, *et al*. Efficacy and safety of the fully human anti-tumour necrosis factor α monoclonal antibody adalimumab (D2E7) in DMARD refractory patients with rheumatoid arthritis: a 12 week, phase II study. *Ann Rheum Dis* 2003;62:1168–77.